

DELHI COLLEGE OF ENGINEERING



सत्यमेव जयते

LIBRARY

Class No. ....

Book No. ....

Accession No. ....

**Borrower is requested  
to check the book and  
get the signatures on the  
torned pages, if any.**

---

**DELHI COLLEGE OF ENGINEERING**  
**Kashmere Gate, Delhi**



**L I B R A R Y**

**DATE DUE**

For each day's delay after the due date a fine of **10 P.** per Vol. shall be charged for the first week, and **50 P.** per Vol. per day for subsequent day. Text Book Re. **1.00.**

Borrower's No.	Date Due	Borrower's No.	Date Due
-------------------	----------	-------------------	----------





# D-C AND A-C MACHINES

## BASED ON FUNDAMENTAL LAWS

BY

MICHAEL LIWSCHITZ-GARIK, Dr-Ing.

*Professor at the Polytechnic Institute of Brooklyn  
Consulting Engineer to the Westinghouse Electric Corporation*

ASSISTED BY

ROBERT T. WEIL, Jr., M.S.

*Professor and Head  
Department of Electrical Engineering  
Manhattan College*



D. VAN NOSTRAND COMPANY, INC.

PRINCETON, NEW JERSEY

TORONTO

NEW YORK

LONDON

D. VAN NOSTRAND COMPANY, INC.  
120 Alexander St., Princeton, New Jersey (Principal office)  
24 West 40th Street, New York 18, New York

D. VAN NOSTRAND COMPANY, LTD.  
358, Kensington High Street, London, W.14, England

D. VAN NOSTRAND COMPANY (Canada), LTD.  
25 Hollinger Road, Toronto 16, Canada

COPYRIGHT © 1952

BY

D. VAN NOSTRAND COMPANY, INC.

Published simultaneously in Canada by

D. VAN NOSTRAND COMPANY (Canada) LTD.

---

*All Rights Reserved*

*This book, or any parts thereof, may not be  
reproduced in any form without written per-  
mission from the authors and the publishers.*

---

Library of Congress Catalogue Card No. 52-6380

01614a10

PRINTED IN THE UNITED STATES OF AMERICA

To my grandchildren,  
**KATHERINE, ALICE, AND PETER,**  
I dedicate my work.



## PREFACE

This text is written for communications as well as power majors taking a one-year course in electric machines. The principal aim of this work is not merely to demonstrate to the student the operation and performance of the electric machine but rather *to teach the student how to deduce machine characteristics from the fundamental laws*, which represent the essence of our knowledge.

It is the author's experience of many years that most students and young engineers are unaware of the fact that the only approach to the solution of a problem lies first in the *selection* of the fundamental laws which refer to the problem and then in the *application* of these laws.

The electric machine consists of several electric circuits interlinked with magnetic fluxes and of one or more magnetic circuits. Therefore, Faraday's law of induction of an emf in a coil interlinked with a magnetic flux, Kirchhoff's mesh law of the electric circuit, and Ampère's law (circuit law) of the magnetic field belong to the fundamental laws which alone can yield the answer to the problem of electric machine operation and performance. Adding to these three laws Biot-Savart's law of the force on a current-carrying conductor in a magnetic field completes the fundamental laws necessary for a perfect understanding of the electric machine as presented in the frame of this book.

In accordance with the aim of the text, the equations of the circuits of the individual machines are set up first and then the operation and performance of the machine are derived from these equations. //

The author hopes that the method of attack applied in this text, i.e., persistently referring to the fundamental laws, will be helpful to the student in solving problems other than those treated in this text. Engineers are too often inclined to start a new problem by setting up an equivalent circuit without deriving it from the fundamental equations. It cannot be emphasized strongly enough that the beginning of beginnings lies in the fundamental laws and that equivalent circuits and geometric loci must follow from equations based upon these laws.

It is not a mere coincidence that the longest chapter in this text is that on the aforementioned four fundamental laws. A thorough study of these

laws is a valuable investment of time, for both the student and the teacher: the progress of study and teaching on a good foundation is fast and fruitful.

The correct sequence in the treatment of the electric machines requires that the d-c machine be treated after the synchronous machine, because the practical d-c machine is an a-c machine with a device (commutator) which permits picking up a fixed instantaneous value of the a-c voltage. In view of the fact that d-c machines are taught first in most colleges, these machines have been discussed immediately after the chapter on fundamental laws.

Although this text is designed for a one-year course, it does not imply that it is necessary to teach the entire text during two semesters. This book, as any other textbook, contains for the sake of completeness a certain amount of material which, at the discretion of the teacher, may be omitted in the classroom and left to the more interested student.

The MKS system of units has not been used in this text, because in the electric machine field engineers think and work in terms of practical (English) units. Final formulae are all given in practical units; derivations are carried out in cgs units. A short conversion table from the practical to the MKS system of units is included at the end of the text.

MICHAEL LIWSCHITZ-GARIK

*Brooklyn, N. Y.*  
*April, 1952*

## ACKNOWLEDGMENTS

The publication of this work has been greatly furthered by the able assistance of Professor Robert T. Weil, Jr., Head of the Electrical Engineering Department of Manhattan College. Professor Weil has contributed several chapters on transformers and a large part of the examples and problems. He has read the manuscript and proofs throughout all stages, has solved many answers to the problems, and supervised the preparation of necessary drawings. I express my sincere appreciation to him for his close and valuable collaboration during the entire preparation of this text.

I am indebted to the Administrations of the Polytechnic Institute of Brooklyn and Manhattan College for their kind assistance in offering the facilities necessary for the completion of this work. To Brother A. Leo, Dean of Engineering at Manhattan College, I express my sincere gratitude for his encouragement and support.

Finally, I wish to express my gratitude to Mr. V. L. Garik, Ph.D., for reading the manuscript; to the Westinghouse Electric Corporation, the General Electric Company, and the National Electric Coil Company for their contribution of data and photographs.

M. L.-G.





# CONTENTS

## 1. THE FUNDAMENTAL LAWS

	PAGE
1-1. Faraday's Law of Induction . . . . .	1
(a) EMF Induced in a Closed Conducting Circuit by a Flux Produced by a Magnet . . . . .	1
(b) EMF of Self-induction and Mutual Induction . . . . .	8
1-2. Kirchhoff's Mesh Law . . . . .	9
(a) $R$ , $L$ , circuit . . . . .	10
(b) $R$ , $L$ , and $M$ Circuit with Constant $L$ and $M$ . . . . .	11
1-3. Circuital Law of the Magnetic Field . . . . .	12
1-4. Forces on Conductors in Magnetic Field . . . . .	14
(a) Magnitude and Direction of the Force . . . . .	14
(b) Direction of the Force in an Electric Machine . . . . .	15
1-5. Summary . . . . .	17
Examples	
Problems	

## 2. MECHANICAL ELEMENTS OF THE DIRECT-CURRENT MACHINE

2-1. Mechanical Elements of the Direct-current Machine . . . . .	21
--	----

## 3. D-C ARMATURE WINDINGS

3-1. Two Types of Closed Windings; Lap and Wave Windings . . . . .	30
3-2. Winding Pitch. Back and Front Pitch . . . . .	31
3-3. Number of Parallel Paths in the Lap and Wave Winding. Number of Brush Studs . . . . .	33
3-4. Operation of the Cummutator . . . . .	40
3-5. Equalizer Connections. Conditions for Symmetry . . . . .	42
3-6. EMF Induced in a D-C Armature Winding . . . . .	44
3-7. Torque Produced by a D-C Machine . . . . .	46
Examples	
Problems	

## 4. THE MAGNETIC CIRCUIT

4-1. The Magnetic Circuit of the D-C Machine . . . . .	50
4-2. No-load Characteristic . . . . .	55

	PAGE
4-3. Armature Reaction . . . . .	55
Example	
Problems	

## 5. METHODS OF EXCITATION

5-1. Methods of Excitation . . . . .	61
(a) Series Excitation . . . . .	61
(b) Shunt Excitation . . . . .	62
(c) Compound Excitation . . . . .	62
5-2. Direction of Rotation of a Shunt and Series Machine as Generator and Motor . . . . .	64

## 6. THE D-C GENERATOR

6-1. The Voltage Equation of the D-C Generator . . . . .	66
6-2. Characteristic Curves of the D-C Generator; Regulation . . . . .	67
6-3. The Separately Excited Generator . . . . .	67
(a) The No-load Characteristic . . . . .	67
(b) The Load Characteristic . . . . .	68
(c) The External Characteristic . . . . .	69
(d) The Regulation Curve . . . . .	70
6-4. The Series Generator . . . . .	70
(a) The No-load Characteristic . . . . .	70
(b) The Load Characteristic . . . . .	70
(c) The External Characteristic . . . . .	71
6-5. The Shunt Generator . . . . .	71
(a) The No-load Characteristic . . . . .	71
(b) The Load Characteristic . . . . .	71
(c) The External Characteristic . . . . .	72
(d) The Regulation Curve . . . . .	73
6-6. The Cumulative Compound Generator . . . . .	74
(a) The No-load Characteristic . . . . .	74
(b) The External Characteristic . . . . .	74
6-7. Parallel Connection and Operation of D-C Generators . . . . .	77
6-8. Applications of the Different Types of Generators . . . . .	79
(a) Separately Excited Generator and Shunt Generator . . . . .	79
(b) Cumulative Compound Generator . . . . .	79
(c) The Differential Generator . . . . .	79
(d) Series Generator . . . . .	79
Examples	
Problems	

## 7. THE D-C MOTOR

	PAGE
7-1. Voltage Equation of the D-C Motor.....	82
7-2. Characteristics of the Shunt Motor.....	84
7-3. Characteristics of the Series Motor.....	87
7-4. Characteristics of the Cumulative Compound Motor.....	88
7-5. Comparison between the Different Types of D-C Motors.....	88
7-6. Speed Control of D-C Motors.....	89
(a) Separately Excited, Shunt, and Cumulative Compound Motor.....	90
(b) Series Motor.....	91
Examples	
Problems	

## 8. COMMUTATION OF THE D-C MACHINE

8-1. The Short-circuited Winding Element. Linear Commutation. Advantage of Accelerated Commutation.....	98
8-2. The EMF of Self-induction of the Short-circuited Winding Element and the EMF due to the Armature Flux. Delayed Commutation.....	101
8-3. Acceleration of Commutation by Means of the Main Flux or Interpoles.....	102
(a) Acceleration of Commutation by the Main Flux.....	103
(b) Acceleration of Commutation by Means of Interpoles.....	104
Problems	

## 9. SOME SPECIAL D-C MACHINES

9-1. Three-wire Generator.....	106
9-2. Dynamotor.....	107
9-3. Dynamic Rotating Amplifiers.....	107
(a) The Amplidyne (Dynamic Amplifier).....	108
(b) Two-stage Rototrol (Rotating Control).....	109

## 10. LOSSES IN D-C MACHINES. HEATING AND COOLING

10-1. Losses in the D-C Machine.....	113
(a) Losses Due to the Main Flux.....	113
(b) Losses Due to the Armature Current (Load).....	115
(c) Friction and Windage Losses.....	116
(d) No Load and Load Losses; Stray Load Losses.....	117
(e) Examples of Loss Distribution and Efficiencies.....	117
10-2. Heating and Cooling of D-C Machines.....	118
Problems	

11. TRANSFORMER CONSTRUCTION		PAGE
11-1.	Transformer Types .....	122
11-2.	Windings .....	125
11-3.	Cooling .....	128
12. THE TRANSFORMER AT NO-LOAD		
12-1.	The Transformer Primary .....	130
12-2.	The EMF Induced by the Main Flux at No-load ( $E$ ) .....	133
12-3.	The Transformer Secondary .....	134
	Problems	
13. THE TRANSFORMER UNDER LOAD		
13-1.	The Behavior of the Transformer Primary Under Load .....	136
13-2.	Reduction of the Secondary Current, Voltage, and Parameters to the Primary .....	137
13-3.	Kirchhoff's Mesh Law for the Secondary .....	139
13-4.	The EMF $E_1 = E_2'$ Induced by the Main Flux Under Load .....	139
14. THE PHASOR DIAGRAM AND EQUIVALENT CIRCUIT OF THE TRANSFORMER UNDER LOAD		
14-1.	The Phasor Diagram of the Transformer under Load .....	141
14-2.	The Equivalent Circuit of the Transformer .....	142
	Example	
	Problems	
15. THE 3-PHASE TRANSFORMER		
15-1.	Advantages, Disadvantages, Construction .....	147
15-2.	Magnetic Circuit .....	148
16. VOLTAGE REGULATION. THE KAPP DIAGRAM		
16-1.	Voltage Regulation. The Kapp Diagram .....	150
17. DETERMINATION OF PARAMETERS FROM A NO-LOAD AND A SHORT-CIRCUIT TEST		
17-1.	The No-load Test .....	154
17-2.	The Short-circuit Test .....	155
17-3.	Transformer Efficiency .....	156

	PAGE
17-4. Per-unit Calculation . . . . .	156
Example	
Problems	

## 18. TRANSFORMER POLARITY. POLYPHASE CONNECTIONS

18-1. Transformer Polarity . . . . .	161
18-2. Polyphase Connections (3-Phase-3-Phase) . . . . .	163
(a) Delta-delta ( $\Delta$ - $\Delta$ ) Connection . . . . .	164
(b) Wye-wye (Y-Y) Connection . . . . .	165
(c) Delta-wye ( $\Delta$ -Y) Connection . . . . .	166
(d) Wye-delta (Y- $\Delta$ ) Connection . . . . .	166
(e) Open-delta (V-V) or V Connection . . . . .	167
(f) T Connection . . . . .	168
18-3. Polyphase Connection: 2-phase to 3-phase, or vice versa . . . . .	168
18-4. Polyphase Connections: 3-phase-6-phase . . . . .	169
(a) Diametrical . . . . .	169
(b) Double-wye . . . . .	170
(c) Double-delta . . . . .	171
Problems	

## 19. PARALLEL OPERATION OF TRANSFORMERS

19-1. Parallel Operation of Transformers . . . . .	174
Example	
Problems	

## 20. THE AUTOTRANSFORMER. INSTRUMENT TRANSFORMERS. CONSTANT-CURRENT TRANSFORMER

20-1. The Autotransformer . . . . .	181
20-2. Instrument Transformers . . . . .	182
20-3. The Constant-current Transformer . . . . .	186
Example	
Problems	

## 21. A-C ARMATURE WINDINGS

21-1. A-C Armature Windings . . . . .	189
(a) Polyphase Lap Windings . . . . .	190
(b) Polyphase Wave Windings . . . . .	193
(c) Single-phase Windings . . . . .	193
(d) Squirrel-cage Windings . . . . .	198
Problems	

## 22. EMF AND MMF OF A-C WINDINGS

PAGE

22-1.	EMF Induced in an A-C Armature Winding; Distribution Factor; Pitch Factor.....	200
22-2.	MMF Produced by an A-C Armature Winding; Alternating Flux; Rotating Flux.....	204
	Examples	
	Problems	

## 23. MECHANICAL ELEMENTS OF THE POLYPHASE INDUCTION MOTOR AND ITS MAGNETIC CIRCUIT

23-1.	Mechanical Elements of the Polyphase Induction Motor and Its Magnetic Circuit.....	214
	(a) Stator.....	214
	(b) Rotor.....	214
	(c) The Magnetic Circuit of the Induction Motor.....	222

## 24. THE POLYPHASE INDUCTION MOTOR AS A TRANSFORMER

24-1.	The Induction Motor at Standstill.....	224
	(a) Rotor Winding Open.....	224
	(b) Rotor Winding Closed.....	227
24-2.	The Induction Motor When Running. The Slip.....	231
	Problems	

## 25. PHASOR DIAGRAM AND EQUIVALENT CIRCUIT OF THE POLYPHASE INDUCTION MOTOR

25-1.	The Phasor Diagram of the Polyphase Induction Motor.....	236
25-2.	The Equivalent Circuit of the Polyphase Induction Motor.....	238

## 26. POWER BALANCE, TORQUE, OPERATION AS A GENERATOR AND AS A BRAKE

26-1.	The Balance of Power in a Polyphase Induction Motor.....	242
26-2.	Torque-speed Characteristic of the Polyphase Induction Motor..	244
26-3.	The Pull-out Torque.....	246
26-4.	Operation as a Generator and Brake.....	246
	Example	
	Problems	

## 27. CIRCLE DIAGRAM OF THE POLYPHASE INDUCTION MOTOR

27-1.	Determination of the Circle Diagram.....	253
27-2.	Developed-mechanical-power Line and Delivered-mechanical-power Line.....	255

27-3.	The Torque-line and the Slip-line.....	256
27-4.	Determination of the Scales for the Power and Torque Lines.....	260
	Problems.....	261

28. DETERMINATION OF PARAMETERS FROM A NO-LOAD AND A LOCKED-ROTOR TEST. INFLUENCE OF PARAMETERS ON PERFORMANCE.  
INFLUENCE OF SKIN-EFFECT AND SATURATION

28-1.	The No-load Test.....	262
28-2.	The Short-circuit (Locked-rotor) Test.....	264
28-3.	Per-unit Values of Parameters.....	265
28-4.	Influence of the Parameters on the Performance of the Motor....	266
	(a) Heating of the Windings and Iron.....	266
	(b) Efficiency.....	266
	(c) Power Factor.....	266
	(d) Pull-out Torque.....	267
	(e) Starting Current (inrush).....	268
	(f) Starting Torque.....	268
28-5.	Influence of Saturation on the Leakage Reactances $x_1$ and $x_2$ ....	269
28-6.	Influence of Harmonics.....	270
	Examples	
	Problems	

29. STARTING AND SPEED CONTROL OF THE POLYPHASE  
INDUCTION MOTOR

29-1.	Starting of a Squirrel-cage Motor.....	278
29-2.	Starting of a Wound Rotor (Slip-ring) Motor.....	280
29-3.	Speed Control of a Wound-rotor Motor.....	282
	(a) Speed Regulation by Means of a Resistance in the Rotor Circuit.....	283
	(b) Speed Control by Changing the Number of Poles.....	283
	(c) Speed Control with the Aid of a Special Regulating Set....	284
	(d) Speed Control by Double Feeding.....	287
	Problems	

30. SOME SPECIAL INDUCTION MACHINES

30-1.	The Synchronous Induction Motor.....	290
30-2.	Induction Motor with a Rotating Flux Produced by a D-C Excited Rotating Pole-structure (Electromagnetic Coupling).....	291
30-3.	Self-synchronizers (Selsyns, Synchronie Apparatus, Autosyns, etc.)	291
30-4.	Position Indicators.....	294



	PAGE
30-5. The Induction Voltage Regulator .....	295
30-6. Resolvers .....	297
Problems	
31. THE SINGLE-PHASE INDUCTION MOTOR	
31-1. Replacement of the Alternating Fluxes by Two Rotating Fluxes..	300
31-2. Torque of the Single-phase Induction Motor .....	301
31-3. Kirchhoff's Mesh Equations of Stator and Rotor Circuits .....	303
31-4. The Equivalent Circuit of the Single-phase Induction Motor .....	303
31-5. The Circle Diagram of the Single-phase Induction Motor .....	304
32. DETERMINATION OF PARAMETERS FROM A NO-LOAD AND A LOCKED-ROTOR TEST	
32-1. The No-load Test .....	307
32-2. The Locked-rotor Test .....	309
32-3. Influence of the Parameters on the Performance of the Motor ....	310
Examples	
Problems	
33. STARTING THE SINGLE-PHASE MOTOR. TYPES OF SINGLE-PHASE MOTORS	
33-1. Starting by Means of a Rotating Flux .....	317
(a) Split-phase Motor .....	318
(b) Resistance-start Split-phase Motor .....	318
(c) Reactor-start Split-phase Motor .....	318
(d) Capacitor-start Split-phase Motor .....	318
(e) Permanent-split Capacitor Motor .....	319
(f) Two-value Capacitor Motor .....	320
33-2. Starting by Means of a Commutator and Brushes .....	321
(a) Repulsion-start Induction Motor .....	321
(b) Repulsion-induction Motor .....	321
33-3. The Shaded-pole Motor .....	322
34. LOSSES IN INDUCTION MOTORS. HEATING AND COOLING	
34-1. Losses in Induction Motors .....	323
(a) Losses due to the Main Flux .....	323
(b) Losses due to the Load Currents .....	324
(c) Friction and Windage Loss .....	325
(d) No-load and Load Loss; Stray-load Loss .....	325
(e) Examples of Loss Distribution and Efficiencies .....	327

	PAGE
34-2. Heating and Cooling of Induction Motors.....	327
Problems	
35. MECHANICAL ELEMENTS OF THE SYNCHRONOUS MACHINE	
35-1. The Salient-pole Machine.....	330
35-2. The Cylindrical Rotor Machine.....	333
36. EQUIVALENT CIRCUIT OF THE SYNCHRONOUS MACHINE	
36-1. General Considerations.....	338
36-2. Equivalent Circuit of the Synchronous Machine.....	348
37. PHASOR DIAGRAMS OF GENERATOR AND MOTOR WITH CYLINDRICAL ROTOR. ARMATURE REACTION. GENERATOR CHARACTERISTICS	
37-1. Phasor Diagrams of Synchronous Generator and Motor with Cylindrical Rotor. Armature Reaction.....	343
(a) Machine Unsaturated.....	343
(b) Machine Saturated.....	345
37-2. Generator Characteristics.....	347
(a) No-load and Air-gap Characteristic.....	347
(b) Short-circuit Characteristic. Potier Triangle.....	347
(c) Load Characteristic.....	349
(d) External Characteristic.....	350
(e) Regulation Curve.....	350
(f) Short-circuit Ratio.....	350
(g) Determination of the Direct-axis Synchronous Reactance $x_d$ .....	351
37-3. Voltage Regulation.....	352
Example	
Problems	
38. PHASOR DIAGRAMS OF SYNCHRONOUS GENERATOR AND MOTOR WITH SALIENT POLES	
38-1. The Two-reaction Theory.....	357
38-2. Phasor Diagrams of the Generator and Motor with Salient Poles. Armature Reaction.....	359
(a) Machine Unsaturated.....	359
(b) Machine Saturated.....	362
38-3. Generator Characteristics. Voltage Regulation.....	364
Examples	
Problems	

### 39. TORQUE AND POWER RELATIONS. PARALLEL OPERATION OF SYNCHRONOUS GENERATORS. SYNCHRONIZING GENERATORS

PAGE

39-1. Torque and Power Relations.....	370
39-2. Parallel Operation of Synchronous Generators.....	373
39-3. Synchronizing of Synchronous Generators.....	375
Problems	

### 40. CIRCLE DIAGRAM OF THE SYNCHRONOUS MACHINE

40-1. Circle Diagram for Constant Torque and Variable Field Current..	378
40-2. Circle Diagram of the Synchronous Machine for Variable Torque and Constant Field Current.....	380
40-3. Influence of Field Current on Overload Capacity and Power Factor. V-Curves of the Synchronous Motor. Synchronous Capacitor...	384
40-4. Starting of a Synchronous Motor.....	386
Examples	
Problems	

### 41. SMALL SYNCHRONOUS MOTORS

41-1. The Reluctance Motor.....	390
41-2. The Hysteresis Motor.....	391

### 42. HUNTING OF A SYNCHRONOUS MACHINE

42-1. The Synchronizing Torque.....	394
42-2. The Ratio of the Amplitude of Oscillation in Parallel Operation to the Amplitude of Oscillation of the Single Machine (The Amplification Factor).....	396
42-3. The Natural Frequency of the Synchronous Machine. The Danger of Resonance.....	399
42-4. Improving Parallel Operation by means of a Damper Winding....	400

### 43. LOSSES IN SYNCHRONOUS MACHINES. HEATING AND COOLING

43-1. The Losses in the Synchronous Machine.....	402
(a) Losses Due to the Main Flux.....	402
(b) Losses Due to the Load Current.....	402
(c) Friction and Windage Losses.....	403
(d) No-load and Load Losses; Stray Load Losses.....	404
(e) Example of Loss Distribution and Efficiency.....	404
43-2. Heating and Cooling of the Synchronous Machine.....	404
Problems	

#### 44. THE SYNCHRONOUS CONVERTER. VOLTAGE AND CURRENT RELATIONS. COPPER LOSSES COMPARED WITH THOSE OF THE D-C MACHINE

	PAGE
44-1. Operation of the Synchronous Converter.....	406
44-2. Voltage and Current Ratios in the Synchronous Converter.....	409
44-3. The Copper Losses in the Synchronous Converter.....	411
44-4. Comparison with D-C Machine.....	412
Problems	

#### 45. COMMUTATION OF THE SYNCHRONOUS CONVERTER. VOLTAGE REGU- LATION. STARTING. PARALLEL OPERATION

45-1. Commutation of the Synchronous Converter.....	415
45-2. Voltage Regulation of the Converter.....	415
45-3. Starting and Parallel Operation of Converters.....	416
45-4. Comparison with the Motor-Generator Set.....	417

#### 46. THE D-C ARMATURE IN AN ALTERNATING MAGNETIC FIELD

46-1. The EMF of Rotation and the EMF of Transformation in the Armature Winding.....	419
(a) The EMF of Rotation in the Armature Winding.....	419
(b) The Transformer EMF in the Armature Winding.....	420
46-2. The Torque of the Single-phase Commutator Motor. The Compen- sating Winding.....	421
46-3. The Transformer EMF of the Short-circuited Winding Element and the Commutating Fluxes in the Single-phase Commutator Motor	424
Problems	

#### 47. THE SINGLE-PHASE SERIES COMMUTATOR MOTOR

47-1. The Voltage Diagram of the Single-phase Series Commutator Motor	428
47-2. Commutation of the Single-phase Series Commutator Motor.....	429
47-3. Torque and Characteristic Curves of the Single-phase Commutator Motor.....	431
47-4. The Universal Motor.....	432
Problems	

#### 48. THE REPULSION MOTOR

48-1. The Voltage Diagram of the Repulsion Motor.....	433
48-2. Commutation of the Repulsion Motor.....	435
48-3. Characteristic Curves of the Repulsion Motor.....	436

## 49. THE 3-PHASE SHUNT COMMUTATOR MOTOR (THE SCHRAGE MOTOR)

PAGE

49-1.	Connection Diagram and Speed Control of the 3-Phase Shunt Commutator Motor.....	439
49-2.	Power-factor Correction of the 3-Phase Shunt Motor.....	442
49-3.	Commutation of the 3-Phase Shunt Motor.....	443
	Problems	

## 50. MOTOR APPLICATION

50-1.	Motor Characteristics.....	444
50-2.	Load Characteristics.....	448
50-3.	Various Motor Types and Their Application.....	449

## 51. DISTRIBUTION OF POWER

51-1.	Systems of D-C Distribution.....	458
51-2.	Systems of A-C Distribution.....	463
	Problems	

## APPENDICES

Appendix 1.	Derivation of Eq. 12-6 from Ampère's Law.....	470
Appendix 2.	Derivation of the Torque of the Polyphase Induction Motor on the Basis of Biot-Savart's Law.....	471
Appendix 3.	Derivation of the Currents of the Polyphase Induction Motor from the Equations for the Electric Circuits and Magnetic Circuit.....	473
Appendix 4.	Derivation of the Circle Diagram of the Polyphase Motor.....	475
Appendix 5.	Curves.....	477
LIST OF SYMBOLS.....		481
CONVERSION TABLE.....		490
REFERENCES.....		491
ANSWERS TO PROBLEMS.....		493
INDEX.....		501

# Chapter 1

## THE FUNDAMENTAL LAWS

*All electric machines operate on the same basic principles and only a few fundamental laws govern the behavior of these machines. A thorough understanding of these fundamental laws is essential for the study of electric machines. These laws are treated in this chapter and are listed below:*

1. Faraday's law of induction.
2. Kirchhoff's law of the electric circuit.
3. Circuital law of the magnetic field (Ampère's law).
4. Law of force on a conductor in a magnetic field (Biot-Savart's law).

**1-1. Faraday's law of induction.** (a) *Electromotive force induced in a closed conducting circuit by a flux produced by a magnet. Faraday's law of induction states: If the magnetic flux linking a closed conducting circuit is changing, an electromotive force is induced in the circuit.*

If  $\phi$  represents the flux linking the circuit and  $d\phi$  the change in flux during the time  $dt$ , then the magnitude of the induced emf is proportional to the rate of change of the flux,  $d\phi/dt$ .

The direction of the induced emf is determined by Lenz's law, which states that the current produced by the induced emf opposes the change in flux. This will be explained by several simple examples.

**Example 1-1.** Consider Fig. 1-1. Shown here are an isolated north pole and a closed circuit of one turn which may be moved relative to this pole. The lines of force proceed outward from the north pole.

It should be noted that the direction of the current and the direction of the lines of force produced by the current bear the same relation to one another as the direction of progress and direction of rotation of a right-hand screw (such as a corkscrew); if the

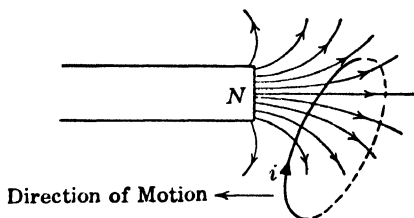


FIG. 1-1. Induction of an emf in a simple circuit.

forward motion of the screw and the direction of the current coincide, then the direction of the lines of force about the conductor is the same as the direction of rotation of the screw.

If the magnet and circuit (Fig. 1-1) are now brought closer to one another so that the flux linking the circuit is increased, the current produced by the induced voltage has a direction as shown by the arrow and tends to produce a flux which reduces the number of lines of force linking the circuit. On the other hand, if the magnet and the circuit are moved further apart so that the number of lines of force linking the circuit is reduced, the induced current  $i$  has the opposite direction and tends to produce a flux which increases the number of lines of force linking the circuit.

**Example 1-2.** Consider an elementary machine (Fig. 1-2). A coil  $ab$  rotates between a north and a south pole. The flux interlinked with the coil is a maximum when the plane of the coil is horizontal and is a minimum when the plane is vertical. When the

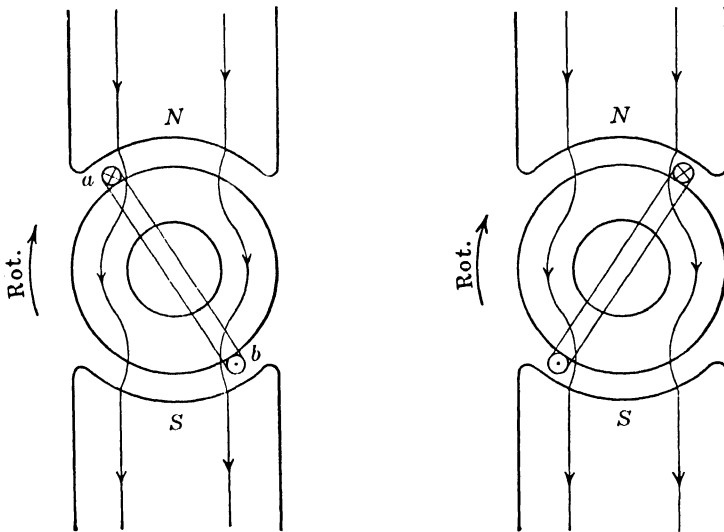


FIG. 1-2. Induction of an emf in a coil of an electric machine.

coil is in the position shown in Fig. 1-2a, the flux linking the coil is decreasing. The induced emf and resultant current, therefore, will have a direction as indicated by the cross and dot\* since current flowing in this direction tends to oppose the reduction in flux linkages.

Fig. 1-2b shows the direction of emf and current for another position of the coil. In this position the flux interlinked with the coil is increasing. The direction of the current is the same as in Fig. 1-2a because a current in this direction tends to oppose the increase in flux linkages.

In both examples considered, the induced emf has the same direction as the current, and therefore this emf must be considered negative with respect to the change of flux interlinkage. If the flux linked with the circuit increases, i.e.,  $d\phi/dt$  is positive, the cur-

\* The cross represents a current flowing away from the observer, and the dot represents a current flowing toward the observer.

rent produced by the induced emf decreases the flux; if the flux linked with the circuit decreases, i.e.,  $d\phi/dt$  is negative, the current produced by the induced emf increases the flux. Accordingly, Faraday's law of induction must be written:

$$e = - \frac{d\phi}{dt} 10^{-8} \text{ volt} \quad (1-1)$$

i.e., *the emf induced in the circuit is equal to the rate of decrease of the flux interlinked with the circuit.* In this equation  $\phi$  is in maxwells and  $t$  in seconds.

**Example 1-3.** Consider Fig. 1-3. A conductor  $ab$  moves downward between two poles. Since the flux interlinked with the circuit is diminishing, for the chosen direction of movement, the current in the conductor will be in the direction from  $b$  to  $a$  because this would oppose the reduction of flux linking the circuit.

For this case, Faraday's law of induction may be expressed in a different way. If the conductor  $ab$  moves downward a distance  $dx$  in a time  $dt$ , the change in flux interlinkage is  $d\phi = -Bl dx$ , where  $B$  is the flux density in gausses and  $l$  is the length of the conductor in centimeters. Hence,

$$e = - \frac{d\phi}{dt} 10^{-8} = Bl \frac{dx}{dt} 10^{-8} \text{ volt}$$

in which  $dx/dt$  is the velocity  $v$  with which the conductor moves. Thus,

$$e = Blv 10^{-8} \text{ volt} \quad (1-2a)$$

$$\text{or} \quad e = \frac{1}{9} Blv 10^{-8} \text{ volt} \quad (1-2b)$$

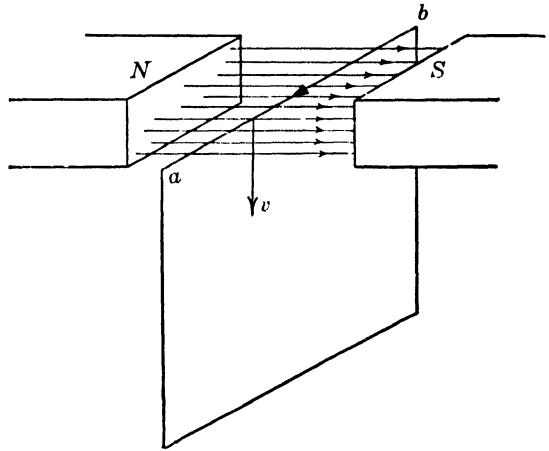


FIG. 1-3. Induction of an emf in a simple circuit.

if  $B$  is expressed in lines per square inch,  $l$  in inches, and  $v$  in feet per minute.  $Bl dx$  is the flux cut by the conductor in the time  $dt$ . Therefore, Eq. 1-2 can be interpreted as follows: *The emf induced in the conductor is equal to the flux cut by it per second.*

Eq. 1-2 can be applied also to the second example where a coil rotates between two poles. It should be noted that Eq. 1-1, which is based on flux interlinkages, is more general, while the flux cutting Eqs. 1-2a and 1-2b are applicable where there is relative motion between conductors and a flux which is constant with time.

The average emf induced in the coil of Fig. 1-2 can be readily determined from Eq. 1-1. When the coil lies in the horizontal, it is interlinked with the total pole-flux  $\Phi$ . When it moves from the horizontal position a quarter of a revolution, it lies in the vertical and its flux interlinkage is zero. A quarter of a revolution further in the same direction brings the coil again in the horizontal; the flux interlinkage is again  $\Phi$  but in the opposite direction. Thus, during a half revolution,  $\Delta\phi = 2\Phi$ . If the



speed of the armature is  $n/60$  rps, ( $n$  in rpm), the duration of a half-revolution is  $\Delta t = 30/n$  seconds and

$$E_{\text{avg}} = \frac{2\Phi}{30/n} 10^{-8} = 4\Phi \frac{n}{60} 10^{-8} \text{ volt} \quad (1-3)$$

The average emf depends upon the total flux per pole and is independent of the flux distribution around the periphery of the armature, i.e., of the magnitude of the flux density  $B$  around the armature. The instantaneous values of the induced emf, on the contrary, depend upon the distribution of  $B$ , as indicated by Eq. 1-2.

Eq. 1-3 assumes that there are only two poles and that the coil consists of two conductors making one turn. If the number of poles is  $p$ , then, during a half revolution,  $\Delta\phi = 2\Phi(p/2)$ , and  $E_{\text{avg}}$  becomes  $p/2$  times the value given by Eq. 1-3. Furthermore, if the number of series-connected turns of the coil is  $N$  and these  $N$  turns are so concentrated that they are

interlinked with the same number of flux lines at any instant of time, then  $E_{\text{avg}}$  is  $N$  times larger than the value given by Eq. 1-3, so that

$$E_{\text{avg}} = \left(4\Phi \frac{p}{2}\right) N \frac{n}{60} 10^{-8} \text{ volt} \quad (1-3a)$$

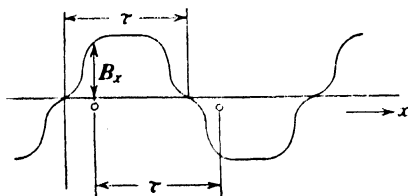


FIG. 1-4. Flux distribution in a d-c machine.

Consider Fig. 1-4 which shows the normal flux distribution of a d-c machine.  $B$  is zero in the middle of the interpolar space (see Fig. 1-2) and is a maximum in the center of the pole. If both coil sides lie at all times in fields of the same strength, the instantaneous value of the emf induced in the coil is (Eq. 1-2)

$$e = 2B_x l v 10^{-8} \text{ volt} \quad (1-4)$$

i.e., it is proportional to  $B_x$ , and the emf curve has exactly the same shape as the  $B$  curve.

If  $D$  = diameter of the armature and  $p$  = number of poles, then the arc

$$\frac{\pi D}{p} = \tau \quad (1-5)$$

is the *pole pitch*. In order that both sides of a coil lie in flux densities of the same strength, its coil span, measured as an arc, must be equal to the pole pitch. This is the case in Fig. 1-2.

When the flux distribution along the armature is *sinusoidal*, the emf

of the coil also will be sinusoidal (Fig. 1-5). The amplitude and the effective value of the emf will now be determined for this case.

Consider again Fig. 1-2. When the angle between the plane of the coil and the horizontal ( $\alpha$ ) is zero, the coil is interlinked with the total pole-flux  $\Phi$ ; when this angle is equal to  $\pi/2$ , i.e., the plane of the coil coincides with the pole-axis, the flux interlinkage of the coil is zero. In any inter-

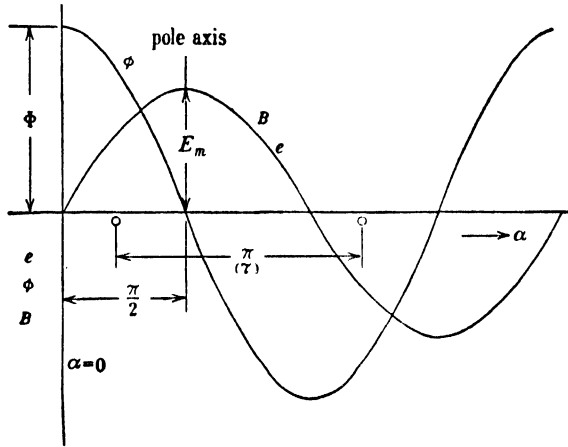


FIG. 1-5. Sinusoidal flux distribution. Flux interlinkage and emf as functions of time showing emf lagging inducing flux by 90 degrees.

mediate position the flux interlinkage is  $\Phi \cos \alpha$ . This can be seen from Fig. 1-5. When the coil sides have the position  $\alpha = 0$  and  $\alpha = \pi$ , the flux interlinked with the coil is proportional to

$$\int_{\alpha=0}^{\alpha=\pi} B_{\alpha} d\alpha$$

When the coil sides have the position  $\alpha$  and  $(\alpha + \pi)$ , the flux interlinked with the coil is proportional to

$$\int_{\alpha}^{(\alpha+\pi)} B_{\alpha} d\alpha$$

The ratio of the latter integral to the former integral is  $\cos \alpha$ , since  $B_{\alpha} = B_{\max} \sin \alpha$ . The curve of flux interlinkage  $\phi$  is shown in Fig. 1-5. From Eq. 1-1:

$$e = -\frac{d\phi}{dt} 10^{-8} = -\frac{d}{dt} (\Phi \cos \alpha) 10^{-8} = \Phi \sin \alpha \frac{d\alpha}{dt} 10^{-8} \text{ volt} \quad (1-6a)$$

where  $d\alpha/dt$  is the angular velocity of rotation of the coil. For a uniform

angular velocity of the coil,  $\alpha = \omega t$

and 
$$e = \omega \Phi 10^{-8} \sin \omega t \quad (1-6b)$$

It can be seen from Fig. 1-5 that the induced emf  $e$  lags the flux interlinkage  $\phi$  by  $90^\circ$ ; when  $\phi$  is maximum ( $\alpha = 0$ ),  $e$  is zero, and  $e$  becomes a maximum, when  $\alpha = \pi/2$  and  $\phi$  is zero. These same conclusions follow from Eq. 1-6. The instantaneous flux interlinkage is

$$\phi = \Phi \cos \omega t = \Phi \sin \left( \omega t + \frac{\pi}{2} \right)$$

which is a function of  $\sin \left( \omega t + \frac{\pi}{2} \right)$ , while the instantaneous emf  $e$  is a function of  $\sin \omega t$ .

Representing the amplitudes (or the effective values) of the sinusoidal functions  $\phi$  and  $e$  by phasors, *that is, quantities whose values are represented by complex numbers, the emf phasor must lag the flux phasor by  $90^\circ$ .*

The amplitude of the induced emf is (Eq. 1-6b)

$$E_m = \omega \Phi 10^{-8} \text{ volt} \quad (1-7a)$$

The period of a sine function is  $2\pi$ . If  $T$  is the time of a period in seconds and  $f$  the frequency in cycles per second, then

$$2\pi = \omega T \quad \text{where} \quad f = \frac{1}{T}$$

and

$$\omega = \frac{2}{T} \pi = 2\pi f$$

Hence

$$E_m = 2\pi f \Phi 10^{-8} \text{ volt} \quad (1-7b)$$

and the effective value of  $e$  is

$$E = \frac{2\pi}{\sqrt{2}} f \Phi 10^{-8} = 4.44 f \Phi 10^{-8} \text{ volt} \quad (1-8)$$

The frequency  $f$  can be expressed in terms of the revolutions per minute of the armature and the number of poles. Consider Fig. 1-2. While the coil is making one revolution, it generates one cycle of the emf (Fig. 1-5). If the armature rotates at  $n$  revolutions per minute, the frequency in cycles per second will be  $f = n/60$ . This applies to a 2-pole machine. If the number of poles is  $p$  instead of 2, it still holds that the emf goes through a complete cycle when it passes two poles of the machine and therefore the frequency is

$$f = \frac{p}{2} \frac{n}{60} = \frac{pn}{120} \text{ cps} \quad (1-9)$$

It has been assumed in Eqs. 1-6a to 1-8 that the coil consists of two conductors making one turn. If the number of series connected turns of the coil is  $N$  and these  $N$  turns are so concentrated that they are interlinked with the same number of flux lines at any instant of time, the induced emf will be  $N$  times that given by Eqs. 1-7 and 1-8, i.e.,

$$E_m = \omega N \Phi 10^{-8} = 2\pi f N \Phi 10^{-8} \text{ volt} \quad (1-10)$$

and 
$$E = 4.44 N f \Phi 10^{-8} \text{ volt} \quad (1-11)$$

**Example 1-4.** A coil with five series-connected turns rotates in a sinusoidally distributed flux at a speed of 1200 rpm. The flux per pole is  $\Phi = 3 \times 10^6$  maxwells; the number of poles is  $p = 6$ . What is the average emf induced in the coil? What is the amplitude and the effective value of the emf induced in the coil? What is the frequency of the emf induced in the coil?

From Eq. 1-3a, with  $p = 6$  and  $N = 5$

$$E_{\text{avg}} = 4 \times 3 \times 10^6 \times \frac{6}{2} \times 5 \times \frac{1200}{60} \times 10^{-8} = 36 \text{ volts}$$

From Eq. 1-9

$$f = \frac{6 \times 1200}{120} = 60 \text{ cps}$$

From Eq. 1-10

$$E_m = 2\pi \times 60 \times 5 \times 3 \times 10^6 \times 10^{-8} = 56.6 \text{ volts}$$

$$E = \frac{56.6}{\sqrt{2}} = 40 \text{ volts}$$

Since the flux is sinusoidally distributed,  $E_{\text{avg}}$  must be  $\frac{2}{\pi} \times E_m$ .

Faraday's law of induction, Eq. 1-1, can also be interpreted in another manner. In this equation  $e$  is the total emf induced in the closed circuit; i.e., if the circuit were opened somewhere and an oscillograph inserted, the value of  $e$  measured at each instant would be for the entire circuit. In reality,  $e$  is the sum of all elemental emf's  $de$  which are induced in the individual elements  $dl$  of the circuit, and Eq. 1-1 can be written:

$$e = \oint E_t dl = - \frac{d\phi}{dt} 10^{-8} \text{ volt} \quad (1-12)$$

where  $E_t$  is the component of the electric field intensity  $\mathbf{E}$  in the direction of  $dl$ . This equation states that every change in the lines of flux linking a circuit produces an electric field within the circuit, and that the line integral of the intensity of this electric field (the induced emf) is equal to  $-\frac{d\phi}{dt}$ . (See references on Electromagnetic Field Theory.)

(b) *Electromotive force of self-induction and mutual induction.* In the previous examples (Figs. 1-1 to 1-3), the flux is produced by a magnet, and the change of flux interlinkage is caused by a relative movement of a coil and a magnet. According to Faraday's law of induction, it is only the *change of flux interlinkage* that causes an emf to appear in a circuit, no matter what the source of the flux. Therefore, an emf will be induced in a circuit if its own flux is changed by changing its current, or if the flux of an adjacent circuit is changed by changing the current in this latter circuit. In the first case this will be an emf of *self-induction*; in the second case, an emf of *mutual induction*.

In the case of self-induction, the flux interlinkage of the circuit is determined by its own current:

$$\phi = Li \quad \text{or} \quad (N\phi) = Li \quad (1-13)$$

depending upon whether the circuit consists of one turn or  $N$  turns all linked with the flux.  $L$  is the *coefficient of self-inductance*. According to Eq. 1-13 it is the *flux interlinkage per unit current*. The magnitude of  $L$  depends upon the geometrical arrangement of the conductors, upon the number of turns, and upon the magnetic nature of the surroundings. The last-mentioned factor plays a great part in the magnitude of the flux  $\phi$  and the flux interlinkage. If the surroundings contain ferromagnetic materials, the magnetic resistance (reluctance) is much lower and the flux  $\phi$  is much larger for the same current than in the case when there are no ferromagnetic materials. This is discussed in Art. 1-3. It is also shown that when there are no ferromagnetic materials, the flux is directly proportional to the magnetizing force (the current), and therefore, in this case, the coefficient of self-inductance  $L$  in Eq. 1-13 is a constant. On the other hand, in ferromagnetic materials flux and magnetizing force are coordinated through the magnetization curve of the material (Fig. 1-8) which has a non-linear character; therefore the coefficient of self-inductance  $L$  is not a constant in this case, but varies with the magnetizing force. For constant  $L$ , according to Eq. 1-1, the emf of self-induction is

$$e_s = - \frac{d\phi}{dt} 10^{-8} = -L \frac{di}{dt} \text{ volt} \quad (1-14)$$

where  $L$  is measured in henries.

If  $i$  is sinusoidal,

$$i = I_m \sin \omega t$$

the emf of self-induction becomes

$$e_s = -I_m \omega L \cos \omega t = I_m \omega L \sin (\omega t - 90^\circ) \quad (1-14a)$$

i.e., the amplitude of the emf of self-induction is equal to  $I_m\omega L$  and the emf of self-induction lags the current by  $90^\circ$ . Note that Eq. 1-14a is in complete accordance with Eq. 1-6b. The latter equation states that the amplitude of the induced emf is equal to  $\omega$  times the maximum flux interlinkage; in Eq. 1-14a,  $I_m L$  is nothing more than the maximum flux interlinkage, for, according to Eq. 1-13,  $L$  is the flux interlinkage per unit current.

In the case of mutual induction, the flux interlinking circuit 1 (the circuit considered) is:

$$(N\phi)_1 = M i_2 \quad (1-15)$$

The coefficient of mutual inductance  $M$  depends upon the same quantities as does  $L$ , and also upon the relative position of both circuits with respect to each other. For constant  $M$ , according to Eq. 1-1, the emf of mutual induction is:

$$e_{M1} = -M \frac{di_2}{dt} \text{ volt} \quad (1-16a)$$

and vice versa

$$e_{M2} = -M \frac{di_1}{dt} \text{ volt} \quad (1-16b)$$

where  $M$  is measured in henries.

**Example 1-5.** A solenoid with 400 turns carries a 60-cycle current of  $I = 6$  amp. The maximum flux interlinked with each of the 400 turns is  $4 \times 10^6$  maxwells. The surrounding is air. What is the coefficient of self-inductance of the coil? What is the effective value of emf of self-induction?

From Eq. 1-13

$$L = \frac{400 \times 4 \times 10^6}{\sqrt{2} \times 6} \times 10^{-8} = 1.886 \text{ henries}$$

From Eq. 1-14a

$$E_s = 6 \times 2\pi \times 60 \times 1.886 = 4270 \text{ volts}$$

**Example 1-6.** The field circuit of a d-c generator has an inductance of 4 henries. Its field current of 8 amp is interrupted in 0.06 sec. What is the average emf induced in the winding?

From Eq. 1-14

$$e_{s, \text{avg}} = 4 \frac{8}{0.06} = 534 \text{ volts}$$

**1-2. Kirchhoff's mesh law.** This law states: In each mesh of a network, the sum of all impressed and induced emf's is equal to the sum of all resistive voltage drops.

$$\sum (V + E) = \sum IR \quad (1-17)$$

(a) *R-L circuit.* Applying Kirchhoff's law to an *R-L* circuit with a constant *L* and an impressed voltage *v*, the equation obtained is

$$v - L \frac{di}{dt} = iR \quad (1-18a)$$

$$v = iR + L \frac{di}{dt} \quad (1-18b)$$

where *v* and *i* are the instantaneous values of impressed voltage and current, respectively.

Eq. 1-18b, which is identical with Eq. 1-18a, can be interpreted in the following way: at any instant of time, the impressed voltage must overcome the resistive voltage drop and the emf of self-induction. While this interpretation is physically correct, it would be entirely wrong to conclude from Eq. 1-18b that  $L(di/dt) = -e_s$  is of the same nature as the resistive voltage drop *iR*. It should not be forgotten that *L* is flux interlinkage associated with an induced emf, but nothing else.

If *v* in Eq. 1-18 is sinusoidal, *i* will also be sinusoidal. A sinusoidal quantity can be represented either by the projections of a rotating phasor on a fixed line or by the projections of a fixed phasor on a rotating

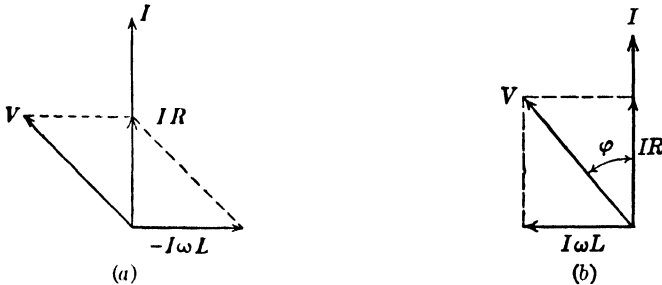


FIG. 1-6. Phasor diagram of voltages in an *R-L* circuit.

line (*time line*). It is customary in the first case to select the counter-clockwise rotation of the phasor; therefore, the time line must rotate clockwise in the second case. The magnitude of the phasor is equal to the amplitude of the sinusoidal quantity. Using this phasor representation, the phasor diagram (Fig. 1-6a) is obtained for Eq. 1-18a. *IR* is the resistive voltage drop in phase with *I*;  $-I\omega L$  is the emf of self-induction,  $90^\circ$  behind *I* in accordance with Eq. 1-14a. The geometric sum of *V* and  $-I\omega L$  is equal to *IR* corresponding to Kirchhoff's law, Eq. 1-17.

The phasor representation of Eq. 1-18b is given by Fig. 1-6b. Here *IωL* is drawn  $90^\circ$  ahead of *I* and is interpreted as the component of *V*

necessary to overcome the emf of self-induction. The geometric sum of  $IR$  and  $I\omega L$  then yields the impressed voltage  $V$ .

The phasor diagram of Fig. 1-6b is the representation usually presented in textbooks.

In the representation of sinusoidal quantities by complex notation, multiplication by  $+j$  rotates the phasor  $90^\circ$  in a positive direction, and multiplication by  $-j$  rotates the phasor  $90^\circ$  in a negative direction. If the current phasor  $I$  is used as a reference, then the phasor diagram of Fig. 1-6a can be expressed as

$$V - jI\omega L = IR \quad (1-19a)$$

and the phasor diagram of Fig. 1-6b as

$$V = IR + jI\omega L \quad (1-19b)$$

Since the emf of self-induction lags the current which produces it by  $90^\circ$ , its amplitude is multiplied by  $-j$  in Eq. 1-19a where the left side represents the sum of  $V$  and  $E_s$ . The component of the impressed voltage necessary to overcome  $E_s$  is shifted  $180^\circ$  with respect to  $E_s$  and is therefore  $90^\circ$  ahead of  $I$ . For this reason  $I\omega L$  appears with multiplier  $+j$  in Eq. 1-19b.

It is customary to use the symbol  $x$ , called *reactance*, for  $\omega L$ . It should be remembered that  $L$  means flux interlinkage and is associated with an induced emf; therefore the reactance  $x$  always is *associated with an induced emf*. Introducing  $x$ , Eqs. 1-19a and 1-19b become

$$V - jIx = IR \quad (1-19c)$$

$$V = IR + jIx \quad (1-19d)$$

(b) *R, L, and M circuit with constant L and M.* Applying Kirchhoff's law to an  $R, L, M$ -circuit with an impressed voltage  $v$ , the voltage equation for the instantaneous values is

$$v_1 - L_1 \frac{di_1}{dt} - M \frac{di_2}{dt} = i_1 R_1^* \quad (1-20)$$

For sinusoidal voltages and currents, the voltage equation for effective values is, corresponding to Eq. 1-19a,

$$V_1 - j\omega L_1 I_1 - j\omega M I_2 = I_1 R_1 \quad (1-21a)$$

\* The emf of mutual induction is introduced here as  $-M(di_2/dt)$ , i.e., with a positive sign for  $M$ . The sign of  $M$  depends, in general, upon the assumed directions of current flow in the coils and upon the manner in which the coils are wound (see references on A-c Circuits). In this text, the directions of the currents and the manner in which the coils are wound will each be assumed so as to yield a positive value for  $M$ .



and, corresponding to Eq. 1-19b,

$$V_1 = I_1(R_1 + j\omega L_1) + j\omega M I_2 \quad (1-21b)$$

Introducing the symbol  $x_1$  for  $\omega L_1$  (primary reactance) and the symbol  $x_m$  for  $\omega M$  (mutual reactance), Eqs. 1-21 become

$$V_1 - jx_1 I_1 - jx_m I_2 = I_1 R_1 \quad (1-22a)$$

$$V_1 = I_1(R_1 + jx_1) + jx_m I_2 \quad (1-22b)$$

In Eqs. 1-19b, 1-21b, and 1-22b, the emf's of self- and mutual induction appear as voltage drops. As pointed out previously, it should not be forgotten that the symbols  $\omega L$ ,  $\omega M$ , and  $x$  are always associated with an induced emf.

It should be noted that Eqs. 1-18 to 1-22 apply only when  $L$  and  $M$  are constants, i.e., when the surroundings do not contain ferromagnetic materials. The case of electric circuits surrounded by iron is treated in connection with the transformer (Art. 12-1).

**1-3. Circuital law of the magnetic field.** A relation similar to Eq. 1-12 also holds for the magnetic circuit, i.e., for a closed circuit carrying a magnetic flux.

If  $H_i$  is the magnetic field intensity at the element  $dl$  of the magnetic circuit,  $N$  the number of turns which are linked by the magnetic flux, and

$I$  the current which flows in the winding, then the equation referred to above is

$$\oint H_i dl = NI \quad (1-23)$$

This equation states that *the line integral of the magnetic field strength along a closed path is equal to the sum of the ampere-turns with which this path is linked.* (See references on Electromagnetic Field Theory.)

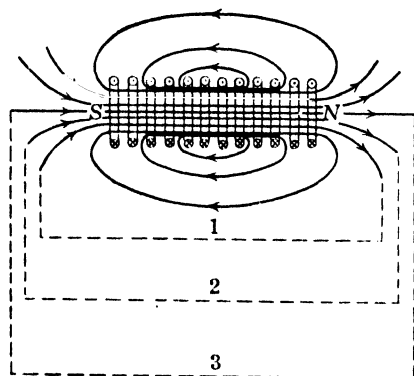


Fig. 1-7. Flux produced by a solenoid.

Fig. 1-7 shows a solenoid and the flux produced by it. The line integral  $\int H_i dl$  is the same for all three closed lines (1, 2, and 3) because all three are linked by the entire turns of the solenoid and therefore  $NI$  is the same for all three. The value of the integral  $\int H_i dl$  is not affected by the shape

or the length of the force line selected. For a long line, such as 3, the number of terms  $dl$  appearing in the sum will increase, but the field intensity becomes smaller as the distance from the coil increases.

Eq. 1-23 can be put easily into a form which is similar to Ohm's law for the electric circuit. For the magnetic induction  $B$ , the relation holds that

$$B = \mu_0 \mu H \quad (1-24)$$

where  $\mu_0$  is a constant equal to  $0.4\pi$ , and  $\mu$  is the relative permeability of the material, i.e., the ratio of its permeability to that of free space

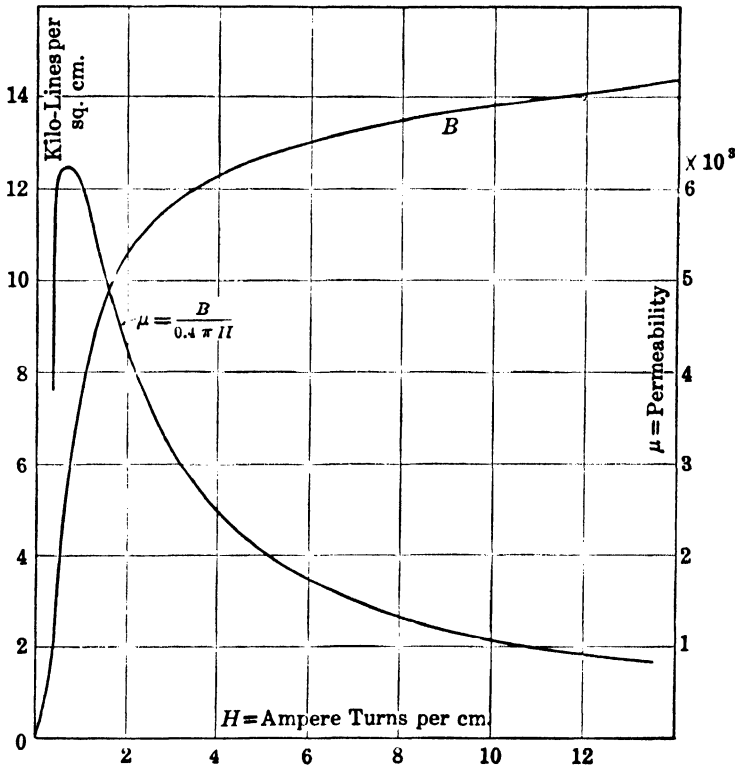


FIG. 1-8. Induction  $B$  and permeability  $\mu$  as a function of field intensity  $H$ .

(vacuum). In Eqs. 1-23 and 1-24, the current  $I$  is expressed in amperes,  $H$  in ampere-turns per centimeter, which, as far as fundamental dimensions are concerned, is the same as amperes per centimeter,  $B$  in gauss, and  $\mu_0$  in gauss centimeter per ampere.

For air  $\mu = 1$ , while for iron  $\mu$  is a variable which depends upon the saturation. As an example, Fig. 1-8 shows the value of  $\mu$  as a function of the field strength  $H$  for electrical sheet steel (1.0% silicon); in this case

$\mu$  has a maximum value of 6100. The values of  $B$  are also shown in Fig. 1-8. The  $BH$  curve is called the *magnetization curve* of the material in question. This curve is used in making calculations for magnetic circuits.

The relation between magnetic flux  $\phi$ , cross-section  $A$ , and magnetic induction  $B$  is given by:

$$\phi = BA \quad (1-25)$$

Substituting Eqs. 1-24 and 1-25 in Eq. 1-23, there results:

$$\phi = \frac{0.4\pi NI}{R_m} \quad (1-26)$$

where

$$R_m = \int \frac{dl}{\mu A} = \Sigma \frac{l}{\mu A} \quad (1-27)$$

Eq. 1-26 is *Ohm's law of the magnetic circuit*. The factor  $NI$  is analogous to the emf in the electric circuit and is called the *magnetomotive force*. It is usually symbolized by  $M$ .  $R_m$  is the magnetic resistance or reluctance of the magnetic circuit.  $R_m$ , similar to the electric resistance, depends upon the length, cross-section, and magnetic conductivity or permeability of the flux path. Notice that  $R_m$  depends upon the value of  $\mu$ . Since in ferromagnetic materials  $\mu$  varies with the magnetizing force,  $R_m$  also varies with the magnetizing force in these materials. An example of the application of the circuital law of the magnetic field is given in Chapter 4.

**1-4. Forces on conductors in a magnetic field.** (a) *Magnitude and direction of the force*. When a current-carrying conductor is placed in a magnetic field, a force is exerted upon it. If the direction of the lines of induction make an angle  $\alpha$  with the direction of the current-carrying conductor (Fig. 1-9), this force is

$$f = 8.85 \times 10^{-8} B l I \sin \alpha \quad \text{lb} \quad (1-28a)$$

where  $l$  is the length of the conductor in inches,  $I$  the current in amperes, and  $B$  the density of the flux (in lines per square inch) in which the conductor is located.

In electric machines, the lines of induction and the conductors are always perpendicular to each other. Thus, in electric machines,

$$f = 8.85 \times 10^{-8} B l I \quad \text{lb} \quad (1-28b)$$

The direction of the force  $f$  on the conductor can be determined with the aid of the left-hand rule: open the left hand, keep the fingers together and the thumb in the same plane as the palm but pointing at right angles to

the fingers. If the fingers point in the direction of current, and the flux enters the palm at right angles to it, the thumb points in the direction of the force.

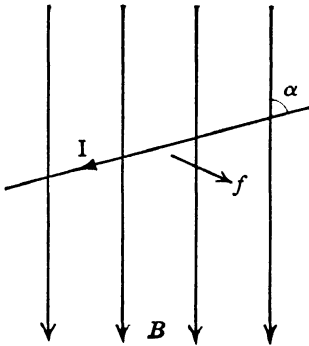


FIG. 1-9. Force on a current-carrying conductor in a magnetic field.

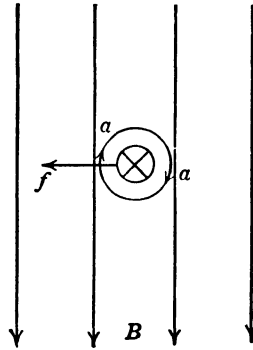


FIG. 1-10. Determination of the direction of the force on a current-carrying conductor in a magnetic field.

Another rule for the determination of the direction of the force  $f$  is the following (Fig. 1-10): draw some lines of induction  $B$ , draw a circle between the lines to represent the cross-section of the conductor, and show by two arrows  $aa$  the direction of the field due to the current in the conductor. The conductor will tend to move toward the region of opposing fields.

It follows from these rules that the force  $f$  is always perpendicular to the plane through  $I$  and  $B$ .

(b) *Direction of the force in an electric machine.* The force on the coil between two poles in Fig. 1-2 will be considered. Fig. 1-11 shows the direction of the forces exerted upon the two coil sides. Because of the large difference between the permeabilities of air and iron, the lines of induction in the air-gap are perpendicular to the iron and therefore the forces are *tangential* to the armature. The forces on both sides act as a couple and tend to rotate the coil about the armature axis. The torque on each conductor, corresponding to the force  $f$ , is equal to  $fR$ , when  $R$  is the radius of the armature. In accordance with

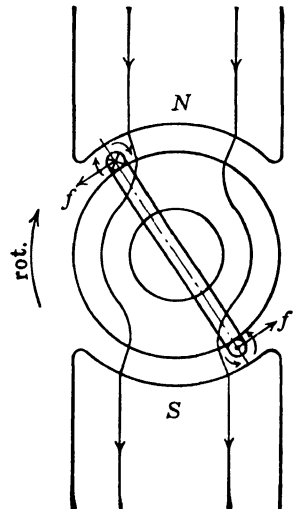


FIG. 1-11. Force on a coil of an electric machine.

the law of action and reaction, this torque acts not only upon the conductors but also upon the magnetic poles.

In the case of an alternating field and a conductor carrying alternating current, the instantaneous values of the flux density  $B$  and the current  $I$  must be used in Eq. 1-28. If the average value of the force is calculated for a single period, it is found to depend upon the effective values of  $B$  and  $I$ , and upon the time phase displacement between these quantities, i.e.,

$$F_{\text{avg}} = 8.85 \times 10^{-8} B_{\text{eff}} I \cos (B, I) \quad (1-29)$$

The torque produced by the couple in Fig. 1-11 is greatest when the flux and current are in time phase. This point will be considered later.

Eq. 1-28 for the force shows that the direction of the torque changes if the direction of either the flux or the current is changed. Changing the direction of the current and flux simultaneously does not change the direction of the torque. This explains why a unidirectional torque is possible in an a-c machine.

The forces shown in Fig. 1-11 refer to a generator driven (by a prime mover) in clockwise direction. Fig. 1-11 also shows the direction of the torque produced by the generated current: it is counterclockwise. Thus, in the case of a generator, the torque developed between the conductors and the flux (the electromagnetic torque) acts in a direction opposite to the direction of rotation and has to be overcome by the prime mover. In the case of a motor, the torque developed between the conductors and the flux is in the same direction as the direction of rotation and is delivered to its shaft. The balance of torques thus occurs in such a manner that in the generator the torque delivered by the prime mover is balanced by the opposing electromagnetic torque of the armature; in the motor the electromagnetic torque produced by the armature is balanced by the opposing torque of the load. It is well to remember that the generator converts mechanical power into electrical power and the motor converts electrical power into mechanical power.

Eq. 1-29 which gives the average value of the tangential force permits the derivation of a useful formula for the *electromagnetic power* of the electric machine. The torque produced by both sides of the coil (Fig. 1-11) is, in lb-ft,

$$T = 2 \times 8.85 \times 10^{-8} B_{\text{eff}} I \cos (B, I) \times \frac{R}{12} \quad (1-30)$$

where  $R = D/2$  is the radius of the rotor in inches. The relation between

torque and power is given by the fundamental equation of mechanics:

$$T = \frac{5250 P_{\text{HP}}}{n} = \frac{7.04 P_{\text{watts}}}{n} \text{ lb-ft} \quad (1-31)$$

Observe that the *area of the flux distribution curve*, i.e., of the  $B$  curve (Fig. 1-4 or Fig. 1-5), is the *flux per pole per unit length*, so that for a sinusoidal flux distribution

$$\Phi = \frac{2}{\pi} \tau l B \quad (1-32)$$

where  $B$  is the amplitude of the sinusoidal  $B$  curve. The pole pitch  $\tau$  is given by Eq. 1-5. The speed  $n$  in Eq. 1-31 can be expressed by the frequency  $f$  using Eq. 1-9 with  $p = 2$ , since a 2-pole structure is considered.

Combining Eqs. 1-30, 1-31, and 1-32 and introducing Eq. 1-11 the following result is obtained for the power  $P$ :

$$P = EI \cos (B, I) \text{ watts}$$

It is seen from Fig. 1-5 that  $E$ , being  $90^\circ$  behind  $\Phi$ , is in phase with  $B$ , so that the electromagnetic power of the electric machine is

$$P = EI \cos \psi \text{ watts} \quad (1-33)$$

where  $\psi$  is the angle between  $E$  and  $I$ .

Eq. 1-33, although derived for an elementary machine with two poles and a single coil under the assumption of a sinusoidal flux distribution, applies also to the actual electric machine. It will be seen later that the angle  $\psi$  is smaller than  $90^\circ$  in a generator and larger than  $90^\circ$  in a motor.

**1-5. Summary.** The four fundamental laws:

1. Faraday's law of induction,
2. Kirchhoff's law of the electric circuit,
3. Circuital law of the magnetic field (Ampère's law),
4. Law of force on a conductor in a magnetic field (Biot-Savart's law),

can be correlated by a simple figure which is very helpful for memorizing the four laws and their relations. This representation has been proposed by L. V. Bewley (see references on A-C Machines).

If, in the triangle of Fig. 1-12, the left side represents the current, the right side represents the voltage, and the base represents the magnetic field intensity  $H$  as well as the flux density  $B = 0.4\pi\mu H$  and also the flux  $\Phi = B \times \text{Area}$ , then the top corner which connects current and voltage

is to be assigned to Kirchhoff's mesh law, the left corner which connects current and  $H$  is to be assigned to Ampère's law (circuital law of the magnetic field), and the right corner which connects flux and voltage is

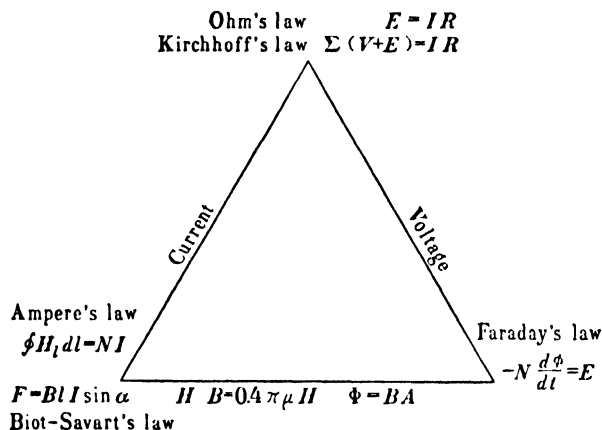


FIG. 1-12. Graphical correlation of the fundamental laws.

to be assigned to Faraday's induction law. Since the left corner connects not only current and  $H$ , but also current and  $B$ , it represents Ampère's law and Biot-Savart's law (law of force on a conductor in a magnetic field).

### PROBLEMS

1. A conductor 10 in. long is moving with a velocity of 80 fpm perpendicular to a magnetic flux whose average density is 60,000 lines per sq. in. Determine the average voltage generated.
2. Determine the velocity of a conductor 15 in. long moving perpendicularly across a magnetic flux of 40,000 lines per sq. in. average density if an average voltage of 0.05 volt is to be induced.
3. A 4-pole generator having a coil of 60 turns on the armature produces a maximum coil voltage of 28.3 volts with a pole flux of  $10^6$  maxwells. The flux distribution is sinusoidal. Determine the generator speed.
4. A conductor is "cutting flux" at an average rate of 150,000 lines per sec. Determine the average voltage induced in the conductor.
5. It is desired to induce an average voltage of 3.5 volts in a coil linking a certain magnetic circuit. The flux changes from +200,000 lines to -200,000 lines in a time interval of  $1/3$  sec. Determine the number of turns on the coil.
6. A 6-pole generator has a flux per pole of  $2 \times 10^6$  maxwells. The armature rotates at 720 rpm. The flux distribution is sinusoidal. Determine the average emf and the maximum emf induced in a full pitch coil of 5 turns.
7. A square coil 10 in. on each edge has 25 turns and rotates at a speed of 1000 rpm in a magnetic field of 2000 lines per sq. in. Determine the maximum flux passing through the coil, and the average emf induced in the coil. What is the voltage if flux and speed are both increased 50%.

8. A 4-pole generator has a flux of  $3.5 \times 10^6$  maxwells per pole. The armature rotates at 600 rpm. (a) Calculate the average voltage generated in a turn when it travels one pole pitch. (b) What is the average voltage generated in one conductor in  $1/4$  revolution of the armature?

9. An armature conductor 15 in. long moves in a flux the density of which is 50,000 lines per sq. in. under the center of the pole. The diameter of the coil of which the conductor is a part is 15 in. and the armature rotates at 1200 rpm. What is the emf induced in the conductor when it lies under the center of the pole?

10. At what speed must the armature of Problem 9 move in order that the emf induced in the conductor be 12 volts.

11. A square coil, 8 in. on each edge, has 50 turns and its plane lies perpendicular to a uniform magnetic flux with a density of 5000 lines per sq. in. The coil rotates  $\frac{1}{4}$  turn about its axis in 0.08 sec. Determine: (a) maximum flux interlinked with the coil; (b) average emf induced during this 0.08 sec; (c) average emf induced if the coil is made to rotate at 150 rpm; (d) instantaneous emf when coil is perpendicular to the flux and also when it is parallel to the flux.

12. A current of 10 amp flowing in a 400-turn coil produced a flux of 8000 lines interlinking these 400 turns. Determine: (a) the flux linkages in maxwell turns; (b) the self-inductance in henries.

13. If the number of turns in the coil of Problem 12 is doubled and the current remains the same, determine the flux linkages and self-inductance in henries. Assume all flux lines link all turns.

14. 1000 turns are wound upon an iron core magnetic circuit of 3 sq. in. cross-section. A current of 9 amp produces a flux density of 85,000 lines per sq. in. and a current of 4 amp produces 65,000 lines per sq. in. Determine the coefficient of self-inductance for each current.

15. The field of a shunt generator has a self-inductance of 35 henries. The current in the field winding is changed from 1.5 amp to 0.80 amp in 0.01 sec. Determine the emf of self-induction.

16. What is the emf of self-induction in Problem 15 if the current changes to zero in the same time?

17. The four shunt field coils of a generator are connected in series and each has 1000 turns. A direct current of 4.0 amp produces  $0.5 \times 10^6$  lines of flux linking each coil. Determine: (a) the coefficient of self-inductance of the entire winding; (b) the total energy storage. If the field circuit is opened and the current decays to zero in 0.25 sec, what is the average value of voltage generated across the field?

18. Two field coils of a 2-pole machine are wound with 1500 turns each. A field current of 3.0 amp produces a flux of  $3 \times 10^6$  maxwells linking each coil. What is the self-inductance of the field circuit?

19. A 4-pole generator having 2000 field turns per pole produces a pole flux of  $3 \times 10^6$  maxwells when the field current is 2.80 amp. Determine: (a) maxwell-turn linkages per pole; (b) total maxwell-turn linkages; (c) coefficient of self-inductance of the field circuit.

20. A mutual inductance of 3.1 henries magnetically couples two circuits. If the current in the first circuit changes from 2.75 to 1.0 amp in 0.015 sec, what is the average voltage induced in the second circuit?

21. A cast-iron ring has a mean diameter of 12 in. and a circular cross-section of 3.5 sq. in. area. Determine the number of ampere-turns required to produce a total flux of 110,000 maxwells.



**22.** Solve Problem 21 for the case where an air gap 0.10 in. is cut in the cast-iron ring. (Neglect fringing.)

**23.** How many additional ampere-turns are required in Problem 21 if the total flux is (a) increased 20%, (b) decreased 20%.

**24.** A cast-steel ring having a mean diameter of 5.5 in. and a circular cross-sectional area of 0.85 sq in. has an air gap 0.10 in. long cut in the ring. (a) Determine the number of ampere-turns necessary to produce fluxes of 30, 50, 80, 100 and 105 kilolines per sq in. (b) If the winding on the ring has 250 turns, plot the curve of total flux vs. exciting current.

**25.** A 200-turn, single-layer coil is wound uniformly upon the entire of a wooden toroidal ring having a mean diameter of 6 in. and a square cross-section of 1 sq. in. area. Determine: (a) flux density in core when coil current is 4 amp; (b) flux density if the wooden ring is replaced by a cast-steel ring of the same dimensions and the coil carries 4 amp.

**26.** A cast-steel ring having a mean radius of 10 in. and a circular cross-section 2 in. in diameter is wound with a coil of 700 turns carrying 10 amp. Determine the flux density and the total flux.

**27.** If an air gap 0.50 in. long is cut in a cast-iron ring of 10 in. mean radius and 3.5 sq. in. circular cross-section, determine the total flux and flux density when 2500 ampere-turns are impressed upon the magnetic circuit.

**28.** A conductor 25 in. long carries a current of 15 amp and is acted upon by a force of 2 lb when placed in a magnetic flux perpendicular to the flux lines. Determine the flux density in gaussess and in lines per square inch.

**29.** Determine the current carried by a conductor 15 in. long if a force of 0.001 lb acts upon it when it is placed in a magnetic flux of 5000 lines per sq in. flux density so that the lines of flux make an angle of  $45^\circ$  with the normal to the conductor.

**30.** A flat, square coil of 20 turns having an area of 60 sq in. is placed in a uniform magnetic flux, so that the plane of the coil is parallel to the flux lines and the two active coil sides lie perpendicular to the lines of flux. The flux density is 5000 lines per sq in. and the coil current is 10 amp. Determine: (a) the force in pounds acting on each side of the coil; (b) the torque in pound-feet acting to turn the coil.

**31.** The coil in Problem 30 is replaced by a 25-turn rectangular coil having dimensions  $12'' \times 18''$ , with the longer sides being the active conductors. Determine the turning torque in pound-feet when the current is 15 amp.

**32.** Repeat Problem 31 with the plane of the coil making an angle of  $45^\circ$  with the direction of the flux lines.

**33.** Repeat Problem 31 with the plane of the coil making an angle of  $60^\circ$  with the direction of the flux lines.

**34.** A 15-in. conductor carrying 20 amp lies in a uniform magnetic flux. A force of 0.25 lb tends to move the conductor perpendicular to the flux and to itself. Determine the flux density.

## Chapter 2

### MECHANICAL ELEMENTS OF THE D-C MACHINE

It follows from Art. 1-4 that the magnetic flux and the current-carrying conductors are the two indispensable elements of the electric machine. The part of the machine on which the conductors producing the tangential forces (Eq. 1-28b) are placed is called the *armature*. In the d-c machine this is the rotating inner part of the machine. The electro-magnets (poles) are stationary and are connected with the outer part of the machine or frame.

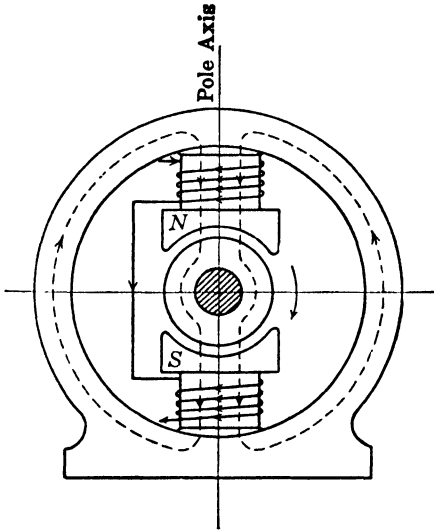


FIG. 2-1. Main flux path of a 2-pole d-c machine.

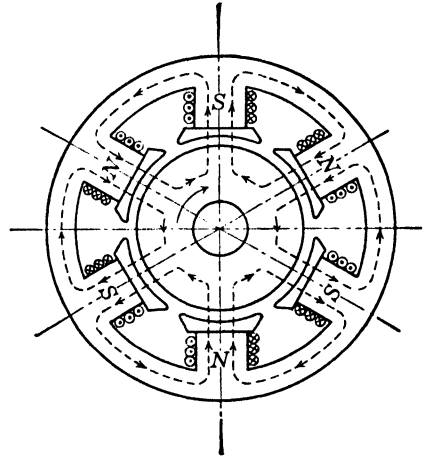


FIG. 2-2. Main flux path of a 6-pole d-c machine.

Figs. 2-1 and 2-2 show the magnetic paths of a 2-pole and of a 6-pole d-c machine. The flux originates in the poles which are mounted on the frame and on which field-exciting coils are placed. The armature is the

inner and rotating part of the machine. The armature conductors are placed in slots punched in the armature laminations. The path of the magnetic flux (Fig. 2-1) consists of: a part of the frame, two poles, two air-gaps between the poles and the armature, two sets of teeth on the armature, and a part of the armature core.

The material of the armature conductors and field coils is copper, since, among the relatively cheap materials, copper has the lowest resistivity and thus the lowest  $I^2R$  losses.

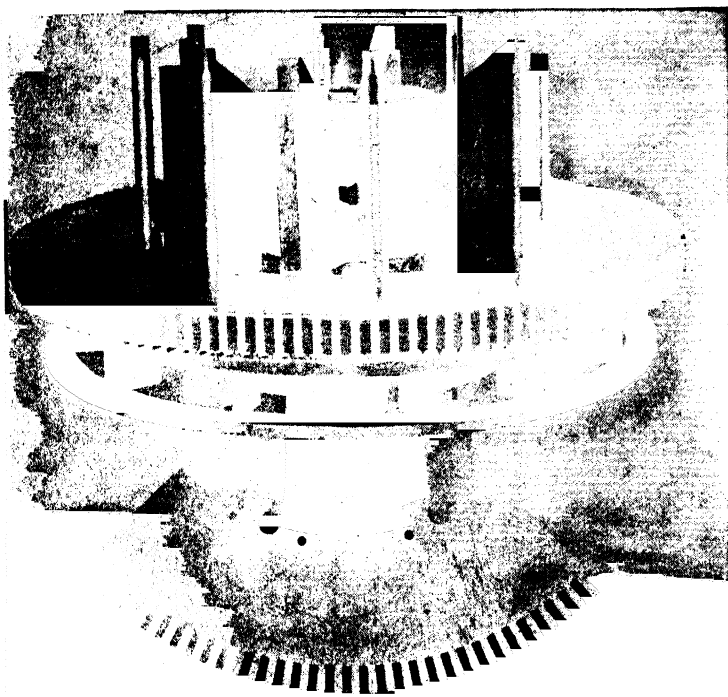


FIG. 2-3. Punched laminated segment and partially assembled stack of laminations of a large d-c machine.

The slots and armature conductors are usually placed parallel to the axis of the armature, but are also sometimes skewed at a slight angle to the axis. The armature iron must be laminated and the laminations insulated; otherwise the pole-flux will induce an emf not only in the conductors but also in the armature iron, which can be considered to consist of iron conductors placed on its surface, parallel to the real conductors in the slots. Currents, thus induced on the surface of the armature iron, will produce high  $I^2R$  losses in the iron without contributing much to the

torque developed by the machine. This kind of  $I^2R$  loss is called an eddy-current loss. For similar reasons (see Art. 10-1) the poles of d-c machines are usually laminated, while the frame is usually solid.

At the bottom of Fig. 2-3 is shown a punched, laminated segment of a large d-c armature and, at the top, the process of stacking such laminations. Fig. 2-4 shows the assembled core for a small, 2-pole, d-c armature with slot insulation inserted. In small machines where the length of the core is small, the entire core consists of a single stack. Fig. 2-5 shows a complete armature core, with commutator, for a large machine. Here the core assembly is divided into five stacks, separated by ventilating ducts. The purpose of these ducts is to transfer the heat developed in the iron (see Chapter 10) to the circulating air. It will be explained in Chapter 3 that the induced emf in a d-c machine is an a-c emf. The purpose of the commutator is to make the machine act, with respect to an external circuit, as though it continually produces a constant voltage.



FIG. 2-4. Assembled armature core for a small d-c machine.

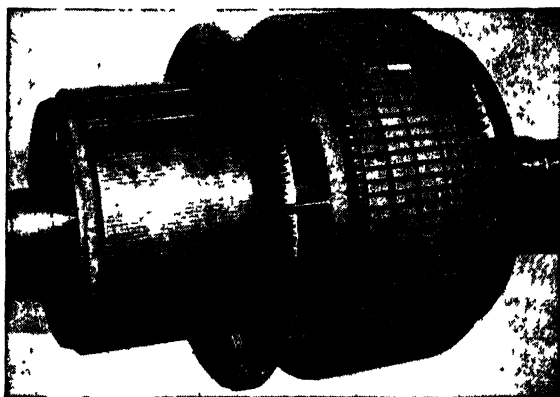


FIG. 2-5. Completely assembled armature core and commutator for a large d-c machine.

Fig. 2-6 shows a partially wound d-c armature. Fig. 2-7 shows a complete armature of a larger machine with the winding connected to the commutator. In Fig. 2-7 some of the wedges which hold the winding in place are partially inserted; the band wires which hold the end windings

have not yet been put on. Fig. 2-8 shows a complete d-c armature for a small machine, with a ventilating fan. The slots are skewed in order to reduce noise.

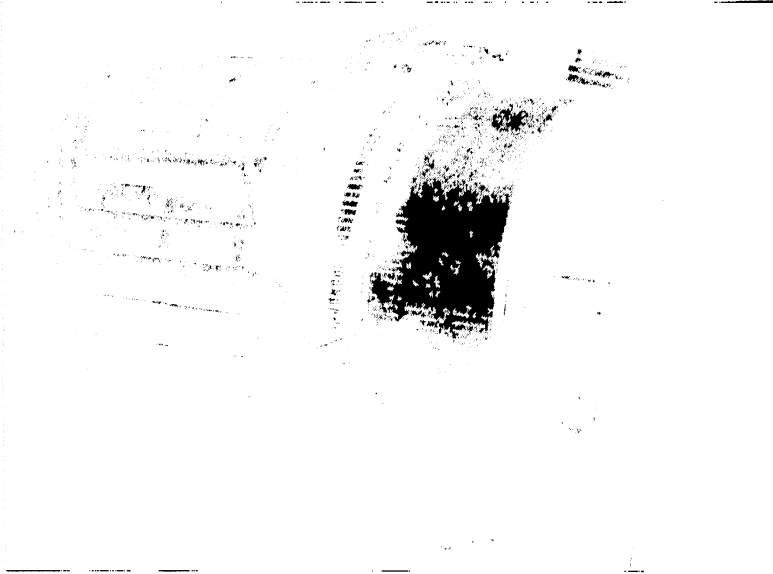


FIG. 2-6. Partially wound d-c armature.

A complete pole, assembled from laminations and held together by rivets, is shown in Fig. 2-9, which also shows a field coil consisting of two



FIG. 2-7. Completely wound d-c armature with slot wedges partially in place.

windings, one a shunt coil of fine wire over which is wound a series coil of heavy wire (see Art. 5-1). Whereas the armature laminations *must* be

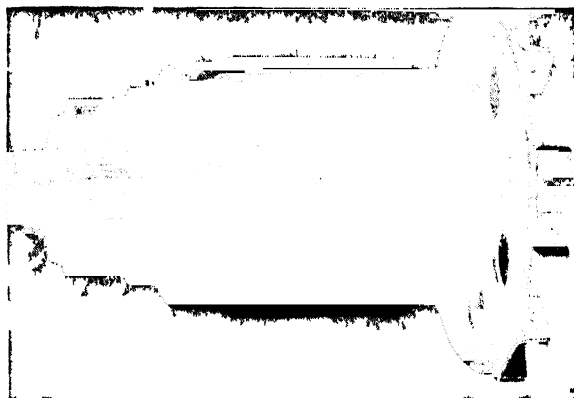


FIG. 2-8. Small d-c armature with skewed slots and ventilating fan.

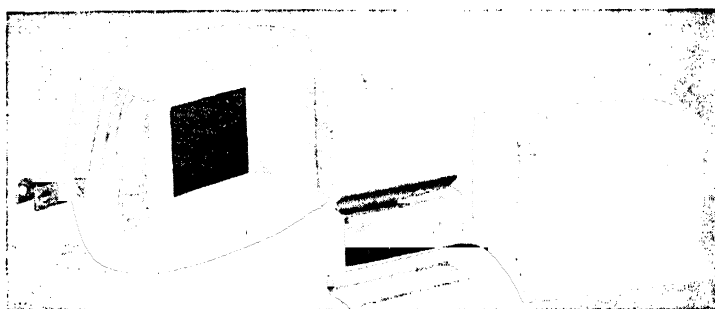


FIG. 2-9. Field coil and field pole for a d-c machine.



FIG. 2-10. Completely assembled pole core and field windings for a d-c machine, showing shunt and series windings.

insulated, the pole laminations are not insulated from each other because they are not influenced by the main flux. Fig. 2-10 shows a complete field pole assembly for a larger d-c machine. Here the series coil is made

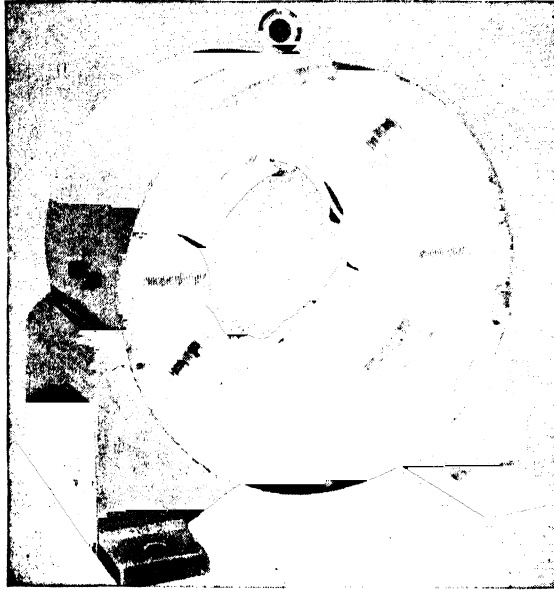


FIG. 2-11. Completely assembled stator for a 50-HP, 850-rpm, 230-volt d-c machine showing main poles and interpoles.

up of copper ribbon. Fig. 2-11 shows a completely assembled stator—that is, the stationary outer part of the machine consisting of the frame, four main poles with their field windings, and four small poles called

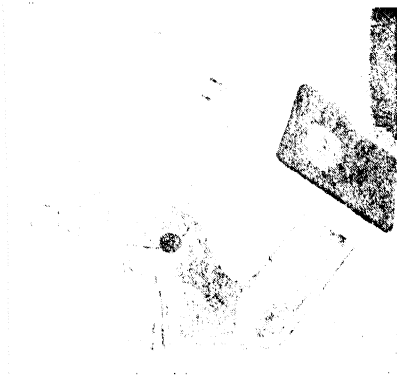


FIG. 2-12. Carbon brush mounted in a brush holder.



FIG. 2-13. Partially assembled brush rigging for a d-c machine.

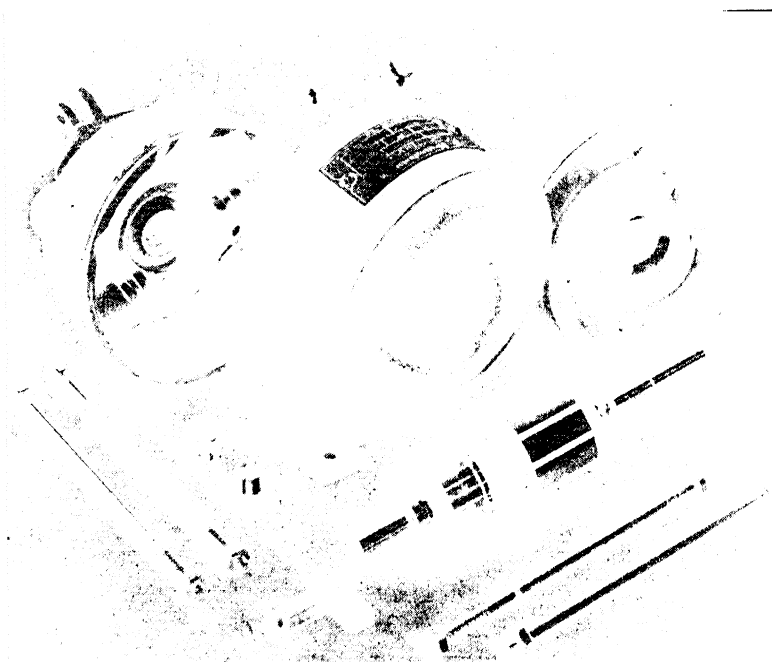


FIG. 2-14. Parts of a 2-pole, fractional-HP d-c motor.

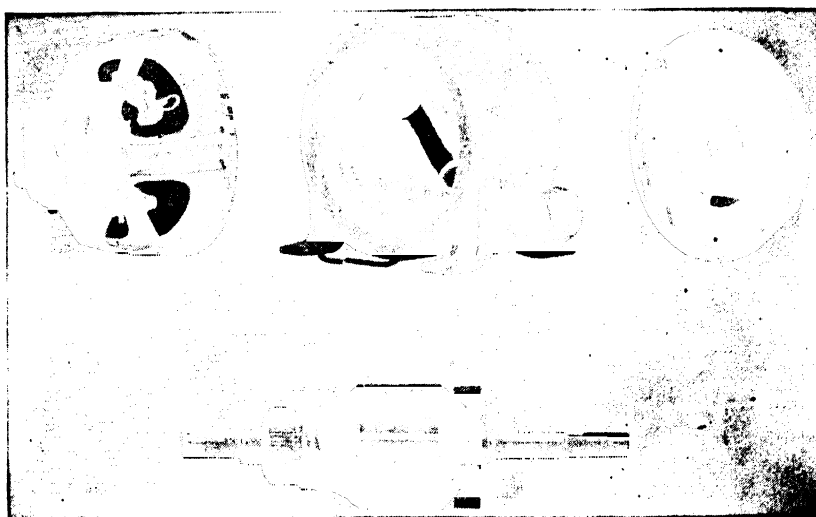


FIG. 2-15. Parts of a small integral-HP d-c motor.



interpoles or commutating poles. The purpose of the interpoles is to avoid sparking at the commutator which may be caused when the armature coils are short-circuited by the brushes on the commutator (see Art. 8-3).

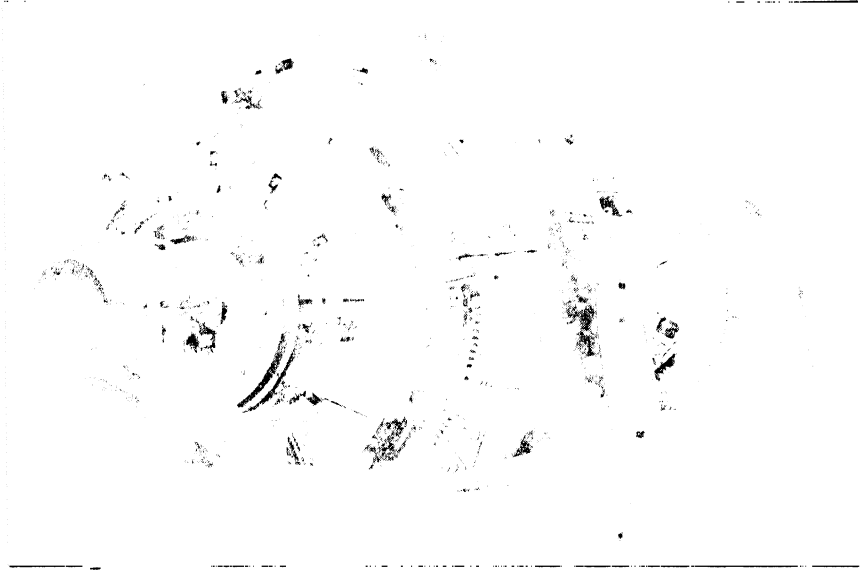


FIG. 2-16. 2500-IHP, 225/450 rpm d-c mill motor.

Fig. 2-12 shows a single carbon brush mounted in a brush holder. The current is conducted from the brush to the brush holder by a flexible copper pigtail. In order to produce the necessary pressure for smooth



FIG. 2-17. Small totally enclosed mill-type motor.

running of the brush on the commutator, an adjustable spring bears on the top of the brush. Fig. 2-13 shows a brush rigging consisting of a rocker ring, four brush studs (one not shown), and four brushes on each stud. Current passes from the brush holder to the stud, which is insulated from the rocker ring. All positive studs are connected together, as well as all negative studs, to form the positive and negative, + and -, terminals of the machine.

Fig. 2-14 shows all the parts of a 2-pole, fractional-horsepower motor with no interpoles. Fig. 2-15 shows the parts of a small, integral-horsepower motor with two main poles and one interpole. Fig. 2-16 shows a large d-c mill motor, and Fig. 2-17 a smaller mill-type motor, which is totally enclosed.

## Chapter 3

### D-C ARMATURE WINDINGS

**3-1. Two types of closed windings: lap and wave windings.** It has already been mentioned that the d-c generator, as used in practice, is an a-c machine with a special device, the commutator, which makes it possible to pick up from the winding a fixed instantaneous value of the a-c voltage. With respect to the external circuit, the voltage then appears as a constant quantity. The same applies to the d-c motor. The operation of the commutator will be studied in Art. 3-4.

In order that the commutator accomplish its purpose, the armature winding must be a *closed* one, i.e., if, starting at a certain point, the winding is followed through all its turns, the starting point is reached again. There are two types of closed windings, the *lap* winding and the *wave* winding.

The *coil span* of any winding must be equal to or approximately equal to a *pole pitch* (see Art. 1-1). Then the winding is most effective, since its turns are able to interlink the total pole-flux (Fig. 1-2). The two conductors of each turn of such a winding always lie under poles of different polarity, so that the emf's induced in the two conductors add.

Fig. 3-1 shows the lap winding. Turn *a* consists of conductors  $a'-a''$ , turn *b* consists of conductors  $b'-b''$ , and so forth. The end of turn *a* ( $a''$ ) is connected with the beginning of turn *b* ( $b'$ ) which lies under the *same* pole as the beginning of turn *a*; the end of turn *b* ( $b''$ ) is connected with the beginning of turn *c* ( $c'$ ), and so forth. The end of the last turn of the winding is then connected with the beginning of the first turn and the winding is closed.

It is important that the end of a turn and the beginning of the next following turn lie under poles of *different* polarity, otherwise the emf's of two consecutive turns will not add. This is achieved in the lap winding, Fig. 3-1, by connecting the end of turn *a* ( $a''$ ) with the beginning of turn *b* ( $b'$ ) which lies under the same pole as the beginning of turn *a* ( $a'$ ).

Apparently the addition of the emf's of consecutive turns can also be achieved in the way shown in Fig. 3-2. Here the end of turn  $a$  ( $a''$ ) which lies under a S-pole is connected with a turn-beginning ( $b'$ ) which lies under a N-pole; however, the latter N-pole is not the N-pole under which the beginning of coil  $a$  ( $a'$ ) lies but the next following N-pole. The coil connection of Fig. 3-2 is that of the wave winding.

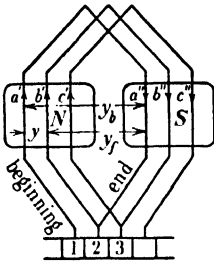


FIG. 3-1. Elements of a lap winding.

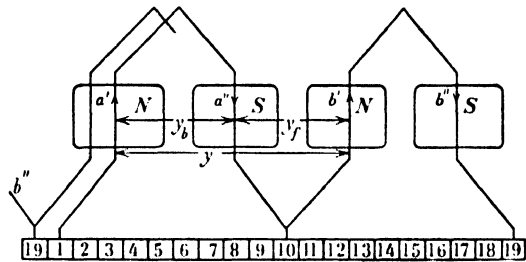


FIG. 3-2. Elements of a wave winding.

Two steps are necessary in order to follow from the beginning of a turn to the beginning of the next following turn. The steps are one forward and one backward step in the lap winding; they are two forward steps in the wave winding.

The wave winding of Fig. 3-2 is a closed winding just as the lap winding is closed. The first wave is connected to the commutator bars 1, 10, 19; the second wave is connected to the commutator bars 19, 9, 18; and so forth. The last wave is connected to commutator bars 12, 2, 11, and the last turn is connected to commutator bars 11 and 1 closing the winding (see also Fig. 3-11).

The lap and wave windings behave differently. For the same number of turns, same pole-flux, and same speed (Eq. 1-3), the lap winding generates a lower voltage than the wave winding. This is due to the fact that the lap winding has more parallel circuits than the wave winding, i.e., fewer coils are connected in series in the lap winding than in the wave winding, thus yielding a lower voltage. This will be explained in some detail in the following articles.

**3-2. Winding pitch. Back pitch and front pitch.** The distance between the beginnings of two consecutive turns is called the *winding pitch* ( $y$ ). The distances which correspond to the two steps necessary to follow from the beginning of a turn to the beginning of the next following turn are called *back pitch* ( $y_b$ ) and *front pitch* ( $y_f$ ). The three pitches are shown in

Figs. 3-1 and 3-2. Corresponding to the fact that in the lap winding one of the two steps necessary to follow from the beginning of one turn to the beginning of the succeeding turn is a forward step, and the other a backward step, the *winding pitch* ( $y$ ) of the lap winding is equal to the difference of back pitch and front pitch.

$$y = y_b - y_f \quad \text{lap winding} \quad (3-1)$$

Since both steps necessary to follow from the beginning of one turn to the beginning of the next succeeding turn in the wave winding are forward steps, the winding pitch of the wave winding is equal to the sum of the back pitch and front pitch.

$$y = y_b + y_f \quad \text{wave winding} \quad (3-2)$$

In larger machines, a turn is the *winding element*. In smaller machines, the winding element may have more than one turn, as shown in Figs. 3-3 and 3-4.

In these latter cases, the statements made in the foregoing with respect to the beginnings and ends of a turn refer to the beginnings and ends of the winding element, i.e., of the coil consisting of several turns. It will

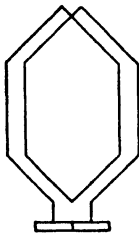


FIG. 3-3. Element of a lap winding with two turns.

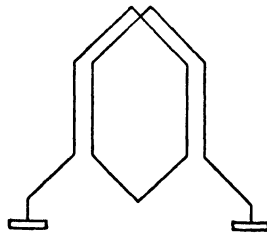


FIG. 3-4. Element of a wave winding with two turns.

become clear from Art. 3-4 that the beginning and the end of each winding element must be connected to a commutator bar. Therefore there are *as many commutator bars as winding elements* for both the lap and wave windings.

Since the commutator is an image of the winding, quantities referring to the winding can be expressed in terms of commutator bars (commutator pitches). Thus the winding pitch, the back pitch, and front pitch can be expressed in commutator bars. It is seen from Fig. 3-1 that the winding pitch of the lap winding is equal to one commutator bar.

$$y = 1 \quad \text{lap winding} \quad (3-3)$$

The winding pitch of the wave winding is approximately equal to the number of commutator bars in *two poles* (see Fig. 3-2).

It is

$$y = \frac{k \mp 1}{p/2} \quad \text{wave winding} \quad (3-4)$$

where  $k$  is the total number of commutator bars. The winding pitch *must deviate* from the number of bars in two poles, otherwise each  $p/2$  winding elements will make a closed circuit and a series connection of the coils will not be achieved.

The *back pitch* of the lap as well as of the wave winding must be equal or approximately equal to the number of *commutator bars per pole*, in order that the coil span be equal or approximately equal to a pole pitch.

**Example 3-1.** 4-pole machine with 36 winding elements and lap winding. What are the back and front pitches of this winding, expressed in commutator bars?

Since there are 36 winding elements, the number of commutator bars is 36. The number of commutator bars per pole is then  $36/4 = 9$ , making the back pitch  $y_b = 9$ ; the front pitch becomes (Eq. 3-1)  $y_f = y_b - 1 = 8$  commutator pitches.

**Example 3-2.** 4-pole machine with 37 winding elements and wave winding. What are the three pitches of this winding expressed in commutator bars?

Since there are 37 winding elements, the number of commutator bars is equal to 37. From Eq. 3-4

$$\text{winding pitch} \quad y = \frac{37 \mp 1}{2} = 18 \text{ or } 19$$

The number of commutator bars per pole is  $37/4 = 9.25$ .

The back pitch is made  $y_b = 9$ .

Therefore (Eq. 3-2) the front pitch is either  $y_f = 18 - 9 = 9$  or  $19 - 9 = 10$  commutator pitches.

**3-3. Number of parallel paths in the lap and wave winding. Number of brush studs.** Direct-current armature windings are usually 2-layer as shown in Fig. 3-5. Each layer may have one, two, or more conductors. There are three conductors in each layer of Fig. 3-5. Each turn of the winding has one conductor in the upper layer and the other conductor in the lower layer. A 2-layer winding with two conductors per layer is shown in Fig. 3-6. The conductors indicated by black circles belong to the same turns.

Fig. 3-7 shows a 4-pole lap winding developed. Fig. 3-8 shows the same winding in a polar diagram. The number of slots is 20, and the number of conductors in each layer of the slot is one. The total number of conductors is  $20 \times 2 = 40$ , and therefore the number of turns (winding elements) as well as the number of commutator bars is 20. A pole

pitch is  $20/4 = 5$  commutator bars, and the back pitch (coil span) is chosen to be equal to 5 commutator bars. Since there is only 1 conductor per layer in the slot, the back pitch is also equal to 5 slot pitches. The front pitch must be equal to 4 commutator bars or slot pitches, in order that the winding pitch is equal to 1, Eq. 3-3.

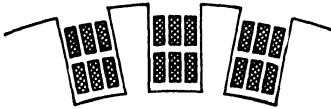


FIG. 3-5. Two-layer winding.

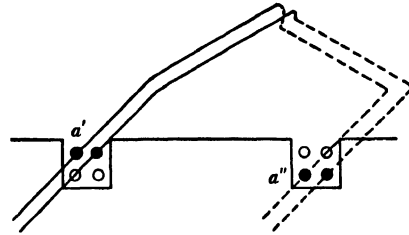


FIG. 3-6. Two-layer winding with two conductors per layer.

In Fig. 3-7, the upper and lower layers are shown next to each other, with the upper layer represented by a full line and the lower layer by a dotted line. Corresponding to the coil span,  $y_b = 5$  commutator bars = 5

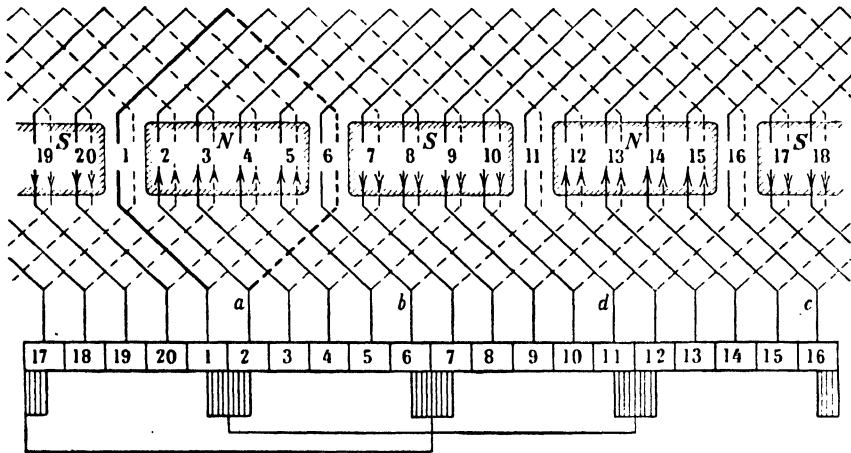


FIG. 3-7. Developed diagram of a 4-pole, 2-layer lap winding with 20 slots and one conductor per layer.

slot pitches, upper conductor 1 is connected to lower conductor  $1 + y_b = 1 + 5 = 6$ , then this lower conductor to upper conductor  $6 - y_f = 6 - 4 = 2$ , and so forth, until the winding is closed.

It follows from Faraday's law, Art. 1-1, Fig. 1-2, that all conductors lying under a pole of certain polarity have emf's of the same direction and that conductors lying under poles of different polarity have emf's

of different directions. For this reason, the emf's of consequent poles have different directions in Fig. 3-7. No emf direction is given to the conductors which lie close to the middle of the interpolar space, because there the flux density is very small and the induced emf negligible (see Fig. 1-4 and Eq. 1-4).

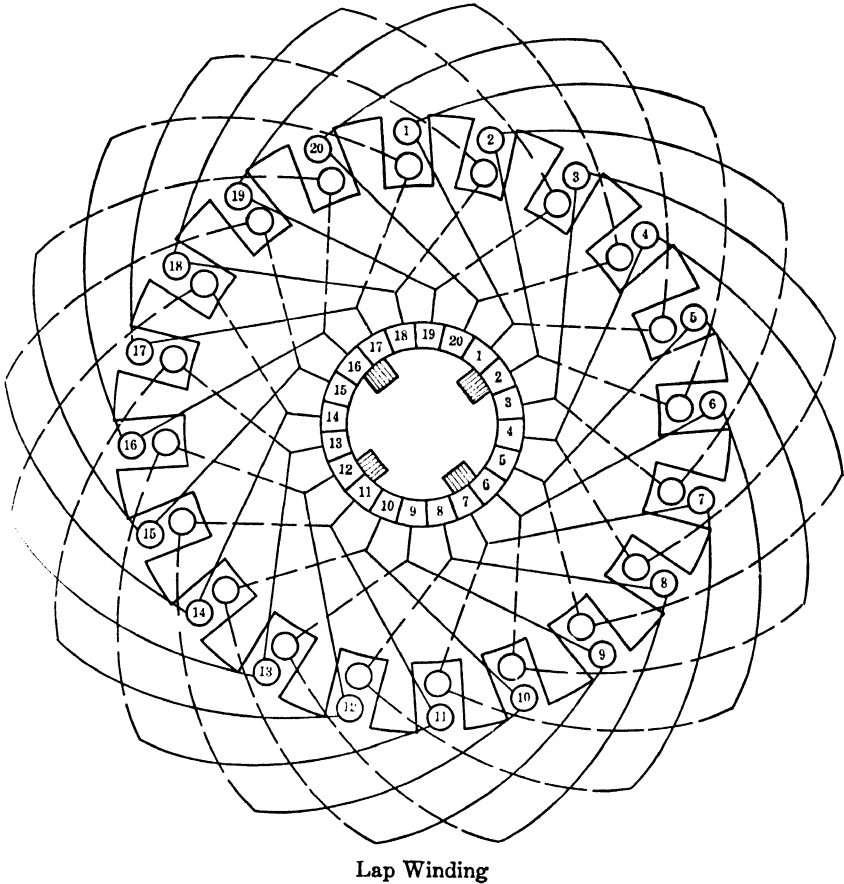


FIG. 3-8. Polar diagram of the winding shown in Fig. 3-7.

Starting at point *a* in Fig. 3-7 and following through the winding, Fig. 3-9 is obtained for the sequence of the upper conductors and for the direction of the induced emf's (indicated by arrows). It is not necessary here to consider the lower conductors, since the coil span is equal to a pole pitch and the emf of each lower conductor is equal to and automatically adds to the emf of its upper conductor. (Conductors lying between poles do not contribute to the emf and are not included.)



Considering Fig. 3-9, there are four groups of turns, each group consisting of four turns in which an emf is induced. A voltage difference exists between the points  $a$  and  $b$ ,  $a$  and  $c$ ,  $d$  and  $b$ , and  $d$  and  $c$ , but there

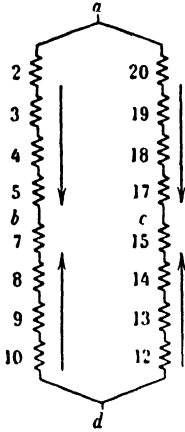


FIG. 3-9. Sequence of upper conductors and direction of the emf's of winding shown in Fig. 3-7.

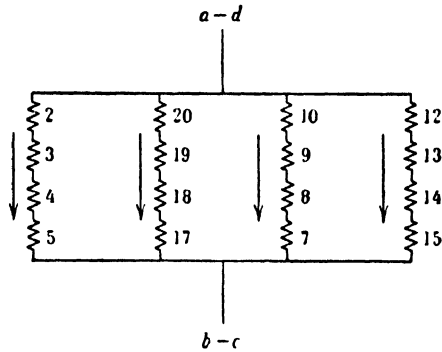


FIG. 3-10. The four parallel circuits of the winding shown in Fig. 3-7.

is no voltage difference between the points  $a$  and  $d$  or between the points  $b$  and  $c$ . Points  $a$  and  $d$  and points  $b$  and  $c$  can be connected, respectively, yielding the grouping Fig. 3-10, which shows that the winding has four parallel circuits, i.e., as many as there are poles. It is a characteristic

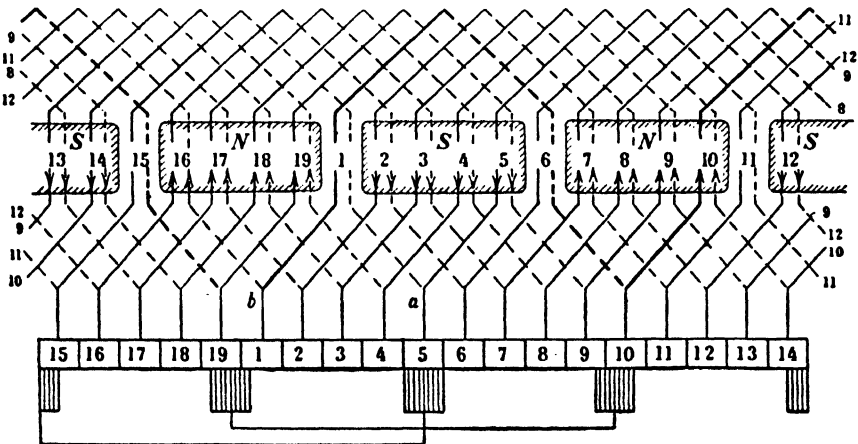


FIG. 3-11. Developed diagram of a 4-pole, 2-layer wave winding with 19 slots and one conductor per layer.

feature of the *lap winding* that *its number of parallel circuits is equal to its number of poles*. Thus, a lap winding will have 8 parallel circuits in an 8-pole machine, 16 parallel circuits in a 16-pole machine, and so forth.

Fig. 3-11 shows a 4-pole wave winding developed, and Fig. 3-12 shows the same winding in a polar diagram. The number of slots is 19 and the

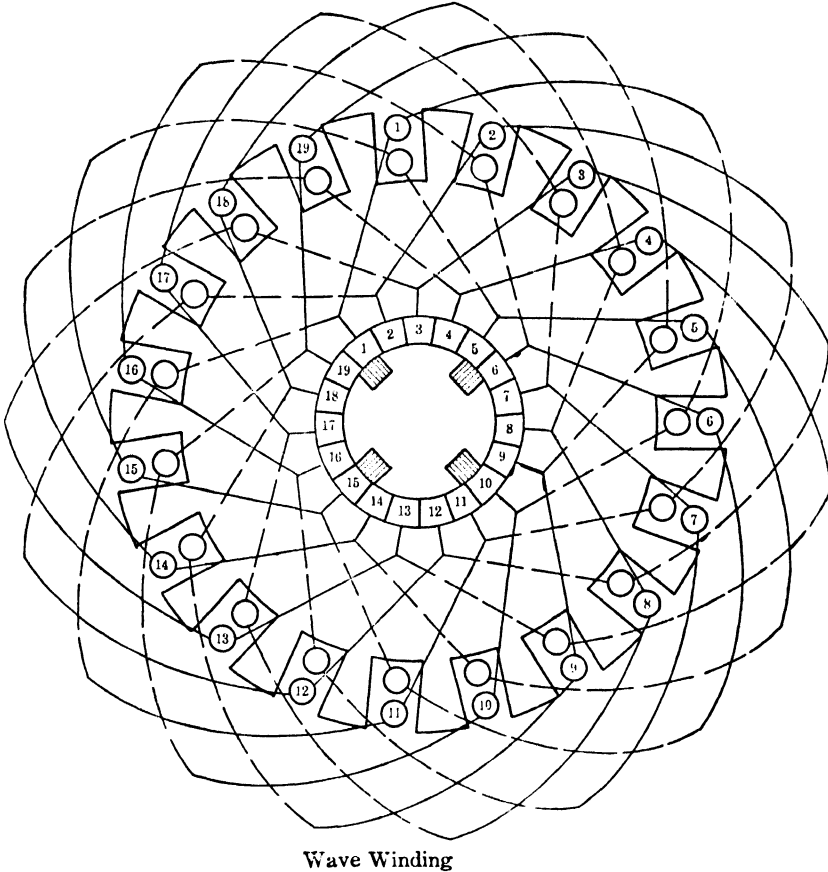


FIG. 3-12. Polar diagram of the winding shown in Fig. 3-11.

number of conductors in each layer of the slot is 1. The total number of conductors is  $19 \times 2 = 38$ , and therefore the number of turns (winding elements) as well as the number of commutator bars is 19. According to Eq. 3-4, the winding pitch is

$$y = \frac{19 - 1}{2} = 9 = y_b + y_f$$

commutator bars. To a pole pitch correspond  $19/4 = 4\frac{3}{4}$  commutator bars. The coil span  $y_b$  is chosen as 5 commutator bars, i.e., close to the pole pitch and somewhat larger than the pole pitch. The forward pitch is then  $9 - 5 = 4$  commutator bars. Since there is only 1 conductor per layer in the slot, the back pitch and front pitch are 5 and 4 slots respectively, if they are expressed in slot pitches. Thus, starting with upper conductor 1, a connection must be made to lower conductor  $1 + y_b = 1 + 5 = 6$  on the side opposite the commutator (back end), then to upper conductor  $6 + y_f = 6 + 4 = 10$  on the commutator side, then again to lower conductor  $10 + y_b = 10 + 5 = 15$ , next to upper conductor  $15 + 4 = 19$ , and so forth, until the winding is closed.

Starting at point *a* in Fig. 3-11 and following through the winding, Fig. 3-13 is obtained for the sequence of the upper and lower conductors

and for the direction of the induced emf's. Upper and lower conductors must be considered here because the coil span is not equal to the pole pitch. It is seen from this figure that here there are only two parallel circuits as compared with the four parallel circuits of the 4-pole lap winding (Fig. 3-7 and 3-10). It is a characteristic feature of the *wave winding*

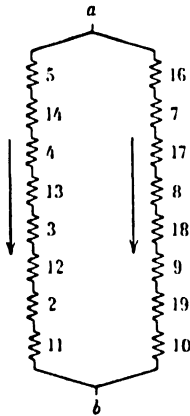


FIG. 3-13. The two parallel circuits of the winding shown in Fig. 3-11.

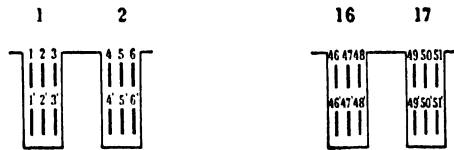


FIG. 3-13a. Example — Arrangement of conductors in slots.

that it has *only two parallel circuits*, regardless of the number of poles. This feature of the wave winding is the reason why it is designated as a *series winding*, and the lap winding is designated as a *parallel winding*.

It is seen from Figs. 3-10 and 3-13 that four external connections to the winding, i.e., four brush studs on the commutator, are necessary for the 4-pole lap winding and only two brush studs for the 4-pole wave winding. In general, the *lap winding* needs as many brush studs as there are poles, since it has as many parallel circuits as poles. Half of the brush studs are of positive polarity; half, of negative. As to the wave winding, two brush studs, one positive and one negative, suffice for any number of poles. However, the wave winding also normally has as many brush studs

as poles. This has the advantage that, for a given current, the commutator is shorter. The positive as well as the negative brush studs are then internally connected by the winding elements short-circuited by the brushes (see Fig. 3-11).

It is seen from Figs. 3-7 and 3-11 that physically the brushes must lie under the center lines of the poles. The active parts (the conductors) of the winding elements short-circuited by the brushes then lie in the interpolar spaces. In schematic diagrams (see Art. 4-3) the brushes are usually placed in the center lines of the interpolar spaces to indicate the conductors to which they are connected. In Figs. 3-7, 3-8, 3-11, and 3-12, the polarity of the brushes is definitely determined by the pole polarities and the direction of rotation of the armature. In the schematic diagrams, the polarity of the brushes is not definitely determined and may be assigned arbitrarily.

It has been mentioned in Art. 3-2 that the winding pitch of the wave winding must deviate from the number of commutator bars in two poles.

In Eq. 3-4 this deviation is  $\mp \frac{1}{p/2}$  commutator bars. If this deviation is made  $\mp \frac{2}{p/2}$  commutator bars, the winding will have four parallel circuits instead of two, independently of the number of poles. Such a winding is called a *duplex wave winding*. Making the deviation equal to  $\mp \frac{3}{p/2}$ , the *triplex wave* winding with six parallel circuits is obtained.

The lap and the simplex wave windings are most commonly used in d-c armatures. Almost all small machines and high-voltage machines are designed with the simplex wave winding.

**Example 3-3.** 8-pole armature with 132 slots. 2-layer winding with three conductors per layer in the slot. Lap winding.

Determine the number of commutator bars and the back and front pitches. Show the sequence in which the conductors are connected.

Since there are three conductors per layer in the slot, the total number of winding elements is  $132 \times 3 = 396$ ; therefore, the number of commutator bars is

$$k = 396$$

The number of commutator bars per pole is  $396/8 = 49\frac{1}{2}$ , and the back pitch must be close to this figure. The number of slots per pole is  $132/8 = 16\frac{1}{2}$ , and the back pitch, if measured in slot pitches, also must be close to this figure. The back pitch is chosen as 16 slot pitches =  $16 \times 3 = 48$  commutator pitches. Fig. 3-13a shows the arrangement of the conductors in the slots. Since the back pitch is 16 slot pitches, upper conductor 1 is connected with a lower conductor lying in slot  $1 + 16 = 17$  and, since it is 48 commutator pitches, upper conductor 1 is connected with lower conductor

$1 + 48 = 49'$ . According to Eqs. 3-1 and 3-3, the front pitch is  $y_f = 47$ . Thus lower conductor  $49'$  must be connected with upper conductor  $49' - 47 = 2$ , and so forth. The sequence in which the conductors are connected is

$$1-49'-2-50'-3-51'-4-52'-5-53' \dots$$

The three turns  $1-49'$ ,  $2-50'$ , and  $3-51'$  lie in the same slots (1 and 17); they are insulated together and placed in the slots together. The same applies for the turns  $4-52'$ ,  $5-53'$ ,  $6-54'$ , and so forth.

**3-4. Operation of the commutator.** Fig 3-14 shows a 2-pole machine with 12 winding elements. It will be assumed that the flux is sinusoidally distributed over the armature. Then the emf's induced in the individual winding elements are sinusoidal functions of time (see Eq. 1-6b).

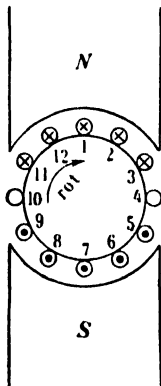


FIG. 3-14. Two-pole machine with 12 winding elements. One layer shown

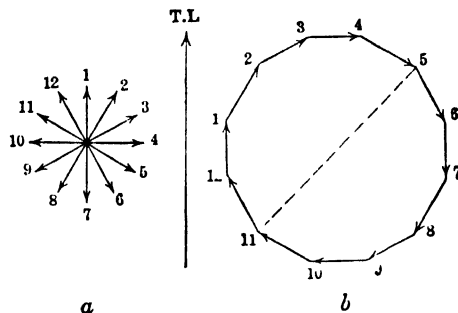


FIG. 3-15. Voltage star and voltage polygon for the 2-pole winding shown in Fig. 3-14.

Only the upper conductors are shown in Fig. 3-14. The lower conductors lie a pole pitch apart from their upper conductors. So, for example, the lower conductor of winding element 1 lies in the same slot as upper conductor 7; the lower conductor of winding element 2 lies in the same slot as upper conductor 8, and so forth. For the position of the conductors shown in Fig. 3-14, winding elements 1 and 7 produce maximum instantaneous emf, since their flux interlinkage is zero (see Fig. 1-5). On the other hand, winding elements 4 and 10 have zero induced emf, since their flux interlinkage is maximum: they are interlinked with the total pole-flux. Since the emf of each winding element is a sinusoidal function, its amplitude can be represented by a phasor (Art. 1-2). The phasors representing the amplitudes of the individual winding elements will be shifted with respect to each other corresponding to their position on the

armature. Thus, the phasors of all winding elements yield a voltage star, as shown in Fig. 3-15a. The time line (T.L.) is placed corresponding to Fig. 13-14, i.e., in such a position that the instantaneous value of the emf is maximum in winding elements 1 and 7.

If the phasors of Fig. 3-15a are arranged in succession in the same order in which they follow one another in the winding, the *voltage polygon* Fig. 3-15b is obtained.

If two arbitrary diametrically opposed points of the winding, for example, the connection points between winding elements 5 and 6, and 11 and 12, are joined to two slip rings *rotating with the winding*, and a voltage is taken from these slip rings by means of brushes, this voltage is a single-phase alternating voltage, the amplitude of which is equal to the length of the connecting line 5-11 in Fig. 3-15b, which in turn is the geometric sum of the individual voltages 12, 1, 2, 3, 4, and 5, or 6, 7, 8, 9, 10, and 11. This alternating voltage is a maximum when the armature winding is so located in the field that the line 5-11 is parallel to the time line, and is zero when the armature winding is so located that the line 5-11 is perpendicular to the time line.

The action is quite different if the voltage is taken from two points which are *at standstill* rather than from two winding points which rotate with the winding. Theoretically, two such points can be obtained, if, at one armature end, the insulation is removed from all conductors and two brushes are held against the bare conductor copper. The voltage between these two brushes will have a *constant value*, namely, that of the instantaneous values of the single-phase emf which corresponds to the position of the two brushes with respect to the time line. The brushes will pick up the amplitude of the single-phase emf, when they are parallel to the time line.

However, it is impractical to remove the insulation at one end of the armature. The practical solution consists in tapping the closed armature winding at all points at which the winding elements are connected to each other and connecting these tap points to bare bars insulated from each other, i.e., a commutator. Brushes resting on the commutator then accomplish the problem of picking up continuously a fixed instantaneous value of the a-c voltage generated in the winding.

The connection between the winding elements and the commutator bars is best shown on the older type of the closed armature winding, the ring winding, Fig. 3-16. In this winding, half of each turn lies inside of the armature iron so that each turn is linked with only *one-half* of the pole flux as compared with the total pole flux in the case of the previously considered 2-layer winding. For the same output the ring winding requires

about twice as much copper as the 2-layer winding and is much more difficult to manufacture.

Fig. 3-16 shows how the winding is tapped at the connection points between the winding elements and how these tap points are connected to the commutator bars.

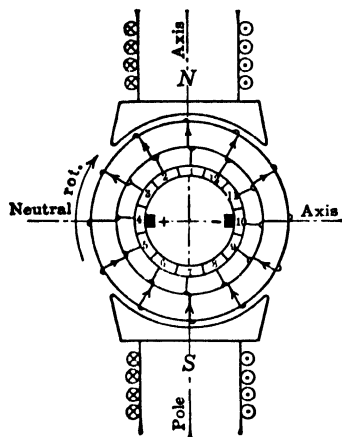


FIG. 3-16. Two-pole d-c machine with ring winding showing connection of winding elements to commutator.

It has been pointed out already (Art. 3-3) that in the 2-layer winding the brushes must lie in the pole axes. In this position they are connected to the conductors which lie in or close to center lines of the interpolar spaces (neutral axes), and pick up from the commutator the maximum value of the a-c voltage.

The voltage at the brushes is not absolutely constant. There is a slight variation in the voltage because the brush covers alternately one or two commutator bars (Fig. 3-7). This changes the form of the voltage polygon with respect to the brushes, as shown in Fig. 3-17. The voltage between the brushes is alternately equal to chord 3-10 or to diameter 4-10. The variation decreases

with an increase in the number of commutator bars (winding elements). With a large number of winding elements the voltage polygon approaches a circle and the variation is very small. Most practical machines closely approach this condition. This variation is commonly referred to as a commutator ripple.

**3-5. Equalizer connections. Conditions for symmetry.** A 2-pole winding is considered in Figs. 3-14 and 3-15. If the voltage polygon is drawn for a 4-pole *lap* winding, it is found that the polygon closes after passing through only two poles (two armature circuits) and that the total winding is represented by two identical polygons which coincide, if placed one above the other. On the other hand, a 4-pole *wave* winding yields only one voltage polygon. In general, there are as many voltage polygons as there are pairs of parallel circuits, i.e.,  $p/2$  polygons in the lap winding and only one polygon, independent of the number of poles, in the simple wave winding. The duplex-wave winding has two identical voltage polygons.

The points of the polygons which coincide when placed one above the other are *in-phase* points. In the case of the 4-pole lap winding, there is a

large number of pairs of in-phase points; in the 6-pole lap winding, there is a large number of triplets of in-phase points and so forth. The simple wave winding has no in-phase points.

If the field (pole) system is not symmetrical or if the armature bearings are eccentric, asymmetry between the pole-fluxes of the machine results. This asymmetry has no effect on the magnitude of the emf's induced in the individual circuits of a simple *wave* winding, because in this winding the winding elements of each parallel path are distributed under

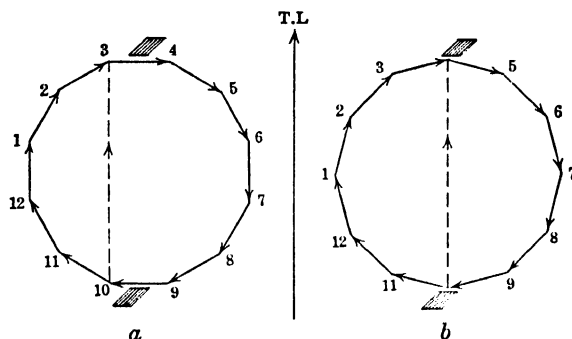


FIG. 3-17. Explanation of the voltage variation of a d-c machine.

*all* poles of the machine. The effect of flux asymmetry is quite different in lap windings. Here the winding elements which belong to an armature path lie only under *two adjacent* poles. Because of the flux asymmetry, the emf's of the individual paths are no longer equal, and the points of the winding which were in-phase points under conditions of complete symmetry are no longer in phase. Since some of these points are connected by brushes of the same polarity, circulating current will flow through the brushes. Sparking at the commutator can result easily in this case, if individual brushes are overloaded.

In order to rid the brushes of these circulating currents, some in-phase points of the winding, between which no voltage difference would exist under conditions of complete symmetry, are tied together by *equalizer* connections of negligible resistance. An alternating current then flows through the winding and equalizers, which leads to an improvement of the commutation but gives rise to additional heating losses.

It follows from the foregoing that equalizer connections should be applied to the multiple-pole lap windings and to the wave windings with more than two parallel circuits (duplex wave windings, triplex wave windings, etc.).

Direct-current armature windings must be symmetrical in order to give



good commutation. The conditions of symmetry for the lap as well as for the wave winding are: the number of slots as well as the number of winding elements (commutator bars) must be divisible by the number of

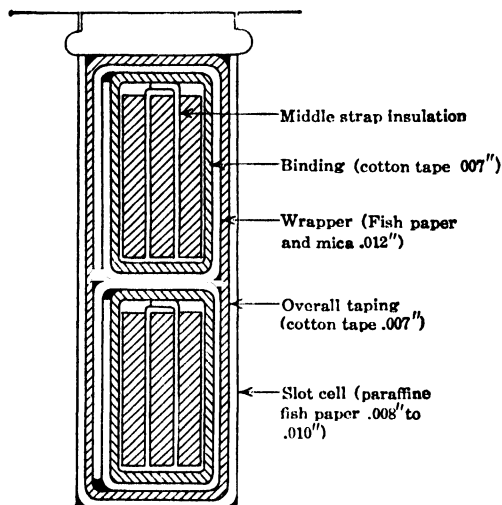


FIG. 3-18. Example of insulation of an armature winding with bare rectangular strap copper.

pairs of parallel circuits. Further, the number of poles must be divisible by the number of parallel circuits in the wave winding with more than two parallel circuits.

Fig. 3-18 shows an example of the insulation of a d-c armature winding.

**3-6. Emf induced in a d-c armature winding.** The emf induced in a d-c armature winding can be obtained either from Eq. 1-11

$$E = \frac{2\pi}{\sqrt{2}} N f \Phi 10^{-8} \text{ volt} \quad (3-5a)$$

for the effective value of the induced emf or from Eq. 1-3a

$$E_{\text{avg}} = 4\Phi \frac{p}{2} N \frac{n}{60} 10^{-8} \text{ volt} \quad (3-5b)$$

for the average value of the induced emf. In both equations  $N$  is the number of turns between two brushes of different polarity (number of turns per circuit). If

$Z$  = total number of conductors of the armature,

$a$  = number of parallel circuits,

then the total number of turns is  $Z/2$ , and the number of turns between two brushes of different polarity (number of turns per circuit) is  $Z/2a$ .

It is presumed in Eqs. 3-5a and 3-5b that the  $N$  turns are concentrated in such a manner that they are all interlinked with the same number of flux lines at any instant of time (see Art. 1-1). This is apparently not the case: the  $Z/2a$  turns of a circuit are shifted with respect to each other and the emf's induced in them are not in phase. Consider the voltage polygon, Figs. 3-15 and 3-17: the brushes pick up a voltage corresponding to the diameter of a circle, while the algebraic sum of the voltages of all winding elements between the brushes is equal to half the circumference of the circle. This means that, because of the shift of the  $Z/2a$  winding elements with respect to each other, the voltage between the two brushes is reduced in the ratio

$$\frac{\text{diameter}}{\text{half of the circle}} = \frac{2}{\pi}$$

and both Eqs. 3-5a and 3-5b must be multiplied by this factor.

Remembering that the brushes are placed in such a position that they pick up the amplitude of the induced a-c voltage, Eq. 3-5a must be multiplied by  $\sqrt{2}$  and Eq. 3-5b by  $\pi/2$ .

Replacing  $N$  by  $Z/2a$  and either multiplying Eq. 3-5a by  $2/\pi$  and  $\sqrt{2}$  or multiplying Eq. 3-5b by  $2/\pi$  and  $\pi/2$ , the emf between two brushes of different polarity of a d-c armature becomes

$$E = Z \frac{p}{a} \frac{n}{60} \Phi 10^{-8} \text{ volt} \quad (3-6)$$

This equation will be discussed once more in connection with the emf induced in an a-c winding (see Art. 22-1).

The derivation of Eq. 3-6 is based on the voltage polygon, Fig. 3-15; this means that sinusoidal flux distribution is assumed. However, this equation holds for any flux distribution, as can be seen from the following discussion which gives another derivation for the emf between brushes of different polarity of the d-c machine.

If  $Z$  is the total number of conductors (in both layers), then the number of conductors per layer per path is  $Z/2a$ . Since an armature path covers a pole pitch ( $\tau$ ), there are  $(Z/2a\tau)dx$  conductors per layer in the arc  $dx$  of the armature circumference. Applying Eq. 1-2a to the conductors lying in the arc  $dx$ , the induced emf is

$$e_x = B_z l v \times 10^{-8} \times \frac{Z}{2a\tau} dx$$

where  $B_x$  is the flux density at the element  $dx$ . The total emf induced in the path per layer is found by integrating  $e_x$  over the length of the path,  $\tau$ . Thus

$$E' = \frac{Zv}{2a\tau} 10^{-8} \int B_x l \, dx$$

The integral is the flux per pole  $\Phi$  (see Fig. 1-4 or 1-5 and also Art. 1-4), so that the emf induced in a path per layer is

$$E' = \frac{Zv}{2a\tau} \Phi \times 10^{-8}$$

If the winding is full-pitch, i.e., if the back pitch of the winding (width of the coil) is equal to the pole pitch, both conductors of a turn (which lie in different layers) lie in flux densities of the same magnitude and the emf's induced in them are equal at any instant of time (see Art. 1-1). Therefore, the total emf per path (for both layers) is  $2 \times E'$ . Introducing for  $v$

$$v = \frac{\pi Dn}{60} = \frac{p\tau n}{60}$$

the resultant emf between two brushes of different polarity is

$$E = Z \frac{p}{a} \frac{n}{60} \Phi 10^{-8} \text{ volt}$$

This is the same as Eq. 3-6. However, the first derivation, on the basis of Eq. 3-5a and the voltage polygon, is general and applies to d-c as well as a-c windings (see Art. 22-1), while the second derivation for  $E$  applies only to the voltage between two brushes of the d-c machine.

D-c armature windings usually are only slightly chorded or full-pitch. Since the pole-flux density is very small in the interpolar space, a little chording does not influence materially the value of  $E$  as given by Eq. 3-6.

**Example 3-4.** Determine the flux necessary to induce an emf of 240 volts in the armature of a 6-pole d-c generator with 72 slots, 6 conductors per slot, 1 turn per winding element.  $n = 1200$ , lap winding.

The total number of conductors is  $Z = 72 \times 6 = 432$ . For the lap winding  $a = p = 6$ . From Eq. 3-6

$$\Phi = \frac{240 \times 10^8}{432} \times \frac{60}{1200} \times \frac{6}{6} = 2.78 \times 10^6 \text{ maxwells}$$

**3-7. Torque produced by a d-c machine.** The electromagnetic torque produced by a d-c machine can be calculated from the basic law of force on a conductor in a magnetic field (Art. 1-4).

According to Eq. 1-28b, the force exerted on a single conductor is

$$f = 8.85 BlI \times 10^{-8} \text{ lb}$$

where  $B$  is in lines per square inch,  $l$  is in inches, and  $I$  is in amperes. In the d-c machine, the current per conductor, i.e., the total armature current  $I_a$  divided by the number of parallel paths  $a$ , has to be introduced for  $I$ . Further, the *effective conductor length*  $l_e$  has to be introduced for  $l$ . In medium-sized and larger machines the armature core is divided into several stacks by radial vents as explained in Chapter 2 (Fig. 2-5). The flux density in the vents is much smaller than that in the gap between poles and armature iron. However, the length of all vents is only 10 to 15% of the core length so that the effective conductor length is only somewhat smaller than the core length.

With the armature diameter  $D$  expressed in inches, the torque in pound-feet produced by a single conductor of a smooth armature is

$$f \times \frac{D}{2 \times 12} = \frac{D}{2 \times 12} \times 8.85 \times B_g l_e \frac{I_a}{a} 10^{-8} \text{ lb-ft} \quad (3-7)$$

where  $B_g$  is the flux density in the air gap around the armature.

The conductors lying under a pole of a fixed polarity all have currents of the same direction and their torques add. Also, all conductors lying under poles of different polarity add their torques (see Art. 1-4). Thus the total torque is obtained by multiplying the torque produced by a single conductor by the total number of conductors of the armature,  $Z$ .

However, it must be taken into account that  $B_g$  is not the same for all conductors. The flux density is small in the interpolar spaces as can be seen from Fig. 1-4 which represents the flux distribution of a d-c machine. If this distribution is replaced by a rectangle of equal area with the value of  $B_g$  under the middle of the pole as its height (Fig. 3-19), then the width of this rectangle is equal to  $b_e$  and the torque of the single conductor, Eq. 3-7, must be multiplied by  $(b_e/\tau)Z$  in order to obtain the total torque.

$B_g b_e$  is the area of the flux distribution curve and is, therefore, equal to

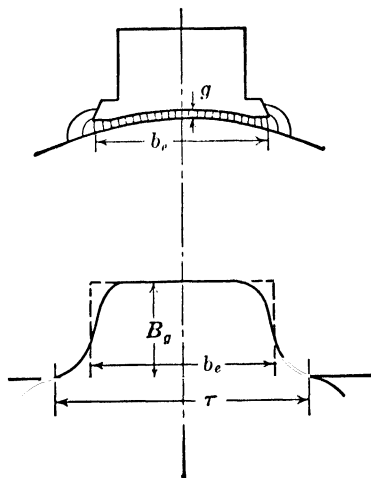


FIG. 3-19. Flux distribution curve of a d-c machine.

the flux per inch of armature length, if  $B_g$  is measured in lines per square inch and  $b_e$  is measured in inches (also see Art. 1-4).  $B_g b_e l_e$  is therefore the flux per pole  $\Phi$ ; i.e.,

$$\Phi = b_e l_e B_g \quad (3-8)$$

Multiplying Eq. 3-7 by  $(b_e/\tau)Z$  and introducing  $\Phi$  for  $B_g b_e l_e$  and  $p\tau$  for  $\pi D$ , the torque produced by a d-c machine becomes

$$T = 0.1174 \times 10^{-8} \frac{p}{a} Z \Phi I_a \text{ lb-ft} \quad (3-9)$$

The electromagnetic torque of the machine is proportional to its total flux ( $p\Phi$ ) and to its total ampere-conductors  $(I_a/a)Z$ . For a given machine  $0.1174 \times 10^{-8}(p/a)Z$  is a constant so that

$$T = C \Phi I_a \quad (3-10)$$

The foregoing derivation of the torque is based on the assumption that the conductors lie directly in the pole-flux (smooth armature). In the actual machine the conductors are placed in slots. The pole flux takes its path mainly through the teeth, and the flux density in the slots, where the conductors lie, is small. Despite this fact, Eq. 3-9 yields correct results for the torque. The proof is beyond the scope of this treatise.

Notice that the torque can be calculated also from the electromagnetic power. It follows from Eqs. 1-31 and 1-33

$$T = \frac{7.04}{n} E I_a \text{ lb-ft} \quad (3-11)$$

This equation also can be obtained from Eq. 3-9 by substituting for  $\Phi$  the value which follows from Eq. 3-6.

### PROBLEMS

1. A 250-kw, 6-pole, 240-volt, 1200-rpm d-c generator, the magnetic circuit of which is treated in Chapter 4, has 72 slots, a 2-layer winding with 6 conductors per slot, one turn per winding element, and  $a = p = 6$ . (a) Determine the number of commutator bars necessary. (b) How many commutator bars would be necessary if each winding element had two turns? (c) Are both windings symmetrical?

2. The flux per pole of the generator in Problem 1 is  $2.78 \times 10^6$  maxwells. Determine the emf induced between brushes for a lap winding with one turn and two turns per winding element.

3. If the generator considered in Problems 1 and 2 is redesigned as a simple wave winding, determine the induced emf at the same speed and pole flux? What will be the ratio of the armature currents for the same load for the simple lap and simple wave windings? Use one turn per winding element and same total number of turns.

4. Draw the developed winding diagram of a 2-layer lap winding for a 24-slot, 4-pole machine with four conductors per slot and one turn per winding element.

5. Draw the developed winding diagram of a 2-layer simple wave winding for a 37-slot 6-pole machine with four conductors per slot, one turn per winding element. Show the position of the brushes. Is the winding symmetrical? If each slot contained two conductors instead of four would the winding be symmetrical?

6. A 500-kw, 250-volt, 4-pole, 900-rpm shunt generator has a 2-layer lap winding with 90 slots and one turn per winding element. The flux per pole is  $\Phi = 4.65 \times 10^6$  maxwells. If the no-load voltage is 250 volts at 900 rpm, determine the number of conductors per slot that are necessary. How many commutator bars are used?

7. An 8-pole d-c generator with  $\Phi = 6 \times 10^6$  maxwells per pole has a 2-layer lap winding with one turn per winding element in 128 slots. If the no-load voltage is 220 volts, determine the speed of operation.

8. A 230-volt, 8-pole, 514-rpm shunt generator has 100 slots and  $\Phi = 3.36 \times 10^6$  maxwells. Each slot contains eight conductors and the winding is 2-layer with one turn per winding element. What type of winding is used and what are the pitches.

9. An 8-pole generator with a simplex 2-layer wave winding has 600 conductors. Each winding element has four turns and a resistance of 0.0025 ohm. What is the armature resistance?

10. A 4-pole generator has a lap-wound armature. Can the armature winding be changed to produce twice the emf at the same speed and pole flux? Explain.

11. A 220-volt, 4-pole, 900-rpm shunt generator has a 2-layer lap winding with 99 slots and two conductors per slot. The pole flux is  $\Phi = 3.7 \times 10^6$  maxwells. Determine the type of winding used to produce 220 volts at no-load, the number of commutator bars, and the front and back pitches.

12. If the current per conductor in Problem 11 is 50 amp, what is the current rating and power output of the machine assuming a full-load voltage drop of 3%?

13. A 4-pole shunt generator is to produce a no-load voltage of 220 volts at 1750 rpm. The armature has a 2-layer wave winding placed in 35 slots with 10 conductors per slot. Determine the flux per pole.

14. A d-c generator has the following data: effective armature length  $l_a = 6.26$  in., effective pole arc  $b_e = 8.1$  in., air gap flux density = 5300 lines per sq in., 8 poles, 72 slots, 6 conductors per slot and a 2-layer lap winding. Determine the torque developed for an armature current of 500 amp.

15. Determine the electromagnetic torque developed by the generator of Problem 14 for an armature current of 1000 amp and a pole-flux  $\Phi = 2 \times 10^6$  maxwells.

16. A 4-pole generator with a simplex wave winding operates at 250 rpm and delivers 250 amp at 550 volts. Assume an armature resistance drop of 3%. Determine the electromagnetic torque developed.

17. Determine the electromagnetic torque developed by a 6-pole d-c machine with 360 conductors arranged in a lap winding. The conductor current is 75 amp, and the flux per pole is  $3.0 \times 10^6$  maxwells.

## Chapter 4

### THE MAGNETIC CIRCUIT

**4-1. The magnetic circuit of the d-c machine.** Figs. 2-1 and 2-2 show a 2-pole and 6-pole machine, respectively, with their magnetic circuits. The magnetic flux of each pole has its path through the stator yoke, pole body, air gap between pole body and armature, armature teeth, armature core, then back through the armature teeth, air gap, and pole body to the stator yoke. The closed circuit passes twice through the air gap, teeth, and pole body. The pole-flux is divided into two parts in the stator yoke as well as in the armature.

The emf to be induced in the armature winding is known: it is approximately equal to the terminal voltage (see Art. 6-1). Then if the magnitude of the emf is known for a given machine, the flux is also known: it is determined by Eq. 3-6. A certain mmf is necessary to drive this flux through the machine structure. The magnitude of the necessary mmf, i.e., the ampere-turns to be placed on the poles, is determined by the basic law, Eq. 1-23; this is the circuital law of the magnetic field. If this law is applied in the form of Eqs. 1-26 and 1-27, it is seen that the sum

$$\Phi \sum \frac{l}{\mu A} = 0.4\pi NI \quad (4-1)$$

has to be extended over five terms for which the permeability  $\mu$ , the length of the magnetic path  $l$ , and the cross-section  $A$  are different. The flux density  $B$  is usually different for the stator yoke, pole body, armature teeth, and armature core; therefore  $\mu$  is also different for these parts of the magnetic circuit; for the air gap,  $\mu$  is equal to 1. Thus Eq. 4-1 can be written in the form

$$\Phi \left( \frac{l_y}{\mu_y A_y} + \frac{2l_p}{\mu_p A_p} + \frac{2g}{A_g} + \frac{2l_t}{\mu_t A_t} + \frac{l_c}{\mu_c A_c} \right) = 0.4\pi NI \quad (4-2)$$

where  $l_p$ ,  $g$ , and  $l_t$  are lengths of the path for 1 pole, 1 air gap, and 1

armature tooth. It follows from Eqs. 1-25 and 4-2

$$\frac{B_y}{0.4\pi\mu_y} l_y + 2 \frac{B_p}{0.4\pi\mu_p} l_p + 2 \frac{B_g}{0.4\pi} g + 2 \frac{B_t}{0.4\pi\mu_t} l_t + \frac{B_c}{0.4\pi\mu_c} l_c = NI \quad (4-3)$$

or

$$H_y l_y + 2H_p l_p + 2H_g g + 2H_t l_t + H_c l_c = NI \quad (4-4)$$

$H$  is the ampere-turns per unit length. Eq. 4-4 states that, in order to find the total ampere-turns  $NI$  necessary to force the flux through the structure, the ampere-turns of each of the five components are to be determined separately and then added up.

Eq. 4-2 to 4-4 describe how to determine the five ampere-turns components. First divide the flux  $\Phi$  by the five cross-sections, i.e., determine the five values of  $B$  to be used in Eq. 4-3. Then determine from the saturation curves of the iron used for the yoke, pole body, and armature, the values of  $H = B/0.4\pi\mu$  which correspond to the values of  $B$  given by Eq. 4-3. Finally, multiply the values of  $H$  found from the saturation curves by their path lengths  $l$  and add the five components. This yields the field (pole) mmf of one complete magnetic circuit. A 2-pole machine has only one magnetic circuit, and the  $NI$  ampere-turns are placed half on each pole. A multipole machine has  $p/2$  magnetic circuits, and the total number of necessary ampere-turns is  $p/2$  times the ampere-turns necessary for one circuit.

The term  $2(B_g/0.4\pi)g = 2H_g g$  which represents the ampere-turns necessary to drive the flux  $\Phi$  twice through the air gap is the largest of the five terms. Its magnitude is 70 to 85% of the total ampere-turns  $NI$ .

The flux  $\Phi$  in Eqs. 3-6 and 4-1 to 4-2 is the flux which is necessary to induce in the armature winding the emf  $E$  of Eq. 3-6, i.e., the flux which crosses the gap and goes through the teeth into the armature where it is *interlinked with the armature winding*. The flux which goes through the pole and stator yoke is larger than this flux  $\Phi$ , owing to leakage. Fig. 4-1 shows the flux distribution between two poles. It is seen that some of the lines of force go from pole tip to pole tip and from pole body to pole body without passing the gap and armature. These lines of force are not interlinked with the armature winding and do not contribute to the armature emf; they represent a *leakage flux*.

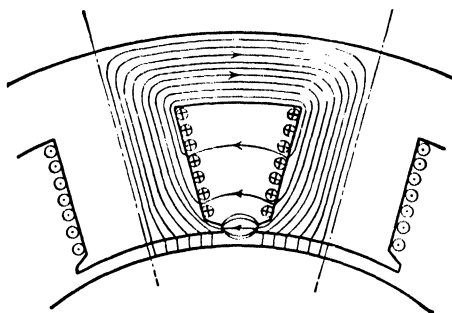


FIG. 4-1. Main flux and leakage flux.



The pole-leakage flux is not small: it can be as high as 15 to 25% of the useful flux  $\Phi$ . Therefore, it is not correct to assume the flux to be the same, namely, equal to  $\Phi$ , for all five parts of the magnetic circuit, as is done in Eqs. 4-1 to 4-3. The flux densities in the yoke and pole,  $B_y$  and  $B_p$ , should be calculated with  $(1.15 \text{ to } 1.25) \times \Phi$ . The calculation of the field ampere-turns  $NI$  will now be demonstrated by an example.

**Example 4-1.** As an example, a 250-kw, 6-pole, 240-volt, 1200-rpm generator will be considered. The dimensions of this generator, in inches, are listed below: (also see Fig. 4-2).

Outside diameter of armature core... $D = 22.5$	Pole length... $l_p = 7.0$
Inside diameter of armature core... $d_i = 12.5$	Pole width... 6.0
Gross core length... $L = 7.0$	Frame $ID$ ... $37\frac{1}{8}$
Number of radial vents... 2	Frame $OD$ ... $42\frac{7}{8}$
Width of each vent... $\frac{3}{4}$	Frame width... 10
Net length of core $l = 7 - 2 \times \frac{3}{8}$ ... 6.25	No. of arm. slots... 72
Single air gap... $g = 0.218$	Slot depth... 2.0
Pole embrace (arc)... $b_p = 7.65$	Slot width... 0.36

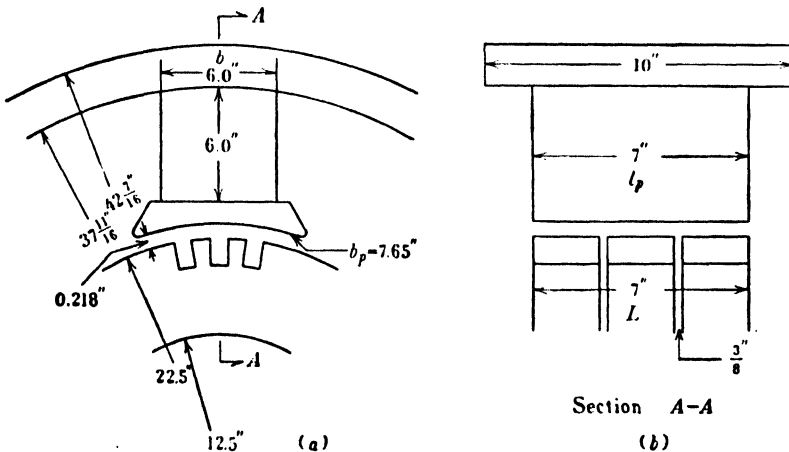


FIG. 4-2. Example — machine dimensions.

Electrical steel is used for the armature. USS hot-rolled steel is used for the poles and frame. The  $B$ - $H$  curves of these materials are given at the end of this text.

(a) *Flux per pole.* The armature has a lap winding and, therefore,  $a = p = 6$ . Each slot has six conductors, three per layer. The total number of conductors is, then,  $Z = 6 \times 72 = 432$ . According to Eq. 3-6, the flux necessary to induce an emf of 240 volts at no-load in the armature winding is

$$\Phi = \frac{240 \times 10^8}{432} \times \frac{60}{1200} \times \frac{6}{6} = 2.78 \times 10^6 \text{ maxwells}$$

(b) *Ampere-turns necessary to drive the pole flux twice through the gap.* Referring to Art. 3-7, the effective core length can be assumed equal to

$$l_e = \frac{L + l}{2} = \frac{7.0 + 6.25}{2} = 6.62 \text{ in.}$$

The effective pole arc  $b_e$ , Fig. 3-19, is larger than the pole arc  $b_p$  by approximately twice the air gap, i.e.,  $b_e = 7.65 + (2 \times 0.218) = 8.1$ . Thus, the cross-section of the gap is equal to  $6.62 \times 8.1$  sq in. From Eq. 3-8.

$$B_g = \frac{2.78 \times 10^6}{6.62 \times 8.1} = 51,800 \text{ lines per sq in.}$$

and the ampere-turns for two gaps (see Eq. 4-3):

$$AT_g = \frac{51,800}{0.4\pi \times (2.54)^2} \times 2 \times 0.218 \times 2.54 \times 1.10 = 7780 \text{ AT}$$

2.54 is the conversion factor from inches to centimeters. The last factor 1.10 takes into account the fact that the gap appears increased at the points opposite the slots, so that the effective air gap is larger than 0.218 in.

(c) *Ampere-turns for the teeth.* The pole flux  $\Phi$  goes into the armature through the teeth lying within the pole arc  $b_e = 8.1$  in. The pole pitch is

$$\tau = \frac{\pi D}{6} = \frac{\pi \times 22.5}{6} = 11.8 \text{ in.}$$

Thus the pole flux  $\Phi$  goes through  $\frac{72}{6} \times \frac{8.1}{11.8}$  teeth. The width of a tooth in the middle of the tooth is equal to 0.534 in. The iron length of the core is somewhat smaller than the net core length  $l = 6.25$  in., because of the insulation between the laminations. Assuming a loss due to insulation of 8%, the cross-section of the teeth per pole is

$$A_t = \frac{72}{6} \times \frac{8.1}{11.8} \times 0.534 \times 6.25 \times 0.92 = 25.3 \text{ sq in.}$$

and

$$B_t = \frac{\Phi}{A_t} = \frac{2.78 \times 10^6}{25.3} = 111,000 \text{ lines per sq in.}$$

The  $B$ - $H$  curve for electrical steel yields for  $B = 110,000$  lines per sq in. 180 AT per in. The length of the magnetic path in a tooth is equal to 2 in. (= slot depth). Thus the AT necessary to drive the flux through the teeth twice is

$$AT_t = 2 \times 2 \times 180 = 720 \text{ AT}$$

(d) *Ampere-turns for the armature core.* The height of the armature core below the teeth is equal to  $\frac{22.5 - 12.5}{2} - 2 = 3.0$  in. The iron length of the core is the same as that of the teeth, i.e.,  $6.25 \times 0.92$  in. The cross-section of the core is thus  $(3 \times 6.25 \times 0.92)$  sq in. Since the pole flux  $\Phi$  divides into two parts within the core

$$B_e = \frac{2.78 \times 10^6}{2 \times 3 \times 6.25 \times 0.92} = 80,600 \text{ lines per sq in.}$$

The  $B$ - $H$  curve for electrical steel yields, for  $B = 80,000$  lines, 10 AT per in. The length of the path in the core is equal to the pole pitch in the middle of the core, i.e., to

$$\frac{\pi(d_i + h_c)}{p} = \frac{\pi(12.5 + 3.0)}{6} = 8.1 \text{ in.}$$

Thus the ampere-turns necessary to drive the flux through the core are

$$\text{AT}_c = 10 \times 8.1 = 81 \text{ AT}$$

(e) *Ampere-turns for the poles.* It will be assumed that the leakage flux between the pole shoes and pole bodies is equal to 20% of the armature flux. Therefore, the flux through the pole and the yoke is

$$\Phi_p = 1.2 \times 2.78 \times 10^6 = 3.34 \times 10^6 \text{ maxwells}$$

The pole laminations are not insulated. The loss of iron thickness due to air layers between the laminations can be assumed 5%. The cross-section of a pole is, therefore, equal to  $(0.95 \times 7 \times 6)$  sq in. (see Fig. 4-2), and the flux density in the pole is

$$B_p = \frac{3.34 \times 10^6}{0.95 \times 7 \times 6} = 83,600 \text{ lines per sq in.}$$

The  $B$ - $H$  curve for USS hot-rolled steel yields, for  $B = 83,000$  lines, 18 AT per in. The length of the path in the pole is assumed equal to the height of the pole without pole shoe (the flux density is low in the pole shoe). This length is equal to 6.0 in., and thus the ampere-turns necessary for two poles are

$$\text{AT}_p = 2 \times 18 \times 6.0 = 216 \text{ AT}$$

(f) *Ampere-turns for the yoke (frame).* The height of the yoke is

$$\frac{(42\frac{7}{8} - 37\frac{1}{16})}{2} = 2\frac{3}{8} \text{ in.}$$

The yoke is of solid steel. Thus the flux density in the yoke is

$$B_y = \frac{3.34 \times 10^6}{2 \times 2.375 \times 10} = 70,000 \text{ lines per sq in.}$$

The  $B$ - $H$  curve for USS hot-rolled steel yields, for  $B = 70,000$  lines, 13.0 AT per in. The length of the magnetic path in the yoke is  $\frac{\pi(42\frac{7}{8} - 2\frac{3}{8})}{6} = 20.9$  in., and the ampere-turns necessary to drive the flux through the yoke are

$$\text{AT}_y = 13 \times 20.9 = 270 \text{ AT}$$

(g) *Total ampere-turns.* The ampere-turns for two poles (for one magnetic circuit) are

$$\begin{aligned} \text{AT}_{\text{cir}} &= \text{AT}_y + \text{AT}_p + \text{AT}_g + \text{AT}_t + \text{AT}_c \\ &= 270 + 216 + 7780 + 720 + 81 = 9067 \text{ AT} \end{aligned}$$

and for all six poles (all three magnetic circuits)

$$\text{AT}_{\text{total}} = 3 \times 9067 = 27,200 \text{ AT}$$

It does not matter whether these AT are produced by a large number of turns on the poles and a small current in the conductors or by a small number of turns and a large

current in the conductors. It is necessary, however, that the product of the number of turns and the current in the conductors is equal to the required number of ampere-turns. The machine considered has 1064 turns per pole. Therefore, the field current necessary to drive a flux  $\Phi = 2.78 \times 10^6$  maxwells through the armature is

$$I_f = \frac{9067}{2 \times 1064} = \frac{27,200}{6 \times 1064} = 4.25 \text{ amp}$$

**4-2. No-load characteristic.** If the field AT are calculated for several values of the armature flux  $\Phi$  and the flux  $\Phi$  is plotted against the field AT, a curve is obtained which is similar to the  $B$ - $H$  curve of iron. Fig. 4-3 shows such a curve which is called the *no-load characteristic*. The emf induced in the armature  $E$  or the flux density in the air gap  $B_g$  can be plotted along the axis of ordinates instead of  $\Phi$ , since both these quantities are proportional to  $\Phi$  for a given machine (see Eqs. 3-6 and 3-8). Along the axis of abscissae, either the total field AT, or the field AT per circuit, or the field AT per pole (half of the AT of a circuit), or only the field current  $I_f$  can be plotted, since all of these quantities are proportional to each other for a given machine.

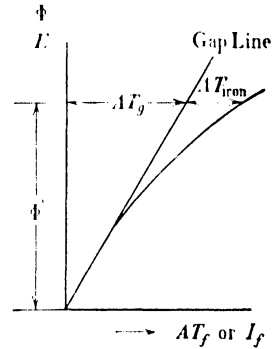


FIG. 4-3. No-load characteristic and air-gap line.

The lower part of the no-load characteristic, Fig. 4-3, follows a straight line. This is due to the fact that, at small values of  $\Phi$ , the AT necessary for the four iron parts of the magnetic circuit are negligible in comparison to those necessary for the air gap. As the flux  $\Phi$  becomes larger, the iron AT increase and the no-load characteristic bends to the right of the *air-gap line*. In Fig. 4-3, the AT necessary for the air gap and the AT necessary for the iron are indicated for a fixed value  $\Phi'$  of the flux.

It has been assumed in the considerations of this article and also of Art. 4-1 that the armature conductors do not carry current, i.e., that the armature is not loaded (this explains the name “no-load characteristic”). If the armature is loaded, not one but two mmf's exist in the machine, namely, the field mmf and the armature mmf. The influence of the armature currents upon the field (the armature reaction) will be discussed in the next article.

**4-3. Armature reaction.** Fig. 4-4 shows the flux distribution of the machine when only the field poles are excited and there is no current in the armature (the leakage fluxes between the poles are omitted). Fig. 4-5

shows the flux distribution for the case when only the armature carries current and the field poles are not excited. As has been explained in Art. 3-3, the physical position of the brushes is in the pole axes. In this position the brushes are connected to the conductors lying in the interpolar spaces, as is indicated in Fig. 4-5. It is seen from this figure that the armature flux is a *cross flux* with respect to the field flux, i.e., it is shifted  $90^\circ$  with respect to the field flux.

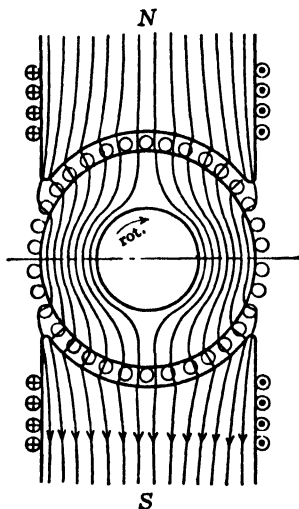


FIG. 4-4. Flux distribution when only the main poles are excited.

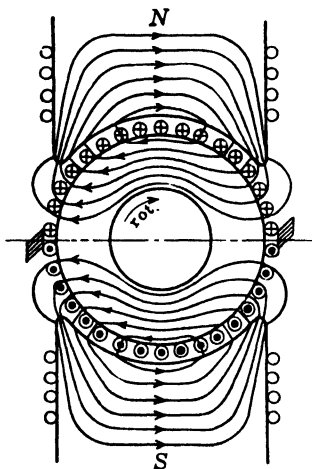


FIG. 4-5. Flux distribution when only the armature carries current.

Fig. 4-6 shows the flux distribution for the case when both windings carry current. It is obtained through superposition of Figs. 4-4 and 4-5. Fig. 4-6 shows *two effects of armature reaction*. The first effect is that the flux is weakened in one half of the pole and strengthened in the other half. When iron is saturated in a certain direction by a given mmf, the increase in flux produced by an additional mmf is less than the decrease of flux when the same additional mmf is applied in the opposite direction. Therefore, the first effect of armature reaction results in a *reduction* of the field flux. If a generator delivers rated voltage at no-load, the voltage will drop when the armature is loaded, and an increase of field current is therefore necessary to sustain the no-load voltage.

The second effect of armature reaction is the *distortion* of the flux in the pole and in the gap. The air-gap flux density under one pole half is greater than that under the other pole half. As a result of this non-

uniform distribution the instantaneous emf induced in the winding elements, while they are in the field of greatest density, may become high enough to cause a spark to take place between the commutator bars in which the winding elements terminate, and may ultimately lead to ring fire (flash-over). For this reason, in large machines and heavy-duty machines, as for example steel-mill rolling motors which are subject to sudden heavy loads and require rapid reversal of rotation, a special winding called a *compensating winding* is used to suppress the armature flux. This winding is placed in the pole shoes, as

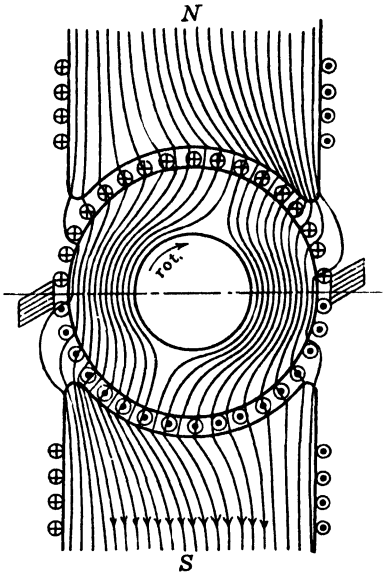


FIG. 4-6. Flux distribution under load.

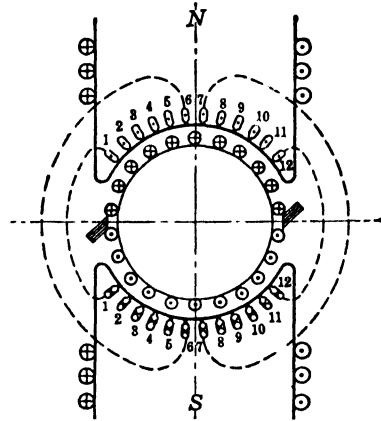


FIG. 4-7. Schematic diagram of a compensating winding in a 2-pole d-c machine.

shown schematically for a 2-pole machine in Fig. 4-7. The back connections are made as follows: top conductor 1 with bottom conductor 1, top conductor 2 with bottom conductor 2, etc. The front connections are: bottom conductor 1 with top conductor 2, bottom conductor 2 with top conductor 3, etc. When so connected the compensating winding produces a cross mmf just as the armature winding. If the armature winding and the compensating winding are now connected in series in such a manner that their mmf's oppose each other, no armature cross-flux will exist in the machine.

Considering Fig. 4-5, the armature behaves magnetically like a solenoid with turns of varying area, the areas being the smallest in the interpolar spaces and the largest in the pole axis. The axis of this solenoid coincides with the brush axis.

In Figs. 4-5 and 4-6, the brushes are placed in a line which is shifted  $90^\circ$  with respect to the pole axis. This is the *neutral axis* of the machine. If the brushes are shifted from the neutral axis, as shown in Fig. 4-8, the armature reaction becomes different from that explained above.

Corresponding to Faraday's law all conductors lying under a pole, N-pole or S-pole, have emf's induced in the *same* direction. If the brushes lie in the neutral axis, the same rule applies also to the currents; thus,

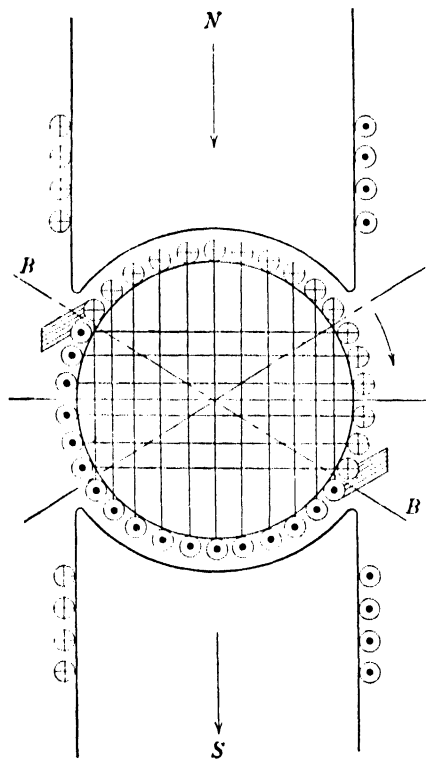


FIG. 4-8. Armature reaction with brushes shifted from the neutral axis.

considering Fig. 4-6, all conductors above (or below) the neutral axis have currents in the same direction. If the brushes are now shifted from the neutral axis, as shown in Fig. 4-8, the rule dictated by Faraday's law for the emf's no longer holds for the currents. This is due to the fact that the brushes determine, and are the connection points between, the parallel circuits. Since the current direction is the same for all conductors of each of the parallel circuits, all conductors lying above (or below) the brush axis (*BB* in Fig. 4-8) must have currents in the same direction, i.e., it is the *brush axis* which determines the direction of the currents in the conductors. Comparing Fig. 4-8 with 4-6, it is seen that, because of the brush shift, some conductors carry a current the direction of which is opposite to the direction of their induced emf.

It is seen from Fig. 4-8 that when the brushes are shifted from the neutral axis the armature again behaves magnetically like a solenoid with turns of varying area, the axis of which coincides with the brush axis. It is a *general rule for all commutator machines that the axis of the armature mmf and flux is determined by the position of the brushes on the commutator.*

In order to study the armature reaction for the case when the brushes are shifted from the neutral axis, Fig. 4-8, it is best to resolve the armature solenoid, the axis of which lies in the brush axis, into two solenoids,

the axes of which coincide with the neutral axis and the pole axis respectively. In Fig. 4-8 the first of the two solenoids is represented by the conductors lying directly under the poles and the second solenoid is represented by the conductors lying in the interpolar spaces. The first solenoid, the axis of which coincides with the neutral axis, produces a cross mmf and *cross flux* with all the consequences mentioned for the case when the brushes lie in the neutral axis, Fig. 4-6. The second solenoid, the axis of which coincides with the pole axis, magnetizes in the same axis as the field coils. In Fig. 4-8 this solenoid opposes the field mmf. Fig. 4-8 refers to a generator and the brushes are moved in the direction of rotation of the armature. In general, if the brushes of a generator are moved *in the direction of rotation, its flux is weakened*; if the brushes are moved opposite to rotation, the flux is strengthened. It will be shown later that in a motor the induced emf and armature current have opposite directions. This means that, for a motor running in the same direction as the generator in Fig. 4-8, all currents will have reversed direction. Therefore, a brush shift in the direction of rotation strengthens the flux in a motor and a brush shift opposite to rotation weakens its flux.

It should be noted that, with respect to commutation, the brushes usually lie in or are close to the neutral axis (see Art. 8-3).

### PROBLEMS

Data and machine dimensions are listed below for several d-c machines. Using Fig. 4-2 and Example 4-1 determine the no-load ampere-turns required at 85% and 100% of rated voltage.

<i>Problem No.</i>	1	2	3	4
Machine. . . . .	Generator	Generator	Generator	Motor
Rating. . . . .	7.5 kw	300 kw	250 kw	1 HP
Volts. . . . .	250	230	275	230
Amperes. . . . .	30	1305	909	4.3
Number of poles. . . . .	4	8	6	2
Speed (rpm). . . . .	1750	514	1200	1750
Outside diameter of armature core ( $D$ ). . . . .	7.50"	38"	22.5"	4.75"
Inside diameter of armature core ( $d_i$ ). . . . .	3.10"	26"	12.5"	1.20"
Gross core length ( $L$ ). . . . .	5"	8"	7"	3"
Number of radial vents. . . . .	0	2	2	0
Width of vents. . . . .		3"	3"	
Net core length. . . . .	5"	7.25"	6.25"	3"
Air gap (single) ( $g$ ). . . . .	0.078"	0.28"	0.125"	0.04"
Pole embrace (arc) ( $b_p$ ). . . . .	4.20"	9.75"	7.70"	4.63"
Pole length ( $l_p$ ). . . . .	5"	7.50"	7"	2.585"



<i>Problem No.</i>	<b>1</b>	<b>2</b>	<b>3</b>	<b>4</b>
Pole width.....	2.25"	8.0"	6"	2.25"
Frame inside diameter (ID)...	14"	59"	37 $\frac{11}{16}$ "	8.0"
Frame outside diameter (OD)	15.75"	64.75"	42 $\frac{7}{8}$ "	9.375"
Frame width.....	8"	13"	10"	4.5"
Number of armature slots....	31	100	75	20
Slot depth.....	0.920"	1.93"	1.97"	0.855"
Slot width (in middle of tooth)	0.318"	0.45"	0.343"	0.30"
Winding.....	wave	lap	lap	wave
Number of circuits ( <i>a</i> ).....	2	8	6	2
Conductors per slot.....	18	8	6	70
Effective air gap (equals air gap times factor).....	1.23	1.1	1.15	1.18
Leakage flux between pole shoes and pole bodies in percent of armature flux.	18%	20%	20%	15%
Height of pole (without pole shoe).....	2.8"	9.6"	7.1"	1.3"
Loss of iron length:				
(a) due to insulation between armature laminations.....	4%	8%	8%	4%
(b) due to air layers in pole.	5%	5%	5%	5%

## Chapter 5

### METHODS OF EXCITATION

**5-1. Methods of excitation.** A d-c motor gets its field current for excitation as well as the armature current from an external source of power. A d-c generator can also be excited from an external source of power: this is the separately excited generator. However, a d-c generator is also able to produce its own excitation, i.e., it is capable of *self-excitation*. This ability is due to the d-c armature and the *residual* magnetism which remains in the field poles after the machine has been once separately excited. It will be shown that under certain conditions the emf induced in the armature winding by the residual magnetism produces a current in such a direction that this residual magnetism is *strengthened*; this increases the armature emf as well as the field current, and the growth of both quantities continues until a voltage is reached whose magnitude depends upon the saturation of the iron of the machine and, for the excitation listed below under (b), also upon the resistance of the field winding (see Art. 6-5).

Thus, the d-c generator may be separately as well as *self-excited*. According to the manner of connection of the field winding with respect to the armature winding, three separate cases of self-excitation are available:

- (a) *Series excitation.*
- (b) *Shunt excitation.*
- (c) *Compound excitation.*

(a) *Series excitation.* For series excitation the field winding and armature winding are connected in series as shown in Fig. 5-1. If the residual magnetism is such that the top pole is a north pole (N) and the bottom

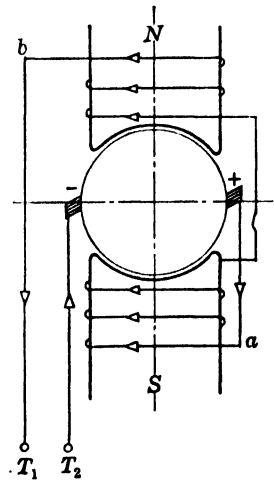


FIG. 5-1. D-c machine with series excitation.

pole a south pole (S), the field winding must be connected in series with the armature so that the field current produces a north pole at the top and a south pole at the bottom. Fig. 5-1 shows the connection of both windings as well as the direction of the current in the field winding.  $T_1$  and  $T_2$  are the terminals of the machine which are connected to the external circuit.

If the field winding is connected in reverse so that end  $b$  of the field winding rather than end  $a$  is connected to the positive pole of the armature, the magnetism will not build up and no voltage will be obtained. An interchange of the terminals of the field winding reverses the field current, provided the residual magnetism has not been completely destroyed, and the machine builds up voltage. If the machine does not build up, a separate source of current must then be employed to restore the residual magnetism. *Self-excitation can result only when the field current aids the residual magnetism.*

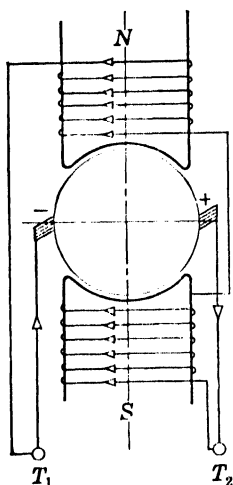


FIG. 5-2. D-c machine with shunt excitation.

(b) *Shunt excitation.* For shunt excitation the field winding is placed in parallel with the armature winding as shown in Fig. 5-2. While the resistance of a series field is made small, in order to prevent a large voltage drop across it, the resistance of the field winding used for shunt excitation is high. Fig. 5-2 shows that the armature furnishes not only the load current but the field current also.

If the resistance of the field were low, it would take a high current and this would load the armature. Normally the field current of shunt-wound machines is 1 to 5% of the armature current, with the higher values applying to small machines.

To produce the field flux a definite value of mmf is necessary. It does not matter whether this mmf is produced by the large current and small number of turns of the series winding or by the low current and correspondingly large number of turns of the shunt winding.

(c) *Compound excitation.* In the case of compound excitation the machine has both a series and a shunt field winding. The greater part of the excitation mmf is usually furnished by the shunt field winding. The series winding serves to make the field flux dependent, within narrow limits, on the load current. The series winding may be connected variously to the armature winding so that it either produces an mmf of the same direction as that of the shunt winding (*cumulative compound connection*)

or an mmf opposite to that of the shunt winding (*differential compound connection*). It will be shown later, Art. 6-6, that the cumulative compound-wound generator, in contrast to the shunt-wound generator, offers the possibility of compensating for the voltage drop in the armature.

The three methods of excitation of a d-c generator as just described are used also in d-c motors. It will be shown in Art. 7-4 that the compound-wound motor, in contrast to the shunt-wound motor, offers the possibility of maintaining the same speed at no-load and rated load.

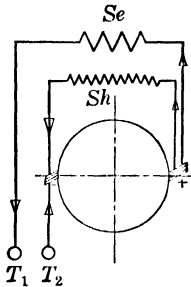


FIG. 5-3a. D-c machine with compound excitation, short-shunt connection.

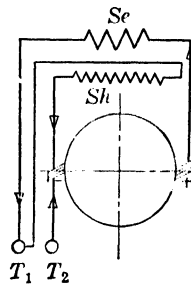


FIG. 5-3b. D-c machine with compound excitation, long-shunt connection.

In the cumulative compound-wound machine the shunt field winding may be connected either directly across the armature terminals (*short-shunt connection*) or across the terminals  $T_1$  and  $T_2$  which connect to the external circuit or the line (*long-shunt connection*). The first case is shown schematically in Fig. 5-3a and the second in Fig. 5-3b.  $Sh$  is the shunt field winding and  $Se$  the series field winding.

The *polarity* of the self-excited d-c generator depends upon its residual magnetism. It has just been shown that the self-excited d-c generator can build up its voltage only when the field winding is connected to the armature winding in such a manner that the field current assists the residual magnetism. An incorrect connection between the field and armature windings will tend to demagnetize the machine and will not build up its voltage. The same demagnetizing effect and resulting failure to build up occur in a machine which has been operating with self-excitation, if the direction of rotation of the armature is reversed, because a reversal of the direction of rotation changes the polarity of the armature.

In order that a self-excited generator may build up its voltage, the manner of connection of the field winding relative to the armature winding and the direction of rotation of the armature must fulfill very definite conditions. If one of these factors is changed in a correctly running

machine, the machine will tend to demagnetize itself. If both factors are changed, the machine builds up its voltage as before.

**5-2. Direction of rotation of a shunt and series machine as generator and motor.** If a generator is to deliver a certain power output, it must receive this power plus its losses from the prime mover. The prime mover must overcome the electromagnetic torque produced by the armature conductors which are rotating in the magnetic field of the generator (see Art. 1-4). The prime mover torque and the armature torque plus the loss torque are always in opposite direction and in equilibrium under all steady load conditions.

Fig. 5-4 shows one pole of the generator previously drawn in Fig. 4-6. The direction of rotation of the armature is clockwise. The prime mover torque  $T_{pm}$  also must be clockwise. The armature torque  $T_{arm}$  is counter-

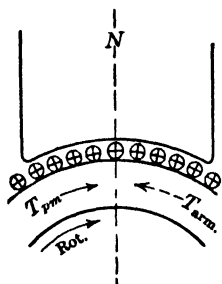


FIG. 5-4. Balance of torques in a generator.

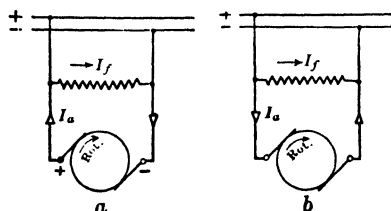


FIG. 5-5. Direction of rotation of a shunt machine as generator and motor.

clockwise and is shown by the dotted arrow. If the prime mover torque is removed and the direction of the field and armature currents is assumed to remain unchanged, the armature will rotate in a direction opposite to that of the prime mover and will produce a motor torque. Therefore, *for the same direction of the field and the armature currents, the direction of rotation of the machine as a motor is opposite to the direction of rotation as a generator.*

Since the direction of the armature torque changes when the direction of either the field or the armature current is changed, it is a simple matter to determine the direction of rotation of the shunt or series machine when operating as a generator and as a motor.

It is assumed for the shunt-wound machine of Fig. 5-5a that, for the direction of rotation shown, it operates as a generator and produces the polarity given in the figure, which must correspond to the polarity of the bus-bars. For this condition of operation, the directions of armature and

field currents are as shown in the figure. If the machine is operated as a motor with the same connection to the line, the armature current reverses while the field current is in the same direction, as shown in Fig. 5-5b. If the field current and armature current maintain their same directions, the direction of rotation of the machine as a motor is opposite to the rotation as a generator. However, since the direction of the armature current reverses when operating as a motor, while the field current remains the same, the direction of rotation as a motor is the same as that as a generator. Consequently the shunt machine will operate in the same direction either as a motor or as a generator, without changing its connections.

Figure 5-6a shows the direction of the current in the armature and field of a series-connected machine when operated as a generator. If the series machine is operated as a motor (Fig. 5-6b), the current is reversed in both the armature and the field winding; therefore, the series machine when operated as a motor without changing the connections rotates in a direction opposite to that as a generator.

If a shunt machine operating as a motor loses the opposing torque of its load, it may be made to operate as a generator in the same direction by supplying it with mechanical power and adjusting the field current so that the induced emf is greater than the line voltage (see Art. 6-7). In the series motor, in order to operate in the same direction as a generator, either the armature current or field current must be reversed in direction.

It follows from the foregoing that the direction of either the armature current or field current must be reversed, in order to reverse the direction of rotation of a motor. Interchanging the connections to the bus-bars will not reverse the direction of rotation, since this reverses the direction of the current in both windings.

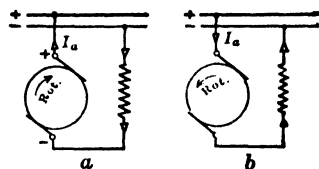


FIG. 5-6. Direction of rotation of a series machine as generator and motor.

## Chapter 6

### THE D-C GENERATOR

**6-1. The voltage equation of the d-c generator.** The emf induced in the armature winding according to Eq. 3-6 does not appear in its full amount at the terminals of the generator. This is due to the fact that, under load, there are voltage drops in the various resistances.

The armature current  $I_a$  flowing in the armature winding produces a voltage drop  $I_a r_a$ . If the machine is series wound or compound wound, the series winding which is connected in series with the armature produces a voltage drop  $I_s r_s$ . It will be shown later, Art. 8-3, that d-c machines have a special winding, the *interpole* winding, for the purpose of improving the commutation. Also, this winding is connected in series with the armature and produces a voltage drop  $I_i r_i$ . If there is a compensating winding, (see Art. 4-3), this winding will also be connected in series with the armature and will produce a voltage drop  $I_c r_c$ . Furthermore, there is a voltage drop in the contact resistance between the brushes and commutator. The voltage drop between all the brushes of each polarity and commutator will be denoted by  $\Delta V$ . Thus, the total voltage drop is

$$I_a r_a + I_s r_s + I_i r_i + I_c r_c + 2\Delta V = \sum I r + 2\Delta V \quad (6-1)$$

Applying Kirchhoff's law to the armature circuit,

$$E = V + (\sum I r + 2\Delta V) \quad (6-2a)$$

where  $V$  is the terminal voltage of the armature = voltage drop of the load. Thus the terminal voltage

$$V = E - (\sum I r + 2\Delta V) \quad (6-2b)$$

The magnitude of the induced emf is given by Eq. 3-6

$$E = Z \frac{p}{a} \frac{n}{60} \Phi 10^{-8} = C \Phi \quad (6-3)$$

where  $C$  is a constant quantity for a given machine running with constant speed  $n$  rpm.

In a shunt generator, the field winding is connected parallel to the armature winding (and load). The armature current ( $I_a$ ) of a shunt generator is, therefore, several percent larger than its load current ( $I_L$ ), i.e.,

$$I_L = I_a - I_f \quad (6-4)$$

The same applies to the compound generator.

**6-2. Characteristic curves of the d-c generator; regulation.** The following characteristic curves of a d-c generator will be considered.

- (a) *No-load characteristic*,  $E = f(I_f)$ ;  $n = \text{constant}$
- (b) *Load characteristic*,  $V = f(I_f)$ ;  $I_a$  and  $n = \text{constant}$
- (c) *External characteristic*,  $V = f(I_L)$ ;  $n = \text{constant}$
- (d) *Regulation curve*,  $I_f = f(I_a)$ ;  $V$  and  $n = \text{constant}$

The no-load characteristic has been treated in Art. 4-2. Its shape depends upon the dimensions of the different parts of the magnetic circuit and the materials used. The shape of all other characteristic curves depends upon the shape of the no-load characteristic and the load.

The influence of the load appears as:

- (a) *Armature reaction* (see Art. 4-3).
- (b) *Voltage drops in the armature, series, interpole, and compensating windings and under the brushes* ( $\sum Ir + 2\Delta V$ , Eq. 6-1).

The voltage drop at the contact surface of the brush ( $\Delta V$ ) depends upon the brush material. For the usual carbon brush it can be assumed equal to one volt for the brushes of each polarity, i.e., to 2 volts for the total machine.

For a generator, besides the characteristic curves, the *voltage regulation* is of importance; that is, the change in voltage from no-load to full-load expressed as a percentage of the full-load voltage. The regulation is a measure of the closeness with which the machine regulates for constant voltage. The regulation is closely related to the external characteristic of the machine and will be determined in connection with the treatment of this characteristic.

The characteristic curves of the different types of generators will be considered in the articles which follow.

**6-3. The separately excited generator.** (a) *The no-load characteristic.* The emf induced in the armature is given by Eq. 6-3.

$$E = C\Phi$$

Since the armature carries no current, the flux  $\Phi$  depends upon only the



field mmf, or, since the number of field turns is constant for a given machine, upon the field current  $I_f$ , i.e.,

$$E = Cf(I_f) \quad (6-5)$$

This is the no-load characteristic; it shows the terminal voltage at no-load,  $V = E_0$ , as a function of the field current and is obtained by using the connections shown in Fig. 6-1a;  $A$  is the armature,  $FW$  the field winding, and  $B$  the source which supplies the field current. The resistance  $R_f$  is used to vary the field current.

In Fig. 6-1b, which shows the no-load characteristic, curve  $a$  shows the voltage  $E_0$  as a function of  $I_f$ , when the field current is increased from zero to  $I_{fm}$ ; curve  $b$  shows the voltage  $E_0$  as a function of  $I_f$  when the exciting current is reduced from the  $I_{fm}$  value to zero. Because of the effect of the

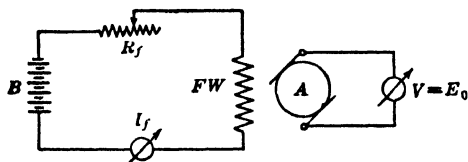


FIG. 6-1a. Connection diagram for the determination of the no-load characteristic of a separately excited generator by test.

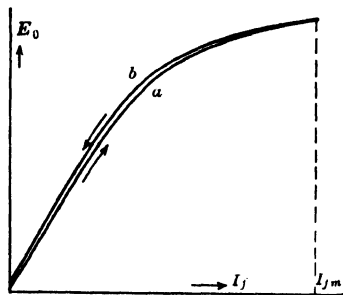


FIG. 6-1b. No-load characteristic of a separately excited generator.

residual magnetism, the two curves do not coincide. The residual magnetism also accounts for the plot of curve  $a$  starting above the zero point for zero field current.

(b) *The load characteristic.* If the armature is loaded, the emf induced in the armature winding is less than that induced at no-load ( $E_0$ , Fig. 6-1b) because of the armature reaction. The terminal voltage  $V$  is smaller than the emf under load by the voltage drops in the windings and under the brushes ( $\sum Ir + 2\Delta V$ ). The curve of terminal voltage as a function of field current for constant speed and constant armature current is known as the *load characteristic*. Fig. 6-2a shows the connections used for taking the load characteristic. The load current is adjusted to the constant value by means of the resistance  $R_L$ .

Curve III in Fig. 6-2b is a load characteristic. Curve I is the no-load characteristic of the same machine. If the quantity  $AB = (\sum Ir + 2\Delta V)$  is added to the load characteristic curve, curve II thus obtained is the

emf induced in the armature winding by the resultant flux. The distance between curve II and the no-load characteristic I is the voltage drop produced by armature reaction. In order to maintain the terminal voltage  $CH$  at both no-load and load,  $CD$  is required as the increase in the field current to compensate for the effect of armature reaction and the voltage drops. The load characteristic (Curve III, Fig. 6-2b) drops more and more below the no-load characteristic as the load current increases.

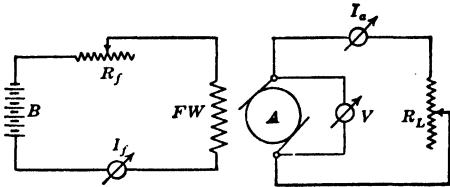


FIG. 6-2a. Connection diagram for the determination of the load characteristic of a separately excited generator by test.

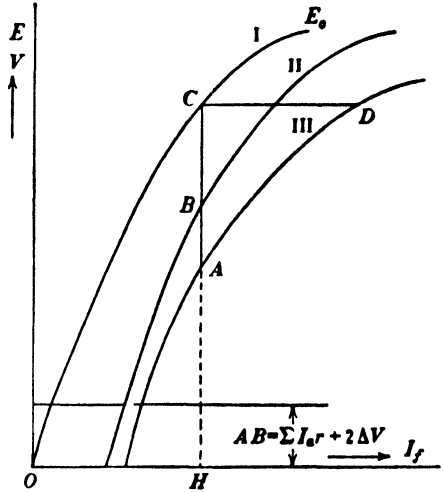


FIG. 6-2b. Load characteristic of a separately excited generator.

(c) *The external characteristic.* The curve showing the terminal voltage as a function of the load current at constant speed and field current,  $V = f(I_L) = f(I_a)$ , is called the *external characteristic* (Curve III, Fig. 6-3). With increasing load current the armature reaction and the resistance drops,  $\sum I_a r$ , increase. Consequently the terminal voltage  $V$  drops with increasing load current.

If the voltage drop  $AB = (\sum I_a r + 2\Delta V)$  is added to the external characteristic, the value of the emf  $E$  induced in the armature winding by the resultant flux is obtained (Curve II).  $BC$ , the difference between the straight-line Curve I which represents the no-load voltage  $E_0$  and Curve II, is the voltage drop caused by the armature reaction. With the aid of the external characteristic the voltage

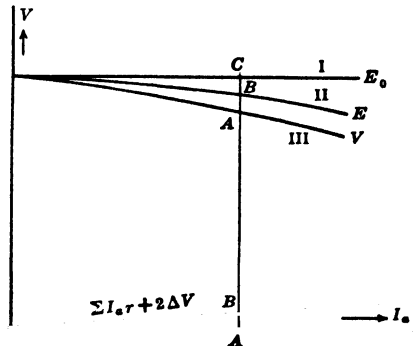


FIG. 6-3. External characteristic of a separately excited generator.

regulation  $\epsilon$  of the machine can be determined

$$\epsilon = \frac{E_0 - AA}{AA} \times 100\%$$

where  $AA$  is the value of terminal voltage at rated load. The connections used to obtain the external characteristic are the same as those used for the load characteristic, Fig. 6-2a.

(d) *The regulation curve.* If the terminal voltage is to remain constant with increasing load current, the field current must be increased; the extent of the increase of the field current depends upon the magnitude of the armature reaction and resistance drops. The regulation curve  $I_f = f(I_L) = f(I_a)$  shows the exciting current as a function of the load current for constant terminal voltage and speed, Fig. 6-4.

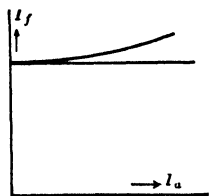


FIG. 6-4. Regulation curve of a separately excited generator.

**6-4. The series generator.** (a) *The no-load characteristic.* For this machine the no-load characteristic can only be taken with separate excitation, because self-excitation would require the armature to carry current, and a no-load characteristic implies no armature current whatever.

(b) *The load characteristic.* The load characteristic of the series generator also must be taken with separate excitation, for with self-excitation the armature and field current would change at the same time. The no-load and load characteristics of the series generator are

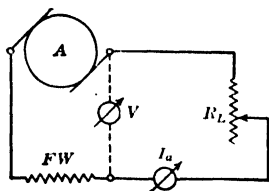


FIG. 6-5a. Connection diagram for the determination of the external characteristic of a series generator by test.

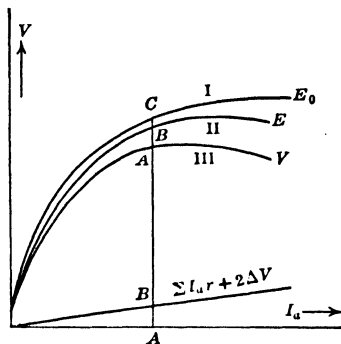


FIG. 6-5b. External characteristic of a series generator.

consequently identical with the no-load and load characteristics of the separately excited generator.

(c) *The external characteristic.* The characteristic features which distinguish the series generator from other types of d-c generators are shown by its external characteristic. Fig. 6-5a shows the connections used to obtain the external characteristic. The load current is varied by means of the load resistance  $R_L$ . Since the armature current is used to excite the field, the field mmf and consequently the induced emf in the armature winding and the terminal voltage  $V$  increase with increasing load current. Curve III of Fig. 6-5b is the external characteristic of a series generator. Curve I is the no-load characteristic of the machine. If the voltage drop  $AB = (\sum I_a r + 2\Delta V)$  is added to Curve III, the Curve II thus obtained is the emf induced in the armature winding by the resultant flux. The difference  $BC$  between Curve II and the no-load characteristic, Curve I, is consequently the voltage drop caused by armature reaction.

**6-5. The shunt generator.** (a) *The no-load characteristic.* Fig. 6-6 shows the connections for obtaining the no-load characteristic of the shunt generator.  $FW$  is the shunt field winding. The field current is varied by

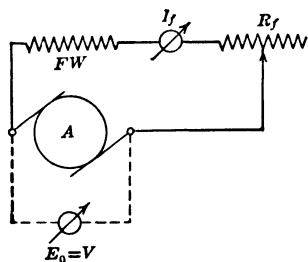


FIG. 6-6. Connection diagram for the determination of the no-load characteristic of a shunt generator by test.

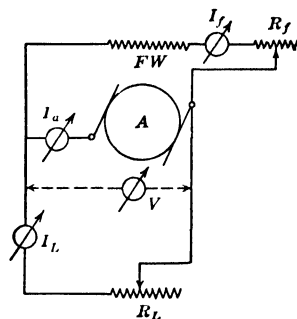


FIG. 6-7. Connection diagram for the determination of the external characteristic of a shunt generator by test.

means of the shunt field rheostat  $R_f$ . In taking the no-load characteristic the armature supplies the field current. Since this current is only a very small percentage of the armature current under load, the voltage drop which it causes in the resistance of the armature winding and under the brushes, as well as the armature reaction, is very small. Consequently the no-load characteristic for self-excitation coincides with that obtained for separate excitation.

(b) *The load characteristic.* The load characteristic of the shunt generator is also almost coincident with that of the separately excited

generator. The trend of the load characteristic curve, therefore, is the same as that of the separately excited generator.

(c) *The external characteristic.* This characteristic is taken with a constant resistance  $R_f$  in the shunt field circuit and at a constant speed, Fig. 6-7. The load current is varied by means of the rheostat  $R_L$  in the external load circuit. Curve III of Fig. 6-8 shows the external

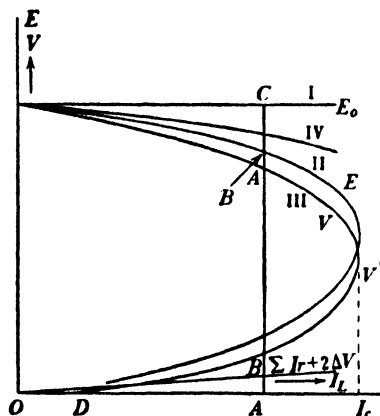


FIG. 6-8. External characteristic of a shunt generator.

characteristic of a shunt generator. The external characteristic of the same generator with separate excitation is illustrated by Curve IV.

With self-excitation, the external characteristic is lower than that obtained with separate excitation, because in the former case the field current decreases with decreasing terminal voltage. Here the shunt field resistance  $R_f$  is constant, whereas, in the case of separate excitation, the field current remains constant. At a definite value of load current, called the critical value  $I_c$ , the external characteristic taken with self-excitation turns back. Up to

the point  $V'$  the load current increased as the external resistance  $R_L$  was decreased. Below this point  $V'$  the current decreases with decreasing values of the resistance  $R_L$ . At short circuit ( $R_L = 0$ ) the terminal voltage is zero and the armature current is  $I_a = OD$ ; this value of current is determined by the residual magnetism of the machine, because when  $V = 0$ , the field current is also zero.

If the voltage drop  $AB = (\sum I_a r + 2\Delta V)$  is added to the external characteristic, Curve II is obtained. The difference  $BC$  between this curve and the straight line I which represents the no-load voltage  $E_0$  of the machine is the voltage drop due to armature reaction and the decrease in the field current.

The regulation is

$$\epsilon = \frac{E_0 - AA}{AA} \times 100\%$$

The external characteristic of the shunt generator is not a single-value curve: for a given value of current  $I_L$  there are two different values of terminal voltage.

If a sudden short circuit ( $R_L = 0$ ) is applied to a shunt generator, the

armature current rapidly falls to the value  $OD$  which is comparatively small. On the other hand, if a short circuit is applied to a series generator, the armature current increases because the field current increases. In comparison with the series generator the shunt generator has the advantage in case of a sudden short circuit in that it does not feed into the short circuit. On the contrary, it rapidly reduces the initial short-circuit current. However, the very high value of the short-circuit current which appears at the instant the short circuit is applied is often sufficient to damage the winding of the shunt generator.

In the shunt generator, the field circuit is connected in parallel with the armature circuit and, therefore, the *terminal voltage is the same* for both circuits under all load conditions. Consider Fig. 6-9.  $OAB$  is the no-load characteristic of the generator. The field current  $OP$  corresponds to the no-load voltage  $PA$  at the armature brushes and also at the terminals of the field circuit. If  $r_f$  is the resistance of the field winding, the total resistance of the field circuit is

$$R_f + r_f = R_{ft} = \frac{AP}{OP}$$

$R_{ft}$  is proportional to  $\tan \alpha$ , Fig. 6-9. If this resistance remains constant, the terminal voltage of the machine for different load currents must always lie on the line  $OL$ . This line is the *field resistance line*. It follows from Fig. 6-9 that the voltage to which the machine builds up at no-load depends on the magnitude of total field resistance. The larger this resistance, the larger  $\tan \alpha$  and the smaller the no-load voltage. For a certain value of the total field resistance the field-resistance line runs tangent to the lower part of the no-load characteristic (coincides with the gap line) and the voltage of the machine is indeterminate. If the total field resistance is made larger than this value, the machine is unable to build up its voltage.

(d) *The regulation curve.* The regulation curve showing the field current as a function of the armature current for constant terminal voltage is the same as that of the separately excited generator, because the voltage drop produced in the armature by the field current is very small and, in

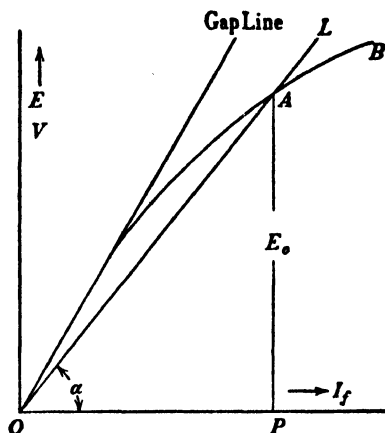


FIG. 6-9. The field resistance line of a shunt generator.

comparison with the voltage drops caused by the load current, can be neglected.

**6-6. The cumulative compound generator.** (a) *The no-load characteristic.* This characteristic of the cumulative compound generator is the same as that of the shunt generator, for at no-load the series winding is not effective.

(b) *The external characteristic.* The characteristic features of the cumulative compound generator can be seen in its external characteristic,

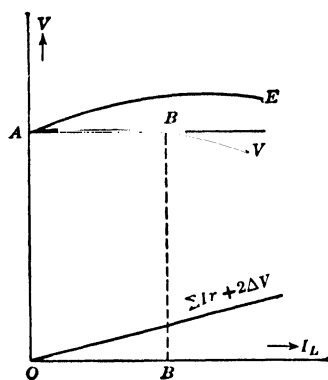


FIG. 6-10. External characteristic of a cumulative compound generator.

Fig. 6-10. The resistance drops in the windings and under the brushes ( $\Sigma Ir + 2\Delta V$ ), as well as the armature reaction, act to decrease the terminal voltage with increasing load current. However, the mmf of the series winding and the flux increase with increasing load current and compensate in part or entirely for the resistance drops as well as the armature reaction. In Fig. 6-10 the mmf of the series winding predominates between A and B, and consequently the terminal voltage is greater than the no-load voltage OA. For load currents greater than OB, the resistance drops and armature reaction predominate and the terminal voltage is less than

that at no-load, OA. Between A and B the generator is *overcompounded*, at B it is *flat-compounded*, and for greater currents it is *undercompounded*.

By a suitable adjustment of the mmf of the series winding it is possible to obtain an external characteristic in which the terminal voltage at rated load is equal to that at no-load (regulation  $\epsilon = 0$ ), or greater than that at no-load (regulation  $\epsilon = \text{negative value}$ ).

**Example 6-1.** For sample calculations the 250-kw, 6-pole, 240-volt, 1200-rpm generator will be considered, the magnetic circuit of which is calculated in Art. 4-1. This machine is designed to operate as a *cumulative compound generator* without a compensating winding.

The resistances of the windings (in ohms at 75° C) are:

Armature.....	0.00366
Interpole.....	0.00163
Series field.....	0.0022
Shunt field.....	47.9 (1064 turns per pole)

The demagnetizing mmf of the armature is 3200 AT per magnetic circuit at rated load (= 1042 amp). The no-load characteristic of the machine as obtained by test at 1200 rpm is shown in Fig. 6-11.

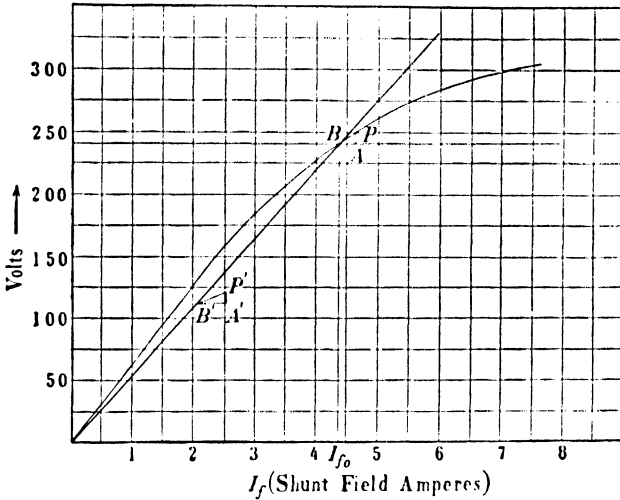


FIG. 6-11. Example 6-1 — No-load characteristic and resistance line.

*Determine:* the field current at no-load, the terminal voltage at rated load current of 1042 amp, and the voltage regulation.

a. The machine first will be treated as a separately excited machine without a series field. Then, for  $E = V = 240$  volts at no-load, from Fig. 6-11,  $I_{f0} = 4.38$  amp and the exciting voltage must be  $47.9 \times 4.38 = 210$  volts.

The voltage drops are  $1042 (0.00366 + 0.00163) + 2 = 7.5$  volts. The demagnetizing armature AT expressed in field amperes are

$$AT_d = \frac{3200}{2 \times 1064} = 1.5 \text{ amp}$$

The resultant mmf, expressed in field amperes, is then  $4.38 - 1.5 = 2.88$  amp which corresponds to an emf of 178 volts. Subtracting the voltage drops ( $\Sigma Ir + 2\Delta V$ ) = 7.5 volts, the terminal voltage is  $V = 178 - 7.5 = 170.5$  volts and the voltage regulation is

$$\epsilon = \frac{240 - 170.5}{170.5} \times 100 = 40.8\%$$

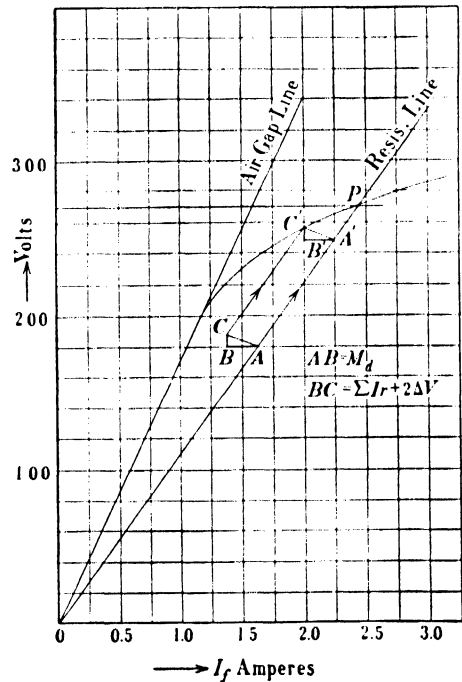


FIG. 6-11a. Example 6-2.

The large voltage regulation obtained for operation as a separately excited machine indicates that this generator is not able to supply 1042 amp as a shunt generator at



240 volts, because in the shunt generator the field current decreases with decreasing terminal voltage.

b. Considering the machine as a cumulative compound generator, the field resistance line must be taken into account since, in the shunt and compound generators, armature and field winding must have the same terminal voltage. The no-load field current is  $I_{f0} = 4.38$  amp, as before, and the armature reaction, in field amperes, is  $AT_d = 1.5$  amp. First, the number of series turns per pole will be determined which is necessary to make the voltage regulation zero (generator flat-compounded at rated load). Since the terminal voltage must be 240 volts at rated load, the total field resistance must be  $240/4.38 = 54.8$  ohms and an external resistance  $R = 54.8 - 47.9 = 6.9$  ohms is necessary. The field resistance line intersects the no-load characteristic at 240 volts (Fig. 6-11).

In order to sustain the no-load voltage of 240 volts at rated load, the series field winding must overcome the armature reaction  $AT_d$  and then supply an additional mmf so that the induced emf is  $E = 240 + (\sum Ir + 2\Delta V)$ . The voltage drops are

$$(0.00366 + 0.00163 + 0.0022) 1042 + 2 = 10 \text{ volts}$$

Thus the induced emf must be 250 volts. Point  $P$  in Fig. 6-11 corresponds to  $E = 250$ , and  $AB$  is therefore the additional mmf of the series field winding necessary to overcome the voltage drops. It is equal to 0.27 field amp. The total mmf of the series field must be  $0.27 + 1.5 = 1.77$  field amp, or  $1.77 \times 1064 = 1885$  AT per pole. Since the current flowing through the series field winding is 1042 amp, the series field winding must have  $1885/1042 = 1.81$  turns per pole. The machine actually was built with two series turns per pole and is somewhat overcompounded. With two turns per pole, the total mmf of the series field per pole is  $2 \times 1042 = 2084$  AT = 1.96 field amp. There remains, after overcoming the armature reaction,  $1.96 - 1.5 = 0.46$  field amp. If a triangle  $P'A'B'$  is constructed (Fig. 6-11) so that  $P'A' = (\sum Ir + 2\Delta V) = 10$  volts and  $B'A' = 0.46$  amp,  $P'A'$  being parallel to the axis of ordinates and  $B'A'$  being parallel to the axis of abscissae, and if this triangle is moved parallel to itself along the field resistance line until  $P'$  hits the no-load characteristic,  $B'$  on the resistance line will yield the terminal voltage  $V$ . This voltage is 246 volts and the voltage regulation is

$$\epsilon = \frac{240 - 246}{246} \times 100 = -2.46\%$$

**Example 6-2.** A 100-kw, 4-pole, 1750-rpm, 250-volt shunt generator has the no-load characteristic shown in Fig. 6-11a and the following data: 1700 turns per pole, field winding resistance at  $75^\circ \text{C} = 80.5$  ohms, armature resistance at  $75^\circ \text{C} = 0.00916$  ohm, interpole winding resistance at  $75^\circ \text{C} = 0.00193$  ohm. The demagnetizing mmf of the armature per pole at full-load is equal to 400 AT. Determine the regulation at full-load.

The rated current is  $100,000/250 = 400$  amp. Therefore, neglecting field current

$$\sum Ir + 2\Delta V = 400(0.00916 + 0.00193) + 2 = 6.43 \text{ volts}$$

The demagnetizing  $AT = 400$  corresponds to a field current of  $400/1700 = 0.235$  amp =  $M_d$ .

Assume that the field rheostat has been adjusted to yield a no-load voltage of 270 volts. Then the resistance line must go through point  $P = 270$  on the no-load characteristic for which  $I_f = 2.42$ . The total resistance of the field circuit must be  $270/2.42 = 116.8$  ohms, i.e., an external resistance of  $116.8 - 80.5 = 36.3$  ohms is necessary.

In order to find the terminal voltage at full-load for the selected field resistance, draw the triangle  $ABC$  with  $AB = M_d = 0.235$  amp and  $BC = \sum Ir + 2\Delta V = 6.43$  volts, as shown in Fig. 6-11a, and move this triangle along the resistance line, parallel to itself, until the point  $C$  hits the no-load characteristic (point  $C'$ ). The full-load terminal voltage is then 248.5 volts, and the regulation is

$$\epsilon = \frac{270 - 248.5}{248.5} \times 100 = 8.6\%$$

The construction shown above is based upon the fact that in the shunt generator the terminal voltage of the armature must be equal to the terminal voltage of the field circuit. For *constant resistance of the field circuit*, the latter terminal voltage is given by the resistance line and therefore the armature terminal voltage must lie on this line for any load. On the other hand, the induced emf must be larger than the terminal voltage by  $(\sum Ir + 2\Delta V)$ . Both conditions are satisfied by the triangle  $C'B'A'$ . The mmf at no-load is given by point  $P$ . The resultant mmf at full-load is given by  $B'$ . The decrease in mmf  $PB'$  is due to the demagnetizing armature mmf  $M_d = AB$  and to the decrease of  $I_f$  caused by the voltage drop  $PB'$  (measured vertically).

**6-7. Parallel connection and parallel operation of d-c generators.** Most of the d-c generators employed are shunt-wound or cumulative compound-wound machines.

If a shunt-wound or compound-wound generator is to be connected in parallel with other generators, it is first necessary to adjust the field current so that its terminal voltage is the same as that of the other generators. The armature is then connected to the bus-bars in such a manner that its positive terminal is connected to the positive bus-bar and its negative terminal to the negative bus-bar. The voltage of the incoming generator and the generators already on the bus-bars are then in opposition and equal, so that no current flows in the circuit between the machines when connected in this manner and the incoming machine delivers no current to the bus-bars.

If the field current of the incoming generator is now increased so that its induced emf is greater than its terminal voltage (which, of necessity, must be equal to the line voltage), the armature delivers a current of such magnitude that the sum of the terminal voltage and the voltage drops in the windings and under the brushes is equal to the emf induced by the resultant flux, Eq. 6-2, and the system is in equilibrium. As the field current of the generator is increased, the current output of its armature is also increased.

*By a variation of the excitation of generators operating in parallel, it is possible to divide the load between the machines in any manner desired.*

Parallel operation of cumulative compound generators is not possible without a special connection. Suppose in the case of cumulative com-

pound generators operating in parallel that the shunt field excitation of one machine is increased somewhat. In order to restore voltage equilibrium in the armature of this machine, its current must increase. However, if the armature current increases, the effect of the series field winding increases and further disturbs the voltage equilibrium, and the armature current must in turn increase still more. In this manner very slight variations

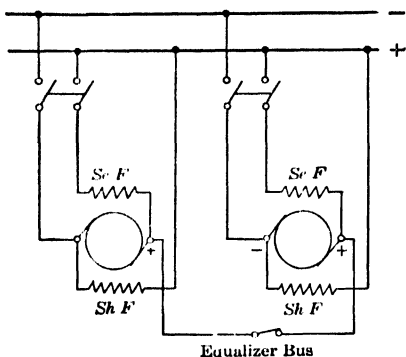


FIG. 6-12. Parallel operation of cumulative compound generators — equalizer bus.

in the shunt field circuit produce great variations in the load distribution.

In order to stabilize the operation of cumulative compound generators operating in parallel, the series field windings of the machines are connected by means of an *equalizer bus* as shown in Fig. 6-12 for two generators. Since the beginnings as well as the ends of the series field windings are connected with each other (the first by the equalizer bus and the latter by the main bus), the voltage drop across the series field windings

of all generators is the same. Therefore, the line current delivered by all generators operating in parallel divides itself among the individual series field windings so that their currents are inversely proportional to their resistances; if the generators are identical, the current is divided equally among the series field windings.

If the armature current of any generator now is increased or decreased, by changing its shunt field excitation, the current in all the series field windings and the armature current of all other generators also will be increased or decreased, since the voltage drop across the series field windings correspondingly increases or decreases. The equalizer bus thus enables all generators operating in parallel to take part in any change in the load on the bus-bars.

When a cumulative compound generator has to be paralleled with other cumulative compound generators, the equalizer switch, Fig. 6-12, has to be closed first or simultaneously with the armature switch.

It is not necessary that generators connected in parallel have the same ratings. It is only essential that the total load be divided among all the generators in proportion to their ratings. This is achieved by proper adjustment of the field currents.

If shunt generators are operating in parallel and a sudden increment of load is placed on the bus-bars, most of the added load will be taken by

the generator which has the lowest voltage drop: since the terminal voltage of all generators, in consequence of the added load, must decrease by the same amount, the generator with the least winding resistance produces this drop with the greatest current. In the case of cumulative compound generators operating in parallel, the equalizer bus serves to divide the increment of load uniformly among the individual generators.

**6-8. Applications of the different types of generators.** (a) *Separately excited generator and shunt generator.* The external characteristic of the separately excited as well as that of the shunt generator, Figs. 6-3 and 6-8, shows that both machines have an inherent tendency to regulate for constant voltage. The regulation, i.e., the voltage drop between no-load and full-load, is small in both types of generators. Since the separately excited generator needs a separate source for excitation whereas the shunt generator is self-excited, the separately excited generator is used mainly in laboratory and commercial testing and in special regulation sets (see Fig. 7-12). The shunt generator is suitable for constant voltage circuits where the load is close to the generator and the voltage drop in the line resistance is not large. For example, a shunt generator may be used as an exciter for the field circuit of a generator, for charging batteries, for supplying current to heating devices, etc.

(b) *Cumulative compound generator.* The cumulative compound generator is the most widely used d-c generator. Its external characteristic usually can be adjusted so as to compensate for the voltage drop in the line resistance. The cumulative compound generator is used for motor drives which require a d-c supply at constant voltage, for supplying current to incandescent lamps, for heavy power service such as electric railways, etc.

(c) *The differential compound generator.* This type of generator has an external characteristic similar to that of a shunt generator with a large demagnetizing armature reaction. It is used in arc welding where a larger voltage drop is desirable when the current increases, in connection with electrically operated shovels where the motor may stall, etc.

(d) *Series generator.* The external characteristic of the series generator (Fig. 6-5b) shows that its voltage increases with increasing load. This makes the series generator suitable only for special purposes; it is used as a voltage booster in certain types of distribution systems, particularly in railway service.

## PROBLEMS

1. The total resistance of the armature circuit in Example 6-1 is 0.00749 ohm at 75°C. Determine the generated voltage at full-load current and the terminal voltage (neglect the shunt field current).

2. Determine the kw generated by the armature winding in Problem 1.

3. Determine the electromagnetic torque developed by the machine in Problem 1 at full-load.

4. Assuming the sum of iron, friction, and windage losses is 3.5 kw, what is the full-load efficiency of the machine in Problem 1.

5. A belt-driven shunt generator is rated at 50 kw, 230 volts. The machine operates at 500 rpm and has an armature resistance of 0.05 ohm. If the pulley at the generator is 20 in., determine the belt pull in pounds.

6. Determine the lb-ft torque required to drive a 500-kw generator which has an efficiency of 92% and operates at 250 rpm.

7. A shunt generator operating at 1750 rpm generates 230 volts at no-load. A 15% reduction in the speed produced a 30% reduction in the no-load voltage. Determine the percent change in the pole flux.

8. If the machine in Example 6-1 is operated at 1500 rpm as a shunt generator, determine the maximum no-load voltage  $R_f = 0$ .

9. Determine the no-load voltage of the machine in Example 6-1 operating as a shunt generator at 1000 rpm.

10. If the machine of Example 6-1 is operating separately excited at 1200 rpm and produces a no-load voltage of 250 volts, determine the terminal voltage for an armature current of 500 amp. Assume the demagnetizing AT of armature reaction to be proportional to the current.

11. Determine the no-load voltage of the machine in Example 6-1 operating as a shunt generator at 1500 rpm with a 12-ohm rheostat in series with the field.

12. The machine in Example 6-1 is operated separately excited at 1200 rpm. Determine (a) the field current required to produce 220 volts at no-load; (b) the field current required to produce 220 volts at full-load current.

13. The following data apply to a d-c generator: 6 poles, 750 rpm, 600 volts, 942 amp, 565 kw, shunt field winding resistance 25.2 ohms at 75°C, interpole plus compensating field winding resistance 0.00602 ohm, armature resistance 0.01083 ohm. The armature has a 2-layer lap winding, 1 turn per element, 87 slots, 8 conductors per slot, 14-slot coil throw. The shunt field has 924 turns per coil, interpole field  $7\frac{1}{2}$  turns per coil, compensating 5 turns per pole pair. The no-load characteristic data are:

$E$ :	210	300	400	500	600	700	750	800
$I_f$ :	1.6	2.42	3.55	4.9	7.2	11.5	14.5	18.0

Assuming that the armature reaction is zero, determine: (a) resistance in field rheostat for shunt excitation at rated load, 600 volts, 942 amp, (b) the no-load voltage for this rheostat setting, (c) the percent voltage regulation.

14. Repeat Problem 13 for speeds of 600 and 900 rpm.

15. For the generator in Problem 13 determine the terminal voltage when delivering an armature current of 1000 amp.

16. Repeat Problem 15 for the generator operating at 900 rpm and delivering 1000 amp.

17. The machine of Problem 13 has an effective armature length  $l_e = 10.9$  in. and an effective pole arc  $b_e = 9.7$  in. Determine the air-gap flux density in lines per square inch.

18. An 8-pole, 500-rpm, separately excited generator has an armature winding with a total of 400 conductors each rated to carry 10 amp and each required to generate 5 volts at no load. If the no-load terminal voltage of the machine is 250 volts and the armature current 80 amp, determine (a) the type of winding; (b) pole-flux; (c) the electromagnetic torque developed.

19. A compensated cumulative compound generator has 900 shunt turns and 15 series turns per pole, a full-load armature current of 72 amp, a no-load voltage of 300, and the total resistance of the armature, series field, interpole winding, and compensating winding is 0.194 ohm. The data for the no-load characteristic are:

$E$ :	192	256	298	338	365	383	398	410	421	430
$I_f$ :	1	1.5	2	3	4	5	6	7	8	9

taken at 1150 rpm. Determine: (a) resistance of the shunt field circuit, (b) shunt ampere-turns per pole at no-load, (c) series ampere-turns per pole at full-load, (d) terminal voltage at full-load, (e) shunt field current at full-load, (f) total field ampere-turns per pole at full-load. Assume complete compensation-armature reaction zero.

20. If the machine of Problem 19 generates a no-load voltage of 300 volts at 950 rpm, determine the field circuit resistance and the terminal voltage at full-load.

21. The series field is removed from the machine in Problem 19 and it is operated as a shunt generator at 1150 rpm with a no-load voltage of 300 volts. If the series field resistance is 0.015 ohm, determine the full-load terminal voltage.

22. A cumulative compound generator operates at no-load with a shunt field current of 1.8 amp; 100 amp through the series field produce rated voltage at the terminals, under load. To maintain the rated voltage with the series field current of 100 amp reversed requires a shunt field current of 2.2 amp. If there are 1500 shunt field turns per pole, determine the number of series turns per pole.

23. A 250-kw and a 750-kw, 550-volt shunt generator operate in parallel, delivering a total load of 1500 amp. The voltage regulation of the smaller machine is 6%, of the larger one 3.5%. Assume the external characteristic curves are straight lines. Determine: (a) the current delivered by each machine, (b) the terminal voltage. Assume each machine delivering rated output when bus load is 1000 kw at 550 volts.

24. Two shunt generators, A and B, having straight-line external characteristics, are operated in parallel, and each has a no-load voltage of 240 volts. The machines are paralleled at no-load. A is rated 500 kw at 230 volts; B is rated 250 kw at 220 volts. For a total load of 600 kw, determine: (a) terminal voltage, (b) kw of each machine, (c) current of each machine.

# Chapter 7

## THE D-C MOTOR

**7-1. Voltage equation of the d-c motor.** In the generator, induced emf  $E$ , terminal voltage  $V$ , and armature current  $I_a$  are all in phase. In a motor induced emf  $E$  and armature current  $I_a$  and, therefore, also induced emf  $E$  and terminal voltage  $V$  are in counter-phase. This will be explained by means of Figs. 7-1 and 7-2.

Fig. 7-1 refers to a generator. The armature is driven in a clockwise direction. For balance of torques, the electromagnetic torque produced

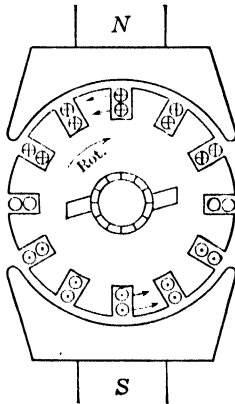


FIG. 7-1. Direction of current and induced emf in a generator.

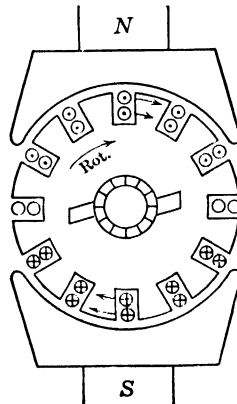


FIG. 7-2. Direction of current and induced emf in a motor.

by the armature must have a counterclockwise direction. This can be accomplished only by currents which have the directions shown in Fig. 7-1, i.e., by currents which flow into the plane of the page under the N-pole and come out of the plane under the S-pole. According to Faraday's law (see Fig. 1-2), the emf's induced in the armature conductors have

the same directions. Thus, in a generator, induced emf  $E$  and armature current  $I_a$  are in phase.

Fig. 7-2 refers to a motor for which it is assumed that the armature rotates in a clockwise direction. Since the electromagnetic torque determines the direction of rotation of the armature of a motor, this torque must be in a clockwise direction. This can be accomplished only by currents which have the directions shown in Fig. 7-2, i.e., by currents which come out of the plane of the page under the N-pole and flow into the plane under the S-pole. The direction of rotation of the armature in Figs. 7-1 and 7-2 is the same and, therefore, the direction of the induced emf's must be the same, namely, that of the currents in Fig. 7-1 which is opposite to the direction of the currents in Fig. 7-2. Thus, in a motor, induced emf  $E$  and armature current  $I_a$  are in counter-phase; the same is true of the induced emf  $E$  and terminal voltage  $V$ .

Thus applying Kirchhoff's law to the motor

$$V - E = (\sum Ir + 2\Delta V) \quad (7-1a)$$

or

$$V = E + (\sum Ir + 2\Delta V) \quad (7-1b)$$

The difference of the signs of  $V$  and  $E$  in Eq. 7-1a is the reason the emf  $E$  is called *counter-emf* in a motor.

The magnitude of the induced emf  $E$  is given for the motor by the same equation as for the generator, Eq. 3-6:

$$E = Z \frac{p}{a} \frac{n}{60} \Phi 10^{-8} = C_1 n \Phi \quad (7-2)$$

where  $C_1$  is a constant quantity for a given machine.

The equation for the torque is Eq. 3-9:

$$T = 0.1174 \times 10^{-8} \frac{p}{a} Z \Phi I_a \text{ lb-ft} \quad (7-3)$$

or Eq. 3-10:

$$T = C_2 \Phi I_a \quad (7-4)$$

where  $C_2$  is a constant quantity for a given machine.

The armature current of the d-c motor (as of other kinds of electric motors) *adjusts itself* to a value corresponding to the opposing torque of the load. If the opposing torque of the load is large, the armature current also is large, Eq. 7-3; conversely, a small value of opposing torque requires a low value of armature current. The same can be seen from Eq. 7-1b which shows that the terminal voltage of a d-c motor is equal to the sum of the counter-emf of the armature and the sum of the voltage



drops. With an increase in the load torque the speed decreases and also the counter-emf induced in the armature,  $E$ . Since the terminal voltage is constant the  $Ir$  drop must therefore increase, i.e., the armature current  $I_a$  must increase. Conversely, a decrease in the load torque results in an increase in speed, an increase in the emf induced in the armature,  $E$ , and a resulting decrease in the  $Ir$  drop and the armature current  $I_a$ .

With a motor operating at rated power, the sum of the voltage drops is about 4 to 10% of the terminal voltage, with the large value applicable to small motors.

Note that the torque given by Eq. 7-3 or Eq. 7-4 is the electromagnetic torque of the machine, designated as *developed torque*. This torque must be distinguished from the *delivered torque*, i.e. the torque delivered to the shaft. This latter torque is smaller than the former by the loss-torque.

Multiplying Eq. 7-1 by the armature current  $I_a$ , the term  $VI_a$  is the power input and the second term on the right is the copper losses in the windings and under the brushes. The difference between  $VI_a$  and the losses  $(\sum Ir + 2\Delta V) \times I_a$  represents the *electromagnetic power* of the machine corresponding to the developed (electromagnetic) torque. Thus

$$\text{Electromagnetic power} = EI_a \quad (7-5)$$

in accordance with the previously derived Eq. 1-33.

The electromagnetic power  $E \times I_a$  and the developed (electromagnetic) torque are connected by the equation of mechanics (Eqs. 1-31, 3-11)

$$T = \frac{7.04EI_a}{n} \text{ lb-ft} \quad (7-6a)$$

or

$$T = \frac{5250\text{HP}}{n} = \frac{5250}{n} \frac{EI_a}{746} \text{ lb-ft} \quad (7-6b)$$

Eq. 7-6 can be verified readily by introducing in it the value of  $E$  from Eq. 7-2: Eq. 7-3 for the torque is then obtained.

Combining Eq. 7-1 with Eq. 7-2, the speed of a motor is

$$n = \frac{V - (\sum Ir + 2\Delta V)}{C_1\Phi} \quad (7-7)$$

**7-2. Characteristics of the shunt motor.** The flux  $\Phi$  of the shunt motor is a function of the current in the shunt field winding,  $I_f$ ,

$$\Phi = f(I_f) \quad (7-8)$$

With the aid of this relation and Eqs. 7-1, 7-2, and 7-7, the behavior of a shunt motor can be determined at starting as well as when running.

If the terminal voltage  $V$  is impressed across a shunt motor at stand-still, the armature current and field flux will produce a torque and the motor will accelerate until it reaches a speed such that the load torque plus the loss torque is exactly balanced by the developed torque.

Eq. 7-7 shows that the speed varies inversely with the flux  $\Phi$ . If it should happen that *sufficient flux  $\Phi$  is not available* (low field current), the motor may *accelerate to a very high speed* and the high mechanical stresses produced may cause it to fly apart. When starting a shunt motor, it is therefore not permissible to connect first the armature circuit and then connect the field circuit across the line. The field circuit must be excited first and then voltage impressed across the armature, or both circuits may be closed simultaneously. In order that the armature current at start may not become too high, a starting resistance is placed in the armature circuit before the line voltage is applied. As the speed and counter-emf rise, the quantity  $(\Sigma Ir + 2\Delta V)$  decreases, the current  $I_a$  decreases, and the starting resistance can be reduced.

Fig. 7-3 shows the basic scheme for starting the shunt motor. One terminal of the field winding  $a$  is connected directly to the power line, and the other terminal  $b$  is connected to the line through a shunt rheostat  $R_f$  and the starting resistance  $R$ . In this manner, both field and armature windings are connected to the line at the same instant. The terminal  $b$  should not be connected to the armature winding directly, without including a part of the starting resistance. To connect the shunt field winding directly across the armature would result in a very low field flux, because the armature terminal voltage is very low at starting.

*The field winding should never be opened suddenly.* Since the field winding has a high self-inductance, the sudden breaking of this circuit produces an emf of self-induction which may be high enough to puncture the insulation. Therefore, the connection of the field winding in parallel with the armature winding and a part of the starting resistance serves as a protection for the field. When the connection of Fig. 7-3 is used and the motor is disconnected, the field circuit is not broken but always remains closed through the armature and a part of the starting resistance. Starting boxes are designed to accomplish this arrangement.

Fig. 7-4 shows the speed of a shunt motor as a function of its armature current at a constant terminal voltage and for three different degrees of

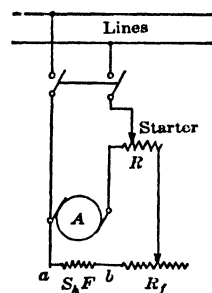


FIG. 7-3. Connections for starting a shunt motor.

saturation (three different field currents). Increasing the armature current increases both the armature reaction and the sum of the voltage drops. Both of these quantities oppose each other in their effect on the speed of the motor. A larger demagnetizing armature reaction produces a smaller resultant flux, and consequently the speed must increase according to Eq. 7-7. A larger voltage drop due to the resistances of the windings means a lower counter-emf and, therefore, a lower speed. With

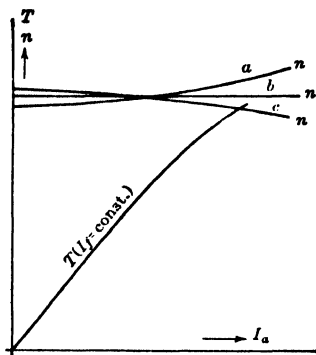


FIG. 7-4. Torque and speed of a shunt motor as a function of armature current for constant field current.

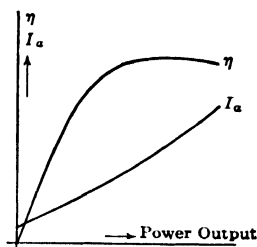


FIG. 7-5. Armature current and efficiency of a shunt motor as a function of power output for constant field current.

increasing armature current, the speed of the shunt motor will vary according to curve *a* or curve *c*: if the armature reaction predominates with increasing current, the speed follows curve *a*; if the voltage drops predominate it follows curve *c*. For a particular excitation, the above two effects may compensate each other approximately and the speed as a function of the armature current then becomes almost parallel to the axis of abscissa (curve *b*). The characteristic shown as *a* is usually not desirable.

According to Eq. 7-4 the torque of a motor is proportional to its armature current:

$$T = C_2 \Phi I_a$$

For a constant field current the torque does not increase linearly with the armature current: as the armature current increases the armature reaction also increases and the resultant flux  $\Phi$  decreases. Fig. 7-4 shows the torque curve for a constant field current. It deviates from a straight line due to the non-linearity of the saturation curve.

Fig. 7-5 shows the armature current  $I_a$  and efficiency as a function of the power output for constant field current and terminal voltage. Since

the current and voltage drops increase with increasing power output, the counter-emf decreases. It was explained above that the product  $E I_a$  represents the electromagnetic power of a motor. Since the quantity  $E$  decreases with increasing power output, the current  $I_a$  must increase more than linearly with increasing power output.

Fig. 7-4 shows that the *shunt motor is essentially a constant speed motor*. Its torque as a function of the armature current is approximately linear.

*Speed regulation* is defined as the ratio of the difference between no-load and full-load speed to the full-load speed. Thus, the speed regulation in per cent is

$$\epsilon = \frac{\text{no-load speed} - \text{full-load speed}}{\text{full-load speed}} \times 100$$

It can be determined from the speed-torque curve or the speed-armature current curve.

**7-3. Characteristics of the series motor.** Eqs. 7-1, 7-2, and 7-7 also apply to the series motor. However, in place of Eq. 7-8 the equation

$$\Phi = f(I_a) \quad (7-9)$$

must be applied, since the field and armature currents are the same in a series motor.

Fig. 7-6 shows the speed and torque of a series motor as a function of the armature current. Since the flux  $\Phi$  is small for low values of armature current, the speed  $n$  consequently must be high in order to satisfy Eq. 7-7. When  $I_a$  is very small, the flux  $\Phi$  is also very small and the speed  $n$  of the motor becomes so high that the machine may destroy itself. *A series motor should never be connected to a line if there is any possibility of losing its entire load (except in the case of fractional-horsepower motors).* Even when starting the series motor, care must be taken to see that a certain opposing torque exists, since at low currents the speed will assume a high value despite the starting resistance. While the speed of a shunt motor varies only a little with the armature current, the speed change of the series motor is very wide.

For low values of armature current, the machine is not saturated and the flux of the series motor is directly proportional to the armature current. Consequently, for low values of armature current, the torque increases as the square of the cur-

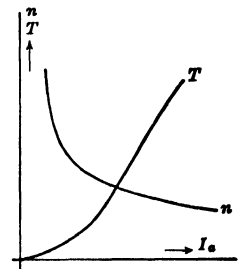


FIG. 7-6. Torque and speed of a series motor as a function of armature current.

rent (see Eq. 7-4). When the armature current is high and the machine is saturated, the flux is almost constant and the torque then varies nearly as the first power of the armature current. For still greater values of armature current, the flux decreases due to the armature reaction, and the torque therefore increases at a rate less than that of the armature current.

**7-4. Characteristics of the cumulative compound motor.** According to the relative strengths of the shunt and series field mmf's, the cumulative compound-wound motor may exhibit characteristics approaching those of the shunt or series motor. If a shunt motor is supplied with a series winding, it is possible to obtain a speed almost independent of the load and therefore almost constant. If the series motor is supplied with a shunt field winding, the possibility of its running away at no-load is thereby avoided.

**7-5. Comparison between the different types of d-c motors.** Figs. 7-7, 7-8, and 7-9 show the speed-current, torque-current, and speed-torque curves of the shunt, cumulative compound, and series motors. These

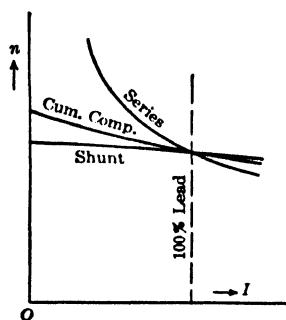


FIG. 7-7. Speed as a function of load current for the different kinds of d-c motors.

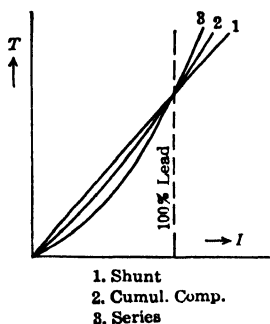


FIG. 7-8. Torque as a function of load current for the different kinds of d-c motors.

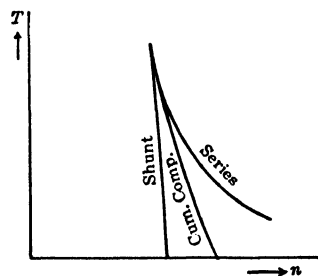


FIG. 7-9. Torque as a function of speed for the different kinds of d-c motors.

curves permit a comparison between the various types of motors. They show that the differences between the torque-current curves are not so marked as the differences between the speed-current and speed-torque curves. Fig. 7-9 can be helpful in deciding the type of motor suitable for a given application.

The characteristic features of the shunt motor are: approximately a constant speed between no-load and full-load, a torque nearly proportional to the armature current (since the flux is almost constant), and the ability to operate as a generator in the same direction of rotation without any change in connections. The last property mentioned makes *dynamic*

*braking possible* with the shunt motor: if the opposing torque of the load is lost and the armature is driven in the same direction as before, the machine acts as a generator, delivers power to the line, produces a torque opposite to the previous motor torque, and therefore acts as a brake.

The outstanding properties of the series motor are: its decreasing speed with increasing torque, a high starting torque varying nearly as the square of the current at low saturation, and a power output affected relatively little by voltage drops in the line.

TABLE 7-1. GENERAL EFFECT OF VOLTAGE VARIATION ON D-C MOTOR CHARACTERISTICS  
+ = Increase      - = Decrease

Voltage Variation %	Starting and Max. Run Torque %	Full-load Speed %	EFFICIENCY			Full-load Current %	Temperature Rise, Full Load	Maximum Overload Capacity %	Magnetic Noise
			Full Load	$\frac{3}{4}$ Load	$\frac{1}{2}$ Load				
SHUNT-WOUND									
120	+30	110	Slight +	No change	Slight -	-17	Main field +. Commutator, i. field and armature -	+30	Slight +
110	+15	105	Slight +	No change	Slight -	-8.5	Main field +. Commutator, i. field and armature -	+15	Slight +
90	-16	95	Slight -	No change	Slight +	+11.5	Main field -. Commutator, i. field and armature +	-16	Slight -
COMPOUND-WOUND									
120	+30	112	Slight +	No change	Slight -	-17	Main field +. Commutator, i. field and armature -	+30	Slight +
110	+15	106	Slight +	No change	Slight -	-8.5	Main field +. Commutator, i. field and armature -	+15	Slight +
90	-16	94	Slight -	No change	Slight +	+11.5	Main field -. Commutator, i. field and armature +	-16	Slight -

Notes: Starting current is controlled by starting resistor.

This table shows general effects, which will vary somewhat for specific ratings.

The characteristics of the cumulative compound motor lie between those of the shunt and series motors. It has a definite no-load speed as does the shunt motor; but, on the other hand, its speed decreases more with increasing torque than that of the shunt motor.

The response of shunt and cumulative compound motors to a variation of the terminal voltage is shown in Table 7-1.

**7-6. Speed control of d-c motors.** It follows from the speed equation of the motor (see Art. 7-1, Eq. 7-7)

$$n = \frac{V - (\sum I r + 2\Delta V)}{C_1 \Phi}$$

that there are three methods for regulating its speed: namely, by varying the voltage  $V$  (*voltage control*), by varying the resistance of the armature circuit (*rheostatic control*), and by varying the flux  $\Phi$  (*flux control*).

(a) *Separately excited, shunt, and cumulative compound motor.* Rheostatic control necessitates an external resistor in the armature circuit. This resistor produces a drop in the speed characteristic. Fig. 7-10 shows speed-torque characteristics for two different values of external resistance. At very small loads, the resistance is not very effective. Therefore, this

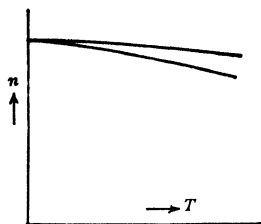


FIG. 7-10. Speed-torque characteristics obtained by rheostatic speed control (separately excited, shunt, and cumulative compound motor).

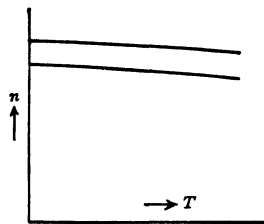


FIG. 7-11. Speed torque characteristics obtained by flux control (separately excited, shunt, and cumulative compound motor).

method makes the speed regulation, i.e., the change of speed between no-load and full-load, large. Furthermore, the efficiency of the motor is reduced by this method of speed control since the copper losses of the armature circuit are increased. For this reason, the *rheostatic control method is seldom used* in industrial installations.

The simplest and cheapest method of speed control is flux control by means of a rheostat in the shunt field circuit. Since the energy required by this circuit is only a small percentage of the machine output, the rheostat is small in size. This method is, therefore, an efficient one. In machines without interpoles (see Chapter 8), where the main flux is used to improve the commutation, the speed may be increased by rheostatic control approximately in the ratio 2 : 1. A further weakening of the main flux may interfere with the commutation, since the armature reaction may reduce the field density at the pole tips beyond the value necessary for good commutation. In machines with interpoles, a ratio of maximum to minimum speed of 5 : 1 or 6 : 1 is fairly common. To a given change in flux (shunt field current), there is a definite shift of the speed characteristic as shown in Fig. 7-11. The speed regulation is affected only slightly by this method of speed control. These considerations apply to the cumulative compound motor only when the series field mmf is small in comparison to the shunt field mmf. In general a shunt motor is used with this type of speed control.

Voltage control is used under certain conditions with separate excita-

tion in the arrangement known as the *Ward-Leonard System*. In Fig. 7-12,  $M$  is the main motor the speed of which is to be regulated. It is supplied with power from the generator  $G$  which is driven by another motor  $M'$ . The field of the generator  $G$  is excited from a constant voltage source and may be adjusted from zero to a maximum value in both directions, by

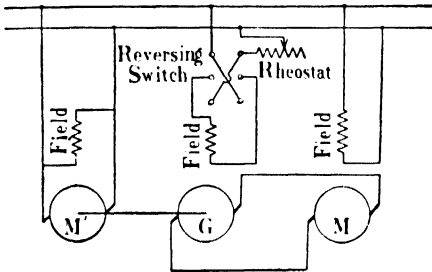


FIG. 7-12. Ward-Leonard system for speed control.

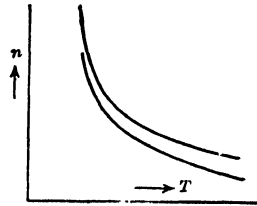


FIG. 7-13. Rheostatic speed control of a series motor.

means of a rheostat and reversing field switch. In this way a smooth variation of the voltage impressed on the main motor is obtained. The motor  $M'$  is very often an a-c motor, though it may be any suitable prime mover.

(b) *Series motor*. Rheostatic control is used for speed variation of the railway series motor. The resistor produces a drop in the speed curve similar to that in the shunt motor. Fig. 7-13 shows speed characteristics for two different values of resistance in the armature circuit. When a car is equipped with two or more motors, as is usually the case, series-parallel control is applied. This is a combined rheostatic and voltage control. At starting, the motors and their resistors are connected in series so that the terminal voltage of each motor is only a part of the line voltage. At full speed, the resistors are cut out and the motors run in parallel so that the terminal voltage of each motor is equal to the total line voltage. At intermediate speeds, the resistors are partially or entirely cut out, or a motor is shorted out of the circuit.

Applications of the different types of d-c motors are discussed in Chapter 50.

**Example 7-1.** The data for the no-load characteristics of a 4-pole, 20-hp, 230-volt shunt motor, taken at 1800 rpm, are:

$E$ :	75	110	140	168	188	204	218	231	240	262	268
$I_f$ :	0.2	0.3	0.4	0.5	0.6	0.7	0.8	0.9	1.0	1.4	1.6

The combined resistance of armature and interpole winding at 75°C is 0.0814 ohm, the



shunt winding has 2800 turns per pole, the total resistance of the shunt field winding circuit is 259 ohms, the full-load current is 76 amp, the demagnetizing effect of full-load armature current (expressed in terms of shunt field current) is  $M_d = 0.1$  amp. Determine: (a) the full-load speed, (b) the full-load torque.

From the no-load characteristic at  $I_f = 230/259 = 0.89 = OP$  (Fig. 7-14) the induced emf  $E = 230$ . Therefore, the no-load speed is 1800 rpm. At full-load current the effective field current is  $OA = 0.89 - 0.1 = 0.79$ , which at speed  $n_0 = 1800$  would give  $E_0 = AA' = 218$  volts. The actual induced emf, however, is  $E = 230 - (76 \times 0.0814 + 2) = 222$  volts. In order to determine the speed consider Eq. 7-2 for the induced emf. If in this equation three corresponding values of  $E_0$ ,  $n_0$  and  $\Phi_0$  are given, then for any three other corresponding values of  $E$ ,  $n$ , and  $\Phi$ ,

$$\frac{n}{n_0} = \frac{E}{E_0} \frac{\Phi_0}{\Phi} \text{ or } n = n_0 \frac{E}{E_0} \frac{\Phi_0}{\Phi}$$

Since  $E_0 = 218$  volts and  $E = 222$  volts and both are induced by the same flux, the speed is

$$n = 1800 \frac{222}{218} = 1832 \text{ rpm}$$

and the torque (Eq. 7-6b)

$$T = \frac{7.04}{1832} (222 \times 76) = 64.8 \text{ ft-lb}$$

Note that Eq. 7-6b for the torque contains the ratio  $E/n$ , i.e., the induced emf per revolution. It follows from Eq. 7-2 for the induced emf that for a *fixed* value of  $\Phi$  the ratio  $E/n$  is a constant. Therefore, in calculating the torque from Eq. 7-6b any pair of values can be used for  $E$  and  $n$ , provided that they correspond to the actual flux. Thus the torque can be calculated here using  $E_0$  and  $n_0$  instead of  $E$  and  $n$ , i.e.,

$$T = \frac{7.04}{1800} (218 \times 76) = 64.8 \text{ ft-lb}$$

Observe also that  $218/1800 = C_1\Phi$  (Eq. 7-2).

This calculation shows that the armature reaction in a shunt motor may raise the speed above its no-load value (see Fig. 7-4). This condition may produce the equivalent of differential compound motor action, and instability at high or sudden overloads. This usually is overcome by a small series winding, sometimes called the *stabilizing winding*.

**Example 7-2.** Assume now that the motor of Example 7-1 has also a series winding of 3.5 turns per pole, making the total resistance of the armature circuit 0.089. Determine the speed and torque at full-load. The series  $AT = 3.5 \times 76 = 266$ , or in terms of shunt field current  $266/2800 = 0.095$ ; therefore, the effective field current now will be  $0.89 + 0.095 - 0.1 = 0.885$  amp. This would give (Fig. 7-14)  $E_0 = 229$  at  $n_0 = 1800$ . The actual induced emf is  $E = 230 - (76 \times 0.089 + 2) = 221.2$ . Therefore the speed

$$n = 1800 \times \frac{221.2}{229} = 1739$$

and the torque (Eq. 7-6b)

$$T = \frac{7.04}{1739} (221.2 \times 76) = 68 \text{ lb-ft}$$

Actual tests showed the full-load speed to be 1730 rpm.

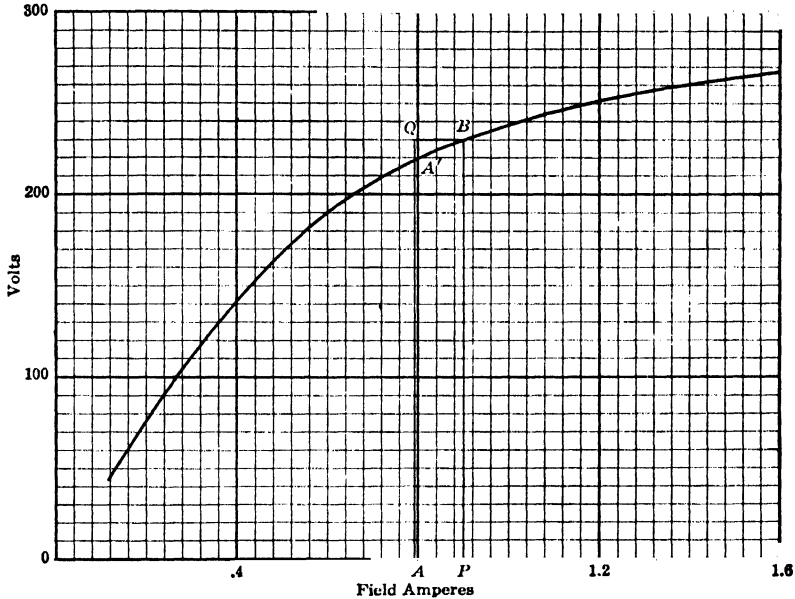


FIG. 7-14. Example 7-1.

**Example 7-3.** Assume that the series turns of this motor were increased to 7.5. Determine the speed and torque. The total armature circuit resistance is now 0.10 ohm. The series  $AT = 7.5 \times 76 = 570$ , or in terms of shunt field current  $570/2800 = 0.203$  amp. Therefore, the effective field current will be  $0.89 + 0.203 - 0.1 = 0.993$  amp. This would give (Fig. 7-14)  $E_0 = 240$  volts at  $n_0 = 1800$ . The actual induced emf is  $E = 230 - (76 \times 0.10 + 2) = 220.4$ . Thus, the speed

$$n = 1800 \frac{220.4}{240} = 1655$$

and the torque (Eq. 7-6b)

$$T = \frac{7.04}{1655} (220.4 \times 76) = 71.3 \text{ lb-ft}$$

This will illustrate the action of the cumulative compound motor.

**Example 7-4.** Assume that the machine of Example 7-1 has been designed as a series motor with 37.5 turns per pole, and that the resistance of the series winding is 0.0636 ohm. Determine the speed and torque at full-load current, half-load current, and at 125% load. It is convenient to plot the no-load characteristic either in field

ampere-turns or in terms of series field current (Fig. 7-15).  $\sum IR + 2 = 13$  volts. The armature-reaction ampere-turns at full-load (Example 7-1) are  $2800 \times 0.1 = 280$ . The effective AT per pole at full-load is then  $76 \times 37.5 - 280 = 2570$ . At  $n_0 = 1800$  rpm,  $E_0 = 233$  volts. The actual induced emf is  $E = 230 - 13 = 217$  volts. Thus, at full-load  $n = 1800 \times (217/233) = 1678$  rpm. The torque is  $T = (7.04/1678) (217 \times 76) = 69.2$  ft-lb. At half-load the effective AT = 1285 and  $E_0 = 148$  at  $n_0 = 1800$ . The

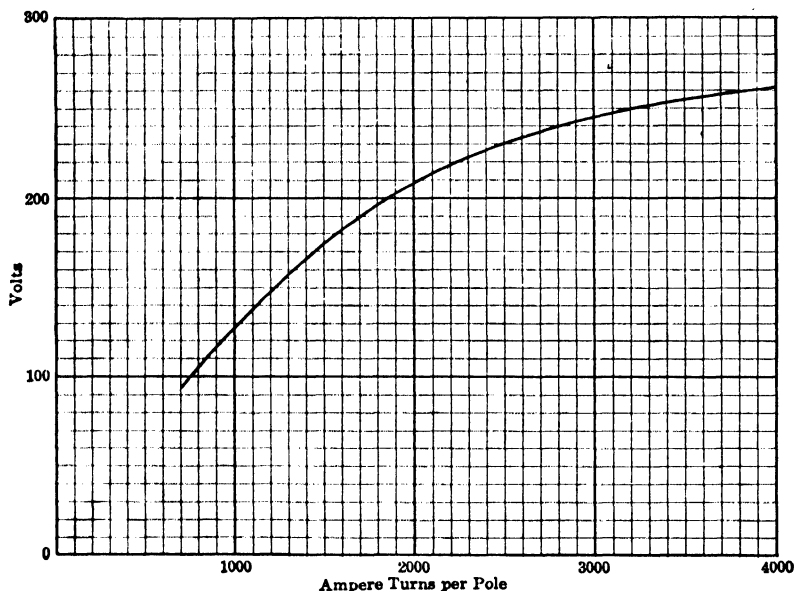


FIG. 7-15. Example 7-4.

actual induced emf  $E = 230 - (0.1450 \times 38 + 2) = 222.5$ , and therefore  $n = 1800 \times 222.5/148 = 2700$ , and  $T = (7.04/2700) (222.5 \times 38) = 22$  ft-lb. At 125% load the effective AT = 3210 and  $E_0 = 248$  at  $n_0 = 1800$ . The actual induced emf  $E = 214.3$  and  $n = 1800 \times 214.3/248 = 1555$ ,  $T = (7.04/1555) (214.3 \times 1.25 \times 76) = 92.1$  ft-lb.

### PROBLEMS

1. If the motor of Example 7-1 operates at a terminal voltage of 250 volts determine: (a) the no-load speed; (b) the full-load speed; (c) the full-load torque developed.
2. Repeat Problem 1 for a terminal voltage of 210 volts.
3. Determine the armature current necessary for the motor of Example 7-1 to develop 60 lb-ft torque at 1800 rpm. What is the field current in amperes?
4. Determine the armature current for the motor of Example 7-1 to develop 70 lb-ft torque at 1600 rpm. Also determine the number of series turns per pole required to produce this torque.
5. The motor in Example 7-1 is operating at rated voltage, rated load, and the voltage is increased to 250 volts. If the torque demand remains unchanged, determine the speed, armature current, and field current.

6. Repeat Problem 5 for a change in voltage from 230 to 210 volts. Explain why the speed is not directly proportional to the voltage.

7. If the motor of Example 7-2 operates at a terminal voltage of 250 volts determine: (a) no-load speed; (b) full-load speed; (c) full-load torque.

8. Repeat Problem 7 for a terminal voltage of 210 volts.

9. If the terminal voltage is 250 volts and the torque demand is the rated full-load value, determine the resistance in ohms which must be placed in series with the armature of the motor in Example 7-2 in order to produce a full-load speed of 1750 rpm.

10. If the motor of Example 7-2 is operated at 230 volts and 0.25 ohm is inserted in the armature circuit, determine the speed and torque at full-load current.

11. Repeat Problem 10 for a terminal voltage of 250 volts.

12. Determine the torque developed by the motor of Example 7-2, and the speed, for a terminal voltage of 230 and armature currents of 20, 40, 60, 80 and 100 amp.

13. The core loss plus the friction and windage loss of the motor in Example 7-2 is 1200 watts, and the stray load loss is 150 watts. Determine the conventional efficiency for rated armature current and full field at 230 volts.

14. If the machine of Example 7-2 is to be operated as a generator using the 3.5 series turns cumulative, determine the speed of operation and the no-load voltage to produce a terminal voltage of 230 volts and an armature current of 75 amp. The shunt field resistance is 260 ohms.

15. Determine the full-load speed of the motor in Example 7-3 if a resistance of 0.25 ohm is inserted in series with the armature.

16. Determine the torque developed by the motor of Example 7-3, and the speed, for armature currents of 20, 40, 60, 80 and 100 amp.

17. If a 230-volt series motor has an armature resistance of 0.20 ohm and a series field resistance of 0.10 ohm, determine the current required to develop a torque of 50 lb-ft at 1200 rpm.

18. A series motor draws 100 amp at 550 volts and runs at 1200 rpm. The armature resistance is 0.08 ohm and the series field resistance 0.035 ohm. When the load current is reduced to 40 amp, the speed is increased to 1950 rpm. Determine the percent reduction in air-gap flux.

19. A 7.5-HP, 230-volt shunt motor has a full-load speed of 1750 rpm and takes a line current of 29 amp. The shunt field resistance is 300 ohms and the armature 0.30 ohm. How much resistance should be inserted in the armature circuit in order to develop 20 lb-ft torque at 1000 rpm?

20. A 5-HP, 230-volt shunt motor takes a rated line current of 20.5 amp. The field resistance is 288 ohms and the armature 0.45 ohm. If the rated speed is 1750 rpm, determine the developed torque and efficiency.

21. The motor of Problem 20 is to be run at 60% reduced torque, at a speed of 1000 rpm and a 10% increase in flux. Determine the armature current and the resistance to be inserted in series with the armature.

22. A 25-HP, 230-volt shunt motor is rated at 900 rpm, 87.5 amp armature current. The armature resistance is 0.05 ohm. Determine the developed torque. What is the resistance in the armature circuit if the torque is 60% of normal at 750 rpm?

23. If a resistance of 1.5 ohms is suddenly inserted in the armature circuit of the motor in Problem 22, determine the developed torque and armature current immediately after the resistance is inserted.

24. A 120-volt, 1150-rpm shunt motor has a rated armature current of 150 amp.

The armature resistance is 0.03 ohm. For constant torque and constant field flux, determine the speed if: (a) the armature voltage is increased 10%; (b) the voltage is decreased 10%.

25. A 220-volt, 15-HP shunt motor has an efficiency of 85%, an armature resistance of 0.20 ohm, and a field resistance of 250 ohms. The full-load speed is 1750 rpm. Determine the torque developed. If a resistance of 0.40 ohm is inserted in series with the armature and the torque remains constant, what is the motor speed?

26. A 3-HP series motor runs at 1750 rpm and 11.6 amp from 230-volt lines.  $\sum r = 0.1$  ohm. Assuming a straight-line saturation curve, determine the speed, at constant torque, when the voltage is: (a) increased 10%; (b) decreased 10%.

27. How must the terminals of a cumulative compound motor be changed in order to reverse the direction of rotation, and still remain cumulatively compounded? Show by diagrams of connections.

28. A 3-HP, 220-volt cumulative compound motor takes an armature current of 10.8 amp and runs at 1750 rpm. The armature and series field resistance are 0.30 and 0.05 ohm respectively. Determine the developed torque. Determine the percent change in flux to produce a speed of 1350 rpm when the armature current is 20 amp and the voltage has been reduced 10%.

29. The data for the no-load characteristic of a shunt dynamo, taken at 450 rpm, are:

$E$ :	20	40	60	70	80	90	100	110
$I$ :	1.8	3.6	5.7	7.0	8.8	11.3	15.7	22.0

This machine operates as a shunt motor from 240-volt lines, the field resistance is 15 ohms, the armature plus interpole field resistance is 0.04 ohm, the full-load armature current is 500 amp, the demagnetizing effect of armature reaction is equivalent to 1 amp of shunt field current. There are 400 shunt field turns per pole. Determine for full-load current: (a) field current, (b) speed, (c) developed torque.

30. The motor of Problem 29 now has 6.5 series turns per pole added to give cumulative action. Assume long-shunt connection, and that the series field has a resistance of 0.01 ohm. Determine the speed and torque for full-load armature current.

31. A 5-HP, 230-volt, adjustable-speed motor has 2500 shunt turns per pole, and 9 series or stabilizing turns per pole. The armature reaction  $M_d = 0.05$  in terms of shunt field current, the armature resistance is 0.30 ohm, and the shunt field resistance 240 ohms. The full-load armature current is 20 amp. The data for the no-load saturation curve taken at 525 rpm are:

$E$ :	40	60	80	100	120	140	160	180	200
$I$ :	0.075	0.12	0.165	0.21	0.27	0.35	0.49	0.75	1.23

When operating at full-load current, the following speeds are desired: 615, 800, 1000, 1200, 1400, 1600, and 1800 rpm. Determine the values of shunt field resistance necessary for each speed.

32. A 120-volt shunt motor with a field resistance of 37 ohms and an armature resistance of 0.07 ohm operates at 750 rpm and takes an armature current of 80 amp. Neglecting armature reaction, at what speed should it operate as a generator to deliver 75 amp at 120 volts?

33. A 230-volt motor has a no-load speed of 1200 rpm, an armature resistance of 0.05 ohm, and a full-load current of 100 amp. Armature reaction reduces the air-gap flux at full-load to 95% of the no-load value. Determine the full-load speed.

34. A 50-HP, 440-volt series motor operates at 1200 rpm with a full-load efficiency of 90%. The armature resistance drop is 12 volts, and the series field drop is 8 volts. Determine: (a) the armature current; (b) torque developed.

35. If the voltage in Problem 34 above is reduced to 350 volts, determine the torque and speed for the rated armature current determined. Assume the air-gap line as the magnetization curve.

36. A 5-HP, 220-volt shunt motor takes a no-load armature current of 3.0 amp and operates at a speed of 1150 rpm. The armature resistance is 0.3 ohm. If the field flux is reduced 20% and a resistance of 1.5 ohms is placed in the armature circuit, the motor operates at 850 rpm when loaded. Determine the armature current and torque developed.

37. An electric hoist with an overall efficiency of 60% is driven by a shunt motor which lifts 5 tons through 45 ft in 30 sec. Determine the HP rating of the motor and the line current. Line voltage = 230 volts, efficiency = 0.88.

38. A 550-volt shunt motor is driving a pump which is delivering 500 gallons of water per minute against a head of 200 ft. The pump efficiency is 75% and the motor 90%. Determine (a) the HP output of the motor; (b) the motor line current; (c) the operating cost per hour with energy at 3.5 cents per kw-hr.

## Chapter 8

### COMMUTATION OF THE D-C MACHINE

**8-1. The short-circuited winding element. Linear commutation. Advantage of accelerated commutation.** If  $I_a$  is the total armature current, the current in each parallel path and also in the conductors of each winding element is

$$i_a = \frac{I_a}{a} \quad (8-1)$$

Consider Figs. 3-7 and 3-11. Rotating in the magnetic field, the winding element changes from one armature path to another thus changing its current from  $+i_a$  to  $-i_a$  (or vice versa). *During the time of reversal the conductors of the winding element lie in the neutral zone and the winding element is short circuited by one brush in a lap winding, or by two brushes of the same polarity in a wave winding with  $p$  brush studs.*

The current flowing in a winding element is thus an alternating current of the shape shown in Fig. 8-1.  $T_c$  is the time of current reversal (of commutation).

Fig. 8-2 shows schematically a winding element of a lap winding with its connections to the commutator bars. It is assumed that the width of the brush is equal to the width of a commutator bar. In this case the brush can short-circuit only one winding element. In Fig. 8-2 the short circuit of the winding element begins when brush edge  $b$  touches commutator bar 1, and ends when the brush edge  $a$  leaves bar 2.  $b$  is the *leading brush edge*, and  $a$  is the *trailing brush edge*.

At the beginning of the short-circuit period  $T_c$  ( $t = 0$ ), the current in the winding element is  $+i_a$  (Fig. 8-1); the brush is then on bar 2 only. At the end of the time  $T_c$  ( $t = T_c$ ), the current in the winding element is  $-i_a$ ; the brush is then on bar 1 only. At intermediate times, the brush lies on both bar 1 and bar 2.

If there are no further influences on the short-circuited winding ele-

ment, the change-over of the current from  $+i_a$  to  $-i_a$  is determined by the magnitude of the contact areas of the brush with the commutator bars 1 and 2 (areas  $A_1$  and  $A_2$  in Fig. 8-2), i.e., the current in the short-circuited winding element is, at any time,

$$i = i_a \left( 1 - \frac{A_1}{A/2} \right) \quad (8-2a)$$

where  $A = A_1 + A_2$  is the total contact area of the brush. At the beginning of the short-circuit period,  $A_1$  is equal to zero and  $i = +i_a$ ; when  $A_1 = A/2$ , i.e., when the brush contacts both commutator bars equally,

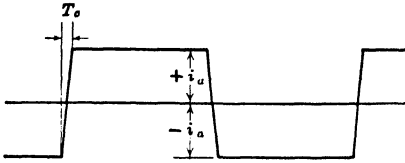


FIG. 8-1. Current in a winding element.

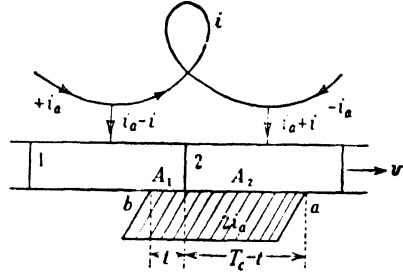


FIG. 8-2. Short-circuited winding element of a lap winding.

$i = 0$  and no current flows in the short-circuited winding element. At times when  $A_1$  is between zero and  $A/2$ , the current  $i$  changes from  $+i_a$  to 0. At times when  $A_1$  is larger than  $A/2$ ,  $i$  becomes negative, and  $i$  reaches the magnitude  $-i_a$  when  $A_1 = A$ . At this instant of time the commutation period is finished.

In Eq. 8-2a, the times  $t$  and  $T_c/2$  can be introduced instead of the areas  $A_1$  and  $A/2$  since these quantities are proportional to each other. Thus

$$i = i_a \left( 1 - \frac{t}{T_c/2} \right) \quad (8-2b)$$

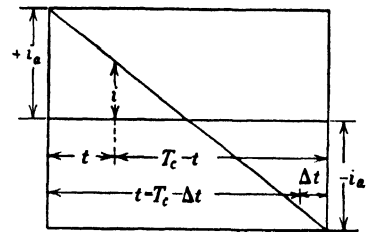


FIG. 8-3. Linear commutation.

Fig. 8-3 shows the current in the short-circuited winding element  $i$  as a function of  $t$ , corresponding to Eq. 8-2b. This is a straight line. The length of the rectangle is equal to the period of commutation  $T_c$ . The distances from the axis of abscissae to the straight line represent the short-circuit currents  $i$ . A curve which represents the short-circuit current  $i$  as a function of time  $t$  is called a *commutation curve*. Fig. 8-3 represents *linear commutation*.



The most dangerous instant of the commutation period is  $t = T_c$ , i.e., the instant at which the trailing brush edge (*a*, Fig. 8-2) leaves commutator bar 2. If the current density becomes too high at the trailing brush edge at the end of the commutation period, then sparking appears under the brush. As a result of this the commutator is pitted, and the sparking becomes progressively worse owing to the poor surface contact between the brush and the commutator.

Besides being dependent upon the efficiency and the heating of the windings and iron, the usefulness of the commutator machine is, above all, dependent upon its commutation. It is necessary, therefore, to have the current density under the trailing brush edge as low as possible; this is the same as saying: *the current flowing through the contact area  $A_2$  at the end of the commutation period must be as small as possible.*

Consider Fig. 8-2. The plus and minus signs before  $i_a$  refer to the winding element considered, but not to the brush. The brush carries the current  $2i_a$ , and the part of this current which flows into the brush through the contact area  $A_2$  is equal to  $i + i_a$  (Fig. 8-2).

The instant of time shortly before the commutation period is finished,  $t = T_c - \Delta t$  (Fig. 8-3), will be considered. For this instant of time,  $A_2$  becomes equal to  $\Delta A_2$ . From Eq. 8-2b for  $t = T_c - \Delta t$

$$i = -i_a \left( 1 - \frac{\Delta t}{T_c/2} \right) = -i_a + \Delta i_a$$

The current which flows through  $\Delta A_2$  at  $t = T_c - \Delta t$  is equal to  $i + i_a = -i_a + \Delta i_a + i_a = \Delta i_a$ . If  $\Delta i_a$  can be made equal to zero at  $t = T_c - \Delta t$ , then no current flows through the contact area  $A_2$  at this time, and the current density at the trailing edge of the brush is zero at the end of the

commutation period. Since the current through  $A_2$  at time  $t = T_c - \Delta t$  is  $i + i_a = +\Delta i_a$ , apparently  $\Delta i_a$  will become zero at this instant of time if  $i$  is equal to  $-i_a$ , i.e., if the current in the short-circuited winding element reaches its end-value  $-i_a$  shortly before the commutation period is over.

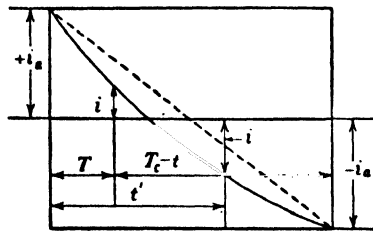


FIG. 8-4. Accelerated commutation.

Fig. 8-4 shows a commutation curve which satisfies this condition. It is *tangent* to the lower horizontal line of the rectangle at times close to  $T_c$ . This type of commutation curve yields better commutation than the linear commutation curve shown in Fig. 8-3.

The straight line which corresponds to linear commutation is drawn in

Fig. 8-4 as a dotted line. Comparing both commutation curves, it is seen that the curve which yields the better commutation effects the change-over from  $+i_a$  to  $-i_a$  faster than the linear curve does. Consider, for example, the times  $t$  and  $t'$ : at  $t$  the positive value of the current  $i$  in the short-circuited winding element is smaller than the positive value which the straight line yields; at  $t'$  the negative value of the current  $i$  is larger than the negative value which corresponds to the straight line. In comparison with the linear commutation of Fig. 8-3, Fig. 8-4 represents *accelerated commutation*.

**8-2. The emf of self-induction of the short-circuited winding element and the emf due to the armature flux. Delayed commutation.** It follows from the previous considerations that accelerated commutation is desirable in order to accomplish sparkless commutation. However, phenomena occur in the short-circuited winding element which *delay* the commutation.

It has been explained previously that the field winding of the d-c machine produces a leakage flux, Fig. 4-1, i.e., a flux which does not go through the main magnetic path of the machine (gap, teeth, and core). The same is true of the armature winding embedded in the armature slots. This winding produces several fluxes which do not go through the main path. One of these leakage fluxes is that around the end-windings, i.e., around the external

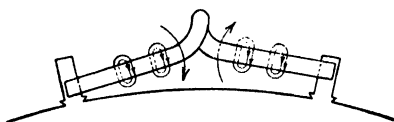


FIG. 8-5. End winding leakage flux.

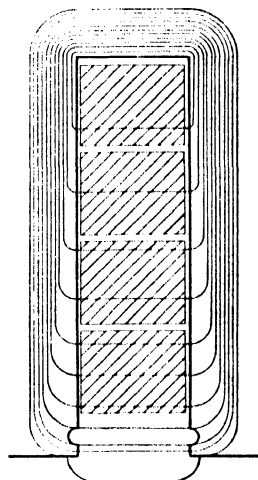


FIG. 8-6. Slot and tooth top leakage fluxes.

connections between the conductors, Fig. 8-5. Another leakage flux is that which crosses the slots without crossing the gap. A third leakage flux is that between the tooth tops in the gap without going through the pole iron. The latter two leakage fluxes are shown in Fig. 8-6.

These three leakage fluxes have no influence on the winding elements as long as their current remains constant (equal to  $+i_a$  or  $-i_a$ ). However, when a winding element goes through the commutation period, i.e., when its current changes from  $+i_a$  to  $-i_a$ , or vice versa, these leakage fluxes which are proportional to the armature current undergo changes and

induce an *emf of self-induction* in the short-circuited winding element. This emf *opposes* any change of the current and, therefore, *delays* the commutation. Fig. 8-7 shows the influence of the emf of self-induction. For comparison the straight line which corresponds to linear commutation

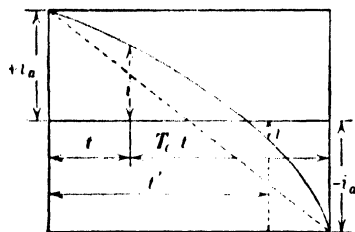


FIG. 8-7. Delayed commutation due to the emf of self-induction in the short-circuited winding element.

is also shown as a dotted line. Comparing both curves it is seen that at time  $t$  the positive value of the current  $i$  in the short-circuited winding element is larger than the positive value which the straight line yields, and that at time  $t'$  the negative value of the current  $i$  is smaller than the negative value which corresponds to the straight line. This is exactly opposite to the desirable accelerated commutation shown in Fig. 8-4.

Refer to Fig. 4-5 which shows the armature flux of a generator. A winding element which lies in the neutral axis and undergoes commutation cuts this flux and an emf is induced in the short-circuited winding element. Consider one of the conductors of the winding element, for example, the conductor lying to the left in the figure; the same result obtained also applies to the other conductor of the winding element. Under the S-pole the lines of force of the field flux go *from the armature* into the pole (Fig. 4-4); the direction of the emf induced by the field flux in the conductor considered, shortly before it reaches the neutral axis, is that shown by the dot. During the commutation period, the conductor emf induced by the field flux changes from the dot corresponding to a S-pole to a cross corresponding to a N-pole. An *acceleration of the commutation* in the conductor is achieved if an emf corresponding to the N-pole is induced in it *while* it undergoes commutation, i.e., *before* the commutation period has ended. Consider the armature flux to the left in Fig. 4-5; it emerges *from the armature* just as the field flux under the S-pole does. This armature flux therefore induces, in the conductor considered, an emf of the same direction as that of the main S-pole, while an emf induced by a N-pole is necessary for acceleration of the commutation. Thus the emf induced in the short-circuited winding element by the armature flux delays the commutation just as the emf of self-induction does. However, *it is mainly the emf of self-induction which causes the sparking in the d-c machine.*

**8-3. Acceleration of the commutation by means of the main flux or interpoles.** It follows from the foregoing that, in order to achieve good commutation, means must be adapted to counteract the delaying action

of the emf of self-induction and the emf induced by the armature flux in the short-circuited winding element, i.e., means must be applied to *accelerate* the commutation. For this purpose either the main flux can be employed or special poles, *interpoles*, which lie between the main poles can be used.

(a) *Acceleration of commutation by the main flux.* It has been explained in the foregoing article that acceleration of the commutation occurs if a voltage corresponding to the next pole ahead is induced in the winding element undergoing commutation. Referring to Fig. 4-5 which represents a generator, this means that an emf corresponding to the N-pole must be induced in the short-circuited winding element while it commutates. This can be achieved by moving the brushes in the direction of rotation (see Fig. 4-8): the short-circuited winding element cuts the lines of force of the main flux during the commutation period, and an emf is induced in it by the main flux which counteracts both the emf of self-induction and the emf induced in the winding element by the armature flux.

The foregoing considerations refer to a generator. The brushes must be shifted *in the direction of rotation*, in order to accelerate the commutation of a *generator*. In a *motor* the brushes must be shifted *opposite to rotation*, in order to accelerate the commutation. This is due to the fact that in a motor the current and the emf induced by the main flux are in counter-phase (see Art. 7-1).

The brush shift method for the purpose of improving commutation is used only in very small machines. The reason for this should be apparent from the following discussion. The *average change of current* in the short-circuited winding element during the commutation period is  $2i_a/T_c$  and is proportional to the armature current  $I_a = ai_a$ . Therefore, the *average emf* of self-induction in the short-circuited winding (which is usually considered in the commutation problem) is also proportional to the armature current. The emf induced in the short-circuited winding by the armature flux also is proportional to the armature current (see Eq. 1-26) since the armature flux is proportional to the armature current. Thus, both emf's delaying commutation in the short-circuited winding element, the emf of self-induction and the emf induced by cutting the armature flux, are proportional to the armature current (to the load). Hence, in order that a counter-acting emf in the short-circuited winding element be effective at all loads, it should be proportional to the armature current (to the load): i.e., this emf must be induced by cutting a flux which is proportional to the armature current.

The main flux is determined mainly by the field winding and is not proportional to the armature current. Therefore, it is not a satisfactory

flux to be used for improvement of commutation. When used for this purpose, the brush shift will improve the commutation only at a fixed load, but not at all loads, because for a fixed position of the brushes there is a corresponding fixed density of the main flux at the armature. Furthermore, the shift of the brushes necessary to improve the commutation (in the direction of rotation for the generator, opposite to the rotation for the motor) weakens the main flux (see Art. 4-3).

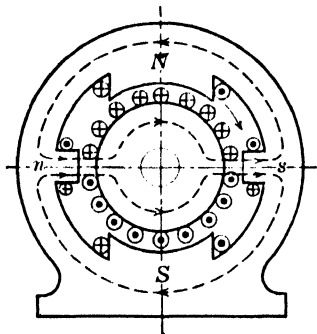


FIG. 8-8. Interpole arrangement for a 2-pole generator.

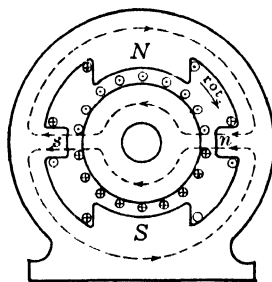


FIG. 8-9. Interpole arrangement for a 2-pole motor.

(b) *Acceleration of commutation by means of interpoles.* Only very small d-c machines do not have interpoles for improvement of the commutation. The axes of the interpoles coincide with the neutral axes (Figs. 8-8 and 8-9). Since the purpose of the interpoles is to *accelerate* the commutation, their polarities (in the direction of rotation) must be those of the *next following* main pole in a *generator* (Fig. 8-8) and those of the *preceding* main pole in a *motor* (Fig. 8-9). The interpole winding is excited by the armature current and is connected in series with the armature winding. The mmf of the interpole winding is adjusted to eliminate the armature mmf in the interpolar spaces and to produce, in addition, an interpole flux sufficient to induce in the short-circuited winding element an emf equal and opposite to the emf of self-induction, thereby accelerating the commutation according to the commutation curve, Fig. 8-4. Since the interpole flux is proportional to the armature current, it improves the commutation at all loads.

### PROBLEMS

1. A 7.5-kw, 250-volt generator has 4 poles, 92 commutator bars, and a lap winding. The full-load current is 30 amp, and the speed is 1750 rpm. The diameter of the commutator is  $5\frac{3}{4}$  in., and the brush thickness is  $\frac{3}{8}$  in. Neglecting insulation thickness between

bars, determine the time of commutation of a single winding element and the average  $di/dt$  at full-load.

2. If the machine in Problem 1 is operated at 1150 rpm with an armature current of 25 amp, determine the time of commutation and the average  $di/dt$  for a single winding element.

3. A  $1\frac{1}{2}$ -HP, 230-volt, 6.3-amp, 1750-rpm, 2-pole shunt motor has 63 commutator bars and a commutator diameter of  $3\frac{3}{8}$  in. The brush width is  $\frac{3}{8}$  in. Determine the time of commutation and the average  $di/dt$  for a single winding element.

4. The 250-kw generator whose dimensions are given in the Example in Chapter IV has a commutator with a diameter of 17.5 in. and 216 commutator bars. The brush width is 2.8 commutator pitches. Determine the time of commutation and the average  $di/dt$  for a single winding element at full load. Neglect the thickness of insulation between bars.

## Chapter 9

### SOME SPECIAL D-C MACHINES

In this chapter some of the special d-c machines will be described, namely:

Three-wire generator.

Dynamotor.

Dynamic rotating amplifiers (Trade names: Amplidyne and Rototrol).

**9-1. Three-wire generator.** A great economy in the use of copper can be realized when power transmission is accomplished at a high voltage and a low current rather than at low voltage and high current. Assume  $V$  to be the voltage at the generator end,  $I$  the current transmitted, and  $R$  the total resistance of the line wires. The power loss in the lines is then  $I^2R$ . If the same power is transmitted at the voltage  $2V$ , the current is  $I/2$ . For the same power loss, the resistance of the lines is then four times larger, and therefore the weight of the copper in the line wires is only one-fourth of its value at the voltage  $V$ .

However, in incandescent lighting, lamps designed for 110 and 115 volts are more efficient than those designed for higher voltage. The *3-wire system* makes it possible to connect lamps and small loads (small motors) to a low voltage, while larger loads (larger motors) can be connected to a voltage twice that of the lamps.

Fig. 9-1 shows the connections of a 3-wire generator devised by Dolivo-Dobrowolsky. A 2-pole generator is assumed, and the armature winding is shown only schematically. A coil of wire  $DE$  wound on an iron core and thus having a high reactance is connected into the armature winding between points  $D$  and  $E$  which lie a pole pitch (180 electrical degrees) apart. The voltage between points  $D$  and  $E$  is alternating (see Art. 3-4). The current in the coil  $DE$  has the frequency  $pn/120$ , and is very small due to the high reactance of the coil. The mid-point  $M$  of the

coil is connected to a slip-ring the brushes of which are connected to a third wire or *neutral wire*. Lamps and small motors are connected between the outer wires and the neutral wire, while larger motors are connected between the outer wires (see Chapter 51).

When both halves of the system are loaded equally, i.e.,  $I_1 = I_2$ , no current flows through the neutral wire. When both halves of the system are loaded unequally, then the difference  $I_1 - I_2$  flows through the neutral wire. This current divides into two parts in the coil  $DE$ , which go through the armature to the positive as well as to the negative brush.

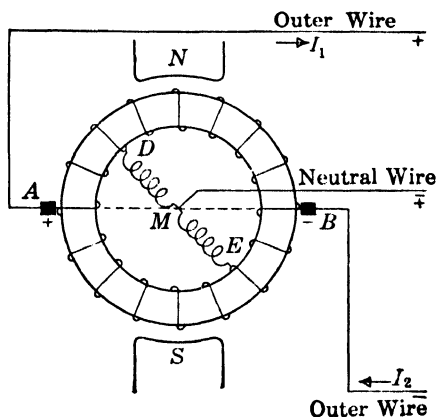


FIG. 9-1. Three-wire generator.

**9-2. Dynamotor.** A generator is often called a *dynamo*. The dynamotor is a combination of a d-c generator and d-c motor in a single unit. The pole structure and armature core are common for both machines, but there are two separate armature windings and two separate commutators with brushes. If voltage is impressed on one of the two armature windings, the machine runs as a motor. The common flux induces emf's in both windings. Therefore, the second armature winding can be loaded as a generator. The emf induced in the motor is determined by the terminal voltage and the voltage drops and is approximately equal to the impressed voltage (see Eq. 7-1). Since speed and flux are the same for both windings, the emf induced in the generator winding is nearly equal to the voltage impressed on the motor times the ratio of number of conductors  $Z_g/Z_m$ , i.e., the generator voltage cannot be regulated independently.

The dynamotor has a higher efficiency than a 2-unit motor-generator. Dynamotors are used mostly for radio and other communication services in ratings of a few hundred watts. The motor power is taken from a storage battery at low voltage. The generator voltage may be as high as 1500 volts.

**9-3. Dynamic rotating amplifiers.** An amplifier is a device which, operated by very little power, is able to control the flow of a much larger quantity of power. With this definition, a d-c generator may be considered as a power amplifier. Consider Fig. 9-2. A prime mover  $M$  drives a d-c generator  $G$  which delivers the power  $P$  to the load. This power is de-



livered by the prime mover, but the generator field can be used to control the power flow to the load, since the voltage and current of the generator depend upon the power of the field.

The field power of a d-c generator with low saturation and a relatively small air gap is about 1% of the power transmitted to the load. Such a d-c generator thus has an amplification of  $100:1 = 100$ , i.e., one watt in the field circuit is able to increase the output by 100 watts. This amplification can be increased by using two d-c machines in series as shown in Fig. 9-3. Here an amplification of  $100 \times 100 = 10,000$  can be achieved. However, an amplifier must have not only a certain amplification but also

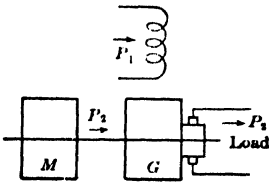


FIG. 9-2. D-c generator as a power amplifier.

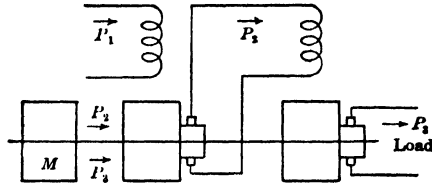


FIG. 9-3. Increase of amplification by using two machines.

a certain rapidity of response; and a system, as shown in Fig. 9-3, is sluggish in this respect due to the fact that it has two separate magnetic circuits. The rotating amplifier should have only one magnetic structure and at least two electric circuits in order to be useful in industrial applications.

There are two solutions to this problem in present-day use. One of them is the Amplidyne; the other, the Rototrol. Both are 2-stage amplifiers.

(a) *The Amplidyne (abbreviated form for dynamic amplifier).* In the Amplidyne, both stages have the same number of poles. Fig. 9-4 shows schematically a 2-pole Amplidyne. Contrary to the normal d-c machine, which has only one set of brushes placed (electrically) in the neutral axis (brushes  $B_1B_1$ ), in the Amplidyne there is another set of brushes ( $B_2B_2$ ) which is shifted with respect to the first set by half a pole pitch, i.e., by 90 electrical degrees. The latter brushes then lie (electrically) in the pole axis. The brushes  $B_1B_1$  are directly connected together.

Separately excited coils  $C$ , called *control coils*, are arranged on the poles. The flux produced by the control coils induces an emf between the brushes  $B_1B_1$ , as in the normal d-c machine. Since these brushes are connected together, a current will flow between them. This is the first stage of amplification. The current flowing between the brushes  $B_1B_1$ , produces an armature flux  $\Phi_1$ , in the axis of these brushes (see Art. 4-3).

The flux  $\Phi_1$  induces an emf between the brushes  $B_2B_2$  which are connected to the load. This is the second stage of amplification. For a power of 1 watt in the control coil there will be a corresponding power of about  $100 \times 100 = 10,000$  watts at the load brushes  $B_2B_2$ .

The load current produces an mmf  $M_2$  in the axis of the brushes  $B_2B_2$  which opposes the mmf of the control coils. Therefore, a compensating winding is necessary which eliminates the armature mmf  $M_2$ . Since the

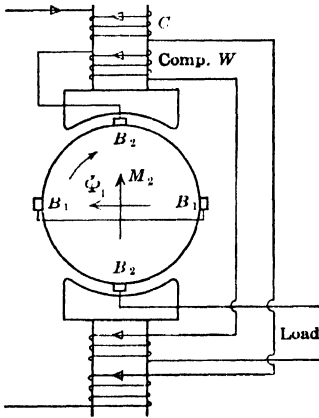


FIG. 9-4. Scheme of 2-pole Amplidyne.

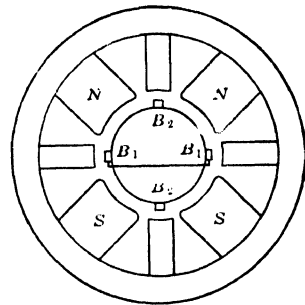


FIG. 9-5. Amplidyne. Split poles and interpoles.

volt-amperes which correspond to  $M_2$  are 10,000 times as great as the volt-amperes in the control circuit, a very exact compensation of the mmf  $M_2$  is necessary; otherwise if a part of the control field is nullified, the amplification will be reduced.

Fig. 9-4 does not show the interpoles which are necessary for a good commutation. Since the Amplidyne has two sets of brushes, it needs twice as many interpoles as the normal d-c machine, namely, four interpoles in a 2-pole Amplidyne. The practical amplifier, therefore, has split poles, as shown in Fig. 9-5, and four interpoles are arranged, two for each brush axis. The coils which compensate  $M_2$  are wound around the poles  $NN$  and  $SS$  so that their axis coincides with the axis of the brushes  $B_2B_2$ .

In order to increase the amplification, the Amplidyne may have, in addition to the control coils and compensating winding, a shunt winding for the axis  $B_1B_1$  connected to the load terminals, and also series windings in both axes as shown in Fig. 9-6.

(b) *Two-stage Rototrol (abbreviated form for rotating control)*. This dynamic amplifier has different numbers of poles for the two stages, the

pole-ratio being 1:2. The first stage has the lesser number of poles; the second stage, the larger number. The smallest numbers of poles for this type of amplifier are, therefore, two for the first stage and four for the second stage. With these numbers of poles the machine has a 4-pole field structure, four interpoles, a 4-pole armature, and four brush studs. The appearance is that of a normal 4-pole generator, except that the field windings are different.

Fig. 9-7 shows schematically the armature, the main poles, and brushes. The interpoles are omitted for the sake of simplicity. The four main poles are designated by 1, 2, 3, and 4, and the four brushes by  $B_1$ ,  $B_2$ ,  $B_3$ ,

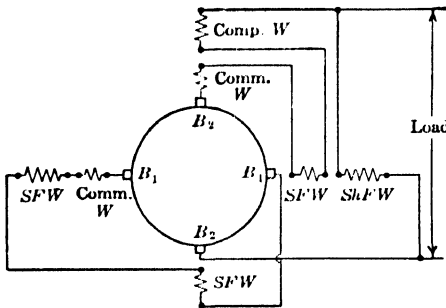


FIG. 9-6. Amplidyne with shunt and series field coils.

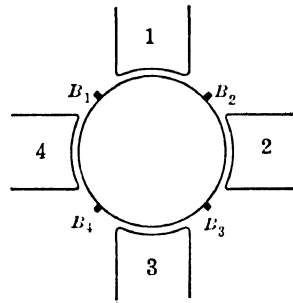


FIG. 9-7. Main poles and brushes of the 2-stage Rototrol.

and  $B_4$ . The armature has a 4-pole lap winding. *Control coils* are placed on poles 1 and 3. These coils will produce a flux in poles 1 and 3 but not in poles 2 and 4. Applying Faraday's law of induction to the armature winding, it will be found that the control flux induces an emf only between the brushes 1 and 3; the resultant emf induced by the control flux between the brushes  $B_2$  and  $B_4$  is zero. The *control coils and the armature between the brushes  $B_1$  and  $B_3$*  make the *first stage* of amplification. Fig. 9-8 shows the poles 1 and 3 with the control coils and the armature with the brushes 1 and 3. The polarity of the brushes is indicated in parentheses.

The voltage between the brushes 1 and 3 due to the 2-pole control flux is now used to excite four field coils placed on all four poles: 1, 2, 3, and 4. These field coils will produce a 4-pole flux distribution and emf's between the four brushes, as in the normal 4-pole d-c machine; if the brushes  $B_1$  and  $B_3$  (Fig. 9-7) have the polarity minus, the brushes  $B_2$  and  $B_4$  will have the polarity plus. The load is connected to the brush-pairs  $B_1B_3$



the four  $C$  coils cumulative compound, the four  $D$  coils will be differential compound, and the load current  $I_4$  will have no effect on the excitation of the 4-pole machine.

Now consider the current  $I_{2B_1B_3}$  produced by the control field in the 2-pole machine between the brushes  $B_1B_3$  (Fig. 9-9). This current flows through the  $C$ -coils and  $D$ -coils in the same direction. Since all coils are wound in the same direction, their mmf's *add up* on each pole producing a strong field for the 4-pole machine, i.e., for the second stage of amplification.

The arrangement described in the foregoing represents a pure amplifier, i.e., the load of the second stage is controlled exclusively by the excitation of the first stage (by the control coils). When the current in the control coils is zero, the output ( $2I_4$ ) of the machine is zero, i.e., under steady state conditions the amplifier delivers no power. It is usually desirable to use the machine as an amplifier for control purposes under transient conditions and as a normal generator under steady state conditions. This can be accomplished by arranging additional series coils on the four poles 1, 2, 3, and 4 and placing them in the load-circuit (for example in the negative load-lead connected between coils 4 and 5 in Fig. 9-9). Instead of series coils, shunt coils on poles 1, 2, 3, and 4 also can be used. As in the Amplidyne, the 2-stage Rototrol also needs a compensating winding to counteract the armature reaction which tends to weaken the control flux.

The type of machine described as the 2-stage Rototrol can be readily made to operate as a 3-stage amplifier. This extended design does not apply to the Amplidyne-type of amplifier.

## Chapter 10

---

### LOSSES IN D-C MACHINES HEATING AND COOLING

---

**10-1. Losses in the d-c machine.** Both main elements of the electric machine, the magnetic circuit and the conductors carrying the armature current, introduce a certain amount of machine losses.

Every electric machine is a *converter of power*: The motor converts electrical power into mechanical power, the generator converts mechanical power into electrical power, and the motor-generator therefore converts electrical power into electrical power. The losses in the machine caused by the flux and currents represent a power loss which reduces the efficiency of the machine. Because of this loss, the input to the machine must, of necessity, be larger than the output. The *efficiency* of a machine is defined as:

$$\eta = \frac{\text{output}}{\text{input}} = \frac{\text{input} - \text{losses}}{\text{input}} = \frac{\text{output}}{\text{output} + \text{losses}} = 1 - \frac{\text{losses}}{\text{input}}$$

The different kinds of losses which appear in the electric machine and especially the d-c machine are considered in the discussions which follow.

(a) *Losses due to the main flux.* Since the armature must rotate relative to the magnetic field in order that the emf be induced in the conductors, the particles of the armature iron are alternately magnetized, first in one direction and then in the other. This leads to the *hysteresis losses*. The magnitude of the hysteresis loss depends upon the area of the hysteresis loop, the number of magnetic cycles per second, and the quality of the iron.

As has been explained in Chapter 2, the armature iron is laminated perpendicular to the direction of the current flow in the armature conductors in order to avoid parasitic (eddy) currents in the iron running parallel to the conductors and causing losses. However, eddy currents do appear in the single laminations and produce heat losses. The eddy-

current losses depend upon the flux density, the number of magnetic cycles per second, the thickness of the laminations, and the quality of the iron.

According to Steinmetz, the hysteresis losses per unit weight can be represented by the following equation:

$$P_h = \sigma_h f B^{1.6} \quad (10-1)$$

where  $B$  is the maximum value of flux density and  $f = pn/120$  is the number of magnetic cycles per second.  $\sigma_h$  is a constant depending upon the quality of the iron. Steinmetz's equation yields low values for the losses when  $B > 65,000$  lines per sq in. A more accurate equation proposed by R. Richter is:

$$P_h = afB + bfB^2 \quad (10-2)$$

where  $a$  and  $b$  are constants corresponding to  $\sigma_h$ . In practice  $B > 65,000$  lines per sq in. In this case the first term of Eq. 10-2 can be disregarded and the following equation used:

$$P_h = \sigma_h \frac{f}{60} \left( \frac{B}{64,500} \right)^2 \quad \text{watts/lb} \quad (10-3)$$

The eddy-current losses are:

$$P_e = \sigma_e \left( \Delta \frac{f}{60} \frac{B}{64,500} \right)^2 \quad \text{watts/lb} \quad (10-4)$$

The constant  $\sigma_e$  depends upon the electric resistivity of the iron.  $\Delta$  is the thickness of the laminations in inches. The total iron losses per pound are

$$P_{h+e} = \sigma_h \frac{f}{60} \left( \frac{B}{64,500} \right)^2 + \sigma_e \left( \Delta \frac{f}{60} \frac{B}{64,500} \right)^2 \quad \text{watts/lb} \quad (10-5)$$

In practice, iron-loss curves are used which represent the loss in watts per pound as a function of the flux density  $B$ . Such curves for different kinds of iron are given at the end of the book. It follows from Eq. 10-5 that the iron loss is proportional to the square of the flux density  $B$ .

The specific loss taken from iron-loss curves or determined from Eq. 10-5 and multiplied by the weight of the teeth and core, respectively, will yield only a part of the iron losses produced by the main flux. This is due to many additional factors which increase the hysteresis as well as the eddy-current losses, but mainly the latter losses. Eq. 10-5 as well as the iron-loss curves presumes that the flux density is sinusoidally distributed in the gap. This is not the case in the d-c machine (see Fig. 3-19). If the flux distribution curve of the d-c machine is resolved into a Fourier

series, it will show a fundamental and considerable harmonics. These harmonics produce iron losses which are not contained in the iron-loss curves. Further factors which produce additional iron losses are: non-uniform distribution of the flux over the cross-section of the armature core, punching of the laminations, and filing of the laminations in order to remove the burrs. The increase of the iron losses, above the value yielded by the iron-loss curves or Eq. 10-5, due to all factors mentioned, may be as high as 40 to 60%.

The iron losses considered are those which appear in the armature iron. However, the main flux also causes iron losses in the poles, namely, on the *pole surface*. This is due to the fact that the *openings of the armature slots* distort the flux curve, Fig. 10-1.

The flux density is larger at points opposite the teeth than at points opposite the slots, owing to the difference of the magnetic reluctance. On the

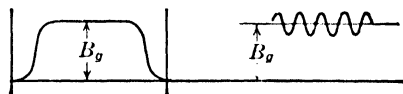


FIG. 10-1. Ripple in the flux distribution curve due to slot openings.

average flux density a ripple is superimposed, the wave length of which is equal to a slot pitch. This ripple moves with respect to the pole and induces eddy currents in the pole surface. The amplitude of the flux pulsations, i.e., the difference between the maximum and average flux densities, depends upon the slot opening. It is much larger in machines with open slots than in machines with semi-closed slots. In machines with open slots the pole-surface losses may be as high as 20 to 50% of the iron losses yielded by Eq. 10-5 or the iron-loss curves.

The existence of the main flux is associated not only with losses in the iron but also with *losses in the copper* of the field winding as well as of the armature winding, even when the latter is not loaded. In order to produce the main flux, a current-carrying field winding is necessary. The copper losses in the field winding are  $I_f^2 R_f$ , where  $I_f$  is the field current and  $R_f$  the total field resistance. The copper losses produced by the main flux in the armature winding are due to the fact that a small part of the main flux goes through the slots and armature conductors as shown in Fig. 10-2. Since the flux interlinkage with the armature conductors changes with the position of the poles, eddy currents are produced in the conductors, and mainly in those which lie in the top of the slot near the air-gap.

In d-c machines the armature winding often is held in place by bands which are placed in grooves made in the armature core. The main flux also induces eddy currents in the steel-wire bands.

(b) *Losses due to the armature current (load)*. The load current produces



copper losses in the armature winding and in the interpole winding which is connected in series with the armature winding. If there is a series field winding and compensating winding, these windings are also connected in series with the armature winding and the load current will produce copper losses in them. A considerable loss is produced by the armature current in the contact resistance between commutator and brushes. This loss is equal to

$$2\Delta V \times I_a = 2 \times I_a \text{ watts}$$

Additional copper losses in the armature winding are caused by the *cross-flux in the slot* (see Fig. 8-6). It has been shown in Art. 8-1, Fig. 8-1, that the current which flows in the conductors of a d-c machine is an alternating current which changes its sign each time the conductor

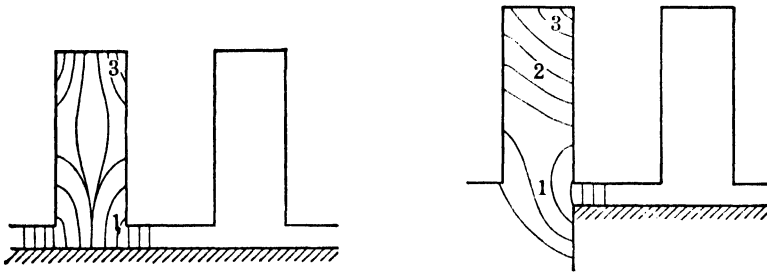


FIG. 10-2. Main flux in the slots of a saturated d-c machine.

changes from one armature path to another path. The frequency of the current is  $pn/120$ , just as for a-c machines (see Eq. 1-9). The change of current causes changes of the slot cross-flux which produce eddy currents in the conductor. These eddy currents are such that they force the current to flow only in the top part of the conductor (*skin effect*) thus decreasing the effective area of the conductor and increasing its resistance. As a result, the  $I^2R$  loss of the conductor is increased.

Another source of additional copper losses is the main flux distortion due to the armature mmf (see Fig. 4-6). The latter increases the flux density under one half of the pole and decreases it under the other half of the pole. This causes eddy-current losses in the armature conductors of the same kind as those produced by the main flux at no-load (see Fig. 10-2). These losses are negligible in machines in which the flux distortion is avoided by means of a compensating winding.

(c) *Friction and windage losses.* Because of rotation, bearing friction losses occur in all machines. The amount of the bearing friction losses

depends upon the pressure on the bearing, the peripheral speed of the shaft at the bearing, and the coefficient of friction between bearing and shaft.

In all commutator machines, brush friction losses must be considered in addition to the bearing friction losses. These brush friction losses are quite large. Like the bearing friction losses they depend upon the brush pressure, the peripheral speed of the commutator, and the coefficient of friction between commutator and brush.

Windage losses also occur because of rotation. The amount of these losses depends upon the peripheral speed of the rotor, the rotor diameter, the core length, and largely upon the construction of the machine.

(d) *No-load and load losses; stray load losses.* A part of the losses considered above occurs when the machine operates at no-load and the remainder appears when the machine is loaded. The former is called *no-load losses*; the latter, *load-losses*. Table 10-1 gives the losses which appear at no-load and the losses which are due to the load.

TABLE 10-1

No-load losses	Iron losses in the armature due to the main flux (1)	Pole surface losses due to slot openings (2)	Windage and bearing friction losses (3)	Brush friction losses at the commutator (4)	Losses in the conductors due to the main flux (5)	Losses in the bands due to the main flux (6)
Load losses	$I^2R$ losses in all windings (1)	Skin-effect losses in the armature conductors (2)	Electric loss in the brush contacts (3)	Loss in the armature conductors due to flux distortion (4)	Losses in the short-circuited winding elements (5)	Iron loss due to flux distortion (6)

The *additional* losses due to the load (items 2, 4, 5, and 6 of the second row) are called *stray load-losses*.

(e) *Examples of loss distribution and efficiencies.* In the following tabulations is shown the loss distribution of two d-c machines, one of which is a 3-HP compound-wound motor and the other a 250-kw compound-wound generator.

<i>Compound Motor</i>		<i>Compound Generator</i>	
3 HP, 115 volts, 1150 rpm		250 kw, 240 volts, 1200 rpm	
4 poles, open type		6 poles, open type	
Armature current	= 24 amp	Armature current	= 1044 amp
Shunt field current	= 0.7 amp	Shunt field current	= 4.25 amp
<hr/>		<hr/>	
Armature $I^2R$	= 210 watts		3800 watts
Interpole field $I^2R$	= 35		1600 (6 interpoles)
(2 interpoles)			
Series field $I^2R$	= 25		400
Brush contact loss	= 48		2100
Stray load loss	= 0		2500
Shunt field loss	= 80		1000
Iron (core) loss	= 100		4400
Brush friction loss	= 20		2000
Bearing friction and			
windage loss	= 80		2500
	598 watts		20,300 watts
<hr/>		<hr/>	
Input = $(24 + 0.7)115 = 2840$ watts		Output = $240 \times 1.04 = 250$ kw	
Output = $2840 - 598 = 2242$ watts		Efficiency = $100 \times \frac{250}{250 + 20.3} = 92.5\%$	
= 3.0 HP			
Efficiency = $100 \frac{2242}{2840} = 78.9\%$			

**10-2. Heating and cooling of d-c machines.** The losses treated in the previous article are of different kinds, but all of them appear in the electric machine in the form of heat. Since the losses are produced mainly in the active parts of the machine, i.e., in the iron which carries the flux and in the conductors which carry the currents, the heat appears mainly in these machine parts. The result is an increase in the temperature of the iron and copper above that of the surroundings.

Tests on various kinds of *insulating* materials have shown that for each material there is a safe continuous-operating temperature which cannot be exceeded without impairing the life of the material. Table 10-2 shows the limiting temperatures for the different kinds of insulation as specified by the AIEE.

The table distinguishes four classes of insulation. Class O insulation consists of cotton, silk, paper, and similar organic materials when neither impregnated nor immersed in oil. Class A insulation consists of cotton, silk, paper, and similar organic materials when impregnated or immersed in oil; also enamel, as applied to conductors. Class B insulation consists of inorganic materials, such as glass, or mica and asbestos in built-up form, combined with binding substances.

A new development in the field of insulating materials is represented by the *silicon* binders and varnishes. These binders and varnishes when used together with the inorganic materials of Class B insulation yield an

TABLE 10-2

Class	Material Classification	Limiting Temperatures, °C for Industrial Apparatus		
		Ther- mometer	Embedded Detector	Hot- spot
O Untreated organics	Untreated fabrics of cotton, silk, linen. Untreated paper, fiber, wood, etc.	75	85	90
A Treated or impregnated organics	Oil, varnish, wax, or compound impregnated fabrics or sheets of cotton, silk, linen, paper, wood, fiber; oil, varnish, bakelite, organic filler compounds.	90	100	105
B Treated or impregnated inorganics	Asbestos, fiberglas, mica tape, oxide films, inorganic fillers, asbestos boards. (A limited amount of organic materials may be used for binding purposes.)	110	120	130
H Treated or impregnated inorganics	Mica, asbestos, fiberglas and similar inorganic materials in built-up form with binding substances composed of silicone compounds, or materials with equivalent properties; silicone compounds in rubbery and resinous forms, or materials with equivalent properties in minute proportions. Class A material may be used only where essential for structural purposes during manufacture.	—	—	180

insulation which is able to withstand much higher temperatures than the standard Class B insulation for the same life of the winding (see class H insulation).

The temperature rise of any part of the machine decreases as the heat conductivity to the surface of the machine part and the heat transfer from the surface of the machine part to the cooling medium (normally air, or hydrogen in some large machines) are increased. *High heat con-*

*ductivity* of all materials used, i.e., of the laminations, conductor material, and insulating materials, and *high heat transfer* from the surfaces of windings and iron to the cooling medium are the necessary conditions for low temperature rises. The heat conductivity of the insulating materials is low.

There are two ways for the heat transfer from the surface to the cooling medium to occur: (1) through radiation and (2) through convection, i.e., heat transportation by the moving air or hydrogen. The radiation is

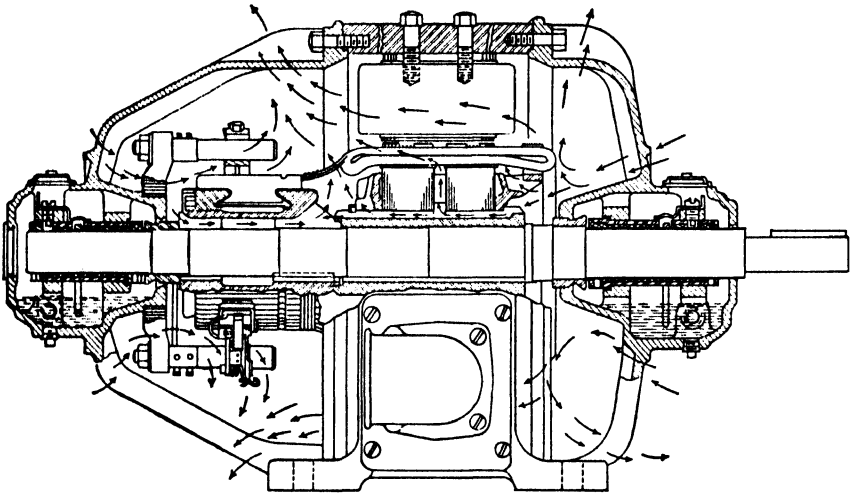


FIG. 10-3. Air flow in an open type d-c machine.

affected by the frame. In totally enclosed machines without an air supply from the outside, convection is also affected only by the frame. In open-type machines and in totally enclosed machines with an air supply from the outside, the winding and the laminations, as well as the frame, are included in the heat transfer by convection. The heat transfer by convection is much larger than that by radiation.

Sufficient ventilation (cooling by convection) of the machine is necessary in order to keep the temperature rises of the iron and copper within the prescribed limits. This ventilation can be achieved when care is taken in the design to insure that good heat transfer will take place from the active iron and copper, where the losses originate, to the cooling medium. For ventilating purposes, the armatures of machines with cores longer than 5 inches are divided into stacks of laminations about 2 in. wide, separated by  $\frac{3}{8}$ -in. ventilating ducts through which the air is forced (see Fig. 2-5). Forcing air through radial ducts facilitates the transfer to the air of the heat due to the losses in the iron and also in the embedded

parts of the windings. Sufficient air circulation must also be present around the end-windings and field coils so that the heat developed there can be transferred to the air.

Of the various kinds of machine construction, the open machine, i.e., one in which there is no restriction to ventilation other than that necessitated by good mechanical construction, is preferred. However, on account of the environment, more or less complete enclosure may be necessary. The different types of enclosures are defined in the NEMA (National Electrical Manufacturers Association) Standards.

Fig. 10-3 shows the air flow in an open-type d-c machine.

### PROBLEMS

1. A 420-kw, 600-volt, 600-rpm long-shunt-connected compound generator has an armature +interpole resistance of 0.03 ohm, a series field resistance of 0.01 ohm, and a shunt field resistance of 45 ohms. The total friction and windage loss is 7 kw, the core loss 3.5 kw, and the stray load loss 1.5 kw. Determine the driving torque and the full-load efficiency.

2. A 400-kw, 600-volt shunt generator has an armature-circuit resistance of 0.032 ohm and a field resistance of 50 ohms. The total friction and windage loss is 3.7 kw, the core loss 3.5 kw, and the stray load loss 4 kw. Determine the generator efficiency at rated output.

3. Assuming the iron losses and the friction and windage losses to be constant (equal to rated load values), and the stray load losses to vary as the square of the armature current, determine the efficiency of the generator in Problem 2 for  $\frac{1}{4}$ ,  $\frac{1}{2}$ ,  $\frac{3}{4}$ ,  $1\frac{1}{4}$ , and  $1\frac{1}{2}$  rated load current. Draw the curve of efficiency vs. armature current and estimate the load at which maximum efficiency occurs. Assume  $I_f$  constant.

4. A 120-volt shunt motor has an armature-circuit resistance of 0.125 ohm and a field resistance of 100 ohms. At no-load it takes 3 amp at 120 volts. At full-load, 120 volts, it takes 40 amp from the line. The stray load loss is 50 watts. Determine the motor output and efficiency at full-load.

5. A shunt motor is tested with a Prony brake, and the following data are recorded: terminal voltage 120, line current 90 amp, speed 1250 rpm, scale reading 23 lb, scale arm 25 in. The armature resistance, including the stabilizing winding and interpole winding, is 0.07 ohm, and the shunt field resistance is 50 ohms. The stray load loss is 150 watts, and the total friction and windage loss is equal to the core loss. Determine: (a) the motor efficiency; (b) the internal power developed; (c) the no-load armature current.

# Chapter 11

## TRANSFORMER CONSTRUCTION

Although the transformer is not classified as an electric machine, the principles of its operation are fundamental for the induction motor and synchronous machine. For this reason it is treated ahead of the a-c machines. Since a-c electric machines are normally built for low frequencies only the low-frequency power transformer will be considered in this text. For transformers operating at higher frequencies, such as those used in transformer-coupled audio amplifiers, and as impedance matching devices in communication circuits, see the listed references.

**11-1. Transformer types.** The construction of single-phase transformers may be divided into three main types: *core type*, *shell type*, and *spiral-core type*. In all types the core is constructed of transformer *sheet steel*

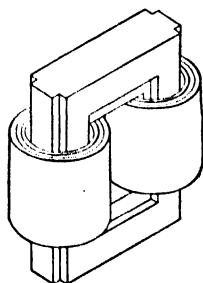


FIG. 11-1a. Coils and laminations of a core-type transformer.

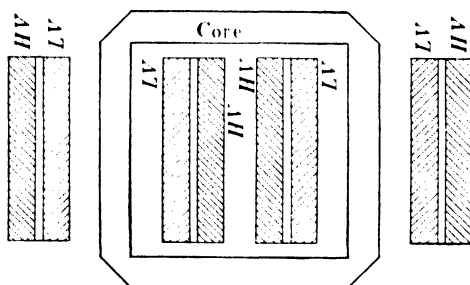


FIG. 11-1b. High- and low-voltage coil grouping of a core-type transformer.

assembled to provide a continuous magnetic circuit with a minimum of air-gap included. The steel used is of high silicon content, sometimes heat-treated to produce a high permeability and a low core loss at the operating flux density.

In core- and shell-type transformers the individual laminations are L or E shaped. The laminations are varnished or coated to insulate them from each other and thereby reduce the circulating currents. Fig. 11-1a shows the general assembly of laminations and coils of the core-type transformer. Fig. 11-1b shows the manner in which high- and low-

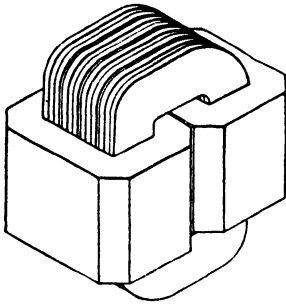


FIG. 11-2a. Coils and laminations of a shell-type transformer.

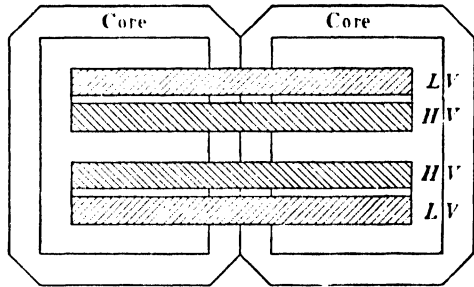


FIG. 11-2b. High- and low-voltage coil grouping of a shell-type transformer.

voltage coils are grouped together on the legs of a core-type transformer. Figs. 11-2a and 11-2b show the general arrangement of coils and laminations in the shell-type transformer. The shell-type transformer may have a simple form of core such as in Fig. 11-2a or a distributed form

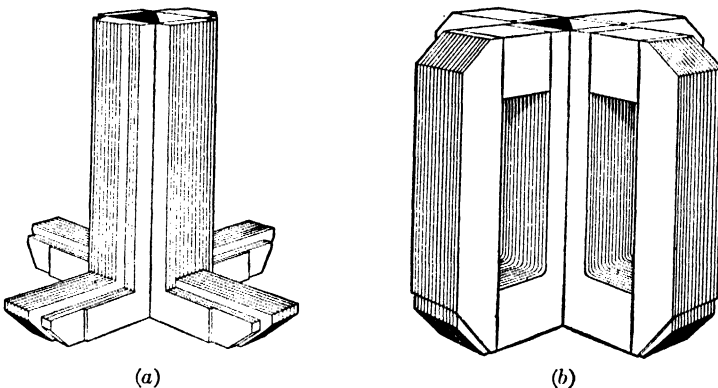


FIG. 11-3. Core construction of a distributed shell-type transformer.

(cruciform). In the shell-type transformer the magnetic circuit encloses the windings. Figs. 11-3a and 11-3b show the core of the *distributed* shell-type transformer; Fig. 11-4 is a view of such a transformer showing



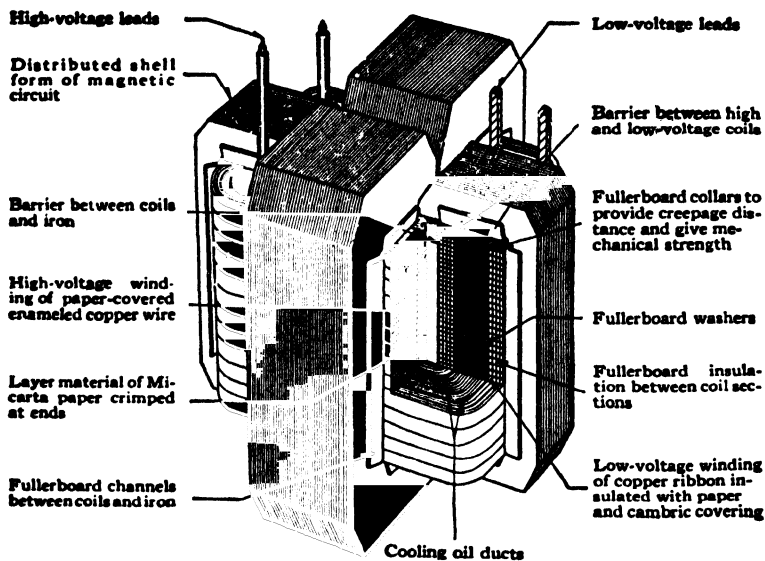


FIG. 11-4. Distributed shell-type (cruciform) transformer showing core, coils, cooling ducts, and insulation.

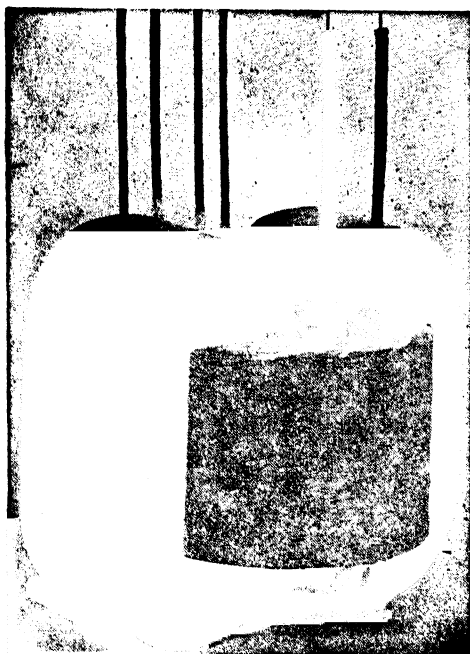


FIG. 11-5. Core and windings of a 10-kva spiral-core transformer.

laminations, coils, insulation, cooling ducts, and high- and low-voltage leads.

The choice of core- or shell-type construction is usually one of cost, for similar characteristics can be obtained with both types. For high-voltage transformers or for multi-winding design some manufacturers prefer the shell-type construction. Usually in this type the iron path is shorter and the mean length of coil turn is longer than in a comparable core-type design. Both core and shell forms are used, and selection is based upon many factors such as voltage rating, kva rating, weight, insulation stress, mechanical stress, and heat distribution.

The spiral core transformer shown in Fig. 11-5 is the newest development in core construction. The core is assembled either of a *continuous* strip of transformer steel wound in the form of a circular or elliptical cylinder, or of a group of short strips assembled to produce the same elliptical-shaped core. By using this construction the core flux always follows along the grain of the iron. Cold-rolled steel of high silicon content enables the designer to use higher operating flux densities with lower loss per pound. The higher flux density reduces the weight per kva.

**11-2. Windings.** The coils used in transformers are form wound and are of the *cylindrical* or *disc* type. The general form for these types may be circular, oval, rectangular, etc. Fig. 11-6 shows a multi-coil rectangular

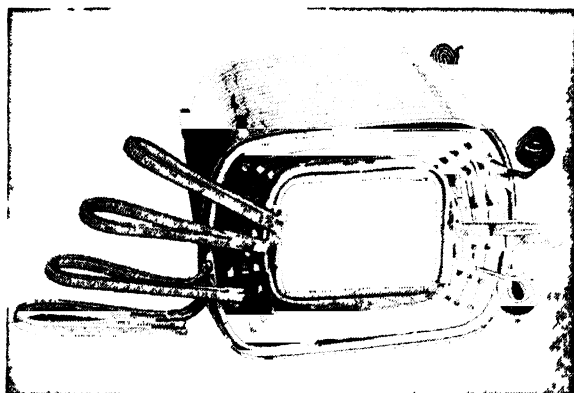


FIG. 11-6. Cylindrical or helical type of form wound coil (multi-coil-winding).

cylindrical type winding, and Fig. 11-7 shows the manner in which a large round cylindrical coil is wound. The circular cylindrical coil has greater mechanical strength and is employed in most core-type power transformers. Cylindrical coils are wound in helical layers with the

layers insulated from each other by paper, cloth, micarta board, or cooling oil ducts. Figs. 11-1a and 11-1b show the general arrangement of these coils with respect to the core. Insulating cylinders of fuller board separate the cylindrical windings from the core and from each other. Since the low-voltage winding is the easiest to insulate, it is placed nearest the core.

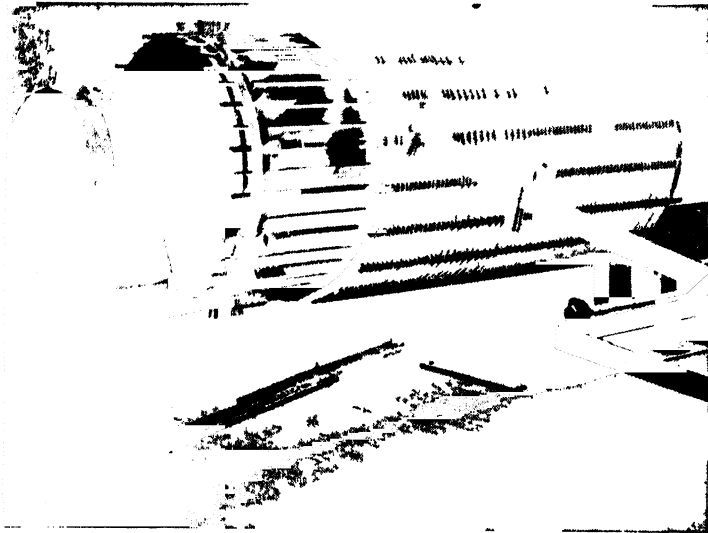


FIG. 11-7 Winding a round cylindrical coil for a 55 000 l v a 287 500 16 320 volt transformer

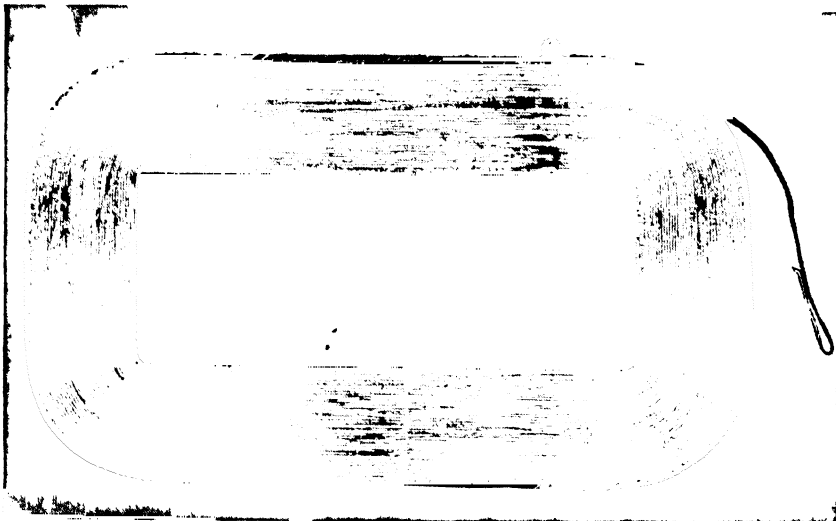


FIG. 11-8 Disc or pancake coil

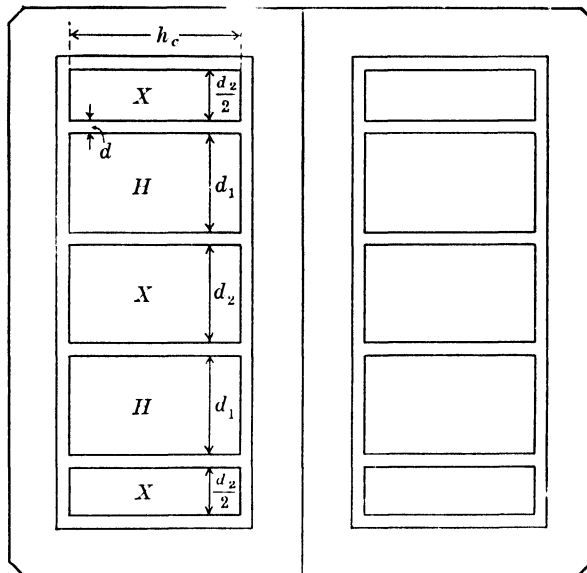


FIG. 11-9. Shell-type transformer showing disc coils.

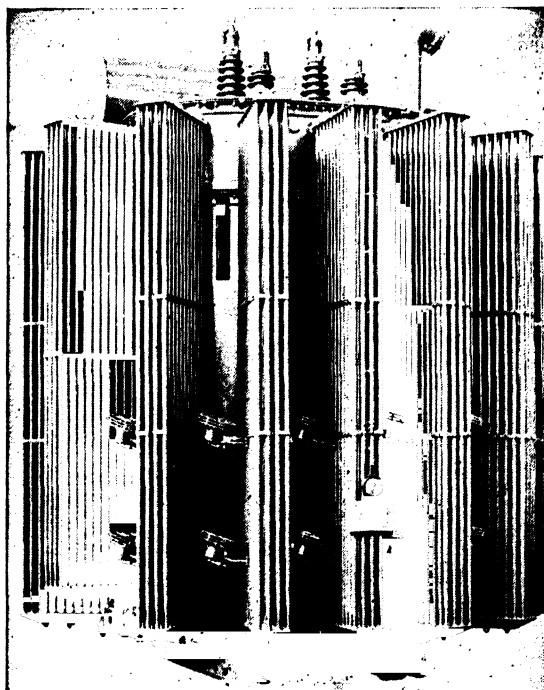


FIG. 11-10. Three-phase 31,250-kva transformer with radiators and cooling fans.

Disc coils, such as that shown in Fig. 11-8, may be of one turn per layer or many turns per layer. Multi-layer discs have the separate layers insulated from each other by paper. A complete winding consists of stacked discs with insulation spaces between the coils as shown in Fig. 11-9; the spaces form horizontal cooling and insulating oil ducts.

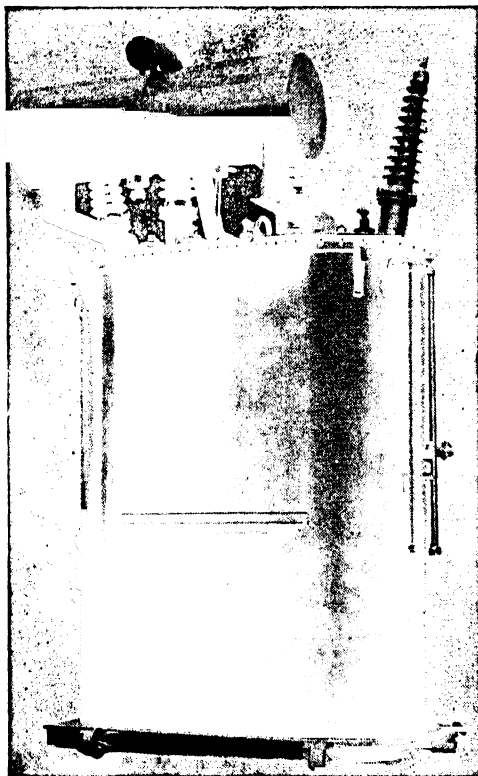


FIG. 11-11. Three-phase 9000-kva, 67,560/6,900-volt water-cooled transformer with conservator tank.

The low- and high-voltage windings are subdivided into a number of discs and stacked alternately, with the end discs being a part of the low-voltage winding. The leakage reactance is reduced if the end discs contain one half as many turns as the remaining low-voltage discs.

Cores and coils must be provided with mechanical bracing to prevent movement and possible insulation damage. Good bracing also reduces vibration and noise during operation.

**11-3. Cooling.** Transformers may be air-cooled, oil-cooled, or water-cooled. Whatever the method of cooling, the essential problem is that of

the heat transfer from the iron and copper of the transformer to the cooling medium (see Art. 10-2). This heat transfer is accomplished by natural oil or air convection, forced oil or air convection, oil-to-air heat transfer or oil-to-water heat transfer. The tanks may be smooth-sided or corrugated to increase the radiating surface area. Fig. 11-10 shows the use of cooling fans with external radiators. Fig. 11-11 shows a water-cooled transformer with an oil conservator tank. The conservator tank serves as an oil reservoir and also limits the surface area of oil exposed to air, thus reducing the formation of sludge within the oil: with the conservator tank, the main tank can be completely filled with oil. Although the oil is used as a cooling medium, it is also employed for its *insulating qualities* and must be dirt and moisture free. Non-inflammable liquids sold under trade names of Pyranol, Inertol, etc. have been developed to remove the hazard of fire associated with oil.

## Chapter 12

### THE TRANSFORMER AT NO-LOAD

The single-phase transformer described in the following paragraphs consists of two electric circuits and one magnetic circuit. Therefore its study must be based on Kirchhoff's mesh law for the electric circuits and on the circuital law of the magnetic field (Ampère's law) for the magnetic circuit.

Once Kirchhoff's mesh equations for the electric circuits and the relations following from Ampère's law are established, the phasor diagram and the equivalent circuit of the transformer can be readily determined.

However, a preliminary study is necessary in order to set up the basic relations of the electric and magnetic circuits.

The transformer will be considered first at no-load, then under load.

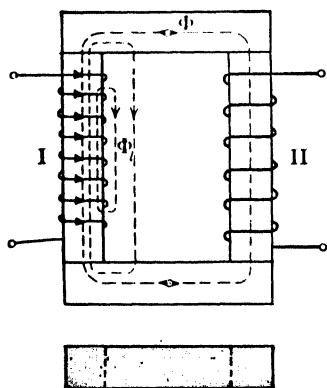


FIG. 12-1. Elementary single-phase transformer.

**12-1. The transformer primary.** Fig. 12-1 shows an iron core assembled of laminations; two coils are wound on the legs. Coil II, the secondary winding, will be considered open in this article. If an alternating voltage is impressed upon the primary winding, coil I, an alternating current  $I_0$  will flow in it, and this current will produce an alternating magnetic flux.

The current  $I_0$ , the *no-load current*, will lag behind the impressed voltage  $V_1$  by an angle  $\varphi_0$  which is about  $90^\circ$ . The active component of  $I_0$ , i.e.,  $I_0 \cos \varphi_0$ , supplies the hysteresis and eddy current losses ( $P_{h+c}$ ) in the core iron and the small amount of copper losses in the primary winding. The reactive component of  $I_0$ , i.e.,  $I_0 \sin \varphi_0$ , which is much larger than the active component  $I_0 \cos \varphi_0$ , is necessary to sustain the alternating

flux. This reactive current  $I_0 \sin \varphi_0$  is small in comparison with the rated primary current of the transformer, because the magnetic circuit of the transformer consists almost entirely of iron (the air gaps at the joints amount to only about 0.0010 to 0.0015 in.). Such a magnetic circuit has a small reluctance and requires a low magnetizing current in order to produce the flux.

The flux alternates at the same frequency as the current and induces an emf of self-induction in the primary winding, coil I. It is expedient to divide this emf of self-induction into two parts corresponding to the two different parts of the flux. By far the greatest part of the flux lines produced by coil I (part  $\Phi$ ) is in the iron. Another part ( $\Phi_l$ ) of the flux, small in comparison to that in the iron, exists in parallel paths through the air as indicated in Fig. 12-1. The part of the flux in the air is directly proportional to the current (see Art. 1-1b) because the path for these lines consists essentially of air, for which the permeability is a constant ( $\mu = 1$ ); on the other hand, the relationship existing between the current and the flux  $\Phi$  in the iron is given by the magnetization curve for the particular kind of laminations used, which has a non-linear character. As has been explained previously (Art. 1-1b), the coefficient of self-inductance is not a constant for the flux in the iron.

The flux in the air is referred to as the *leakage flux* ( $\Phi_l$ ) and that in the iron as the *main flux*  $\Phi$ . It is only the main flux which links with the turns of secondary coil II.

Dividing the emf of self-induction into two components, the component due to the leakage flux is  $-j\omega L_l I$  (Eq. 1-19a); the component due to the main flux will be denoted by  $E$ . Thus Kirchhoff's mesh law for the primary circuit is

$$\mathbf{V}_1 + \mathbf{E}_1 - j\omega L_l \mathbf{I}_1 = \mathbf{I}_1 r_1 \quad (12-1)$$

where  $L_l$  is the coefficient of self-inductance of the primary *leakage* flux and  $r_1$  is the ohmic resistance of the primary winding. The subscript 1 indicates the primary circuit. Since no load is considered,  $I_1 = I_0$ . Introducing the *primary leakage reactance*  $x_1$ ,

$$\omega L_l = x_1 \quad (12-2)$$

Eq. 12-1 becomes

$$\mathbf{V}_1 + \mathbf{E}_1 - j\mathbf{I}_1 x_1 = \mathbf{I}_1 r_1 \quad (12-3)$$

or

$$\mathbf{V}_1 = -\mathbf{E}_1 + j\mathbf{I}_1 x_1 + \mathbf{I}_1 r_1 \quad (12-3a)$$

In the latter form  $-E_1$  is the component of the primary voltage necessary to overcome the emf induced in the winding by the main flux;  $+jI_1 x_1$  is



the component of the primary voltage necessary to overcome the emf induced by the primary leakage flux; and  $I_1 r_1$  is the component of the primary voltage necessary to drive the current  $I_1$  through the resistance  $r_1$ .

Eq. 12-3a also can be interpreted in the following way: the voltage impressed on the primary winding I is balanced by the negative value of the emf induced in it by the main flux,  $-E_1$ , and by the voltage drops due to the leakage reactance and the resistance.

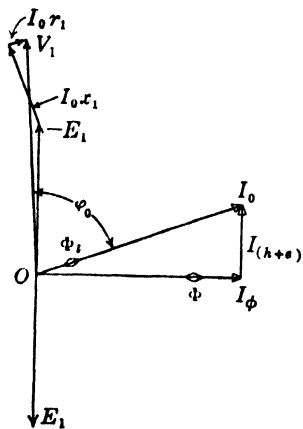


FIG. 12-2. No-load phasor diagram.

It will be seen later (Chapter 13) that only the main flux  $\Phi$  is useful in transferring power from the primary to the secondary winding, while the leakage flux does not contribute to the power transfer. Likewise, only the emf  $E_1$  is useful and not the emf produced by the leakage flux.

The phasor diagram of the voltages corresponding to Eq. 12-3a is shown in Fig. 12-2.

The emf  $E_1$  induced in coil I by the main flux  $\Phi$  lags this flux by  $90^\circ$ . To produce the flux  $\Phi$  a current component *in phase with*  $\Phi$ , i.e., a current component leading  $E_1$  by  $90^\circ$ , is required. Another current component, in phase with  $-E_1$ , is required to supply the hysteresis and eddy current losses due to the main flux. The first current component, designated by  $I_\phi$ , is the reactive component of the magnetizing current  $I_m$ ; the second current component, designated by  $I_{h+c}$ , is the active component of the magnetizing current  $I_m$ . Thus

$$I_m = I_\phi + I_{h+c} \quad (12-4)$$

The active component of the no-load current  $I_0$ , namely,  $I_0 \cos \varphi_0$ , is larger than  $I_{h+c}$  by a small amount corresponding to the copper loss  $I_0^2 r_1$  in the primary winding. However, the copper loss at no-load is negligible in comparison with the hysteresis and eddy current losses in the core iron and, therefore, with a very close approximation

$$I_0 \approx I_m \quad (12-5)$$

If the reactive component  $I_\phi$  of the magnetizing current is drawn along the horizontal (Fig. 12-2) and is directed to the right, the flux  $\Phi$  is in phase with  $I_\phi$ ; the emf  $E_1$  lags  $\Phi$  by  $90^\circ$  and is therefore directed downward; and consequently the voltage component necessary to overcome  $E_1$  ( $= -E_1$ ) leads the flux and the current  $I_\phi$  by  $90^\circ$  and is directed upward. The leakage reactance drop  $I_0 x_1$ , i.e., the component of the

terminal voltage necessary to overcome the emf due to the leakage flux, is perpendicular to  $I_0$  and leads  $I_0$  by  $90^\circ$ , and the component to overcome the ohmic resistance drop  $I_0 r_1$  is in phase with the current. The geometric sum of the three voltages,  $-E_1$ ,  $I_0 x_1$ , and  $I_0 r_1$ , is the primary applied voltage  $V_1$ . The phase displacement angle between the current  $I_0$  and the terminal voltage  $V_1$  is nearly  $90^\circ$ ;  $I_0$  is almost a pure reactive current with respect to  $V_1$ . It should be realized that the values of  $I_0 r_1$  and  $I_0 x_1$  are in reality very much smaller in proportion to  $-E_1$  and  $V_1$  than those shown in Fig. 12-2.

**12-2. The emf induced by the main flux at no-load ( $E_1$ ).** It follows from the phasor diagram (Fig. 12-2) that the main flux is produced by the current  $I_\phi$ . Corresponding to Eq. 1-13

$$N_1 \Phi = L_m \sqrt{2} I_\phi \quad (12-6)$$

where  $L_m$  is the coefficient of self-inductance for the main flux. Since the path of the main flux lies in iron,  $L_m$  is not a constant but depends upon the magnitude of  $I_\phi$ , as has been explained in Art. 1-1 and Art. 12-1.

It follows from Eqs. 1-10 and 12-6 that

$$E_1 = -j\omega N_1 \Phi \frac{10^{-8}}{\sqrt{2}} = -j\omega L_m I_\phi = -jx_m I_\phi \quad (12-7)$$

This expression for the emf induced by the main flux  $E_1$  is in accordance with the expression for emf induced by the leakage flux,  $-j\omega L_{l1} I_0 = -jx_1 I_0$ , with the difference that the magnitude of  $x_m$ , just as the magnitude of  $L_m$ , depends upon the saturation of the iron.  $x_m$  is called the *main flux reactance*.

Eqs. 12-6 and 12-7 characterize the *magnetic circuit* of the transformer. Eq. 12-6 can be derived from the circuital law of the magnetic field (Ampère's law), as shown in App. 1.

In order to get the relation between  $E_1$  and the magnetizing current  $I_m = I_\phi + I_{h+c}$  (Fig. 12-2), Eq. 12-7 is written as

$$I_\phi = jc_1 E_1$$

Further, from Fig. 12-2,

$$I_{h+c} = -c_2 E_1$$

so that

$$I_m = I_\phi + I_{h+c} = -E_1 (c_2 - jc_1)$$

The quantity in parentheses is an admittance. It is called the *main flux admittance* and will be denoted by  $Y_m$ . Instead of  $c_1$  and  $c_2$  the symbols

$g_m$  and  $b_m$  will be used; thus

$$\mathbf{I}_m = -\mathbf{E}_1 \mathbf{Y}_m = -\mathbf{E}_1 (g_m - jb_m) \quad (12-8)$$

$g_m$  is the *main flux conductance*;  $b_m$  is the *main flux susceptance*. Writing

$$-\mathbf{E}_1 = \frac{\mathbf{I}_m}{\mathbf{Y}_m} = \mathbf{I}_m \mathbf{Z}_m = \mathbf{I}_m (r_m + jx_m) \quad (12-9)$$

$r_m$  takes into account the iron losses produced by the main flux and  $x_m$  is the same as in Eq. 12-7; neglecting the iron losses ( $r_m = 0$ ,  $I_{h+c} = 0$ ,  $I_m = I_\phi$ ), Eq. 12-9 becomes identical with Eq. 12-7.  $\mathbf{Z}_m$  is the *main flux impedance*. Since  $\mathbf{Z}_m = 1/\mathbf{Y}_m$

$$r_m = \frac{g_m}{g_m^2 + b_m^2} \quad x_m = \frac{b_m}{g_m^2 + b_m^2} \quad (12-10)$$

**12-3. The transformer secondary.** Consider coil II, the secondary winding, with the winding open (no-load) just as in the foregoing discussion. The lines of force of the alternating main flux  $\Phi$  go through the iron, link this secondary winding, and induce an emf  $E_2$  in it. Since the main flux and its frequency are the same for both primary and secondary windings, the emf's induced in the two windings are respectively proportional to their numbers of turns  $N_1$  and  $N_2$ :

$$\frac{E_1}{E_2} = \frac{N_1}{N_2} = a \quad (12-11)$$

According to Eq. 1-11,

$$E_1 = 4.44 N_1 f \Phi 10^{-8} \text{ volt} \quad (12-12)$$

$$E_2 = 4.44 N_2 f \Phi 10^{-8} \text{ volt} \quad (12-13)$$

The ratio  $N_1/N_2$  is called the *ratio of transformation*. Since the no-load current  $I_0$  is small, the resistance drop as well as the leakage reactance drop is small at no-load, and  $E_1$  is almost equal to the terminal voltage  $V_1$ . Accordingly, the ratio of transformation is often given with sufficient accuracy by the ratio of terminal voltages at no-load:

$$\frac{N_1}{N_2} = \frac{E_1}{E_2} \approx \frac{V_1}{V_2} \quad (12-14)$$

### PROBLEMS

1. A transformer having 480 primary turns and 120 secondary turns takes a power input of 80 watts and a current of 1.40 amp when the primary is connected to a 120-volt, 60-cycle line and the secondary is on open circuit. The primary resistance is 0.25 ohm. Determine the iron loss in watts, the no-load power factor, and the maximum

core flux assuming the resistance and reactance drops as negligible. Draw the phasor diagram.

2. A 5-kva, 110/220-volt, 60-cycle transformer has 120 turns on the primary winding, and a core having a cross-section of 4.70 sq in. and a mean length of 31 in. Using the curves for transformer steel given in the Appendix, determine the effective value of the magnetizing current and the maximum value of the flux density.

3. If the flux density in a given 2300/230-volt, 60-cycle transformer is not to exceed 60,000 lines per sq in., determine the number of primary turns when the core cross-section is 26.5 sq in.

4. A 7.5-kva, 1100/110-volt, 60-cycle transformer is connected across an 1100-volt line with the secondary open. The power input is 120 watts and the no-load current  $I_0$  is 0.40 amp.  $N_1 = 800$  turns,  $N_2 = 80$  turns,  $r_1 = 4$  ohms and  $r_2 = 0.04$  ohm.  
(a) If the primary leakage reactance drop is neglected, what is the magnitude of the primary and secondary induced voltages? (b) Draw the phasor diagram to scale.  
(c) What is the maximum value of core flux?

5. If, in Problem 4, the primary leakage flux at no-load is 0.15% of the total flux calculated in part (c), determine the primary and secondary induced voltages. Draw the phasor diagram to scale.

6. A 50-kva, 2300/230-volt, 60-cycle transformer takes 200 watts and 0.30 amp at no-load when 2300 volts is applied to the high-voltage side. The primary resistance is 3.5 ohms. Neglecting the leakage reactance drop determine: (a) no-load power factor; (b) primary induced voltage  $E_1$ ; (c)  $I_{h+e}$ ; (d)  $I_\phi$ . Draw the phasor diagram to scale.

7. A 1000-kva, 25-cycle, 27,000/2200-volt transformer is designed to operate at a maximum flux density of 75,000 lines per sq in. and an induced voltage of 20 volts per turn. Determine the primary turns  $N_1$ , secondary turns  $N_2$ , and the cross-section area of the core in square inches.

8. Repeat Problem 7 for a 25-cycle, 66,000/1100-volt transformer.

9. The core of a 500-kva transformer has a mean length of 66 in. and a cross-section of 260 sq in. The primary consists of four identical coils.

(a) If 15,000 volts at 60 cycles is impressed across the four primary coils in series, and the maximum flux density is to be 75,000 lines per sq in., determine  $I_{h+e}$ ,  $I_\phi$ ,  $I_0$  and the no-load power factor. Use the curves for transformer steel given in the Appendix.

10. Repeat Problem 9 if 7500 volts at 60 cycles is impressed across two coils connected in series.

11. Repeat Problem 9 if 3750 volts at 60 cycles is impressed across the four coils in parallel.

## Chapter 13

### THE TRANSFORMER UNDER LOAD

**13-1. The behavior of the transformer primary under load.** Consider the transformer to be loaded, for example, with a resistor placed across the secondary winding. Since an induced emf ( $E_2$ ) exists at the terminals of the secondary winding, a current  $I_2$  will flow through the load resistance and the secondary winding. When the transformer losses (copper losses in both windings and hysteresis and eddy-current losses in the core iron) are disregarded, then, according to the law of conservation of energy, the power taken by the primary winding from the lines is equal to the power delivered to the external circuit placed across the secondary winding: i.e., if the secondary is loaded, the current taken by the primary winding from the lines must *increase* or *decrease* as the secondary load current is *increased* or *decreased*. The transfer of power from the primary to the secondary is accomplished by means of the main flux  $\Phi$ . The main flux is an *indispensable element in the transformer* as well as in all electric machines.

As a result of the increase in the primary current due to the load, the three components of voltage which balance the primary terminal voltage (Eq. 12-3a) also change: the resistance drop and the leakage reactance drop are greater, and therefore the voltage  $E_1$  induced by the main flux  $\Phi$  is correspondingly smaller. However (in ordinary power transformers) the resistance and leakage reactance drops are usually small in comparison to the emf  $E_1$  even at rated load, so that  $E_1$  has approximately the same value for the loaded as well as the unloaded transformer; since the main flux  $\Phi$  is determined by  $E_1$  (see Eq. 12-12), this means that the main flux  $\Phi$  varies only slightly between no-load and full-load. Therefore, practically the same magnetomotive force ( $I_\phi N_1$ , see Fig. 12-2) and the same magnetizing mmf ( $I_m N_1$ ) are necessary in the primary to produce the main flux  $\Phi$  under conditions of load and no-load. The main flux  $\Phi$  is

largest at no-load and smallest under short-circuit conditions (see Art. 17-2).

When the secondary is loaded, *two mmf's act on the transformer*, the mmf of the primary winding and the mmf of the secondary winding; the magnitude of the main flux is determined by the *resultant* of these two mmf's. As explained, this mmf changes little between no-load and full-load. Fig. 13-1 shows the mmf diagram of a loaded transformer in which, corresponding to a resistive load, the secondary current  $I_2$  lags the emf  $E_2$  induced in the secondary winding by the main flux.  $E_2$  as well as  $E_1$  lags behind the flux  $\Phi$  by  $90^\circ$ . The geometric sum of the primary mmf  $I_1 N_1$  and the secondary mmf  $I_2 N_2$  yields the resultant magnetizing mmf  $I_m N_1$  which is necessary to produce the main flux  $\Phi$ .

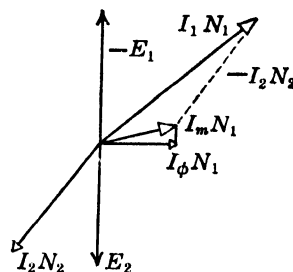


FIG. 13-1. Mmf diagram under load.

Since the reluctance of the magnetic circuit of the transformer is comparatively low, the magnetizing mmf is only about 5 to 10% of the primary mmf under conditions of rated load; this is the same as saying that the magnetizing current is about 5 to 10% of the rated line current. Therefore, it can be approximated that  $I_1 N_1 \approx I_2 N_2$ , or

$$\frac{I_2}{I_1} \approx \frac{N_1}{N_2} = \frac{E_1}{E_2} \quad (13-1)$$

The currents in the two windings, therefore, are approximately inversely proportional to the induced emf's. This is in conformity with the law of conservation of energy (disregarding losses), for according to this law  $V_1 I_1 \cos \varphi_1 = V_2 I_2 \cos \varphi_2$ . It will be seen from the following text that  $\cos \varphi_1 \approx \cos \varphi_2$  for the fully loaded transformer.

**13-2. Reduction of the secondary current, voltage, and parameters to the primary.** The mmf diagram of Fig. 13-1, the phasor diagram of the loaded transformer, and its equivalent circuit become simpler if the assumption is made that *the secondary winding has the same number of turns as the primary winding*, i.e., that  $N_2 = N_1$ . Such an assumption will be permissible if care is taken that the secondary quantities, with  $N_1$  turns, are such that:

1. The mmf of the secondary winding retains its original value, i.e., that the resultant mmf and the main flux  $\Phi$  remain unchanged,
2. The kva of the secondary retain the original value,

3. The  $I^2R$  loss of the secondary retains its original value,
4. The magnetic energy ( $\frac{1}{2}L_{12}I_2^2$ ) of the secondary leakage flux which appears when the secondary carries current retains its original value.

The secondary quantities expressed in  $N_1$  turns are designated as *referred to the primary*. They will be indicated by a *prime*.

The first condition means that the secondary current referred to the primary ( $I_2'$ ) must be such that

$$I_2'N_1 = I_2N_2 \quad (13-2)$$

or

$$I_2' = I_2 \frac{N_2}{N_1} = \frac{I_2}{a} \quad (13-2a)$$

The second condition requires that

$$E_2'I_2' = E_2I_2 = E_2'I_2 \frac{N_2}{N_1}$$

or

$$E_2' = E_2 \frac{N_1}{N_2} = E_2a = E_1 \quad (13-3)$$

This means that the secondary and primary emf's induced by the main flux are equal. This corresponds to the assumption that the number of turns of the secondary winding is equal to that of the primary winding.

The third condition means that

$$I_2'^2r_2' = I_2^2r_2$$

Inserting the value of  $I_2'$  from Eq. 13-2

$$r_2' = \left(\frac{N_1}{N_2}\right)^2 r_2 = a^2r_2 \quad (13-4)$$

The fourth condition requires that

$$\frac{1}{2}I_2'^2x_2' = \frac{1}{2}I_2^2x_2$$

where  $x_2$  is the actual leakage reactance of the secondary. Inserting the value of  $I_2'$  from Eq. 13-2

$$x_2' = \left(\frac{N_1}{N_2}\right)^2 x_2 = a^2x_2 \quad (13-5)$$

Thus, calculating with the referred quantities  $E_2'$ ,  $I_2'$ ,  $r_2'$  and  $x_2'$  instead of the actual quantities  $E_2$ ,  $I_2$ ,  $r_2$ , and  $x_2$  does not change anything in the magnetic and electric behavior of the transformer.

It follows from Eqs. 13-2 to 13-5 that the reduction factors to the primary are:  $N_1/N_2 = a$  for voltage,  $N_2/N_1 = 1/a$  for current, and  $(N_1/N_2)^2 = a^2$  for resistance and reactance.

**13-3. Kirchhoff's mesh law for the secondary.** Kirchhoff's mesh law for the primary is given by Eq. 12-3 or 12-3a. Kirchhoff's mesh equation for the secondary is

$$\mathbf{E}_2 = \mathbf{I}_2(r_2 + jx_2) + \mathbf{I}_2(R_2 + jX_2) = \mathbf{I}_2(r_2 + jx_2) + \mathbf{V}_2 \quad (13-6)$$

where  $R_2$  and  $X_2$  are the load resistance and reactance respectively and  $V_2$  is the voltage at the load terminals. With all quantities referred to the primary, Eq. 13-6 becomes

$$\begin{aligned} \mathbf{E}_2' = \mathbf{E}_1 &= \mathbf{I}_2'(r_2' + jx_2') + \mathbf{I}_2'(R_2' + jX_2') \\ &= \mathbf{I}_2'(r_2' + jx_2') + \mathbf{V}_2' \end{aligned} \quad (13-7)$$

**13-4. The emf  $E_1 = E_2'$  induced by the main flux under load.** According to Eq. 13-2,  $\mathbf{I}_2'N_1 = \mathbf{I}_2N_2$ .  $\mathbf{I}_2'$  is, therefore, a current which, flowing in the  $N_1$  turns of the primary winding, will produce the same mmf as the current  $\mathbf{I}_2$  produces flowing in  $N_2$  turns of the secondary winding. By using  $\mathbf{I}_2'$  it is possible to replace the mmf diagram under load, shown in Fig. 13-1, with a *current* diagram, because the secondary and primary mmf's have the same number of turns. It follows from Fig. 13-1

$$\mathbf{I}_1N_1 + \mathbf{I}_2N_2 = \mathbf{I}_mN_1 \quad (13-8)$$

Introducing  $\mathbf{I}_2'N_1$  for  $\mathbf{I}_2N_2$ ,

$$\mathbf{I}_1N_1 + \mathbf{I}_2'N_1 = (\mathbf{I}_1 + \mathbf{I}_2')N_1 = \mathbf{I}_mN_1 \quad (13-8a)$$

or

$$\mathbf{I}_1 + \mathbf{I}_2' = \mathbf{I}_m \quad (13-9)$$

At no-load the core is magnetized by the mmf  $\mathbf{I}_mN_1$  with  $\mathbf{I}_m \approx \mathbf{I}_0 = \mathbf{I}_{1(\text{no-load})}$ . At load the core is magnetized by  $(\mathbf{I}_1 + \mathbf{I}_2')N_1$ . At no-load the reactive component of  $\mathbf{I}_m(I_\phi)$  produces the main flux and the active component of  $\mathbf{I}_m(I_{h+c})$  supplies the iron losses due to the main flux. At load the reactive component of  $(\mathbf{I}_1 + \mathbf{I}_2')$  produces the main flux and the active component of  $(\mathbf{I}_1 + \mathbf{I}_2')$  supplies the iron losses. Therefore Eqs. 12-6, 12-7, and 12-8 apply also to the loaded transformer, if  $(\mathbf{I}_1 + \mathbf{I}_2')$  is substituted for  $\mathbf{I}_m$ , i.e., for load,

$$\mathbf{I}_1 + \mathbf{I}_2' = -\mathbf{E}_1\mathbf{Y}_m = -\mathbf{E}_2'\mathbf{Y}_m \quad (13-10)$$

or

$$-\mathbf{E}_1 = -\mathbf{E}_2' = (\mathbf{I}_1 + \mathbf{I}_2')\mathbf{Z}_m \quad (13-10a)$$



$Y_m$  and  $Z_m$  are given by Eqs. 12-8 and 12-9. The relations between  $g_m$ ,  $b_m$ ,  $r_m$ , and  $x_m$  are given by Eq. 12-10.

Eq. 13-8 has been derived from Fig. 13-1 which refers to a resistive load. This equation and the following equations derived from it apply to any kind of load.

Since Kirchhoff's mesh equations of both electric circuits (Eqs. 12-3a and 13-7) and the equation which characterizes the magnetic circuit (Eq. 13-10) are now established, the *phasor diagram of the transformer under load* can be drawn and its equivalent circuit determined.

## Chapter 14

### THE PHASOR DIAGRAM AND EQUIVALENT CIRCUIT OF THE TRANSFORMER UNDER LOAD

**14-1. The phasor diagram of the transformer under load.** In the phasor diagram,  $E_2'$  and  $E_1$  are in phase since both emf's are induced by the same flux  $\Phi$ . The phase displacement between the secondary terminal voltage  $V_2'$  and the secondary current  $I_2'$  is determined entirely by the character of the external load circuit. The component of the secondary emf  $E_2'$  necessary to overcome the secondary leakage reactance drop  $I_2'x_2'$  leads the current  $I_2'$  by  $90^\circ$ . The ohmic voltage drop  $I_2'r_2'$  is in phase with  $I_2'$ . According to Eq. 13-7, the geometric sum of  $I_2'r_2'$ ,  $I_2'x_2'$ , and  $V_2'$  must yield  $E_2' = E_1$ .

Fig. 14-1 shows the phasor diagram of the transformer loaded with a pure resistance. The phasors  $I_\phi$ ,  $I_{h+c}$ ,  $I_m$ ,  $\Phi$ , and  $E_1$  are drawn as for the unloaded transformer (see Fig. 12-2).  $E_2'$  is equal to and in phase with  $E_1$ . Since the load is purely resistive, the secondary current  $I_2'$  and the terminal voltage  $V_2'$  are in phase, so that  $V_2'$  and  $I_2'$  are drawn in the same direction. The emf  $E_2'$  induced in the secondary by the main flux is obtained by adding to  $V_2'$  the quantities  $I_2'r_2'$  in phase with  $I_2'$  and  $I_2'x_2'$  perpendicular to  $I_2'$  and leading it by  $90^\circ$ .

From Eq. 13-9

$$I_1 = I_m + (-I_2') \quad (14-1)$$

Thus, in the phasor diagram of Fig. 14-1, the current  $I_1$  is obtained by adding  $-I_2'$  to  $I_m$ . The phasor  $-E_1$ , which is the component of the primary voltage necessary to overcome the emf induced in it by the main

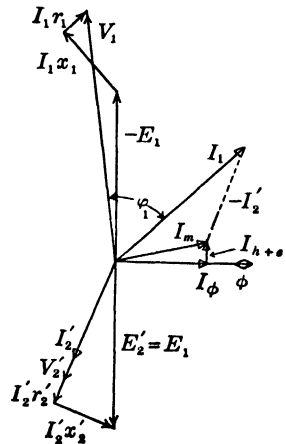


FIG. 14-1. Voltage and (mmf) current diagram of the transformer loaded with a pure resistance.

flux, is drawn upward and  $90^\circ$  ahead of  $\Phi$ . Adding to  $-E_1$  the primary resistance drop  $I_1 r_1$  in phase with  $I_1$  and the leakage reactance drop  $I_1 x_1$  perpendicular to  $I_1$  and leading it by  $90^\circ$ , the primary voltage  $V_1$  is obtained.

$\varphi_1$  is the phase-displacement angle of the primary, i.e., the angle between primary terminal voltage and current. Despite the in-phase condition of voltage and current at the secondary terminals, the magnetizing current and the leakage of both windings cause a slight phase displacement between the primary terminal voltage and current.

Fig. 14-2 shows the voltage and current (mmf) diagram for a transformer with an inductive load, i.e., the secondary current lags the secondary terminal voltage  $V_2'$  by an angle  $\varphi_2$ , the secondary phase dis-

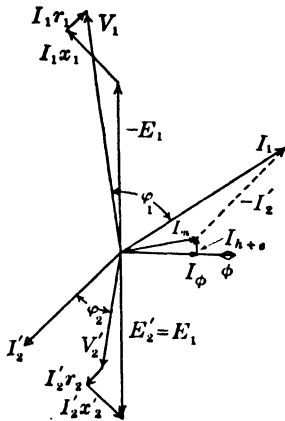


FIG. 14-2. Voltage and (mmf) current diagram of the transformer loaded with an inductive load.

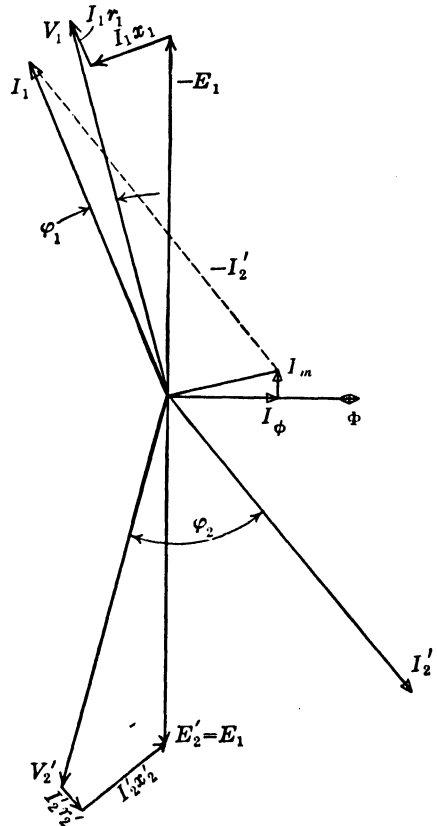


FIG. 14-3. Voltage and (mmf) current diagram of the transformer loaded with a capacitive load.

placement angle;  $\varphi_1$  increases with increased inductive load, i.e., with increased angle  $\varphi_2$ . For a capacitive load the situation may be reversed partly, as shown in Fig. 14-3.

**14-2. The equivalent circuit of the transformer.** From the phasor diagrams shown by Figs. 14-1 to 14-3 it may be observed that the applica-

tion of the voltage  $V_1$  to the primary of the transformer results in a primary current  $I_1$  lagging behind or leading  $V_1$  by an angle  $\varphi_1$ . The angle  $\varphi_1$  depends upon the load as well as upon the internal action within the transformer. As far as the source of power is concerned, the transformer and load appear as an equivalent impedance of such value that it takes the current  $I_1$  at the angle  $\varphi_1$ . The character or make-up of this equivalent impedance may be obtained from Kirchhoff's mesh equations for the two electric circuits (Eqs. 12-3a and 13-7) and from Eq. 13-10 or 13-10a which characterize the magnetic circuit (see Art. 12-2). These equations are:

$$V_1 = -E_1 + I_1(r_1 + jx_1) \quad (14-2)$$

$$E_2' = E_1 = I_2'(r_2' + jx_2') + I_2'(R_2' + jX_2') \quad (14-3)$$

$$I_1 + I_2' = I_m = -E_1 Y_m = -E_2' Y_m \quad (14-4)$$

These are three equations with three unknown quantities ( $E_1$ ,  $I_1$ , and  $I_2'$ ). The solution for  $I_1$  by eliminating  $E_1$  and  $I_2'$  will yield the equivalent impedance, i.e., the equivalent circuit. Introducing the abbreviations

$$r_1 + jx_1 = Z_1 \quad (14-5)$$

$$(r_2' + R_2') + j(x_2' + X_2') = Z_2' \quad (14-6)$$

Eqs. 14-2 to 14-6 yield

$$\begin{aligned} E_1 &= I_2' Z_2' = (I_m - I_1) Z_2' = -E_1 Y_m Z_2' - I_1 Z_2' \\ E_1(1 + Y_m Z_2') &= -I_1 Z_2' \quad \text{or} \quad E_1 = -\frac{I_1}{\frac{1}{Z_2'} + Y_m} \end{aligned} \quad (14-7)$$

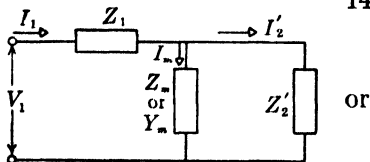
Therefore,

$$V_1 = I_1 Z_1 + \frac{I_1}{\frac{1}{Z_2'} + Y_m} = I_1 \left[ Z_1 + \frac{1}{\frac{1}{Z_2'} + Y_m} \right] \quad (14-8)$$

Eq. 14-8 gives the relation between the primary applied voltage, primary current, and the parameters of the transformer and the load. The quantity in the brackets is the *total impedance, looking into the primary terminals*. It includes the primary and secondary impedance of the transformer, the load impedance, and the main flux admittance  $Y_m$ .

Eq. 14-8 is the equation which applies to a circuit such as that represented in Fig. 14-4. This circuit is the *equivalent circuit* of the transformer and load. In this circuit, as Eq. 14-8 shows, the secondary impedance  $Z_2'$  is in parallel with the main flux admittance  $Y_m$ , giving a resultant

admittance  $\mathbf{Y}_m + 1/\mathbf{Z}_2'$  or a resultant impedance  $1/(\mathbf{Y}_m + 1/\mathbf{Z}_2')$ . Breaking up  $\mathbf{Z}_1$  and  $\mathbf{Z}_2'$  into their components according to Eqs. 14-5 and 14-6 and introducing from Eq. 12-8



$$\mathbf{Y}_m = g_m - jb_m \quad (14-9)$$

$$\mathbf{Z}_m = \frac{1}{\mathbf{Y}_m} = (r_m + jx_m) \quad (14-10)$$

FIG. 14-4. Equivalent circuit of the transformer.

the circuit of Fig. 14-4 becomes that shown in Figs. 14-5 and 14-6 which is more commonly known as the equivalent circuit of the transformer.

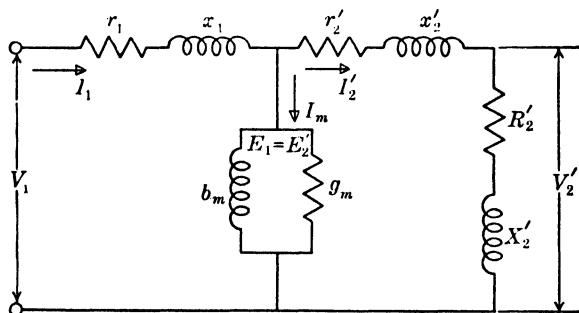


FIG. 14-5. Equivalent circuit of the transformer.

It has been pointed out in Art. 12-2 that the magnitude of  $x_m(b_m)$  depends upon the saturation of the iron which is dependent upon the

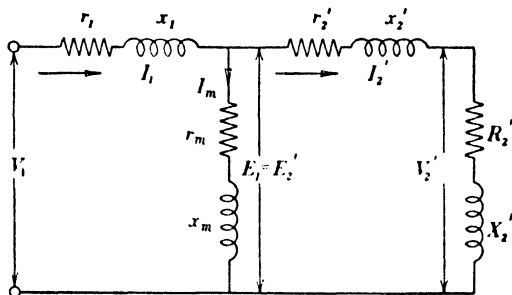


FIG. 14-6. Equivalent circuit of the transformer.

magnitude of the main flux  $\Phi$ . Since the main flux of the transformer remains almost constant between no-load and full-load (Art. 13-1),  $x_m(b_m)$  can be considered as a constant.

It will be shown in Chapter 17 how the parameters  $r_1$ ,  $x_1$ ,  $r_2'$ ,  $x_2'$ ,  $r_m$  and  $x_m$  (or  $g_m$  and  $b_m$ ) can be determined from no-load and short-circuit tests.

Having an equivalent circuit is of great assistance in making performance calculations of the transformer such as current, power factor, power, etc., especially when a calculating board is used on which the equivalent circuit can be set up.

**Example.** The parameters of the equivalent circuit of a 100-kva, 2200/220-volt, 60-cycle transformer are given at 75°C as follows:

$$\begin{aligned} r_1 &= 0.286 \text{ ohm} & r_2' &= 0.319 \text{ ohm} \\ x_1 &= 0.73 \text{ ohm} & x_2' &= 0.73 \text{ ohm} \\ r_m &= 302 \text{ ohms} \\ x_m &= 1222 \text{ ohms} \end{aligned}$$

It will be shown in Arts. 17-1 and 17-2 how the above parameters have been determined from no-load and short-circuit tests. If the load impedance on the low-voltage side of the transformer is  $Z_L = 0.387 + j0.290$  ohm, solve the equivalent circuit when the voltage  $V_1$  is 2300 volts.

$$a = \frac{2200}{220} = 10$$

$$Z_L' = R_L' + jX_L' = a^2(R_L + jX_L) = 38.7 + j29.0 = 48.4 \angle 36.8$$

From Eq. 14-6

$$Z_2' = (0.319 + 38.7) + j(0.73 + j29.0) = 39.02 + j29.73 = 49.0 \angle 37.3$$

$$Z_m = 302 + j1222 = 1258 \angle 76.1$$

$$Y_m = \frac{1}{Z_m} = 0.795 \times 10^{-3} \angle -76.1$$

From Eq. 14-8

$$\begin{aligned} I_1 &= \frac{V_1}{Z_1 + \frac{1}{\frac{1}{Z_2'} + Y_m}} = \frac{2300 \angle 0}{\left[ 0.286 + j0.73 + \frac{1}{\frac{1}{49.0 \angle 37.3} + 0.795 \times 10^{-3} \angle -76.1} \right]} \\ &= \frac{2300 \angle 0}{48.2 \angle 39.2} = 47.7 \angle -39.2 \end{aligned}$$

$$\begin{aligned} I_2' &= I_1 \times \frac{Z_m}{Z_2' + Z_m} = 47.7 \angle -39.2 \times \frac{1258 \angle 76.1}{1258 \angle 76.1 + 49.0 \angle 37.3} \\ &= 46.2 \angle -40.5 \end{aligned}$$

$$I_m = I_1 \times \frac{Z_2'}{Z_m + Z_2'} = 1.80 \angle -76.7$$

Input power factor	= $\cos 39.2^\circ$	= 0.775 lagging
Power input	= $2300 \times 47.7 \times 0.775$	= 85.0 kw
Power output	= $(46.2)^2 \times 38.7$	= 82.7 kw
Primary copper losses	= $(47.7)^2 \times 0.286$	= 650 watts
Secondary copper losses	= $(46.2)^2 \times 0.319$	= 680 watts
Core losses	= $(1.80)^2 \times 302$	= 980 watts
$\eta$ efficiency	= $\frac{82.7}{85.0} \times 100$	= 97.3%
Voltage across load	= $46.2 \times 48.4$	= 2240 volts
Regulation	= $\frac{2300 - 2240}{2240} \times 100$	= 2.68%

### PROBLEMS

Equivalent circuit parameters are listed below for four transformers. Assume all values to be corrected to 75°C.

	A	B	C	D
	10 kva	15 kva	500 kva	1000 kva
	240/120	2300/230	11,000/2300	66,000/6600
<i>ohms</i>	60 <i>cycles</i>	60 <i>cycles</i>	60 <i>cycles</i>	60 <i>cycles</i>
$r_1$	0.14	2.5	0.830	22
$x_1$	0.20	10	3.80	105
$r_2$	0.03	0.022	0.035	0.20
$x_2$	0.048	0.095	0.160	1.12
$r_m$	80	1500	2800	25,000
$x_m$	250	8850	11,500	165,000
$a$	2	10	4.78	10

#### LOAD IMPEDANCE (ohms)

$R_L$	1.40	3.54	9.5	35
$X_L$	0	0	5.0	26

1. For transformer A, determine the primary current, primary power factor, magnetizing current, and efficiency. Assume  $V_1$  fixed at name plate value.
2. Repeat Problem 1 for transformer B.
3. Repeat Problem 1 for transformer C.
4. Repeat Problem 1 for transformer D.

## Chapter 15

### THE 3-PHASE TRANSFORMER

**15-1. Advantages, disadvantages, construction.** Transformation of 3-phase voltages may be accomplished by means of three single-phase transformers arranged in banks so that each phase requires a separate transformer, or by means of a single 3-phase transformer unit. The first

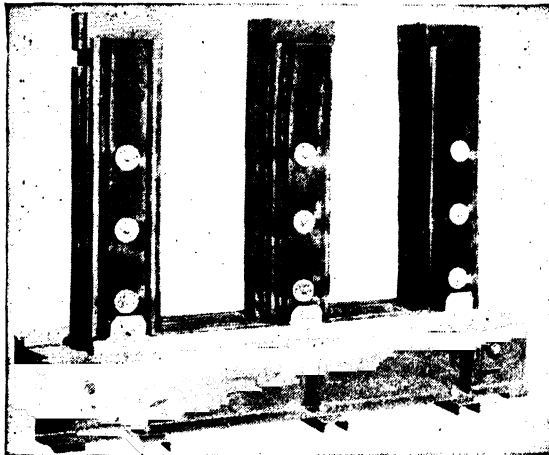


FIG. 15-1. Core for a 3-phase transformer.

method was common practice years ago, for it enabled the use of a single reserve unit of one-third the bank capacity for stand-by or emergency spare. Thus the replacement investment is only  $33\frac{1}{3}\%$  of the first cost of the bank. However, the reliability of modern transformers is such that the necessity for reserve capacity is no longer a demand in many cases. System interconnection frequently provides all the necessary reserve needed. Also, it is sometimes a simple matter to install small or medium portable substations as reserve when required,



Considerable advantages are to be gained from the use of a single-unit 3-phase transformer in place of three single-phase units of the same total capacity. The advantages are: increased efficiency, reduced size, reduced weight, and less cost. A reduction in space is an advantage from the structural point of view in generating stations or substations.

Disadvantages include the greater cost of spares where spare capacity is demanded, usually a greater repair cost when subject to a short-circuit

fault, and greater weight and size for reserve than a single-phase unit of a bank of transformers.

Fig. 15-1 shows the core of a large 3-phase core-type transformer. A final-assembled 3-phase core-type unit is shown in Fig. 15-2 where the low-voltage cylindrical coils are nearest the core and the high-voltage coils are on the outside. The shell-

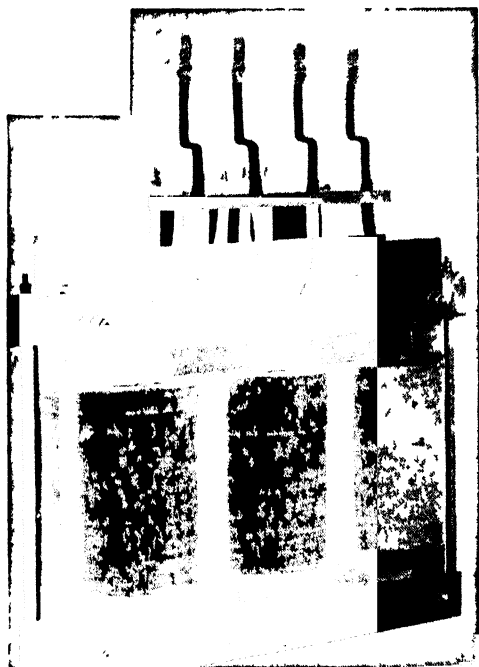


FIG 15-2 Three-phase, core-type distribution transformer, 37.5 kva, 2400/240 volts, Y-connected

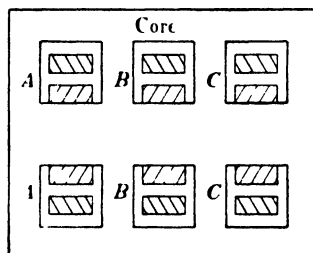


FIG 15-3 Shell-type construction

type as well as the distributed shell-type core construction, discussed in Article 11-1, may also be used for 3-phase transformers. The shell-type construction is one in which the windings are embedded within the iron core. Fig. 15-3 shows the general arrangement of coils in the shell-type 3-phase transformer.

**15-2. Magnetic circuit.** The three cores of the 3-phase transformer are connected on both ends by common yokes. This is permissible. It should be remembered that the three voltages impressed upon the three primary windings make a symmetrical 3-phase voltage system, and this means

that the three fluxes due to the three voltages also make a symmetrical system, i.e., the three fluxes are shifted in time by  $120^\circ$  and  $240^\circ$  respectively. Since the sum of the instantaneous values of the three fluxes is therefore equal to zero at any instant of time, it follows that the three magnetic circuits can be connected just as the three current circuits of a 3-phase electric system, for instance in a star in which the return conductor can be omitted. It can be seen by examining Fig. 15-1 that the connection of the three magnetic circuits is that of a star.

It is also seen from Fig. 15-1 that the magnetic path is not the same for all three fluxes, being longer for the outer cores than for the inner core. As a consequence, the magnetizing current is not the same in the three phases. However, since the magnetizing current is small, the 3-phase transformer can be considered as a symmetrical 3-phase system, i.e., the three phases can be treated as being equal. It then follows that the voltage diagrams derived in Chapters 12, 13, and 14 for the single-phase transformer also apply to *one phase* of the 3-phase transformer. The same is true of the equivalent circuit of the single-phase transformer. Also the no-load and short-circuit tests used to determine the parameters of the single-phase transformer (see Chapter 17) hold equally well for the 3-phase transformer.

If, in general,  $m_1$  is the number of primary phases and  $m_2$  the number of secondary phases, then the power output of the secondary of the transformer is

$$P_2 = m_2 V_2 I_2 \cos \varphi_2 \quad (15-1)$$

and the primary power input

$$P_1 = m_1 V_1 I_1 \cos \varphi_1 \quad (15-2)$$

$V_1$ ,  $V_2$ ,  $I_1$ , and  $I_2$  are respectively phase voltages and currents.

## Chapter 16

---

### VOLTAGE REGULATION: THE KAPP DIAGRAM

**16-1. Voltage regulation: the Kapp diagram.** An important factor in transformer operation is the *voltage regulation*. The regulation is defined as the change in secondary voltage, expressed as a percent of rated secondary voltage, which occurs when rated kva output (at a specified power factor) is reduced to zero, with the primary impressed terminal voltage maintained constant. The defining equation for percent regulation is

$$\epsilon = 100 \frac{V_{2 \text{ no-load}} - V_{2 \text{ rated}}}{V_{2 \text{ rated}}}$$

If the multiplying factor 100 is omitted, the regulation will be given in per-unit (the per-unit method of calculation is explained in detail in Chapter 17). If all voltages are referred to the primary, as in the phasor diagrams previously used, the regulation will be

$$\epsilon = 100 \frac{V_1 - V_2'_{\text{rated}}}{V_2'_{\text{rated}}} \quad (16-1)$$

Since the voltage regulation is defined in terms of full-load conditions and since the full-load current is large in comparison to the magnetizing current  $I_m$ , it frequently is permissible to neglect the effect of  $I_m$  in considering the voltage regulation. This may not be done, however, if calculations are made for small loads.

If  $I_m$  is neglected, it will be observed from Eq. 12-8 that this means  $Y_m$  is assumed zero, or in other words that  $Y_m \ll 1/Z_2'$  which is practically true at full-load. Eq. 14-8 then becomes

$$\mathbf{V}_1 = \mathbf{I}_1(\mathbf{Z}_1 + \mathbf{Z}_2') \quad (16-2)$$

Since

$$\mathbf{Z}_2' = r_2' + jx_2' + R_2' + jX_2'$$

Eq. 16-2 may be written as

$$\begin{aligned} \mathbf{V}_1 &= \mathbf{I}_1[(r_1 + r_2') + j(x_1 + x_2')] + \mathbf{I}_1(R_2' + jX_2') \\ &= \mathbf{I}_1\mathbf{Z}_e + \mathbf{V}_2' \end{aligned} \quad (16-3)$$

where

$$\mathbf{Z}_e = (r_1 + r_2') + j(x_1 + x_2') = R_e + jX_e \quad (16-4)$$

$\mathbf{Z}_e$  is the *equivalent impedance* of the transformer referred to the primary,  $R_e$  is the *equivalent resistance*, and  $X_e$  the *equivalent leakage reactance*. How these values may be determined from a short-circuit test is explained in Chapter 17. The phasor diagram for Eqs. 16-3 and 16-4 is shown in Fig. 16-1; it is often referred to as the *Kapp Transformer Diagram*. In this diagram the current  $I_2' = I_1$  is assumed to be the rated full-load current, and  $V_2' = OA$  is rated secondary terminal voltage, drawn at angle  $\varphi_2$  to  $I_2'$ , as given by the load power factor. Further  $AB = I_2'R_e$  and  $BC = I_2'X_e$ .  $V_1 = OC$  is the primary-terminal voltage. If a circle with radius  $OC$  and center at  $O$  cuts  $OA$  extended at  $D$ , then the regulation in per-unit is  $\epsilon = AD/V_2'$ .

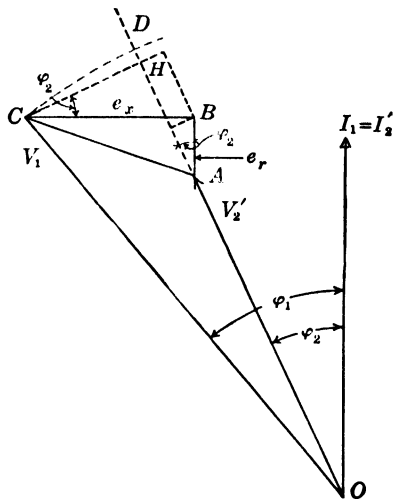


FIG. 16-1. Kapp diagram of a transformer.

In order to calculate the per-unit regulation using this diagram, Fig. 16-1, it is convenient to assume that the unit voltage is equal to the rated secondary voltage  $V_2'$ , i.e.,  $V_2' = OA = 1$ , then  $AD = \epsilon$ . Let

$$\frac{I_2'R_e}{V_2'} = AB = e_r, \quad \frac{I_2'X_e}{V_2'} = BC = e_x;$$

$e_r$  and  $e_x$  then are the per-unit voltage drops in the transformer. From Fig. 16-1,

$$AH = e' = e_r \cos \varphi_2 + e_x \sin \varphi_2$$

$$HC = e'' = e_x \cos \varphi_2 - e_r \sin \varphi_2$$

Therefore, the primary voltage in per-unit is:

$$V_1 = \sqrt{(1 + e')^2 + e''^2} \approx (1 + e') + \frac{e''^2}{2(1 + e')}$$

Observing that  $2 \gg 2e'$ , this equation may be written as

$$V_1 = (1 + e') + \frac{e''^2}{2}$$

so that

$$\epsilon = \frac{V_1 - V_2'}{V_2'} = \frac{V_1 - 1}{1} = e' + \frac{e''^2}{2}$$

The regulation thus is

$$\epsilon = e_r \cos \varphi_2 \pm e_x \sin \varphi_2 + \frac{(e_x \cos \varphi_2 \mp e_r \sin \varphi_2)^2}{2} \quad (16-5)$$

where the upper signs are used for lagging current and the lower for leading current. This is the AIEE Standards approximate equation for transformer regulation.

TABLE 16-1.

APPROXIMATE REGULATION FOR 60-CYCLE,  
3-PHASE, POWER TRANSFORMERS AT FULL-LOAD

kv	Lagging Power Factor	Percent Regulation		
		1000 kva	10,000 kva	100,000 kva
15	80	4.2	3.9	
	90	3.3	3.1	
	100	1.1	0.7	
34.5	80	5.0	4.8	
	90	4.0	3.7	
	100	1.2	0.8	
69	80	6.1	5.7	5.5
	90	4.9	4.4	4.2
	100	1.4	0.9	0.6
138	80	7.7	7.2	7.0
	90	6.2	5.6	5.4
	100	1.8	1.2	0.9
230	80		9.7	9.4
	90		7.6	7.3
	100		1.7	1.3

For a given power-factor angle  $\varphi_2$ , the voltage regulation increases as  $I_1 R_s$  and  $I_1 X_s$  increase. Moreover, the effect of the leakage reactance is considerably greater than that of the resistance. A low value of voltage

regulation requires low reactances. Furthermore, the voltage regulation increases with the power-factor angle. For unity- and lagging-power-factor loads the voltage at the terminals of the secondary increases as the load is decreased; for some leading-power-factor loads the voltage decreases as the load is decreased. The change in the displacement angle between the primary and secondary terminals ( $\varphi_1 - \varphi_2$ ) also decreases as the reactance  $x_e$  is decreased. Also, in order to keep the power-factor angle of the primary small, the magnetizing current carried by the primary should be low.

Nomographic charts have been prepared to determine the regulation of transformers, given the per-unit resistance, per-unit reactance, and power-factor.

Table 16-1\* shows the typical regulation of 3-phase transformers of various voltage and kva rating.

\* From *Westinghouse Electrical Transmission and Distribution Reference Book*, Fourth Edition.

# Chapter 17

## DETERMINATION OF PARAMETERS FROM A NO-LOAD AND A SHORT-CIRCUIT TEST

It is possible with a no-load test and a short-circuit test to determine the six parameters of the transformer and, from these, its regulation and efficiency.

**17-1. The no-load test.** In this discussion only the 2-winding transformer will be considered. Rated voltage  $V_1$  is impressed upon either winding of the transformer, with the other winding open, and the no-load power

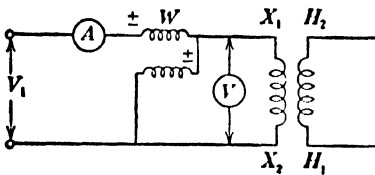


FIG. 17-1. Test circuit for no-load.

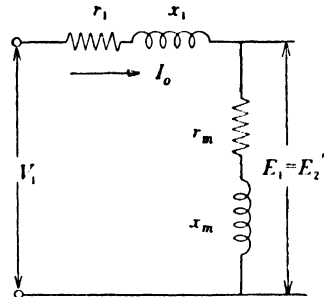


FIG. 17-2. Equivalent circuit for no-load.

input  $P_0$  and the no-load current  $I_0$  are recorded. Usually, rated voltage is applied to the low-voltage winding. Fig. 17-1 shows the test circuit used.  $r_1$ , the resistance of the winding excited, is measured with d-c, and the temperature of the cooling medium is recorded.

Fig. 17-2 shows the equivalent circuit of the transformer at no-load. This may be easily deduced from Fig. 14-4; at no-load the load impedance is infinite and the circuit reduces to that of Fig. 17-2. Given  $V_1$ ,  $P_0$ ,  $I_0$ , and  $r_1$ , the parameters  $x_m$  and  $r_m$  may be determined.

The core loss  $P_{h+c}$  is approximately equal to the no-load loss  $P_0$  since the copper loss  $I_0^2 r_1$ , due to the no-load current, is usually small. From Eq. 12-3

$$\mathbf{E}_2' = \mathbf{E}_1 = \mathbf{V}_1 - I_0 \mathbf{Z}_1$$

or

$$E_1 \approx V_1 - I_0 x_1 \quad (17-1)$$

where  $x_1$  is the leakage reactance of the primary winding, the determination of which is discussed in Art. 17-2 which follows.

Since  $E_1$  is the voltage across the main flux impedance  $Z_m$  (Fig. 17-2), and  $r_m$  is small in comparison with  $x_m$ ,

$$x_m \approx \frac{E_1}{I_0} \quad (17-2)$$

The main flux resistance  $r_m$  is given by Eqs. 14-9 and 14-10

$$r_m = \frac{g_m}{g_m^2 + b_m^2} \approx \frac{g_m}{b_m^2} \approx g_m x_m^2 \quad (17-3)$$

where  $g_m$ , the main flux conductance is

$$g_m = \frac{P_{h+c}}{E_1^2} \approx \frac{P_0}{V_1^2} \quad (17-4)$$

Thus both  $r_m$  and  $x_m$  can be readily determined if  $x_1$  is known. It should be noted that the parameters determined from the no-load readings are in terms of the winding in which the readings were taken.

**17-2. The short-circuit test.** In this test a reduced voltage is applied to one winding, usually the high-voltage winding, with the other winding solidly short-circuited. The reduced voltage  $V_{sc}$ , frequently called the impedance voltage, is selected so that the short-circuit current  $I_{sc}$  will not damage the windings.

Fig. 17-3 shows the circuit employed for this test, and Fig. 17-4 shows the equivalent circuit for short-circuit conditions. Since  $V_2 = 0$  and  $(r_2' + jx_2')$  is small in comparison with  $x_m$ , very little current will flow through the magnetizing branch. Therefore, the main flux and the iron losses are very small, and the power  $P_{sc}$  consists essentially of the copper losses in both windings.

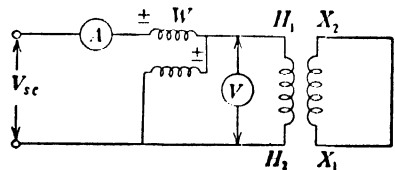


FIG. 17-3. Test circuit for short-circuit.



The power at short circuit is the total copper loss of the transformer. Because of skin-effect (see Art. 10-1b),  $P_{sc}$  may be greater than the ohmic copper losses. The skin-effect will be neglected in this chapter.

From Fig. 17-4

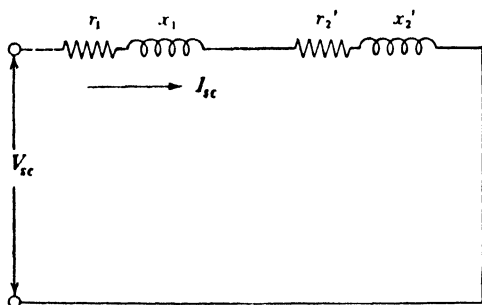
$$Z_e = \frac{V_{sc}}{I_{sc}} \quad (17-5)$$

$$R_e = \frac{P_{sc}}{(I_{sc})^2} \quad (17-6)$$

$$X_e = \sqrt{Z_e^2 - R_e^2} \quad (17-7)$$

$Z_e$ ,  $R_e$ , and  $X_e$  are called *equivalent impedance*, *equivalent resistance*, and *equivalent leakage reactance* respectively. It is generally assumed that

$$x_1 = x_2' = \frac{X_e}{2} \quad (17-8)$$



Once again it should be noted that the parameters are in terms of the winding in which the instrument readings were taken.

Since the equivalent resistance  $R_e$  is the sum of  $r_1$  and  $r_2'$ , it follows that

FIG. 17-4. Equivalent circuit for short circuit.

$$r_2' = R_e - r_1 \quad (17-9)$$

According to AIEE Standards the resistances must be corrected to 75°C when calculating the regulation and efficiency from the equivalent circuit. This will be shown in the example of Art. 17-5.

Normally at rated current the voltage  $V_{sc}$  is 2 to 4% of rated voltage for low-voltage transformers (up to 2300 volts) and from 5 to 16% for high-voltage transformers (up to 275 kv).

**17-3. Transformer Efficiency.** The efficiency of a transformer may be obtained by direct loading or by the method of losses. The method of losses is used exclusively in commercial work. If the no-load losses ( $P_0 \approx P_{h+c}$ ) and the load losses ( $\approx I_1^2 R_e$ ) are known, at rated voltage and rated current respectively, the efficiency is

$$\eta = \frac{\text{output}}{\text{output} + \text{losses}} = \frac{\text{kva} \times 10^3 \times \cos \phi}{\text{kva} \times 10^3 \times \cos \phi + I_1^2 R_e + P_{h+c}} \quad (17-10)$$

**17-4. Per-unit calculation.** When the parameters, voltage drops, losses, etc., of a transformer are expressed in ohms, volts, and watts, they apply

only to the transformer being considered. It is possible to express the parameters, voltage drops, etc., of the transformer so that these quantities, although determined for a certain case, become general, i.e., applicable to a wide range of ratings, sizes, voltages, etc. For this reason certain *units* (base values) have to be defined and the quantities mentioned above expressed as fractions of these units. The quantities so expressed are then referred to as resistances, reactances, voltage drops, etc., on a per-unit basis or *in p-u*.

It is usual to assume the following units:

Unit voltage = primary voltage

Unit current = primary full-load current

$$\text{Unit impedance} = \frac{\text{unit voltage}}{\text{unit current}} = \frac{\text{primary voltage}}{\text{primary full-load current}}$$

Unit power = primary input

The advantages of the per-unit calculation are shown by the following example:

Consider a transformer designed for two different voltages and having the following data:

(a) 500 kva, 42,000/2400 volts, 60 cycles,

$$\begin{aligned} r_1 &= 19.5 \text{ ohms}, r_2 = 0.55 \text{ ohm}, x_1 = 39.5 \text{ ohms}, x_2 = 0.120 \text{ ohm}, \\ a &= 42,000/2400 = 17.5, \quad a^2 = 306.3, \quad r_2' = 0.055 \times 306.3 = \\ &16.84 \text{ ohms}, x_2' = 0.120 \times 306.3 = 36.8 \text{ ohms, and} \end{aligned}$$

(b) 500 kva, 84,000/2400 volts, 60 cycles,

$$r_1 = 78.0 \quad r_2' = 67.4 \quad x_1 = 158 \quad x_2' = 147.2 \text{ ohms.}$$

If each of these transformers is treated on the p-u basis, the results will be:

(a) Unit current =  $500/42 = 11.91$  amp; unit impedances =  $42,000/11.91 = 3528$  ohms.

Therefore

$$\begin{aligned} r_1 &= 19.5/3528 = 0.00553 & r_2' &= 16.84/3528 = 0.00478 \\ x_1 &= 39.5/3528 = 0.0118 & x_2' &= 36.8/3528 = 0.01043. \end{aligned}$$

(b) Unit current =  $500/84 = 5.95$ ; unit impedance =  $84,000/5.95 = 14130$  ohms.

$$\begin{aligned} r_1 &= 78/14,130 = 0.00552 & r_2' &= 67.4/14,130 = 0.00478 \\ x_1 &= 158/14,130 = 0.0118 & x_2' &= 147.2/14,130 = 0.01043. \end{aligned}$$

Both transformers have different ratings and therefore different constants

when expressed in ohms. However, when expressed in p.u, the parameters of both transformers are equal.

**Example.** A 100-kva, 2200/220-volt, 60-cycle transformer is tested on open-circuit at no-load and short-circuit at 25°C and the following readings are recorded:

*Open circuit* (H.V. winding open)

$$V_1 = 220 \text{ volts}$$

$$I_0 = 18 \text{ amp}$$

$$P_0 = 980 \text{ watts}$$

*Short circuit* (L.V. winding short-circuited)

$$V_{sc} = 70 \text{ volts}$$

$$I_{sc} = 45.5 \text{ amp} = I_1 \text{ rated}$$

$$P_{sc} = 1050 \text{ watts}$$

The resistance of the high-voltage winding after the short-circuit test was 0.24 ohm, and the temperature was 25°C.  $a = 2200/220 = 10$ .

*Required:* the parameters of the equivalent circuit, the regulation at full-load unity p.f. and 0.80 p.f. lagging, and the efficiency at unity p.f. and 0.80 p.f. lagging:

$$I_1(\text{rated}) = \frac{100,000}{2200} = 45.5 \text{ amp}$$

$$Z_e(25^\circ\text{C}) = \frac{70}{45.5} = 1.54 \text{ ohms}$$

$$R_e(25^\circ\text{C}) = \frac{1050}{(45.5)^2} = 0.507 \text{ ohm}$$

$$X_e = \sqrt{(1.54)^2 - (0.507)^2} = 1.46 \text{ ohms}$$

$$R_e(75^\circ\text{C}) = 0.507 \times \frac{234.5 + 75}{234.5 + 25} = 0.605 \text{ ohm}$$

$$r_1(75^\circ\text{C}) = 0.24 \times \frac{234.5 + 75}{234.5 + 25} = 0.286 \text{ ohm}$$

$$r_2' = R_e - r_1 = 0.605 - 0.286 = 0.319 \text{ ohm}$$

$$x_1 = x_2' = 0.73 \text{ ohm}$$

$$P_{h+e} = 980 - (1.80)^2 \times 0.286 = 979 \text{ watts}$$

$$E_1 = 2200 - 1.80 \times 0.73 \approx 2200 \text{ volts}$$

$$x_m = \frac{2200}{1.80} = 1222 \text{ ohms}$$

$$g_m = \frac{979}{(2200)^2} = 0.000202 \text{ mho}$$

$$r_m = 0.000202 \times (1222)^2 = 302 \text{ ohms}$$

$$\text{Unit voltage} = 220 \times 10 = 2200 \text{ volts } (V_2')$$

$$\text{Unit current} = 45.5 \text{ amp}$$

$$\text{Unit impedance} = 48.4 \text{ ohms}$$

$$e_r = \frac{0.605}{48.4} = 0.0125$$

$$e_x = \frac{1.46}{48.4} = 0.0302$$

Regulation at unity p.f. (Eq. 16-5):

$$\begin{aligned}\text{Reg.} &= 0.0125 + \frac{(0.0302)^2}{2} \\ &= 0.0125 + 0.000455 = 0.0130\end{aligned}$$

Regulation at 0.80 p.f. lagging (Eq. 16-5):

$$\begin{aligned}\text{Reg.} &= 0.80 \times 0.0125 + 0.60 \times 0.0302 + \frac{(0.80 \times 0.0302 - 0.60 \times 0.0125)^2}{2} \\ &= 0.0100 + 0.0181 + 0.000139 \\ &= 0.0282\end{aligned}$$

Efficiency:

$$\text{Load losses (75°C)} = 1050 \times \frac{234.5 + 75}{234.5 + 25} = 1252 \text{ watts}$$

Efficiency at rated load unity p.f.:

$$\eta = \frac{100}{100 + 0.980 + 1.25} = 0.977$$

Efficiency at rated load 0.80 p.f. lagging:

$$\eta = \frac{100 \times 0.80}{100 \times 0.80 + 0.980 + 1.25} = 0.973$$

Efficiency at  $\frac{3}{4}$  load 0.80 p.f. lagging:

$$\eta = \frac{100 \times \frac{3}{4} \times 0.80}{100 \times \frac{3}{4} \times 0.80 + 0.980 \times (\frac{3}{4})^2 + 1.25} = 0.972$$

### PROBLEMS

Open-circuit and short-circuit tests were taken on three single-phase transformers, and the following data were recorded.

	E	F	G
	10 kva	90 kva	5000 kva
	2200/110	11,000/2200	14,000/4000
	60 cycles	60 cycles	60 cycles
$V_1$ volts	110	2200	4000
$I_0$ amp	0.90	1.70	55.3
$P_0$ watts	68	1010	28,100
$V_{sc}$ volts	112	550	895
$I_{sc}$ amp	4.55	8.18	357
$P_{sc}$ watts	218	995	37,800
$r_1$ ohms (at 25°C)	5.70	8.0	0.16

1. Determine the six parameters of the equivalent circuit for transformer *E*.
2. Repeat Problem 1 for transformer *F*.
3. Repeat Problem 1 for transformer *G*.
4. Determine the regulation and efficiency of transformer *E* at rated load current, unity and 0.80 lagging p.f. Determine the efficiency at  $\frac{1}{4}$ ,  $\frac{1}{2}$  and  $\frac{3}{4}$  load unity and 0.80 lagging p.f.
5. Repeat Problem 4 for transformer *F*.
6. Repeat Problem 4 for transformer *G*.
7. Using the Kapp diagram, determine the regulation of transformer A, Chapter 14 (p. 146), at unity, 0.80 lagging and 0.80 leading p.f.
8. Repeat Problem 7 for transformer B, Chapter 14 (p. 146).
9. Repeat Problem 7 for transformer C, Chapter 14 (p. 146).
10. Repeat Problem 7 for transformer D, Chapter 14 (p. 146).
11. A 500-kva 42,000/2400-volt, 60-cycle transformer has parameters  $r_1 = 19.5$ ,  $r_2 = 0.055$ ,  $x_1 = 39.5$ , and  $x_2 = 0.120$ . The core loss and copper loss are equal at full-load. Determine the regulation and efficiency at unity, 0.80 lagging and 0.80 leading p.f.
12. A 500-kva, 2300/230-volt, 60-cycle transformer services both a lighting and a power load. The copper loss is 0.0105 p-u and the core loss 0.0102 with rated full-load current. The transformer is connected continuously to the supply mains. The load is 350 kw at 0.80 p.f. lagging for 10 hr, 450 kw at 0.95 p.f. lagging for 2 hr, and idle the remainder of the day. What is the all-day efficiency?

$$\text{All-day efficiency} = \frac{\text{Total kw-hr output in 24 hr}}{\text{Total kw-hr input in 24 hr}}$$

13. Determine the all-day efficiency of a 100-kva transformer having core and copper losses at full-load current equal to 0.011 p-u, and supplying the following load cycle

<i>kw</i>	<i>p.f.</i>	<i>hr</i>
80	0.85	5
45	0.75	4
100	1.0	2
idle		13

14. A 75-kva 230/115-volt 60-cycle single-phase transformer was tested at no-load and short-circuit, and the following p-u data were recorded:

$V_1 = 1.0$	$V_{sc} = 0.041$
$I_0 = 0.025$	$I_{sc} = 1.0$
$P_0 = 0.01$	$P_{sc} = 0.016$

Determine the regulation and efficiency at full-load, unity p.f., 0.80 p.f. lagging, and 0.80 p.f. leading.

What is the efficiency of this transformer at  $\frac{1}{4}$ ,  $\frac{1}{2}$ ,  $\frac{3}{4}$ , and  $1\frac{1}{4}$  load current, 0.80 p.f. lagging?

15. Prove by means of the calculus that maximum transformer efficiency occurs when copper losses are equal to core losses.

16. What is the primary voltage  $V_1$  required if the transformer of Problem 14 is to deliver 50 kva at 115 volts at 0.80 p.f. lagging?

## Chapter 18

### TRANSFORMER POLARITY POLYPHASE CONNECTIONS

**18-1. Transformer polarity.** Transformers, single-phase or polyphase, have all leads marked with a standard system of lettering designating the transformer polarity. In order to connect windings of the same transformer in parallel, or to interconnect two or more transformers in parallel, or to connect single-phase transformers for polyphase transformation of voltages, it is necessary to know the lead marking. Transformer manufacturers usually follow a standard marking scheme.

Transformer *polarity marking* designates the relative instantaneous directions of current in the transformer leads. High-voltage leads are designated with the letter  $H$ , low-voltage leads with  $X$ , and tertiary leads with  $Y$ , each with a suitable subscript 1, 2, 3, 4, etc., depending upon the number of leads. Fig. 18-1 shows the directions of instantaneous currents and induced voltages for power supplied to the high-voltage winding and a load connected to the low-voltage winding. In Fig. 18a both windings are wound in the same direction; in Fig. 18b, in opposite directions. The currents are indicated by closed arrows, and the induced voltages by open arrows. A high- and a low-voltage lead have the same polarity if, at a given instant, the current enters the high-voltage lead and leaves the low-voltage lead (or vice versa), thus giving the effect as though the two leads belonged to a continuous circuit. Thus, in Fig. 18-1,  $H_1$  and  $X_1$

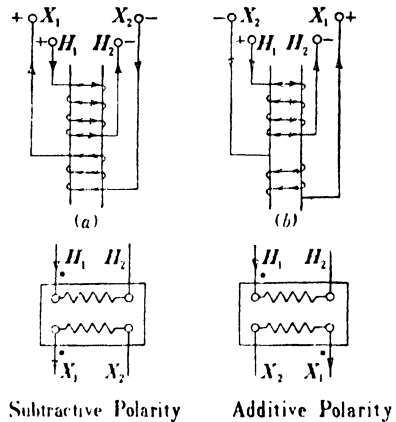


Fig. 18-1. Transformer polarity designation.

have the same polarity. This means that in single-phase transformers the marking of the leads is such that when  $H_1$  and  $X_1$  are connected together and voltage applied to either side of the transformer, the voltage measured between the highest subscript  $H$ -lead and the highest subscript  $X$ -lead is always less than the voltage of the complete high-voltage winding. Instantaneously the terminal voltage from  $H_1$  to  $H_2$  in Fig. 18-1 is in time phase with the voltage  $X_1$  to  $X_2$ .

Viewing the transformer from the high-voltage side, the  $H_1$ -lead is usually brought out on the right side as shown in Fig. 18-1. When the  $H_1$  and  $X_1$  leads are adjacent, the polarity is said to be *subtractive*, and when  $H_1$  is diagonally opposite  $X_1$ , the polarity designation is *additive*. Fig. 18-1 shows both subtractive and additive polarity designations.

Tests to determine the polarity of unmarked transformers are quite simple to perform. Two of the adjacent high- and low-voltage terminals are connected together, as shown in Fig. 18-2, and the voltage between

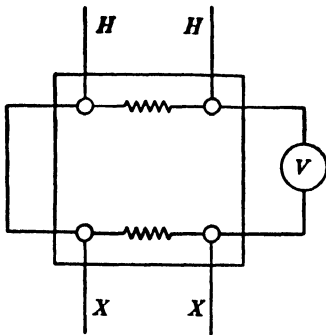


FIG. 18-2. A-c polarity test of a transformer.

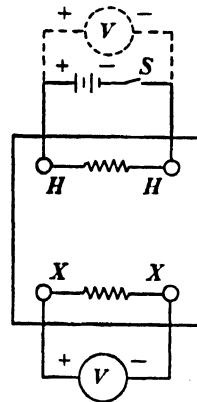


FIG. 18-3. D-c polarity test of a transformer.

the other two adjacent terminals measured when an a-c voltage is impressed on the high-voltage winding. If the voltmeter reading is greater than the voltage impressed on the high-voltage winding, the polarity is additive; if less, the polarity is subtractive.

Fig. 18-3 shows a method of determining polarity using a dry cell, a switch, and a d-c voltmeter. Either winding of the transformer is placed across the battery with the switch  $S$  in the circuit, and the voltmeter is placed across the same terminals to read upscale. The voltmeter terminals are then transferred directly across to adjacent terminals of the other winding. The switch  $S$  is suddenly opened, and the meter deflection

is observed: an upscale deflection indicates additive polarity; a downscale deflection, subtractive polarity. This test is advantageous when the turn ratio is very high but must be used with caution because of the high voltages of self-induction which may appear when the switch is opened.

Fig. 18-4 shows the manner of connection for a transformer having a single H-V winding and two L-V windings, such as a transformer rated at 440-220/110 volts. Fig. 18-4a shows the L-V winding connected in

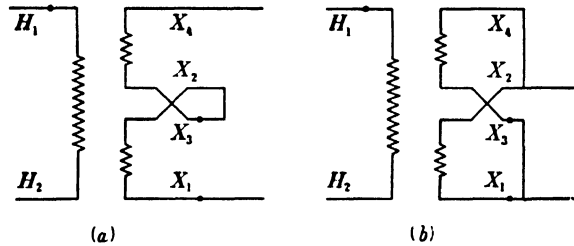


FIG. 18-4. Series and parallel connection of the secondary windings of dual voltage transformers

series for 220 volts and Fig. 18-4b shows the parallel connection for 110 volts. In instrument transformers the windings are frequently merely *spotted*, as shown in Figs. 18-1 and 18-4. The spots are indicative of terminals having the same polarity. The sequence  $X_1, X_3, X_2, X_4$ , in Fig. 18-4 is deliberate in order to simplify the scheme of connections for either series or parallel operation of the L-V windings.

**18-2. Polyphase connections (3-phase-3-phase).** The generation of large-scale power is usually 3-phase at generator voltages of 13.2 kv or slightly higher. Transmission is accomplished at higher voltages (66, 110, 132, 220, 275 kv), and transformers are therefore necessary to step-up the generator voltages to that of the transmission line. At load centers the transmission voltage must be reduced to distribution voltages (6600, 4600, 2300 volts) and, at most consumers, the distribution voltages must be reduced to utilization voltages of 440, 220, or 110 volts.

Polyphase transformation of 3-phase voltages may be accomplished either by using banks of interconnected single-phase transformers or by using polyphase transformers. Years ago the use of single-phase transformers in banks was the accepted method, but today, with improvement in transformer design and manufacture, the polyphase transformer is commonly used. Various methods of transforming 3-phase voltages to higher or lower 3-phase voltages are available. The most common con-



nections are: (a) delta-delta; (b) wye-wye; (c) delta-wye; (d) wye-delta; (e) open-delta; (f) T.

(a) *Delta-delta ( $\Delta$ - $\Delta$ ) connection.* Fig. 18-5 shows the  $\Delta$ - $\Delta$  connection of three identical single-phase transformers. The secondary winding  $ab$  corresponds to the primary  $AB$ ; the polarity of terminal  $a$  is the same as that of  $A$ . The phasor diagrams neglect the magnetizing current and impedance drops in the transformers and are drawn for unity power factor

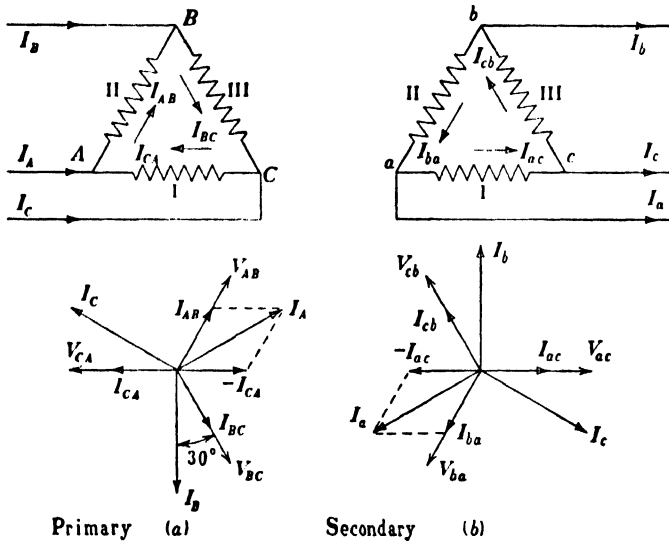


FIG. 18-5. Delta-delta connection of transformers.

between *phase* voltage and *phase* current. Thus  $I_{AB}$  is in phase with  $V_{AB}$ . As in previous diagrams, primary and secondary terminal voltages, and also primary and secondary currents, are opposite in phase so that  $V_{ba}$  corresponds to  $V_{AB}$ . Corresponding to  $\cos \varphi = 1$  between phase voltage and phase current,  $I_{ba}$  is in phase with  $V_{ba}$ . The phasor diagrams are shown for a balanced load. It should be noted that the line currents are  $\sqrt{3}$  times the phase currents and are displaced  $30^\circ$  behind the phase currents; the  $30^\circ$  displacement angle always exists for all balanced loads regardless of power factor. For identical transformers, having equal ratios of transformation and equal impedances, no circulating current exists within either primary or secondary delta, and the transformers will share the total load equally; for example, three transformers supplying a 300-kva load will each assume 100 kva of the load. The ratio of transformation between banks is the same as that of the individual transformer.

In order for the output voltage to be sinusoidal, the magnetizing cur-

rent of a transformer must contain a third-harmonic component. Since the third-harmonic components of current of the three phases are displaced from each other by  $3 \times 120 = 360^\circ$ , they are all in phase and produce a single-phase third-harmonic current circulating within the  $\Delta$ ; this current produces the sinusoidal flux, and the secondary voltage is therefore sinusoidal.

The  $\Delta$ - $\Delta$  connection offers an added advantage in that it may be operated in open-delta should one transformer be lost; the capacity available is then reduced; this is explained under (e).

(b) *Wye-Wye (Y-Y) connection.* For this connection the phasor diagrams can be drawn in the same manner as for the  $\Delta$ - $\Delta$  connection. The line voltage is  $\sqrt{3}$  times the phase voltage, and the two are displaced by  $30^\circ$ . The transformation ratio between primary and secondary line voltages or line currents is the same as that of the individual transformer.

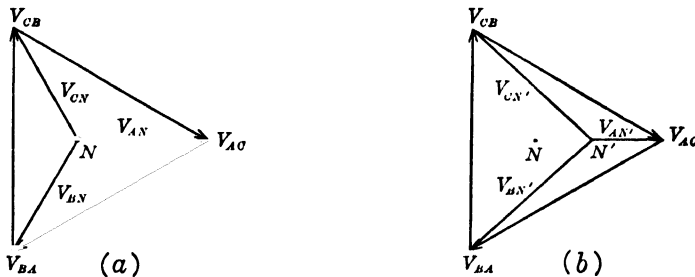


FIG. 18-6. Wye-wye connection with isolated neutral; (a) balanced load; (b) unbalanced load.

Y-Y banks are operated with grounded neutrals, i.e., the neutral of the primary is connected to the neutral of the power source. With an isolated neutral any unbalance in load or any single-phase load connected across one transformer or between lines will cause the electrical neutral to shift position and the phase voltages will become unbalanced. A grounded neutral prevents this very unsatisfactory condition of operation. Fig. 18-6 shows the conditions existing when the neutral is isolated. In Fig. 18-6a the load is balanced, and in Fig. 18-6b the load is unbalanced.

With an isolated neutral the third-harmonic components of current in the primary cancel and the transformer flux is non-sinusoidal, thus producing non-sinusoidal phase voltages; however, the line voltages are sinusoidal. Such harmonic voltages are undesirable because of the stresses which they may produce on the insulation of the windings. The use of a grounded neutral or a tertiary  $\Delta$  winding will allow a path for the third-harmonic current and thus produce a sinusoidal flux and a sinusoidal phase voltage.

(c) *Delta-wye ( $\Delta$ -Y) connection.* Fig. 18-7 shows the connections and phasor diagrams for the  $\Delta$ -Y arrangement supplying a balanced unity power factor load. The phasor diagrams may be deduced from the diagram of Fig. 18-5. Primary and secondary line voltages and line currents are observed to be out of phase with each other by  $30^\circ$ . The ratio of primary to secondary line voltages is  $1/\sqrt{3}$  times the transformation ratio for one transformer of the bank. No difficulty regarding third-harmonic currents

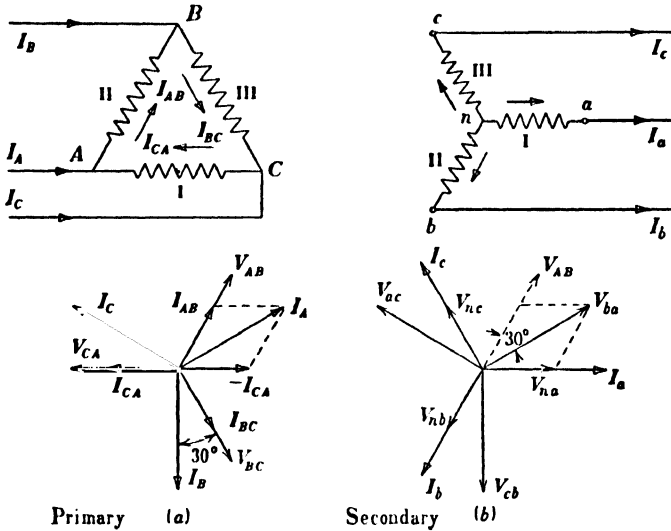


FIG. 18-7. Delta-wye connection of transformers.

appears since the existence of a  $\Delta$  connection allows a path for these currents. The use of such a bank permits a grounded neutral on the secondary side, thus providing a 4-wire 3-phase service. Unbalance in loadings causes very slight voltage unbalance since the transformer primaries are connected in delta.

Because of the  $30^\circ$  shift in primary and secondary voltages, it is not possible to parallel such a bank with a  $\Delta$ - $\Delta$  or Y-Y bank of transformers.

The secondary phasor diagrams of Fig. 18-7 may not appear to be completely consistent with those of Fig. 18-5 unless rotated through  $180^\circ$ , thus causing  $V_{ba}$  to be  $(180^\circ + 30^\circ)$  out of phase with  $V_{AB}$ . This is entirely due to the arbitrarily assumed positive directions of currents in the wye.

(d) *Wye-delta (Y- $\Delta$ ) connection.* This connection is very similar to that of the  $\Delta$ -Y connection. A  $30^\circ$  shift in line voltages appears between primary and secondary, and third-harmonic currents flow within the  $\Delta$  to

provide a sinusoidal flux. The ratio between primary and secondary voltages is  $\sqrt{3}$  times the transformer turn ratio. When operated in Y- $\Delta$ , it is customary and desirable to ground the primary neutral, thus connecting it 4-wire.

(e) *Open-delta (V-V) or V connection.* An advantage of the  $\Delta$ - $\Delta$  connection is found in the fact that if one of the transformers be removed from the bank, due to a fault or otherwise, the remaining two will continue

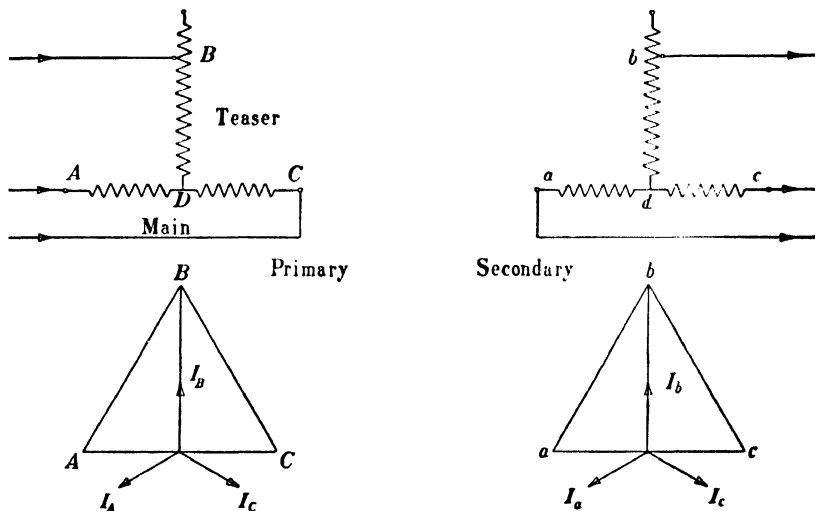


FIG. 18-8. T connection of transformers.

to deliver a 3-phase output to the load. If transformer I be removed from the bank on both primary and secondary sides in Fig. 18-5, the same line voltages  $V_{AB}$ ,  $V_{BC}$ ,  $V_{CA}$ ,  $V_{ba}$ ,  $V_{cb}$ ,  $V_{ac}$ , appear in the phasor diagrams.  $V_{AB}$  and  $V_{ba}$  appear as the sum of the voltages of transformers II and III. If the same unity-power-factor load is applied as in the discussion for the  $\Delta$ - $\Delta$  bank, the currents  $I_a$ ,  $I_b$  and  $I_c$  must appear in the same phase relationship to the line voltages as in Fig. 18-5. Therefore, the phase voltages and phase currents are out of phase by  $30^\circ$ , since phase and line currents are identical in the V connection. As a result, at unity-power-factor the transformers II and III operate at a power factor of 0.866.

In the open-delta connection the combined capacity of the two transformers, i.e.,  $\frac{2}{3}$  of the 3-phase output, is not available if the transformers are not to be overloaded. If the  $\Delta$ - $\Delta$  bank supplies a load of  $\sqrt{3} V_L I_L$  volt-amperes, then the open-delta bank is able to supply  $\sqrt{3} V_L (I_L / \sqrt{3})$  volt-amperes at the same copper losses since the line current becomes the transformer current in the open-delta connection. The ratio of the open-

delta to  $\Delta$ - $\Delta$  volt-amperes is thus  $1/\sqrt{3} = 0.577$ . Hence only 0.866 of the combined single-phase capacity is available ( $0.577/0.667$ ) when two transformers are used in open-delta. This factor is sometimes called the *utility factor*.

(f) Fig. 18-8 shows the *T connection* employing two transformers for 3-phase to 3-phase transformation. The main transformer requires a center tap and the teaser transformer an 0.866 tap, or it may be wound with 86.6% of the turns on the main transformer. For loads of unity power-factor the teaser and each half of the main transformer all operate at different power factors, thus producing voltage unbalance. Where the teaser is wound with the proper number of turns (no top), the utility factor is 0.928; when the top is employed and 0.134 turn is unused, the utility factor is 0.866. It is possible to use two identical transformers using the same number of turns in main and teaser if some slight unbalance is not objectionable in cases of emergency.

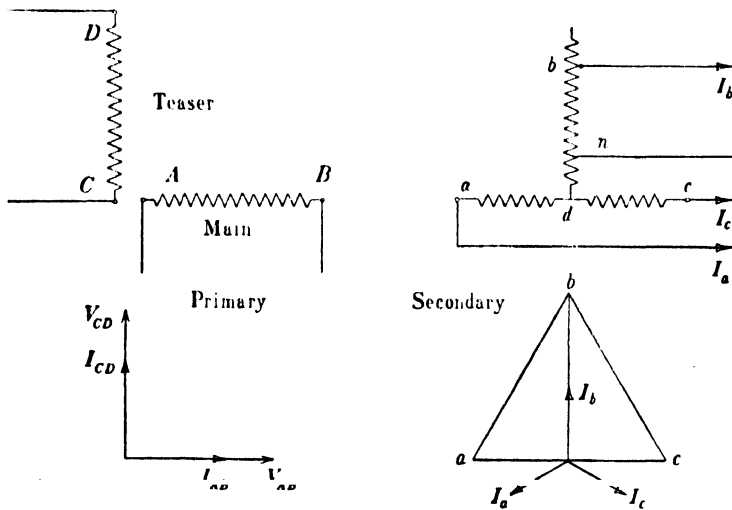


FIG. 18-9. Scott connection (2- to 3-phase transformation, or vice versa).

**18-3. Polyphase connection: 2-phase to 3-phase, or vice versa.** This connection known as the *Scott Connection* is shown in Fig. 18-9. Modern distribution systems are 3-phase, but where older 2-phase systems are in use the Scott Connection enables transformation to 3-phase power, either 3- or 4-wire. The connection is best studied with an example: in Fig. 18-9 the main transformer is rated at 2400/208 volts and has a center tap on the secondary side; the teaser transformer can be identical but requires an 86.6% tap point, providing a voltage of 180 volts. For these trans-

formers supplying a 100-kw unity-power-factor load with losses neglected, the following results are tabulated:

$I_1$ load	$= \frac{100,000}{\sqrt{3} \times 208} = 278 \text{ amp}$
Teaser power factor	= unity
Main power factor (dc)	= 0.866
Main power factor (da)	= 0.866
Power (teaser)	= $180 \times 278 = 50 \text{ kw}$
Power (main)	= $2(104 \times 278 \times 0.866) = 50 \text{ kw}$
Ratio of transformation (teaser)	= $2400/180 = 13.33$
Ratio of transformation (main)	= $2400/208 = 11.53$
Primary current (teaser)	= 20.8 amp
Primary current (main)	= 24.1 amp

It is noted that the teaser operates at unity p.f. while each half of the main operates at a p.f. of 0.866. Had the load p.f. been 0.866 lagging, the current phasors on the load phasor diagram would rotate  $30^\circ$  clockwise and the power factors would become: teaser 0.866, one half of main 0.50, other half of main 1.00. Because of the different power output from the teaser and the two halves of the main transformer, voltage unbalance results.

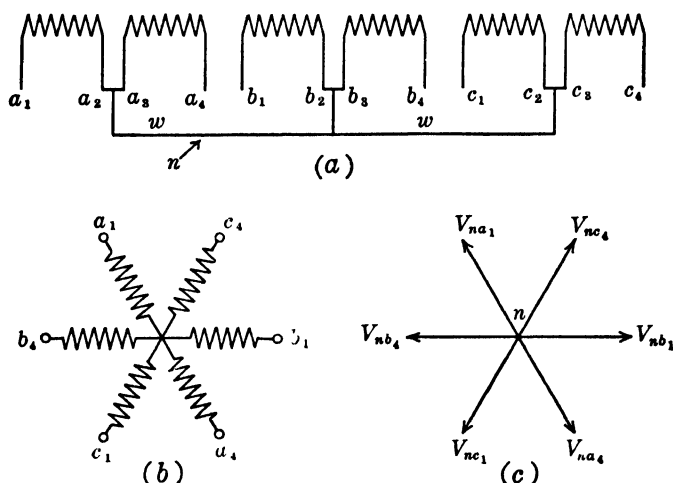


FIG. 18-10. Three to 6-phase transformation; diametrical connection.

**18-4. Polyphase connections: 3-phase to 6-phase.** Where synchronous converters or mercury arc rectifiers require 6-phase power, transformation may be accomplished by the following three common schemes of connections: (a) diametrical connection; (b) double-wye; (c) double-delta.

(a) Fig. 18-10 shows the *diametrical connection* (only the secondaries

shown). Three transformers, having center-tapped secondaries, are necessary. The leads  $a_1c_4b_1a_4c_1b_4$  are connected to the rings of a 6-phase converter or the anodes of a mercury arc rectifier. This connection is a *true* 6-phase connection which yields 6-phase voltages between the six leads regardless of whether or not a load is connected. The neutral of the bank may be grounded and used as the neutral wire of a 3-wire d-c system employing a converter. When the transformers are used with a mercury arc rectifier, the neutral constitutes the negative side of the d-c output.

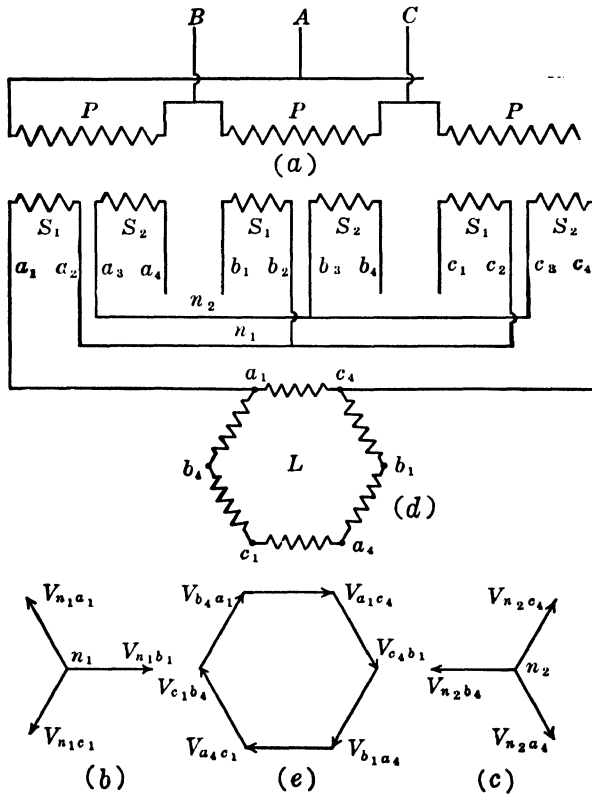


FIG. 18-11. Three to 6-phase transformation; double-wye connection.

(b) Fig. 18-11 shows the *double-wye* connection. Each transformer requires two identical secondary windings. Two separate wye connections are arranged as shown in Fig. 18-11 so that the voltages available from terminals  $a_1b_1c_1$  are opposite in phase to the voltages available from  $a_4b_4c_4$ . With the neutrals  $n_1$  and  $n_2$  connected, the system becomes identical with the diametrical arrangement of the previous discussion and is a *true* 6-phase system yielding voltages between terminals both with and

without a load connected. With the neutrals  $n_1$  and  $n_2$  separate, the two secondary wyres are not interconnected until a symmetrical 6-phase load is applied to terminals  $a_1c_4b_1a_4c_1b_4$ . Such an arrangement is not considered *true* 6-phase, but operates 6-phase when the load is present. When used with a 6-phase mercury arc rectifier, the double-wye connection is employed with a center-tapped reactance coil (called an interphase transformer) connecting  $n_1$  and  $n_2$ . The center tap constitutes the negative side of the d-c output. By using this arrangement two anodes are always

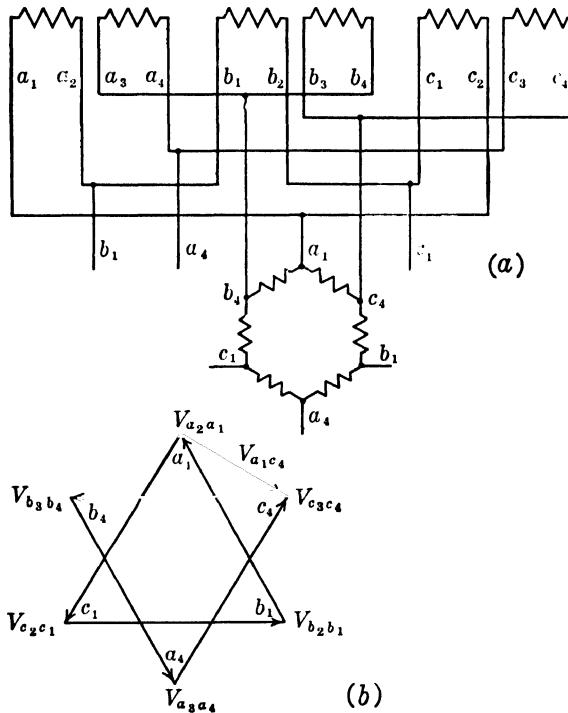


FIG. 18-12. Three- to 6-phase transformation; double-delta connection.

firing together, each overlapped with the other by 60 electrical degrees. With a solid connection between  $n_1$  and  $n_2$  just one anode fires at a time.

(c) Fig. 18-12 shows the *double-delta* connection. Again two identical secondaries are necessary on each transformer. Two independent deltas are formed, and the load is necessary to make 6-phase operation complete. Without the load, 6-phase voltages are not obtainable between the terminals  $a_1c_4b_1a_4c_1b_4$ .

A double-T connection employing two transformers also may be used for 3- to 6-phase transformation. The *main* requires a center-tapped



primary and two identical center-tapped secondaries; the *teaser* requires an 86.6% tap on the primary and similar taps on each of two identical secondaries.

By means of the Scott connection it is possible to transform from 2- to 6-phase, using main and teaser transformers each having a single primary winding and two secondary windings, the main with center-tapped secondaries, and the teaser with 86.6% tapped windings.

It should be noted here that phase transformation from single phase to polyphase cannot be accomplished with static transformers, and requires rotating equipment.

### PROBLEMS

1. A 10,000-kva, 13,200-volt, 3-phase generator supplies power to a 3-phase, 220-volt load by means of three single-phase transformers connected in a 3-phase bank. Determine the voltage, current, and kva ratings, and also the ratio of transformation for:

- (a) Y- $\Delta$  bank
- (b) Y-Y bank
- (c)  $\Delta$ -Y bank
- (d)  $\Delta$ - $\Delta$  bank

2. Three identical 60-cycle power transformers are connected in a Y- $\Delta$  bank to transform voltages from a 440-volt, 3-phase, 3-wire distribution system, in order to supply a 220-volt 3-phase 3-wire load. If the operating flux density is 70,000 lines per sq in. and the mean core area 40 sq in., determine the number of turns in the primary and secondary windings.

3. Three single-phase transformers are to be arranged in a 3-phase bank to supply a 120-volt, 4-wire system from a 3-wire, 6600-volt distribution line. The transformers are connected  $\Delta$ -Y with the neutral grounded on the secondary side. If a balanced 300-kw unity power factor lighting load is supplied by this bank, determine:

- (a) Primary current and voltage ratings.
- (b) Secondary current and voltage ratings.
- (c) Ratio of transformation.

4. A Y- $\Delta$  bank of transformers supplies a balanced load of 500 kw, 1100 volts, 0.85 power factor lagging. Determine primary and secondary voltages and currents. Draw a complete phasor diagram for primary and secondary. Line voltage = 11,000.

5. Repeat Problem 4 for a  $\Delta$ -Y connection.

6. Repeat Problem 4 for a  $\Delta$ - $\Delta$  connection.

7. The leads of three special 220/81-volt transformers lack polarity markings and it is necessary to connect them in a  $\Delta$ -Y bank in order to supply a 3-phase synchronous converter requiring a ring voltage of 140 volts. How would you proceed to connect the transformers using a single lamp as the only test equipment available?

8. If a fully loaded 50-HP, 208-volt, 4-pole induction motor having an efficiency of 91% and a power factor of 90% is placed in parallel with the lighting load of Problem 3 above determine:

- (a) Secondary current.
- (b) Primary current.
- (c) Transformer power factor.

9. A 4600/440-volt  $Y-\Delta$  bank of three identical transformers supplies three balanced 3-phase loads connected in parallel: (a) 75 kw at unity power factor; (b) 100 kva at 0.90 power factor lagging; (c) 50 kva at 0.85 power factor leading. Determine the transformer ratings necessary.

10. A  $\Delta-\Delta$  bank of identical transformers carries a balanced 3-phase load of 100 kva, 0.866 power factor lagging, and a single-phase load of 40 kw, unity power factor. Specify the kw and kva of each transformer.

11. A 300-kw, 440-volt, 3-phase, 3-wire balanced load operating at 0.85 power factor lagging is to be supplied from a 4600-volt, 2-phase, 4-wire system. Determine the ratio of transformation and kva ratings for both the main and teaser transformers.

12. How much power is delivered by each transformer in Problem 11?

13. It is necessary to supply a balanced 2-phase, 220-volt load of 50 kw, 0.90 power factor lagging from a 3-phase, 1100-volt system. Specify the voltages and currents for the transformers necessary.

14. A  $\Delta-\Delta$  bank of transformers supplies a balanced unity power load of 150 kw. If one transformer is removed, specify the operating power factor and kw load for each of the two remaining transformers operating in open delta.

15. Repeat Problem 14 for a balanced load of 150 kw operating at 0.866 power factor lagging.

16. A 3-phase, 1100-volt system supplies 1000 kva to a 220-volt balanced 3-phase load by means of T-connected transformers. Specify the voltage and current ratings of the transformers and the ratios of transformation.

17. Two 230/115-volt transformers having center taps on both primary and secondary windings, but lacking 86.6% taps, are connected in T on both primary and secondary sides. If the primary side is connected to a balanced 230-volt, 3-phase system, determine the line to line voltages on the secondary side, and specify the displacement angles between them. Neglect exciting currents and impedance drops.

18. A 2-phase, 440-volt, 60-cycle, 50-HP motor having an efficiency of 91% and operating at a power factor of 0.88 takes power from a 2300-volt, 3-phase system through a Scott-connected bank of transformers. Determine the kva loading for each transformer on both primary and secondary sides.

19. Two 50-kva transformers are connected in open delta and supply a balanced load of 0.80 power factor lagging. What is the maximum kw load permitted if the transformers are allowed to operate at 15% overload?

20. How much additional load of the same 0.80 power factor can be carried if a third 50-kva transformer is added in Problem 19 to produce a full  $\Delta-\Delta$  bank?

21. A 6-phase, 625-volt synchronous converter receives power from an 11,500-volt 3-phase distribution system. If the power input is 500 kva at unity power factor, and the transformer bank supplying the converter is connected  $\Delta$  on the primary side and diametrical on the secondary, determine the voltage, current, and kva ratings of both primary and secondary windings. Also specify the ratio of transformation.

22. Repeat Problem 21 for a  $\Delta$ -double  $\Delta$  transformer bank.

23. Repeat Problem 21 for a  $\Delta$ -double Y transformer bank.

# Chapter 19

## PARALLEL OPERATION OF TRANSFORMERS

**19-1. Parallel operation of transformers.** When two or more transformers are to be operated in parallel in order to deliver power to a load over common bus-bars, it is necessary to satisfy very definite conditions of

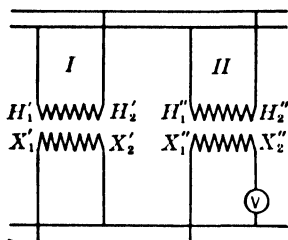


FIG. 19-1. Two transformers in parallel.

operation. In the analysis of this chapter just two transformers will be considered in parallel.

The first condition to be satisfied is that primary and secondary windings be connected to their respective bus-bars with due regard to the polarity: at any instant all transformer *terminals connected to a given bus must have the same polarity*. In Fig. 19-1 two transformers are shown in parallel and a voltmeter  $V$  is shown between the terminal  $X_2''$  (or  $X_1''$  or  $X_2'$  or  $X_1'$ ) and the bus-bar to which this terminal is

connected: it is assumed that the  $H$  terminals constitute the primary windings and the  $X$  terminals are connected to the common bus-bars supplying the load. If the voltmeter  $V$  reads zero, the condition of proper polarities is satisfied; otherwise, the voltmeter would read double secondary voltage indicating improper polarities.

Further conditions for parallel operation can be derived from the current voltage relations of the simplified Kapp diagram (Fig. 16-1) and the corresponding equivalent circuit of Fig. 19-2 which neglects the magnetizing current. In this discussion the influence of the transformation ratio will also be introduced. For this purpose the secondary voltage will be expressed as  $V_2 = aV_t$  where  $V_t$  is the actual secondary voltage. All currents and impedances are referred to the primary side. Thus for transformer I

$$\mathbf{V}_1' = a'\mathbf{V}_t' + \mathbf{I}_2'\mathbf{Z}_{c1}' \quad (19-1)$$

and for transformer II

$$\mathbf{V}_1'' = a''\mathbf{V}_t'' + \mathbf{I}_2''\mathbf{Z}_{c1}'' \quad (19-2)$$

But since primaries and secondaries are connected to common buses

$$\mathbf{V}_1' = \mathbf{V}_1'' = \mathbf{V}_1 \quad \text{and} \quad \mathbf{V}_t' = \mathbf{V}_t'' = \mathbf{V}_t \quad (19-3)$$

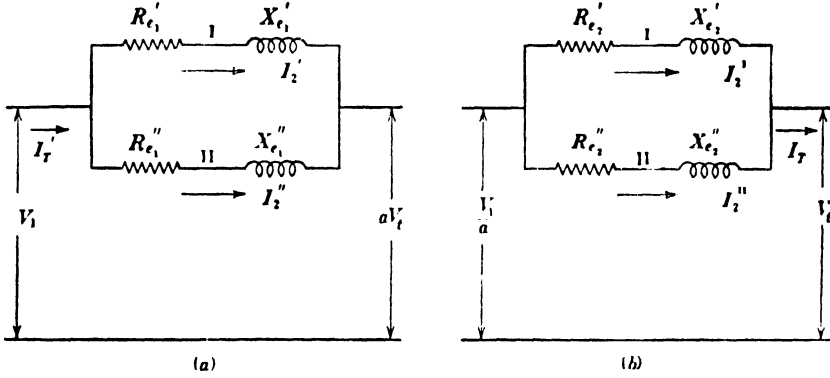


FIG. 19-2. Equivalent circuit of two transformers in parallel: (a) in terms of primary; (b) in terms of secondary.

$\mathbf{Z}_{c1}'$  and  $\mathbf{Z}_{c1}''$  are the equivalent impedances in terms of the primary (short-circuit impedances with secondary short-circuited). The total load current (on the primary side) is the sum of the transformer currents, or

$$\mathbf{I}_T' = \mathbf{I}_2' + \mathbf{I}_2'' \quad (19-4)$$

From Eqs. 19-1 to 19-4 the following relations may be obtained:

$$\mathbf{I}_2' = \frac{-\mathbf{V}_t(a' - a'') + \mathbf{I}_T'\mathbf{Z}_{c1}''}{\mathbf{Z}_{c1}' + \mathbf{Z}_{c1}''} \quad (19-5)$$

$$\mathbf{I}_2'' = \frac{+\mathbf{V}_t(a' - a'') + \mathbf{I}_T'\mathbf{Z}_{c1}'}{\mathbf{Z}_{c1}' + \mathbf{Z}_{c1}''} \quad (19-6)$$

The only quantity in Eq. (19-1) to (19-6) not referred to the primary is  $\mathbf{V}_t$ . All other quantities are, as mentioned previously, referred to the primary.

If  $\mathbf{Z}_{c2}'$  and  $\mathbf{Z}_{c2}''$  are the equivalent impedances referred to the secondary and  $\mathbf{I}_T$  is the total load current on the secondary side the voltage equations become

$$\frac{\mathbf{V}_1'}{a'} = \mathbf{V}_t' + \mathbf{I}_2'\mathbf{Z}_{c2}' \quad (19-7)$$

$$\frac{\mathbf{V}_1''}{a''} = \mathbf{V}_t'' + \mathbf{I}_2''\mathbf{Z}_{c2}'' \quad (19-8)$$

and 
$$I_T = I_2^I + I_2^{II} \quad (19-9)$$

Eq. 19-3 and Eqs. 19-7 to 19-9 yield

$$I_2^I = \frac{-V_t(a' - a'') + a''I_T Z_{e2}''}{a'Z_{e2}' + a''Z_{e2}''} \quad (19-10)$$

$$I_2^{II} = \frac{+V_t(a' - a'') + a'I_T Z_{e2}'}{a'Z_{e2}' + a''Z_{e2}''} \quad (19-11)$$

where  $I_2^I$  and  $I_2^{II}$  are now the actual transformer currents on the load or secondary side.

The equations for  $I_2'$  and  $I_2''$  and also  $I_2^I$  and  $I_2^{II}$  show that the current of each transformer consists of two components. The magnitude of the first component is the same in each transformer but opposite in phase, i.e., these two currents represent an *internal current* circulating between the transformers and never reaching the external circuit. The sum of the second components of  $I_2'$  and  $I_2''$  or  $I_2^I$  and  $I_2^{II}$  gives the load current at the primary or secondary bus-bars, depending upon which set of equations is employed.

The circulating current results from a difference in the transformation ratios ( $a' - a''$ ) and is independent of the load current. It also exists at no load ( $I_T'$  or  $I_T = 0$ ).

From Eqs. 19-5 and 19-6 with transformers having equal transformation ratios ( $a' = a''$ )

$$\frac{I_2'}{I_2''} = \frac{Z_{e2}''}{Z_{e2}'} \quad (19-12)$$

i.e., if two transformers of the same rating and same transformation ratio are to divide the load equally, their short-circuit impedances must be equal. In general, for transformers of different rating but the same transformation ratio, the equivalent impedances must be inversely proportional to the ratings, if each transformer is to assume a load in proportion to its rating. Thus, a transformer in parallel with another of twice the capacity must have an impedance twice that of the larger transformer in order that the load be properly divided between them.

It should be noted that satisfying Eq. 19-12 does not necessarily require equal power factors for the currents  $I_2'$  and  $I_2''$ . Consider two transformers of the same rating and same transformation ratio having  $Z_{e2}' = Z_{e2}''$  (Fig. 19-3). It is assumed that the short-circuit resistances (equivalent resistances) are not equal; consequently the short-circuit reactances are also unequal. Since  $I_2'R_{e2}'$  and  $I_2''R_{e2}''$  make different angles with  $V_t' = V_t''$ , then  $I_2'$  and  $I_2''$  must have different angles with  $V_t$ , i.e., the transformers operate with equal currents at different power

factors (Fig. 19-3). Thus the proper distribution of active and reactive current components requires that the ratios of short-circuit resistances and reactances be equal, i.e.,  $X_e'/R_e' = X_e''/R_e''$ . If this condition is not satisfied, the total loss of the two transformers will not be a minimum.

Summarizing, the conditions for proper parallel operation of single-phase transformers are the following: (a) proper connections to the bus-bars with regard to polarity, (b) identical voltage ratings, (c) equal transformation ratios, (d) ratio of the equivalent impedances inversely proportional to the ratio of current ratings, (e) ratio of equivalent resistances equal to ratio of equivalent reactances.

For parallel operation of 3-phase transformers, conditions have to be satisfied similar to those for single-phase transformers. The secondary voltages of 3-phase transformers to be connected in parallel are in phase if, for the same winding directions of primary and secondary, the connections of primary and secondary windings are the same: for example, all primaries connected star and all secondaries connected delta, or vice versa. Consider a single 3-phase transformer; if its primary and secondary windings are connected the same (both star or both delta), then the line voltages are displaced from each other by almost  $180^\circ$ . On the other hand, if the primary winding is connected in star and the secondary in delta, or vice-versa, the line voltages are displaced from each other by about  $(180^\circ \pm 30^\circ)$ . It therefore follows that transformers having the same primary connections (all star or all delta) and different secondary connections (some star and some delta) cannot be connected in parallel. However, a transformer with its windings connected in star may be connected in parallel with a transformer having its windings connected in delta.

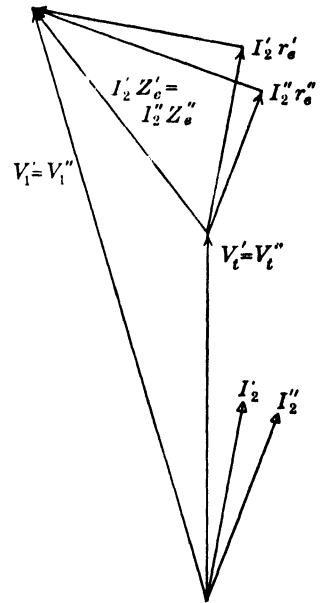


FIG. 19-3. Phasor diagram of two transformers in parallel.

**Example.** The data below apply to two single-phase transformers:

Transformer	Rating (kva)	Voltage	Short-circuit test (at rated current)	
			Voltage	Watts
A.....	200	2300/230	160	1400
B.....	300	2300/225	100	1700

The transformers operate in parallel on both sides and deliver a total load of 400 kva at 0.80 power factor lagging. Determine: (a) the current delivered by each to the load bus; (b) the power delivered by each; (c) the power factor of each.  $V_t = 230$  volts.

## Transformer A

$$I_1 = \frac{200,000}{2300} = 87$$

$$a' = \frac{2300}{230} = 10$$

$$Z_{e1}' = \frac{160}{87} = 1.84$$

$$R_{e1}' = \frac{1400}{(87)^2} = 0.185$$

$$X_{e1}' = 1.83$$

$$Z_{e1}' = 0.185 + j1.83 = 1.84 \angle 84.23$$

$$Z_{e2}' = \frac{Z_{e1}'}{(a')^2} = 0.00185 + j0.0183$$

$$Z_{e2}' = 0.0184 \angle 84.23$$

## Transformer B

$$I_1 = \frac{300,000}{2300} = 130.5$$

$$a'' = \frac{2300}{225} = 10.22$$

$$Z_{e1}'' = \frac{100}{130.5} = 0.767$$

$$R_{e1}'' = \frac{1700}{(130.5)^2} = 0.0998$$

$$X_{e1}'' = 0.760$$

$$Z_{e1}'' = 0.0998 + j0.760 = 0.767 \angle 82.5$$

$$Z_{e2}'' = \frac{Z_{e1}''}{(a'')^2} = 0.000955 + j0.00727$$

$$Z_{e2}'' = 0.00734 \angle 82.5$$

$$I_T = \frac{400,000}{230} = 1740 \text{ amp}$$

$$I_T = 1740 \angle -36.8 = 1392 - j1044$$

$$I_2^I = \frac{-230 \angle 0(10 - 10.22) + 1740 \angle -36.8 \times 10.22 \times 0.00734 \angle 82.5}{10 \times 0.0184 \angle 84.23 + 10.22 \times 0.00734 \angle 82.5}$$

$$= \frac{50.6 + j0 + 91.2 + j93.5}{0.0283 + j0.0257} = \frac{170 \angle 33.4}{0.259 \angle 83.73}$$

$$= 657 \angle -50.33 = 418 - j506$$

$$I_2^{II} = \frac{230 \angle 0(10 - 10.22) + 1740 \angle -36.8 \times 10 \times 0.0184 \angle 84.23}{0.259 \angle 83.73}$$

$$= \frac{-50.6 + j0 + 21.6 + j235}{0.259 \angle 83.73} = \frac{288 \angle 54.8}{0.259 \angle 83.73}$$

$$= 1112 \angle -28.93 = 974 - j538$$

$$(check) \quad I_2^I + I_2^{II} = 1392 - j1044$$

$$\text{Power Factor A} = \cos 50.33^\circ = 0.638 \text{ lagging}$$

$$\text{Power Factor B} = \cos 28.93^\circ = 0.875 \text{ lagging}$$

$$\text{Power A} = 230 \times 657 \times 0.638 = 96 \text{ kw}$$

$$\text{Power B} = 230 \times 1112 \times 0.875 = 224 \text{ kw}$$

$$(check) \quad 96 + 224 = 320 = 400 \times 0.80$$

If the load on these transformers was reduced to zero the currents would become

$$\begin{aligned} \mathbf{I}_2^{\text{I}} (\text{no-load}) &= \frac{-230 \angle 0(10 - 10.22)}{0.259 \angle 83.73} = \frac{50.6 \angle 0}{0.259 \angle 83.73} \\ &= 195.5 \angle -83.73 = 21.3 - j194 \\ \mathbf{I}_2^{\text{II}} (\text{no-load}) &= \frac{230 \angle 0(10 - 10.22)}{0.259 \angle 83.73} = \frac{50.6 \angle 180}{0.259 \angle 83.73} \\ &= 195.5 \angle 96.27 = -21.3 + j194 \end{aligned}$$

The current above is the circulating current and exists under all conditions of loading. Thus, under load, the component of  $\mathbf{I}_2^{\text{I}}$  supplying the load is

$$\begin{aligned} \mathbf{I}_2^{\text{I}} (\text{load component}) &= (418 - j506) - (21.3 - j194) \\ &= 396.7 - j312 \end{aligned}$$

and

$$\begin{aligned} \mathbf{I}_2^{\text{II}} (\text{load component}) &= (974 - j538) - (-21.3 + j194) \\ &= 995.3 - j732 \end{aligned}$$

The sum of the above two currents is as it should be,  $\mathbf{I}_T = 1392 - j1044$

If the transformation ratios of the two transformers had been the same, and if the equivalent impedances  $Z_{e2}'$  and  $Z_{e2}''$  were unchanged, the circulating current would disappear and  $\mathbf{I}_2^{\text{I}}$  and  $\mathbf{I}_2^{\text{II}}$  would become:

$$\begin{aligned} \mathbf{I}_2^{\text{I}} &= \frac{91.2 + j93.5}{0.259 \angle 83.73} = \frac{131 \angle 45.7}{0.259 \angle 83.73} \\ &= 506 \angle -38.0 = 397 - j312 \\ \mathbf{I}_2^{\text{II}} &= \frac{216 + j235}{0.259 \angle 83.73} = \frac{319 \angle 47.4}{0.259 \angle 83.73} \\ &= 1233 \angle -36.33 = 995 - j732 \end{aligned}$$

The sum of the above two currents is  $\mathbf{I}_T = 1392 - j1044$

## PROBLEMS

1. The short-circuit test data for two single-phase, 22,000/440-volt, 60-cycle transformers are given below in p-u:

Transformer	Rating (kva)	Short-circuit Test		
		Voltage	Current	Power
I .....	100	0.025	1.0	0.01
II .....	500	0.035	1.0	0.008

Unit voltage = 22,000

Unit current = rated current

Unit power = rated kva

Determine for each transformer



- (a) Impedance, resistance, and reactance in ohms and p-u.
- (b) Full-load efficiency at unity, 0.80 lagging and 0.80 leading power factor, assuming the core loss and copper loss equal at full load.
- (c) Regulation at unity, 0.80 lagging and 0.80 leading power factor.

2. The transformers of Problem 1 are operated in parallel on both the primary and secondary sides and supply a load of 500 kw at unity power factor at 440 volts. Determine:

- (a) Current delivered by each transformer.
- (b) Power output of each transformer.
- (c) Power factor at which each transformer operates.
- (d) Circulating current.

3. Repeat Problem 2 above for a 500-kva load at 0.8 power factor lagging. Carry out all calculations in p-u. Use common base of 600 kva.

4. Two single-phase, 66,000/6600-volt, 60-cycle, transformers are tested on short circuit, and the following p-u data are recorded (unit power = transformer rating in kva):

<i>Transformer</i>	<i>Rating</i>	<i>Voltage</i>	<i>Current</i>	<i>Watts</i>
I.....	1000	0.05	1.0	0.008
II.....	3000	0.06	1.0	0.007

The transformers are connected in parallel on both sides and supply a load of 3500 kva at 0.85 power factor lagging, 6600 volts. Determine:

- (a) Current delivered by each transformer.
- (b) Power output of each transformer.
- (c) Power factor of each transformer.
- (d) Circulating current.

Carry out all calculations on a p-u basis using a common base of 4000 kva.

5. The data of short-circuit tests at *rated current* on two transformers are given as:

<i>Transformer</i>	<i>Rating</i>		<i>S.C. Test</i>	
	<i>Kva</i>	<i>Voltage</i>	<i>Volts</i>	<i>Power (watts)</i>
A.....	100	11,000/2300	265	1000
B.....	500	11,000/2350	340	3400

The transformers are connected in parallel on both sides to 11,000- and 2300-volt buses, and supply a total load current of 275 amp at 0.90 power factor lagging to the 2300-volt bus. Determine:

- (a) Current delivered by each transformer.
- (b) Power delivered by each transformer.
- (c) Power factor of each transformer.
- (d) Circulating current.

6. If the ratios of transformation of the transformers in Problem 5 were the same, namely, 11,000/2300, determine:

- (a) Current delivered by each transformer.
- (b) Power delivered by each transformer.
- (c) Power factor of each transformer.
- (d) Circulating current.

7. Compare the transformer copper losses in Problems 5 and 6. Explain the difference.

## Chapter 20

### THE AUTOTRANSFORMER INSTRUMENT TRANSFORMERS CONSTANT-CURRENT TRANSFORMER

**20-1. The Autotransformer.** Chapters 11 to 19 discussed the general theory of the 2-winding transformer. The *autotransformer* using a single winding on an iron core, with a part of the winding common to both the primary and secondary, is frequently used. For certain types of service the autotransformer is superior to the 2-winding transformer, offering better regulation, reduced weight and size per kva, lower cost, higher efficiency, and lower magnetizing current.

In the autotransformer only a part of the kva input is transformed from the primary to the secondary by transformer action, while the remainder is transferred directly from the primary lines to the secondary lines. The relative amounts of power transformed and power transferred depend upon the ratio of transformation. Autotransformers offer the greatest advantage when the ratio of transformation is small; the smaller the ratio of transformation, the smaller the physical size of the autotransformer required to supply a given load.

However, the autotransformer has a disadvantage in that the low-voltage side has a metallic connection to the high-voltage side contrary to the 2-winding transformer. Thus a ground on the high-voltage side of an autotransformer may subject the low-voltage circuit to the high voltage of the high-voltage line.

Fig. 20-1 shows the schematic diagram of an autotransformer with a primary impressed voltage  $V_1$  and a load voltage  $V_2$ . Just as in the

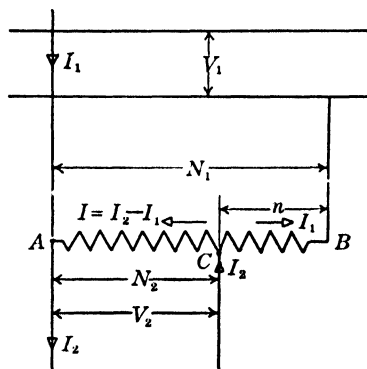


FIG. 20-1. Schematic diagram of an autotransformer.

2-winding transformer the core flux is determined by the induced emf  $E_1$  ( $\approx V_1$ ), the number of primary turns  $N_1$ , and the line frequency. The ratio of transformation is given by:

$$a = \frac{E_1}{E_2} = \frac{N_1}{N_2} \approx \frac{V_1}{V_2} \approx \frac{I_2}{I_1} \quad (20-1)$$

The common part of the winding between  $A$  and  $C$  carries a current which is the difference between  $I_2$  and  $I_1$ . If the magnetizing current is ignored the difference  $I_2 - I_1$  may be taken algebraically.

It follows from Fig. 20-1 that:

$$\begin{aligned} \frac{I_2}{I_1} &= a & \frac{E_1}{E_2} &= a \\ \frac{I}{I_1} &= a - 1 & \frac{E_n}{E_1} &= \frac{n}{N_1} = \frac{a - 1}{a} \\ \frac{I}{I_2} &= \frac{a - 1}{a} & \frac{E_n}{E_2} &= a - 1 \end{aligned} \quad (20-2)$$

$$\frac{\text{Rating as an autotransformer}}{\text{Rating as a 2-winding transformer}} = \frac{a}{a - 1} \quad (20-3)$$

$$\frac{\text{Full-load losses in \% of autotransformer rating}}{\text{Full-load losses in \% of 2-winding transformer rating}} = \frac{a - 1}{a} \quad (20-4)$$

$$\frac{\text{Magnetizing current as an autotransformer}}{\text{Magnetizing current as a 2-winding transformer}} = \frac{a - 1}{a} \quad (20-5)$$

$$\frac{\text{Impedance drop as an autotransformer}}{\text{Impedance drop as a 2-winding transformer}} = \frac{a - 1}{a} \quad (20-6)$$

$$\frac{\text{Short-circuit current as an autotransformer}}{\text{Short-circuit current as a 2-winding transformer}} = \frac{a}{a - 1} \quad (20-7)$$

$$\frac{\text{Regulation as an autotransformer}}{\text{Regulation as a 2-winding transformer}} = \frac{a - 1}{a} \quad (20-8)$$

**20-2. Instrument transformers.** Instrument transformers are divided into two classes: potential transformers and current transformers. Each serves two purposes: (1) to insulate the high-voltage circuit from the measuring circuit, in order to protect the measuring apparatus and the operator; (2) to make possible the measurement of high voltages, with low-voltage instruments (usually 115 volts), or large currents with low-

current ammeters (usually 5 amp), which procedure simplifies the measuring problem greatly. These transformers also are used to operate relays, solenoids, circuit-breakers, or other controlling devices. The principle of the instrument transformer is fundamentally the same as that of the power transformer.

The potential transformer has the high voltage applied to the primary, and the secondary, usually rated at 115 volts, is connected to the voltmeter. From Figs. 14-1 and 14-2 it is observed that the ratio of primary to secondary terminal voltage is not the same as the turn ratio, but also depends upon the character of the load, upon the impedance of the windings, and upon the magnetizing current  $I_m$ . The phase angle between primary and secondary terminal voltages is not exactly  $180^\circ$ , or zero if the phasor  $V_2'$  is reversed (see Fig. 16-1). In order to keep the ratio of primary to secondary voltage constant, or practically so, the potential transformer is designed with as small a leakage reactance and resistance as possible. The flux density in the core is also lower than that used in power transformers. Thus, in order to keep the ratio and phase-angle errors small, the instrument transformer is much larger than a power transformer of the same rating. Instrument transformers usually are rated from 25 to 500 volt-amperes according to the *burden* or secondary load. As far as heating is concerned, their rating as a power transformer would be from two to four times the rating as instrument transformers.

From Fig. 14-1 it should be clear that  $V_1/V_2'$  is more nearly unity, or  $V_1/V_2$  more nearly equal to  $a$ , the smaller the load current, or the greater the load impedance. Also  $\varphi_1$  is more nearly equal to  $\varphi_2$  under these same conditions. It also is clear that, for a given secondary burden, the ratio and phase angle can be specified accurately. Thus, the ratio and phase angle of instrument transformers usually are specified for a certain burden, and correction factors are applied, if necessary, for other burdens. Usually the departure from the specified values is very small. Fig. 20-2 shows a typical correction curve for a potential transformer. The phase-angle error is the angle of departure of  $V_1$  from  $V_2$  reversed, so it is nearly zero and not  $180^\circ$ . The phase-angle error is of importance only in power measurements, while the ratio error is important in both voltage and power measurements. Fig. 20-3 shows a typical voltage transformer, rated 2400/120 volts. Note the fuses and bushings on the primary side. The low-voltage secondary terminals are shown on the front of the case.

Current transformers perform somewhat the same service in a-c measurements as shunts do in d-c, and in addition they perform the important function, in high-voltage circuits, of insulating the measuring devices from the high-voltage lines. The important characteristic required in a current

transformer is a constant ratio between secondary and primary current, as well as a small phase angle between primary and secondary current. From the discussion of Art. 13-1 and from Figs. 14-1 and 14-2, it is observed that  $I_2'$  and  $I_1$  are more nearly equal, or  $I_2 = aI_1$  when the

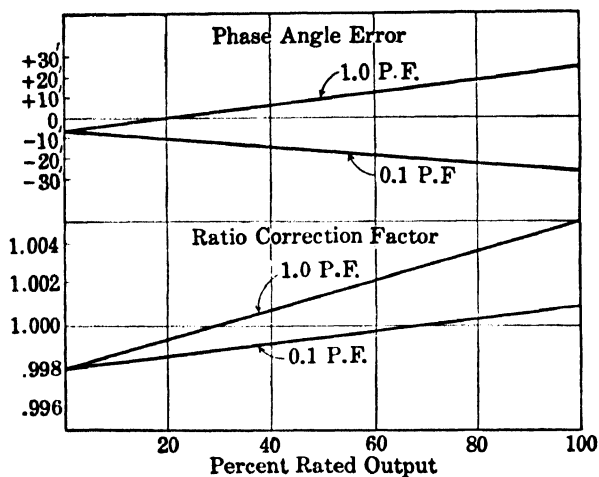


FIG. 20-2. Potential transformer correction curves.

magnetizing current  $I_m$  is small in comparison to  $I_2'$ . The ratio of  $I_2$  to  $I_1$  differs from the turn ratio  $a$  when  $I_m$  is large, although it is not affected appreciably by the impedance of the windings. Ratio and phase-angle correction often must be applied to current transformers also, and the manufacturers will supply them when required. Thus, in instrument transformers, it is necessary to use high-grade laminations for the core, and to operate at relatively low flux densities.

The secondary current of the current transformer depends mainly upon the primary current, and is nearly independent of the impedance of the instruments connected to the secondary. Primary current flows independent of whether the secondary circuit is open or closed; it is determined entirely by the line current. If the secondary circuit is open, no secondary current can flow, and hence there is no opposing mmf provided by secondary current. The result is that the primary current is then entirely a magnetizing current  $I_m$  (see Fig. 12-2). This results in a very high flux density and a high induced voltage in the secondary, as well as a high impedance drop across the primary. The voltage may be sufficient to damage the secondary insulation, or to shock severely an operator coming in contact with the secondary terminals. *Therefore, it is important that the secondary of current transformers be short-circuited when there are no*

*instruments connected to it. This is an important consideration. Many portable current transformers have a shorting switch mounted directly on the transformer.*

The primary of the current transformer has only a few turns, often only one, while the secondary has many turns, the number of them depending on the ratio desired. Fig. 20-4 shows a current transformer in



FIG. 20-3. Potential transformer 2400/120 volts.



FIG. 20-4. Current transformer 200/5 amp.

which the primary consists only of a single bar of copper around which is placed the secondary winding. The secondary of both the current and potential transformer, as well as the iron core, always should be grounded.

**20-3. The constant-current transformer.** Street lighting circuits, using arc or incandescent lamps, frequently employ lamps connected in series (see Chapter 51). All lamps in series have the same current which must

be carefully regulated and maintained constant in order to insure maximum lamp life. The circuit current is the same as that of the lamps and is much lower than would be the case with lamps in parallel. However, the circuit voltage is usually rather high and depends upon the number of lamps in series.

Constant-current transformers are designed to maintain a constant current in the series lamp circuits, regardless of the number of lamps connected in series across the secondary winding of the transformer. A common secondary current rating is 6.60 amp, but other ratings such as 7.5 or 20 amp also are used. Regulation of the current to within  $\pm \frac{1}{2}\%$  of the rated value between  $\frac{1}{4}$  and  $1\frac{1}{4}$  load is readily accomplished. Primary transformer voltages are usually 2400 or 4800 volts, and the secondary voltages under load may be as high as 4000 volts.

The *moving coil* constant-current transformer may be an oil-immersed



FIG. 20-5. Constant current transformer, 20 kw, 2400-volt primary, 6.6 amp secondary, 60 cycles, equipped with compound balancing lever and micrometer weight adjustment. Hinge-end view.

transformer, or a dry-type, air-cooled, indoor transformer. The primary winding is stationary and the secondary is free to move with respect to the primary; counterweights are used to effect a balance between the weight of the secondary coil and the force of repulsion between the primary and secondary. Fig. 20-5 shows a constant-current transformer.

In operation a constant voltage is applied to the primary, and the secondary adjusts its position relative to the primary so that the secondary

voltage across the series lamp circuit produces the rated lamp current. At this position a mechanical balance results between coil weight, counterweights, and the electromagnetic force of repulsion. Should a single lamp in the series string burn out, it is automatically shorted by an oxide film device in the lamp base, and the transformer secondary moves farther away from the primary. As the secondary winding moves farther away from the primary winding, the leakage flux increases and the secondary terminal voltage decreases to the value required to produce rated lamp current. At all positions of the coils the force of repulsion is essentially constant.

Constant-current transformers are designed to have a high leakage reactance while power transformers of similar voltage rating have a much lower leakage reactance.

**Example.** A 100-kva, 2300-to-230-volt, 60-cycle, 2-winding transformer is used as an autotransformer having a single winding in order to step up the voltage of a 2300-volt line by 10%. If the transformer has 2% losses, a 2.2% regulation, and a 3.3% impedance ( $Z_e$ ) as a 2-winding transformer, its characteristics as a 2300/2530-volt autotransformer are:

Primary voltage	= 2300 volts
Load voltage	= 2530 volts
Ratio of transformation	= $\frac{10}{11}$
$I_1$ (as 2-winding transformer)	= $\frac{100,000}{2300} = 43.5$ amp
$I_2$ (as 2-winding transformer)	= $\frac{100,000}{230} = 435$ amp
$I_2$ (as autotransformer)	= 435 amp
$I$ (as autotransformer)	= 43.5 amp
$I_1$ (as autotransformer)	= 478.5 amp
Output (as autotransformer)	= $2530 \times 435 = 1100$ kva
Losses	= $\frac{1}{11} \times 0.02 = 0.00182$
Regulation	= $\frac{1}{11} \times 0.022 = 0.002$
Impedance	= $\frac{1}{11} \times 0.033 = 0.003$

Assume 230-volt winding to be insulated for 2300 volts.



### PROBLEMS

1. An autotransformer is required to supply 200 amp at 220 volts from a 240-volt single-phase line. Neglecting losses and impedance drops, determine: (a) ratios  $N_1/N_2$  and  $N_2/n$ ; (b) currents  $I_1$ ,  $I_2$  and  $I$ ; (c) percentage of power transferred directly; (d) percentage of power transformed.

2. A two-winding, 1100/220-volt, 60-cycle transformer is used as an autotransformer to boost the voltage of a single-phase, 1100-volt line 20%. If the transformer was rated at 10 kva (2 winding), determine the output as an autotransformer and the currents  $I_1$ ,  $I_2$  and  $I$ . How much power is transferred directly and how much power is transformed.

3. A short-circuit test is taken on a 10-kva, 2300/115-volt, 60-cycle, two-winding transformer, and the following data are recorded:

$$V_{sc} = 118 \text{ volts}$$

$$I_{sc} = 4.35 \text{ amp}$$

$$P_{sc} = 225 \text{ watts}$$

If this transformer is connected as an autotransformer to boost the voltage of a 2300-volt line 5%, and a short circuit occurs on the 2415-volt output side, determine the theoretical short-circuit current which would flow.

4. Calculate the regulation of the autotransformer in Problem 3 for full-load, 0.80 power factor lagging.

5. A 15-kva, 2300/230-volt, 60-cycle transformer has the following constants:

$$r_1 = 2.5 \text{ ohms}$$

$$r_2 = 0.021 \text{ ohm}$$

$$x_1 = 10.2 \text{ ohms}$$

$$x_2 = 0.10 \text{ ohm}$$

Neglecting the magnetizing current determine the regulation of this transformer when used as an autotransformer to boost the 2300-volt line 10%. The load is 16.5 kw, unity power factor.

6. What voltage impressed across the 2300-volt side of the autotransformer in Problem 5 will produce rated current when the 2530-volt side is short-circuited?

7. Is it possible to arrange two autotransformers in a Scott connection and supply a 2-phase load from a 3-phase system? If a 2-phase, 230-volt, 4-wire, 60-cycle load is to be supplied from a 3-phase, 3-wire, 208-volt, 60-cycle system by means of two autotransformers, specify the transformer requirements (voltages, taps) and show the manner of connection.

8. Transformation of voltages from 3-phase to 6-phase may be accomplished by means of three autotransformers properly connected. A 6-phase converter requiring ring voltages of 150 volts from a 230-volt, 60-cycle, 3-phase, 3-wire system is to be supplied by means of autotransformers. Specify the transformers necessary and show the diagram of connections.

## Chapter 21

### A-C ARMATURE WINDINGS

**21-1. A-c armature windings.** A-c armature windings can be *single-phase* or *polyphase* (2 or 3 or more phases): the polyphase windings will be considered first in this chapter.

As for d-c armature windings, polyphase armature windings are usually 2-layer. The single-layer polyphase winding is used in the wound rotors of small induction motors, Art. 23-1b, but seldom in the stators of these motors.

As for d-c armature windings, polyphase armature windings can be of the *lap* or *wave* type, see Art. 3-1. The wave-type polyphase winding is used mainly in wound rotors of medium size and larger induction motors.

While d-c armature windings are wound continuously and are *closed* windings, polyphase armature windings are arranged in groups of two or more single coils, the number of groups being determined by the number of poles and the number of phases. It is the *number of slots per pole per phase*,  $q$ , which determines the *number of single coils in a group*, and it is the *product of the number of poles and the number of phases*,  $p \times m$ , which determines the *number of groups* in the winding.

This will be explained by two examples. A 3-phase, 2-pole winding with  $Q = 12$  slots has  $q = 12/(2 \times 3) = 2$  slots per pole per phase and each coil group will consist of two single coils. There will be a total of  $p \times m = 2 \times 3 = 6$  groups in this winding, two groups per phase. Fig. 21-1 shows this winding. A 3-phase, 4-pole winding with  $Q = 24$  slots also has  $q = 24/(4 \times 3) = 2$  single coils per group, but the total number of groups is now  $4 \times 3 = 12$ , 4 groups per phase. Figs. 21-4 and 21-8 show 3-phase, 4-pole windings, each with  $Q = 24$  slots; Fig. 21-4 is a lap winding and Fig. 21-8 a wave winding.

The number of slots per pole per phase

$$q = \frac{Q}{p \times m} \quad (21-1)$$

and the product  $p \times m$  are the determining factors in the layout of polyphase armature windings.

(a) *Polyphase lap windings.* Fig. 21-1 shows a 2-pole, 3-phase, 2-layer lap winding placed in 12 slots. The number of slots per pole per phase is  $q = 2$ . If slots 1 and 2 are assigned to phase I, slots 3 and 4 must be

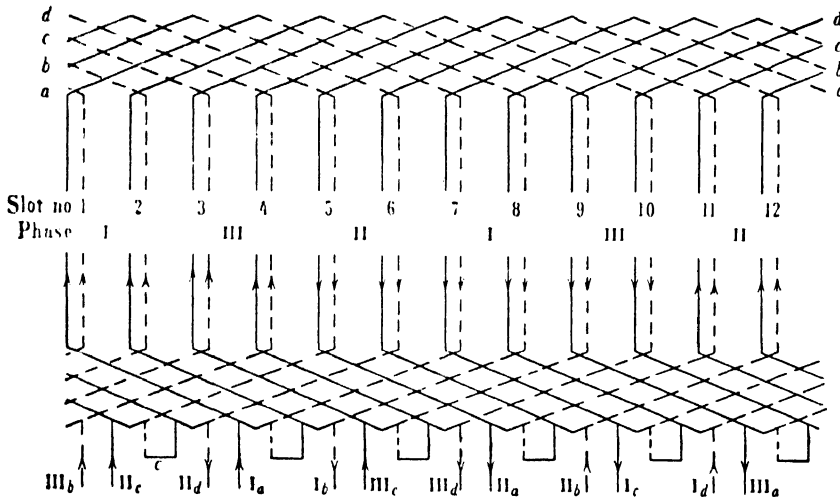


FIG. 21-1. Three-phase, 2-pole, 2-layer lap winding with two slots per pole per phase.

assigned to phase III, slots 5 and 6 to phase II, slots 7 and 8 again to phase I, etc. The reason for the phase sequence I, III, II is given in the following.

Considering the upper coil side in slot 1, the lower coil side which makes a complete coil with it lies in slot 7. The distance between both coil sides, the *coil span*, is  $7 - 1 = 6$  slot pitches. There are  $Q = 12$  slots (total) and the number of poles is  $p = 2$ , i.e., there are 6 slots per pole. Thus the coil span is equal to the pole pitch: the winding is *full-pitch* or *not chorded*. Chorded or fractional-pitch windings will be discussed later in this chapter.

*All coils have the same coil span: this is always the case in a 2-layer winding.* All connections, i.e., those between single coils, between coil groups, and from the winding to the terminals, lie on the same side of the winding. Considering the coils at the end opposite the connections, upper coil side 1 is connected with lower coil side  $1 + 6 = 7$ ; upper coil side 2 with lower coil side  $2 + 6 = 8$ , and so forth. A coil may consist of one or more turns (see Fig. 21-6). It is assumed in Fig. 21-1 that the coil has more than one turn. The short connectors *C* at the connection end con-

nect the last turn of the first coil of a group with the first turn of the second coil of the same group. Thus the first connector *C* from the left connects the end of coil (upper 1-lower 7) with the beginning of coil (upper 2-lower 8).

Each phase has two coil groups. Phase I consists of the coil groups terminating in  $I_a I_b$  and  $I_c I_d$ ; phase II of the coil groups terminating in  $II_a II_b$  and  $II_c II_d$ ; and phase III of the coil groups terminating in  $III_a III_b$  and  $III_c III_d$ . In each case *a* or *c* represents the beginning of a coil group and *b* or *d* its end. According to the voltage to be produced in the case of a generator, or the voltage impressed in the case of a motor, the coil groups assigned to each phase are connected either in series or in parallel.

The beginnings (as well as the ends) of the three phases must be displaced from each other by *120 electrical degrees*. That is,  $I_a$ ,  $II_a$ ,  $III_a$  in Fig. 21-1 are displaced from each other by 120 electrical degrees. A 2-pole machine corresponds to 360 electrical degrees. Therefore, since a slot pitch is equal to  $360/12$ , or 30 electrical degrees, the beginnings of the three phases must be displaced from each other by  $120/30 = 4$  slots. Hence if slot 1 is taken as the start of phase I, then phase II must start in slot  $1 + 4 = 5$ , and phase III must start in slot  $5 + 4 = 9$ .  $I_a$ ,  $II_a$ , and  $III_a$  are then the beginnings of the three phases.  $I_c$ ,  $II_c$ ,  $III_c$  also could be taken as the beginnings of the three phases since they also are displaced by 120 electrical degrees. Note that it is the displacement of the beginnings of the phases by 120 electrical degrees which makes the sequence of the phases I, III, II, Fig. 21-1.

For any *instant of time*, the direction of currents or emf's in the windings can be found for alternating current *in the same way as for direct current*. However, the currents or emf's in the three phases are displaced in time phase from each other by 120 electrical degrees. For example, if the instant is chosen when the current in phase I is a maximum, Fig. 21-2, the current in the other two phases, II and III, is  $\frac{1}{2}$  the magnitude of the current in phase I and flows in the opposite direction, i.e., if the current in the coil group  $I_a I_b$  of phase I flows from  $I_a$  to  $I_b$ , the current in the coil group  $II_a II_b$  of phase II flows from  $II_b$  to  $II_a$  and in the coil group  $III_a III_b$  of phase III from  $III_b$  to  $III_a$ . Further, it is important to note that 2 upper (or 2 lower) conductors which lie a pole pitch (in the considered example, 6 slot pitches) apart carry currents of opposite

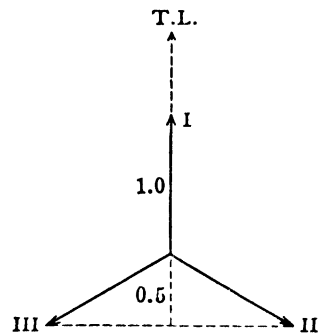


FIG. 21-2. Determination of the direction of current in a 3-phase winding for a fixed instant of time.

current in the coil group  $I_a I_b$  of phase I flows from  $I_a$  to  $I_b$ , the current in the coil group  $II_a II_b$  of phase II flows from  $II_b$  to  $II_a$  and in the coil group  $III_a III_b$  of phase III from  $III_b$  to  $III_a$ . Further, it is important to note that 2 upper (or 2 lower) conductors which lie a pole pitch (in the considered example, 6 slot pitches) apart carry currents of opposite

directions. Thus if the arrow goes upward in upper conductor 1, it must go downward in upper conductor  $1 + 6 = 7$ .

In Fig. 21-1 the current directions are shown corresponding to the instant of time assumed in Fig. 21-2. Note that in a 2-pole winding half of the conductors carry currents shown by an upward arrow followed by the other half which carry currents downward. In a  $p$ -pole winding this change occurs  $p/2$  times, see Fig. 3-7.

For a series connection of the coil groups of a phase, two coil ends which carry current in opposite directions have to be connected with each

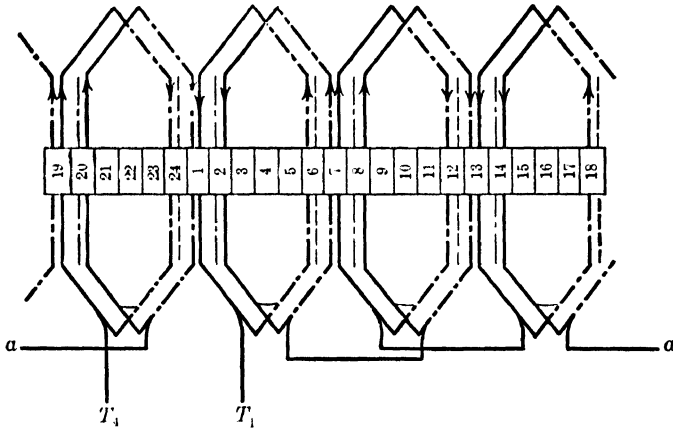


FIG. 21-3. One phase of a 4-pole, 3-phase, 2-layer, fractional-pitch lap winding with two slots per pole per phase.

other; on the other hand, for a parallel connection of the coil groups, ends carrying current in the same direction have to be connected together. Therefore, for a series connection  $I_b$  is connected to  $I_d$  in phase I,  $II_b$  to  $II_d$  in phase II, and  $III_b$  to  $III_d$  in phase III. For a parallel connection of the coil groups  $I_a$  is connected to  $I_d$ , and  $I_b$  to  $I_c$  in phase I;  $II_a$  to  $II_d$  and  $II_b$  to  $II_c$  in phase II; etc.

The coil span in Fig. 21-1 is equal to a pole pitch ( $= 6$  slot pitches) and the winding is full pitch. Normally, 2-layer windings are *chorded* (*fractional pitch*). Chording has an advantage in that the shape of the emf induced in the winding and the mmf produced by the winding is closer to a sinusoidal curve than in a full-pitch winding. Fig. 21-3 shows one phase of a 4-pole 2-layer chorded lap winding with  $q = 2$  slots per pole per phase. Upper coil side 1 is connected with lower coil side 6 (not with 7 as in Fig. 21-1). The coil span is equal to  $6 - 1 = 5$  slot pitches. The chording is equal to 1 slot pitch. Fig. 21-4 shows the complete winding. There are  $p \times m = 4 \times 3$  coil groups. The four coil groups of each phase are

connected in series, leaving two leads for each phase. The directions of the currents shown in the leads correspond to the instant of time when the current in phase I is a maximum, see Fig. 21-2.

The end-windings as shown in Figs. 21-1, 21-3, and 21-4 are away from the iron. In smaller machines the coils have a rectangular shape with

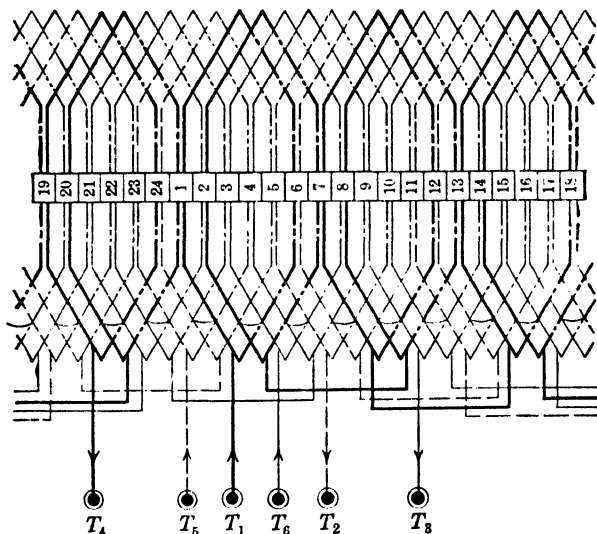


FIG. 21-4. Three-phase, 4-pole, 2-layer fractional-pitch lap winding with two slots per pole per phase.

round ends and the end-windings lie directly at the iron, Fig. 21-5. In larger machines the coils are diamond-shaped, as shown in Fig. 21-6. This coil has 7 turns (7 conductors per coil side) and each conductor consists of 2 parallel strands.

The general considerations outlined in the preceding for 3-phase lap windings also hold for 2-phase lap windings. The only difference is that the 2-phase winding has  $2p$  coil groups while the 3-phase winding has  $3p$  coil groups.

(b) *Polyphase wave windings.* Fig. 21-7 shows one phase of a 4-pole, 3-phase, 2-layer wave winding with  $q = 2$  slots per pole per phase; Fig. 21-8 shows the complete winding. If this winding is compared with the lap winding in Fig. 21-4, it is evident that fewer end connections are necessary. While the diamond lap winding has loops on both ends of the coil, Fig. 21-6, the wave winding has a loop on only one end; on the connection side of the coil the ends go in different directions, Fig. 21-7.

(c) *Single-phase windings.* The single-phase winding is used mostly in the stator of single-phase, fractional-horsepower, induction motors (see

Chap. 31). It is designed in the form of the *hand* or *mould* winding, Fig. 21-9, or the *skein* winding, Fig. 21-10. The single coils are connected in groups as in the polyphase windings, but the coils belonging to a group have *different coil spans*, Fig. 21-9. There are as many coil groups as there are poles.

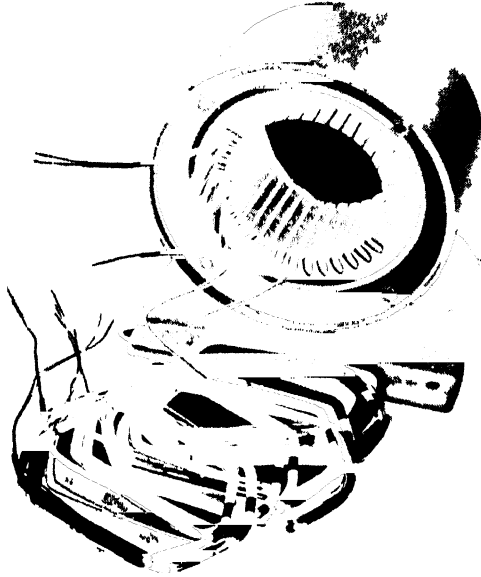


FIG 21-5 Stator of small induction motor in process of winding

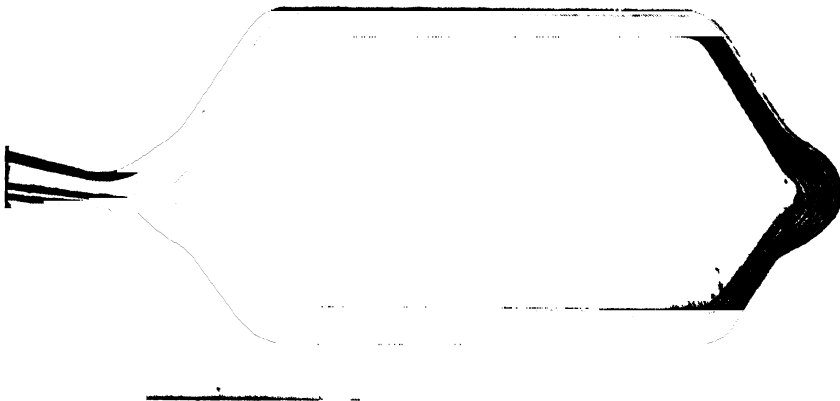


FIG 21-6 Diamond coil

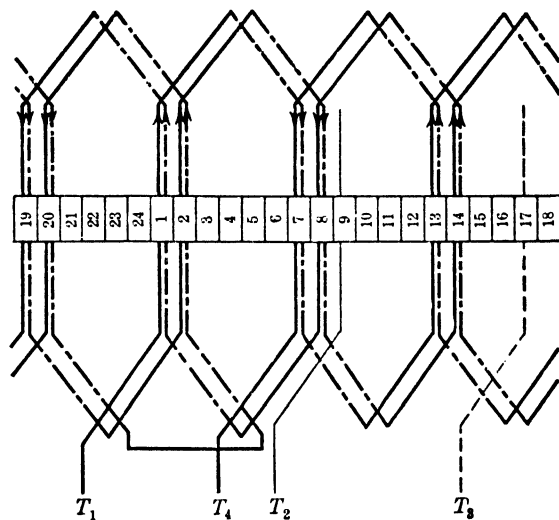


FIG. 21-7. One phase of a 4-pole, 3-phase, 2-layer wave winding with two slots per pole per phase.

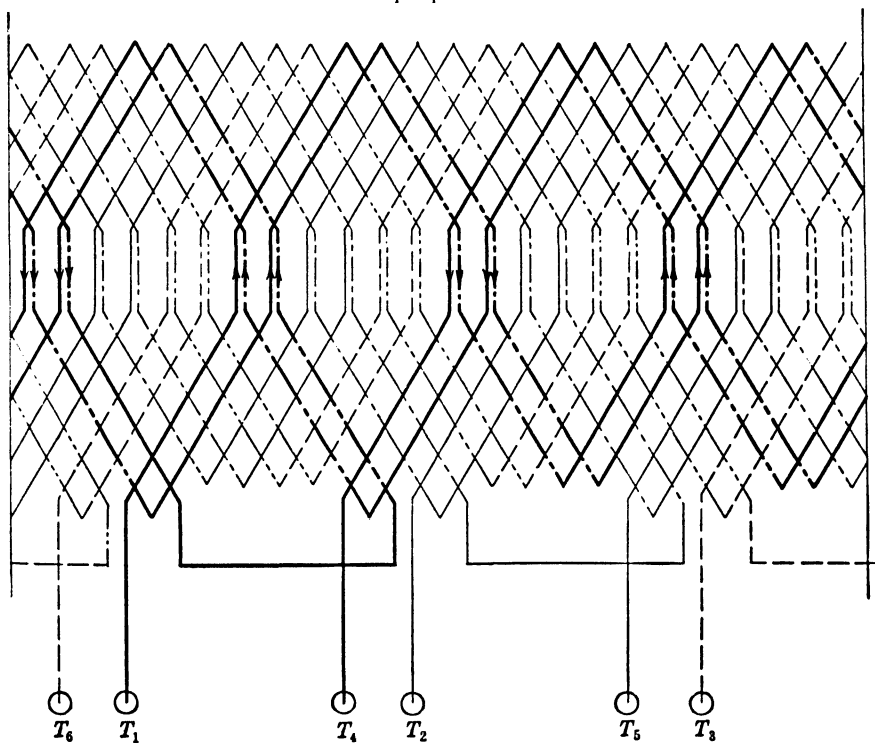


FIG. 21-8. Three-phase, 4-pole, 2-layer wave winding with two slots per pole per phase.





FIG. 21.9 Mould winding

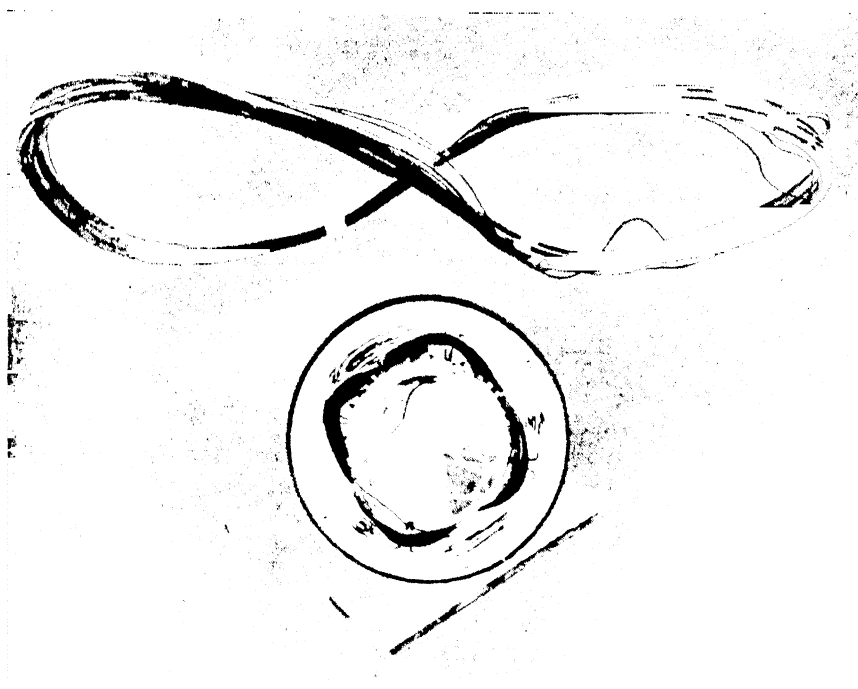


FIG. 21.10 Skin winding

In the hand winding, the wire is placed in the slot one turn at a time, starting with the inner coil (coil with the smallest span). In the mould winding, the coils are first wound on a mould and then placed in the slots. In the skein winding, a skein of wires is looped a number of times through the slots to form a pole.

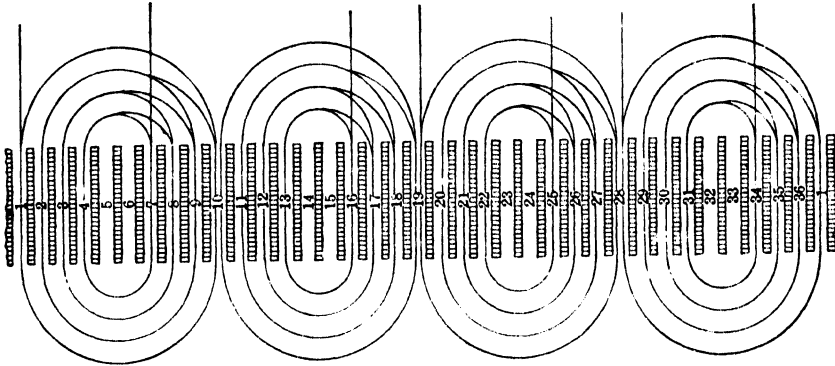


FIG. 21-11. Mould winding diagram for a single-phase, 4-pole motor with 36 slots.  
Main winding only.

Single-phase induction motors have two single-phase windings, the *main* winding and the *starting* winding, see Art. 33-1. For the main winding, any one of the three kinds of windings discussed is used; for the starting winding, the skein winding is preferred.

Fig. 21-11 shows the diagram of a mould winding for a 4-pole motor with 36 slots. Only the main winding is shown. There are  $p = 4$  coil groups each with 4 coils of different coil spans. Notice that the winding is not placed in all slots.

Slot No.	1	2	3	4	5	6	7	8	9	10	11	12	13	14	15	16	17	18	19	20	21	22	23	24	25	26	27	28	29	30	31	32	33	34	35	36
Main Winding	1	2	2	1			1	2	2	$\frac{1}{1}$	2	2	1			1	2	2	$\frac{1}{1}$	2	2	1			1	2	2	$\frac{1}{1}$	2	2	1			1	2	2
Starting Winding				1	1	1	1							1	1	1	1						1	1	1	1					1	1	1	1		

FIG. 21-12. Winding distribution for a single-phase 4-pole motor with 36 slots.

Figs. 21-12 and 21-13 show the winding distribution and winding diagram for a 4-pole 36-slot motor with a skein winding. The numbers in the second row of Fig. 21-12 indicate the number of times the loop of the skein passes through the slot. The numbers in the third row indicate the same for the starting winding. Fig. 21-13 shows the main winding only.

Here, also, each of the two windings is placed only in a part of the slots. The axes of the two windings are displaced by 90 electrical degrees.

(d) *Squirrel-cage windings.* The rotors of most induction motors have squirrel-cage windings. These windings have solid, uninsulated bars in

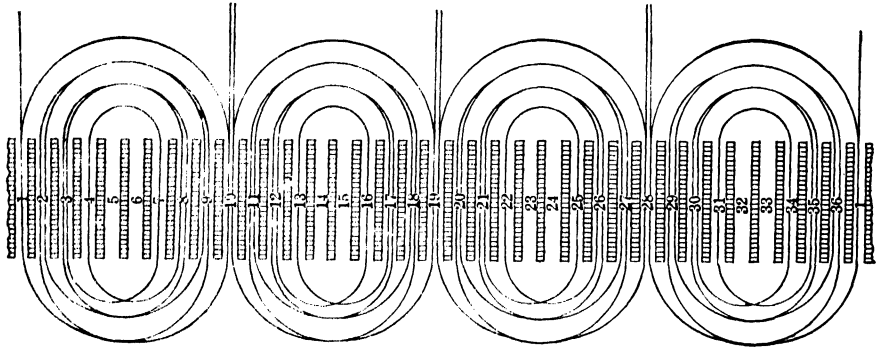


FIG. 21-13. Skein winding diagram corresponding to the winding distribution of Fig. 21-12. Main winding only.

the slots and are connected on each end of the rotor by a short-circuiting ring. In small rotors (up to 30 HP) the bars and rings are usually die-cast with aluminum, Fig. 23-7; in larger rotors the bars are usually made of copper, Fig. 21-14.

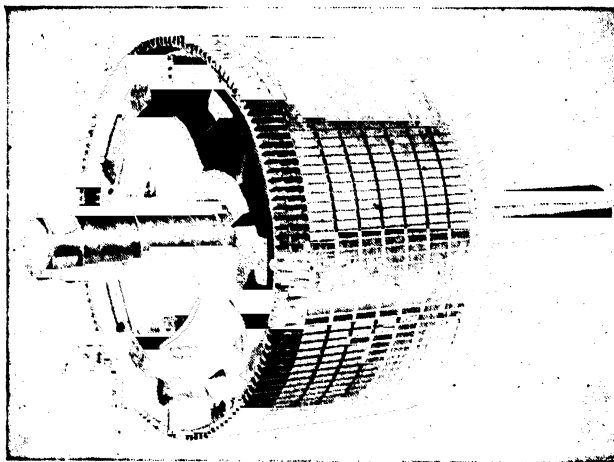


FIG. 21-14. Complete squirrel-cage rotor of a large induction motor.

## PROBLEMS

1. Draw the developed winding diagram of a 3-phase, 2-layer lap winding for a 4-pole machine with 3 slots per pole per phase and a 77.8% chording.
2. Repeat Problem 1 for a wave winding.
3. Draw the developed winding diagram of a 2-phase, 2-layer lap winding for a 4-pole machine with 4 slots per pole per phase. Chording is 87.5%.
4. A 2-pole, 24-slot, single-phase motor has the following winding distribution:

Slot No.	1	2	3	4	5	6	7	8	9	10	11	12	13	14	15	16	17	18	19	20	21	22	23	24
Main Winding	1	2	2	2	1				1	2	2	2	1	2	2	2	1				1	2	2	2
Starting Winding			1	2	2	2	1	2	2	2	1				1	2	2	2	1	2	2	2	1	

Draw the main winding diagram for the skein winding.

5. Draw the main winding diagram for a mould winding for the factor of Problem 4. The numbers in the table indicate in this case the ratios of turns in the individual coils.
6. Suggestions for further armature winding layouts for 3-phase machines are:

	<i>poles p</i>	<i>q</i>	<i>chording</i>	<i>winding</i>
a. ....	2	6	61.1%	lap
b. ....	6	2	83.3	lap
c. ....	6	2	83.3	wave
d. ....	6	4	83.3	lap
e. ....	6	4	75	wave
f. ....	8	2	83.3	lap
g. ....	8	3	77.8	wave

## Chapter 22

### EMF AND MMF OF A-C WINDINGS

**22-1. Emf induced in an a-c armature winding; distribution factor; pitch factor.** The effective value of the emf induced in a single *turn* by a *sinusoidally distributed flux* is given by Eq. 1-8

$$E = \frac{\omega}{\sqrt{2}} \Phi 10^{-8} = 4.44 f \Phi 10^{-8} \text{ volt} \quad (22-1)$$

If the coil consists of  $n_c$  turns which lie close to each other and are at all times interlinked with the same flux the effective emf induced in the *coil* is

$$E_c = 4.44 f n_c \Phi 10^{-8} \text{ volt} \quad (22-2)$$

Eqs. 22-1 and 22-2 presume that the coil pitch is equal to the pole pitch (= 180 electrical degrees) because only in this case is the maximum flux interlinkage of the turn equal to the total pole-flux (see Art. 3-1). If the coil pitch is less than the pole pitch, i.e., if the winding is *chorded*, the effective emf induced in the coil will be less than that given by Eq. 22-2: it will be equal to the voltage of the full-pitch coil times the ratio of the cross-hatched area to the total area of Fig. 22-1, i.e., times the ratio

$$\sin\left(\frac{W}{\tau}\right)\left(\frac{\pi}{2}\right) / \sin \frac{\pi}{2} = \sin \frac{W}{\tau} \frac{\pi}{2}$$

$W$  is the coil span in units of  $\tau$  (inches or slot pitches). The factor

$$k_p = \sin \frac{W}{\tau} \frac{\pi}{2} \quad (22-3)$$

is called the *pitch factor* of the winding. When the winding is not chorded (full pitch), then  $W = \tau$  and  $k_p = \text{unity}$ . The pitch factor is less than unity in all chorded windings. Taking into account the pitch factor, Eq. 22-2 for the emf induced in the *coil* is

$$E_c = 4.44 f n_c k_p \Phi 10^{-8} \text{ volt} \quad (22-4)$$

Consider Fig. 21-1, or Fig. 21-4, or Fig. 21-8: each phase consists of as many coil groups as there are poles. The coil groups are shifted with respect to each by a pole pitch (180 electrical degrees) and, therefore, lie in flux densities ( $B$ ) of the *same strength*. In Fig. 21-1, for example, the upper coil sides 7 and 8 of the second coil group of phase  $A$  are each shifted one pole pitch ( $= 6$  slot pitches) with respect to the upper coil sides 1 and 2 of the first coil group of this phase; also the lower coil sides (1, 2 and 7, 8) of both coil groups are shifted with respect to each other by one pole pitch. Fig. 21-1 refers to a full-pitch winding. However, the same is also true of chorded windings (see Fig. 21-4): the upper coil sides of all coil groups are shifted with respect to each other a pole pitch and the lower coil sides, considered by themselves, are also shifted a pole pitch. It follows, therefore, that the corresponding coil sides of all coil groups lie, at any instant of time, in flux densities ( $B$ ) of the same strength and that the magnitude and the time phase of the induced emf are the *same for all coil groups*. Therefore, it is sufficient to determine the emf induced in one coil group in order to know the emf induced in the total phase, for the winding of a phase consists of the series or parallel connection of its coil groups.

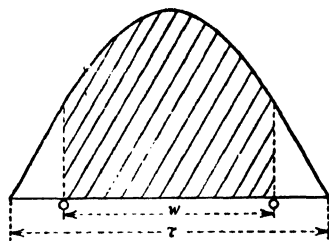


FIG. 22-1. Explanation of the pitch factor.

Eq. 22-4 refers to a single coil. A coil group consists of  $q$  ( $=$  number of slots per pole per phase) single coils connected in *series*. The *magnitude* of the induced emf is the *same* for all individual coils of a coil group. However, the time phase is not the same, because the individual coils of a coil group lie in different slots and therefore their emf's are shifted with respect to each other. The time phase shift between the emf's of the individual coils is equal to the angle between two slots (in electrical degrees), i.e., to the angle  $\alpha = (p \times 180)/Q = 180/mq$ . The resultant emf of a coil group is therefore not equal to the algebraic sum of the emf's of all single coils, but to the geometric sum of these emf's.

Consider as an example a 3-phase winding with  $q = 4$ . The angle between two slots is  $\alpha = 180/(3 \times 4) = 15^\circ$ . Fig. 22-2 shows the voltage polygon of the induced emf's in the four coils of the group. Each phasor  $AB, BC, CD, DE$  is equal in magnitude and represents the maximum value of the emf induced in a coil ( $E_c$ ).  $AE$  is the maximum value of the resultant emf ( $E_r$ ), i.e., of the emf induced in the coil group. The ratio

$$\frac{\text{resultant effective emf}}{\text{sum of effective emf's of individual coils}} = \frac{E_r}{qE_c} = k_d \quad (22-5)$$

is called the *distribution factor*. It is smaller than 1 and expresses the reduction of the resultant emf of the coil group (winding) caused by the distribution of the turns belonging to a coil group over several ( $q$ ) pairs of slots rather than placing them in one single pair of slots.

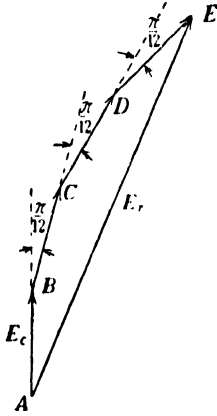


FIG. 22-2. Explanation of the distribution factor.

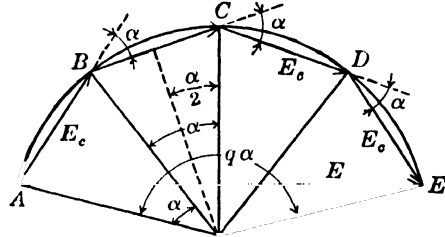


FIG. 22-3. Determination of the distribution factor.

Fig. 22-3, which is the same as Fig. 22-2, is drawn in polar form and yields for the distribution factor

$$k_d = \frac{E_r}{qE_c} = \frac{2R \sin q \frac{\alpha}{2}}{2Rq \sin \frac{\alpha}{2}} = \frac{\sin q \frac{\alpha}{2}}{q \sin \frac{\alpha}{2}} \quad (22-6)$$

Introducing  $\alpha = 180/mq$

$$k_d = \frac{\sin \frac{90}{m}}{q \sin \frac{90}{mq}} \quad (22-7)$$

Eqs. 22-6 and 22-7 apply only to the polyphase windings treated in Arts. 21-1a and 21-1b.

Eqs. 22-4 and 22-5 yield for the effective emf induced in a *coil group* of a *polyphase winding*:

$$E_g = qk_d E_c = 4.44fn_c qk_d k_p \Phi 10^{-8} \text{ volt} \quad (22-8)$$

where  $n_c q$  is the number of turns in a coil group ( $N_g$ ); therefore,

$$E_g = 4.44fN_g k_d k_p \Phi \times 10^{-8} \text{ volt} \quad (22-9)$$

Consider Fig. 21-1: if the two coil groups of a phase are connected in parallel, the emf induced in the phase is given by Eq. 22-9; if the two coil groups of a phase are connected in series, the emf of a phase will be twice the value given by Eq. 22-9. Consider Fig. 21-4 or 21-8. In both cases the four coil groups are connected in series and the emf induced in a phase is four times the value given by Eq. 22-9. If the four coil groups were connected in two parallel parts, each part consisting of two coil groups in series, the emf of a phase would be twice the value given by Eq. 22-9 and, finally, the emf of a phase would be that given by Eq. 22-9 if the four coil groups were connected in parallel.

The number of *series-connected* turns *per phase* will be denoted by  $N$ .  $N$  is then equal to  $N_g$  times the number of coil groups connected in series and the emf per phase is

$$E = 4.44fNk_dk_p \cdot 10^{-8} \text{ volt} \quad (22-10)$$

The quantity  $Nk_dk_p$  can be considered as the number of *effective turns per phase*. It is smaller than the actual number of turns per phase  $N$ , owing to the distribution of the winding over several slots under each pole and to the chording of the coils. The product  $k_p k_d$  is often called the *winding factor*.

Some values of the distribution factor are given in the following table:

Slots per pole per phase	2	3	4	5	6	8	$\infty$
Three-phase	0.966	0.960	0.958	0.957	0.957	0.956	0.955
Two-phase	0.924	0.910	0.906	0.904	0.903	0.901	0.900

It is seen from this table that the distribution of the winding causes a turn-loss of 3.5 to 4.5% in 3-phase windings and a loss of 7.5 to 10% in 2-phase windings. In single-phase windings the loss is 15 to 17%.

The preceding considerations are based on the assumption of a sinusoidal flux distribution. The induced emf is then sinusoidal, i.e., a sinusoidal function of time (see Art. 1-1). It is desirable that the generators of power stations yield a sinusoidal voltage. Harmonics in the power supply voltage produce unnecessary losses and may also interfere with telephone lines. In modern generating stations the *synchronous generator* (see Art. 35-1) supplies power to the distribution system. There are two types of synchronous generators: cylinder rotor (turbine generator, Fig. 35-2) type and the salient pole (Fig. 35-1) type. The former type has a flux distribution which is closely sinusoidal. The flux distribution of the latter type is usually similar to that of a d-c generator (see Fig. 1-4). If this



latter flux distribution curve is resolved into a Fourier series, it is evident that the harmonic fluxes, which move with the same speed as the fundamental flux but have a larger number of poles than the fundamental flux, will induce undesirable emf's in the winding of high frequency (see Eq. 1-9). A thorough analytical investigation and also experience shows that the harmonic emf's are small in comparison with the emf induced by the fundamental flux and can be disregarded except in certain cases, such as that of telephone interference mentioned above. It has been pointed out that chording of the coils reduces the harmonics. Also a larger value of  $q$  decreases the harmonics.

It has been explained in Art. 3-1 that the d-c machine is nothing more than an a-c machine with a device (commutator) which permits a continuous pick up of the amplitude of the a-c voltage. If this is true, then Eq. 3-6 for the emf induced between the brushes of a d-c machine must follow from the general Eq. 22-10 for the emf induced in an a-c machine. This is shown to be true if, for the d-c machine,  $(p \times n)/120$  is substituted for  $f$ ,  $Z/2a$  for  $N$ , and unity for  $k_p$ . Regarding  $k_d$ , the d-c armature winding between two consecutive brushes ( $= 1$  parallel circuit of the winding) is distributed over a pole pitch. In the phasor diagram of Fig. 22-2 the ratio  $E_r/qE_c$  is then equal to the ratio of the diameter of a circle to the length of one half the circumference, i.e., to  $2/\pi$ . This means that  $k_d$  for the d-c armature winding is equal to  $2/\pi$ . When these substitutions are made in Eq. 22-10 and the right side of Eq. 22-10 is multiplied by  $\sqrt{2}$  to account for the amplitude of the induced a-c emf, Eq. 3-6 for the d-c armature winding is obtained.

**22-2. Mmf produced by an a-c armature winding; alternating flux; rotating flux.** Consider an elementary single-phase machine with a single coil (Fig. 22-4) and let the number of turns of the coil be  $n_c$  and the current in the conductors be  $i$ . Applying the circuital law of the magnetic field (Eq. 1-23) to this elementary machine, the mmf  $n_c i$  is the same for all lines of force because each line of force is interlinked with the same ampere-turns  $n_c i$ . Therefore, the representation of the mmf as a function of space around the stator between the coil sides will be a rectangle with the height  $n_c i$ .

For reasons which will immediately become obvious, it is expedient to represent as a function of space not the total mmf  $n_c i$  but one half of it ( $n_c i/2$ ), corresponding to half a line of force, in such a manner that the half which drives the flux *into* the rotor is assumed positive and the half which drives the flux *from* the rotor into the gap is assumed negative (or vice versa). This yields the graphical representation shown in Fig. 22-5.

If it is assumed that the iron is not saturated, then its permeability  $\mu$  is very high (see Fig. 1-8) and, for any finite value of the flux density  $B = 0.4\pi\mu H$  in the iron, only a very small value of field intensity  $H$  in the iron is necessary. This means, when the saturation is low, the path in the iron contributes but little to the line integral  $\oint H dl$ , and it can be assumed that  $\oint H dl = H_g 2g$ , i.e.,  $n_c i = H_g 2g$  ( $g$  = air gap). Since  $B_g = 0.4\pi H_g$ ,  $B_g = 0.4\pi n_c i / 2g = 0.4\pi (n_c i / 2) (1/g)$ . Thus if  $g$  is a constant quantity, as is the case in all induction motors, Fig. 22-5 represents not only the mmf-curve but, to another scale, also the flux distribution in the

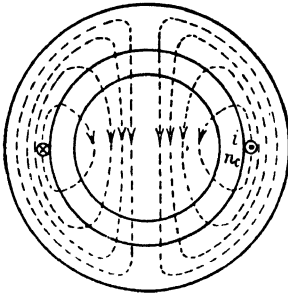


FIG. 22-4. Elementary 2-pole, single-phase machine with a single coil.

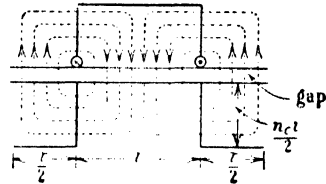


FIG. 22-5. Mmf curve of the elementary machine of Fig. 22-4.

gap (the  $B$  curve). The representation of the latter curve must consist of areas above and below the axis of abscissae which are equal to each other, because the area of the  $B$ -distribution curve is the flux per unit length of the core (see Art. 1-4, Eq. 1-32) and the flux going into the rotor (positive area) must be equal to the flux leaving the rotor (negative area). Thus the representation of the mmf-curve with positive and negative areas, as shown in Fig. 22-5, has the advantage that it also yields the  $B$ -distribution curve which must contain positive and negative areas.

If the Fourier series is applied to the rectangular mmf-curve of Fig. 22-5, a fundamental wave and harmonic waves are obtained as shown in Fig. 22-6. The length of the fundamental wave is the same as that of the rectangular mmf-curve, namely,  $2\tau$ . The amplitude of the fundamental wave is  $4/\pi$  times the height of the rectangular wave, i.e.,  $(4/\pi)(n_c i / 2)$ . Introducing  $i = \sqrt{2} I \sin \omega t$ , the equation of the fundamental mmf wave becomes

$$f = \frac{\sqrt{2}}{2} \frac{4}{\pi} n_c I \sin \omega t \cos \frac{\pi}{\tau} x \quad (22-11)$$

For a fixed instant of time  $t$ , this mmf and also the  $B$ -distribution produced by it are *cosine functions of space* ( $x$ ) around the stator. For a fixed point  $x$ , both the mmf and  $B$  are a maximum when the current is a maximum and are zero when the current is zero. If the direction of the current is reversed, the direction of the mmf and  $B$  is also reversed. Such an mmf and flux are referred to as *alternating mmf* and *alternating flux*. The alternating flux thus can be characterized as a flux which is *fixed in space* while its *magnitude varies* from a positive maximum to a negative maximum (standing wave). Such an alternating flux has already been considered in the single-phase transformer.

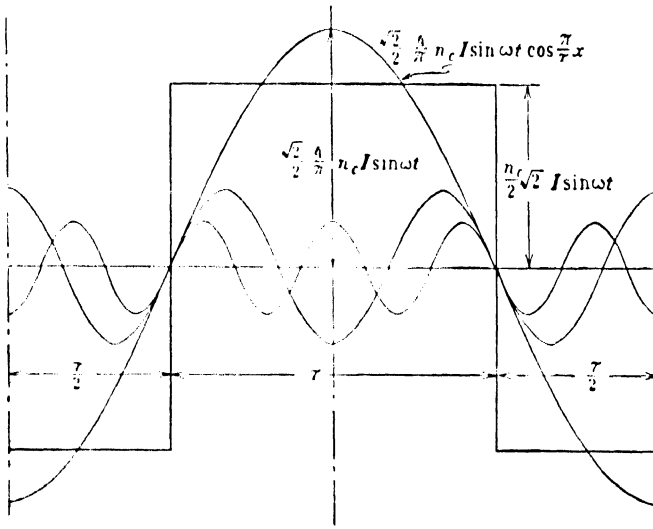


FIG. 22-6. Mmf curve of the 2-pole, single-phase winding of Fig. 22-4 with the fundamental and two harmonics.

Fig. 22-4 refers to an elementary single-phase machine since there is only one coil fed by a single-phase current. Fig. 22-7 shows an elementary 2-pole 3-phase machine: here three coils are displaced from each other in space by 120 electrical degrees and it will be assumed that they are fed by three currents shifted from each other 120° in time. Each of the three coils will produce a rectangular mmf as that shown in Fig. 22-6 of which only the fundamental will be considered. The three fundamental waves produced by the three coils will be displaced from each other in space by 120° since the three coils are displaced from each other by this angle. Using coil (phase) I as a reference and placing the  $x = 0$  point, as before in Fig. 22-6, in the axis of this coil, the three mmf waves produced

by the three coils are

$$\begin{aligned}
 f_I &= \frac{\sqrt{2}}{2} \frac{4}{\pi} n_c I \sin \omega t \cos \frac{\pi}{\tau} x \\
 f_{II} &= \frac{\sqrt{2}}{2} \frac{4}{\pi} n_c I \sin (\omega t - 120) \cos \left( \frac{\pi}{\tau} x - 120 \right) \\
 f_{III} &= \frac{\sqrt{2}}{2} \frac{4}{\pi} n_c I \sin (\omega t - 240) \cos \left( \frac{\pi}{\tau} x - 240 \right)
 \end{aligned} \quad (22-12)$$

The first of these three equations is identical with that derived for the single coil (Eq. 22-11.)

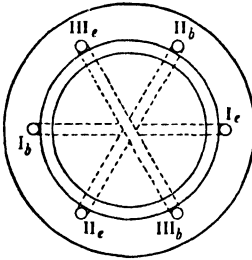


FIG. 22-7. Elementary 2-pole 3-phase machine.

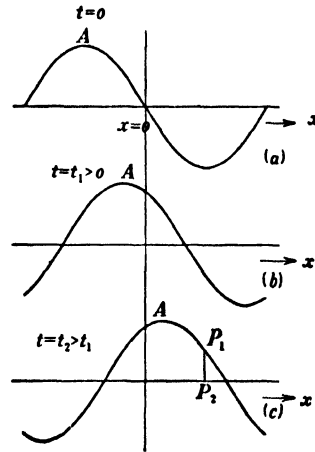


FIG. 22-8. The function  $\sin \left( \omega t - \frac{\pi}{\tau} x \right)$  at different instants of time.

In order to obtain the resultant mmf produced by all three phases, the sum  $f_I + f_{II} + f_{III}$  is to be taken. Observing that  $\sin \alpha \cos \beta = \frac{1}{2} \sin (\alpha - \beta) + \frac{1}{2} \sin (\alpha + \beta)$  the final result obtained is:

$$f = \frac{3}{2} \frac{\sqrt{2}}{2} \frac{4}{\pi} n_c I \sin \left( \omega t - \frac{\pi}{\tau} x \right) \quad (22-13)$$

The resultant mmf contains a sine function of time and of space. The meaning of this function can be seen readily from Fig. 22-8 which represents its position around the stator (in the air gap) for three different instants of time. Fig. 22-8a refers to  $t = 0$ , Fig. 22-8b refers to  $t = t_1 > 0$ ,

and Fig. 22-8c to  $t = t_2 > t_1$ . Observe the position of a fixed point of the wave, for example point  $A$ , at the different instants of time: as time elapses this point moves to the right in the positive direction of the  $x$ -axis. This means that the function  $\sin\left(\omega t - \frac{\pi}{\tau} x\right)$  represents a *traveling wave*.

Referring to Eq. 22-13, the amplitude of the traveling mmf wave  $\left(\frac{3}{2} \frac{\sqrt{2}}{2} \frac{4}{\pi} n_c I\right)$  is a constant quantity. Thus the resultant *mmf of a 3-phase (polyphase) winding is an mmf which travels around the stator (in the gap) with constant amplitude*. Such an mmf and the flux produced by it are referred to as a *rotating mmf* and a *rotating flux*.

A comparison of the rotating mmf or flux with the alternating mmf or flux shows that the former has a constant amplitude and moves around in the gap of the machine while the latter has a variable amplitude and is fixed in space.

A rotating mmf and flux can be produced in another way. Consider Fig. 35-1 which shows the rotor of a synchronous machine. The field coils on the salient poles are fed by a direct current. When this pole structure is driven by a Diesel engine or a waterwheel, the effect of its rotation is a rotating mmf and flux. However, a prime mover is necessary to produce this effect, whereas in the discussion considered above the rotating mmf and flux were produced by non-moving coils and polyphase currents. The discovery of the possibility of producing a rotating flux by non-moving coils and polyphase currents was a turning point in the development of the electric machine, because the induction motor, which is the most commonly used electric machine, operates on the basic principle of producing a rotating flux by fixed coils.

The velocity of propagation of the mmf wave represented by Eq. 22-13 and of the flux produced by it can be determined from Eq. 22-13. Imagine an observer traveling with the mmf wave and sitting on point  $P_1$  of the wave (see Fig. 22-8c). For this observer, the magnitude of the mmf will always have the same value  $P_1 P_2$ , i.e., for him the right side of Eq. 22-13 is a constant quantity. Since the factor  $\frac{3}{2} \frac{\sqrt{2}}{2} \frac{4}{\pi} n_c I$  has a constant value, the condition that exists for the observer is:

$$\sin\left(\omega t - \frac{\pi}{\tau} x\right) = \text{constant}$$

and, therefore,

$$\omega t - \frac{\pi}{\tau} x = \text{constant}$$

Differentiating this equation with respect to  $t$ , the velocity of propagation of the mmf wave  $dx/dt$  is obtained as

$$\frac{dx}{dt} = \omega \frac{\tau}{\pi} = 2f\tau \quad (22-14)$$

This equation states that the wave moves, during one cycle of the current, a distance twice the pole pitch, i.e., its wave length.

For rotating machines it is customary to express the velocity of propagation in rpm rather than as a distance. The distance covered by the wave in one minute is  $2f\tau \times 60$ . The distance which corresponds to one revolution of the rotor is  $p\tau$ . Thus the speed in rpm is

$$n = \frac{2f\tau \times 60}{p\tau} = \frac{120f}{p} \quad (22-15)$$

Note that this is the *same equation* which has been derived for the frequency of the a-c emf induced in an armature winding moving with  $n$  rpm relative to a pole-structure with  $p$  poles (Eq. 1-9).

Applying the relation  $\sin \alpha \cos \beta = \frac{1}{2}[\sin(\alpha - \beta) + \sin(\alpha + \beta)]$  to Eq. 22-11, there results

$$f = \frac{1}{2} \left( \frac{\sqrt{2}}{2} \frac{4}{\pi} n_c I \right) \sin \left( \omega t - \frac{\pi}{\tau} x \right) + \frac{1}{2} \left( \frac{\sqrt{2}}{2} \frac{4}{\pi} n_c I \right) \sin \left( \omega t + \frac{\pi}{\tau} x \right) \quad (22-16)$$

Comparing this equation with Eq. 22-13, it is seen that an alternating mmf can be replaced by two rotating mmf's traveling in *opposite* directions and each having an amplitude equal to half of that of the alternating mmf. Use of this concept, to replace an alternating mmf by two rotating mmf's, is made in the treatment of the single-phase motor (Art. 31-1).

Eqs. 22-11 and 22-13 were derived under the assumption that there is only one coil per pole pair per phase (see Figs. 22-4 and 22-7), i.e., one slot per pole per phase ( $q = 1$ ). If there are  $q > 1$  slots per pole per phase, i.e., a coil group of  $q$  coils per pole pair per phase, then the resultant mmf is obtained by treating the mmf given by Eq. 22-11 and also that given by Eq. 22-13 as phasors. This is permissible because they are sinusoidal functions. The phasors representing the amplitudes of the mmf's of the individual coils of the coil group are shifted with respect to each other by the electrical angle which corresponds to a slot pitch, and the resultant mmf is obtained by a geometric addition of the mmf's of the  $q$  single coils. This is the same consideration as that applied to the determination of the resultant emf of a coil group with  $q$  coils (see Figs. 22-2 and 22-3). It leads to the introduction of the *distribution factor*  $k_d$  as given by Eqs.

22-6 and 22-7, and the resultant mmf is that given by Eq. 22-11 or that given by Eq. 22-13 times  $k_d q$ .

Eqs. 22-11 and 22-13 refer to a full-pitch winding. This can be seen from Figs. 22-4 and 22-7 in which the coil pitch (measured as an arc) is equal to the pole pitch. If the winding is chorded, then the *pitch factor* must be introduced as was done for the determination of the emf of a chorded winding.

Compare Eqs. 22-11 and 22-13. The factor  $\frac{3}{2}$  in Eq. 22-13 is due to the fact that a 3-phase winding has been considered as an example (Fig. 22-7). If an  $m$ -phase ( $m > 1$ ) winding were considered, the factor  $m/2$  would appear in Eq. 22-13. Multiplying Eqs. 22-11 and 22-14 by  $qk_d$  in order to include the case of a coil group with  $q$  single coils, and further, multiplying these equations by the pitch factor  $k_p$  in order to include the case when the coils are chorded, and finally introducing into Eq. 22-13  $m/2$  instead of  $\frac{3}{2}$ , the amplitude of the fundamental of the mmf of a single-phase winding becomes

$$F = 0.9 n_c q k_d k_p I \quad (22-17)$$

and that of the polyphase winding ( $m > 1$ )

$$F = 0.45 m n_c q k_d k_p I \quad (22-17a)$$

$n_c q$  in Eqs. 22-17 and 22-17a is the number of turns per pole pair. The total number of *turns per phase*  $N$  is

$$N = \frac{p}{2} n_c q \quad (22-18)$$

Introducing  $n_c q$  from this equation into Eqs. 22-17 and 22-17a the *amplitude of the fundamental of the mmf of a single phase winding* is

$$F = 1.8 \frac{N}{p} k_d k_p I \quad (22-19)$$

and the *amplitude of the fundamental of the mmf of a polyphase winding* ( $m > 1$ ) is

$$F = 0.9m \frac{N}{p} k_d k_p I \quad (22-20)$$

Only the fundamental mmf wave has been considered throughout this article. The harmonics (see Fig. 22-6) have been disregarded. An investigation of the harmonic mmf's in the same manner, as has been done for the fundamental wave, shows that a single-phase winding produces harmonic alternating mmf's and fluxes and that a polyphase winding produces harmonic rotating mmf's and fluxes. The speed of the rotating

harmonic mmf's and fluxes is different from that of the fundamental wave, Eq. 22-15. Some of the rotating harmonic mmf's (fluxes) travel in the same direction as the fundamental mmf (flux) and some travel in opposite directions. A 3-phase winding does not produce mmf harmonics of the order 3 or a multiple of 3.

The useful torque of the machine is produced by the fundamental flux. All harmonic fluxes are undesirable, especially in induction motors, where they produce not only additional losses (see Art. 26-1) but may produce vibration and noise. They may also distort the torque-speed curve and cause locking torques. The harmonic mmf's which produce the harmonic fluxes must be kept as small as possible. This may be achieved by a *chording* of the coils and a value of  $q$  which is not too small. These same means are also used to keep down the harmonics of the induced emf (see foregoing article). Chording reduces the harmonics of low order (5th and 7th). *Skewing* of the rotor or stator is very helpful for the reduction of the influence on the rotor of the harmonic fluxes of high order and is used in small and medium-sized induction motors for this purpose (see Fig. 23-5).

**Example 22-1.** A 250-HP, 2300-volt, 3-phase, 60-cycle,  $\cos \varphi = 0.80$ , 14-pole, salient-pole, wye-connected synchronous motor has a stator with 84 slots and a 2-layer winding with 18 conductors per slot. The coil throw is 5 slots.

Determine the flux per pole necessary to induce a voltage of 2300 volts between terminals at no-load.

$$N = \frac{18 \times 84}{2 \times 3} = 252$$

Since  $q = 84 / (3 \times 14) = 2$ ,  $k_{d1} = 0.966$ . For the throw of 83.3%  $k_{p1} = \sin \frac{5}{6} \times 90 = 0.966$ .

Thus  $k_{dp1} = 0.934$  and from Eq. 22-10

$$\Phi = \frac{2300}{\sqrt{3}} 10^8 \times \frac{1}{4.44 \times 60 \times 252 \times 0.934} = 2.12 \times 10^6 \text{ maxwells}$$

**Example 22-2.** Assume that the machine of Example 22-1 has a no-load flux density distribution represented by:

$$B_x = 100 \sin \frac{\pi}{\tau} x - 14 \sin 3 \frac{\pi}{\tau} x - 20 \sin 5 \frac{\pi}{\tau} x + 1 \sin 7 \frac{\pi}{\tau} x$$

The emf induced at no-load will now be determined on a relative basis. Let  $\Phi_1 = 100$ . Then since  $B_3/B_1 = 0.14$  and  $\tau_3/\tau_1 = \frac{1}{3}$ ,

$$\Phi_3 = \frac{1}{3} \times 14 = 4.67$$

and also

$$\Phi_5 = \frac{1}{5} \times 20 = 4$$

$$\Phi_7 = \frac{1}{7} \times 1 = 0.143$$



If  $n$  is the order of the harmonic, the distribution and pitch factors are (see Eqs. 22-3 and 22-6)

$$k_{pn} = \sin n \frac{W}{\tau} \frac{\pi}{2} \quad k_{dn} = \frac{\sin nq \frac{\alpha}{2}}{q \sin n \frac{\alpha}{2}} \quad (22-21)$$

$n$	1	3	5	7
$k_{pn}$	0.966	0.707	0.259	0.259
$k_{dn}$	0.966	0.707	0.259	0.259

The ratios of the emf's are, according to Eq. 22-10,

$$\begin{aligned} \frac{E_3}{E_1} &= \frac{\Phi_3}{\Phi_1} \cdot \frac{f_3}{f_1} \cdot \frac{k_{dp3}}{k_{dp1}} = \frac{4.67}{100} \times 3 \times \frac{0.500}{0.934} = 0.075 \\ \frac{E_5}{E_1} &= \frac{\Phi_5}{\Phi_1} \cdot \frac{f_5}{f_1} \cdot \frac{k_{dp5}}{k_{dp1}} = \frac{4}{100} \times 5 \times \frac{0.0671}{0.934} = 0.0145 \\ \frac{E_7}{E_1} &= \frac{\Phi_7}{\Phi_1} \cdot \frac{f_7}{f_1} \cdot \frac{k_{dp7}}{k_{dp1}} = \frac{0.143}{100} \times 7 \times \frac{0.0671}{0.934} = 0.00072 \end{aligned}$$

**Example 22-3.** The total mmf of a 3-phase 2-pole winding with 2 slots per pole per phase will be determined. It will be assumed that the winding is fractional-pitch, the coil span 5 slot pitches; the mmf will be determined for the instant shown in Fig. 22-9, i.e., when the current in phase III is zero while in phases I and II the currents are equal and of opposite sign.

The circles in Fig. 22-10a represent coil sides and this figure shows the slot distribution over the two poles.  $I_b$ ,  $II_b$ , and  $III_b$  are the beginnings of the three phases. Since the currents in phases I and II are opposite, the beginning of phase II must be marked by a dot

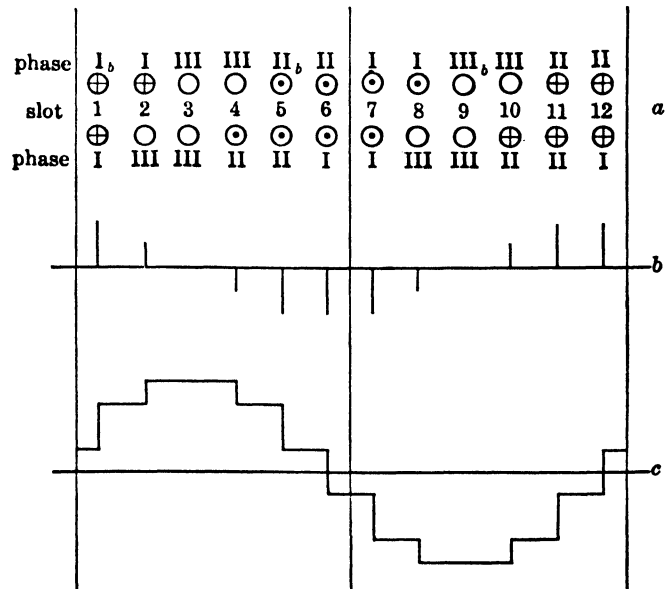
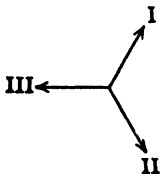


FIG. 22-9. Example.

FIG. 22-10. Mmf-curve of a 3-phase winding. ( $q = 2$ .)

if the beginning of phase I is marked by a cross. This determines the current directions in the top and bottom layers around the machine. Fig. 22-10b is the ampere-conductor distribution of the winding. It is obtained by adding the currents of Fig. 22-10a, observing the signs and magnitudes of the individual currents. In the case considered, the magnitudes of all currents are equal. Fig. 22-10c is the total mmf of the winding. It is obtained through graphical integration of Fig. 22-10b. The integration can be started at any point and a line then is drawn in such a manner that the positive and negative areas of the mmf curve are equal.

### PROBLEMS

1. A 24-pole, 60-cycle, 3-phase synchronous generator has a total of 216 slots, 18 conductors per slot in a 2-layer winding, a 3-parallel wye connection and a coil throw of 0.778. If the no-load generated voltage is 2300 volts between terminals, determine the no-load flux per pole. What is the line voltage for the same pole flux if the machine is reconnected 2-parallel delta?

2. For the machine of Example 22-1 determine the pitch and distribution factors for the 7th, 11th, and 13th harmonics. (See Eq. 22-21.)

3. For the machine of Problem 1 determine the pitch and distribution factors for the 5th, 7th, 11th, and 13th harmonics. (See Eq. 22-21.)

4. For the machine of Problem 2, Chapter 21, determine the pitch and distribution factors of the 11th and 13th harmonics.

5. A 60-cycle generator is assumed to have a square-wave flux distribution under the poles and zero flux in the interpolar spaces. The flux per pole is  $12 \times 10^6$  maxwells. If the coil pitch is equal to the pole pitch, what will be the voltage induced in a single turn (a) for a pole arc of 75% and, (b) for a pole arc of 65%? Draw the flux and emf curves for both cases.

6. With normal excitation the pole flux in a 60-cycle generator is  $6 \times 10^6$  maxwells per pole and is sinusoidally distributed along the air gap. For a coil pitch of unity determine the generated armature voltage per turn. What is the form factor and shape of this emf? If the coil throw is 0.833, what is the emf induced per turn?

7. With normal excitation the pole flux in a 60-cycle generator is  $10 \times 10^6$  maxwells and is sinusoidally distributed along the air gap. The armature has a 2-layer, 3-phase winding with 12 slots per pole and 6 conductors per slot. What is the emf induced in the winding per pole if the coil throw is: (a) 1.0, (b) 0.833, (c) 0.75? All conductors are connected in series.

8. A 7500-kva, 3-phase, 25-cycle, wye-connected generator is rated to deliver its output at 11,800 volts between terminals. The field structure has 12 poles, and the armature 180 slots containing a 2-layer winding with 4 conductors per slot. All conductors are connected in series. What is the no-load terminal voltage when the pole flux is 52 megalines per pole and the generator is driven at rated speed? The coil throw is 12 slots.

9. Show the shape of the total mmf of the 3-phase winding of Problem 1, Chapter 21, for the instant of time: (a) when the current in phase I is zero; (b) when the current in phase I is a maximum.

10. Repeat Problem 9 for the 2-phase winding of Problem 3, Chapter 21.

*Note*—Problem 6, Chapter 21, offers added suggestions for problems on determining the shape of the mmf wave of 3-phase windings.

## Chapter 23

### MECHANICAL ELEMENTS OF THE POLYPHASE INDUCTION MOTOR AND ITS MAGNETIC CIRCUIT

It has been explained in Chapter 2 that all electric machines have *two indispensable elements, the magnetic flux and the conductors carrying current* (the armature). In the induction motor the flux is produced by the outer part, the *stator*, while the rotating inner part of the machine, the *rotor*, is its armature.

As in the d-c machine, the armature conductors are placed parallel to the axis of the armature or they are skewed at a slight angle to the axis and the armature iron is laminated. Since the stator is excited by alternating currents which produce rotating fluxes, the stator iron must also be laminated.

(a) *Stator*. Fig. 23-1 shows laminated segments of large induction motors: *A* represents a stator segment, *B* a segment of a squirrel cage rotor, and *C* a segment of a phase-wound rotor. The difference between these two rotor types is explained later. Fig. 23-2 shows a complete stack of stator laminations for a smaller induction motor with semi-open slots; the laminations of small motors are usually punched from one piece.

The stator or primary winding of the induction motor is connected to a source of power, is placed in the stator slots, and is completely insulated corresponding to the voltage of the power supply. Fig. 23-3 shows the connection end of a partially wound stator, and Fig. 23-4 shows the complete stator for a larger motor (also see Fig. 21-5).

(b) *Rotor*. The rotor or secondary winding of the induction motor is its armature winding. It is placed in the slots of the rotor. While in the d-c machine both the field and the armature winding are connected to a source of power, this is not the case in the induction motor. Here the armature winding is not connected to a source of power but gets its power by induction from the flux produced by the stator winding—hence the name *induction motor*.

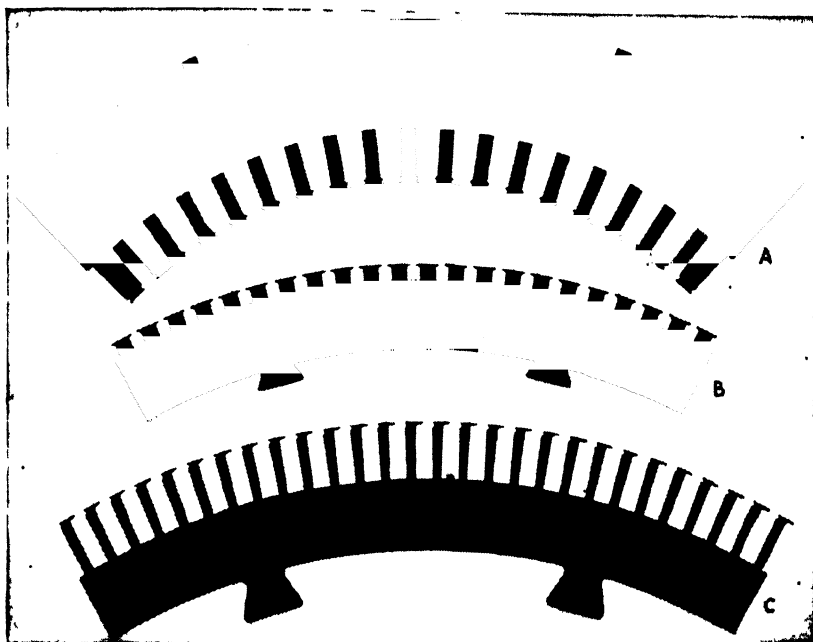


FIG. 23-1 Laminated segments of stator and rotor of large induction motors.

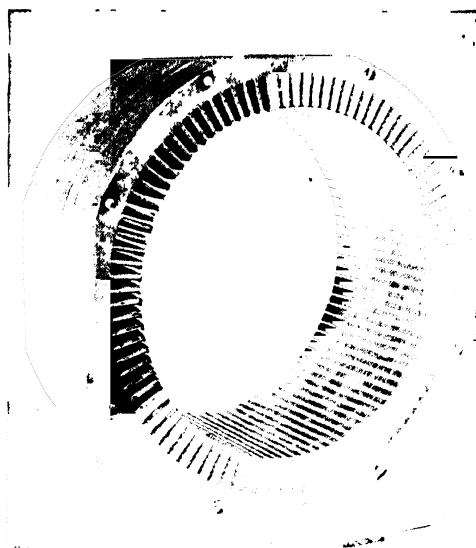


FIG. 23-2. Complete stack of stator laminations of a small induction motor with semi-open slots.

There are two general kinds of rotor windings, one the squirrel-cage winding, the other the phase winding similar to that of the stator. The

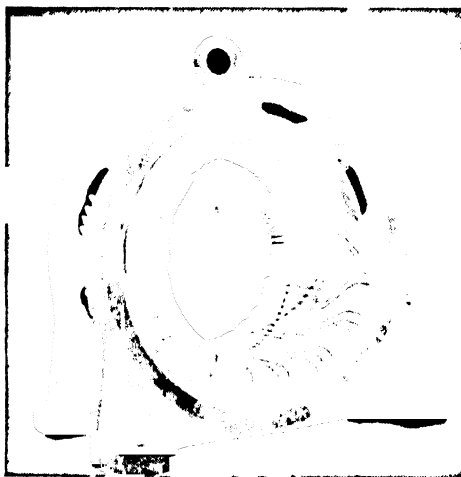


FIG. 23-3. Partially wound stator of an induction motor.

squirrel-cage winding consists of bare bars put in the slots and connected together at each end by a ring. A complete squirrel-cage rotor for a larger

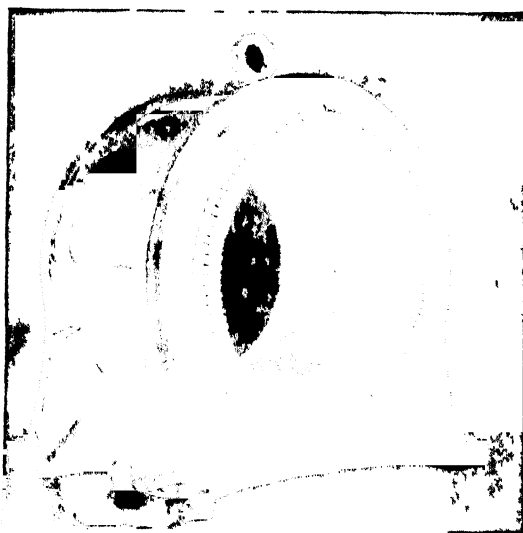


FIG. 23-4. Complete stator of a medium size induction motor.

induction motor was shown in Fig. 21-14. A laminated segment of a squirrel-cage rotor similar to that shown in Fig. 21-14 is shown in Fig.

23-1B. The slots are shallow and semi-open. This produces a definite speed-torque characteristic. In order to produce a different speed-torque characteristic, the slots and bars often are narrow and much deeper, as shown in Fig. 23-5, which represents a complete rotor of a small induction motor, equipped with ventilating fans. The slots here are skewed in order

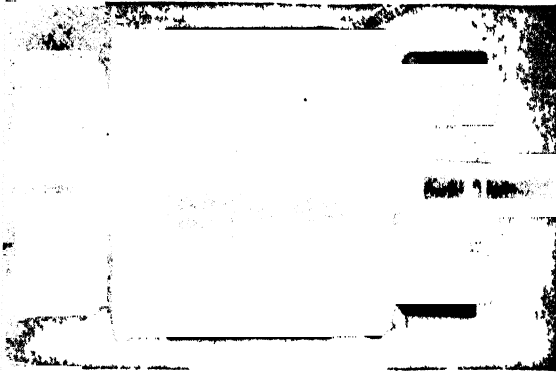


FIG. 23-5. Complete rotor of a squirrel-cage motor with deep bars.

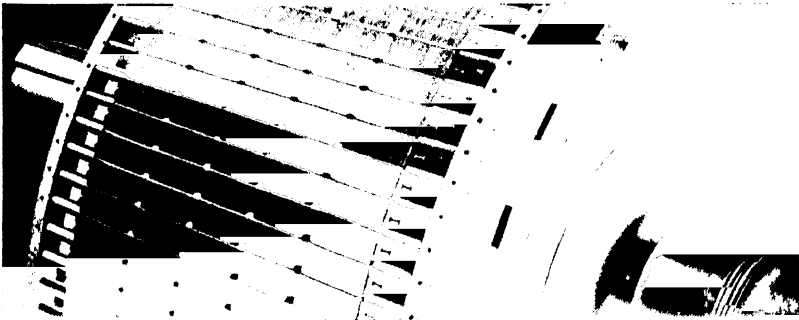


FIG. 23-6. Squirrel-cage rotor with round bars.

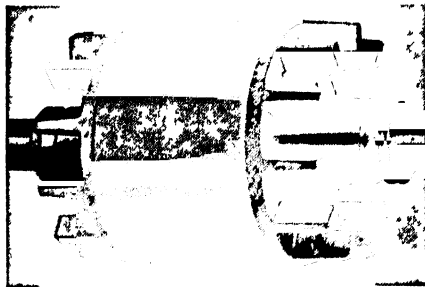


FIG. 23-7. Complete squirrel-cage rotor with die-cast aluminum bars, end rings, and ventilating fans.

to produce better starting performance and to avoid noise. Fig. 23-6 shows a squirrel-cage motor with round bars. Fig. 23-7 shows a complete rotor of a smaller motor, in which the rotor bars as well as the rings and ventilating fans are cast in aluminum.

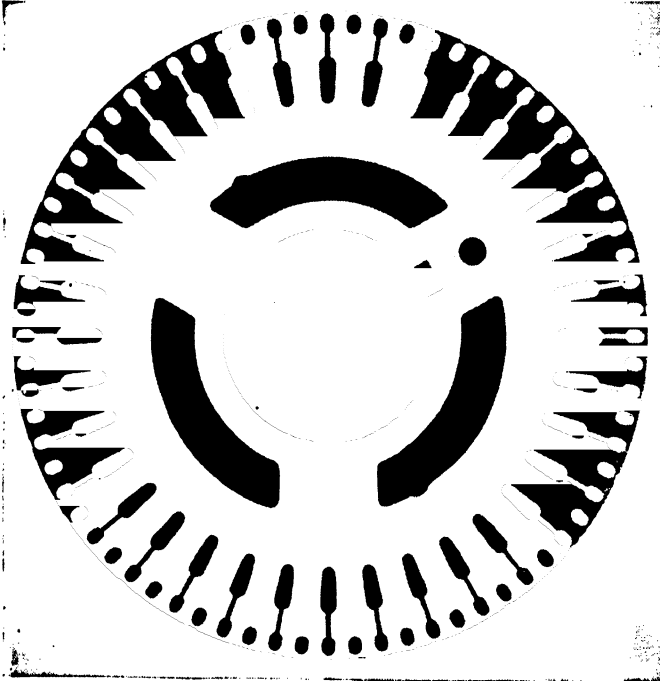


FIG. 23-8. Punching of a double cage rotor.

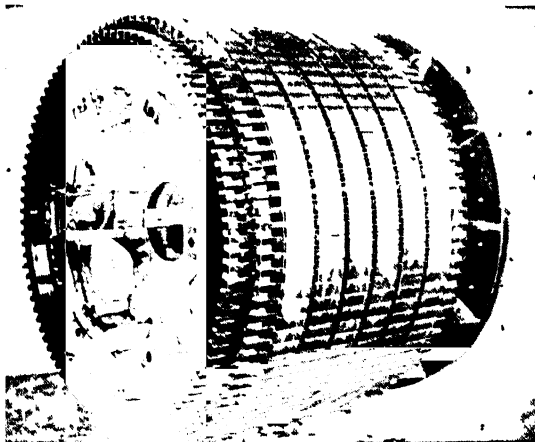


FIG. 23-9. Complete double-cage rotor.

Certain desirable operating characteristics can be achieved by the use of two squirrel cages in the same rotor. Different shapes of slots for double-

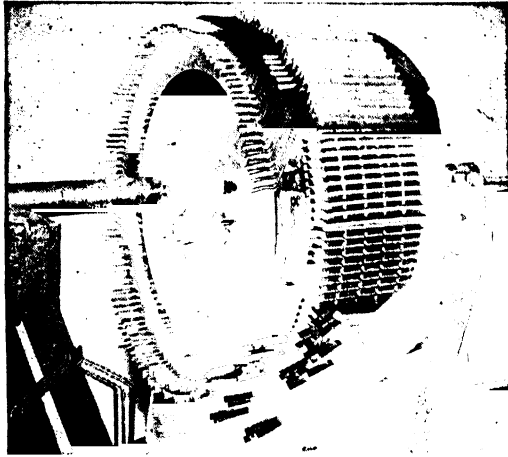


Fig. 23-10. Partially wound rotor with phase winding.

cage rotors are shown in Fig. 28-4. Fig. 23-8 shows the rotor punching for a double-cage rotor, having twice as many slots in the upper cage as in the lower one. Fig. 23-9 shows a complete double-cage rotor.

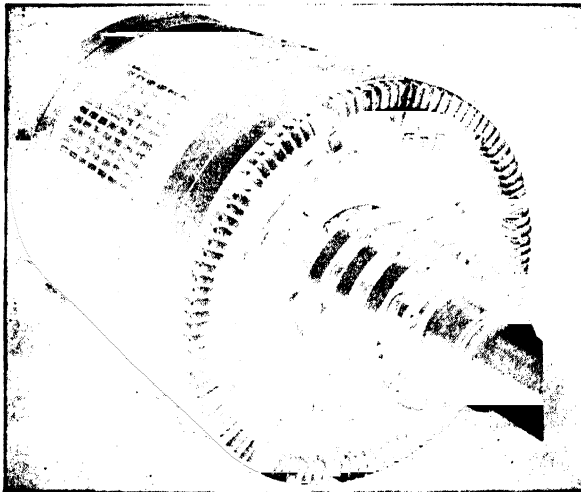


Fig. 23-11. Complete wound rotor of a larger induction motor.

A punching of a phase-wound rotor is shown in Fig. 23-1. Fig. 23-10 shows a partially wound rotor with phase winding, and Fig. 23-11 shows



a complete phase-wound rotor. These rotors are usually 3-phase. In order to connect the rotor to an external rheostat, for starting and control purposes, the beginnings of the phases are connected to slip rings; a 3-phase motor has three slip rings. Brushes riding on the slip rings provide

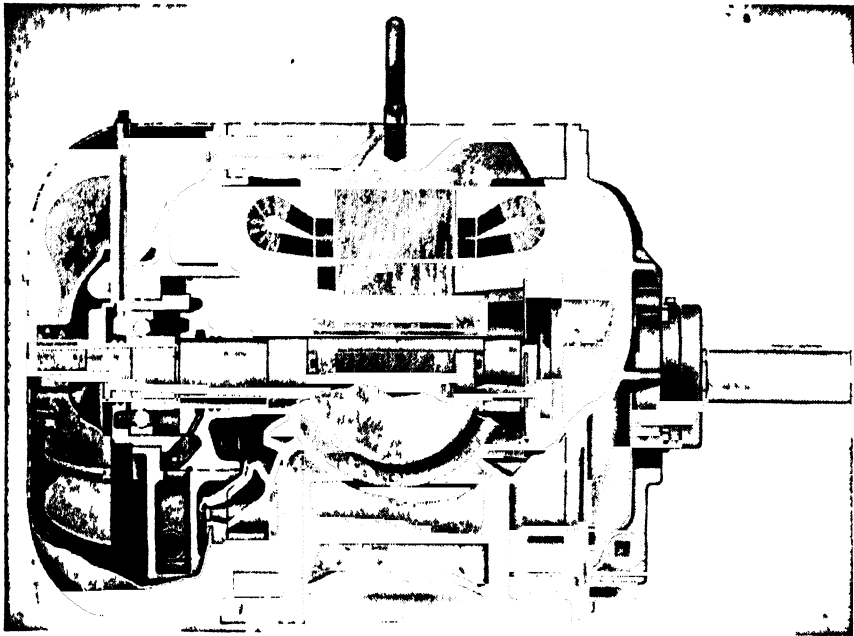


FIG 23-12 Cutaway section of a totally enclosed fan-ventilated squirrel-cage induction motor



FIG. 23-13. Parts of a small 3-phase squirrel-cage induction motor with cast aluminum bars.

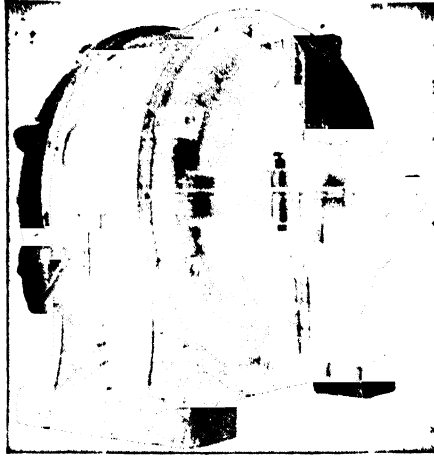


FIG. 23-14. Open-type polyphase induction motor.

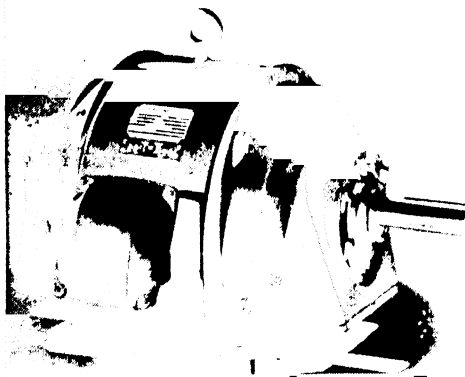


FIG. 23-15. Splashproof, ball-bearing, squirrel-cage induction motor.

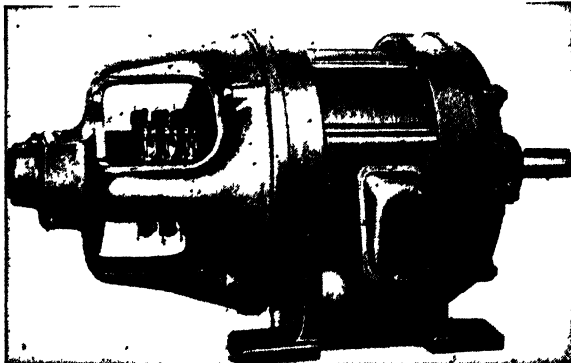


FIG. 23-16. Medium-sized phase-wound induction motor.

the connection to the rheostat. The phase-wound rotor is called simply a *wound rotor or also slip-ring rotor*.

Fig. 23-12 shows a cutaway section of a squirrel-cage induction motor, totally enclosed type, fan-ventilated. The flow of air for this motor is

TABLE 23-1. HORSEPOWER AND SYNCHRONOUS SPEED RATINGS FOR  
GENERAL-PURPOSE POLYPHASE INDUCTION MOTORS

Cycles	60	60	60	60	60	60	60	25	25	25
Hp	Rpm	Rpm	Rpm	Rpm	Rpm	Rpm	Rpm	Rpm	Rpm	Rpm
$\frac{1}{2}$	....	....	....	...	...	...	...	....	750	...
$\frac{3}{4}$	....	....	1200	...	...	...	...	....	750	..
1	....	1800	1200	...	...	...	...	*1500	750	...
$1\frac{1}{2}$	*3600	1800	1200	...	...	...	...	*1500	750	...
2	*3600	1800	1200	900	...	...	...	*1500	750	...
3	*3600	1800	1200	900	...	...	...	*1500	750	...
5	*3600	1800	1200	900	...	...	...	*1500	750	...
$7\frac{1}{2}$	*3600	1800	1200	900	...	...	...	*1500	750	...
10	*3600	1800	1200	900	...	600	...	*1500	750	500
15	*3600	1800	1200	900	...	600	...	*1500	750	500
20	*3600	1800	1200	900	...	600	...	*1500	750	500
25	....	1800	1200	900	...	600	...	*1500	750	500
30	....	1800	1200	900	...	600	...	*1500	750	500
40	....	1800	1200	900	...	600	...	*1500	750	500
50	....	....	1200	900	...	600	...	....	750	500
60	....	....	1200	900	...	600	...	....	750	500
75	....	....	1200	900	...	600	...	....	750	500
100	....	....	....	900	...	600	450	....	750	500
125	....	....	....	900	720	600	450	....	750	500
150	....	....	....	...	720	600	450	....	750	500
200	....	....	....	...	720	600	...	....	...	500

\* NOTE — The 3600 and 1500 rpm ratings apply to squirrel-cage motors only.

(NEMA MG9-512)

shown in Fig. 34-2. Fig. 23-13 shows the parts of a small 3-phase induction motor, with cast-aluminum rotor, and ventilating fan. Fig. 23-14 shows a complete induction motor, open type, and Fig. 23-15 shows a splash-proof motor. Fig. 23-16 shows a complete medium-sized motor with phase-wound rotor.

The standard ratings of polyphase induction motors are given in Table 23-1.

(c) *The magnetic circuit of the induction motor.* Fig. 23-17 shows the

magnetic paths of a 4-pole induction motor. Each of the four paths includes a part of the stator core, two sets of stator teeth, two air-gaps, two sets of rotor teeth, and a part of the rotor core. The circuital law of the magnetic field (Eq. 1-23 or Eq. 4-1) is the basic relation for the study of the magnetic circuit of the induction motor as it is for the magnetic

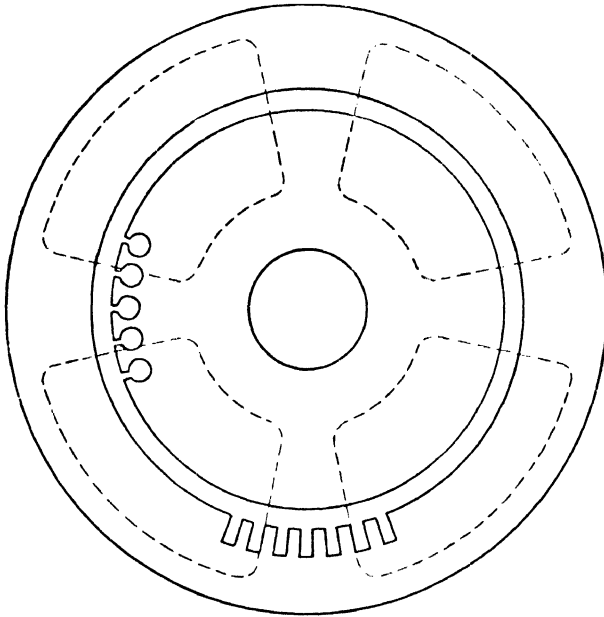


FIG. 23-17. Main flux paths of a 4-pole induction motor.

circuit of the d-c machine and any other magnetic circuit. Comparing the magnetic circuits of the induction motor and the d-c machine, Art. 4-1, each consists of five terms and the only difference is that the term which represents the pole bodies of the d-c machine ( $2H_p l_p$ , Eq. 4-4) is to be replaced by a term which represents the stator teeth of the induction motor. Otherwise the determination of the mmf necessary to drive a given flux through a given structure follows exactly the pattern shown for the d-c machine. The current in the polyphase winding necessary to produce a certain mmf is determined by Eq. 22-20.

## Chapter 24

### THE POLYPHASE INDUCTION MOTOR AS A TRANSFORMER

It has been pointed out already that in the induction motor, contrary to other electric machines, only one machine part, the stator, is connected to a source of power. The rotor of the induction motor is not connected to any power line, but receives its emf and current by means of *induction*: energy is transferred to the rotor by means of the magnetic flux. This same feature also applies to the transformer, and it will be shown in the following that the *induction motor operates on the transformer principles*.

The stator winding of the polyphase induction motor is usually 3-phase, seldom 2-phase. The rotor winding is either of the squirrel-cage type (Fig. 23-6) or wound 3-phase type (Fig. 23-11) connected to three slip rings. When the rotor winding is phase-wound, it must be wound for the same number of poles as the stator winding. It will be shown in Art. 24-2 that a squirrel-cage winding automatically assumes the same number of poles as the stator.

**24-1. The induction motor at standstill.** (a) *Rotor winding open.* Consider a 3-phase motor with a 3-phase wound rotor, Fig. 24-1, the slip rings of which are at first *open*. In this case the induction motor behaves exactly as a transformer with an open secondary (no-load). The impressed line voltage forces currents into the stator windings which produce a rotating flux. The magnitude of the currents and of the flux is such that Kirchhoff's mesh law is satisfied (see Eq. 12-3). There are, besides the impressed voltage, two emf's in the stator circuit, one of them produced by the *main flux*, the other by the *leakage fluxes* of the stator.

As in the transformer, the main flux is that flux which is interlinked with *both* windings, i.e., the stator and *rotor* winding. Its path consists of the stator and rotor cores, stator and rotor teeth, and twice the air

gap  $g$ . The leakage fluxes of the stator are those fluxes which are inter-linked with the stator winding only. The stator winding is embedded in slots, and its leakage fluxes are similar to those of the d-c armature winding (see Art. 8-2), namely;

1. Slot leakage flux, Fig. 8-6.
2. Tooth-top leakage flux, Fig. 8-6.
3. End-winding leakage flux, Fig. 8-5.

In a-c machines there is an additional leakage flux which does not exist in the d-c machine. This is the *harmonic* leakage flux. It has been explained in Art. 22-2 that an a-c winding produces a fundamental mmf

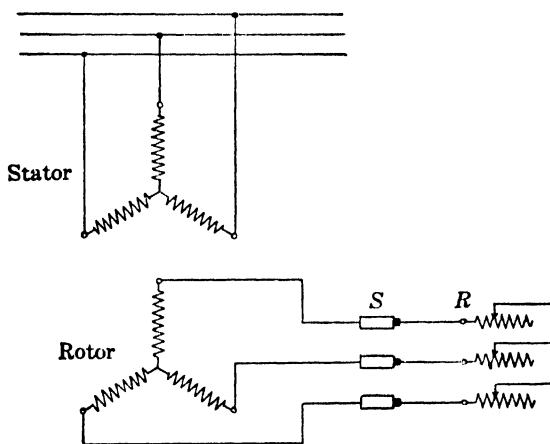


FIG. 24-1. Schematic diagram of a 3-phase, wound-rotor induction motor.

wave, the length of which is equal to twice the pole pitch of the machine  $2\tau$ , and harmonic mmf waves. Only the flux produced by the fundamental mmf wave produces the useful torque of the machine. The harmonic fluxes are parasitic fluxes and are to be considered as leakage fluxes. Thus for a-c windings there exists, in addition to the leakage fluxes enumerated under 1, 2, and 3, a fourth leakage flux, namely, the *harmonic or differential leakage flux*. The designation "differential" means that the difference between the *total* mmf and the *fundamental* wave is to be considered as leakage. The fundamental wave is called the *main wave* or *synchronous wave*.

Only the end-winding flux is a real leakage flux. The three other leakage fluxes together with the fundamental flux constitute the total flux of the machine. Physically only a single flux exists in the machine, namely, the total flux. The division into the main flux and leakage flux is necessary for the same two reasons which were stated for the transformer.

The main reason is that it is only the flux interlinked with *both* windings which transfers power from the stator or primary winding to the rotor or secondary winding. The second reason is that the two kinds of flux have paths with entirely different reluctances (see Art. 12-1). While the reluctance of the leakage fluxes is determined mainly by air ( $\mu = 1$ ) resulting in a high reluctance path, (see Eq. 1-27), the main flux path lies in the iron with a high  $\mu$  and in the air gap which is small relative to the air paths of the leakage fluxes 1, 2, and 3.

The fact that the reluctance of the paths of the leakage fluxes is determined mainly by air ( $\mu = 1$ ) and is therefore almost constant makes the magnitude of the leakage fluxes *directly proportional* to the current (mmf) producing them. This does not apply to the main flux, the path of which lies in the air gap *and iron* (see Art. 12-1). The magnitude of the main flux is determined by the mmf producing it, by the length of the air gap, and by the permeability of the iron. Since the last changes with the mmf according to the saturation curve of the iron used, the main flux is not proportional to the mmf producing it.

Referring again to Fig. 24-1 with the rotor winding open, the two emf's induced in the stator winding are: (a) the emf induced by the main flux; (b) the emf induced by the leakage fluxes. Both emf's lag their fluxes by  $90^\circ$ . As in the transformer (see Art. 12-1) the main flux is produced by the reactive component  $I_\phi$  of the magnetizing current  $I_m$ , while the leakage fluxes are produced by the total stator current which, with the rotor open, is only a little larger than  $I_m$ . As in the transformer, the magnetizing current  $I_m$  has an active component  $I_{h+c}$  in counter-phase with the emf induced by the main flux  $E_1$ , which is necessary to supply the hysteresis and eddy-current losses due to the main flux. As in the transformer,

$$I_\phi + I_{h+c} = I_m \quad (24-1)$$

As in the transformer (see Eq. 12-3), Kirchhoff's mesh law for the stator winding is

$$V_1 + E_1 - jI_1x_1 = I_1r_1 \quad (24-2)$$

or

$$V_1 = -E_1 + jI_1x_1 + I_1r_1 \quad (24-2a)$$

The subscript 1 indicates the primary (stator) winding.  $V_1$ ,  $E_1$ ,  $I_1$  and the parameters  $r_1$  and  $x_1$  are assumed to be *phase* values, so that the voltages in Eqs. 24-2 and 24-2a are per-phase quantities.

The relations between  $I_\phi$  and  $E_1$  and  $I_m$  and  $E_1$  are the same as for the transformer, i.e., Eqs. 12-7 to 12-10 also hold here.

The emf  $E_1$  induced by the main flux in the stator winding is equal to (see Eq. 22-10)

$$E = 4.44 N_1 f_1 \Phi k_{d1} k_{p1} 10^{-8} \text{ volt} \quad (24-3)$$

The main flux induces a voltage not only in the stator winding but also in the rotor winding. The speed of the rotating flux\* produced by the stator currents is, *with respect to the stator* (see Eq. 22-15),

$$n_s = \frac{120f_1}{p} \quad (24-4)$$

The speed  $120f_1/p$  is called the *synchronous speed*, and the subscript  $s$  indicates this fixed value of the speed. Generally, when the rotor rotates with a speed  $n$  in the direction of the rotating flux, the relative speed between the rotating flux and the rotor winding is  $n_s - n$ . Since the rotor is considered here at standstill  $n = 0$ , the relative speed between the rotating flux and rotor is equal to  $n_s$ , i.e., the frequency of the emf induced in the rotor winding is (see Eq. 1-9)

$$f_2 = \frac{n_s p}{120} = f_1$$

Thus the emf induced in the rotor winding, at standstill, is

$$E_2 = 4.44 N_2 f_1 \Phi k_{d2} k_{p2} 10^{-8} \text{ volt} \quad (24-5)$$

and

$$\frac{E_2}{E_1} = \frac{N_2 k_{d2} k_{p2}}{N_1 k_{d1} k_{p1}} \quad (24-6)$$

i.e., the ratio of the emf's induced in both windings by the main flux is equal to the ratio of their effective turns, just as in the transformer.

The magnetizing current  $I_m$  drawn from the lines by the polyphase induction motor with an open secondary (rotor) is much larger than that drawn by the transformer. This current is from 18 to 40% of the rated current in the induction motor and only 3% to 15% of the rated current in the transformer. The larger magnetizing current of the induction motor is caused by the air gap, i.e., by the higher reluctance of the main flux path of the induction motor: a larger mmf is necessary to drive the same main flux through the induction motor than through the transformer.

(b) *Rotor winding closed.* It will be assumed in this discussion that the rotor winding is closed but that the rotor is *blocked* so that it can not rotate. In this case the emf  $E_2$  induced in the rotor by the main flux,

\* Here and in following discussions the rotating flux means the main flux.



Eq. 24-5, will produce polyphase currents in the rotor winding. These currents yield rotating mmf's consisting of a main wave and harmonics just as the polyphase currents in the stator winding yield a main mmf wave and harmonics. Just as in the stator, the harmonic fluxes of the rotor produced by its harmonic mmf's are considered as leakage fluxes (rotor leakage), and only the main wave of the rotor is to be taken into account because only it contributes to the useful torque. For this reason the rotor mmf considered in the following discussion refers to the main wave only.

It has been explained that the frequency  $f_2$  of the rotor currents at standstill is equal to the stator frequency  $f_1$ . Therefore the speed of the rotor mmf with respect to the rotor, at standstill, is

$$n_s' = \frac{120f_2}{p} = \frac{120f_1}{p} = n_s$$

This equation shows that the speed of the rotor mmf relative to the rotor is identically the same as the speed of the stator mmf relative to the stator, namely,  $n_s' = n_s$ . Thus it follows that at standstill the mmf waves of stator and rotor are stationary with respect to each other. It will be shown in the next article that this is also true when the rotor rotates, no matter what the speed of rotation. *Standstill of stator and rotor mmf waves with respect to each other is a necessary condition for the existence of a uniform torque in the machine.*

The rotor winding is the armature winding of the induction motor. When currents flow in the rotor winding, an mmf wave is produced by them, and this wave reacts upon the stator mmf wave which is always at standstill with respect to the rotor wave. Just as in the transformer the secondary mmf reacts upon the primary mmf (see Art. 13-1). The reaction of the rotor mmf, i.e., the armature reaction, is such that it opposes the stator mmf and tends to reduce the main flux and  $E_1$ . In accordance with Kirchhoff's equation (Eq. 24-2) the stator is forced to draw more current from the lines, thus compensating for the armature reaction and sustaining the main flux, i.e., the emf  $E_1$ . The terms  $I_1 r_1$  and  $j I_1 x_1$  increase with increasing primary current  $I_1$ . However, these terms are, in the normal range of operation, small in comparison with the emf induced by the main flux,  $E_1$ , so that the main flux varies but little in the normal range of operation, just as in the transformer.

When the rotor carries current, there are two mmf's in the machine, and the main flux is determined by the resultant mmf. The two mmf's are (see Eq. 22-20):

$$F_1 = 0.9m_1 \frac{N_1}{p} k_{s1} k_{p1} I_1 \quad (24-7)$$

and

$$F_2 = 0.9m_2 \frac{N_2}{p} k_{d2}k_{p2}I_2 \quad (24-8)$$

As in the transformer, a simplification of the formulas, the phasor diagram, and the equivalent circuit is achieved when the secondary quantities are "*referred to the primary*" or, in other words, when it is assumed that the rotor winding is identical with the stator winding, i.e., that it has the same number of phases  $m_1$  and the same number of effective turns  $N_1k_{d1}k_{p1}$  as the stator winding.

Such an assumption will be permissible if care is taken that the referred quantities of the rotor are such that (see Art. 13-2):

1. The rotor retains the original value of its mmf as given by Eq. 24-8, i.e., the main flux is not changed.
2. The kva of the rotor retains its original value.
3. The  $I^2R$  loss of the rotor retains its original value.
4. The magnetic energy of the leakage fluxes of the rotor ( $\frac{1}{2}L_lI^2$ ) retains its original value.

Rotor quantities referred to the stator will be indicated by a *prime*. The first condition above means that the rotor current referred to the stator,  $I_2'$ , must be such that

$$0.9m_1 \frac{N_1}{p} k_{d1}k_{p1}I_2' = 0.9m_2 \frac{N_2}{p} k_{d2}k_{p2}I_2$$

or

$$I_2' = \frac{m_2}{m_1} \frac{N_2k_{d2}k_{p2}}{N_1k_{d1}k_{p1}} I_2 \quad (24-9)$$

$I_2'$  is a current which, flowing in the stator winding, will produce the same mmf as the current  $I_2$  produces flowing in the rotor winding. The second condition means that

$$m_1E_2'I_2' = m_1E_2' \frac{m_2N_2k_{d2}k_{p2}}{m_1N_1k_{d1}k_{p1}} I_2 = m_2E_2I_2$$

or

$$E_2' = \frac{N_2k_{d2}k_{p2}}{N_1k_{d1}k_{p1}} E_2 = E_1 \quad (24-10)$$

i.e., that the secondary and primary emf's induced by the main flux are equal. This is in accordance with the assumption that the number of effective turns of the secondary winding is equal to that of the primary winding.

The third condition means  $m_1 I_2'^2 r_2' = m_2 I_2'^2 r_2$  or, inserting the value of  $I_2'$  from Eq. 24-9,

$$r_2' = \frac{m_1}{m_2} \left( \frac{N_1 k_{d1} k_{p1}}{N_2 k_{d2} k_{p2}} \right)^2 r_2. \quad (24-11)$$

The fourth condition means that

$$\frac{1}{2} m_1 I_2'^2 x_2' = \frac{1}{2} m_2 I_2'^2 x_2$$

where  $x_2 = \omega L_{l2} = 2\pi f_1 L_{l2}$  is the leakage reactance of the rotor at line frequency  $f_1$ . Inserting into this equation the value of  $I_2'$ ,

$$x_2' = \frac{m_1}{m_2} \left( \frac{N_1 k_{d1} k_{p1}}{N_2 k_{d2} k_{p2}} \right)^2 x_2 \quad (24-12)$$

It follows from Eqs. 24-9 to 24-12 that the *reduction factors* to the primary are:

$$\begin{array}{ll} \frac{N_1 k_{d1} k_{p1}}{N_2 k_{d2} k_{p2}} & \text{for voltage} \\ \frac{m_2}{m_1} \frac{N_2 k_{d2} k_{p2}}{N_1 k_{d1} k_{p1}} & \text{for current} \end{array} \quad (24-13)$$

and

$$\frac{m_1}{m_2} \left( \frac{N_1 k_{d1} k_{p1}}{N_2 k_{d2} k_{p2}} \right)^2 \quad \text{for resistance and reactance}$$

Since these reduction factors satisfy conditions 1 to 4, calculations made with the referred quantities  $E_2'$ ,  $I_2'$ ,  $r_2'$  and  $x_2'$  do not change anything in the magnetic or electric behavior of the machine.

The total mmf which produces the main flux  $\Phi$  is given by the geometric sum of the mmf's of both windings  $F_1$  and  $F_2$ , Eqs. 24-7 and 24-8. This geometric sum yields the magnetizing mmf (see Eq 13-8)

$$0.9m_1 \frac{N_1 k_{d1} k_{p1}}{p} \mathbf{I}_1 + 0.9m_2 \frac{N_2 k_{d2} k_{p2}}{p} \mathbf{I}_2 = 0.9m_1 \frac{N_1 k_{d1} k_{p1}}{p} \mathbf{I}_m \quad (24-14)$$

Substituting for  $I_2$  the value from Eq. 24-9, the result is the same as that for the transformer

$$\mathbf{I}_1 + \mathbf{I}_2' = \mathbf{I}_m \quad (24-14a)$$

Therefore, the same considerations apply as for the transformer (see Art. 13-4) and Eq. 13-10 and 13-10a, derived for the transformer, also apply to the induction motor, the secondary of which carries current. However, it should not be forgotten that the rotor is considered here to be at standstill, at which operating condition stator and rotor mmf's

are at standstill with respect to each other. Eqs. 13-10 and 13-10a can be considered applicable to the machine during running only when proof is given that stator and rotor mmf's are at standstill with respect to each other at any rotor speed.

Kirchhoff's mesh equations for the stator and rotor are, (see Eq. 24-2a)

$$\mathbf{V}_1 = -\mathbf{E}_1 + \mathbf{I}_1(r_1 + jx_1) \quad (24-15)$$

$$\mathbf{E}_2' = \mathbf{E}_1 = \mathbf{I}_2'(r_2' + jx_2') \quad (24-15a)$$

The second equation for the rotor applies only to the case considered here, i.e., to the rotor at standstill.

The foregoing considerations refer to the induction motor with a phase wound rotor and an external resistance in the rotor circuit, Fig. 24-1. The same considerations also apply to the squirrel-cage rotor, but in this case no external resistance can be inserted into the rotor; therefore, the squirrel-cage rotor corresponds to the case of a wound rotor with an external resistance equal to zero. The squirrel-cage rotor and the wound rotor with no external resistance behave at standstill as a transformer the secondary of which contains only its own resistance and leakage reactance, i.e. as a transformer at short-circuit. For this condition the main flux of the transformer and induction motor is small, and the current is high and limited mainly by the leakage reactances and resistances of the primary and secondary windings (see Art. 28-2). Due to the fact that the leakage reactances of the induction motor are much higher than those of the transformer, the short-circuit current (current at standstill) of the induction motor is much smaller than that of the transformer. The short-circuit current is 3.5 to 8 times rated current in the induction motor and 7 to 40 times rated current in the transformer.

**24-2. The induction motor when running. The slip.** When the blocked rotor, with closed winding, is released, it starts rotating because the rotating flux exerts tangential forces on its current-carrying conductors. The direction of rotation of the rotor is the same as that of the rotating flux which rotates at the constant speed  $n_s = 120f_1/p$  relative to the stator, i.e., at synchronous speed (Eq. 24-4). When the rotor is at standstill, the *relative* speed between the rotating flux and rotor is equal to the synchronous speed  $n_s$  and the emf induced in the rotor is  $E_2' = E_1$ . When the rotor rotates at a speed  $n$ , the *relative* speed between the rotating flux and the rotor is  $n_s - n$ . Since it is the relative speed between the flux and rotor winding which determines the magnitude and frequency of the emf induced in the rotor, the magnitude of the emf induced in the

rotor winding at the speed  $n$  is

$$E_{2s}' = \frac{n_s - n}{n_s} E_2' \quad (24-16)$$

and the frequency of this emf is

$$f_2 = \frac{n_s - n}{n_s} f_1 \quad (24-17)$$

The quantity  $(n_s - n)/n_s$  is called the *slip*, i.e., the slip is defined as:

$$s = \frac{n_s - n}{n_s} \quad (24-18)$$

The slip gives the relative speed between the rotating flux and the rotor as a fraction of the synchronous speed  $n_s$ . At standstill,  $n = 0$  and  $s = 1$ ; at synchronous speed  $n = n_s$  and  $s = 0$ . At synchronous speed the relative speed between the rotating flux and the rotor is equal to zero and no emf is induced in the rotor. Therefore, there is no current in the rotor and no tangential force is exerted on the rotor at synchronous speed. An induction motor is not able to reach the synchronous speed; it will run with a slip sufficient enough to induce the current necessary to produce the tangential force and torque required by the load. *The slip is the basic variable of the induction motor.*

Introducing Eq. 24-18 into Eqs. 24-16 and 24-17, the emf induced in the rotor by the rotating flux as a function of slip  $s$  is

$$E_{2s}' = sE_2' \quad (24-19)$$

and the frequency of this emf is

$$f_2 = sf_1 \quad (24-20)$$

At standstill of the rotor ( $s = 1$ ) the frequency of the rotor emf is equal to the line frequency; this is in accordance with the result obtained previously.

Thus, for the rotor running with the speed  $n$  the quantity  $sE_2' = sE_1$  is to be introduced for  $E_2' = E_1$  in Kirchhoff's mesh Eq. 24-15a. In the same equation,  $x_2'$  is the rotor leakage reactance at line frequency  $f_1$ . Since, at the rotor speed  $n$ , the frequency of the rotor current is  $f_2 = sf_1$ , the quantity  $sx_2'$  instead of  $x_2'$  is to be introduced for the running rotor. Hence Kirchhoff's mesh equation of the rotor circuit becomes

$$sE_2' = sE_1 = I_2'(r_2' + jsx_2') \quad (24-21)$$

Eq. 24-15a which applies only to standstill is a special case of Eq. 24-21, obtained from the latter equation by setting  $s = 1$ .

According to Eq. 24-20 the speed of the mmf wave produced by the rotor, relative to the rotor is

$$n_s' = \frac{120f_2}{p} = \frac{120f_1s}{p} = sn_s = n_s - n$$

Since the rotor speed is equal to  $n$ , the speed of the rotor mmf relative to the stator is  $n + n_s' = n_s$ . This is the same as the speed of the stator mmf wave relative to the stator, i.e., rotor and stator mmf waves are stationary with respect to one another at any rotor speed  $n$ . It has been pointed out in the foregoing article that this is the condition for the existence of a uniform torque in the polyphase machine. *Thus the polyphase induction motor is able to produce a uniform torque at any rotor speed.* It will be seen later, see Art. 36-1, that the synchronous motor does not possess the ability to produce a uniform torque at any speed.

With the proof given that stator and rotor mmf's are at standstill with respect to each other at any rotor speed, just as at standstill of the rotor, Eqs. 24-14 and 24-14a also apply to the running motor and consequently Eqs. 13-10, 13-10a hold for the running motor, i.e., no matter what the speed of the rotor,

$$\mathbf{I}_m = \mathbf{I}_1 + \mathbf{I}_2' = -\mathbf{E}_1\mathbf{Y}_m = -\mathbf{E}_2'\mathbf{Y}_m \quad (24-22)$$

$$\mathbf{E}_1 = \mathbf{E}_2' = -\mathbf{I}_m\mathbf{Z}_m = -(\mathbf{I}_1 + \mathbf{I}_2')\mathbf{Z}_m \quad (24-22a)$$

Considering the rotor, the number of rotor poles has been assumed to be the same as that of the stator. Stator and rotor must have the same number of poles in all electric machines. In the phase-wound rotor the equality of numbers of poles is achieved simply by winding the rotor for the same number of poles as the stator. It has been mentioned that the squirrel-cage rotor automatically produces the same number of poles as that of the stator.

Consider Fig. 24-2. The rotating flux is sinusoidally distributed as shown by the  $B$ -curve. This flux moves with the speed  $n_s$  while the rotor rotates at speed  $n$ . With respect to the rotor the rotating flux moves at a relative speed  $n_s - n$ . Applying Faraday's law in the  $Blv$  form, the emf's induced in the individual bars of the squirrel cage are also sinusoidally distributed as shown in Fig. 24-2. In order to simplify the explanation the assumption will be made that the rotor speed  $n$  is close to the synchronous

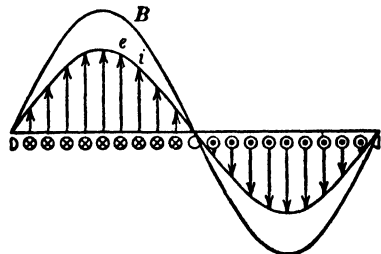


FIG. 24-2. Explanation of the number of poles of a squirrel-cage rotor.

speed  $n_s$ , as is generally the case for operation at rated output. The rotor leakage reactance  $sx_2'$  then becomes very small, and it can be assumed that the current and emf of the individual rotor bars are in phase. Therefore the emf's of the individual bars in Fig. 24-2 represent, to another scale, the currents of the individual bars and, if the currents are indicated by crosses under the positive half-wave of the  $B$  curve, they must be indicated by dots under the negative half-wave of the  $B$  curve. It is seen that the flux wave produces a 2-pole current distribution and hence also a 2-pole mmf distribution in the squirrel-cage rotor. Since the number of poles of the flux wave is the same as that of the stator winding, the squirrel-cage rotor produces the same number of poles as that of the stator.

The current distribution shown in Fig. 24-2 repeats each *pole pair*. The emf's of the individual bars, within a pole pair, have a time shift with respect to one another which corresponds to the angle between two bars, i.e., the time shifts between the emf's of the bars are equal to their space shifts. This means that a *squirrel-cage rotor represents a symmetrical polyphase system with as many phases as there are bars in a pole pair*. If  $Q_2$  is the number of slots of the rotor, then  $m_2 = Q_2/(p/2)$  and  $p/2$  phases are connected in parallel. The number of turns per phase is  $N = \frac{1}{2}$  because each phase consists of 1 conductor. The distribution and pitch factors are equal to 1. Thus for the squirrel-cage rotor

$$m_2 = \frac{2Q_2}{p}; N_2 = \frac{1}{2}; k_{d2} = 1; k_{p2} = 1 \quad (24-23)$$

These quantities are to be introduced for the squirrel-cage rotor in Eqs. 24-5 to 24-14.

Dividing Eq. 24-21 by the slip  $s$ , Kirchhoff's mesh equation of the rotor becomes

$$\mathbf{E}_2' = \mathbf{E}_1 = \left( \frac{r_2'}{s} + jx_2' \right) \mathbf{I}_2' \quad (24-24)$$

which also can be written as

$$\mathbf{E}_2' = \mathbf{E}_1 = (r_2' + jx_2') \mathbf{I}_2' + \left( \frac{1-s}{s} \right) r_2' \mathbf{I}_2' \quad (24-25)$$

Comparing this equation and Eq. 24-15 for the stator with the corresponding mesh equations of the transformer, it is seen that they are of the same character and that the mechanical power of the induction motor can be represented as the power dissipated in a pure resistive load, the resistance being equal to  $\left( \frac{1-s}{s} \right) r_2'$ , i.e., the *induction motor, when*

*running, behaves as a transformer loaded with a pure ohmic resistance.* It could be expected that the load circuit of the induction motor, considered as a transformer, contains only resistance and no reactance, since the developed power of a rotating induction motor is a mechanical power which can only be represented by a resistance, and not by a reactance.

The similarity of the fundamental equations of the induction motor and the transformer must lead to a similarity of both their phasor diagrams and equivalent circuits.

The phasor diagram of the running polyphase induction motor can now be drawn and its equivalent circuit determined, since Kirchhoff's mesh equations of both electric circuits (Eqs. 24-2a and 24-21) and the equation which characterizes its magnetic circuit (Eq. 24-22) have been established.

### PROBLEMS

1. Determine the frequency of the rotor currents in an 8-pole, 60-cycle, 3-phase, squirrel-cage induction motor when operating at speeds of 890, 885, 870 and 850 rpm.

2. A 30-HP, 10-pole, 60-cycle induction motor operates at a rated speed of 704 rpm. Determine: (a) full-load slip; (b) the number of space degrees during one cycle.

3. For the motor of Problem 2 determine: (a) the speed of the stator mmf with respect to the stator; (b) the speed of the rotor mmf with respect to the rotor; (c) the speed of the rotor mmf with respect to the stator; (d) the difference between speeds (a) and (c). Remember that the result of (d) is the necessary condition for the existence of a uniform torque in the induction motor.

4. A 4-pole, 3-phase, Y-connected induction motor has 48 stator slots and 10 series conductors per slot. The coil throw is 10 slots. (a) Determine the pitch and distribution factors. (b) Determine the maximum flux per pole when connected to a 230-volt line neglecting resistance and reactance drops in the stator winding.

5. If the rotor of the motor described in Problem 4 has a Y-connected winding with 36 slots, six series conductors per slot, and a coil throw of 9 slots, determine the ratio of transformation.

6. Determine the emf generated in a single conductor rotating in the air gap of the machine of Problem 5 at 1740 rpm. Neglect resistance and reactance drops.

7. A 6-pole, 3-phase, Y-connected induction motor has 54 stator slots, 12 series conductors per slot and a coil throw of 7 slots. (a) Determine pitch and distribution factors; (b) determine the maximum flux per pole when connected to a 230-volt line, neglecting resistance and reactance drops in the stator winding.

8. The rotor of the motor in Problem 7 has four slots per pole per phase with four series conductors per slot. The winding is full pitch. Determine the ratio of transformation.

9. Determine the emf generated in a single conductor rotating in the air gap of the machine of Problem 7 at 1160 rpm. Neglect resistance and reactance drops.



## Chapter 25

### PHASOR DIAGRAM AND EQUIVALENT CIRCUIT OF THE POLYPHASE INDUCTION MOTOR

---

**25-1. The phasor diagram of the polyphase induction motor.** Kirchhoff's mesh equations for the primary and secondary electric circuits (Eqs. 24-2a and 24-21) and Eqs. 24-22 and 24-22a for the magnetic circuit yield the phasor diagram of (mmf's) currents and voltages shown in Fig. 25-1.

The main flux  $\Phi$  is in phase with the reactive component of the magnetizing current  $I_\phi$ . The emf's induced by the main flux in both windings,  $E_1$  and  $E_2'$  respectively, are equal and in phase, and lag the main flux  $\Phi$  by  $90^\circ$ .

The active component of the magnetizing current  $I_{h+e}$  which supplies the hysteresis and eddy-current losses due to the main flux is in counter-phase with  $E_1$ . The geometric sum of  $I_\phi$  and  $I_{h+e}$  is the magnetizing current  $I_m$ . In the transformer this current is practically equal to the no-load current  $I_0$ . In the induction motor, running at no-load, the difference between the no-load current  $I_0$  and  $I_m$  is larger than in the transformer.

The secondary emf  $E_2' = E_1$  is equal to the geometric sum of  $I_2' \frac{r_2'}{s} = I_2' \left( r_2' + r_2' \left( \frac{1-s}{s} \right) \right)$ , in phase with  $I_2'$ , and the secondary leakage reactance drop  $I_2' x_2'$  which leads  $I_2'$  by  $90^\circ$ . The angle  $\psi_{2s}$  between rotor (secondary) current  $I_2'$  and rotor emf  $E_2'$  is

$$\psi_{2s} = \tan^{-1} \frac{x_2'}{r_2'/s} \quad (25-1)$$

The magnitude of  $\psi_{2s}$  depends on the slip. The slip of the induction motor operating at its *rated torque* is usually small, from 0.01 to 0.05; the larger

value applies to small motors and the smaller value to large motors. For this slip the angle  $\psi_{2s}$  is very small and the rotor current is almost in phase with its emf  $E_2'$ .

The primary current  $I_1$  is found as the geometric sum of  $I_m$  and  $-I_2'$ . The stator terminal voltage  $V_1$  is the geometric sum of  $-E_1$  (the counter emf) and the voltage drops  $I_1 r_1$  and  $I_1 x_1$ , the former in phase with  $I_1$  and the latter  $90^\circ$  ahead of  $I_1$ .

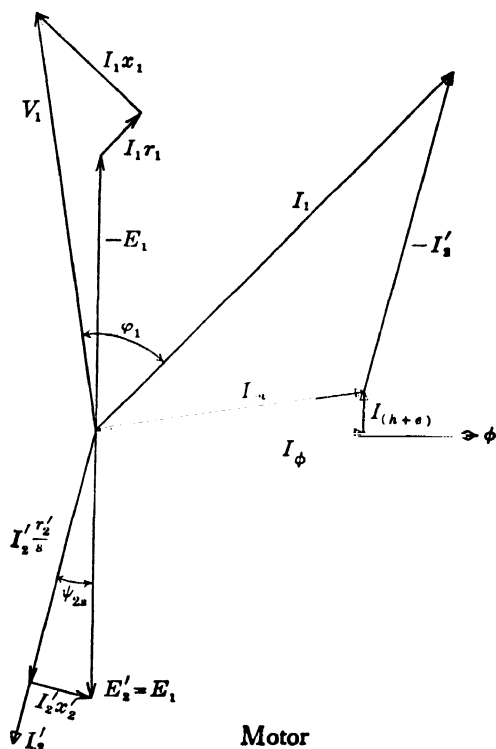


FIG. 25-1. Phasor diagram of voltages and mmf's (currents) of the polyphase induction motor under load.

The phasor diagram of (mmf's) currents and voltages of the running induction motor is identical with that of a transformer loaded with a pure resistance (see Fig. 14-1). The power factor angle  $\phi_1$  between the primary current  $I_1$  and primary voltage  $V_1$  is *always lagging* in the induction motor, while it can be lagging, zero, or leading in the transformer, depending upon the character of the load (see Fig. 14-3). The lag of  $I_1$  with respect to  $V_1$  is caused by the magnetizing current and by the leakage reactance drops. *Reactive current is required to sustain both the main flux*

as well as the leakage fluxes. Induction motors and transformers are the main consumers of reactive current from the power lines. These reactive currents are a necessary evil since they do not contribute to the power transfer but increase the copper losses in the induction motors and transformers, in the wires transferring the power and in the generators producing the power.

**25-2. The equivalent circuit of the polyphase induction motor.** The equivalent circuit of the polyphase induction motor can be derived exactly in the same manner as that of the transformer, namely, from Kirchhoff's mesh equations of both electric circuits (Eqs. 24-2a and 24-21) and from Eq. 24-22 which refers to the magnetic circuit (see Art. 13-4). These equations are

$$\mathbf{V}_1 = -\mathbf{E}_1 + \mathbf{I}_1(r_1 + jx_1) \quad (25-2)$$

$$\mathbf{E}_2' = \mathbf{E}_1 = \mathbf{I}_2' \left( \frac{r_2'}{s} + jx_2' \right) \quad (25-3)$$

$$\mathbf{I}_1 + \mathbf{I}_2' = \mathbf{I}_m = -\mathbf{E}_1 \mathbf{Y}_m = -\frac{\mathbf{E}_1}{\mathbf{Z}_m} \quad (25-4)$$

where (see Art. 12-2)

$$\mathbf{Y}_m = g_m - jb_m \quad (25-5)$$

and

$$\mathbf{Z}_m = r_m + jx_m \quad (25-6)$$

are the main flux admittance and the main flux impedance respectively. From Eq. 12-10, Art. 12-2,

$$r_m = \frac{g_m}{g_m^2 + b_m^2} \quad x_m = \frac{b_m}{g_m^2 + b_m^2} \quad (25-7)$$

Kirchhoff's mesh equations, Eqs. 25-2 and 25-3, can be written as

$$\mathbf{V}_1 = -\mathbf{E}_1 + \mathbf{I}_1 \mathbf{Z}_1 \quad (25-8)$$

$$\mathbf{E}_2' = \mathbf{E}_1 = \mathbf{I}_2' \mathbf{Z}_2' \quad (25-9)$$

where

$$\mathbf{Z}_1 = r_1 + jx_1$$

$$\mathbf{Z}_2' = \frac{r_2'}{s} + jx_2' = r_2' + r_2' \left( \frac{1-s}{s} \right) + jx_2'$$

These two equations combined with Eq. 25-4 yield

$$\mathbf{E}_1 = \mathbf{I}_2' \mathbf{Z}_2' = (\mathbf{I}_m - \mathbf{I}_1) \mathbf{Z}_2' = -\mathbf{E}_1 \mathbf{Y}_m \mathbf{Z}_2' - \mathbf{I}_1 \mathbf{Z}_2'$$

$$\mathbf{E}_1 (1 + \mathbf{Y}_m \mathbf{Z}_2') = -\mathbf{I}_1 \mathbf{Z}_2' \quad \text{or} \quad \mathbf{E}_1 = -\frac{\mathbf{I}_1}{\frac{1}{\mathbf{Z}_2'} + \mathbf{Y}_m}$$

Therefore,

$$\mathbf{V}_1 = \mathbf{I}_1 \mathbf{Z}_1 + \frac{\mathbf{I}_1}{\frac{1}{\mathbf{Z}_2'} + \mathbf{Y}_m} = \mathbf{I}_1 \left[ \mathbf{Z}_1 + \frac{1}{\frac{1}{\mathbf{Z}_2'} + \mathbf{Y}_m} \right] \quad (25-10)$$

The quantity in the brackets is the total impedance of the polyphase induction motor looking into the primary terminals. This impedance is the same as that of the transformer (see Eq. 14-8). Hence the equivalent circuit of the polyphase induction motor is, in general, the same as that of the transformer and is given by Fig. 14-4. The main difference lies in the expression for  $\mathbf{Z}_2'$ : in the induction motor the resistance  $r_2'$  is associated with the slip  $s$  while it is a constant in the transformer.

Breaking up the impedances  $\mathbf{Z}_1$ ,  $\mathbf{Z}_2$ ,  $\mathbf{Z}_m$ , and the admittance  $\mathbf{Y}_m$  into their components, four *identical* forms of the equivalent circuit of the polyphase induction motor are obtained, as shown in Figs. 25-2 to 25-5.

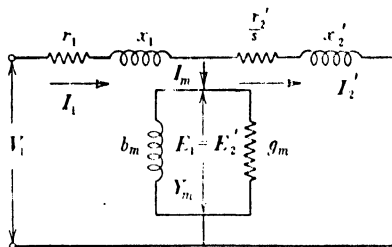


FIG. 25-2. Equivalent circuit of the polyphase induction motor.

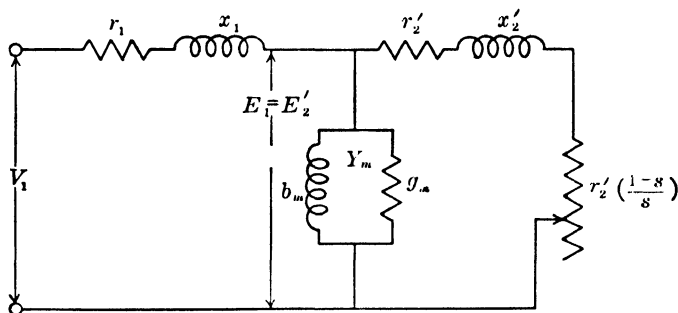


FIG. 25-3. Equivalent circuit of the polyphase induction motor.

It has been pointed out in Art. 12-2 that the magnitude of  $x_m(b_m)$  depends upon the saturation of the iron, i.e., upon the magnitude of the main flux  $\Phi$ . Since the main flux changes little between no-load and full-load,  $x_m(b_m)$  can be treated as a constant, especially for medium-sized and larger-sized motors.

It will be shown in Chapter 28 how the parameters  $r_1$ ,  $x_1$ ,  $r_2'$ ,  $x_2'$ ,  $r_m$  and  $x_m$  (or  $g_m$  and  $b_m$ ) can be determined from the no-load and the blocked rotor tests.

The equivalent circuit is very helpful in making calculations with fixed parameters or with varying parameters, especially when the circuit is

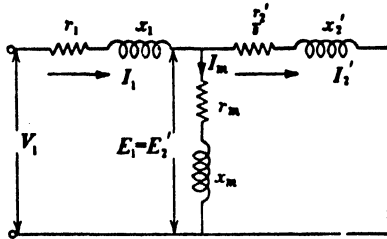


FIG. 25-4. Equivalent circuit of the polyphase induction motor.

set up on a calculating board. It should be kept in mind that an equivalent circuit does not necessarily represent the *actual behavior of all parts* of the apparatus to which it is equivalent. The equivalent circuit of the transformer does not yield the actual values of the secondary voltage and current but “referred” quantities. The equivalent circuit of the induction motor is even

further removed from the actual behavior of its secondary circuit than in the transformer. The differences can be seen from the following tabulation:

#### *Equivalent Circuit*

1. Magnitude of the secondary emf independent of the slip
2. Secondary leakage reactance constant
3. Frequency of secondary emf and current equal to line frequency ( $f_1$ )

#### *Actual Behavior*

1. Magnitude of the secondary emf proportional to the slip
2. Secondary leakage reactance proportional to the slip
3. Frequency of secondary emf and current equal to slip frequency ( $sf_1$ )

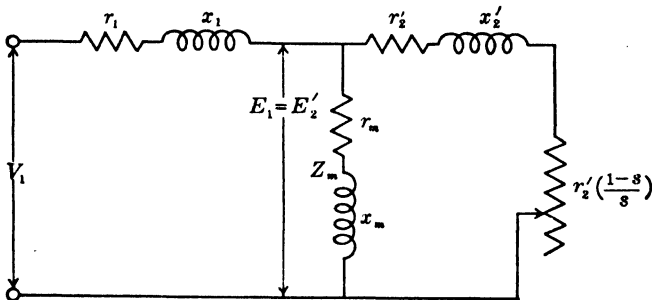


FIG. 25-5. Equivalent circuit of the polyphase induction motor.

A polyphase induction motor connected to a 60-cycle line has, at rated load, rotor currents of  $60(0.05 \text{ to } 0.01) = 3 \text{ to } 0.6$  cycles, while the rotor current of its equivalent circuit is line frequency, i.e., 60 cycles. However, calculations based on the equivalent circuit yield correct results. This is due to the fact that  $I_2'$  is not the actual rotor current but a current

which, *flowing in the stator winding, produces the same mmf as the actual rotor current flowing in the rotor winding*, see Art. 24-1. The substitution of an equivalent stator current of line frequency for the actual rotor current of slip frequency is possible because the *rotor mmf is at standstill with respect to the stator mmf at any rotor speed*, i.e., independent of the frequency of the rotor current.

Note that, as in the case of the transformer, the phasor diagram of voltages and mmf's and the equivalent circuit are derived on the basis of Kirchhoff's mesh equations of the electric circuits, and Eq. 25-4 which is based on Ampère's law of the magnetic circuit (see Art. 12-2). Therefore calculations using the basic equations directly yield the same results as calculations using the equivalent circuit. Formulas for the secondary current, primary current, primary power angle, etc., derived from the basic equations are given in App. 1. For performance calculations some engineers use the equivalent circuit while others use the basic formulas. The main advantage of the equivalent circuit is that it can be set up on a calculating board.

## Chapter 26

### POWER BALANCE TORQUE OPERATION AS A GENERATOR AND AS A BRAKE

**26-1. The balance of power in a polyphase induction motor.** Fig. 26-1 shows the power distribution in a polyphase induction motor. The power input of the stator is:

$$P_{in} = m_1 V_1 I_1 \cos \varphi_1 \quad \text{watts} \quad (26-1)$$

A part of this power, the stator copper loss  $m_1 I_1^2 r_1$  and the iron loss due to the main flux  $P_{h+c}$ , are consumed by the stator. The balance is transferred by the rotating field to the rotor, so that the latter power is

$$P_{rot.f} = P_{in} - (m_1 I_1^2 r_1 + P_{h+c}) \quad (26-2)$$

It can be seen from the equivalent circuit of Fig. 25-2 that the power transferred by the rotating field is also equal to

$$P_{rot.f} = m_1 E_2' I_2' \cos \psi_{2s} = m_2 E_2 I_2 \cos \psi_{2s} = m_1 \frac{I_2'^2 r_2'}{s} \quad \text{watts} \quad (26-3)$$

$\psi_{2s}$  is given by Eq. 25-1.

A part of the power  $P_{rot.f}$  is consumed by the rotor as electric power ( $P_e$ ). This is the copper loss in the rotor  $m_1 r_2' I_2'^2$ . It follows from Eq. 26-3 that

$$P_e = m_1 r_2' I_2'^2 = s P_{rot.f} \quad (26-4)$$

The difference between the power transferred by the rotating field,  $P_{rot.f}$ , and the electric power of the rotor,  $P_e$ , is the *developed* mechanical power of the rotor. Thus

$$P_{m.dev} = P_{rot.f} - P_e = (1 - s) P_{rot.f} = m_1 \frac{1 - s}{s} r_2' I_2'^2 \quad (26-5)$$

The last expression for  $P_{m.dev}$  also follows directly from the equivalent circuit of Fig. 25-3.

The mechanical power delivered at the shaft ( $P_{m \text{ del}}$ ) is less than the mechanical power developed by the amount of the mechanical losses of the rotor. There are three kinds of losses which are supplied mechanically by the rotor:

- (a) Bearing friction and windage losses ( $P_{F+W}$ ).
- (b) Losses due to the slot openings ( $P_{\text{iron}}$  due to rotation).
- (c) Losses due to the flux harmonics ( $P_{\text{iron}}$  due to rotation).

The slot openings of the rotor produce a ripple in the flux density curve, (see Fig. 10-1) which causes eddy-current and hysteresis losses on the

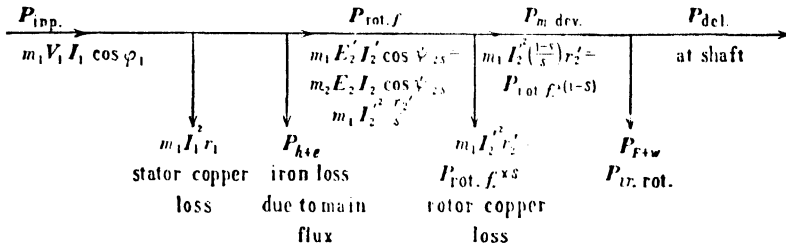


FIG. 26-1. Balance of power in a polyphase induction motor.

surface of, and in the teeth of, the stator. These losses are similar to those produced by the slot openings of the d-c armature in the pole shoes of the d-c machine (see Art. 10-1). In the same manner the slot openings of the stator cause eddy-current and hysteresis losses on the surface of, and in the teeth of, the rotor. These iron losses, due to the slot openings of stator and rotor, occur at no-load as well as at load.

It has been explained in Art. 22-2 that a polyphase winding carrying alternating currents produces, besides the main (useful) rotating flux, a series of parasitic rotating fluxes which travel with different speeds, some in the direction as the main flux and some opposite to the main flux. These parasitic fluxes cause iron losses similar to those caused by the slot openings: the harmonic fluxes produced by the stator winding cause eddy-current and hysteresis losses on the surface of, and in the teeth of, the rotor; and the harmonic fluxes produced by the rotor winding, in turn, cause eddy-current and hysteresis losses on the surface of, and in the teeth of, the stator. The harmonic fluxes are produced by the currents and occur mainly at load; they are small at no-load when the current is low. The iron losses due to the harmonic fluxes are frequently called "stray load losses."

The iron losses due to the slot openings and to the harmonic fluxes are zero at standstill of the rotor and increase with increasing rotor speed, just as the friction and windage losses increase with the rotor speed.



Therefore, these iron losses are to be considered as mechanical losses, i.e., in the same category as the friction and windage losses.

The mechanical power delivered to the shaft is

$$P_{m.del} = P_{m.dev} - (P_{F+W} + P_{ir.rot}) \quad (26-6)$$

where the subscript  $ir.rot$  indicates that these iron losses are due to rotation (rotational iron losses).

**26-2. Torque-speed characteristic of the polyphase induction motor.** Using the basic relation of mechanics

$$T = \frac{7.04}{n} P_{watts} \text{ lb-ft}$$

the developed torque of the polyphase induction motor is obtained from Eq. 26-5 for the developed power as

$$T_{dev} = \frac{7.04}{n} m_1 I_2'^2 r_2' \left( \frac{1-s}{s} \right)$$

where  $n$  is the rotor speed. From Eq. 24-18

$$n = n_s(1-s)$$

and therefore

$$T_{dev} = \frac{7.04}{n_s} m_1 I_2'^2 \frac{r_2'}{s} \text{ lb-ft} \quad (26-7)$$

This last equation characterizes the induction motor. It states that the *developed torque of the polyphase induction motor is determined by the secondary copper loss divided by the slip*. From Eqs. 26-7 and 26-3

$$T_{dev} = \frac{7.04}{n_s} P_{rot.f(watts)} \text{ lb-ft} \quad (26-7a)$$

i.e., the developed *torque* of the polyphase induction motor is directly *proportional* to the *power* transferred by the *rotating field*.

Eq. 26-7 does not apply to the synchronous machine (see Chapter 39) because in the latter machine both machine parts are connected with a source of power.

Eq. 26-7 yields the *developed* torque. The torque delivered at the shaft is less than the developed torque by the loss torque which corresponds to  $P_{F+W}$  and  $P_{ir.rot}$  (see Eq. 26-6).

The fundamental equation for the torque, Eq. 26-7, has been derived on the basis of the equivalent circuit. The same equation for the torque can also be derived on the basis of the fundamental law of forces on current

carrying conductors in a magnetic field, see Art. 1-4. This is shown in App. 2.

When the motor parameters are given,  $I_2'$  can be determined from the equivalent circuit and the developed torque,  $T_{dev}$ , from Eq. 26-7.

The shape of the torque-speed characteristic depends upon the magnitudes of the machine parameters. Therefore, motors designed for different purposes will have parameters of different magnitudes. Three different shapes of torque-speed characteristics of squirrel-cage motors are shown

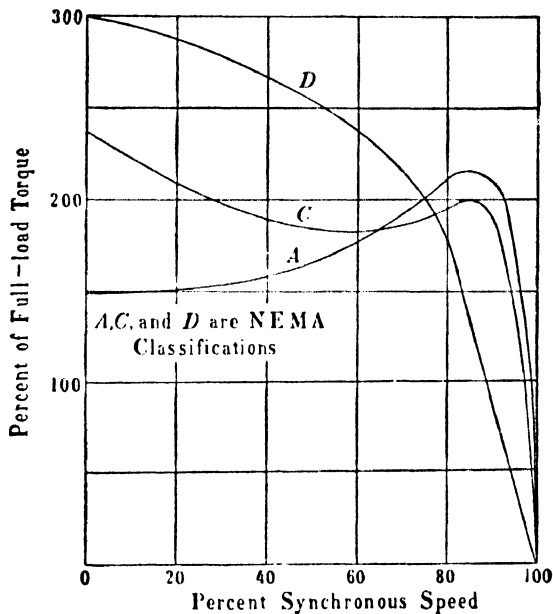


FIG. 26-2. Torque-speed curves of a polyphase induction motor — NEMA classification.

in Fig. 26-2. Designs C and D are special designs and have the purpose of high starting torques, i.e., high torques at standstill ( $n = 0$ ); design A is that of the general-purpose motor, see Table 50-4, ("Characteristics and Applications of Polyphase 60-Cycle A-c Motors").

The motor of design A shows a maximum torque, called *pull-out torque*, at a definite slip. When the load torque becomes larger than the pull-out torque, the motor comes to standstill. The slip of the general-purpose motor at rated load is small, between 1% and 5%, i.e., the speed at rated load is between 95% and 99% of the synchronous speed (the larger slip applies to small motors, the smaller slip to large motors). The slip at which the pull-out torque occurs, the *pull-out slip*, is about 5 to 7 times the slip at rated load.

**26-3. The pull-out torque.** The ratio of pull-out torque to rated torque determines the *overload capacity* of the motor. The Standards of the NEMA prescribe a certain overload capacity for the different motor types (see Table 50-2). In order to determine the pull-out torque, without calculating a number of points of the torque-speed curve, Eq. 26-7 can be used. For this purpose  $I_2'$  must be expressed in terms of the primary voltage  $V_1$ , the parameters of the motor, and the slip. This can be done by eliminating  $E_1$  and  $I_1$  from Eqs. 25-2 to 25-4 as shown in App. 3. This yields

$$I_2' = V_1 \frac{1}{\sqrt{l^2 + m^2}} \quad (26-8)$$

where

$$l = (1 + \tau_2)r_1 + (1 + \tau_1) \frac{r_2'}{s}; \quad m = x_1 + (1 + \tau_1)x_2' - \frac{\tau_1}{x_m} \frac{r_2'}{s} \quad (26-9)$$

$$\tau_1 = \frac{x_1}{x_m} \quad \tau_2 = \frac{x_2'}{x_m} \quad (26-10)$$

Inserting the value of  $I_2'$  from Eq. 26-8 in Eq. 26-7 and differentiating with respect to the slip yields the pull-out slip at which the pull-out torque occurs:

$$s_{p.o.} \approx \frac{(1 + \tau_1)r_2'}{x_1 + (1 + \tau_1)x_2'} \quad (26-11)$$

Now in order to find the pull-out torque, calculate  $I_2'$  for  $s_{p.o.}$  from Eq. 26-8 or from the equivalent circuit and then determine the torque for  $s_{p.o.}$  from Eq. 26-7.

**26-4. Operation as a generator and brake.** It has been pointed out that an induction motor is able to run only at subsynchronous speeds. At synchronous speed of the rotor the relative speed between the rotating flux and the rotor winding is zero, and the rotor emf and current are zero. Therefore, no torque exists at synchronous speed.

If an induction motor is driven by another machine and brought above its synchronous speed, then, according to Eq. 24-18, the slip becomes *negative* and the mechanical power of the rotor also becomes negative, (see Eq. 26-5). This means that at supersynchronous speeds the rotor does not supply mechanical power to the shaft but *consumes mechanical power* from the shaft, i.e., the machine operates as a *generator*. Thus an induction motor, driven by a prime mover above its synchronous speed operates as an induction generator. It is a characteristic feature of all

electric machines that they are able to operate both as a *motor* and a *generator*. It is not difficult to show that the torque changes its sign when the rotor speed becomes larger than the synchronous speed: at a sub-synchronous speed an emf is induced in the rotor winding corresponding to the relative speed between the rotating flux and the rotor,  $(n_s - n)$ . At synchronous speed ( $n = n_s$ ) this emf becomes zero because the relative

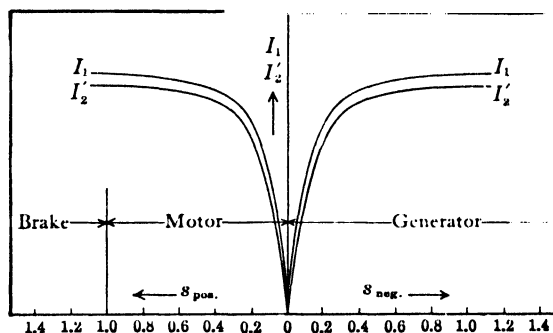


FIG. 26-3. Stator and rotor currents as a function of slip for motor, generator, and brake operation.

speed between rotating flux and rotor is zero. At supersynchronous speeds ( $n > n_s$ ) the relative speed between rotating flux and rotor changes its sign as compared to subsynchronous speeds, and therefore  $E_2'$  and  $I_2'$  change their signs. Since torque is determined by the product of flux and armature current, see Eq. A2-2, the torque changes sign at supersynchronous speed. This also follows directly from Eq. 26-7 in which  $s$  is negative for generator operation.

Note that the equivalent circuit and all equations of the induction motor which contain  $s$  as a variable also apply to the induction generator when the slip is introduced with a negative sign.

There is still another kind of operation of an induction motor. Assume that a 3-phase motor runs with a certain speed and that the connections to two of the three power lines are suddenly interchanged. This changes the direction of rotation of the rotating flux and the rotor is now running *opposite to the direction of the rotating flux*. Therefore, the rotor speed  $n$  appears in Eq. 24-18 for the slip with a negative sign, with the result that the slip becomes larger than 1 and positive. Considering Eq. 26-5 the mechanical power of the rotor is now negative, as in the case of the induction generator, i.e., mechanical power is *supplied to the shaft*. However, since there is no prime mover, this mechanical power can be taken only from the kinetic energy of the rotating mass and this mass will soon come to a

standstill. After coming to a standstill the machine again operates as a normal induction motor; it accelerates in the direction of the new rotating flux to a subsynchronous speed corresponding to the load torque. It is evident that during the period from the interchange of line connections to standstill of the rotor the machine operates as a *brake*. This operation is known as *plugging*. Plugging of induction motors for the purpose of stopping, or of stopping and reversing, is used frequently.

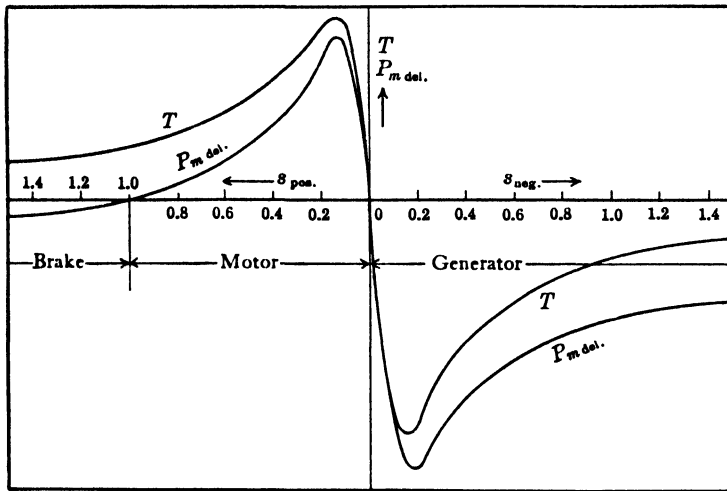


FIG. 26-4. Torque and mechanical power at the shaft as a function of slip for motor, generator, and brake operation.

Curves which show the current  $I_1$  and  $I_2'$  as a function of slip for motor, generator, and brake operation are shown in Fig. 26-3. Both currents change little at high slips. At  $s = 0$ ,  $I_1 = I_0$ . Fig. 26-4 shows the torque  $T$  and the mechanical power at the shaft,  $P_{m.del}$ , as a function of slip for motor, generator, and brake operation.  $T$  and  $P_{m.del}$  are negative at negative values of  $s$  (generator operation).  $T$  is positive for all positive values of  $s$  but  $P_{m.del}$  changes its sign for  $s = +1$  where the range of operation as a brake starts. This will be demonstrated once more in Chapter 27 which deals with the circle diagram of the induction motor.

**Example.** A 3-HP, 440/220-volt, 3-phase, 60-cycle, 4-pole, 1750-rpm squirrel-cage induction motor has the following data and parameters. The data and parameters given will be determined later, in Chapter 28, from a no-load and a locked-rotor test.

(a) *Parameters for starting*

$$r_1 = 2.69 \text{ ohms} = 0.0311 \text{ p-u}$$

$$r_2' = 2.79 \text{ ohms} = 0.0322 \text{ p-u}$$

$$x_1 = x_2' = 3.40 \text{ ohms} = 0.0393 \text{ p-u}$$

$$x_m = 103 \text{ ohms} = 1.19 \text{ p-u}$$

$$r_m = 3.66 \text{ ohms} = 0.0423 \text{ p-u}$$

(b) *Parameters for running*

$$r_1 = 2.69 \text{ ohms} = 0.0311 \text{ p-u}$$

$$r_2' = 2.14 \text{ ohms} = 0.0248 \text{ p-u}$$

$$x_1 = 4.36 \text{ ohms} = 0.0505 \text{ p-u}$$

$$x_2' = 4.50 \text{ ohms} = 0.052 \text{ p-u}$$

$$x_m = 103 \text{ ohms} = 1.19 \text{ p-u}$$

$$r_m = 3.66 \text{ ohms} = 0.0423 \text{ p-u}$$

(The difference between starting and running parameters is explained in Chapter 28.)

It is required to determine the performance at start and during running conditions. The friction and windage loss is 44 watts, total no-load iron loss (due to main flux and rotation) 122 watts, and the stray-load loss 48 watts. The no-load current is 2.36 amp at 440 volts. Assume iron loss due to main flux equal one half of total no-load iron losses.

(a) *Starting performance:*

$$r_2' \left( \frac{1-s}{s} \right) = 0$$

$$Z_1 = 2.69 + j3.40 = 4.33 / 51.6$$

$$Z_2' = 2.79 + j3.40 = 4.40 / 50.6$$

$$Z_m = 3.66 + j103 = 103 / 87.96$$

from Eq. 25-10

$$254 \angle 0 = I_1 \left[ Z_1 + \frac{Z_m Z_2'}{Z_m + Z_2'} \right]$$

$$I_1 (\text{inrush}) = \frac{254 \angle 0}{8.59 / 51.8} = 29.6 / -51.8$$

$$I_2' = I_1 \times \frac{Z_m}{Z_m + Z_2'}$$

$$I_2' = 29.6 \angle -51.8 \times \frac{103 / 87.96}{6.45 + j106.4}$$

$$I_2' = 29.6 \angle -51.8 \times \frac{103 / 87.96}{107.5 / 86.56}$$

$$= 28.4 \angle -50.4 \text{ amp}$$

$$T_{\text{start}} = \frac{7.04}{1800} \times 3 \times (28.4)^2 \times 2.79 = 26.4 \text{ lb-ft}$$

(b) *Running performance:* assume  $s = 0.03$

$$r_2' \left( \frac{1-s}{s} \right) = 2.14 \left( \frac{1-0.03}{0.03} \right) = 69.2 \text{ ohms}$$

$$\mathbf{Z}_1 = 2.69 + j4.36 = 5.13 \angle 58.3$$

$$\mathbf{Z}_2' = (2.14 + 69.2) + j4.50 = 71.4 \angle 3.60$$

$$\mathbf{Z}_m = 3.66 + j103 = 103 \angle 87.96$$

from Eq. 25-10

$$\begin{aligned} \mathbf{I}_1 &= \frac{254 \angle 0}{\mathbf{Z}_1 + \frac{\mathbf{Z}_m \mathbf{Z}_2'}{\mathbf{Z}_m + \mathbf{Z}_2'}} = \frac{254 \angle 0}{60.8 \angle 38.2} \\ &= 4.18 \angle -38.2 \end{aligned}$$

Input power factor =  $\cos 38.2^\circ = 0.785$

$$\begin{aligned} \mathbf{I}_2' &= \mathbf{I}_1 \times \frac{\mathbf{Z}_m}{\mathbf{Z}_m + \mathbf{Z}_2'} \\ &= 4.18 \angle -38.2 \times \frac{103 \angle 87.96}{103 \angle 87.96 + 71.4 \angle 3.60} \\ &= 4.18 \angle -38.2 \times \frac{103 \angle 87.96}{131 \angle 55.5} \\ &= 3.28 \angle -5.74 \text{ amp} \end{aligned}$$

$$T_{\text{dev}} = \frac{7.04}{1800} \times 3 \times (3.28)^2 \times \frac{2.14}{0.03} = 9.0 \text{ lb-ft}$$

$$\text{Mechanical loss-torque} = \frac{7.04}{1800} \times (48 + 44 + 61) = 0.60 \text{ lb-ft}$$

$$T_{\text{del}} = T_{\text{dev}} - T_{\text{loss}} = 8.40 \text{ lb-ft}$$

Power input =  $3 \times 254 \times 4.18 \times 0.785 = 2500 \text{ watts}$

Losses

$m_1 I_1^2 r_1$	= 141 watts
$m_1 I_2'^2 r_2'$	= 69
no-load iron (main flux and rotation)	= 122
stray load	= 48
friction and windage	= 44
Total loss	<u>424 watts</u>

Power delivered =  $2500 - 424 = 2076 \text{ watts} = 2.78 \text{ HP}$

$$\text{Efficiency} = \frac{2076}{2500} = 0.83$$

$$\begin{aligned}\text{Slip} &= \frac{69}{2500 - (141 + 61)} = \frac{69}{2298} = 0.03 \text{ (check)} \\ \text{Speed} &= \frac{120 \times 60}{4} (1 - 0.03) = 1746 \text{ rpm} \\ T_{\text{del}} &= \frac{5250}{1746} \times 2.78 = 8.40 \text{ lb-ft}\end{aligned}$$

which checks with value previously determined.

It should be noted that normal slip is slightly greater than 0.03 since the calculated output for  $s = 0.03$  is 2.78 HP. An approximation of the normal slip is:

$$s_n = \frac{3.0}{2.78} \times 0.03 = 0.0324$$

From Eq. 26-11

$$\begin{aligned}\text{pull-out slip} &\approx \frac{1.042 \times 2.14}{4.36 + 1.042 \times 4.50} = 0.246 \\ \text{at } s &= 0.246 \quad r_{20}' \left( \frac{1-s}{s} \right) = 6.56 \\ \mathbf{Z}_2' &= (2.14 + 6.56) + j4.50 = 9.81 \angle 27.3 \\ \mathbf{I}_1 &= \frac{254 \angle 0}{\mathbf{Z}_1 + \frac{\mathbf{Z}_m \mathbf{Z}_2'}{\mathbf{Z}_m + \mathbf{Z}_2'}} = \frac{254 \angle 0}{14.1 \angle 41.1} = 18.0 \angle -41.1 \\ \mathbf{I}_2' &= \mathbf{I}_1 \times \frac{\mathbf{Z}_m}{\mathbf{Z}_m + \mathbf{Z}_2'} = 17.2 \angle -36.6 \\ T_{\text{p.o.}} &= \frac{7.04}{1800} \times 3 \times (17.2)^2 \times \frac{2.14}{0.246} = 30.2 \text{ lb-ft}\end{aligned}$$

$$\text{Normal torque} = \frac{3.0}{2.78} \times 8.40 = 9.05 \text{ lb-ft}$$

$$\frac{T_{\text{st}}}{T_n} = \frac{26.4}{9.05} = 2.92$$

$$\frac{T_{\text{p.o.}}}{T_n} = \frac{30.2}{9.0} = 3.36$$

## PROBLEMS

Parameters for the starting and running performance for three 3-phase squirrel-cage induction motors are listed below. All values are given in ohms per phase. Also included are the friction and windage, no-load iron, and stray-load losses as a fraction of the output rating. Assume the iron losses due to the main flux =  $\frac{1}{2}$  (total no-load iron losses).



Determine the complete starting and running ( $s = 0.025$ ) performance for each motor.

	Problem 1	Problem 2	Problem 3
	10-HP	15-HP	20-HP
	220-volt	220-volt	440-volt
	2-pole	4-pole	6-pole
	60-cycle	60-cycle	60-cycle
<i>Starting:</i>			
$r_1$ . . . . .	0.142	0.138	0.259
$r_2'$ . . . . .	0.188	0.121	0.352
$x_1 = x_2'$ . . . . .	0.350	0.233	0.842
$x_m$ . . . . .	11.7	8.64	20.7
$r_m$ . . . . .	0.194	0.130	0.390
<i>Running:</i>			
$r_1$ . . . . .	0.142	0.138	0.259
$r_2'$ . . . . .	0.168	0.104	0.324
$x_1$ . . . . .	0.421	0.281	1.04
$x_2'$ . . . . .	0.440	0.302	1.17
$x_m$ . . . . .	11.7	8.64	20.7
$r_m$ . . . . .	0.194	0.130	0.390
<i>Losses:</i>			
Friction and windage . . . . .	0.015	0.01	0.008
No-load iron . . . . .	0.02	0.024	0.024
Stray-load . . . . .	0.02	0.015	0.015

## Chapter 27

### CIRCLE DIAGRAM OF THE POLYPHASE INDUCTION MOTOR

**27-1. Determination of the circle diagram.** The same equations of both electric circuits and of the magnetic circuit (Eqs. 25-2 to 25-4) which led to the phasor diagram of mmf's and voltages and to the equivalent circuit of the polyphase induction motor also lead to the geometric locus of the end-point of its primary current.

Consider Eq. 25-10 derived from the basic equations mentioned above. The quantity in the brackets of this equation represents the *total* impedance of the polyphase induction motor looking into its primary terminals. Eq. 25-10 can be written as

$$I_1 = V_1 Y_t = V_1 (g_t - jb_t) \quad (27-1)$$

where  $Y_t$  is the total admittance,  $g_t$  the total conductance, and  $b_t$  the total susceptance, looking into the primary terminals.  $g_t$  and  $b_t$  are *functions* of the six parameters of the machine *and of the slip*.

Assuming the real and imaginary axes as shown in Fig. 27-1, and further introducing a Cartesian system of coordinates  $y'$ ,  $x'$  so that  $y'$  lies in the real axis and  $x'$  lies in the imaginary axis, and placing the phasor  $V_1$  arbitrarily in the real axis,

$$V_1 = V_1 \quad (27-2)$$

$$I_1 = y' - jx' \quad (27-3)$$

In the latter equation,  $y'$  and  $x'$  are the coordinates of the end-point of  $I_1$ . It follows from Eqs. 27-1 and 27-3 that

$$y' = V_1 g_t = \psi_1 \quad (27-4)$$

$$x' = V_1 b_t = \psi_2 \quad (27-5)$$

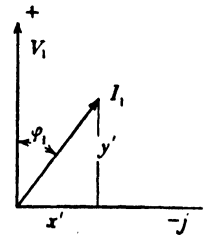


FIG. 27-1 Derivation of the circle diagram.

where  $\psi_1$  and  $\psi_2$  are two different functions of the six parameters and the slip. Eliminating the slip  $s$  from Eq. 27-4 with the aid of Eq. 27-5, or vice

versa, a quadratic equation for  $y'$  and  $x'$  is obtained (see App. 4) which is the equation of a circle, showing that the end-point of the primary current  $I_1$  moves on a circle. Using the rules of analytic geometry, the coordinates of the center-point and the radius of the circle can be determined. Having the coordinates of the center-point  $C'$ , the angle ( $\alpha$ ) which the imaginary axis makes with the line connecting the origin of coordinates and the center-point  $C$  (Fig. 27-2) can be determined:

$$\tan \alpha = \frac{y_c'}{x_c'} \approx \frac{2\tau_1}{x_m(1 + 2\tau_1 + \tau_2)} \quad (27-6)$$

$\tau_1$  and  $\tau_2$  are given by Eq. 26-10.

In practical problems, two points of the circle are given either by test (see Chapter 28) or by computation. These points are the no-load point  $P_0$  and the short-circuit (locked-rotor) point  $P_L$  (Fig. 27-2).  $P_0$  corresponds to the current  $I_0$  which the motor draws from the lines at no-load;

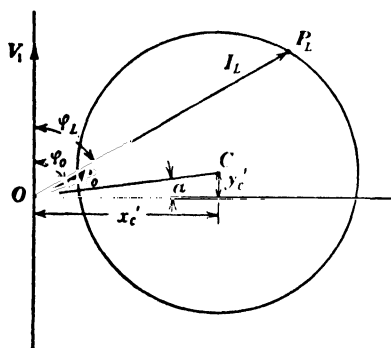


FIG. 27-2. Construction of the circle diagram.

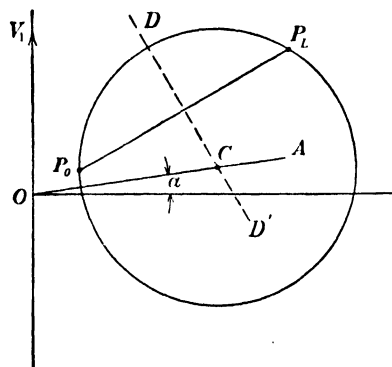


FIG. 27-3. Construction of the circle diagram.

$P_L$  corresponds to the current which the motor draws from the lines at standstill (rotor locked). The perpendicular bisector  $DD'$  (Fig. 27-3) of the line which connects  $P_0$  and  $P_L$  must go through the center-point of the circle. Since the center-point must also lie on the line  $OA$  which makes the angle  $\alpha$  (Eq. 27-6) with the imaginary axis, the perpendicular bisector  $DD'$  intersects the line  $OA$  in the center-point. Thus the circle on which the endpoint of  $I_1$  moves is determined by the no-load and short-circuit (locked rotor) currents and by the angle  $\alpha$ .

Each point of the circle corresponds to a certain value of the primary current  $I_1$  and therefore also to a certain value of the slip  $s$ .

Notice that  $\alpha$  increases with increasing primary resistance. In larger

machines,  $\alpha$  is small, and the center-point can be assumed to lie on the imaginary axis.

**27-2. Developed-mechanical-power line and delivered-mechanical-power line.** There are four characteristic points on the circle. These are: the no-load point and the points which correspond to  $s = 0$ ,  $s = 1$  and  $s = \pm \infty$ .

$s = 0$  means  $n = n_s$ , i.e., the rotor runs synchronously with the rotating flux and the rotor current is zero (see Art. 26-4). It has been explained that the rotor is not able to achieve this speed by itself but

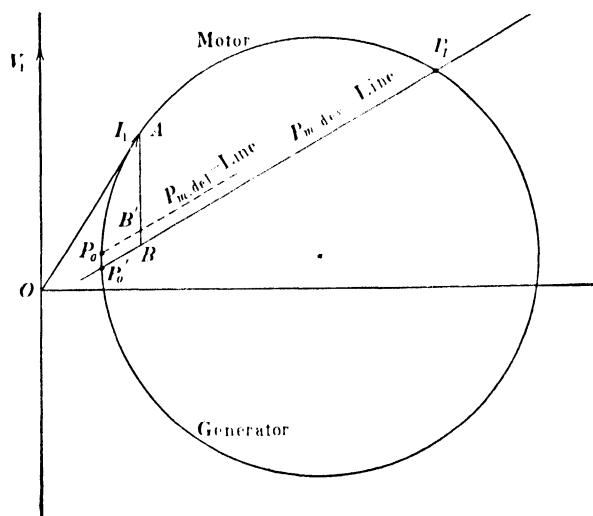


FIG. 27-4. Construction of the mechanical-power-lines.

must be brought up to this speed by another machine, and this machine will have to supply the mechanical losses of the rotor, i.e., the friction and windage losses and the rotational iron losses. The active component of the stator current at  $s = 0$  is smaller than that at no-load ( $I_0 \cos \varphi_0$ ) by the amount corresponding to these losses. The point on the circle which corresponds to  $s = 0$  will be denoted by  $P_0'$ . It lies on the circle below the point  $P_0$  (see Fig. 27-4).

$s = 1$  means  $n = 0$ , i.e., standstill (locked rotor). Consider the equivalent circuit, Fig. 25-3 or Fig. 25-5. The resistive load  $\frac{1-s}{s} r_2' I_2'^2$  which represents the developed mechanical power is zero at  $s = 1$ , i.e., the mechanical power is zero. This is in agreement with  $n = 0$ . The

resistance  $\frac{1-s}{s} r_2'$  which corresponds to the load is zero, and the motor draws a large current from the lines, limited practically only by the resistances and leakage reactances of both windings (see Art. 28-2). The point of the circle which corresponds to  $s = 1$  has been denoted by  $P_L$  (Figs. 27-2 and 27-3).

At  $s = 0$  the rotor current is zero and the developed mechanical power of the rotor is zero. At  $s = 1$ ,  $n = 0$  and again the mechanical power is zero. It can be shown that if a straight line is drawn through the points  $P_0'$  and  $P_L$  (Fig. 27-4), the distance from any arbitrary point on the circle to this line is proportional to the mechanical power developed at the stator current or slip which corresponds to this point of the circle. Thus for the point  $A$  of the circle (Fig. 27-4), i.e., for the current  $OA$  and the slip which correspond to the point  $A$ , the developed-mechanical-power is proportional to the distance  $AB$ . The line through  $P_0'$  and  $P_L$  is called the *developed-mechanical-power line* ( $P_{m.\text{dev}}$ -Line).

The developed-mechanical-power is positive for the part of the circle which lies above the  $P_{m.\text{dev}}$ -Line and is negative for the part of the circle which lies below this line. This means that mechanical power is available at the shaft, and the machine operates as a *motor* on the part of the circle which lies *above* the  $P_{m.\text{dev}}$ -Line; inversely, the machine accepts mechanical power from the shaft and operates as *generator* or *brake* on the part of the circle below the  $P_{m.\text{dev}}$ -Line. The range of operation as a brake will be discussed below.

At no-load the developed-mechanical-power of the motor is equal to its mechanical losses (friction and windage losses and rotational iron losses). At no-load the mechanical power delivered to the shaft is zero. The *delivered-mechanical-power line*,  $P_{m.\text{del}}$ -Line, is obtained with good approximation by drawing a straight line parallel to the  $P_{m.\text{dev}}$ -Line through the no-load point  $P_0$  (Fig. 27-4). The distance from any point on the circle to the  $P_{m.\text{del}}$ -Line is then proportional to the delivered mechanical power. The  $P_{m.\text{del}}$ -Line thus drawn applies only up to the maximum value of  $P_{m.\text{del}}$ ; the point on the circle corresponding to maximum  $P_{m.\text{del}}$  and maximum  $P_{m.\text{dev}}$  is determined by the tangent to the circle which is parallel to the  $P_{m.\text{del}}$  and  $P_{m.\text{dev}}$  lines.

**27-3. The torque-line and the slip-line.** Of interest is the point on the circle at which  $s = \pm \infty$ . Consider the equivalent circuit, Fig. 25-3 or 25-5. The load of the induction motor,  $\frac{1-s}{s} r_2' I_2'^2$ , which represents its developed mechanical power, is the same at  $s = +\infty$  and  $s = -\infty$ ,

namely,  $-I_2'^2 r_2'$ . This means that  $s = +\infty$  and  $s = -\infty$  are represented by the same point on the circle. The developed mechanical power at this point is negative, i.e., mechanical power is supplied to the shaft. The magnitude of this mechanical power supplied to the machine is equal to  $I_2'^2 r_2'$ , which is equal to the copper loss in the rotor. This means that at  $s = \pm \infty$  the rotor copper loss is supplied from outside and that the *rotating field does not transfer any power to the rotor*. Since the power transferred by the rotating field to the rotor is proportional to the torque on the rotor (see Art. 26-2), the torque on the rotor is zero at  $s = \pm \infty$ .

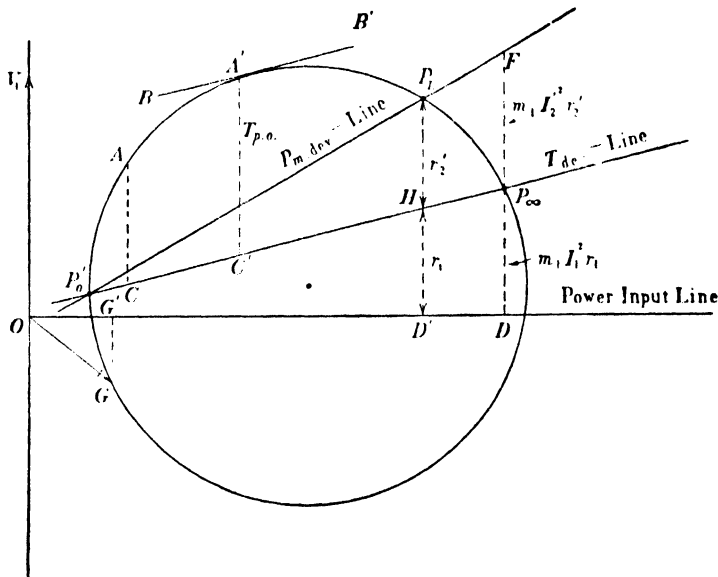


FIG. 27-5. Construction of the torque line.

The torque on the rotor is also zero at  $s = 0$ , because at  $s = 0$  the rotor current is zero. Thus the circle points at which  $s = 0 (P_0')$  and  $s = \pm \infty (P_\infty)$  are those at which the torque is zero, and it can be shown that when a straight line, the *Torque-Line*, is drawn through these two points (Fig. 27-5), the distance from any circle-point to this line represents the developed torque of the machine for the point considered. Thus in Fig. 27-5 the distance  $AC$  from point  $A$  on the circle to the  $T_{dev}$ -Line represents, to a certain scale, the developed torque of the motor at the slip or the primary current which corresponds to the point  $A$ . If a tangent  $BB'$  to the circle is drawn parallel to the  $T_{dev}$ -Line, the distance  $A'C'$  represents the pull-out torque (maximum torque) of the motor.

The circle-point  $P_\infty$  can be found approximately in the manner de-

scribed below. Observe first that the distance from any point on the circle to the imaginary axis is  $I_1 \cos \varphi_1$  and, therefore, a measure of the power input (or power output) of the stator. The imaginary axis can be called the *power-input Line*. Consider Fig. 27-5. The distance  $P_\infty F$  is the developed mechanical power at  $s = \pm \infty$ , i.e.,  $P_\infty F$  is equal to  $I_2'^2 r_2'$ . The distance  $P_\infty D$  is the power input of the stator at  $s = +\infty$ . Consider further the equivalent circuit Fig. 25-4. At  $s = 1$  the secondary impedance ( $r_2' + jx_2'$ ) is much smaller than the main flux impedance ( $r_m + jx_m$ ) and only a little magnetizing current flows through the latter impedance. This means that at  $s = 1$  the main flux is small, and the iron losses due to the main flux are negligible (see Art. 28-2). The same applies to other points on the circle for which the slip is large. Therefore, the power input at  $s = \pm \infty$  consists mainly of the stator copper losses  $I_1^2 r_1$ , and no power is transferred to the rotor by the rotating flux. It then follows that the distance  $FD$  (Fig. 27-5) is divided by the point  $P_\infty$  in the ratio  $I_2'^2 r_2' (P_\infty F)$  to  $I_1^2 r_1 (P_\infty D)$ . The magnetizing current is small at large values of slip:  $I_2' \approx I_1$ . Hence it can be assumed that the point  $P_\infty$  divides the distance  $FD$  in the ratio  $r_2'$  to  $r_1$ . The same ratio applies approximately to the perpendicular  $P_L D'$  drawn from the point  $P_L (s = 1)$ , i.e., the  $T_{\text{dev}}$ -Line divides the distance  $P_L D'$  in the ratio  $r_2'$  to  $r_1$ . This enables the construction of the  $T_{\text{dev}}$ -Line and the location of the point  $P_\infty$ : drop a perpendicular to the imaginary axis from point  $P_L (s = 1)$  which is usually known; divide this perpendicular in the ratio  $r_2'$  to  $r_1$  in order to locate the point  $H$  on this perpendicular; draw the straight line through the points  $P_0'$  and  $H$  which is the  $T_{\text{dev}}$ -Line.

When the primary copper losses are neglected ( $r_1 = 0$ ), the distance  $P_\infty D$  and also the distance  $HD'$  become zero, i.e., in this case the  $T_{\text{dev}}$ -Line coincides with the power-input line.

It has been explained (Art. 26-4) that when the motor operates as a brake the slip is positive and larger than 1. Apparently, the range of operation as a brake lies between the points  $P_L$  and  $P_\infty$ .

Consider point  $G$  in Fig. 27-5. This point lies below the point  $P_0'$  for which  $s = 0$  and, therefore, corresponds to a negative slip. The machine operates here as a generator. Accordingly, the active component  $GG'$  of the current  $I_1 = OG$  is negative, i.e., power is supplied by the induction machine to the lines. Note that, while the active component of the primary current is reversed, its reactive current component  $OG'$  remains unchanged, and, therefore, reactive current must be supplied by the lines in order to sustain the main flux and the leakage fluxes of the generator.

The main consumers of reactive currents from power lines are induction

motors and transformers and the generators must supply the reactive currents. The *asynchronous (induction) generator* is unable to supply reactive current; on the contrary, it *requires reactive current*. This is the reason the induction generator is seldom used. The induction generator is not able to operate as an independent unit. It must operate in parallel with one or more synchronous generators which supply the reactive current not only for the consumers but also for the induction generator.

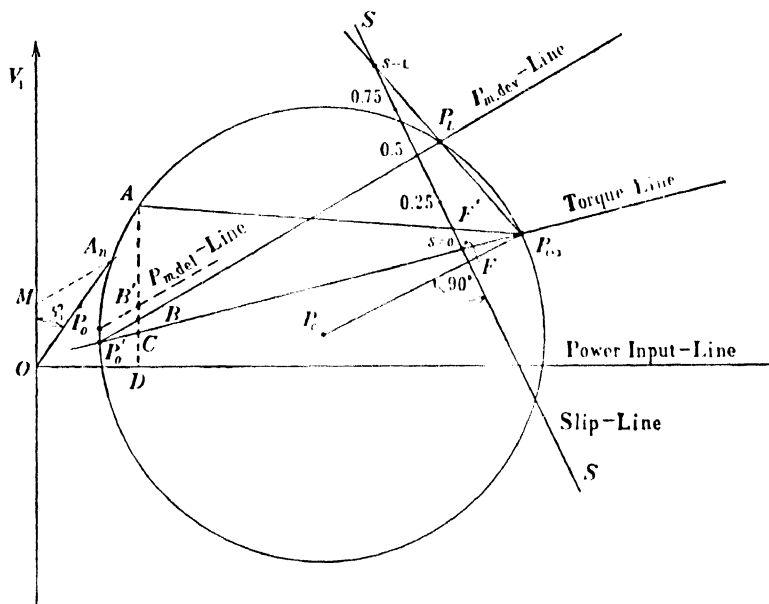


FIG. 27-6. Construction of the slip-line.

Fig. 27-6 shows how the slip-line, as well as the slip for any point on the circle, can be determined. The slip-line is found in the following way: connect the center-point of the circle  $P_c$  with the point  $P_\infty$  and draw at random a perpendicular  $SS$  to this line  $P_cP_\infty$ . The line  $SS$  is the *slip-line*. The point  $s = 0$  is given by the intersection of the slip-line with the line  $P_0'P_\infty$ , i.e., with the torque-line. The point  $s = 1$  is given by the intersection of the slip-line and a line drawn through  $P_\infty P_L$ . The slip is distributed uniformly over the slip-line, i.e., the point  $s = 0.5$  is in the center between  $s = 0$  and  $s = 1$ , and so on. The slip for any point  $A$  of the circle (Fig. 27-6) is found by connecting this point with the point  $P_\infty$ ;  $FF'$  is the slip which corresponds to the point  $A$ .

It will be observed in Fig. 27-6 that the following proportionalities exist for the point  $A$ :



$AD \sim P_1$	(primary power input)
$AC \sim P_{\text{rot. f}}$	(power transferred by the rotating field)
$AC \sim T_{\text{dev}}$	(developed torque)
$AB \sim P_{m. \text{dev}}$	(developed mechanical power of the rotor)
$AB' \sim P_{m. \text{del}}$	(mechanical power delivered at the shaft)
$CD = (AD - AC) \sim (P_1 - P_{\text{rot. f}})$ $= m_1 I_1^2 r_1 + P_{h+c}$	(primary copper losses and iron losses due to the main flux)
$CB = (AC - AB) \sim (P_{\text{rot. f}} - P_{m. \text{dev}})$ $= m_2 I_2^2 r_2$	(secondary copper losses)
$BB' = (AB - AB') \sim (P_{m. \text{dev}} - P_{m. \text{del}})$ $= P_{F+w} + P_{\text{ir. rot}}$	(friction + windage losses and rotational iron losses)

**27-4. Determination of the scales for the power and torque lines.** If the current scale of the circle diagram is chosen so that  $1'' = a$  amp, the power scale is such that  $1'' = m_1 V_1 a$  watts, since  $m_1$  and  $V_1$  are constant quantities. This power scale applies to the distances between the point on the circle and the power input line (imaginary axis), the  $P_{\text{rot. f}}$ -Line (torque line), the  $P_{m. \text{dev}}$ -Line, and the  $P_{m. \text{del}}$ -Line.

The distance between the point of the circle and the  $P_{m. \text{del}}$ -Line which corresponds to the *rated* (normal) output at the shaft is equal to

$$\frac{HP \times 746}{m_1 \times V_1} \text{ amp} = \frac{HP \times 746}{m_1 V_1 a} \text{ inches} = OM \text{ (Fig. 27-6)}$$

where  $HP$  is the rated horsepower of the motor. Drawing a line parallel to the  $P_{m. \text{del}}$ -Line at the distance  $OM$  inches from this line yields the normal operating point on the circle (point  $A_n$ , Fig. 27-6). The rated primary current of the motor is then  $OA_n$  and  $\varphi_1$  is the primary power factor angle.

Since (see Eq. 26-7a)

$$T_{\text{dev}} = \frac{7.04}{n_s} P_{\text{rot. f (watts)}} \text{ lb-ft}$$

the scale for the developed torque is

$$1'' = m_1 V_1 a \frac{7.04}{n_s} \text{ lb-ft}$$

### PROBLEMS

1. (a) Construct the circle diagram of the 3-HP, 440/220-volt, 3-phase, 60-cycle, 4-pole, squirrel-cage motor treated in the Example of Chapter 26, using the parameters for running, and determine from this diagram the rated primary current, power factor, pull-out torque, starting current, and starting torque.

(b) Construct the circle diagram using the parameters for starting and determine the rated primary current, power factor, pull-out torque, starting current, and starting torque.

(c) Compare the results obtained from the circle diagrams with those obtained from the equivalent circuit in Chapter 26.

2. Repeat Problem 1 for the 10-HP, 220-volt, 3-phase, 60-cycle, 2-pole, squirrel-cage motor the parameters of which are given in Problem 1 of Chapter 26.

3. Repeat Problem 1 for the 15-HP, 220-volt, 3-phase, 60-cycle, 4-pole, squirrel-cage motor the parameters of which are given in Problem 2 of Chapter 26.

4. Repeat Problem 1 for the 20-HP, 440-volt, 3-phase, 60-cycle, 6-pole, squirrel-cage motor the parameters of which are given in Problem 3 of Chapter 26.

These problems will show that the circle diagram constructed with the parameters for running, yields inaccurate values for the starting performance; also, that the circle diagram constructed with the parameters for starting, yields inaccurate results for the running performance and the pull-out torque.

## Chapter 28

### DETERMINATION OF PARAMETERS FROM A NO-LOAD AND A LOCKED-ROTOR TEST. INFLUENCE OF PARAMETERS ON PERFORMANCE. INFLUENCE OF SKIN-EFFECT AND SATURATION

It has been mentioned previously that the six parameters of the induction motor can be determined from a no-load and a locked-rotor (short-circuit) test, just as in the case of the transformer. This is shown in the following.

**28-1. The no-load test.** During this test the load on the motor shaft is zero and the following measurements are taken:

- (a) the primary voltage  $V_1$  which is usually equal to the rated voltage,
- (b) the primary current  $I_0$ ,
- (c) the power input  $P_0$ .

The power  $P_0$  is equal to the motor losses at no-load. These are the copper losses  $m_1 I_0^2 r_1$  in the stator winding, the hysteresis and eddy-current losses due to the main flux  $P_{h+c}$ , the friction and windage losses of the rotor  $P_{F+W}$ , and the rotational iron losses due to the *slot-openings* (see Arts. 10-1a and 34-1), i.e.,

$$P_0 = m_1 I_0^2 r_1 + P_{h+c} + P_{F+W} + P_{ir.rot} \quad (28-1)$$

Since all these losses are small the active component of  $I_0$  is small in comparison with its reactive component  $I_\phi$  and, therefore, the power factor at no-load

$$\cos \varphi_0 = \frac{P_0}{m_1 V_1 I_0} \quad (28-2)$$

is also small, about 0.05 to 0.15.

Only a very small rotor current is necessary to account for  $P_{F+W} + P_{ir.rot}$ , and the secondary circuit can therefore be considered to be open.

This may also be deduced from the magnitude of the resistance which represents the mechanical power of the rotor,  $r_2' \frac{1-s}{s}$ : this resistance becomes very high because the slip at no-load is negligibly small, i.e., the rotor circuit is practically open at no-load. Thus the equivalent circuit of the motor at no-load is represented by Fig. 28-1.

A knowledge of  $P_{h+c}$  is necessary in order to determine  $r_m$ , for the latter represents these losses.  $P_{h+c}$  can be separated from the other no-load losses by two tests. One test requires that the rotor be driven by another machine at *synchronous speed* ( $s = 0$ ). In this case the rotor current is exactly zero and the losses  $P_{F+W}$  and  $P_{ir,rot}$  are supplied by the driving machine. The power input of the stator of the induction motor is then equal to

$$P_0' = m_1 I_0'^2 r_1 + P_{h+c} \quad (28-3)$$

where  $P_0'$  and  $I_0'$  are the power input and stator current at  $s = 0$ . Having determined  $r_1$  by another test, the loss  $P_{h+c}$  can be calculated. ( $I_0'$  is the current which corresponds to the point  $P_0'$  on the circle diagram (see Fig. 27-6).

The emf  $E_1$  induced by the rotating flux in the stator winding at no-load is approximately

$$E_1 \approx V_1 - I_0 x_1 \quad (28-4)$$

As in the transformer (see Art. 12-2) the conductance of the main flux path is

$$g_m = \frac{P_{h+c}}{m_1 E_1^2} \quad (28-5)$$

From the equivalent circuit at no-load (Fig. 28-1),

$$x_m \approx \frac{E_1}{I_0} \quad (28-6)$$

The main flux resistance  $r_m$  (see Eq. 25-7)

$$r_m = \frac{g_m}{g_m^2 + b_m^2} \approx \frac{g_m}{b_m^2} \approx g_m x_m^2 \quad (28-7)$$

Thus the no-load test yields the main flux parameters  $r_m$  and  $x_m$  (or  $g_m$  and  $b_m$ ), provided that the primary leakage reactance  $x_1$  in Eq. 28-4 is

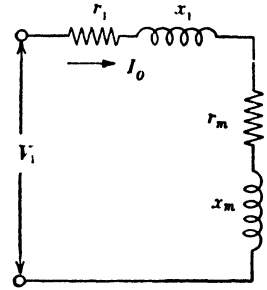


FIG. 28-1. Equivalent circuit of the induction motor at no-load.

known. This reactance and the secondary parameters  $r_2'$  and  $x_2'$  are obtained with the aid of the short-circuit test.

**28-2. The short-circuit (locked-rotor) test.** During this test the rotor is blocked and the following measurements are taken:

- (a) the primary voltage  $V_L$  which is less than the rated voltage for the reason given below,
- (b) the primary current  $I_L$ ,
- (c) the power input  $P_L$ .

At standstill the slip  $s$  is equal to unity, and the equivalent circuit of the motor is given by Fig. 28-2. Since the secondary impedance  $r_2' + jx_2'$  is small in comparison with  $x_m$  and the primary voltage drop is large,

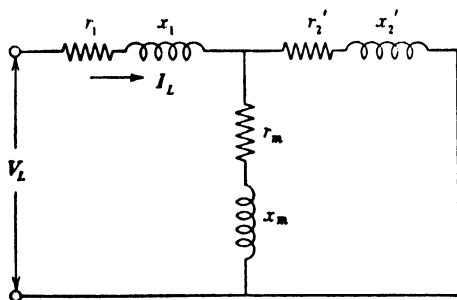


FIG. 28-2. Equivalent circuit of the induction motor at standstill.

only a small current flows through the main flux circuit, and the *main flux* and also the iron losses due to the main flux are *small*.

At standstill there is no mechanical power  $\left(\frac{1-s}{s} r_2' = 0\right)$  and

there are no mechanical losses ( $P_{F+W} = 0, P_{ir.rot} = 0$ ) in the machine. Therefore, the power input at standstill  $P_L$  is consumed mainly by the copper losses of both windings.

It is seen from Fig. 28-2 that at standstill the primary current is practically determined by the sum of the primary and secondary impedances  $r_1 + jx_1$  and  $r_2' + jx_2'$ . It is the counter-emf  $E_1$  which reduces the primary current when the motor runs ( $s \ll 1$ ). But there is only a small counter-emf present at standstill. Therefore, the primary current becomes high, about 4 to 8 times the rated current, if rated line voltage  $V_1$  is applied to the stator during the short-circuit test. In order to avoid over-heating of the windings the short-circuit test is taken at a voltage  $V_L$  which is about 30 to 50% of rated voltage.

The power factor at standstill

$$\cos \varphi_L = \frac{P_L}{m_1 V_L I_L} \quad (28-8)$$

is larger than that at no-load (see Fig. 27-2) but is still small due to the high reactive current component necessary to produce the stator and rotor leakage fluxes.

The measured quantities  $V_L$ ,  $I_L$ , and  $P_L$  determine the short-circuit impedance  $Z_L$ , the short-circuit resistance  $R_L$ , and the short-circuit reactance  $X_L$ .

$$Z_L = \frac{V_L}{I_L} \quad R_L = \frac{P_L}{m_1(I_L)^2} \quad X_L = \sqrt{Z_L^2 - R_L^2} \quad (28-9)$$

On the other hand, the equivalent circuit Fig. 28-2 yields

$$R_L \approx r_1 + r_2' \quad X_L = \frac{x_1}{1 + \tau_2} + x_2' - \frac{r_1 r_2'}{x_m} \quad (28-10)$$

where  $\tau_2 = x_2'/x_m$  (Eq. 26-10)

The stator resistance  $r_1$  is normally measured in connection with the no-load test. Since  $R_L$  is known from Eq. 28-9

$$r_2' \approx R_L - r_1 \quad (28-11)$$

For the separation of  $x_1$  and  $x_2'$  observe that  $\tau_2$  is small, about 0.03 to 0.06, and also that the quantity  $r_1 r_2'/x_m$  is small, so that with fair approximation

$$X_L \approx x_1 + x_2' \quad \text{and} \quad x_1 \approx x_2' \approx \frac{X_L}{2} \quad (28-12)$$

With this value of  $x_1$  the main flux parameters  $x_m$  and  $r_m$  can now be determined (Eqs. 28-4 to 28-7).

**28-3. Per-unit values of the parameters.** The parameters can be expressed either in ohms or in "per-unit", i.e., as fractions of a fixed unit of impedance. The advantage of the "per-unit" expression of the parameters for transformers has been explained in Art. 17-4. The same advantage exists here. When expressed in "per-unit", the parameters apply to a wide range of induction motors, i.e., to induction motors of different sizes, different speeds, different voltages, etc. When expressed in ohms, the parameters apply to a specific motor having a fixed speed, fixed output, fixed voltage, etc. The unit of impedance in which the parameters of induction motors are expressed, is defined as follows:

Unit voltage = rated voltage per phase.

Unit current = current per phase which corresponds to the output at

$$\text{the shaft} = I_{HP} = \frac{HP \times 746}{m_1 V_1}.$$

Unit impedance = unit voltage/unit current.

Unit power = unit current  $\times$  unit voltage.

When expressed as fractions of the so defined unit of impedance, the

parameters of polyphase induction motors are approximately:

$$r_1 = 0.01 \text{ to } 0.05 \quad r_2' = 0.01 \text{ to } 0.05 \quad r_m = 0.02 \text{ to } 0.03$$

$$x_1 = 0.06 \text{ to } 0.12 \quad x_2' = 0.08 \text{ to } 0.12 \quad x_m = 1.5 \text{ to } 3.5$$

The larger values of  $r_1$  and  $r_2'$  apply to small motors, the smaller values to large motors. The smaller values of  $x_1$  and  $x_2'$  apply to high-speed machines; the larger values, to lower-speed machines. The lower values of  $x_m$  apply to lower-speed machines; the higher values, to high-speed machines.

**28-4. Influence of the parameters on the performance of the motor.** The performance of an induction motor is determined by the following six quantities:

- (a) Heating of the windings and iron.
- (b) Efficiency.
- (c) Power factor.
- (d) Pull-out torque.
- (e) Starting current (inrush).
- (f) Starting torque.

The requirements, with respect to the magnitudes of the parameters, are not the same for all six quantities; they partially contradict each other, so that *compromises must be made by the designer*. These contradictions should be carefully noted in the discussions below.

(a) The heating of the windings and iron depends upon the  $I^2R$  losses and the iron losses. Since the currents are determined by the load the  $I^2R$  losses become small when  $r_1$  and  $r_2'$  are made small, i.e., when as much winding material as possible is arranged in the available space. It will be shown under (f) that a large value of  $r_2'$  is necessary to produce a high starting torque. In order to make the iron losses due to the main flux small, without increasing the motor size, it is necessary to make the main flux small. However, since the torque is determined by the main flux and the rotor currents, a small main flux is not permissible if the designer is to satisfy the necessary pull-out torque. With respect to heating the rotational iron losses should be made as small as possible.

(b) The efficiency is determined by the total losses of the motor. The lower the losses at a given load the higher will be the efficiency at this load. The consideration for low  $I^2R$  and iron losses is given in (a) above.

(c) Consider Fig. 28-3. The point *A* on the circle corresponds to a certain load: *OA* is the total current at this load and *BA* is the reactive

current component of  $OA$ . At no-load (point  $P_0$ ) the current  $I_0$  is almost equal to the current  $I_\phi$  which sustains the main flux (see Art. 28-1). In the circle diagram  $I_\phi$  is practically equal to the reactive current  $OF$ . Considering the reactive current at load  $BA$ , it consists of two parts,  $BF' = OF = I_\phi$  and  $F'A$ . The first part is necessary to sustain the main flux, and the second part is necessary to sustain the leakage fluxes of stator and rotor. If there were no leakage fluxes, only the reactive current  $I_\phi$  would appear (at all loads) and the geometric locus of the end-point of the primary current  $I_1$  would be a straight line through the point  $F$ . These are the leakage fluxes which make the geometric locus of the end-point of  $I_1$  become a circle.

For a high power factor a low reactive current is necessary, i.e., a low value of  $I_\phi$  and small leakage reactances  $x_1$  and  $x_2'$  are necessary. For a low value of  $I_\phi$  the air gap must be small and the flux must be small. For this reason the air gap of induction motors is kept as small as mechanically permissible. A small flux is not permissible with respect

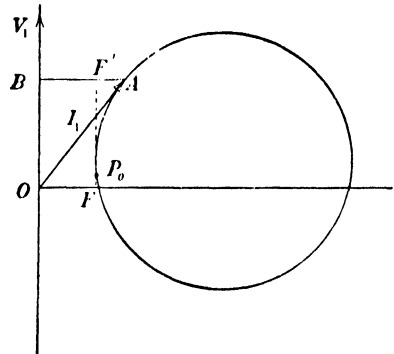


FIG. 28-3. Reactive current of the induction motor.

to the requirements for the pull-out torque. It will be seen under (e) that the leakage reactances cannot be made too small if the starting current (inrush) requirements are to be satisfied.

(d) Consider Fig. 27-5. The distance between the point  $P_\infty$  and the imaginary axis,  $P_\infty D$ , is equal to the primary copper losses  $m_1 I_1^2 r_1$ . The higher these copper losses, the more the point  $P_\infty$  moves up the circle, and the smaller becomes the pull-out torque. With respect to a high pull-out torque the primary resistance must be small. Physically this can be explained in the following way: the torque is determined by the power transferred by the rotating flux to the rotor, and the higher the primary losses for a given power input, the smaller is the power transferred by the rotating flux to the rotor.

It can be seen from Fig. 27-5 that the pull-out torque increases with increasing diameter of the circle, just as the locked-rotor current (starting current) increases with increasing diameter of the circle. Consider Fig. 28-2 which represents the equivalent circuit of the motor at locked rotor. Here, as at all large slips, the magnitude of the primary current is determined mainly by the stator and rotor leakage reactances. The smaller the values of  $x_1$  and  $x_2'$ , the larger is the diameter of the circle and the



pull-out torque. However, small values of  $x_1$  and  $x_2'$  are not permissible with respect to the locked-rotor (starting) current.

The secondary resistance  $r_2'$  has no influence on the magnitude of the pull-out torque because  $r_2'$  has no influence on the power transferred by the rotating flux to the rotor. The magnitude of  $r_2'$  influences only the slip at which the pull-out torque occurs (the pull-out slip, see Eq. 26-11).

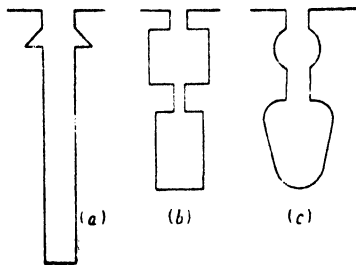


FIG. 28-4. Skin-effect rotors.

(e) It has been explained under (d) that the starting current is determined mainly by the leakage reactances  $x_1$  and  $x_2'$  (in the smallest polyphase motors also by  $r_1$  and  $r_2'$ ). A high starting current is not desirable because of the voltage drop which it produces in the supply lines, and standards, limiting the inrush current, have been established for small and medium-size motors

by the NEMA (National Electric Manufacturers Association). The leakage reactances  $x_1$  and  $x_2'$  must have certain values in order to meet these standards. Thus the limitations with respect to the starting current are contrary to the requirements for a high power factor and high pull-out torque.

(f) Eq. 26-7 for the torque shows that at standstill the torque is directly proportional to the copper losses of the rotor  $m_1 I_2'^2 r_2'$ . A high starting torque is only possible when the copper losses of the rotor at standstill are high. At standstill  $I_2' \approx I_1$ , i.e., at standstill  $I_2'$  is almost equal to the locked-rotor current. This current is limited by the source of power supply, and the leakage reactances  $x_1$  and  $x_2'$  must be such as to meet the standards for the starting current. Thus for a high starting torque the rotor resistance  $r_2'$  must be high. A high rotor resistance contradicts the requirements for a high efficiency.

There are certain rotor-slot arrangements which enable the designer to achieve a *high resistance at starting and a low resistance during running*, thus satisfying the requirements for a high starting torque and a high efficiency. These rotor-slots arrangements are shown in Fig. 28-4. The first one consists of a deep bar (*deep-bar rotor*), and the second one (Fig. 28-4, b and c) consists of two cages (*double-cage or Boucherot rotor*). The operation of these rotors is based upon the *skin-effect* phenomenon which, at higher frequencies, allows the current to flow only in the top part of the conductor in the case of the deep-bar rotor and mainly in the upper conductor in the case of the double-cage rotor. At standstill the rotor frequency is equal to the stator frequency (see Eq. 24-20) and, therefore,

equal to the line frequency. At this frequency the rotor current flows only in a *part of the cross-section* of the rotor conductor and the rotor resistance appears high. At rated load the rotor frequency is small and there is no skin-effect. Therefore, at rated load the whole cross-section of the rotor conductor is effective and the rotor resistance is small.

The skin-effect influences, at starting, not only the rotor resistance ( $r_2'$ ) but also the rotor leakage reactance ( $x_2'$ ). The latter is smallest at high slips and increases with increasing speed of the rotor. Its change with slip is thus opposite to that of the resistance.

It should be noted that the geometric locus of the end-point of the primary current is not a circle when the motor parameters vary with the slip. Therefore, the circle diagram discussed in the previous chapter does not apply to the skin-effect motors.

The deep-bar rotor is used in most of the larger induction motors.

**28-5. Influence of saturation on the leakage reactances  $x_1$  and  $x_2'$ .** It has been explained in Arts. 12-2 and 24-1 that the magnitude of the main flux reactance,  $x_m$ , depends upon the saturation of the main flux path. However this reactance changes little between no-load and full-load. At high slips, for example at starting, the magnitude of the main flux reactance is of little importance since it is always large in comparison with the rotor impedance at high slips (see Fig. 28-2), so that little current flows through it and its presence can be disregarded (see Art. 28-2). The result is that  $x_m$  can be treated as a constant parameter, although it may have different values at full-load and at high slips.

The leakage reactances,  $x_1$  and  $x_2'$ , have been tacitly treated as constants (except the case of the skin-effect motor in which  $x_2'$  is a variable (see foregoing article). The magnetic path of the leakage fluxes lies, to a great part, in the air for which the permeability  $\mu$  is a constant (see Art. 24-1), so that  $x_1$  and  $x_2'$  are practically constant between no-load and over-load, i.e., as long as the stator and rotor currents are not too high. At larger slips, and especially at standstill, these currents are high and saturate, more or less, the iron part of the leakage-flux path. Because of this fact,  $x_1$  and  $x_2'$  may be considerably smaller at starting than at running with full-load, namely, about 75 to 85% of the latter values. When this is the case, the starting and running performance must be calculated with different values of  $x_1$  and  $x_2'$  (see Example 26-1).

Determining the parameters from a no-load and a locked-rotor test, the latter test should be made at both a low voltage ( $V_L$ ) and at the normal voltage ( $V_L = V_1$ ), i.e., with low currents in the windings and also with large currents (see Example which follows).

**28-6. Influence of harmonics.** It has been explained in Art. 22-2 that an a-c winding produces a main wave and harmonics. The useful torque is produced by the main wave. The harmonics produce parasitic torques

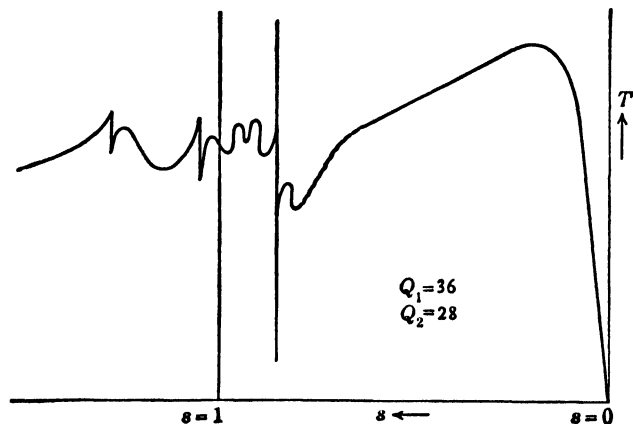


FIG. 28-4a. Speed torque curve with cusps due to harmonics.

which, more or less, distort the torque-speed characteristic; they may prevent a motor from starting or not permit the motor to bring its load up to full speed. Such a distorted torque-speed characteristic of a poorly designed motor is shown in Fig. 28-4a.

**Example 28-1.** The six parameters of a 3-HP, 440/220-volt, 3-phase, 60-cycle, 4-pole squirrel-cage induction motor will be determined from a no-load and a locked-rotor test. The stator resistance at 25°C is 2.26 ohms, and the friction and windage loss is 44 watts. Stray load loss = 48 watts

*No-load test—75°C*

$$V_1 = 440 \text{ volts}$$

$$I_0 = 2.36 \text{ amp}$$

$$P_0 = 211 \text{ watts}$$

*Locked-rotor test (full voltage)—75°C*

$$V_L = 440 \text{ volts} = V_1$$

$$I_L = 29.1 \text{ amp}$$

$$P_L = 13.92 \text{ kw}$$

*Locked-rotor test (reduced voltage)*

$$V_L = 76 \text{ volts}$$

$$I_L = 4.25 \text{ amp}$$

The skin-effect factor for  $r_2'$  is 1.30 and for  $x_2'$  is 0.97 (see Fig. 28-5).

Saturated reactances

$$Z_L = \frac{440}{\sqrt{3} \times 29.1} = 8.73 \text{ ohms}$$

$$R_L = \frac{13,920}{3 \times (29.1)^2} = 5.48 \text{ ohms}$$

$$X_L = \sqrt{Z_L^2 - R_L^2} = 6.80 \text{ ohms}$$

$$r_1(\text{at } 75^\circ\text{C}) = 2.26 \times \frac{234.5 + 75}{234.5 + 25} = 2.69 \text{ ohms}$$

$$r_2' = 5.48 - 2.69 = 2.79 \text{ ohms}$$

$$x_1 = x_2' = 3.40 \text{ ohms}$$

Unsaturated reactances

$$Z_L = \frac{76}{\sqrt{3 \times 4.25}} = 10.3 \text{ ohms}$$

$$X_L = \sqrt{(10.3)^2 - (5.48)^2} = 8.72 \text{ ohms}$$

$$x_1 = \frac{8.72}{2} = 4.36 \text{ ohms}$$

The ratio of unsaturated leakage reactance to saturated leakage reactance (4.36/3.40) is called the *saturation factor*.

In order to determine the running performance from the equivalent circuit it is necessary to correct  $r_2'$  and  $x_2'$  for skin-effect since the unsaturated parameters above were taken at 60 cycles.

$$(\text{corrected}) = \frac{2.79}{1.30} = 2.14 \text{ ohms} = r_2'$$

$$(\text{corrected}) = \frac{4.36}{0.97} = 4.50 \text{ ohms} = x_2'$$

$$x_m = \frac{254 - 2.36 \times 4.36}{2.36} = \frac{243.7}{2.36} = 103 \text{ ohms}$$

$$P_{h+e} + P_{\text{ir.rot}} = 211 - 3(2.36)^2 \times 2.69 - 44 = 122 \text{ watts}$$

It will be assumed that one half of the iron losses are due to the main flux so that:

$$P_{h+e} = 61 \text{ watts}$$

$$g_m = \frac{61}{3 \times (243.7)^2} = 3.43 \times 10^{-4} \text{ mho}$$

$$r_m = g_m x_m^2 = 3.43 \times 10^{-4} \times (103)^2 = 3.66 \text{ ohms}$$

$$(\text{check}) \quad m_1 I_0^2 r_m = 3 \times (2.36)^2 \times 3.66 = 61 \text{ watts}$$

$$r_m = \frac{61}{3 \times (2.36)^2} = 3.66 \text{ ohms}$$

The parameters determined above are tabulated in Ex. 26-1.

**Example 28-2.** The example of Chapter 26 will now be solved on a per-unit basis.

$$\text{Unit voltage} = \frac{440}{\sqrt{3}} = 254 \text{ volts}$$

$$\text{Unit current} = \frac{3 \times 746}{3 \times 254} = 2.94 \text{ amp} = I_{HP}$$

$$\text{Unit impedance} = \frac{254}{2.94} = 86.5 \text{ ohms}$$

$$\text{Unit power} = 254 \times 2.94 = 746 \text{ watts} = 1 \text{ HP}$$

$$\text{Unit speed} = 1800 \text{ rpm}$$

$$\text{Unit torque} = 7.04 \times 3 \times \frac{\text{unit power}}{\text{unit speed}} = 8.80 \text{ lb-ft}$$

(a) *Parameters for starting (p-u)*

$$r_1 = 0.0311$$

$$r_2' = 0.0322$$

$$(x_1 = x_2') = 0.0393$$

$$x_m = 1.19$$

$$r_m = 0.0423$$

(b) *Parameters for running (p-u)*

$$r_1 = 0.0311$$

$$r_2' = 0.0248$$

$$x_1 = 0.0505$$

$$x_2' = 0.0520$$

$$x_m = 1.19$$

$$r_m = 0.0423$$

(a) *Starting performance (p-u)*

$$r_2' \left( \frac{1-s}{s} \right) = 0$$

$$Z_1 = 0.0500 / \underline{51.6}$$

$$Z_2' = 0.0508 / \underline{50.6}$$

$$Z_m = 1.19 / \underline{87.96}$$

From Eq. 25-10

$$1/\underline{0} = \underline{I_1} \left[ 0.0500 / \underline{51.6} + \frac{0.0508 / \underline{50.6} \times 1.19 / \underline{87.96}}{0.0508 / \underline{50.6} + 1.19 / \underline{87.96}} \right]$$

$$\underline{I_1} = 10.05 / \underline{-51.8}$$

(p-u)

$$(check) \quad I_1(\text{amp}) = 10.05 \times 2.94 = 29.6$$

$$\begin{aligned} I_2' &= 10.05 \angle -51.8 \times \frac{1.19 \angle 87.96}{0.0508 \angle 50.6 + 1.19 \angle 87.96} \\ &= 9.66 \angle -50.4 \end{aligned}$$

The starting torque on a p-u basis is the same as  $P_{\text{rot.f}}$  on a p-u basis (see Eq. 26-7a):

$$P_{\text{rot.f}} = (9.66)^2 \times \frac{0.0322}{1.0} = 3.0$$

$$T_{\text{st p-u}} = 3.0$$

$$(check) \quad T_{\text{st}} (\text{lb-ft}) = 3.0 \times 8.80 = 26.4$$

$$(b) \text{ Running performance} \quad s = 0.03$$

$$r_2' \left( \frac{1-s}{s} \right) = 0.80$$

$$Z_1 = 0.0593 \angle 58.3$$

$$Z_2' = 0.825 \angle 3.60$$

$$Z_m = 1.19 \angle 87.96$$

from Eq. 25-10

$$\begin{aligned} I_1 &= \frac{1.0 \angle 0}{\left[ 0.0593 \angle 58.3 + \frac{0.825 \angle 3.60 \times 1.19 \angle 87.96}{0.825 \angle 3.60 + 1.19 \angle 87.96} \right]} \\ &= 1.42 \angle -38.2 \end{aligned}$$

$$\text{Input power factor} = \cos 38.2^\circ = 0.785$$

$$\begin{aligned} I_2' &= 1.42 \angle -38.2 \times \frac{1.19 \angle 87.96}{0.825 \angle 3.60 + 1.19 \angle 87.96} \\ &= 1.115 \angle -5.74 \end{aligned}$$

$$P_{\text{rot.f}} = (1.115)^2 \times \frac{0.0248}{0.03} = 1.025$$

$$T_{\text{dev}} = 1.025$$

$$(check) \quad T_{\text{dev}} (\text{lb-ft}) = 1.025 \times 8.80 = 9.05$$

$$\text{Mech. loss torque (p-u)} = \frac{7.04 \times \frac{(48 + 44 + 61)}{1800}}{8.80} = 0.068$$

$$T_{\text{del}} (\text{p-u}) = 1.025 - 0.068 = 0.957$$

(check)  $T_{\text{del}} (\text{lb-ft}) = 0.957 \times 8.80 = 8.40$

Power input  $= 3 \times 1.0 \times 1.42 \times \cos 38.2^\circ = 3.35$

Losses

$$m_1 I_1^2 r_1 = 0.189$$

$$m_1 I_2'^2 r_2' = 0.093$$

$$\text{no-load iron} = 0.163$$

$$\text{stray load} = 0.064$$

$$\text{Friction and windage} = 0.059$$

$$\text{Total} = 0.568$$

$$P_{\text{del}} = 3.35 - 0.568 = 2.78$$

(check)  $P_{\text{del}} (\text{watts}) = 2.78 \times 746 = 2076 = 2.78 \text{ HP}$

$$\text{Efficiency} = \frac{2.78}{3.35} = 0.83$$

$$\text{slip} = \frac{0.093}{3.35 - (0.189 - 0.082)} = 0.03 \quad (\text{check})$$

$$s_{\text{normal}} = \frac{3.0}{2.78} \times 0.03 = 0.0324$$

From Eq. 26-11

$$s_{\text{p.o.}} = \frac{1.042 \times 0.0247}{0.0505 + 1.042 \times 0.0520} = 0.246$$

$$r_2' \left( \frac{1-s}{s} \right) = 0.0758$$

$$Z_2' = 0.1133 / \underline{27.3}$$

From Eq. 25-10

$$I_1 = 6.12 / \underline{-41.4}$$

$$I_2' = 5.85 / \underline{-36.6}$$

$$P_{\text{rot.f}} = (5.85)^2 \times \frac{0.0248}{0.246} = 3.44$$

$$T_{\text{p.o.}} = 3.44$$

(check)  $T_{\text{p.o.}} (\text{lb-ft}) = 3.44 \times 8.80 = 30.2$

The normal torque delivered by this machine at 3.0 HP output,  $s = 0.0324$ , is

$$T = \frac{5250}{1800(1 - 0.0324)} \times 3 = 9.05 \text{ lb-ft}$$

$$= 1.025 \text{ p-u}$$

$$\frac{T_{\text{st}}}{T_{\text{n}}} = \frac{3.0}{1.025} = 2.92$$

$$\frac{T_{\text{p.o.}}}{T_{\text{n}}} = \frac{3.44}{1.025} = 3.36$$

## PROBLEMS

For the influence of skin-effect on  $r_2'$  and  $x_2'$  use Fig. 28-5. For saturation factors use Fig. 28-6.

The *saturation factor* is defined as the ratio of the unsaturated values of  $x_1$  and  $x_2'$ , to the saturated values of these reactances.

1. For the motor of Examples 28-1 and 28-2 calculate the primary current and primary power factor for slips of 1.0, 0.8, 0.6, 0.4, 0.2, 0.1, and 0.03.

2. Determine the developed torque-speed characteristic for the motor of Examples 28-1 and 28-2, using the slips specified in Problem 1. Calculate on a p-u basis.

3. Repeat Problem 1 for 115% rated voltage.

4. Repeat Problem 1 for 85% rated voltage.

5. Repeat Problem 2 for 115% rated voltage.

6. Repeat Problem 2 for 85% rated voltage.

7. Construct the circle diagram for the motor of Examples 28-1 and 28-2, using the unsaturated values of  $x_1$  and  $x_2'$ . From this diagram determine the developed torque-speed characteristic for slips of 1.0, 0.8, 0.6, 0.4, 0.2, 0.1, and 0.03 and compare with Problem 2.

8. The motor of Examples 28-1 and 28-2 is required to develop a higher starting torque. To do this the end rings of the squirrel cage were turned down in a lathe so that the rotor resistance at standstill, as well as at running, was increased 25%. Determine the starting performance.

9. Determine the running performance of the motor in Problem 8 at a slip of 0.04.

10. Determine the pull-out slip and pull-out torque for the motor in Problem 8.

11. It is required to reduce the starting line current of the motor in Examples 28-1 and 28-2 by 28%.

(a) If an autotransformer is used determine the turn ratio.

(b) If series reactors are used determine their value in ohms.

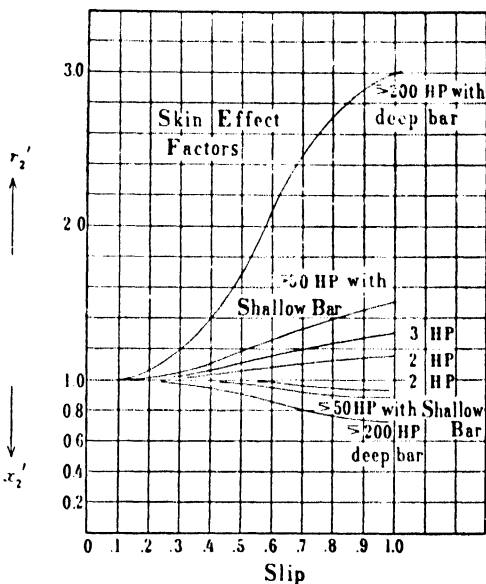


FIG. 28-5.

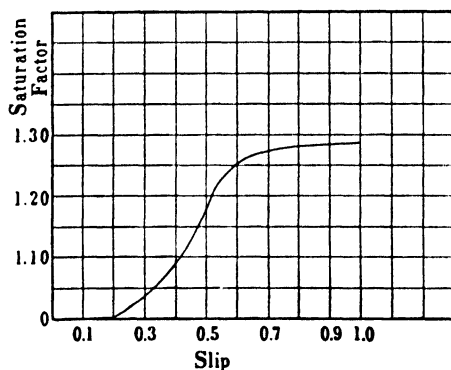


FIG. 28-6.



(c) What is the new starting torque developed (express as a percentage of starting torque developed in Examples 28-1 and 28-2).

12. The six parameters of an 800-HP, 2300-volt, 3-phase, 60-cycle, 8-pole, shallow-bar, squirrel-cage induction motor are to be determined from the no-load and locked-rotor tests given below. The stator resistance is 0.103 ohm per phase at 75°C; the stator is wye-connected. (Neglect skin effect.)

<i>No-load test</i>	<i>Locked-rotor test (full voltage)</i>
$V_1 = 2300$ volts	$V_L = 2300$ volts
$I_0 = 43$ amp	$I_L = 1200$ amp
$P_0 = 12.5$ kw	$P_L = 1060$ kw
<i>Locked-rotor test (reduced voltage)</i>	
	$V_L = 600$ volts
	$I_L = 240$ amp

The friction and windage loss is 4.4 kw, and the iron losses due to the main flux are 40% of the total no-load iron losses. Assume the temperature of the stator winding at no-load and locked-rotor tests is 75°C.

13. The stray-load losses of the motor of Problem 12 are 6.0 kw. Determine the running performance for a slip of 0.013. Calculate throughout in p-u.

14. Determine the starting performance of the motor of Problem 12.

15. Determine the primary current and power factor at slips of 1.0, 0.8, 0.6, 0.4, 0.2, 0.1, and 0.013 for the motor of Problem 12. Plot.

16. Plot the developed torque-speed characteristic for the motor of Problem 12 at slips of 1.0, 0.8, 0.6, 0.4, 0.2, 0.1 and 0.013.

17. Repeat Problem 15 for 115% rated voltage.

18. Repeat Problem 15 for 85% rated voltage.

19. Repeat Problem 16 for 115% rated voltage.

20. Repeat Problem 16 for 85% rated voltage.

21. Determine the pull-out slip and pull-out torque for the motor of Problem 12.

22. It is desired to reduce the starting current of the motor in Problem 12 by 30%.

(a) Determine the series resistors which will accomplish this reduction in current.

(b) For reactor starting what magnitude of reactance is needed?

23. No load and locked-rotor tests were taken on a  $7\frac{1}{2}$ -HP, 440-volt, 3-phase, 60-cycle, 6-pole, wye-connected, squirrel-cage induction motor, and the following data were recorded:

<i>No-load test</i>	<i>Locked-rotor test (full voltage)</i>
$V_1 = 440$ volts	$V_L = 440$ volts
$I_0 = 5.84$ amp	$I_L = 60.4$ amp
$P_0 = 600$ watts	$P_L = 24.16$ kw
<i>Locked-rotor test (reduced voltage)</i>	
	$V_L = 120$ volts
	$I_L = 13.5$ amp

The stator resistance per phase is 1.2 ohms at 75°C. The friction and windage loss is 60 watts and the iron losses due to the main flux are 50% of the total no-load iron losses. Assume the temperature of the stator winding at both no-load and locked-rotor tests to be 75°C.

Determine the six parameters of the equivalent circuit in ohms and p-u for both starting and running performance.

24. The stray load losses of the motor in Problem 23 are 93 watts. Determine the running performance at  $s = 0.024$

25. Determine the starting performance of the motor in Problem 23.

26. Determine the primary current and power factor for the motor of Prob. 23 for slips of 1.0, 0.8, 0.6, 0.4, 0.2, 0.1 and 0.024. Calculate in p-u. Plot.

27. Determine the developed speed-torque characteristic in p-u for the motor of Problem 23 at slips of 1.0, 0.8, 0.6, 0.4, 0.2, 0.1 and 0.024.

28. Calculate the pull-out slip and pull-out torque (in p-u) for the motor of Problem 23.

29. Repeat Problem 26 for 115% rated voltage.

30. Repeat Problem 26 for 85% rated voltage.

31. Repeat Problem 27 for 115% rated voltage.

32. Repeat Problem 27 for 85% rated voltage.

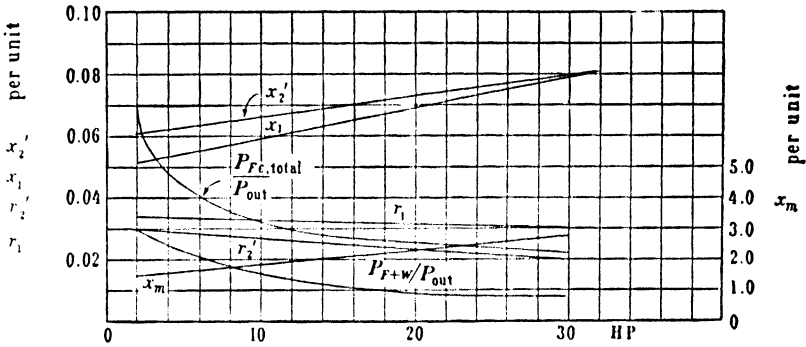


FIG. 28-7.

33. Fig. 28-7 refers to 3-phase, 4-pole, 60-cycle, 230-volt induction motors. This figure can be used for preparation of problems on performance of polyphase induction motors. Resistances and reactances are in per-unit. Losses are given as a fraction of power output.  $x_1$  and  $x_2'$  are saturated values.

## Chapter 29

---

### STARTING AND SPEED CONTROL OF THE POLYPHASE INDUCTION MOTOR

---

---

**29-1. Starting of a squirrel-cage motor.** Curve  $T_M$  in Fig. 29-1 represents the torque-speed curve of a squirrel-cage motor. Once the squirrel-cage motor is constructed, nothing can be changed regarding its parameters, and its torque-speed characteristic is fixed. During the starting period the motor goes through the total torque-speed curve  $T_M$ , Fig. 29-1, until it reaches the speed at which the motor torque is equal to the load torque. At no speed should the load torque  $T_L$  be larger than the motor torque  $T_M$ ; otherwise the motor will be unable to reach its rated speed. The difference ( $T_M - T_L$ ) is used to accelerate the rotating masses. The larger this difference, the shorter is the accelerating period.

It has been explained previously (see Eqs. 26-7 and 26-8) that the torque of the induction motor varies with the square of its terminal voltage. Thus an increase in the terminal voltage of 10% raises the torque curve  $T_M$ , Fig. 29-1, 21% and, vice versa, a decrease of the terminal voltage of 10% lowers the torque curve 19%. A reduction of the terminal voltage is used when a low starting current is necessary to reduce the voltage drop in the lines and a relatively small starting torque is required, as, for example, in the case of a fan drive.

Three means are employed in order to lower the terminal voltage of the squirrel-cage motor during starting.

- (a) Series resistor.
- (b) Series reactor.
- (c) Autotransformer, Fig. 29-2.

When a series resistor or reactor is used, the starting current of the motor, which in this case is equal to the line current, is reduced directly with the terminal voltage while the starting torque is reduced with the square of the terminal voltage. For example, with a series resistor or reactor which produces a voltage drop of 30%, the line (motor) current will be 70% of

its original value and the starting torque of the motor will be 49% of its original value.

When an autotransformer is used, Fig. 29-2, the line current and the motor current are not equal; the line current is the primary current of the transformer while the motor current is the secondary current; therefore, the ratio of line current to motor current must be the same as the ratio of motor voltage (secondary voltage of the transformer) to line voltage

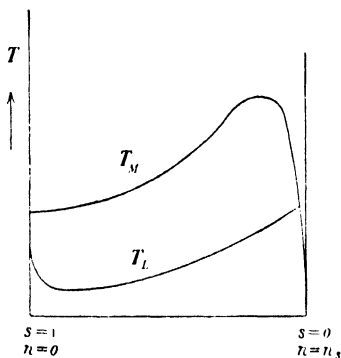


FIG. 29-1. Torque-speed characteristics of a squirrel-cage motor and its load.

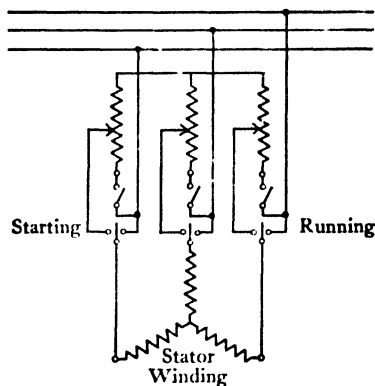


FIG. 29-2. Starting of a squirrel-cage motor with the aid of an autotransformer.

(primary voltage of the transformer), for the primary and secondary kva must be the same ( $V_1 I_1 \approx V_2 I_2$ ). For example, if the secondary voltage of the transformer is 70% of the line voltage, the motor current is 70% of its original value and the line current is  $0.7(V_2/V_1) = 0.7 \times 0.7 = 0.49 = 49\%$  of the motor current at full voltage. At 70% voltage the motor torque is 49% of its original value as in the case of the series resistor or reactor. Comparing resistor or reactor starting with autotransformer starting at 70% voltage at the motor terminals, the following table holds:

	<i>Resistor or Reactor</i>	<i>Autotransformer</i>
Motor current.....	70%	70%
Line current.....	70%	49%
Motor torque.....	49%	49%

The autotransformer reduces the line current with the square of the terminal voltage while the resistor or reactor reduces the line current, at the same starting torque, directly with the terminal voltage. For the same starting torque the autotransformer yields a larger reduction of

the line current than the resistor or reactor, but is more expensive than the latter.

The influence of voltage and frequency variation on the performance of polyphase induction motors is shown in Table 29-1.

**29-2. Starting of a wound-rotor (slip-ring) motor.** In the wound-rotor motor the rotor resistance is not fixed as is the case in the squirrel-cage motor; it can be varied between an infinitely large value (open slip rings) and the resistance of the rotor winding  $r_2'$  (slip rings short-circuited). The secondary resistance of the wound-rotor motor is in general  $r_2' + r_{ext}' = r_t'$ , where  $r_{ext}'$  is the external rotor resistance referred to the stator. Therefore, in the equivalent circuit for the wound-rotor motor the quantity  $r_t' = r_{ext}' + r_2'$  is to be introduced, while only  $r_2'$  is introduced for the squirrel-cage motor, for in the latter  $r_{ext}' = 0$ .

Consider the equivalent circuit Fig. 25-4. The only quantity which changes with the load torque is  $r_2'/s$ ; in the wound-rotor motor it is the quantity  $r_t'/s$ . When the motor is loaded, the rotor assumes a slip of such a magnitude that the ratio  $r_t'/s$  yields the values of secondary current and flux, i.e., the value of torque, necessary to overcome the load torque. *It is the ratio  $r_t'/s$  which is of prime importance.* For the same load torque the slip becomes twice as large if the rotor resistance is made  $r_t' = 2r_2'$  instead of  $r_2'$ . In general, the slip for a given torque is directly proportional to the rotor resistance.

In a squirrel-cage motor the rotor resistance is fixed ( $= r_2'$ ) and the ratio  $r_2'/s$  is determined only by the slip  $s$ . This yields a *single* torque-speed curve as shown in Fig. 29-1. In the wound-rotor motor the rotor resistance ( $= r_2' + r_{ext}'$ ) can be varied. Since the slip for a given torque is proportional to the rotor resistance, each value of  $r_{ext}'$  determines another torque-speed curve. Fig. 29-3 shows several such torque-speed curves. Curve I corresponds to  $r_{ext}' = 0$  (this is the *natural* torque-speed curve) while the other three curves correspond to  $r_{ext}' = 3r_2'$ ,  $5.5r_2'$  and  $8.5r_2'$  respectively. The pull-out torque is independent of the rotor resistance and is therefore the same for all torque-speed curves (see Art. 28-4). A line drawn parallel to the axis of ordinates shows that different torques can be developed at the same slip.

The latter statement applies also to standstill ( $s = 1$ ): it is possible to start a wound-rotor motor with any torque between 0 and the pull-out torque, while the starting torque of the squirrel-cage motor is fixed. The external resistance necessary to start a wound-rotor motor with a given value of torque can be easily determined. As an example, the case will be considered where it is desirable that the motor develop rated torque at

TABLE 29 L. GENERAL EFFECT OF VOLTAGE AND FREQUENCY VARIATION ON INDUCTION-MOTOR CHARACTERISTICS  
+ = Increase      - = Decrease

	Starting and Maximum Running Torque	Syn-chronous Speed	% Slip	Full-load Speed	EFFICIENCY			POWER FACTOR			Full-load Current	Starting Current	Temperature Rise, Full Load	Maximum Overload Capacity	Magne- netic Noise, No Load in Par- ticu- lar
					Full Load	$\frac{1}{2}$ Load	$\frac{1}{4}$ Load	Full Load	$\frac{1}{2}$ Load	$\frac{1}{4}$ Load					
Voltage Variation	120% Voltage	No change	-30%	+ 1.5%	Small +	- $\frac{1}{4}$ to 2 points	- 7 to 20 points	- 5 to 15 points	- 10 to 30 points	- 15 to 40 points	-11%	+25%	- 5 to 6 C	+44%	Notice- able +
	110% Voltage	No change	-17%	+1%	+ $\frac{1}{4}$ to 1 point	Prac- tically no change	- 1 to 2 points	- 3 to 4 points	- 5 to 6 points	- 5 to 6 points	-7%	+10 to 12%	- 3 to 4 C	+21%	Slight +
	Function of Voltage	Con- stant	1 (Voltage) <sup>1</sup>	(Syn speed, slip)								Voltage		(Voltage) <sup>2</sup>	
	90% Voltage	No change	+23%	-1½%	- 2 points	Prac- tically no change	+ 1 to 2 points	+ 1 point	+ 2 to 3 points	+ 4 to 5 points	+11%	- 10 to 12%	+ 6 to 7 C	-19%	Slight -
Fre- quency Variation	105% Fre- quency	+5%	Practically no change	+ 5%	Slight +	Slight +	Slight +	Slight +	Slight +	Slight +	Slight -	- 5 to 6%	Slight -	Slight -	
	Function of Fre- quency	Frequen- cy		(Syn speed, slip)								1			
	95% Fre- quency	-5%	Prac- tically no change	- 5%	Slight -	Slight -	Slight -	Slight -	Slight -	Slight -	Slight +	+ 5 to 6%	Slight +	Slight +	Slight +

NOTE: This table shows general effects, which will vary somewhat for specific ratings.

standstill ( $s = 1$ ). Refer to the equivalent circuit Fig. 25-4. At rated torque it is desirable that  $r_{ext} = 0$  in order to avoid a reduction in efficiency through additional copper losses in the external resistance. If the slip at rated torque is equal to  $s_n$ , then at rated torque the ratio  $r_t'/s$  is equal to  $r_2'/s_n$ . In order that rated torque appear at standstill where  $s = 1$ , the ratio  $r_t'/s$  must be the same as at rated torque, i.e.,

$$\frac{r_2' + r_{ext}'(s = 1)}{1} = \frac{r_2'}{s_n} \quad \text{or} \quad r_{ext}'(s = 1) = r_2' \left( \frac{1 - s_n}{s_n} \right)$$

If  $s_n = 0.02$ , the external resistance must be  $0.98/0.02 = 49$  times the resistance of the rotor winding.

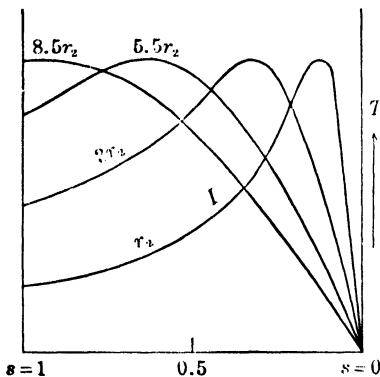


FIG. 29-3. Torque-speed characteristics of a wound-rotor motor for various values of secondary resistance.

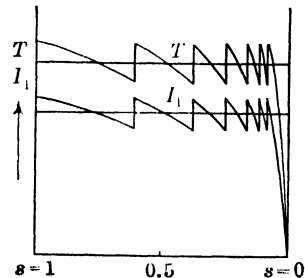


FIG. 29-4. Starting of a wound-rotor motor.

The squirrel-cage motor must go through its whole torque-speed curve during the starting period, up to the point where the motor torque is equal to the load torque. On the other hand, it is possible to keep the torque of a wound-rotor motor constant during the entire starting period. This is achieved by keeping the ratio  $r_t'/s$  constant, i.e., by a gradual reduction of the external resistance during acceleration. The torque during the starting period is then a line parallel to the axis of abscissae in Fig. 29-3. Since the starting resistance cannot be changed gradually but in steps, the torque and current during starting also change in steps, as shown in Fig. 29-4.

**29-3. Speed control of a wound-rotor motor.** Speed control over a wide range is only possible with the wound-rotor motor. The speed regulation can be achieved in several ways, some of which will be described in the following paragraphs.

(a) *Speed regulation by means of a resistance in the rotor circuit.* Consider Fig. 29-3. Any line parallel to the axis of abscissae corresponds to speed regulation at constant torque. Assume that a wound-rotor motor has to drive a mill which requires a constant torque at variable speed. At the highest speed the motor operates on its natural torque-speed curve (Curve I,  $r_{ext}' = 0$ ), and a fixed point on this curve corresponds to the required torque. Let the slip at this point be  $s_1$ ; the ratio  $r_t'/s$  for this point is then equal to  $r_2'/s_1$ . If the rotor resistance ( $r_2' + r_{ext}'$ ) is now changed, the motor automatically assumes a slip  $s_2$  of such a magnitude that the ratio  $(r_2' + r_{ext}')/s_2$  is equal to  $r_2'/s_1$ , because to a fixed value of torque there corresponds a fixed ratio of  $r_t'/s$  (see foregoing article). Thus variable speed can be obtained by means of a variable resistor in the rotor circuit.

However, this kind of speed control is not economical. Consider Eq. 26-4 which states that the electric power of the rotor, i.e., the power dissipated in the rotor as copper losses, is equal to the slip times the power transferred to the rotor by the rotating flux. In the case of the constant-torque drive considered above the power transferred to the rotor by the rotating flux remains constant, i.e., independent of the slip, since, according to Eq. 26-7a, the torque is equal to a constant quantity times the power transferred by the rotating flux. Also the power input to the motor changes little with rotor speed when the torque remains constant (see Fig. 26-2). Therefore, the higher the slip, the larger the part of the power input dissipated as copper losses in the rotor circuit and the lower the efficiency of the motor. The percent decrease in efficiency is almost equal to the percent decrease in speed.

(b) *Speed control by changing the number of poles.* Assuming a constant line frequency, speed variation in a few steps may be obtained by varying the number of poles of the motor, since, according to Eq. 24-4,

$$n_s = \frac{120f}{p}$$

Special windings are capable of producing different numbers of poles by a regrouping of coils. The most common winding of this kind is that with the pole ratio 1:2. Such a winding for 4 and 8 poles with  $f_1 = 60$  cycles yields two synchronous speeds of 1800 and 900 rpm respectively. If more than two speeds are desired, two separate windings can be arranged in the stator slots. Normally a squirrel-cage rotor is used for this kind of speed variation, or otherwise the rotor must have the same kind of winding as the stator, which then necessitates a larger number of slip rings than the normal three. If a slip-ring rotor is used, variation of speed



between steps (synchronous speeds) can be accomplished by inserting resistance in the rotor circuit.

(c) *Speed control with the aid of a special regulating set.* With the aid of a regulating set it is possible to obtain a continuous and economic speed regulation of the wound-rotor motor. The operation of such a set is based upon the considerations discussed in the following paragraphs.

To overcome a given opposing torque at the shaft of the motor a definite rotor current is necessary, i.e., there must be a definite induced emf  $E_{2s}$  and with it a corresponding slip. Consider Fig. 29-5a which

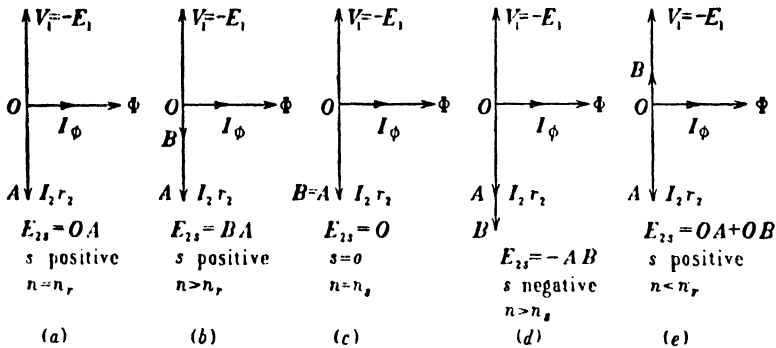


FIG. 29-5. Phasor diagrams for explanation of speed control of a polyphase wound-rotor induction motor.

represents a simplified phasor diagram of the induction motor with  $r_1$ ,  $x_1$  and  $x_2$  assumed to be negligible. In this case, the induced emf  $E_{2s}$  is consumed by the resistance drop  $I_2 r_2$ . In Fig. 29-5b, the value of  $I_2 r_2$  is the same as in Fig. 29-5a and, therefore, the values of  $I_2$  and of the torque are the same as for Fig. 29-5a. However, in Fig. 29-5b a voltage  $OB$  is impressed upon the slip rings of the rotor in phase with  $I_2 r_2$ . Since the total emf necessary to produce the current  $I_2$  is equal to  $OA$ , and since a voltage  $OB$  is introduced from the outside through the slip rings, the emf to be induced in the rotor by the rotating flux of the machine must be  $OA - OB = BA$ . This is less than  $OA$ , and therefore the slip will be less than in the case of Fig. 29-5a.

Figs. 29-5c, d, and e refer to the same current  $I_2$ , i.e., to the same torque as Figs. 29-5a and b. In Fig. 29-5c, the voltage impressed upon the slip rings,  $OB$ , is equal to  $OA = I_2 r_2$  and no emf induced in the rotor by the rotating flux is necessary; in this case the slip will be zero and the rotor speed will be the same as that of the rotating flux, namely, the synchronous speed  $n_s$ . In Fig. 29-5d, the impressed voltage  $OB$  is larger than the voltage drop  $I_2 r_2$  necessary for the required torque. This forces

the rotor to run above the synchronous speed, i.e., with a negative slip so that  $E_{2s}$  becomes negative. The magnitude of  $E_{2s}$  is equal to  $OB - OA$ . Here the machine operates as a motor above the synchronous speed. In Fig. 29-5e the impressed voltage  $OB$  is in counter-phase with  $I_2 r_2$ . This forces the rotor to run with a higher slip than without the impressed voltage, because the induced rotor emf has to overcome the opposing voltage  $OB$  and also supply the voltage drop  $I_2 r_2$ .

Thus it is possible to regulate the speed of a wound-rotor induction motor below as well as above its synchronous speed, if a voltage is impressed on its rotor which is opposite in-phase to or in-phase with the emf induced in the rotor by the rotating flux.

Fig. 29-6 shows a regulating set consisting of a synchronous converter ( $RC$ ) and a d-c machine ( $DC$ ).  $IM$  is the induction motor the speed of which is to be regulated. The synchronous converter is a combination of a synchronous machine and a d-c machine (see Art. 44-1). The slip rings of the induction motor are connected with the slip rings of the synchronous converter. The commutator of the synchronous converter is connected with the commutator (armature) of the d-c machine, which is coupled to the induction motor. The starter is short-circuited during running.

When the induction motor operates at a certain slip  $s$ , the electric power of the rotor ( $sP_{rot.f}$ , see Eq. 26-4) is consumed by the synchronous converter ( $RC$ ) and delivered to the d-c machine ( $DC$ ). The synchronous part of the converter consumes power from the induction motor and operates as a synchronous motor. Therefore the d-c part of the synchronous converter operates as a d-c generator, and the d-c machine ( $DC$ ) which consumes power from the converter operates as a d-c motor. Thus the electric power of the rotor of the induction motor is delivered back to its shaft as mechanical power.

The speed variation is accomplished by varying the excitation of the d-c machine ( $DC$ ). The greater the excitation, the lower the speed of the induction motor. The regulating set does not operate near synchronous speed because the voltage at the slip rings becomes too small to cause the rotary converter to rotate.

The arrangement shown in Fig. 29-6 in which the d-c machine is coupled to the induction motor is used when increasing torque with decreasing speed is required (constant HP drive). When the torque is

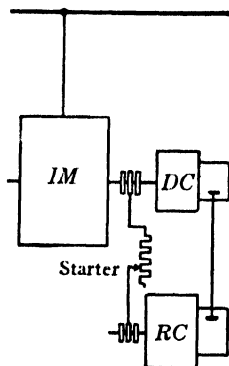


FIG. 29-6. Speed regulation of a wound-rotor motor with the aid of a rotary converter and a d-c machine (Kramer cascade).

constant or decreases with speed (fan drive), the d-c machine (*DC*) is not coupled with *IM*, but with a synchronous machine which then operates as a generator and delivers the electric power of the rotor of the induction motor to the line.

It is possible to correct the power factor of the induction motor with the aid of the excitation of the synchronous converter, because a synchronous motor when over-excited is able to deliver reactive current (see Art. 40-3). At a certain excitation of the synchronous converter the total reactive power required by the induction motor is supplied to its rotor by the converter, and the phase displacement at the stator terminals of the induction motor becomes zero ( $\cos \varphi_1 = 1$ ).

The synchronous converter set is able to vary the speed only below synchronism. There are other sets employing a-c commutator machines which permit speed control below and above synchronism.

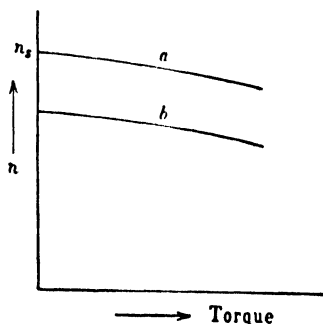


FIG. 29-7. Torque-speed characteristics of an induction motor controlled by a regulating set.

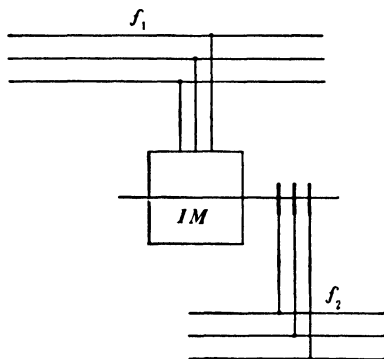


FIG. 29-8 Doubly fed induction motor.

With all these sets the rotor frequency is determined by both the induction motor and the regulating set. The rotor frequency (rotor slip) varies with the load just as in the ordinary induction motor. In Fig. 29-7 curve *a* shows the natural torque-speed characteristic of an induction motor, i.e., the characteristic for no impressed voltage on the slip rings (see Fig. 29-5a). The slip increases, i.e., the speed decreases slightly with increasing torque (as in a d-c shunt motor). Curve *b* of Fig. 29-7 shows the torque-speed characteristic when a constant voltage is impressed upon the rotor which is opposite in-phase to the emf induced in the rotor by the rotating flux. Such a voltage forces the rotor to increase the slip at all values of torque (see Fig. 29-5c). However, the trend of the torque-speed characteristic remains the same as for the natural characteristic, i.e., the speed decreases slightly with increasing torque.

(d) *Speed control by double feeding.* The machine behaves entirely differently when the secondary frequency is determined not by the induction motor and its regulating set but by another source of power with *fixed* frequency. In this case the induction machine is referred to as a *doubly fed induction motor*. Fig. 29-8 shows such an arrangement. The rotor as well as the stator is connected to a source of power. The fixed frequencies of both sources are  $f_1$  and  $f_2$ , respectively. It will be assumed, as an example, that the motor has four poles and that  $f_1 = 60$  cycles while  $f_2 = 25$  cycles.

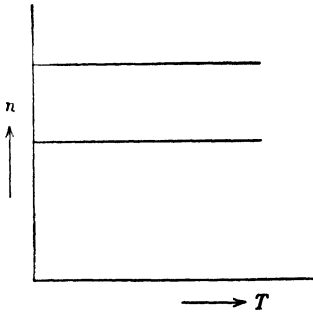


FIG. 29-9. Torque-speed characteristics of a doubly fed induction motor.

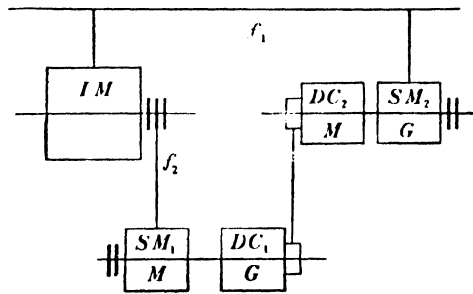


FIG. 29-10. Speed control of an induction motor by double feeding.

It has been previously explained, see Art. 24-1, that, for the development of a uniform torque, stator and rotor mmf waves must be at standstill with respect to each other. In the example considered, the speed of the stator mmf with respect to the stator is  $n_{s1} = (120 \times 60)/4 = 1800$  rpm, and the speed of the rotor mmf with respect to the rotor is  $n_{s2} = (120 \times 25)/4 = 750$  rpm. If the rotor is fed in such a manner that its mmf rotates in the same direction as the stator mmf, then the condition for a uniform torque is satisfied only when the rotor speed is  $n_{s1} - n_{s2} = 1800 - 750 = 1050$  rpm. On the other hand, if the rotor is fed in such a manner that its mmf rotates in opposite direction to the stator mmf, then the condition for a uniform torque is satisfied only when the rotor speed is  $n_{s1} + n_{s2} = 1800 + 750 = 2550$  rpm.

Thus the doubly fed induction motor has *two fixed speeds* at which a uniform torque exists. Expressed by a formula, these two speeds are

$$n = \frac{120(f_1 \mp f_2)}{p} \quad (29-1)$$

At each of these two speeds the machine is able to develop uniform torques of different magnitudes, as shown in Fig. 29-9. Apparently a continuous speed control can be achieved if one of the two frequencies of Eq. 29-1 can be continuously varied. Such an arrangement is shown in Fig. 29-10.

$IM$  is the induction motor the speed of which is to be controlled. The stator is connected to the supply lines; its rotor is connected to a synchronous machine  $SM_1$ , which is coupled to a d-c machine  $DC_1$ . The latter is connected electrically with another d-c machine  $DC_2$ , which is coupled to a synchronous machine  $SM_2$ , connected to the lines. The electric power of the rotor of the induction motor is consumed by the synchronous machine  $SM_1$  which operates as a motor. The d-c machine  $DC_1$ , therefore, operates as a generator, and the d-c machine  $DC_2$  operates as a motor. The synchronous machine  $SM_2$  operates as a generator and returns the electric power of the induction motor to the lines.

The speed control of the induction motor in the above arrangement is accomplished by changing the excitation of the d-c machine  $DC_2$ . This produces a change in speed of the set  $SM_1 - DC_1$  and therefore a change in the frequency  $f_2$ .

If  $f_2$  is zero, i.e., if one of the sources of power is d-c, Eq. 29-1 yields only a *single speed* at which the machine is able to produce a uniform torque. This is the case in the *synchronous machine* which will be treated later.

### PROBLEMS

1. A 15-HP, 4-pole, 3-phase, 60-cycle, 440-volt, Y-connected wound-rotor induction motor has the following per-unit parameters at  $s = 1$  ( $x_1, x_2'$  sat. values):

$$\begin{array}{lll} r_1 = 0.018 & r_m = 0.17 & r_2' = 0.023 \\ x_1 = 0.09 & x_m = 3.5 & x_2' = 0.085 \end{array}$$

Determine the external resistance (in ohms per phase) necessary to start this motor with 130% rated torque. The rated speed is 1756 rmp.

2. For the wound-rotor motor of Problem 1 determine the external resistance (in ohms per phase) necessary to start the motor with its pull-out torque. Can the motor start with a torque larger than the pull-out torque? (Sat. factor = 1.2.)

3. Determine the starting torque of the motor of Problem 2 for an external resistance three times as large as that necessary to start the motor with its pull-out torque.

4. Determine the starting performance of the motor of Problem 1 for an external resistance = 0. Is the starting performance with external resistance = 0 satisfactory?

5. For the motor of Problem 1 determine the external resistance necessary to start the motor with rated torque, and also the stator current which occurs at this resistance. Compare this stator current with that of a squirrel-cage motor.

6. A 125-HP, 6-pole, 3-phase, 60-cycle, 2300-volt, Y-connected, squirrel-cage induction motor has the following per-unit parameters at  $s = 1$  ( $x_1, x_2'$  unsat. values):

$$\begin{array}{lll} r_1 = 0.017 & r_m = 0.20 & r_2' = 0.018 \\ x_1 = 0.095 & x_m = 3.1 & x_2' = 0.10 \end{array}$$

The saturation factor of the leakage paths at  $s = 1$  and starting with full voltage is 1.23. Determine the voltage ratio of an autotransformer necessary to reduce the starting

current to 60% of the value which occurs at starting with full voltage. (Assume that the saturation of the leakage paths at 60% starting current is 1.1.) What will be the starting torque at that voltage ratio?

7. Determine for the motor of Problem 6 the series ohmic resistance in the stator circuit necessary to reduce the starting current to 60% of the value which occurs at starting with full voltage. What is the loss in this resistance?

8. Refer to Problem 7. What is the starting torque with the resistance which reduces the starting current to 60% of the value which occurs at full voltage?

9. Determine for the motor of Problem 6 the series inductive reactance in the stator circuit necessary to reduce the starting current to 60% of the value which occurs at starting with full voltage.

10. Refer to Problem 9. What is the starting torque with the inductive reactance which reduces the starting current to 60% of the value which occurs at full voltage?

11. With 2300 volts at the terminals of a 3-phase, wound-rotor induction motor the emf measured at the open-rotor slip rings at standstill is 640 volts. For a blocked rotor test with 780 volts at the stator terminals and the slip rings short-circuited, the line current is 275 amp and the power input is 115 kw. What resistance (in ohms) should be connected, (a) in star and (b) in delta, to the rotor slip rings so that, with 2300 volts applied to the stator, the rotor current at standstill will be unchanged? What is the ratio of the torques developed in the two cases? (Neglect the magnetizing branch and assume that the stator and rotor parameters are equal. Further, neglect the voltage drops in the stator for the open-rotor test.)

12. It is to be decided whether to start a squirrel-cage induction motor by means of an autotransformer or a series resistance in the stator circuit. In each case, the line current at full voltage must be equal to the rated current of the motor. For a blocked rotor test with 25% rated voltage at the terminals of the motor, the motor current is equal to the rated current and the power factor is 0.20. Compare the starting torques for the two methods of starting. (Neglect the magnetizing branch and assume equal parameters for stator and rotor.)

13. A 500-HP, 3-phase, 25-cycle, 2300-volt, 12-pole induction motor has a slip of 1.8% at full-load. The resistance of the rotor winding per phase, referred to the stator, is 0.5 ohm. What is the rotor current at full-load? What is the ratio of delivered to developed torque? What is the starting torque, if the terminal voltage is adjusted so that the rotor current is twice its full-load value? (Total rotational losses = 2.5%.)

14. A 500-HP, 3-phase, 60-cycle, 2300-volt induction motor has full-load copper losses in the stator and rotor windings equal to 2.4% and 2.6%, respectively. The total iron loss is 8.6 kw. The iron loss due to the fundamental flux is 3.5 kw. The friction and windage losses are 8 kw. The magnetizing current is 20 amp. The leakage reactances of the windings at  $s = 1$  are 4.5 times their resistances. Determine the terminal voltage of this motor if the starting current is to be 200 amp. (Neglect the skin-effect in the rotor winding. Stray load loss = 5.5 kw.) (Full-load  $\cos \phi = 0.90$  in.)

15. A 2000-HP, 24-pole, 3-phase, 60-cycle, 6600-volt, star-connected wound-rotor induction motor has a turn ratio 8.05. The rotor is star-connected. The speed of this motor is controlled by a 3-phase a-c commutator machine set between rated speed and -30% of rated speed. Determine the approximate values of voltage and the kva of the commutator machine, neglecting voltage drops due to resistance and leakage reactance of the stator winding, and leakage reactance of the rotor winding.

## Chapter 30

### SOME SPECIAL INDUCTION MACHINES

Some of the machines described below have only the construction but not the behavior in common with the induction motor. This is pointed out in the discussion of the individual machines.

**30-1. The synchronous induction motor.** Consider Eq. 29-1. If the frequency  $f_2$  of the line to which the rotor is connected is equal to zero, the rotor speed becomes

$$n = \frac{120f_1}{p} = n_s$$

i.e., *there is only one speed, the synchronous speed, at which a uniform torque is developed.* Thus a wound rotor motor, the rotor of which is

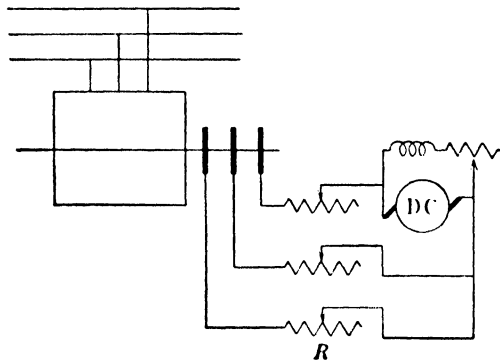


FIG. 30-1. Connection diagram of the synchronous induction motor.

excited with direct current, runs with synchronous speed and operates as a synchronous motor (see Art. 29-3d). Fig. 30-1 shows the connection diagram of the synchronous induction motor.  $R$  is the starting resistance which is cut out during running;  $DC$  is the exciter of the induction motor.

Field current is applied by the exciter after the motor comes up to speed. The d-c excitation then pulls the motor into "step", i.e., into synchronous speed (see Art. 40-4).

The synchronous induction motor has been used for many applications, especially in Europe. The advantage of this type of machine lies in a better starting performance as compared with that of the salient-pole synchronous motor (see Art. 40-4). On the other hand, low-voltage exciters with high current ratings have to be used for these machines; this is necessitated by the limited starting voltage at the slip rings of induction motors; such a limited voltage requires a small number of rotor turns and therefore a low rotor resistance so that  $I_2 r_2$  is small.

**30-2. Induction motor with a rotating flux produced by a d-c excited rotating pole-structure (electromagnetic coupling).** The rotating flux of the conventional induction motor is produced by polyphase windings carrying polyphase currents. A rotating flux can also be produced by a rotating pole-structure excited by direct current, and such a rotating flux has the same effect as that produced by polyphase a-c windings. Use is made of this where an a-c source is not available, as for example, on shipboard. An induction motor of this kind must have additional bearings so that *both* members, the primary and the secondary, can rotate independently. The primary has a d-c excited pole-structure, while the secondary member has a single- or double-cage winding. When placed between a Diesel and a geared propeller shaft on shipboard, this machine prevents the transmission of torque pulsations to the gears.

**30-3. Self-synchronizers (Selsyns, Synchrotie Apparatus, Autosyn, etc.).** In many power applications, as for example in lift-bridge drives, printing-press drives, etc., it is desirable to tie together two or more parallel drives, by a *pure electrical* interconnection, in such a manner that the speeds as well as the space-phase alignments of the different drives are the same. For this purpose wound rotor induction motors can be used. Consider Fig. 30-2 in which the stators of two 3-phase wound-rotor induction motors are connected to a *common* source of power and the rotors are electrically interconnected. Since each of the machines is connected to two sources of power, both will behave as synchronous machines (see Art. 29-3d), and each machine will influence the speed of the other machine in such a manner that both machines will always run synchronously. Assume, for example, that the line frequency in Fig. 30-2 is 60 cycles, that the machines are 2-pole, and that the rotor of one machine operates at a speed  $n_1 = 1780$  rpm while the rotor of the other



machine runs at speed  $n_2 = 1820$  rpm. The rotor frequencies corresponding to these two speeds are (see Eq. 24-17)

$$f_{r1} = \frac{3600 - 1780}{3600} 60 = 30.35$$

$$f_{r2} = \frac{3600 - 1820}{3600} 60 = 29.65$$

The first rotor which runs at the lower speed will be forced, by the second machine, to assume the speed (see Eq. 29-1)

$$n_1' = \frac{60 - 29.65}{2} 120 = 1820 \text{ rpm}$$

i.e., to increase its speed, and the second rotor which has the higher speed will be forced by the first machine to assume the speed

$$n_2' = \frac{60 - 30.35}{2} 120 = 1780 \text{ rpm}$$

i.e., to decrease its speed. Thus, synchronizing forces will make both machines always run synchronously *with the same speed*.

Now consider the machines at a fixed speed. There is only *one* relative position of both rotors at which the secondary emf's will be exactly opposed with respect to the circuit of the two rotors, so that no current

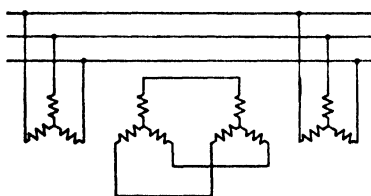


FIG. 30-2. Connection diagram of two 3-phase self-synchronizers.

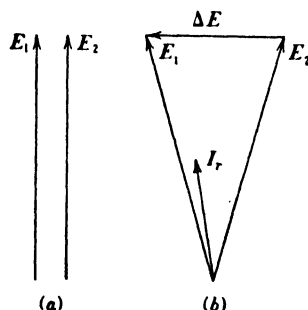


FIG. 30-3. Phasor diagram of the rotors of two self-synchronizers.

will flow in the secondary windings (Fig. 30-3a). For all other positions of the two rotors, there will be a resultant voltage ( $\Delta E$ , Fig. 30-3b) which will produce a current and torque tending to turn the rotors to that position where the rotor emf's are opposed. One of the two machines operates as a *generator (transmitter)* and the other as *motor (receiver)*, the

generator tending to reduce the angle by which its rotor is advanced, and the motor tending to reduce the angle by which its rotor is behind.

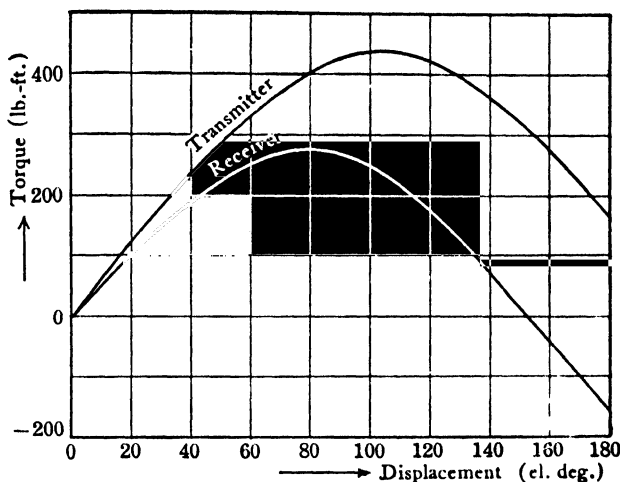


FIG. 30-4. Torque as a function of displacement for two self-synchronizers.

Fig. 30-4 refers to two 25-hp, 8-pole, 60-cycle, 3-phase self-synchronizers and shows the transmitter and receiver torques as a function of the displacement of the two rotors for a fixed speed.

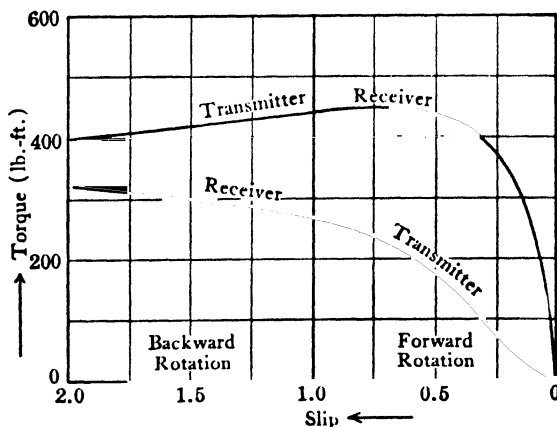


FIG. 30-5. Torque as a function of slip for two self-synchronizers.

It is evident that the torques which line up the self-synchronizers will be small when their rotors run in the direction of their rotating fluxes at low slip, because at low slip the rotor emf's are small (see Eq. 24-19)

and the current in the circuit of the two rotors will be small. Large rotor emf's and large synchronizing torques are obtained at high slips, and also when the rotors run opposite to the direction of their rotating fluxes. In the latter case  $s > 1$ . Fig. 30-5 refers to the same two machines as in Fig. 30-4 and shows the torque as a function of slip for a fixed displacement of the two rotors.

Note that Fig. 30-4 refers to a value of slip larger than 1, i.e., to rotors running opposite to the direction of their rotating fluxes.

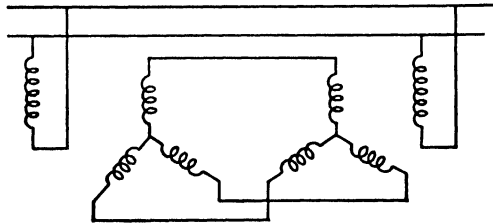


FIG. 30-6. Connection diagram of two single-phase position indicators.

**30-4. Position indicators.** In many applications, for example elevators, hoists, generator rheostats, gates or valves, etc., an indication of position is desirable. In these cases units are used with 3-phase stators and single-phase rotors. The connection diagram of two position indicators is shown in Fig. 30-6. The 3-phase stator windings are directly connected together.

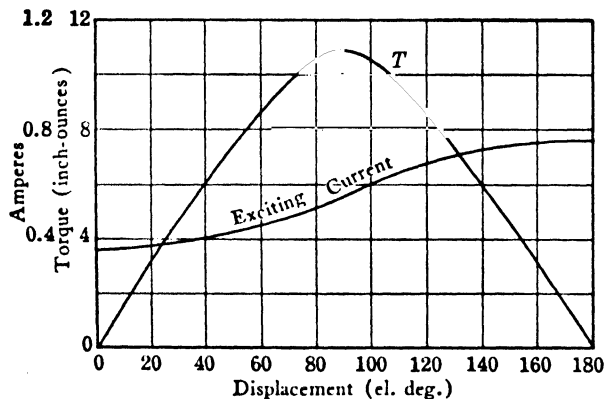


FIG. 30-7. Torque as a function of displacement for two salient-pole position indicators.

The rotor windings are excited by a-c. One of the machines operates as a transmitter and the other as a receiver. For reasons explained in the foregoing article, if the rotor of the transmitter is turned through a certain

angle, the rotor of the receiver will follow by the same angle. Fig. 30-7 shows a typical torque-displacement curve for two units.

The rotors are usually of the salient-pole type, as in the synchronous machine (see Fig. 35-1), because the saliency introduces the advantage of increasing the synchronizing torque by the reluctance torque (see Arts. 39-1 and 41-1). Fig. 30-7 refers to salient-pole rotors.

Position indicators are usually of fractional-horsepower rating while the 3-phase self-synchronizers of the wound rotor type described in the foregoing article are built as larger units (up to 100 HP).

**30-5. The induction voltage regulator.** The induction voltage regulator is an induction motor which is used as a transformer to regulate the voltage of an outgoing circuit from a central station having many single circuits. The rotor does not rotate continuously but may be rotated through a range of 180 electrical degrees.

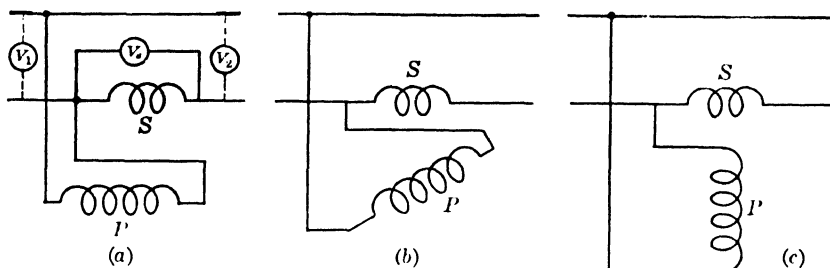


FIG. 30-8. Schematic diagram showing the principle of operation of a single-phase induction regulator.

As in the case of the induction motor the induction voltage regulator may be either single-phase or polyphase. Since it has to add or subtract an increment of line voltage, *its secondary is in series with the line*. Fig. 30-8 shows the coil arrangement of a single-phase induction regulator with single-phase windings on both the stator and the rotor. The primary  $P$  (usually the rotor) is connected to the power line as in the ordinary transformer. The secondary  $S$  is in series with the line.  $V_1$  is the non-regulated voltage;  $V_2$ , the regulated.  $V_s$  is the secondary voltage of the induction regulator. Thus

$$V_2 = V_1 \pm V_s \quad (30-1)$$

The magnitude of  $V_s$  depends upon the mutual inductance between the secondary and primary windings of the induction regulator, i.e., upon the angle between the axes of the windings  $P$  and  $S$ .  $V_s$  is a maximum when the axes of the two windings coincide (Fig. 30-8a);  $V_s$  is zero when

the axes of the windings are shifted 90 electrical degrees with respect to each other (Fig. 30-8c). The angle between the positive and negative maximum of  $V_s$  is 180 electrical degrees.

Consider Fig. 30-8c in which the axes of the windings are perpendicular to each other. The voltage  $V_s$  of the secondary winding due to the transformer flux is zero, but, since this winding carries the load current which is an alternating current, an emf of self-induction is induced in it. Hence, the secondary winding appears in the load circuit as a reactor which would reduce the load voltage  $V_2$  if its reactive voltage drop were not nullified. Fig. 30-9 shows the actual coil arrangement of the single-phase induction regulator. The rotor has, in addition to the primary winding which is connected to the line, a short-circuited winding  $SC$  the axis of which is

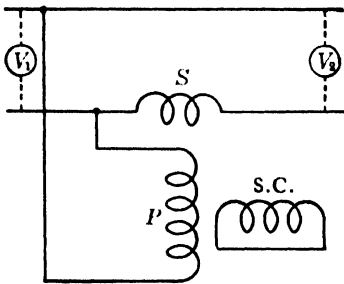


FIG. 30-9. Coil arrangement in the single-phase induction regulator.

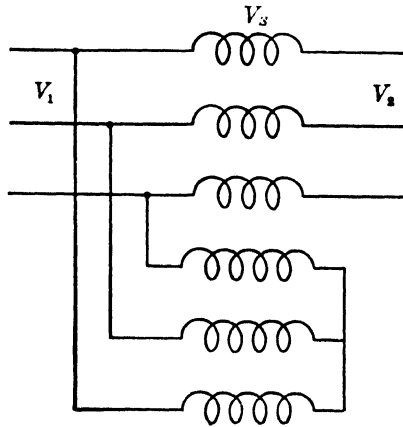


FIG. 30-10. Schematic diagram of the 3-phase induction regulator.

shifted 90 electrical degrees with respect to the primary winding. Fig. 30-9 shows the primary and secondary windings in the same position as Fig. 30-8c. However, it can be seen from Fig. 30-9 that the flux produced by the load current in the secondary winding  $S$  also will link the short-circuited winding  $SC$ , because the axes of these windings coincide. Since the winding  $SC$  is short-circuited, the secondary winding  $S$  and the winding  $SC$  behave as a transformer under short-circuit conditions, i.e., the flux in the axis of the secondary winding  $S$  is small and the voltage drop in the line is caused only by the relatively small leakage fluxes of the secondary winding  $S$  and the winding  $SC$ .

The voltage drop in the line due to the secondary  $S$  of the regulator at the position shown in Fig. 30-8c could appear to a lesser degree (corresponding to the sine of the angle between the axes of the coils  $P$  and  $S$ ) at any intermediate position between those of Fig. 30-8a and Fig. 30-8c. However, since the compensating winding  $SC$  has a fixed position with

respect to the primary winding  $P$ , it has the same effect on the secondary  $S$  and the line at intermediate positions as for the position shown in Fig. 30-9.

Fig. 30-10 shows the coil arrangement of a 3-phase induction regulation. The primary winding can be connected star or delta while the secondary is again in series with the line. The action is somewhat different from that of the single-phase induction regulator. The primary currents produce a *rotating flux* which induces a voltage  $V_s$  in the secondary winding. The magnitude of this induced voltage is independent of the relative position of the windings. However, the relative position of the windings determines the *phase* of the secondary voltage  $V_s$  with respect to the primary voltage  $V_1$ . The relation here is

$$V_2 = V_1 + V_s \quad (30-2)$$

i.e., the regulated voltage is the geometric sum of  $V_1$  and  $V_s$ . Fig. 30-11 shows the voltage diagram of the polyphase induction regulator. As in the single-phase induction regulator, the maximum regulated voltage is  $V_1 + V_s$ , and the minimum regulated voltage is  $V_1 - V_s$ . For intermediate positions of rotor and stator the end-point of  $V_s$  and also of  $V_2$  moves on a circle. A short-circuited compensating winding (see Fig. 30-9) is not required for the polyphase induction regulator.

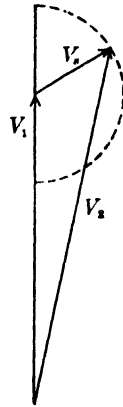


FIG. 30-11. Voltage diagram of the polyphase induction regulator.

Induction regulators usually are built as vertical 2-pole machines, or in the larger sizes as vertical 4-pole machines. The smaller the number of poles, the larger the mechanical angle which corresponds to 180 electrical degrees, and the easier the voltage adjustment. The gradual rotation of the rotor is accomplished by a worm-gear drive with the gear on the shaft of the rotor. The worm is usually operated by a motor controlled automatically by voltage relays. Since the rotor of the induction regulator does not rotate, it may be cooled by oil just as any ordinary transformer. This is of decided advantage when the induction regulator is used to regulate a high-voltage line.

**30-6. Resolvers.** Resolvers are used to perform trigonometric operations in analog computing devices and control systems. One of the common operations is the production of a *pure sinusoidal* voltage as a function of the angle between stator and rotor windings.

Resolvers are built 2-pole for an output of few millivolt-amperes.

Both stator and rotor have two single-phase windings. Fig. 30-12 shows a schematic diagram of the windings of a resolver. As in the induction voltage regulator the rotor does not rotate continuously but may be rotated through a range of 180 electrical degrees.

The single-phase voltage impressed upon the two primary windings (stator or rotor windings) produce two alternating fluxes shifted 90 degrees with respect to each other in space.

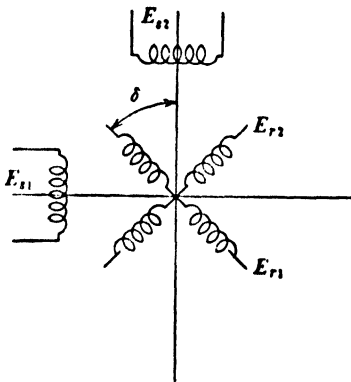


FIG. 30-12. Winding arrangement of a resolver.

It will be assumed that the primary windings lie in the stator and the secondary windings in the rotor. If the emf's induced by the two stator fluxes in the stator windings are  $E_{s1}$  and  $E_{s2}$ , then for a displacement  $\delta$  of the axes of stator and rotor windings, the emf's induced in the rotor windings are (Fig. 30-12)

$$E_{r1} = aE_{s1} \cos \delta + aE_{s2} \sin \delta$$

$$E_{r2} = -aE_{s1} \sin \delta + aE_{s2} \cos \delta$$

where  $a$  is the ratio of rotor turns to stator turns.

It is required that the secondary voltages  $E_{r1}$  and  $E_{r2}$  be purely sinusoidal. This necessitates sinusoidal flux distribution and a *sinusoidal*

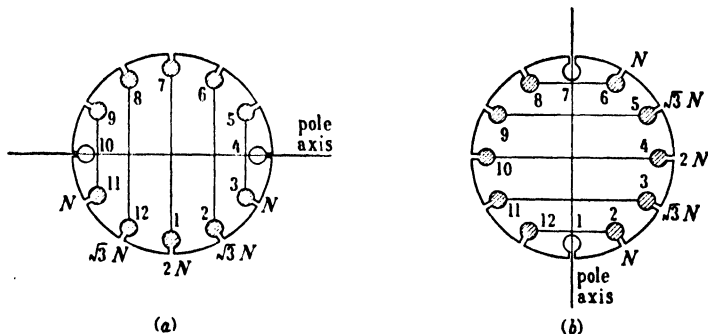


FIG. 30-13. Conductor distribution in the primary of a resolver for sinusoidal flux distribution.

*distribution* of the rotor (secondary) conductors. The sinusoidal flux distribution can be achieved through a sinusoidal distribution of the stator (primary) conductors. Fig. 30-13 shows such a conductor distribution for a rotor with 12 slots. One of the two windings lies in the

slots 1-7, 2-6, 12-8, 3-5, and 11-9 and has its pole axis through the slots 4-10; the other winding lies in the slots 4-10, 5-9, 3-11, 6-8, and 2-12 and has its pole axis through the slots 1-7. The angle between 2 slots is  $360/12 = 30$  degrees. Considering the first winding (Fig. 30-13a), the number of turns in slots 1-7 is  $2N$ , the number of turns in slots 2-6 and 12-8 is  $2N \cos 30^\circ = \sqrt{3}N$ , the number of turns in slots 3-5 and 11-9 is  $2N \cos 60^\circ = N$ , and the number of turns in slots 4 and 10 is  $2N \cos 90^\circ = 0$ . The second winding has exactly the same distribution but shifted 90 degrees.

In order to eliminate the influence of the harmonics of high order, rotor or stator slots must be skewed (see Art. 22-2).

### PROBLEMS

1. A 40-kw, unity power factor, 440-volt, single-phase load is fed through an induction voltage regulator which is boosting the primary line voltage 15%. Determine the currents in each winding of the regulator neglecting the magnetizing current.

2. A 2-kva induction voltage regulator is designed to operate on either a 115-volt or a 230-volt supply circuit. There are two primary windings and two secondary windings which give 100% buck or boost on the load side when voltage is applied to the regulator. Specify the coil currents for each connection and show properly labeled diagrams of connections. Neglect magnetizing current.

3. A 230-volt, 3-phase, 60-cycle, wound-rotor, Y-connected induction motor has a slip-ring voltage of 120 volts at standstill with the slip rings open. This motor is to be used as a 3-phase induction voltage regulator to boost the 230-volt line voltage 15%. Determine the angle between stator and rotor voltages necessary to achieve this boost, neglecting the magnetizing current and the resistance and reactance drops in the machine.

4. Repeat Problem 3 for 5% and 10% boost in voltage.

5. Repeat Problem 3 for 5, 10, and 15% voltage buck.

6. Referring to Problem 3, what are the maximum and minimum voltages (available on the regulated side) which this machine can produce? Neglect the magnetizing current and the resistance and reactance drops.



## Chapter 31

### THE SINGLE-PHASE INDUCTION MOTOR

Any 3-phase induction motor can be made to operate as a single-phase induction motor by opening one of the three stator phases. The two remaining stator phases constitute a single-phase winding distributed over  $\frac{2}{3}$  of the pole pitch. A 3-phase winding is ordinarily a 2-layer winding (see Art. 21-1a), while the actual winding of the single-phase motor is usually single layer and of the chain type (see Art. 21-1c).

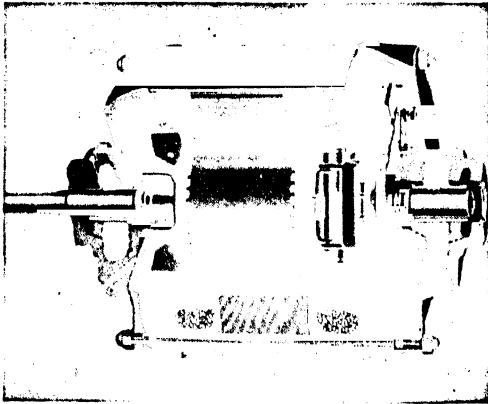


FIG. 31-1. Cutaway view of a single-phase induction motor with centrifugal switch.

Fractional-horsepower motors are usually single-phase, and there are many types of such single-phase motors. The differences between them are described in Chapter 33. However the *mechanical elements* of the single-phase induction motor are the same as those of the polyphase induction motor, except that a centrifugal switch is used in certain types of single-phase motors, in order to cut out a winding

used only for starting (see Chap. 33). Fig. 31-1 shows the cutaway view of a single-phase motor with centrifugal switch. The rotor of the single-phase induction motor is usually of the squirrel-cage type.

**31-1. Replacement of the alternating flux by two rotating fluxes.** The single-phase stator winding of the single-phase motor produces an alternating flux (see Art. 22-2) which is at standstill with respect to the stator. It has been shown in Art. 22-2 that an alternating flux is equivalent in its

operation to two rotating fluxes traveling in *opposite* directions, each having an amplitude equal to half of that of the alternating flux. Use will be made of this property for the analysis of the single-phase motor.

The rotating flux which travels in the same direction of rotation as the rotor is called the *forward rotating flux*, while the rotating flux which travels in the opposite direction to the rotor is called the *backward rotating flux*.

Contrary to the polyphase induction motor, where the rotor emf is induced by only one rotating flux, it is induced here by two rotating fluxes, and the influence of each flux on the rotor is to be considered separately. The effect of *each* of the two rotating fluxes on the rotor of the single-phase motor is the same as that of the single rotating flux on the rotor of the polyphase motor.

Assume that the rotor has a speed  $n$  rpm. Then, according to the definition of the slip  $s$  (see Eq. 24-18), the slip of the rotor with respect to the forward rotating flux is

$$s = \frac{n_s - n}{n_s} = 1 - \frac{n}{n_s} \quad (31-1)$$

Since the backward rotating flux rotates opposite to the rotor, the slip of the rotor with respect to this backward rotating flux is

$$s_b = \frac{n_s - (-n)}{n_s} = 1 + \frac{n}{n_s} = 2 - s \quad (31-2)$$

In order to make clear the influence of the two rotating fluxes on the rotor it will be assumed that  $n < n_s$ . Then, with respect to the forward rotating flux, and according to Eq. 31-1,  $s$  is positive and smaller than 1. Considering the circle diagram of the polyphase motor Fig. 27-5, it is seen that the rotor, under the influence of the forward rotating flux, operates as in a *motor*. With  $s$  positive and smaller than 1, the slip of the rotor with respect to the backward rotating flux is, according to Eq. 31-2, positive and larger than 1. Again considering the circle diagram of Fig. 27-5 it is seen that the rotor, under the influence of the backward rotating flux, operates as in the region of brake operation. Thus the two rotating fluxes have an opposite influence upon the rotor.

**31-2. Torque of the single-phase induction motor.** The relation for the *developed* torque, Eq. 26-7, derived for the polyphase induction motor can be applied to each of the two rotating fluxes of the single-phase induction motor. Thus the torque developed by the rotor under the in-

fluence of the forward rotating flux is

$$T_f = \frac{7.04}{n_s} \frac{I_{2f}'^2 r_2'}{s} \text{ lb-ft} \quad (31-3)$$

and the torque developed by the rotor under the influence of the backward rotating flux is

$$T_b = -\frac{7.04}{n_s} \frac{I_{2b}'^2 r_2'}{2-s} \text{ lb-ft} \quad (31-4)$$

$I_{2f}'$  and  $I_{2b}'$  are the currents produced in the rotor by the forward and backward fluxes respectively. The *resultant* developed torque is the sum of  $T_f$  and  $T_b$ . Thus

$$T_r = T_f + T_b \quad (31-5)$$

Fig. 31-2 shows both torques and the resultant torque for slips between 0 and +2. The resultant torque is *zero at standstill* in accordance with the fact that an alternating flux is not able to start an induction motor: only

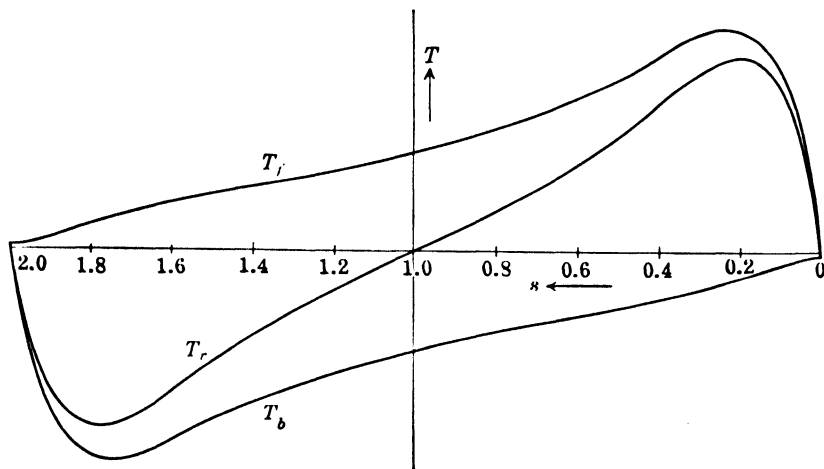


FIG. 31-2. Forward, backward, and resultant torque of a single-phase induction motor.

a rotating flux is able to do this. At standstill  $s = 1$  and  $2 - s = 1$  and both rotating fluxes have equal but opposite influence on the rotor; therefore  $T_f = -T_b$  and  $T_r = 0$ . However, at any other slip,  $|T_f| \neq |T_b|$  and there exists a driving torque  $T_r$ . This means that there is no torque on the rotor when it is at standstill ( $s = 1$ ), but as soon as the rotor starts rotating ( $n > 0$ ), *regardless of the direction of rotation*, a driving torque is present which will bring the rotor up to about synchronous speed ( $n_s = 120f_1/p$ ) as in the polyphase motor. At synchronous speed ( $s = 0$ ) the resultant torque has a small negative value.

**31-3. Kirchhoff's mesh equations of the stator and rotor circuits.**

It is now simple to derive, on the basis of the foregoing, Kirchhoff's mesh equations for both rotor and stator. The two rotating fluxes induce two emf's and two currents ( $I_{2f}'$  and  $I_{2b}'$ ) of the frequencies  $sf_1$  and  $(2 - s)f_1$  respectively, in the rotor. Since the *frequencies are different*, the two emf's and their currents must be considered separately, i.e., *two* Kirchhoff's mesh equations must be set up *for the rotor*, namely, (see Eq. 25-3).

$$\mathbf{E}_{2f}' = \mathbf{I}_{2f}' \left( \frac{r_2'}{s} + jx_2' \right) \quad (31-6)$$

and

$$\mathbf{E}_{2b}' = \mathbf{I}_{2b}' \left( \frac{r_2'}{2 - s} + jx_2' \right) \quad (31-7)$$

Neglecting at first the iron losses due to the main flux, the emf's  $E_{2f}'$  and  $E_{2b}'$  become, according to the Eqs. 25-4 and 25-6,

$$\mathbf{E}_{2f}' = -j(\mathbf{I}_1 + \mathbf{I}_{2f}')x_m \quad (31-8)$$

and

$$\mathbf{E}_{2b}' = -j(\mathbf{I}_1 + \mathbf{I}_{2b}')x_m \quad (31-9)$$

$(\mathbf{I}_1 + \mathbf{I}_{2f}')$  is the resultant mmf, i.e., the magnetizing current of the forward rotating flux;  $(\mathbf{I}_1 + \mathbf{I}_{2b}')$  is the magnetizing current of the backward rotating flux. All quantities in Eqs. 31-6 to 31-9 are referred to the stator. Therefore the emf's induced in the stator winding by the two rotating fluxes are also equal to  $E_{2f}'$  and  $E_{2b}'$  (see Eq. 24-10), and Kirchhoff's mesh equation for the stator is (see Eq. 25-2)

$$\mathbf{V}_1 = \mathbf{I}_1(r_1 + jx_1) + j(\mathbf{I}_1 + \mathbf{I}_{2f}')x_m + j(\mathbf{I}_1 + \mathbf{I}_{2b}')x_m \quad (31-10)$$

**31-4. The equivalent circuit of the single-phase induction motor.** The equivalent circuit of the single-phase motor is obtained from Eq. 31-10 by eliminating the rotor currents  $I_{2f}'$  and  $I_{2b}'$  with the aid of Eqs. 31-6 to 31-9. Introducing the abbreviations

$$\begin{aligned} \mathbf{Z}_1 &= r_1 + jx_1 & \mathbf{Z}_{2f}' &= \frac{r_2'}{s} + jx_2'; \\ \mathbf{Z}_{2b}' &= \frac{r_2'}{2 - s} + jx_2' & \text{and } jx_m &= \mathbf{Z}_m \end{aligned} \quad (31-11)$$

Eq. 31-10 becomes

$$\mathbf{V}_1 = \mathbf{I}_1 \left[ \mathbf{Z}_1 + \frac{\mathbf{Z}_m \mathbf{Z}_{2f}'}{\mathbf{Z}_m + \mathbf{Z}_{2f}'} + \frac{\mathbf{Z}_m \mathbf{Z}_{2b}'}{\mathbf{Z}_m + \mathbf{Z}_{2b}'} \right] \quad (31-12)$$

The second term in the bracket is the impedance of  $\mathbf{Z}_m$  and  $\mathbf{Z}_{2f}'$  connected

in parallel; the third term in the bracket is the impedance of  $Z_m$  and  $Z_{2b}'$  connected in parallel. Therefore, the equivalent circuit of the single-phase induction motor is as shown in Fig. 31-3, or more explicitly as shown in Fig. 31-4. The iron losses due to the main flux were neglected in the previous considerations. Taking these losses into account the equivalent circuit of the single-phase induction motor becomes as shown in Fig. 31-5 (see Fig. 25-4).

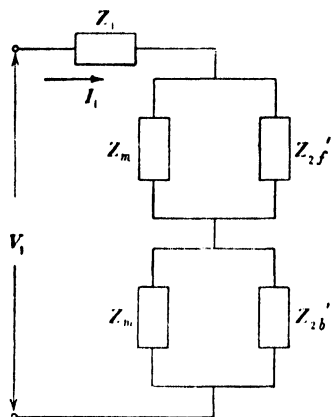


FIG. 31-3. Equivalent circuit of the single-phase induction motor.

With the parameters given, it is possible to determine from the equivalent circuit the primary current, the primary power factor, and the rotor currents  $I_{2f}'$  and  $I_{2b}'$ . Then, with the aid of Eqs. 31-3 to 31-5, the forward and backward torques and the resultant torque can be calculated.

Fig. 31-6 shows the forward rotor current  $I_{2f}'$ , the backward rotor current  $I_{2b}'$ , and the

stator current  $I_1$  as a function of slip. The backward current  $I_{2b}'$  is a mirror image of the forward current  $I_{2f}'$  with respect to the axis of ordinates through  $s = 1$ .  $I_{2f}'$  is zero at  $s = 0$ ;  $I_{2b}'$  is zero at  $s = 2$ .

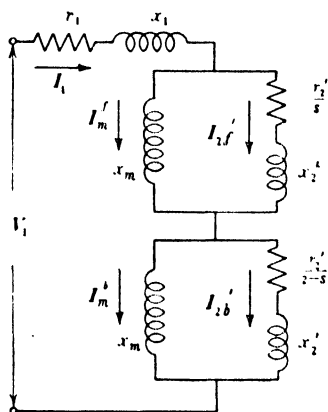


FIG. 31-4. Equivalent circuit of the single-phase induction motor — iron losses due to the main flux neglected.

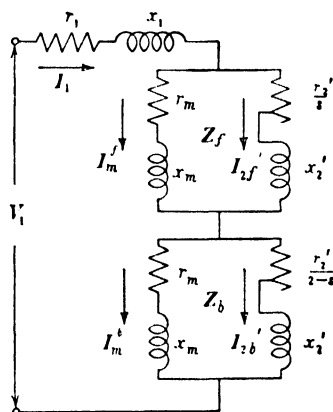


FIG. 31-5. Equivalent circuit of the single-phase induction motor — iron losses due to the main flux considered.

**31-5. The circle diagram of the single-phase induction motor.** It can be shown by a consideration similar to that for the polyphase motor (see

Art. 27-1) that Eq. 31-12 yields a circle for the geometric locus of the end-point of the primary current, just as in the polyphase motor. The equations for the radius and for the coordinates of the center point are very

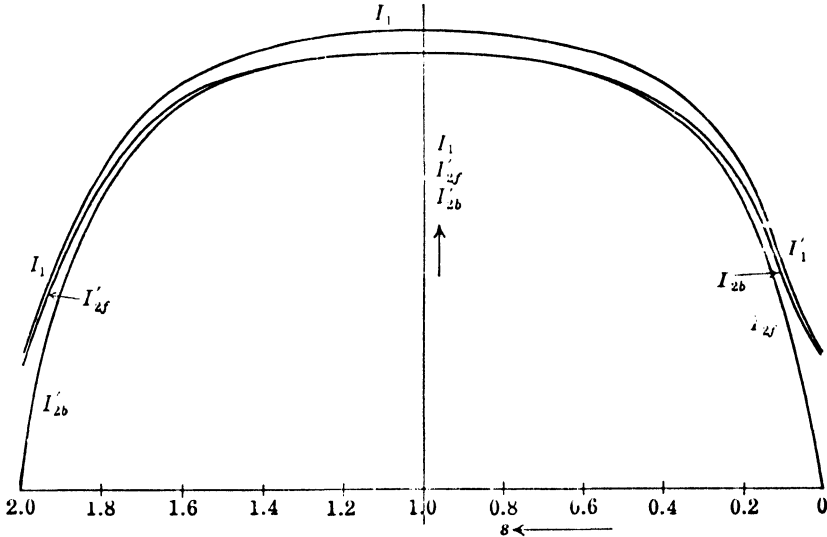


FIG. 31-6. Forward rotor current, backward rotor current, and primary current as a function of slip.

complicated. The circle is therefore best constructed from the three characteristic points,  $s = 0$ ,  $s = 1$ , and  $s = \infty$ , for which the currents can be determined from the equivalent circuit. If no-load and locked-rotor tests are available, only the current for the point  $s = \infty$  is to be determined from the equivalent circuit. Fig. 31-7 shows the circle diagram of the single-phase motor.  $P_0'$  corresponds to  $s = 0$ ,  $P_L$  to  $s = 1$ , and  $P_\infty$  to  $s = \infty$ .  $P_0$  is the no-load point.

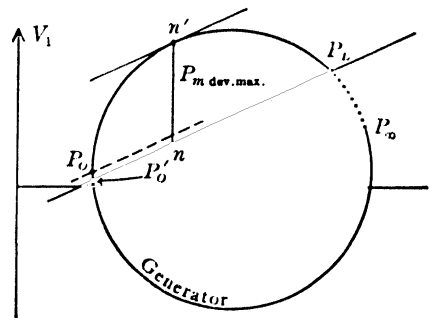


FIG. 31-7. Circle diagram of the single-phase induction motor.

There is a small negative torque at  $s = 0$  due to the backward rotating flux. However, the line through  $P_0'$  and  $P_L$  represents with fair approximation the  $P_{m.dev.}$ -Line (see Fig. 27-4), and the distance from any point of the circle to this line is a measure of the developed mechanical power. As in the polyphase motor,

the  $P_{m.del}$ -Line can be found by drawing a line parallel to the  $P_{m.dev}$ -Line, through the point  $P_0$  (see Fig. 27-4).

The circle diagram of the single-phase motor does not include a torque line since the torque of the single-phase motor is zero not only at a point close to  $s = 0$  ( $P_0'$ ) and  $s = \infty$  ( $P_\infty$ ) but also at standstill ( $s = 1$ ,  $P_L$ ). The determination of the torque-speed curve from the circle diagram is not possible for the single-phase motor; as a result the circle diagram of the single-phase motor is of little value.

The single-phase motor can operate as a generator, but it *cannot operate as a brake* (dotted part of the circle between  $P_L$  and  $P_\infty$ ). Operation as a brake means that the rotor rotates in a direction opposite to that of the rotating flux. Considering the fact that the forward and backward fluxes rotate in opposite directions, the single-phase motor has no defined direction of rotation; it is capable of coming up to speed from standstill ( $s = 1$ ) in either direction and there is no possibility for its rotor to run against its rotating flux.

## Chapter 32

### DETERMINATION OF PARAMETERS FROM A NO-LOAD AND A LOCKED-ROTOR TEST

**32-1. The no-load test.** The no-load test is run at rated voltage  $V_1$  with the starting winding open (see Art. 33-1), and  $I_0$  and  $P_0$  are measured. Fig. 32-1 shows the equivalent circuit for no-load ( $s \approx 0$ ). At synchronous speed no current flows in the rotor of the *polyphase motor* (see Fig. 28-1) because the relative speed between the rotating flux and the rotor is zero. However, it is quite different with the single-phase motor, for at  $s = 0$  there is no difference in speed between the rotor and the forward rotating flux, but there is a difference in speed equal to twice the synchronous speed between the rotor and the backward rotating flux. Therefore current  $I_{2b}'$  flows in the rotor of the single-phase motor at  $s = 0$ . At no-load the rotor current of the polyphase motor is negligible. As can be seen from Fig. 32-1 this is not the case with the single-phase motor.

At no-load the stator of the polyphase motor carries only the magnetizing current necessary to sustain the main flux since there is no armature reaction from the rotor. The stator current of the single-phase motor at no-load is about twice the magnetizing current, owing to the armature reaction from the rotor current  $I_{2b}'$ . As a result, the stator copper losses of the single-phase motor at no-load are larger than those of the polyphase motor. At no-load the copper losses in the rotor of the polyphase motor are  $\approx 0$ , but there are copper losses at no-load in the rotor of the single-phase motor due to the current  $I_{2b}'$ .

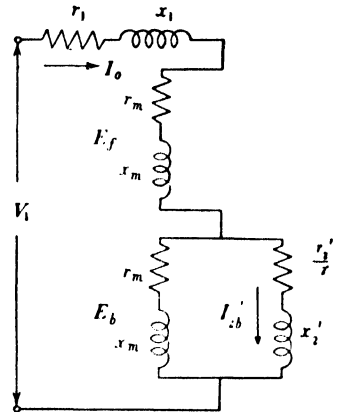


FIG. 32-1. Equivalent circuit of the single-phase motor at no-load.



Since  $(r_m + jx_m)$  is large in comparison with  $\left(\frac{r_2'}{2} + jx_2'\right)$ ,  $I_{2b}' \approx I_0$  at no-load (see Fig. 32-1 and also Fig. 31-6). It will be shown in the following article that  $r_2' \approx r_1/2$ . Hence the rotor copper losses at no-load can be assumed equal to  $0.5r_1I_0^2$ .

Thus the power input at no-load  $P_0$  consists of the iron losses due to the main flux, the friction and windage losses, the rotational iron losses, the copper losses in the stator winding  $I_0^2r_1$  and the copper losses in the rotor winding  $\approx 0.5I_0^2r_1$ . Subtracting from  $P_0$  the sum  $(P_{F+W} + I_0^2r_1 + 0.5I_0^2r_1)$ , the remainder is the sum of  $P_{h+c} + P_{ir,rot}$ . It can be assumed with fair approximation that the iron losses due to the main flux are equal to  $\frac{1}{2}(P_{h+c} + P_{ir,rot})$ . Thus the iron losses due to the main flux, which are necessary for the determination of the parameter  $r_m$ , are known.

It follows from the equivalent circuit of Fig. 32-1 that, for no-load ( $s \approx 0$ ),

$$V_1 \approx I_0 \frac{x_m}{k_2} (2k_2^2 - 1) \quad (32-1)$$

where

$$k_2 = 1 + \frac{x_2'}{x_m} \quad (32-2)$$

or

$$x_m \approx \frac{V_1}{I_0} \frac{k_2}{2k_2^2 - 1} \quad (32-3)$$

$x_m$  cannot be determined from Eq. 32-3 because  $k_2$  is unknown. However,  $k_2$  varies within narrow limits, usually between 1.03 and 1.07, and a certain value for  $k_2$  can be assumed at first. This value can be checked later (see the following article). A knowledge of  $x_m$  is necessary for the determination of  $r_m$ .

As for the polyphase motor, Eqs. 28-5 and 28-4,

$$g_m = \frac{P_{h+c}}{E_1^2} \quad (32-4)$$

$$E_1 \approx V_1 - I_0x_1 \quad (32-5)$$

$E_1$  consists here of two parts: the voltage across the forward branch  $E_{2f}'$ , and the voltage across the backward branch  $E_{2b}'$ , Fig. 32-1. Since  $(r_m + jx_m)$  is large in comparison with  $\left(\frac{r_2'}{2} + jx_2'\right)$ , the voltage  $E_{2f}'$  is large in comparison with the voltage  $E_{2b}'$ . It can be assumed that the

ratio of the two voltages is the same as that of the two impedances  $(r_m + jx_m) \approx jx_m$  and  $\left(\frac{r_2'}{2} + jx_2'\right)$ , i.e.,

$$\frac{E_{2f}'}{E_{2b}'} = \frac{x_m}{\sqrt{\left(\frac{r_2'}{2}\right)^2 + x_2'^2}} = C \quad (32-6)$$

Since  $\mathbf{E}_1 = \mathbf{E}_{2f}' + \mathbf{E}_{2b}'$

$$E_{2f}' \approx E_1 \frac{C}{1 + C} \quad (32-6a)$$

Assuming that the iron losses are produced by the forward rotating flux only, because the backward emf is small and the backward rotating flux therefore weak

$$g_m \approx \frac{P_{h+c}}{E_{2f}'^2} \quad (32-7)$$

Further from Eq. 28-7

$$r_m \approx g_m x_m^2 \quad (32-8)$$

Thus the no-load test yields the main flux parameters  $x_m$  and  $r_m$ , provided that the resistances  $r_1$  and  $r_2'$  and the leakage reactances  $x_1$  and  $x_2'$  are known. These parameters can be obtained from the short-circuit (locked-rotor) test.

**32-2. The locked-rotor test.** This test is made with the starting winding open, and  $V_L$ ,  $I_L$ , and  $P_L$  are measured. As for the polyphase motor, Eq. 28-9,

$$\begin{aligned} Z_L &= \frac{V_L}{I_L} & R_L &= \frac{P_L}{I_L^2} \\ X_L &= \sqrt{Z_L^2 - R_L^2} \end{aligned} \quad (32-9)$$

The equivalent circuit for the locked rotor, Fig. 32-2, yields with fair approximation

$$\mathbf{Z}_{(s=1)} \approx \left(r_1 + \frac{2r_2'}{k_2^2}\right) + j(x_1 + 2x_2') \quad (32-10)$$

i.e., at locked rotor, the equivalent resistance of the motor is approximately equal to the primary resistance plus twice the rotor resistance,

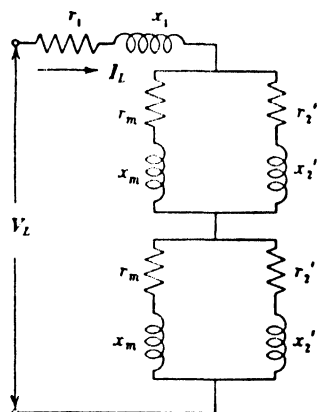


FIG. 32-2. Equivalent circuit of the single-phase motor at standstill.

and the equivalent reactance of the motor is approximately equal to the primary reactance plus twice the rotor reactance.

$r_1$  is measured separately. Then, using the measured locked-rotor resistance  $R_L$ ,

$$r_2' = \frac{R_L - r_1}{2} k_2^2 \quad (32-11)$$

For the separation of  $x_1$  and  $x_2'$ , it is usually assumed that

$$x_1 \approx 2x_2' = \frac{X_L}{2} \quad (32-12)$$

With these values of  $x_1$  and  $x_2'$ , the previously assumed value for  $k_2$  can be checked, and the resistance  $r_2'$ , the quantity  $C$  (Eq. 32-6), and the resistance  $r_m$  can be determined.

### 32-3. Influence of the parameters on the performance of the motor.

The influence of the parameters on the performance of the single-phase motor is, in general, the same as that on the polyphase motor. However, the existence of the backward rotor current  $I_{2b}'$  results in an increase in the stator current and mainly of its reactive component. This makes the *power factor* of the single-phase motor *lower* than that of the polyphase motor. Also the efficiency of the single-phase motor is influenced by the increased copper losses in both the stator and rotor.

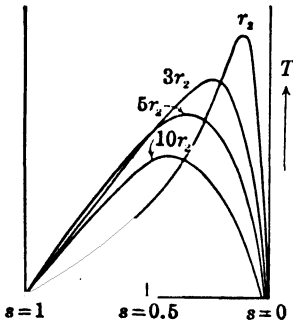


FIG. 32-3. Influence of the rotor resistance on the torque-speed curve of the single-phase motor.

A further difference between the polyphase and single-phase motor appears in the influence of the secondary resistance on the pull-out torque. The rotor resistance does not affect the magnitude of the pull-out torque in the polyphase motor (see Art. 28-4d); it affects only the pull-out slip, i.e., the slip at which the pull-out torque appears. Because of the backward rotating flux, the rotor resistance influences not only the pull-out slip of the single-phase motor but also the magnitude of the pull-out torque.

Fig. 32-3 shows speed-torque curves of a single-phase motor for different values of  $r_2'$ . The larger the rotor resistance, the smaller is the pull-out torque. Speed control of a single-phase motor with a wound rotor by means of a resistance in the rotor circuit is therefore possible only within a narrow range.

**Example 32-1.** The determination of the parameters from a no-load and locked-rotor test will be demonstrated on  $\frac{1}{8}$ -HP 6-pole 60-cycle split-phase motor for 110 volts.

(a) *No-load test* (starting winding open) shows

$$V_1 = 110 \text{ volts, } P_0 = 63.0 \text{ watts, } I_0 = 2.70 \text{ amp}$$

$r_1$  after the test = 2.65 ohms;  $P_{F+W} = 3.0$  watts (ball-bearing motor)

(b) *Locked-rotor test* (starting winding open) shows

$$V_L = 110 \text{ volts; } P_L = 851 \text{ watts; } I_L = 11.65 \text{ amp}$$

$r_1$  after the test = 2.54 ohms

(The difference in the magnitude of  $r_1$  is due to the fact that the tests were made at different times and at different ambient temperatures.)

Assume  $k_2 = 1.05$ ; then from Eq. 32-3

$$x_m = \frac{110}{2.70} \cdot \frac{1.05}{2 \times (1.05)^2 - 1} = 35.5 \text{ ohms}$$

$r_m$  can be determined when the other parameters are known.

From Eq. 32-9

$$Z_L = \frac{110}{11.65} = 9.44 \text{ ohms; } R_L = \frac{851}{(11.65)^2} = 6.27 \text{ ohms;}$$

$$X_L = \sqrt{(9.44)^2 - (6.27)^2} = 7.03 \text{ ohms}$$

From Eq. 32-12

$$x_1 \approx 2x_2' \approx \frac{7.03}{2} = 3.51 \text{ ohms}$$

$$x_2' = 1.75 \text{ ohms}$$

Checking (Eq. 32-2)

$$k_2 = 1 + \frac{1.75}{35.5} = 1.0493$$

which value is very close to the assumed  $k_2 = 1.05$ .

From Eq. 32-11

$$r_2' = \frac{6.27 - 2.54}{2} \times (1.05)^2 = 2.06$$

The five parameters as determined from the no-load and locked-rotor tests are (in ohms)

$$r_1 = 2.54$$

$$r_2' = 2.06$$

$$x_m = 35.5$$

$$x_1 = 3.51$$

$$x_2' = 1.75$$

For the calculation of the performance of the motor the hot resistances of the windings at full-load should be used; if full-load data are not available the resistances at 75°C must be used. For the motor considered,  $r_1$  at full-load was 2.85 ohms, while in the locked-rotor test the resistance was 2.54 ohms. It can be assumed that the resistance

of the rotor is increased by the load in the same ratio as the stator resistance. Thus at full-load  $r_2' = 2.06(2.85/2.54) = 2.31$ , and the motor parameters for performance calculations are (in ohms)

$$r_1 = 2.85 \qquad r_2' = 2.31$$

$$x_m = 35.5$$

$$x_1 = 3.51 \qquad x_2' = 1.75$$

$r_m$  can now be determined. The no-load losses of the motor are 63 watts. They consist of copper losses in both windings, iron losses (due to the main flux + rotational losses), and friction and windage losses. The latter losses are 3.0 watts. The resistance of the stator winding after the no-load test was 2.65 ohms, and thus the loss in the stator copper is

$$P_{\text{co},1} = 2.65 \times (2.7)^2 = 19.3 \text{ watts}$$

From the locked-rotor test,  $r_1 = 2.54$  and  $r_2' = 2.06$ . Since at no-load  $r_1 = 2.65$ , it can be assumed that at no-load

$$r_2' = 2.06 \frac{2.65}{2.54} = 2.15 \text{ ohms}$$

It has been explained previously (see Art. 32-1 and Fig. 31-6) that the rotor current at no-load is approximately equal to  $I_0(I_{2b}' \approx I_0)$ . Therefore the losses in the rotor winding at no-load are

$$P_{\text{co},2} = 2.15 \times (2.7)^2 = 15.7 \text{ watts}$$

The total iron losses are then

$$P_{\text{ir}} = 63.0 - (3.0 + 19.3 + 15.7) = 25.0 \text{ watts}$$

The rotational iron losses at no-load are relatively larger in the single-phase motor than in the polyphase motor. As in the latter motor, the slot openings cause tooth-surface and tooth-pulsation losses in the single-phase motor (see Art. 34-1a). However, contrary to the polyphase motor, the single-phase motor has a large no-load current which does not differ very much from the full-load current. In consequence of this, the harmonics produce additional tooth-surface and tooth-pulsation losses (see Art. 34-1b) at no-load. As has been explained, all of these additional iron losses are caused by the rotation of the rotor and must be supplied by the rotor. It can be assumed that the losses due to the main flux are approximately half of the total iron losses, i.e.,  $P_{h+\epsilon} \approx 13$  watts. This loss determines the magnitude of  $r_m$ . From Eqs. 32-5, 32-6, and 32-6a

$$E_1 = 110 - 2.70 \times 3.51 = 100.6$$

$$C = \frac{35.5}{\sqrt{\left(\frac{2.15}{2}\right)^2 + (1.75)^2}} = 17.3 \qquad E_{2f}' = 100.6 \frac{17.3}{18.3} = 95.2$$

Eqs. 32-7 and 32-8 yield

$$g_m = \frac{13}{(95.2)^2} = 0.0014$$

$$r_m = 0.0014 \times (35.5)^2 = 1.77 \text{ ohms}$$

The six parameters for performance calculations are (in ohms)

$$\begin{aligned} r_1 &= 2.85 & r_m &= 1.77 & r_2' &= 2.31 \\ x_1 &= 3.51 & x_m &= 35.5 & x_2' &= 1.75 \end{aligned}$$

*Note.*—In general the saturation of the leakage paths should be taken into account when evaluating the locked rotor test (see Art. 28-5 and Ex. 28-1). The saturation of the leakage paths has been neglected here.

**Example 32-2.** The parameters computed in Example 32-1 for a  $\frac{1}{8}$ -HP 6-pole split-phase motor will be used to determine the performance of the motor.

(a) First the iron losses due to the main flux will be neglected, i.e., assume  $r_m = 0$ , and the primary current, power factor, and torque will be determined for approximately normal slip. Since no simple formula is available for the normal slip of a single-phase motor, a value of slip will be assumed, the torque corresponding to this slip will be computed, and finally the real slip will be determined from the ratio of rated output to calculated output. The normal slip of the single-phase motor lies between 0.025 and 0.05, the smaller value occurring in larger motors.

The calculations below will be carried through for a slip of  $s = 0.038$ . Since the iron losses are neglected, the resultant impedance of the forward branch of the equivalent circuit is

$$\begin{aligned} Z_f &= \frac{Z_m Z_{2f}'}{Z_m + Z_{2f}'} = \frac{35.5/90 \left( \frac{2.31}{0.038} + j1.75 \right)}{j35.5 + \left( \frac{2.31}{0.038} + j1.75 \right)} \\ &= \frac{35.5/90 \times 60.8/1.65}{60.8 + j37.25} = \frac{2160/91.65}{71.4/31.5} \\ &= 30.3/60.15 = 15.1 + j26.2 \end{aligned}$$

and the impedance of the backward branch

$$\begin{aligned} Z_b &= \frac{Z_m Z_{2b}'}{Z_m + Z_{2b}'} = \frac{35.5/90 \left( \frac{2.31}{1.962} + j1.75 \right)}{j35.5 + \left( \frac{2.31}{1.962} + j1.75 \right)} \\ &= \frac{35.5/90 \times 2.11/56.0}{1.178 + j37.25} = \frac{74.9/146.9}{37.3/88.2} \\ &= 2.01/57.8 = 1.07 + j1.70 \\ Z_t &= Z_1 + Z_f + Z_b = 19.0 + j31.4 = 36.8/58.8 \\ I_1 &= \frac{110/0}{36.8/58.8} = 2.99/-58.8 \end{aligned}$$

$$\cos 58.8^\circ = 0.517$$

$$V_{2f}' = I_1 Z_f = 2.99 \times 30.3 = 90.6 \text{ volts}$$

$$V_{2b}' = I_1 Z_b = 2.99 \times 2.01 = 6.01 \text{ volts}$$

$$I_{2f}' = \frac{V_{2f}'}{Z_{2f}'} = \frac{90.6}{\sqrt{\left(\frac{2.31}{0.038}\right)^2 + (1.75)^2}} = 1.49 \text{ amp}$$

$$I_{2b}' = \frac{V_{2b}'}{Z_{2b}'} = \frac{6.01}{\sqrt{\left(\frac{2.31}{1.962}\right)^2 + (1.75)^2}} = 2.85 \text{ amp}$$

From Eqs. 31-3, 31-4, 31-5 the developed torque is

$$T = \frac{7.04}{1200} \times 2.31 \left[ \frac{(1.49)^2}{0.038} - \frac{(2.85)^2}{1.962} \right] \times 16 = 11.8 \text{ oz-ft}$$

Since part of this developed torque is necessary to supply the iron losses due to rotation and the friction and windage losses, the load torque is therefore less than the 11.8 oz-ft developed.

(b) The iron losses due to the main flux will now be taken into account and the resultant impedance determined as in part (a), Fig 31-5.

$$\begin{aligned} \mathbf{Z}_m &= r_m + jx_m = 1.77 + j35.5 \\ \mathbf{Z}_f &= \frac{(1.77 + j35.5) \left( \frac{2.31}{0.038} + j1.75 \right)}{1.77 + j35.5 + \frac{2.31}{0.038} + j1.75} \\ &= \frac{35.5 / 87.15 \times 60.8 / 1.65}{62.6 + j37.25} = \frac{2160 / 88.8}{72.8 / 30.8} \\ &= 29.7 / 58.0 = 15.7 + j25.2 \\ \mathbf{Z}_b &= \frac{35.5 / 87.15 \left( \frac{2.31}{1.962} + j1.75 \right)}{1.77 + j35.5 + \frac{2.31}{1.962} + j1.75} \\ &= \frac{35.5 / 87.15 \times 2.11 / 56.0}{2.95 + j37.25} = \frac{74.9 / 143.2}{37.3 / 85.46} \\ &= 2.01 / 57.7 = 1.07 + j1.70 \\ \mathbf{Z}_t &= \mathbf{Z}_1 + \mathbf{Z}_f + \mathbf{Z}_b = 19.6 + j30.4 \\ &= 36.2 / 57.2 \\ \mathbf{I}_1 &= \frac{110 \angle 0}{36.2 / 57.2} = 3.04 \angle -57.2 \end{aligned}$$

$$\cos 57.2^\circ = 0.542$$

$$V_{2f}' = I_1 Z_f = 3.04 \times 29.7 = 90.2 \text{ volts}$$

$$V_{2b}' = I_1 Z_b = 3.04 \times 2.01 = 6.11 \text{ volts}$$

$$I_{2f}' = \frac{V_{2f}'}{Z_{2f}'} = \frac{90.2}{\sqrt{\left(\frac{2.31}{0.038}\right)^2 + (1.75)^2}} = 1.49 \text{ amp}$$

$$I_{2b}' = \frac{V_{2b}'}{Z_{2b}'} = \frac{6.11}{\sqrt{\left(\frac{2.31}{1.962}\right)^2 + (1.75)^2}} = 2.89 \text{ amp}$$

The developed torque is

$$T = \frac{7.04}{1200} \times 2.31 \left[ \frac{(1.49)^2}{0.038} - \frac{(2.89)^2}{1.962} \right] \times 16 = 11.67 \text{ oz-ft}$$

The iron losses due to rotation were assumed to be 12 watts and the friction and windage loss 3.0 watts, totaling 15 watts. The delivered torque for the assumed slip of 0.038 is therefore

$$T_{\text{del}} = 11.67 - \frac{7.04}{1200} \times 15 \times 16 = 10.26 \text{ oz-ft}$$

To determine the efficiency at slip  $s = 0.038$

$$P_{\text{co},1} = (3.04)^2 \times 2.85 = 26.3 \text{ watts}$$

$$P_{\text{co},f} = (1.49)^2 \times 2.31 = 5.1$$

$$P_{\text{co},b} = (2.89)^2 \times 2.31 = 19.3$$

$$P_{\text{ir. total}} = 25$$

$$P_{F+W} = 3$$

$$\text{Total} = 78.7 \text{ watts}$$

$$\text{Input} = 110 \times 3.04 \times 0.542 = 181.4 \text{ watts}$$

$$\text{Output} = 181.4 - 78.7 = 102.7 \text{ watts}$$

$$= 0.137 \text{ HP}$$

$$\eta = \frac{102.7}{181.4} \times 100 = 56.6\%$$

Since the rated output is 0.166 HP, the normal slip is approximately

$$\frac{0.166}{0.137} \times 0.038 = 0.046$$

Therefore normal speed is approximately

$$1200(1 - 0.046) = 1144 \text{ rpm}$$

It should be noted that no stray load losses were included in the efficiency calculation. This is justified by the fact that the no-load current of the single-phase motor is high and therefore stray load losses occur at no-load and are included with the rotational iron losses.

## PROBLEMS

In all problems following take into account the iron losses due to the main flux and neglect saturation of leakage paths.



1. Determine the running performance of the motor of Examples 32-1 and 32-2 at a slip of 0.045.
2. Calculate and plot for the motor of Examples 32-1 and 32-2 the primary current and power factor for slips of 0.30, 0.25, 0.20, 0.10, 0.075 and 0.046.
3. Calculate and plot for the motor of Examples 32-1 and 32-2 the developed torque-speed characteristic for slips of 0.30, 0.25, 0.20, 0.10, 0.075, and 0.046.
4. Repeat Problem 3 for a 25% increase in  $r_2'$ .
5. The no-load test and locked-rotor test of a  $\frac{1}{2}$ -hp split-phase motor for 110 volts, 60 cycles, 4 poles, and approximately 1725 rpm, show the following:

*No-load Test*

$$V_1 = 110 \quad I_0 = 3.55 \quad P_0 = 86.0 \\ r_1 = 1.58$$

*Locked-rotor Test*

$$V_L = 110 \quad I_L = 21.0 \quad P_L = 1592 \\ r_1 = 1.55$$

Friction and windage losses = 7.0 watts. Hot resistance at full-load:  $r_1 = 1.71$ . Determine for this motor its six constants. Assume that half of the iron losses are due to the main flux

6. Determine for the motor of Problem 5 the running performance at a slip  $s = 0.043$ .
7. For the motor of Problem 5 calculate and plot the primary current and power factor for slips of 0.30, 0.25, 0.20, 0.10, 0.075 and 0.043.
8. Calculate and plot the developed torque-speed characteristic for the motor of Problem 5 at slips of 0.30, 0.25, 0.20, 0.10, 0.075 and 0.043.
9. A  $\frac{1}{4}$ -hp split-phase motor designed for 110 volts, 60 cycles, 4 poles, and approximately  $n = 1720$  has the following constants:

$$\begin{array}{lll} r_1 = 3.8, & r_2' = 2.325 & I_0 = 1.86 \\ x_m = 52.9, & x_2' = 2.1 & r_2' = 2.1 \text{ at no-load} \\ x_1 = 4.2, & & \end{array}$$

Friction and windage losses = 10 watts. Total iron losses = 19 watts of which half can be assumed as main flux losses. Determine the main flux resistance  $r_m$ .

10. Determine the running performance for the motor of Problem 9 at a slip of 0.045.
11. Calculate and plot for the motor of Problem 9 the primary current and power factor for slips of 0.30, 0.25, 0.20, 0.10, 0.075 and 0.045.
12. Calculate and plot the developed torque-speed characteristic for the motor of Problem 9 at slips of 0.30, 0.25, 0.20, 0.10, 0.075, and 0.045.
13. The no-load and locked-rotor tests of a  $\frac{1}{4}$ -hp split-phase motor for 110 volts, 60 cycles, 4 poles, and approximately 1725 rpm, show the following:

*No-load Test*

$$V_1 = 110 \quad I_0 = 2.75 \quad P_0 = 59.5 \\ r_1 = 2.41$$

*Locked-rotor Test*

$$V_L = 110 \quad I_L = 14.6 \quad P_L = 1123 \\ r_1 = 2.21$$

Friction and windage losses = 5.4 watts. Hot resistance at full-load:  $r_1 = 2.44$ . Determine for this motor its six constants. Assume that half of the iron losses are due to the main flux.

14. Determine the running performance of the motor in Problem 13 for a slip of 0.045.
15. Calculate and plot the primary current and power factor of the motor in Problem 13 for slips of 0.30, 0.25, 0.20, 0.10, 0.075 and 0.045.
16. Calculate and plot the developed torque-speed characteristic for the motor of Problem 13 at slips of 0.30, 0.25, 0.20, 0.10, 0.075, and 0.045.

## Chapter 33

### STARTING THE SINGLE-PHASE MOTOR TYPES OF SINGLE-PHASE MOTORS

It has already been mentioned that the single-phase motor has *no starting torque* in contrast to the polyphase motor or the a-c commutator motor. In order to start the single-phase motor, either a *rotating flux* such as that in the polyphase motor has to be produced, or a *commutator* with brushes

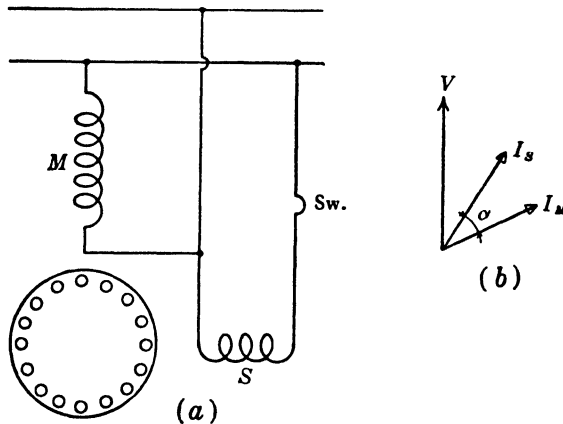


FIG. 33-1. Connection and current diagram of the split-phase motor (for starting).

has to be included with the rotor. The split-phase motor (Fig. 33-1) and the repulsion-start motor (Fig. 33-5) are examples of these two methods of starting the single-phase motor.

**33-1. Starting by means of a rotating flux.** In order to produce a rotating flux at standstill a second winding (*starting or auxiliary winding*) is necessary in the stator in addition to the main winding. The axis of the starting winding has to be *displaced in space* with respect to the axis of the main

winding, and the current in the starting winding has to be *out of time phase* with the current in the main winding.

The main winding leaves one slot or several slots empty and several slots only partly filled (see Fig. 21-12). The starting winding is placed in these empty and partly filled slots so that the axes of both windings are displaced by 90 electrical degrees.

A number of different methods are employed to achieve the time phase shift between the currents in the main and starting windings.

(a) *Split-phase motor.* The connection diagram for this type of motor is shown in Fig. 33-1.  $M$  is the main winding,  $S$  is the starting winding,  $Sw$  is a centrifugal switch. The main winding has a relatively low resistance and high reactance, while the starting winding has a high resistance and low reactance. This results in an angle  $\alpha$  of about  $30^\circ$  between the currents in the two windings (Fig. 33-1b) and in a small rotating flux superimposed on the alternating flux. The starting torque is therefore limited. The starting winding cannot remain in the circuit continuously, or overheating and noise will occur. Usually a centrifugal switch on the rotor (see Fig. 31-1) automatically disconnects the starting winding at about 70% of the synchronous speed.

It can be shown that the starting torque is, in general,

$$T = \frac{450.8}{n_s} \frac{\tau_2'}{\left(1 + \frac{x_2'}{x_m}\right)^2} \frac{N_S k_{WS}}{N_M k_{WM}} I_M I_S \sin \alpha \text{ oz-ft} \quad (33-1)$$

where the subscripts  $M$  and  $S$  refer to the main and starting windings respectively.  $k_{WM}$  and  $k_{WS}$  are the winding factors of both windings (see Art. 22-1).  $\tau_2'$  and  $x_2'$  are both referred to the main winding, and  $\alpha$  is the angle between the currents  $I_M$  and  $I_S$ .

The magnitude of the current drawn from the line ( $I_M + I_S$ ) is limited and fixed by the NEMA standards. Hence higher starting torques can be achieved mainly by increasing the angle  $\alpha$  between  $I_M$  and  $I_S$ .

(b) *Resistance-start split-phase motor.* An increase of the angle  $\alpha$  and of the starting torque can be achieved by inserting a resistance in series with the starting winding. This resistance must be cut out together with the starting winding at about 70% of the synchronous speed.

(c) *Reactor-start split-phase motor.* Inserting of a reactor in series with the main winding has the same effect as the insertion of a resistance in series with the starting winding. This reactor must be short-circuited, or otherwise made ineffective, when the starting winding circuit is opened by the centrifugal switch.

(d) *Capacitor-start motor.* A very considerable increase of the angle

$\alpha$  between  $I_M$  and  $I_S$  can be achieved when a capacitor is placed in series with the starting winding (Fig. 33-2). The capacitor causes the current in the starting winding to lead the terminal voltage (Fig. 33-2b) and, with an appropriate capacitor, the angle  $\alpha$  may approach  $90^\circ$ .

Capacitor-start motors are built from  $\frac{1}{8}$  to 10 HP. For a line voltage of 110 volts the size of the capacitor is 70–90 $\mu$ f for  $\frac{1}{8}$ -HP motors, 120–150 $\mu$ f for the  $\frac{1}{4}$ -HP motor, 230–280 $\mu$ f for the  $\frac{1}{2}$ -HP motor, and 340–410 $\mu$ f for

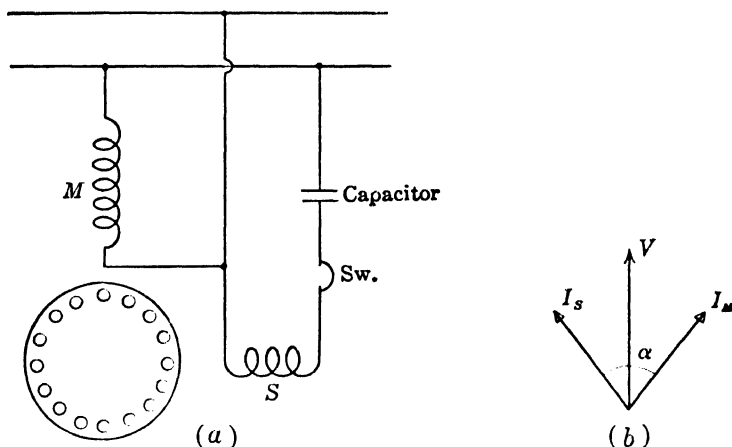


FIG. 33-2. Connection and current diagram of the capacitor-start motor.

the 1-HP motor. The starting torques, which depend on the size of the capacitor, are about 350 to 400% of rated torque at  $n = 3450$  rpm, 400 to 475% at  $n = 1725$  rpm, and 285 to 390% at  $n = 1140$  rpm.

The capacitor used for starting purposes is the relatively inexpensive electrolytic capacitor which is fit for intermittent duty only. As in the split-phase motor the starting winding of the capacitor motor is opened by a centrifugal switch at about 70% of the synchronous speed.

(c) *Permanent-split capacitor motor.* In this type of motor the starting winding and the capacitor are designed for *permanent operation*, giving an unbalanced 2-phase motor. For satisfactory running performance only a small capacitance is necessary. For example, for 110 volts the capacitor of a  $\frac{1}{20}$ -HP motor is 3 $\mu$ f, of a  $\frac{1}{8}$ -HP motor 5 $\mu$ f, of a  $\frac{1}{4}$ -HP motor 8 $\mu$ f, of a  $\frac{1}{2}$ -HP motor 15 $\mu$ f. This is much less than the capacitance necessary for high starting torque (see "Capacitor-start motor"). However, the permanent-split capacitor motor uses the same capacitor for starting and running and, therefore, has a small starting torque of about 35 to 50% of the rated torque.

Since the electrolytic capacitor cannot be used for continuous operation,

the more expensive oil or pyranol-insulated foil-paper capacitor must be used for this type of motor.

(f) *Two-value capacitor motor.* In order that the 2-phase motor described under (e) be able to develop a high starting torque and at the same time

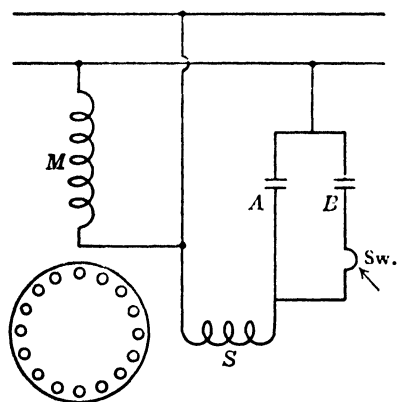


FIG. 33-3. Connection diagram of the 2-value capacitor motor with two capacitors.

have a satisfactory running performance, it is necessary to use different values of capacitance for starting and running. This can be accomplished either by using two capacitors, an electrolytic capacitor for starting and an oil capacitor for running, or by using a single oil capacitor in connection with an autotransformer.

The arrangement with two separate capacitors is shown in Fig. 33-3. *A* is an oil capacitor; *B* is an electrolytic capacitor. A centrifugal switch (*Sw.*) on the rotor shaft or a relay disconnects the electrolytic capacitor after starting is accomplished.

The arrangement with one capacitor and an autotransformer is shown in Fig. 33-4. The capacitor is connected across the terminals of the auto-

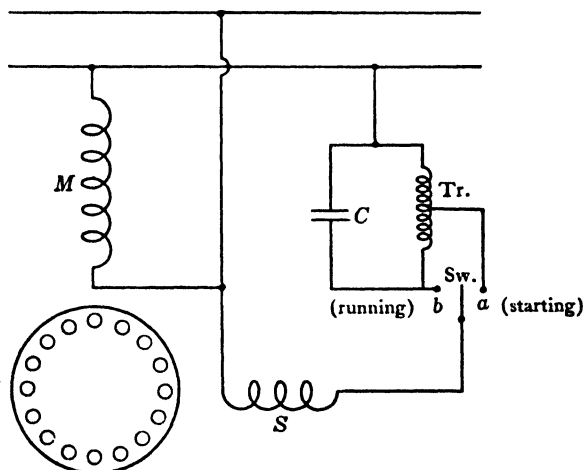


FIG. 33-4. Connection diagram of the 2-value capacitor motor with transformer.

transformer which has a mid-tap used for starting. When starting, the voltage across the capacitor is twice as large as when running, thus giving an effective capacitance at start which is four times the running capacitance.

The permanent-split capacitor motor and the 2-value capacitor motor both operate as unbalanced 2-phase motors and offer advantages in comparison with the split-phase motor and capacitor-start motor, which are pure single-phase motors. The latter motors produce a pulsating torque resulting in vibration and noise under certain conditions. The former motors develop a more uniform torque and are, therefore, quieter than the pure single-phase motors.

**33-2. Starting by means of a commutator and brushes.** This method of starting a single-phase induction motor is based upon the properties of the *repulsion motor* which is a single-phase a-c commutator motor. Its connection diagram is shown in Fig. 33-5. The stator has a single-phase winding similar to that of the single-phase induction motor, and the rotor has a d-c armature winding with commutator and brushes. The brushes are short-circuited. It will be shown in Art. 48-3 that this motor has series-motor characteristics and is, therefore, able to develop a high starting torque.

Reversal of the repulsion motor can be achieved either by shifting the brushes (see Art. 48-3), or by arranging two identical single-phase windings in the stator, one for each direction of rotation.

Two types of single-phase motors employing the repulsion motor properties for starting are available: the repulsion-start induction motor and the repulsion induction motor.

(a) *Repulsion-start induction motor.* This motor is built exactly as the repulsion motor. However, when the rotor has reached about  $\frac{2}{3}$  of the synchronous speed, a centrifugal mechanism short-circuits the commutator segments so that the armature acts as a squirrel-cage winding in a single-phase stator. A view of such a motor, disassembled, is shown in Fig. 33-6. The centrifugal mechanism is sometimes designed to lift the brushes from the commutator at the same time that a bracelet short-circuits the commutator segments. The repulsion-start induction motor starts as a repulsion motor but operates as an induction motor with an approximately constant-speed characteristic.

(b) *Repulsion-induction motor.* The stator is the same as that of the repulsion (single-phase) motor. In addition to the d-c armature winding with commutator and brushes a squirrel-cage winding is also included in the rotor. No centrifugal mechanism is used to short-circuit the d-c armature winding so that both rotor windings always operate in parallel.

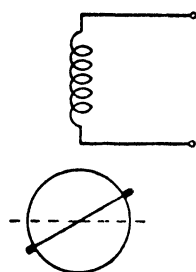


FIG. 33-5. Connection diagram of the repulsion motor.

Depending upon the design of the windings, the motor may have either an approximately constant speed characteristic, as the induction motor, or a varying speed characteristic, as the repulsion (series) motor.

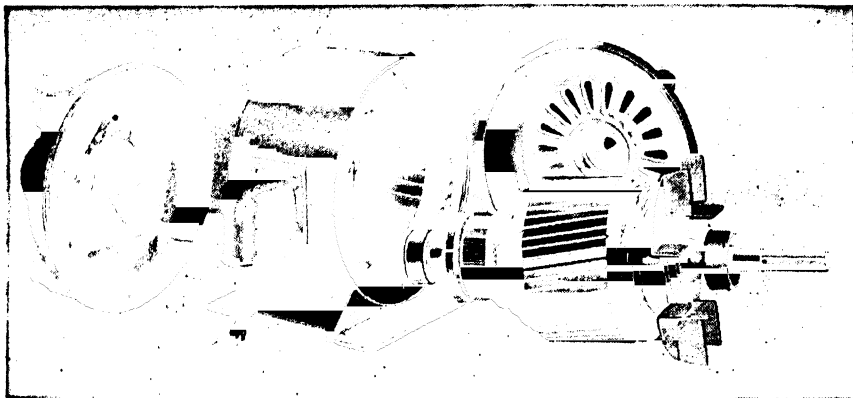


FIG. 33-6. Disassembled small repulsion-start single-phase motor.

**33-3. The shaded-pole motor.** For a very small output and a small starting torque the construction shown in Fig. 33-7 is used. The main

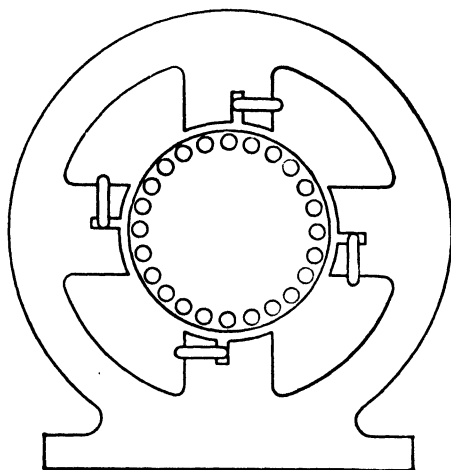


FIG. 33-7. Shaded-pole motor.

winding, not shown in the figure, is a concentrated single-phase winding placed on salient poles. Around a portion of each pole a copper strap (called *shading coil*) is placed, thus forming a short circuit. The rotor is of the squirrel-cage type.

The main winding produces an alternating flux. However, the flux will not be in time-phase over the whole pole area: within the part of the pole lying *inside* the shading coil the flux will be delayed with respect to the flux in the part of the pole lying *outside* the shading coil. This is due to the induced current in the shading coil which delays the change of flux

interlinkage within this coil. This means that the flux is a maximum in the shaded portion of the pole later than in the unshaded portion, which is identical with a progressive shift of the flux in the direction of the unshaded pole-portion to the shaded pole-portion. The effect of this progressive shift of the flux is the same as that of a weak rotating flux.

## Chapter 34

---

### LOSSES IN INDUCTION MOTORS HEATING AND COOLING

---

---

**34-1. Losses in induction motors.** As in d-c machines (see Chapter 10) the losses are produced by the flux as well as by the currents in the stator and rotor.

(a) *Losses due to the main flux.* Hysteresis and eddy-current losses due to the main flux appear in both the stator and rotor, because both are subject to magnetization in alternate directions (see Art. 10-1). However, the frequency of magnetization is constant for the stator, namely, equal to the line frequency  $f_1$ , and variable for the rotor, since it is the relative speed between the rotating flux of the machine and the rotor which determines the frequency of magnetization of the rotor. In the rotor the frequency is  $f_2 = sf_1$ . At rated speed  $s$  is small and there are practically no hysteresis or eddy-current losses due to the main flux in the rotor.

As in d-c machines the iron losses due to the main flux are larger than those obtained from Eq. 10-5, or from the iron loss curves (given at end of text), due to the non-sinusoidal flux distribution (non-sinusoidal  $B$  curve), non-uniform distribution of the flux over the cross-section of the armature core, punching of the laminations, and the filing of the laminations in order to remove the burrs. The increase of the iron losses due to these factors may be as high as 30 to 40%.

Consider Fig. 10-1. It has been pointed out that the *slot openings* produce a *ripple* superimposed on the average flux density which causes high-frequency iron losses. In induction motors both the rotor and stator are slotted. Therefore, the stator slot openings produce surface losses in the rotor and the rotor slot openings produce surface losses in the stator. Medium-sized and larger induction motors have open slots in the stator and semi-open slots in the rotor; smaller induction motors have semi-open slots in both parts. The surface losses are larger in machines with open stator slots.



Due to the fact that both the rotor and stator have slots, another kind of loss appears in the induction motor: the flux pulsation due to the slot openings *penetrates the teeth* themselves and produces eddy currents as well as hysteresis losses in the teeth. The frequency of these pulsations is the same as that of the tooth surface losses, i.e., for the stator  $Q_2 n/60$  and for the rotor  $Q_1 n/60$ . The magnitude of the variation of the flux density in the teeth depends upon the saturation in the teeth. The total losses due to the slot openings are larger in induction motors than in d-c machines (and synchronous machines). These losses, as a percentage of the iron losses due to the main flux, (Eq. 10-5), are approximately: 80 to 120% in squirrel-cage motors with semi-open slots in stator and rotor, 150 to 200% in squirrel-cage motors with open slots in stator and semi-open slots in rotor, and 180 to 220% in wound rotor motors.

The flux ripple produced by the slot openings induces parasitic currents not only in the iron but also in the bars of a squirrel-cage rotor. The currents induced in these bars may become considerable and the copper losses in the bars high, if the slot pitch of the cage is much different from the stator slot pitch. A difference up to 30% between the slot pitches keeps the losses at a low level. Equal slot pitches cannot be used because this would produce locking torques which may prevent starting of the motor.

(b) *Losses due to the load currents.* The load currents produce  $I^2 R$  losses in the stator and rotor windings. Furthermore, the *cross-flux in the slot* may produce additional copper losses through *skin-effect* (see Art. 10-1) which forces the current to flow in the top part of the conductor, thus decreasing the effective area of the conductor and increasing its resistance which results in an increase of the copper losses. The skin-effect is proportional to the square root of the frequency. It is negligible at rated load in the rotor since the frequency of the rotor currents at rated load is very small. Although the stator frequency is always equal to the line frequency, i.e., usually 60 cycles, the skin-effect loss in the stator is usually small (in medium-sized and larger motors about 5 to 15% of the stator  $I^2 R$  losses).

It has been shown in Art. 22-2 that the mmf of a distributed winding consists of a main wave and harmonics. While the main wave produces the main flux, the harmonics produce parasitic fluxes which travel with different speeds than the main flux and some in an opposite direction to the main flux. The amplitudes of these rotating fluxes are proportional to the current in the winding and inversely proportional to the length of air-gap. Since the induction motor has a smaller air-gap than the other a-c machines, in order to keep down its magnetizing current, the harmonic fluxes are stronger in it than in the other a-c machines with larger air-gaps.

At no-load the stator current of the induction motor is small and, therefore, the stator mmf and the harmonic fluxes are also small. At full-load the harmonic fluxes may become considerable, depending upon the design of the winding (see Art. 22-2). Since the stator harmonic fluxes travel with respect to the rotor, they produce rotor surface losses and tooth-pulsation losses in the same way as the slot opening ripple produces losses (Fig. 10-1). The same consideration also applies to the rotor: at load the rotor currents produce harmonic fluxes which travel with respect to the stator and cause stator tooth-surface and tooth-pulsation losses. These losses are mainly eddy-current losses.

In well-designed induction motors the losses due to the harmonic fluxes of stator and rotor mmf are 0.6 to 3.0% of the motor output. The larger value applies to small motors; the lower value, to large motors. A motor of 1000-HP output has about 1% harmonic losses. In poorly designed induction motors the harmonic losses may be 4 to 5 times as high as the values given above.

Just as the flux ripple due to the slot openings induces currents in the bars of the squirrel-cage rotor, the flux harmonics of the stator induce currents in the squirrel-cage bars. In well-designed induction motors these current losses usually are small, about 0.03 to 0.05% of the output.

In large machines the leakage fluxes around the end-windings of the stator, due to the load current, are considerable and, since they move with respect to the stator, they induce eddy currents in metallic parts, such as the end plates, finger plates, bolts, etc. These losses can be neglected in small machines.

(c) *Friction and windage losses.* The friction and windage losses in the induction motor are the same as in the d-c machine (see Art. 10-1).

(d) *No-load and load losses; stray-load losses.* The losses which appear at no-load and those which appear at load are shown in Table 34-1.

TABLE 34-1

No-load losses	Iron losses in the stator due to the main flux.	Surface and tooth pulsation losses in stator and rotor due to slot openings.	Copper losses in the squirrel cage due to the slot openings.	Windage and bearing friction losses.
Load losses	$I^2R$ losses in the stator and rotor windings.	Surface and tooth pulsation losses in stator and rotor due to harmonic fluxes.	Skin effect losses in the stator winding.	Losses in the structural parts due to leakage fluxes.

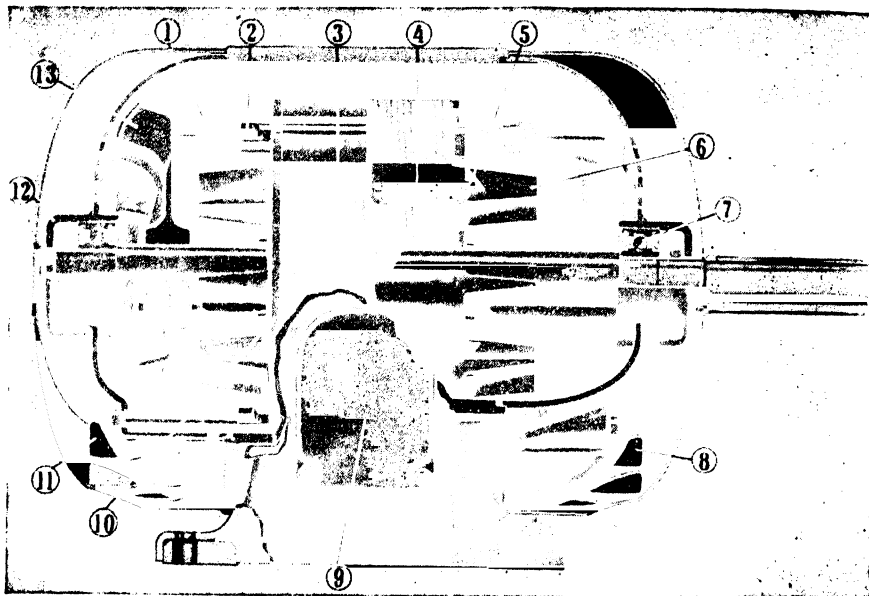


FIG. 34-1. Cutaway view of a splash proof ball-bearing, squirrel-cage motor.

- |                            |                               |
|----------------------------|-------------------------------|
| 1. End turn of stator coil | 7. Prelubricated ball bearing |
| 2. Locking bar             | 8. Ventilation openings       |
| 3. Stator core             | 9. Conduit box                |
| 4. Rotor                   | 10. End plates                |
| 5. Balancing lug           | 11. End brackets              |
| 6. Rotor blades            | 12. Bearing hub               |
|                            | 13. Fan                       |

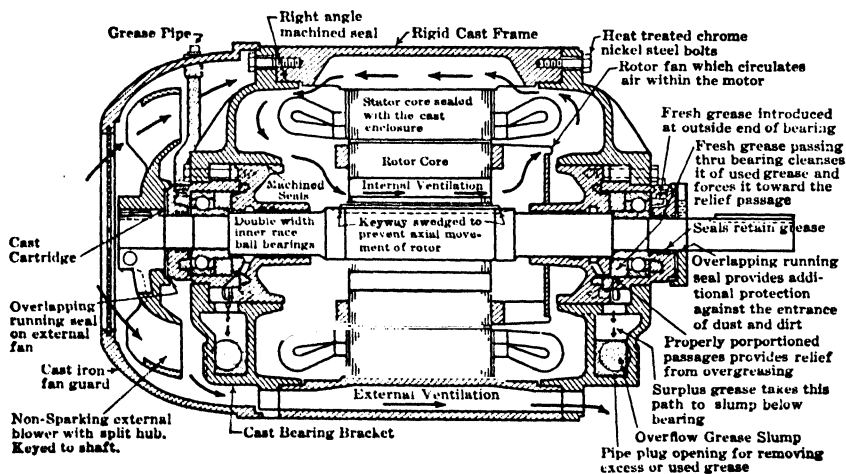


FIG. 34-2. Air flow in a totally enclosed fan-cooled, squirrel-cage motor.

The additional losses due to the load (these are items 2, 3, and 4 of the second row) are called *stray load-losses*, as in the d-c machine.

(e) *Examples of loss distribution and efficiencies.* In the following tabulation is shown the loss distribution of three induction motors, one of which is single-phase and the other two polyphase.

$\frac{1}{6}$ HP, 4 poles, single phase, 60 cycles, 110 volts, $n = 1720$ rpm	
Stator winding $I^2R$ . . . . .	25 watts
Rotor winding $I^2R$ . . . . .	20
Total iron loss (including stray load loss) . . . . .	20
Bearing friction and windage loss . . . . .	10
	<u>75 watts (Total)</u>

Output  $\frac{1}{6}$  HP = 124.5 watts

$$\text{Efficiency} = 100 \frac{124.5}{124.5 + 75} = 62.3\%$$

3 HP, 4 poles, 60 cycles,

3 phase, 220/440 volts, 1745 rpm

250 HP, 8 poles, 60 cycles,

3 phase, 2300 volts, 883 rpm

	<i>Aluminum cast squirrel-cage Rotor</i>	<i>Squirrel-cage Rotor</i>
Stator winding . . . . .	140 watts	4300 watts
Rotor winding . . . . .	80	3600
Stray load loss . . . . .	50	1900
Iron loss . . . . .	120	2700
Bearing friction and windage loss . . . . .	<u>50</u>	<u>2000</u>
	440 watts (Total)	14,500 watts (Total)

Output =  $746 \times 3 = 2238$  watts

$$\text{Efficiency} = 100 \frac{2238}{2238 + 440} = 83.6\%$$

Output =  $746 \times 250 = 186.5$  kw

$$\text{Efficiency} = 100 \frac{186.5}{186.5 + 14.5} = 92.8\%$$

**34-2. Heating and cooling of induction motors.** The discussion of Art. 10-2 with respect to the insulation, limiting temperatures, heat conductivity, heat transfer and cooling of the d-c machine also applies to the induction motor. Sufficient cooling must be provided in order to dissipate the heat due to the losses. Fig. 34-1 shows a cutaway section of an open splash-proof squirrel-cage motor. Fig. 34-2 shows the air flow in a totally enclosed fan-cooled squirrel-cage motor. Note the internal and external ventilation separated from each other and flowing in opposite directions. A cutaway section of a totally enclosed fan-cooled squirrel-cage motor is shown in Fig. 23-12.

## PROBLEMS

1. A 7.5-HP, 230-volt, 4-pole, 3-phase, 25-cycle, squirrel-cage induction motor was loaded by means of a Prony brake and the following data were recorded for three different loads. Power was measured by the 2-wattmeter method.

	(1)	(2)	(3)
Voltage .....	230	230	230
Line current .....	25.1	14.4	9.55
Watts $W_1$ .....	5500	2950	1550
Watts $W_2$ .....	2920	1120	-490
Scale reading (lb) .....	36.8	17.3	4.0
Speed (rpm) .....	682	710	733

A brake arm 24 in. long was used, and the tare reading on the scale was 1.61 lb. Determine the performance for each point including HP output, slip, torque, power factor, and efficiency.

2. A 5-HP, 230-volt, 4-pole, 60-cycle, 3-phase, squirrel-cage induction motor is delivering rated output. The iron loss is 150 watts of which 65 watts are due to the main flux; stator copper loss, 125 watts; rotor copper losses, 130 watts; friction and windage losses, 90 watts; stray load losses, 95 watts. Determine: (a) power transferred by rotating field; (b) mechanical power in watts developed by rotor; (c) power input in watts; (d) efficiency; (e) slip; (f) torque in pound-feet.

3. Repeat Problem 2 for a 6-HP output assuming the following: stator copper loss, rotor copper loss and the stray load loss vary as the square of the output, and the core and friction and windage loss remain constant.

4. A 100-HP, 3-phase, 4-pole, 440-volt, 60-cycle, squirrel-cage induction motor is operating at full-load at a slip  $s = 0.02$ . The full-load stator current is 130 amp and the stator hot resistance is 0.032 ohm per phase. The no-load current is 1135 amp and the no-load power input 4580 watts. Forty percent of the total iron losses can be assumed to be the iron losses due to the main flux. The friction and windage losses are 1.7% of the output and the stray load loss 1.5% of the output. Determine the full-load efficiency and power factor.

5. The motor of Problem 4 takes 92 amp when delivering  $\frac{3}{4}$  rated output and 150 amp when delivering  $\frac{1}{2}$  rated output. The iron losses due to the main flux can be assumed the same as at full-load. Also, the friction and windage losses remain unchanged. The stray load losses vary as the square of the primary current, and the slip is proportional to the output. Determine the efficiency and power factor at  $\frac{3}{4}$  and  $\frac{1}{2}$  load. Combine with Problem 4 and draw curves of efficiency and power factor vs. load.

6. A 2300-volt, 3-phase, 8-pole, 60-cycle, squirrel-cage induction motor takes a power input of 361 kw when delivering rated output. The rated line current is 103 amp and the speed 879 rpm. At rated output, friction and windage losses are 4.40 kw, stray load losses 3.36 kw, and the iron losses are 5.0 kw of which 2.2 kw are due to the main flux. The stator resistance at 75°C is 0.158 ohm per phase. Determine the output, efficiency and power factor at full-load.

7. Determine the output, efficiency and power factor of the motor in Problem 6 for power inputs of 275 and 450 kw. The respective line currents are 80 and 129.5 amp. The stray load losses are proportional to the square of the power input; the iron losses, iron losses due to main flux, and friction and windage losses are the same as for full-load in Problem 6. Assume slip proportional to power input. Combine with Problem 6 and draw curves of efficiency and power factor vs. output.

## Chapter 35

### MECHANICAL ELEMENTS OF THE SYNCHRONOUS MACHINE

As in the d-c machine the flux of the synchronous machine is produced by a direct current. However, quite different from the d-c machine, the pole structure of the synchronous machine is the inner part of the machine which rotates, while the armature is the outer part and is stationary. As in the induction motor, the stationary part is called the stator and the

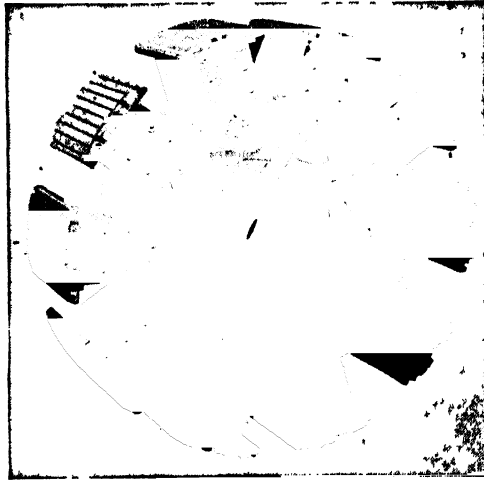


FIG. 35-1 Salient-pole rotor of a 10-pole synchronous machine (field coils not shown)

rotating part the rotor. Thus, of the three main kinds of electric machines—namely the d-c machine, induction motor, and synchronous machine—in the d-c machine and the synchronous machine the flux is produced by a direct current, while in the induction motor the flux is produced by an alternating current.

It will be explained in the following that the synchronous machine is

a special case of the induction motor. On the other hand, the d-c machine is nothing more than a synchronous machine with an added special device, the commutator.

A distinction must be made between synchronous machines having six or more poles and those having two and four poles. The rotors of the former are of the salient-pole type (*salient-pole rotors*), as in the d-c

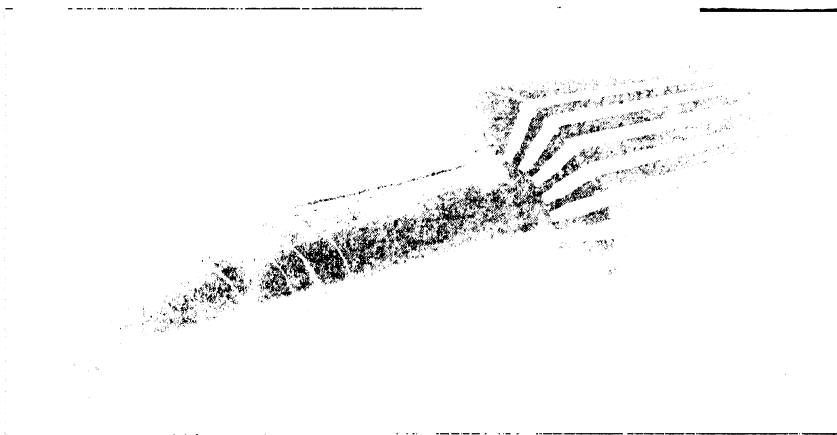


FIG. 35-2. Cylindrical rotor of a 2-pole synchronous machine.

machine. Fig. 35-1 shows a salient-pole rotor, without the field coils, for a 10-pole synchronous machine. Two-pole and 4-pole 60-cycle machines rotate at 3600 and 1800 rpm respectively. When used as generators, they are driven by steam turbines. The rotors are subject to high mechanical stresses and for this reason are built of high-grade steel in a cylindrical shape (*cylindrical rotors*). Fig. 35-2 shows a cylindrical rotor (without winding) of a 2-pole synchronous machine. The d-c field winding is placed in slots and held in place by heavy metal wedges. The two large teeth correspond to the salient poles of the salient-pole rotor. It should be mentioned that small 4-pole machines are built with salient poles.

While the field winding of the salient-pole machine consists of concentrated coils as in the d-c machine, the field winding of the cylindrical rotor machine is distributed similar to a single-phase winding (see Fig. 21-9).

**35-1. The salient-pole machine.** Fig. 35-3 shows the main flux paths of a 4-pole salient-pole machine. The general shape and construction of the stator is very similar to that of the induction motor. The core is laminated just as in the induction motor and the d-c machine, and for the same

reason. Fig. 35-4 shows a partially wound stator of a larger salient-pole machine, and Fig. 35-5 shows a complete stator.

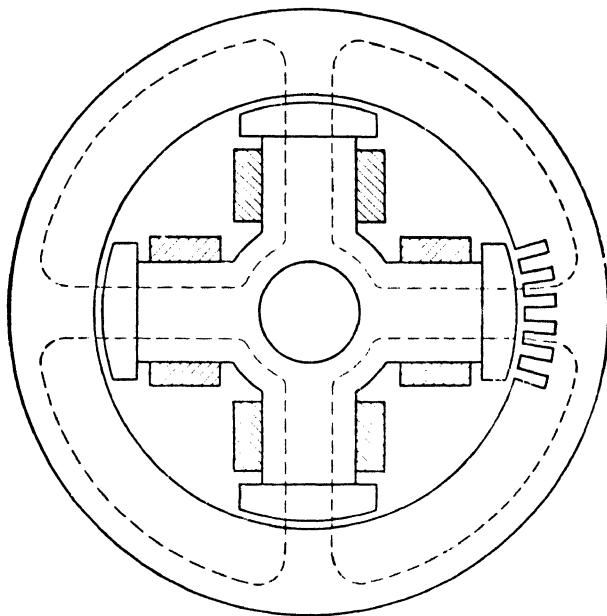


FIG. 35-3. Main flux paths of a 4-pole, salient-pole synchronous machine.

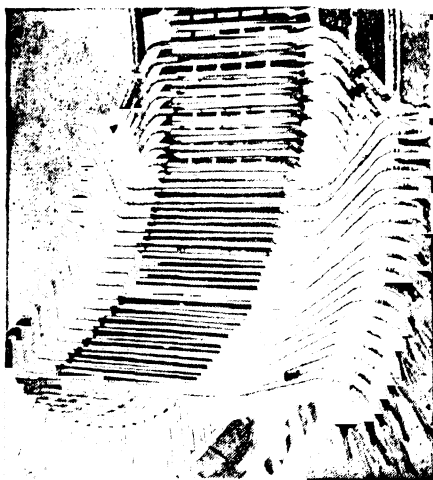


FIG. 35-4. Partially wound stator of a large synchronous machine with salient poles.

Fig. 35-6 shows a punching of a salient-pole machine, with slots for a squirrel-cage winding which is called a *dampcr* or an *amortisseur* winding.



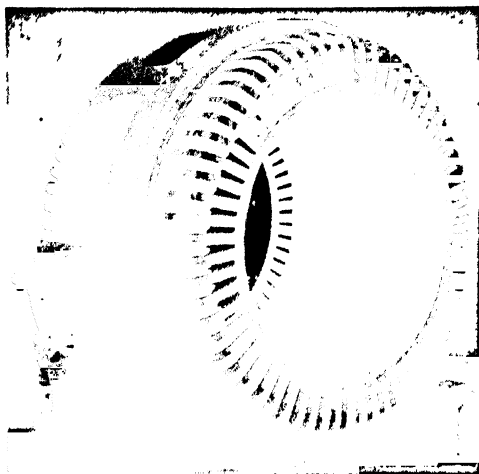


FIG. 35-5. Complete stator of a 3-phase, salient-pole synchronous motor, 1000 HP, 2200 volts, 514 rpm

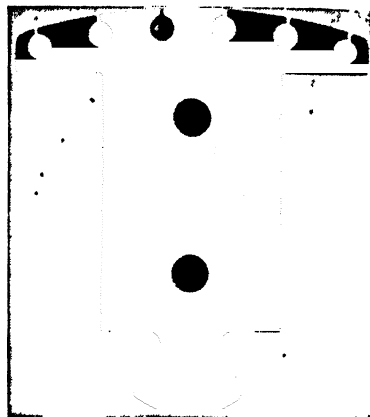


FIG 35-6 Pole punching of a salient-pole machine with slots for the damper winding

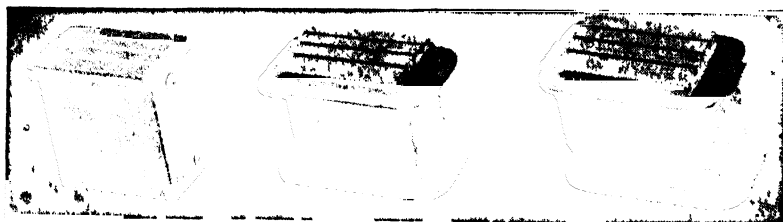


FIG. 35-7. Salient pole in three stages of assembly.

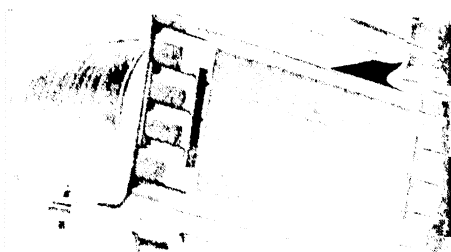


FIG. 35-8. Details of a damper winding.

This winding is necessary in all synchronous motors for starting purposes (see Art. 40-4) and is often used in synchronous generators to damp out oscillations which may occur during parallel operation (see Art. 42-4).

Fig. 35-7 shows a salient pole in three stages of assembly: the bare pole, the insulated pole, and the complete pole. Fig. 35-8 shows details



FIG. 35-9. Complete rotor of a 4-pole, salient-pole, synchronous machine.

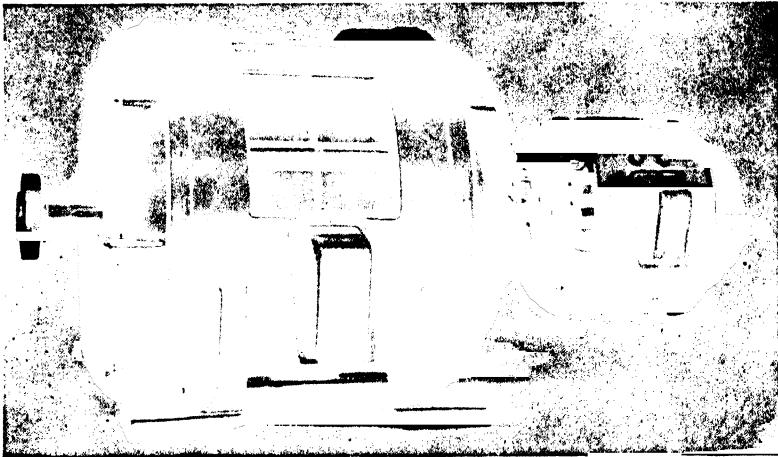


FIG. 35-10. Complete synchronous machine coupled with exciter.

of a damper winding: the bars of each pole are connected to segments which (in all motors) are bolted together making a complete ring connection around the rotor. Fig. 35-9 shows a complete salient-pole rotor of a 4-pole generator. Fig. 35-10 shows a complete synchronous machine coupled with its exciter.

**35-2. The cylindrical rotor machine.** Fig. 35-11 shows a punched stator segment of a 2-pole machine with a cylindrical rotor. Fig. 35-12 shows a stator core assembly of a cylindrical rotor machine without winding. Fig. 35-13 shows the complete stator of a 3-phase cylindrical rotor generator, rated at 80,000 kw, 1800 rpm, 22,000 volts.

A complete 2-pole rotor, without winding, was shown in Fig. 35-2.

In this figure the bottom part of each slot does not contain conductors but is used for ventilation purposes. The grooves at the top of each slot are designed to hold the wedges.

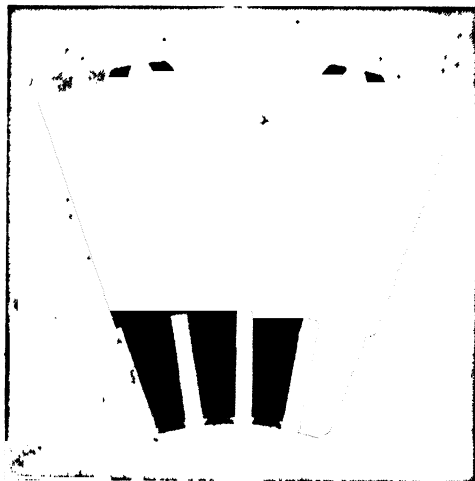


FIG. 35-11. Punched stator segment of a 2-pole machine with cylindrical rotor.

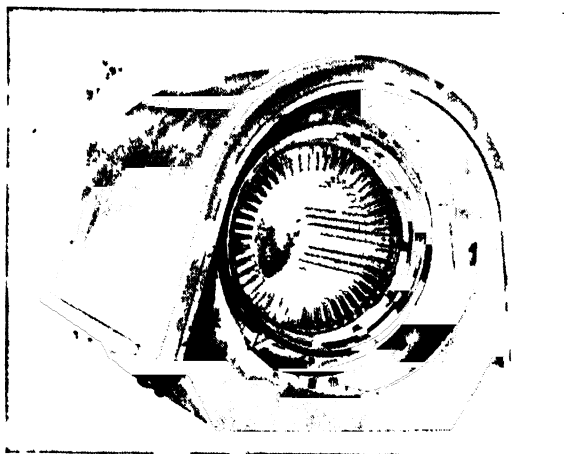


FIG. 35-12. Stator core assembly without winding, for a cylindrical rotor machine.

Fig. 35-14 demonstrates the process of assembling the rotor winding. Fig. 35-15 shows a rotor with the winding and wedges assembled. Fig. 35-16 shows part of a complete rotor: to the left, the end-winding retaining ring; in the center, the ventilation fan; to the right, the slip rings through which the d-c exciting current is introduced.

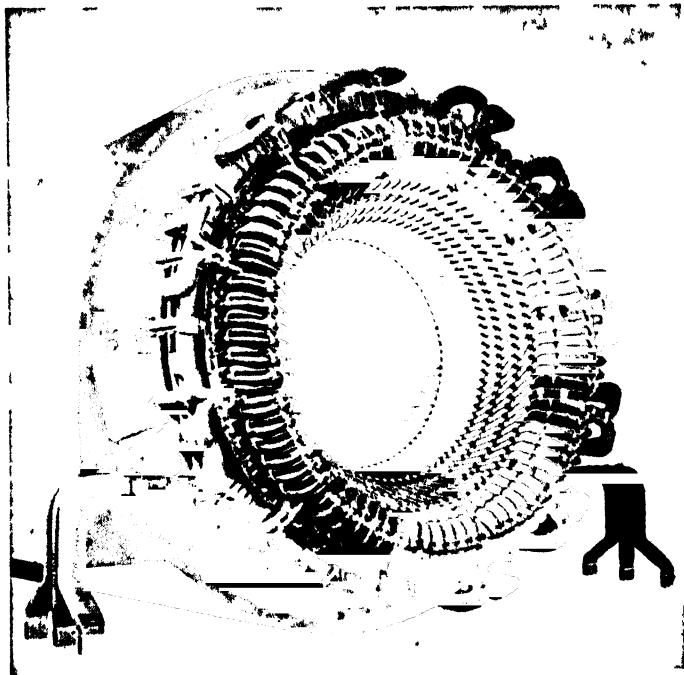


FIG. 35-13. Complete stator of a 3-phase cylindrical rotor generator, 80,000 kw, 85% p.f., 22,000 volts, 1800 rpm.



FIG. 35-14. Winding the coils of a 2-pole cylindrical rotor.



FIG. 35-15. Cylindrical rotor complete with winding and slot-wedges.



FIG. 35-16. Part of a cylindrical rotor for a 12,500-kva machine showing the end winding retaining ring, ventilating fan, and slip rings.

Fig. 35-17 shows a 2-pole cylindrical rotor generator with its turbine and exciter. The rating of this unit is 31,250 kva at 14,440 volts, 0.80 power factor, 60 cycles.

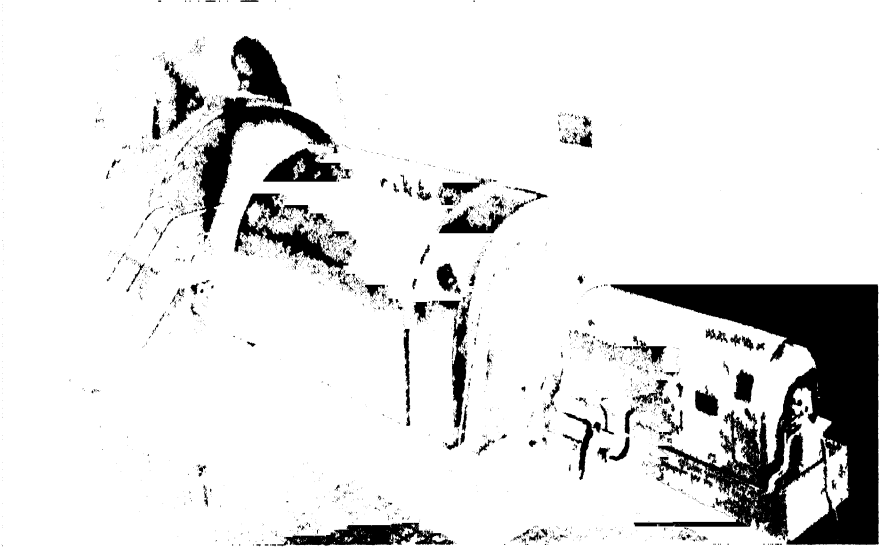


FIG. 35-17. Three-phase cylindrical rotor generator, 31,250-kva, 14,440 volts, 80% p.f., 3600 rpm, with turbine and exciter.

No distinction has been made in the foregoing between the synchronous generator and synchronous motor because the synchronous machine is able to operate both as a generator and as a motor, just as the d-c machine. The cylindrical rotor machine is chiefly used as a generator while most synchronous motors are of the salient-pole type.

## Chapter 36

### EQUIVALENT CIRCUIT OF THE SYNCHRONOUS MACHINE

**36-1. General considerations.** The stator as well as the rotor of the synchronous machine is connected to a source of power. Therefore, as for the doubly fed induction motor (see Art. 29-3d), a uniform torque cannot be developed at *any* rotor speed, because the stator and rotor mmf's are not at standstill with respect to each other at all rotor speeds. In

general, the doubly fed machine has two speeds at which the torque is uniform. These speeds are given by Eq. 29-1:

$$n = \frac{120(f_1 \mp f_2)}{p} \quad (36-1)$$

Since the rotor is connected to a d-c source of power in the case of the synchronous machine,  $f_2 = 0$ , and there is only a *single speed* at which a uniform torque exists, namely,

$$n_s = \frac{120f_1}{p} \quad (36-2)$$

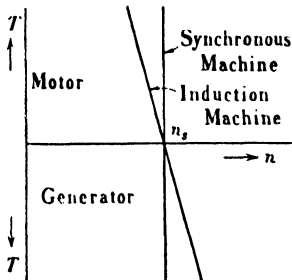


FIG. 36-1. Torque-speed characteristic of the synchronous machine and induction machine.

This is the *synchronous* speed of the machine. The synchronous machine is bound to its synchronous speed. Its torque-speed characteristic is a vertical line, as shown in Fig. 36-1. For comparison, the torque-speed characteristic of the induction machine is also shown in this figure.

When a synchronous generator is operating as a single unit, it is necessary for the rotor speed to remain *constant* and *independent* of the torque in order that the *frequency* remain *constant*.

The synchronous machine represents a special case of the doubly fed induction machine and is therefore a special case of the transformer.

However, it has the character of a *current transformer*, while the induction machine has the character of a *voltage transformer*. The voltage transformer operates with a constant primary voltage and therefore with almost a constant flux from no-load to full-load, since its voltage drop is small. The current transformer when operated with a constant primary current has a large flux variation between no-load and full-load: at no-load its flux is fixed by the mmf of the primary current alone; at load its flux is determined by the resultant of the primary *and* secondary mmf's. The primary current of the synchronous machine is the direct current of the field winding; the secondary current is the armature current.

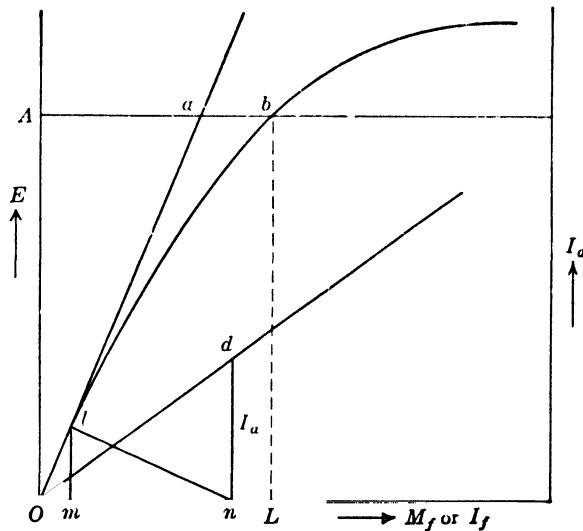


FIG. 36-2. No-load and short-circuit characteristic of a synchronous machine.

Since there is no direct proportionality between mmf and flux in iron, the magnetization curve of the material has to be used for a study of the current transformer. The same reasoning applies to the synchronous machine, i.e., the saturation curve (*no-load characteristic*) of the magnetic circuit of the synchronous machine has to be used for the study of its behavior and performance. This is the same as in the d-c machine, especially the d-c series machine, which also operates with a variable flux. The no-load characteristic is indispensable for a study of the d-c machine but was not mentioned in the foregoing study of the induction motor. It was not necessary in the case of the induction motor because this machine behaves as a voltage transformer and operates with almost a constant flux between no-load and full-load, i.e., it operates at a single



point of the no-load characteristic and the entire curve is therefore unnecessary.

Curve *Olb* in Fig. 36-2 is a no-load characteristic: as for the d-c machine, the field ampere-turns (field mmf,  $M_f$ ) or the field current  $I_f$  is shown on the axis of abscissae and the pole-flux  $\Phi$  or the armature (stator) emf  $E$  is shown on the axis of ordinates. At low values of  $\Phi$  the no-load characteristic is a straight line because the mmf required for the iron parts of the magnetic path (see Art. 4-2) is negligible in comparison with the mmf required to maintain the flux  $\Phi$  in the air-gap between the rotor and stator. The straight line *Oa* which coincides with the lower part of the no-load characteristic is called the *air-gap line* (see Art. 4-2). The field mmf necessary to induce a certain emf *OA* in the stator winding is equal to *Ab*. The part *Aa* of this mmf is necessary to drive the flux, which corresponds to  $E = OA$ , through the air-gap, and the part *ab* is necessary to drive the flux through the iron parts of the magnetic path.

**36-2. Equivalent circuit of the synchronous machine.** The rotor of the synchronous machine runs at the speed given by Eq. 36-2, i.e., if the rotor has  $p$  poles and the stator current has a frequency  $f_1$ , the rotor speed is  $n_r = 120f_1/p$ . The stator winding must be wound for the same number of poles as that of the rotor. The speed of the stator mmf with respect to the stator is given by Eq. 24-4, which is identical with Eq. 36-2, i.e., stator and rotor mmf's are at standstill with respect to each other. This is to be expected since Eq. 36-2 has been derived for the condition of a uniform torque.

Thus the main flux of the machine, which is produced by the stator and rotor mmf's, travels at synchronous speed  $n_s$  with respect to the stator and zero speed with respect to the rotor, i.e., the main flux induces emf's in the stator winding but none whatever in the rotor windings (field winding and damper winding). The rotor windings appear open with respect to the main flux and therefore the equivalent circuit of the synchronous machine is given by Fig. 36-3. The same result can be obtained from the equivalent circuit of the induction motor, Fig. 25-4, since for the synchronous machine  $s = 0$ .

In Fig. 36-3,  $r_a$  is the armature resistance,  $x_l$  the leakage reactance of the armature, and  $x_{ad}$  the main flux reactance. The corresponding symbols for the induction machine are  $r_1$ ,  $x_1$ , and  $x_m$ . The reason for using the symbol  $x_{ad}$  instead of  $x_m$  will become clear from the discussion which follows (see Art. 38-1).

The equivalent circuit Fig. 36-3 of the synchronous machine is simple,

but difficulties arise with its use because of the main flux reactance  $x_{ad}$ . It has been previously explained that the synchronous machine, as a current transformer, operates with a variable main flux between no-load and full-load; this means that the permeability of the main flux path is a variable quantity and therefore  $x_{ad} = \omega L_{ad}$  is a variable quantity (see Art. 12-2). Hence the equivalent circuit of Fig. 36-3 will yield correct results only for the unsaturated machine operating on the air-gap line, where the permeability is constant; otherwise the value of  $x_{ad}$  must be changed with changing load. It is different with the induction motor which operates on the *voltage transformer* principle; the flux of the induction motor changes little between no-load and full-load and therefore its  $x_m$  can be treated as a constant, especially for medium-sized and larger-sized motors (see Art. 25-2).

Since the current flowing in the reactance  $x_{ad}$  (Fig. 36-3) is the armature current  $I_a$ , the quantity  $-jI_a x_{ad}$  is the emf induced in the armature winding by the flux produced by the armature winding *alone*. This means that the equivalent circuit of Fig. 36-3 assumes that two *separate* fluxes exist in the main path of the machine, one produced by the field winding, and the other produced by the armature winding. This again indicates that the equivalent circuit of Fig. 36-3 is applicable only for the unsaturated machine, because only in this machine is it permissible to calculate with separate fluxes. In a saturated machine only one flux is to be considered, namely, that produced by the resultant mmf of the machine.

Thus it is observed that the equivalent circuit of Fig. 36-3 has a limited application. Furthermore, it applies only to the machine with a cylindrical rotor. It cannot be applied to a salient-pole machine: this is due to the fact that this machine, with salient poles followed by interpolar spaces, has a variable reluctance around the stator bore. As a consequence of this variable reluctance an entirely different method of treatment must be applied to the salient-pole synchronous machine.

The axis going through the center of the pole is called the *direct axis*, and the axis going through the center of the interpolar space is called the *quadrature axis*. These two axes are very important in the treatment of the salient-pole machine. In the cylindrical rotor machine only the direct axis through the center of the pole is to be considered. The subscript  $d$  in  $x_{ad}$  indicates the direct axis:  $x_{ad}$  is the reactance of the main flux

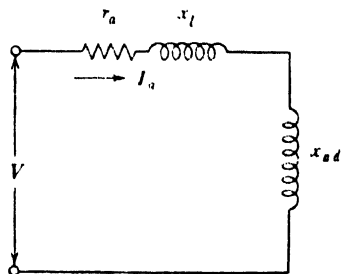


FIG. 36-3. Equivalent circuit of the synchronous machine.

which has an axis of symmetry coinciding with the center-line of the pole.

Note that the equivalent circuit of the synchronous machine shown in Fig. 36-3 does not contain the resistance  $r_m$  (see Arts. 14-2 and 25-2) which corresponds to the iron losses due to the main flux and which appears in the equivalent circuits of both the transformer and induction motor. This is explained by the fact that the primary winding of the synchronous machine is the field winding and that the iron losses due to the main flux are supplied mechanically by the rotor.

## Chapter 37

### PHASOR DIAGRAMS OF GENERATOR AND MOTOR WITH CYLINDRICAL ROTOR. ARMATURE REACTION. GENERATOR CHARACTERISTICS

**37-1. Phasor diagrams of synchronous generator and motor with cylindrical rotor. Armature reaction.** First the unsaturated machine, i.e., the machine operating on its air-gap, will be considered; then the saturated machine.

(a) *Machine unsaturated.* In this case the equivalent circuit of Fig. 36-3 can be used. Kirchhoff's mesh equation for generator operation is,

$$\mathbf{E}_f - j\mathbf{I}_a x_{ad} - j\mathbf{I}_a x_l = \mathbf{I}_a r_a + \mathbf{V} \quad (37-1)$$

and for motor operation,

$$\mathbf{V} + \mathbf{E}_f - j\mathbf{I}_a x_{ad} - j\mathbf{I}_a x_l = \mathbf{I}_a r_a \quad (37-2)$$

$E_f$  is the emf induced in the armature winding by the *field* flux. In the case of the generator the sum of the three emf's balances the voltage drop in the armature resistance and in the load. In the case of the motor, the sum of the impressed voltage and the three emf's balances the voltage drop in the armature resistance.

Eq. 37-1 for the generator can be rewritten as

$$\mathbf{V} + \mathbf{I}_a r_a + j\mathbf{I}_a (x_l + x_{ad}) = \mathbf{E}_f \quad (37-3)$$

and Eq. 37-2 for the motor can be rewritten as

$$\mathbf{V} = -\mathbf{E}_f + \mathbf{I}_a r_a + j\mathbf{I}_a (x_l + x_{ad}) \quad (37-4)$$

$\mathbf{E}_f$  appears in the latter equation with a minus sign, being the counter-emf of the motor, just as in the d-c motor and induction motor.  $x_{ad}$  is the reactance corresponding to the main flux, the axis of which is the direct axis, and is called the *armature reaction reactance of the direct axis*. The sum

$$x_l + x_{ad} = x_d \quad (37-5)$$

is called the *direct-axis synchronous reactance*.

The phasor diagrams which correspond to Eqs. 37-3 and 37-4 are shown in Figs. 37-1 and 37-2, both for lagging current. Since  $E_f$  is 90 electrical degrees behind the flux  $\Phi_f$  producing it and since this flux is in

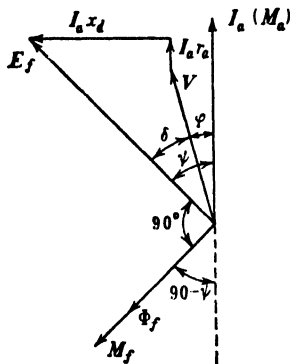


FIG. 37-1. Phasor diagram of an unsaturated synchronous generator with a cylindrical rotor—lagging current.

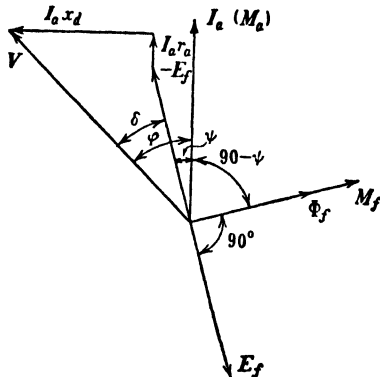


FIG. 37-2. Phasor diagram of an unsaturated synchronous motor with a cylindrical rotor—lagging current.

phase with the field mmf  $M_f$ , both  $\Phi_f$  and  $M_f$  are readily drawn in the phasor diagrams. Figs. 37-3a and 37-3b show the phasor diagrams for a leading current.

The following observations can be made on the four phasor diagrams. First,  $V$  is behind  $E_f$  in a generator and  $V$  is ahead of  $-E_f$  in a motor. Furthermore, considering the generator diagrams of Figs. 37-1 and 37-3a, the angle between the armature mmf  $M_a$  (see Eq. 22-20)

$$M_a = 0.9m \frac{N_a}{p} k_d k_p I_a, \quad (37-5a)$$

which is in phase with  $I_a$ , and the field mmf  $M_f$  is larger than  $90^\circ$  for a lagging current and less than  $90^\circ$  for a leading current. This means that a lagging current in a generator opposes its field mmf, while a leading current supports its field mmf. It can be seen from the motor diagrams of Figs. 37-2 and 37-3b that the opposite is true of a motor: lagging current in a motor supports the field mmf, while leading current opposes the field mmf.

These considerations yield the following important *rules of armature reaction* in the synchronous machine: *lagging current opposes the field mmf in a generator and supports the field mmf in a motor; leading current supports the field mmf in a generator and opposes the field mmf in a motor.*

However, it should be observed that it is not the power factor angle

$\varphi$  between  $I_a$  and  $V$  which determines the character and the magnitude of the armature reaction but the angle  $\psi$  between  $I_a$  and  $E_f$  or  $-E_f$ , because the position of  $M_f$  in the phasor diagram is determined by  $E_f$ .

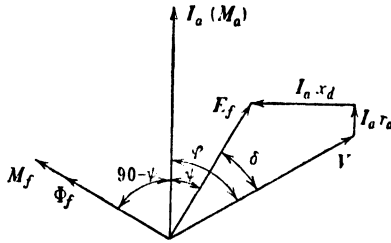


FIG. 37-3a. Phasor diagram of an unsaturated synchronous generator with a cylindrical rotor—leading current.

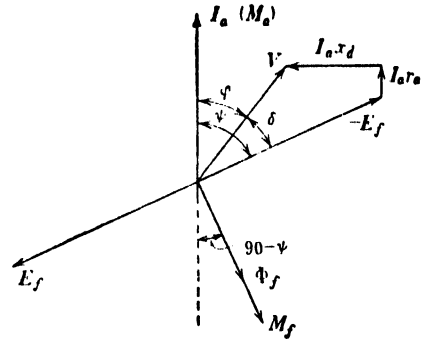


FIG. 37-3b. Phasor diagram of an unsaturated synchronous motor with a cylindrical rotor—leading current.

It is seen from Figs. 37-1 to 37-3 that the angle between the field mmf  $M_f$  and the armature mmf  $M_a$  is  $(90 - \psi)^\circ$ . Neglecting harmonics, the field mmf and the armature mmf are sinusoidal waves, the amplitudes of which can be treated as phasors. In the phasor diagrams (Figs. 37-1 to 37-3)  $M_f$  and  $M_a$  are the phasors which represent the amplitudes of both mmf's. Since the amplitude of a sinusoidal mmf coincides with the center-line of the flux produced by it, i.e., with its pole axis (see Fig. 37-4), the angle  $(90 - \psi)^\circ$  is the angle between the pole axes of rotor and stator.

Attention must be called to the angle  $\delta$  between  $V$  and  $E_f$  or  $-E_f$  in the phasor diagrams. It will be shown later (see Art. 39-1) that this angle is the *basic variable* of the synchronous machine, just as the slip is the basic variable of the induction motor. A torque-angle characteristic therefore takes the place of the torque-speed characteristic of the induction motor, and it is the angle  $\delta$  which determines the magnitude of the torque.

(b) *Machine saturated.* When the machine is saturated, the resultant mmf of the field and armature windings and the flux produced by it must

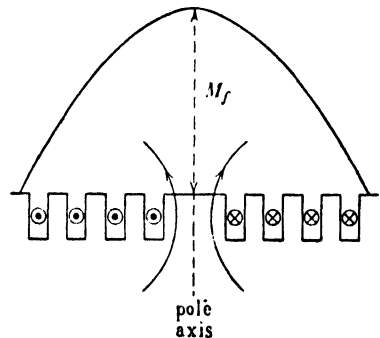


FIG. 37-4. Field mmf distribution and field pole axis.

be considered. The armature reaction reactance  $x_{ad}$  does not appear in this case, because it is taken care of by the armature mmf which is a component of the total mmf. Only the leakage reactance  $x_l$  of the armature is to be considered and a no-load characteristic must be available (see Art. 36-1).

Kirchhoff's mesh equation for generator operation is (see Eq. 37-3)

$$\mathbf{V} + \mathbf{I}_a r_a + j\mathbf{I}_a x_l = \mathbf{E} \quad (37-6)$$

and for motor operation (see Eq. 37-4)

$$\mathbf{V} = -\mathbf{E} + \mathbf{I}_a r_a + j\mathbf{I}_a x_l \quad (37-7)$$

$E$  is entirely different from  $E_f$ .  $E_f$  is the emf induced in the armature winding by the field flux (of an unsaturated machine) *alone*.  $E$  is the emf induced in the armature winding by the flux due to the resultant mmf of armature and rotor.

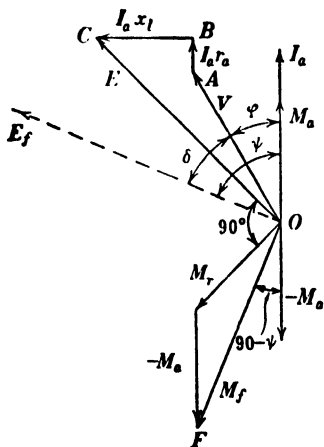


FIG. 37-5. Phasor diagram of a saturated synchronous generator with a cylindrical rotor—lagging current.

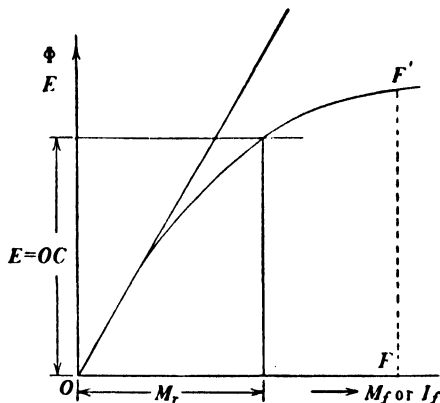


FIG. 37-6. Determination of the resultant mmf from the no-load characteristic.

Fig. 37-5 shows the phasor diagram of a generator with a cylindrical rotor for a lagging current.  $OC$ , the resultant of  $V$ ,  $I_a r_a$ , and  $I_a x_l$ , is the emf  $E$  to be induced in the armature by the flux produced by the *resultant* mmf ( $M_r$ ). This resultant mmf must lead the emf  $OC = E$  by  $90^\circ$ . Its magnitude is to be determined from the no-load characteristic as shown in Fig. 37-6. Having found  $M_r$  from the no-load characteristic, the field mmf  $M_f$  is determined from the equation

$$\mathbf{M}_r = \mathbf{M}_f + \mathbf{M}_a \quad (37-8)$$

or

$$\mathbf{M}_f = \mathbf{M}_r + (-\mathbf{M}_a) \quad (37-8a)$$

as shown in Fig. 37-5. The angle between  $M_f$  and  $-M_a$  is  $(90 - \psi)^\circ$ . If the generator, loaded corresponding to the phasor diagram of Fig. 37-5, should suddenly lose its load, the voltage at its terminals would be the no-load voltage  $E_f$  which corresponds to the field mmf  $M_f = OF$  (equal to  $FF'$  in Fig. 37-6). The direction of  $E_f$  is indicated in the phasor diagram.

The phasor diagram of a motor with a cylindrical rotor and a leading current, taking into account saturation, is shown in Fig. 37-7. The resultant mmf  $M_r$  is found from the no-load characteristic in the manner shown in Fig. 37-6 for the generator.  $M_f$  is again determined from Eq. 37-8a.

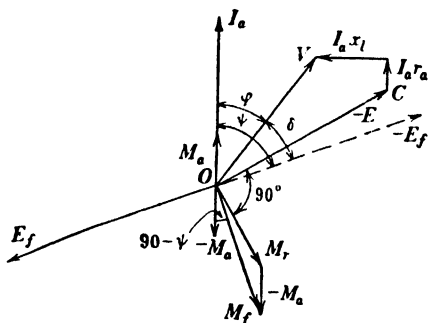


FIG. 37-7. Phasor diagram of a saturated synchronous motor with a cylindrical rotor—leading current.

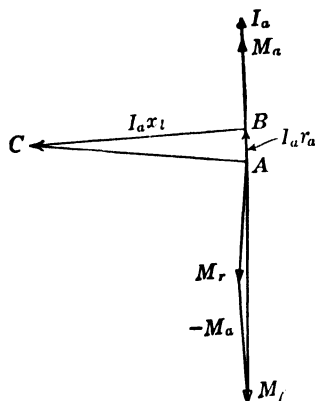


FIG. 37-8. Phasor diagram of a short-circuited generator with a cylindrical rotor.

**37-2. Generator characteristics.** The characteristics described in the following paragraphs are of importance for establishing good concepts of generator operation.

(a) *No-load and air-gap characteristic.* These characteristics have already been shown in Fig. 36-2.

(b) *Short-circuit characteristic. Potier triangle.* The short-circuit characteristic represents the armature current  $I_a$  as a function of the field current  $I_f$  or of the field mmf  $M_f$  with the armature terminals short-circuited. It is taken at synchronous speed of the generator. Referring to Fig. 37-5 the short-circuited generator appears to be loaded with an almost pure inductance because the resistance of the armature winding  $r_a$  is small in comparison to its leakage reactance  $x_l$ . Fig. 37-8 shows the



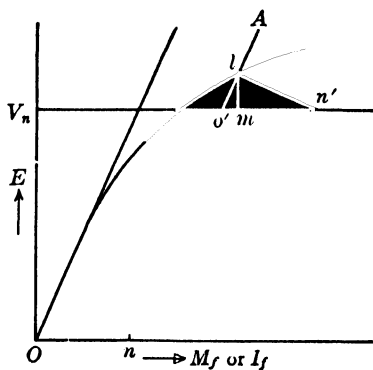


reaction mmf ( $mn = M_a$ ) and the leakage reactance  $x_l \approx z_a = lm/I_a$ . This triangle is called the *Potier triangle*.

(c) *Load characteristic.* This characteristic represents the terminal voltage  $V$  as a function of field current  $I_f$  or field mmf  $M_f$  for a constant load current  $I_a$  and a constant phase angle  $\varphi$ . Fig. 37-9 shows three such characteristics for the same constant load current  $I_a$  but for different values of a lagging angle  $\varphi$ .

Let  $OA$  be the normal terminal voltage  $V_n$  of the generator. The field current necessary to produce this voltage at no-load is  $Aa$ . At a fixed load current the field current required to sustain the no-load voltage increases rapidly with decreasing  $\cos \varphi$ . This increase of field current is necessary to counterbalance the voltage drop  $I_a z_a$  but mainly to counteract the armature reaction which increases with increasing lagging angle  $\varphi$ . The  $\cos \varphi = 0$  load characteristic can be readily constructed if the no-load characteristic and the Potier triangle are available. This is based upon the fact that, at  $\cos \varphi = 0$ , the armature mmf is in almost direct opposition to the field mmf, just as at short-circuit, Fig. 37-8. Then at constant current  $I_a$  the voltage drop remains the same ( $= lm$ ) for all values of  $V$  and the armature reaction mmf also remains the same ( $= mn$ ) for all values of  $V$ . Thus the  $\cos \varphi = 0$  characteristic can be found by moving the Potier triangle  $lmn$  parallel to itself with the vertex  $l$  on the no-load characteristic; the point  $n$  describes the  $\cos \varphi = 0$  characteristic, Fig. 37-9. For the voltage  $OA = V_n$ , as an example, the emf induced by the main flux is  $(OA + ml)$ ; the resultant mmf is  $Am$  and the field mmf is  $An$ . For the voltage  $OA'$  the induced emf is  $(OA' + ml)$  and the resultant field mmf is  $A'n$ .

It has been shown that the  $\cos \varphi = 0$  load characteristic can be determined from the no-load characteristic and the Potier triangle. Inversely, the Potier triangle can be determined from the no-load characteristic and two points of the  $\cos \varphi = 0$  load characteristic. It will be noted in Fig. 37-9 that the Potier triangle  $lmn$  fixes the angle  $lOn$ , since  $On$  is parallel to the axis of abscissae and  $Ol$  is parallel to the air-gap line. Let  $n$  and  $n'$  in Fig. 37-10 be two experimentally determined points of the  $\cos \varphi = 0$  load characteristic, the point  $n$  being determined with the



**FIG. 37-10.** Determination of Potier triangle from no-load characteristic and two points of zero power factor characteristic determined by test.

armature short-circuited and the point  $n'$  being determined at normal voltage  $V_n$  with full-load current. Then, if  $n'O'$  is made equal to  $nO$  and the line  $O'A$  is drawn through  $O'$  parallel to the air-gap line, the intersection of  $O'A$  and the no-load characteristic will yield the Potier triangle  $lmn$ .  $lm$  is the leakage reactance drop and  $lm/I_a$  is the leakage reactance  $x_l$ .  $mn'$  is the armature reaction mmf  $M_a$ .

(d) *External characteristic.* This characteristic represents the terminal voltage  $V$  as a function of the load current  $I_a$  at constant field current  $I_f$ ,

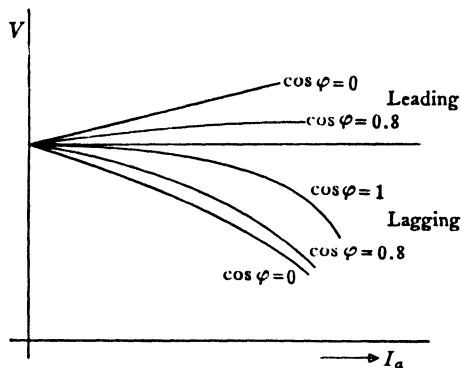


FIG. 37-11. External characteristics for lagging and leading current.

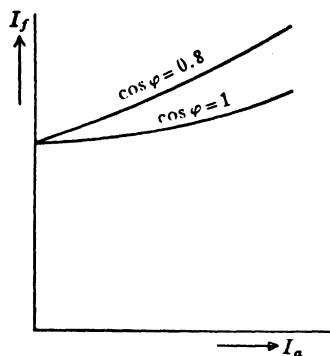


FIG. 37-12. Regulation curves for constant power factor.

and constant power factor  $\cos \varphi$ . Fig. 37-11 shows the trend of the external characteristic for lagging as well as leading current. For a lagging current the voltage drop increases as the power factor decreases.

(e) *Regulation curve.* This curve shows the field current  $I_f$  as a function either of the load current  $I_a$  at constant power factor, or of the power factor at constant load current  $I_a$ . In both cases the terminal voltage is kept constant. Fig. 37-12 shows regulation curves for two fixed values of power factor and variable  $I_a$ ; Fig. 37-13 shows a regulation curve for a fixed value of the load current and variable  $\cos \varphi$ . The trend of these curves, as well as that of the other characteristics of the machine under load, can be explained by the rules of armature reaction (see foregoing article).

(f) *Short-circuit ratio.* The short-circuit ratio (SCR) of a synchronous machine is defined as the ratio of field current required to produce rated voltage on open circuit to the field current required to produce rated current on short circuit. Fig. 37-14 shows a no-load characteristic and a short-circuit characteristic. The armature current is expressed in per-

unit of rated current. According to the definition

$$\text{SCR} = \frac{OF_0}{OF_s} = \frac{LF_0}{KF_s} = \frac{LF_0}{1} = LF_0$$

The short-circuit ratio determined in this manner is the *saturated* SCR. The *unsaturated* SCR is equal to  $L'F_0'$ ; it is determined from the no-load field current which corresponds to the air-gap characteristic and is smaller than the saturated SCR.

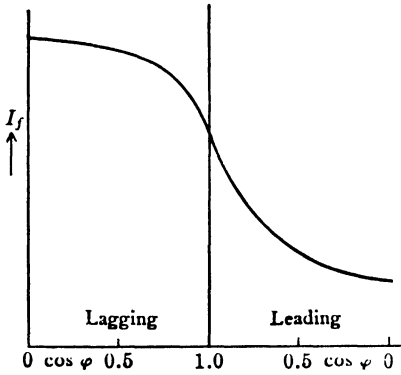


FIG. 37-13. Regulation curve for constant load current.

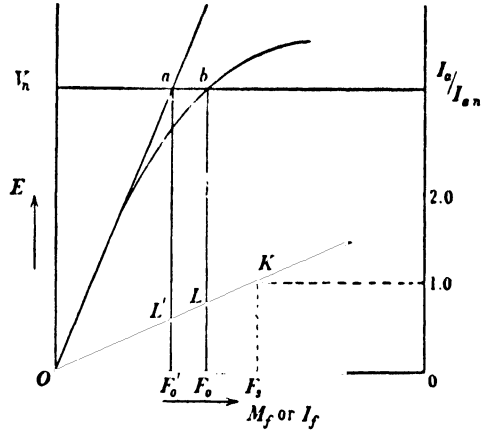


FIG. 37-14. Determination of the SCR.

The short-circuit ratio is an important factor for the synchronous machine for the following reasons. The field mmf  $OF_s$ , Fig. 37-14, necessary to produce the rated current at short circuit is larger the larger the armature reaction mmf and the  $I_a x_l$  drop (see Fig. 37-8). A small SCR indicates a large armature reaction, i.e., a machine sensitive with respect to load variations. A large SCR indicates a small armature reaction, i.e., a machine less sensitive to load variations.

(g) *Determination of the direct-axis synchronous reactance  $x_d$ .* This reactance can be determined from the no-load and short-circuit characteristics. Consider Fig. 37-14. The field current  $OF_0'$  induces the emf  $F_0'a = V_n$  in the stator at open circuit. When the stator is short-circuited at the same field current  $OF_0'$ , the induced emf in the stator is the same but it is consumed by the drop due to the synchronous impedance (see Fig. 37-1) i.e.  $E_f = F_0'a = V_n = I_a z_d$ . Since  $r_a$  is small in comparison with  $x_d$

$$x_d \approx \frac{V_n}{I_a} \approx \frac{V_n}{F_0' L'} \quad (37-9)$$

where  $I_a = F_0' L'$  is the short-circuit current which corresponds to  $I_f = OF_0'$ .  $F_0' L'$  is expressed in Fig. 37-14 in per-unit, the unit being the normal current. If, in Fig. 37-14, the voltage is also expressed in per-unit with the normal voltage  $V_n$  as the unit value

$$x_d \approx \frac{1}{F_0' L'}$$

As has been shown under (f),  $F_0' L'$  is the unsaturated short-circuit ratio. Thus

$$x_d = \frac{1}{\text{SCR}} \quad (37-10)$$

i.e., the synchronous reactance in per-unit is equal to 1 divided by the unsaturated short-circuit ratio.

**37-3. Voltage regulation.** The voltage regulation is defined as the per-unit voltage rise which takes place at the terminals when the load is dropped and the field current and the speed remain unchanged. In this case the no-load voltage corresponding to the field current appears at the machine terminals; this voltage can be determined from the no-load characteristic. In Fig. 37-9 the field mmf which corresponds to the voltage  $V_n$  and  $\cos \varphi = 0.8$  is  $Ab$ . The no-load voltage  $E_f$  produced by this mmf is  $cd$  and consequently the per-unit voltage regulation is:

$$\epsilon = \frac{db}{cb} = \frac{E_f - V_n}{V_n} \text{ in p-u} \quad (37-11)$$

or

$$\epsilon = \frac{E_f - V_n}{V_n} \times 100 \text{ in percent} \quad (37-11a)$$

The voltage regulation increases with increasing load current  $I_a$  and with increasing lagging angle  $\varphi$ . For capacitive loads the voltage regulation may be negative. Fig. 37-15 shows the voltage regulation for a constant-load current and variable power factor.

Similar to the short-circuit ratio, the voltage regulation is determined partly by the voltage drop  $I_a z_a$  but mainly by the armature reaction. It is an important factor for the synchronous machine. There are several methods employed for the determination of the magnitude of the voltage regulation. The following empirical method is recommended by the AIEE.

The no-load characteristic and two points of the  $\cos \varphi = 0$  load characteristic are determined by tests, one of the two points being at normal current and short-circuited armature (point  $n$  Fig. 37-10), the other

point being at normal current and normal voltage (point  $n'$  Fig. 37-10). From this the Potier triangle can be determined as explained in the foregoing article. Referring to Fig. 37-16a where the load current  $I_a$  is assumed along the horizontal, draw the voltage diagram of the three phasors  $V_n$ ,  $I_a r_a$ , and  $I_a x_l$ , i.e., determine the emf  $E$  to be induced in the armature by the flux due to the resultant mmf (see Fig. 37-5).  $I_{fs}$  is then the difference in field amperes between the air-gap line and the no-load characteristic for the voltage  $E$ , and it represents the effect of saturation.

In order to find the field current  $I_{ft}$  which corresponds to the load current  $I_a$ , the rated voltage  $V_n$ , and the fixed value of the angle  $\varphi$ , draw  $I_{f0}$  horizontally (Fig. 37-16b), lay off the value of the field current  $I_{fsh}$

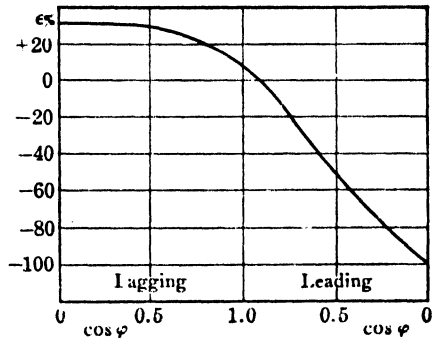


FIG. 37-15. Voltage regulation as a function of power factor for constant lagging and leading current.

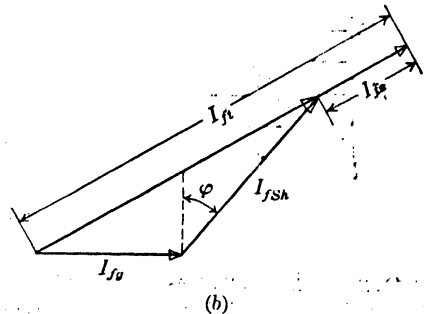
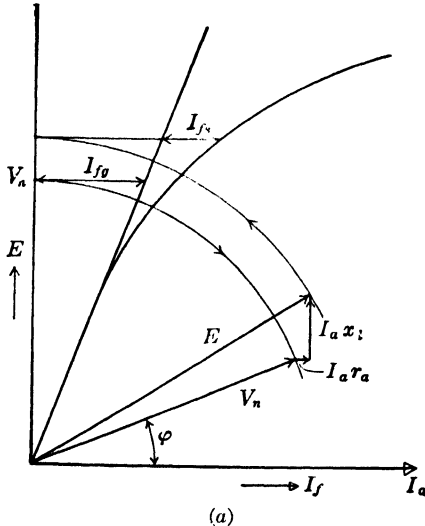


FIG. 37-16. Empirical AIEE method for determination of regulation.

required to produce the current  $I_a$  in the short-circuited armature (On Fig. 36-2 or On Fig. 37-9 or  $O'n'$  Fig. 37-10) at the power factor angle  $\varphi$  to the vertical, and add  $I_{fs}$  directly to the phasor sum of these two

phasors. The no-load voltage  $E_f$  corresponding to  $I_{f1}$  determines the voltage regulation.

**Example.** The no-load and the full-load zero-power-factor characteristics of a 3-phase, 6500-kva, 5500-volt, Y-connected turbogenerator are shown in Fig. 37-17. The ordinate is plotted in volts per phase.

$$V_n = \frac{5500}{\sqrt{3}} = 3180 \text{ volts per phase}$$

$$I_a = \frac{6500}{\sqrt{3} \times 5.5} = 683 \text{ amp}$$

Following the methods of Art. 37-2, the triangle  $O'ln$  is constructed, and the Potier triangle  $lmn$  is determined. From this,  $mn = 71$  is the armature reaction  $M_a$  expressed

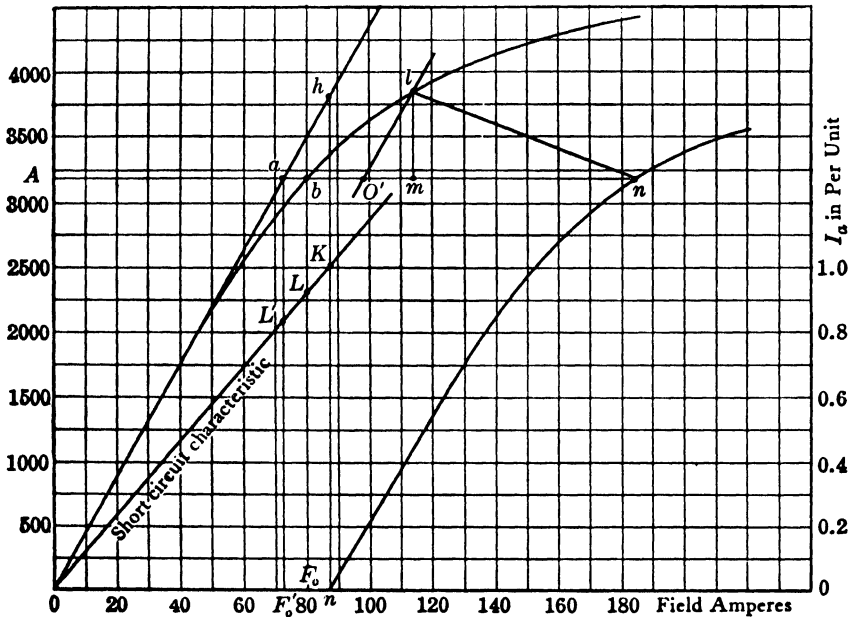


FIG. 37-17.

in terms of field amperes,  $lm = 660$  volts is the leakage-reactance voltage; therefore  $x_l = 660/683 = 0.968$  ohm. The leakage reactance in p-u is  $660/3180 = 0.208$ . The short-circuit ratio (unsaturated) SCR is  $Aa/On = 73/87 = 0.84$ , and the saturated value is  $Ab/On = 80/87 = 0.92$  (for the saturation at rated voltage). Also from the short-circuit characteristic (on per-unit basis) the SCR =  $F_0'L' = 0.84$ ; the saturated value SCR =  $F_0L = 0.92$ . Therefore  $x_d = 1/0.84 = 1.19$  in per-unit. The unit impedance is  $3180/683 = 4.66$  ohms; therefore  $x_d = 1.19 \times 4.66 = 5.54$  ohms. Also by definition  $x_d = nh/683 = 3780/683 = 5.54$  ohms. The armature-reaction react-

ance  $x_{ad} = x_d - x_l$  (Eq. 37-5); hence  $x_{ad} = 5.54 - 0.968 = 4.57$  ohms, or  $4.57/4.66 = 0.98$  p.u.

The per-unit voltage regulation of this machine now will be determined for (1) unity power factor, (2) 0.8 power factor lagging, using the AIEE method in Art. 37-3 (see also Fig. 37-16). (Armature resistance is neglected.) From Fig. 37-5 it follows that  $E = \sqrt{(V_a \cos \varphi)^2 + (V_a \sin \varphi + I_a x_l)^2}$ ; hence for  $\varphi = 0$ ,  $E = \sqrt{(3180)^2 + (660)^2} = 3250$ . From Fig. 37-17 the value of  $I_{fo} = Aa = 73$ ,  $I_{fsh} = 87$ , and  $I_{fs} = 8.0$ .

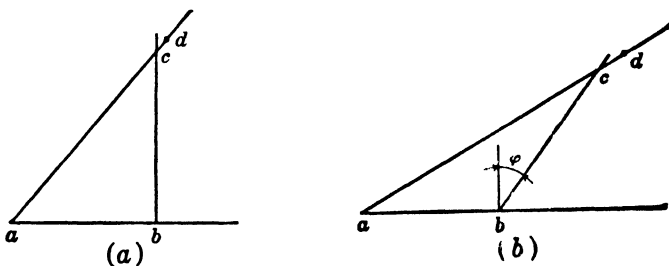


FIG. 37-18.

Fig. 37-16b is now constructed as shown in Fig. 37-18a in which  $ab = I_{fo} = 73$ ,  $bc = I_{fsh} = 87$ ; then  $ac = \sqrt{73^2 + 87^2} = 113.6$ ,  $cd = 8$ , and hence  $I_{ft} = ad = 121.6$ . This value of field current produces  $E_f = 3950$  at no-load (see Fig. 37-17). Hence  $\epsilon = (3950 - 3180)/3180 = 0.242$  at unity power factor. For  $\cos \varphi = 0.8$  lagging current

$$E = \sqrt{(3180 \times 0.8)^2 + (3180 \times 0.6 + 660)^2} = 3615 \text{ volts}$$

From Fig. 37-17,  $I_{fo} = 73$ ,  $I_{fsh} = 87$ ,  $I_{fs} = 16$ . Fig. 37-16b now appears as shown in Fig. 37-18b. Here  $ab = 73$ ,  $bc = 87$ ,  $cd = 16$ ,  $ad = 159.2$  amp. This  $I_f$  produces  $E_f = 4280$  volts at no-load; hence

$$\epsilon = \frac{4280 - 3180}{3180} = 0.346$$

With the information given in this example it is instructive to draw the phasor diagram of Fig. 37-5 for this machine. This is done only for 0.8 power factor lagging (Fig. 37-19). The figure is drawn to scale, so that  $V = 3180$ ,  $E = 3615$ ,  $M_r = 100$ ,  $M_a = 71$ ,  $M_f = 159.2$ ,  $\cos \varphi = 0.8$ .

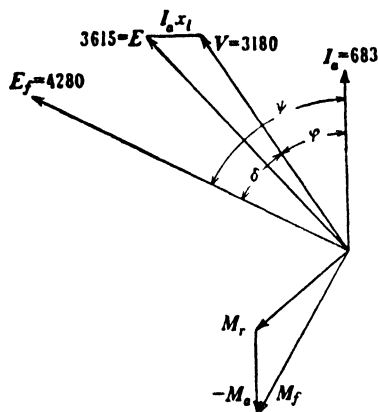


FIG. 37-19.

## PROBLEMS

1. For the machine of Example 37-1, determine the voltage regulation for 0.8 power factor leading, and draw the voltage and mmf diagrams.
2. The no-load and full-load zero-power-factor curves for a 12.0-kv 5000-kva



3-phase Y-connected 60-cycle turbogenerator are as follows, *the voltage being per-phase* (neglect armature resistance):

$I_f$ (amp):	10	20	30	40	43.0	50	60	70	80	90	100	110
$V$ (no-load):	1750	3500	5120	6360	6700	7260	7860	8280	8580	8780	—	—
$V$ (full-load):	—	—	—	—	0	1080	2720	4250	5380	6180	6750	7080

(a) Construct the Potier triangle and determine  $x_l$  in ohms and in per-unit.

(b) Determine the armature reaction  $M_a$  in terms of field amperes.

(c) Determine  $x_d$  in ohms and in p-u.

3. Using the AIEE method, determine the voltage regulation for the machine of Problem 2 in p-u for unity power factor and for 0.8 lagging and 0.8 leading.

4. For the machine of Problem 2 draw the short-circuit characteristic and determine the saturated and unsaturated SCR.

5. The no-load and full-load zero power factor characteristics for a 23,500-kva, 13,800-volt, 3-phase, 60-cycle, 2-pole, 0.85-p.f. lagging hydrogen-cooled turbogenerator are given below in p-u values.

#### No-load characteristic

$I_f$ :	0.10	0.20	0.40	0.60	0.80	1.0	1.2	1.4	1.6
$V$ (no-load):	0.13	0.23	0.45	0.69	0.87	1.0	1.09	1.15	1.21

#### Zero-power-factor characteristic

$I_f$ :	1.2	1.3	1.4	1.6	1.7	1.8	2.0	2.2	2.4	2.6
$V$ (full-load):	0.015	0.13	0.25	0.49	0.61	0.69	0.83	0.92	0.99	1.25

Unit field amperes = 183

Unit voltage = 13,800

Neglect armature resistance.

(a) Construct the Potier triangle and determine  $x_l$  in ohms and p-u.

(b) Determine the armature reaction  $M_a$  in terms of field amperes.

(c) Determine the value of  $x_d$  in both ohms and p-u.

6. For the machine of Problem 5 determine the voltage regulation for 0.80 p.f. lagging and 0.80 p.f. leading, using the AIEE method.

Draw emf and mmf phasor diagrams.

7. Determine the saturated and unsaturated SCR for the machine of Problem 5.

8 A 70,600-kva, 13,800-volt, 3-phase, 60-cycle, 2-pole, 0.85-p.f. lagging hydrogen-cooled turbogenerator has no-load and full-load zero power characteristics identical with those of Problem 5, on a p-u basis. However, for this generator:

Unit field amperes = 350

Unit voltage = 13,800

(a) Construct the Potier triangle and determine  $x_l$  in ohms and p-u.

(b) Determine the armature reaction  $M_a$  in field amperes.

(c) Determine the value of  $x_d$  in ohms and p-u.

9. For the machine of Problem 8 determine the regulation at unity, 0.80 lagging and 0.8 leading power factor, using the AIEE method.

Construct emf and mmf phasor diagrams.

## Chapter 38

### PHASOR DIAGRAM OF SYNCHRONOUS GENERATOR AND MOTOR WITH SALIENT POLES

**38-1. The two-reaction theory.** It has been mentioned in Art. 36-2 that the salient-pole machine, because of its interpolar spaces, must be treated differently than the machine with a cylindrical rotor. Contrary to the latter machine which has only one axis of symmetry (the pole axis or the direct axis), the salient-pole machine has two axes of symmetry, namely, the pole axis and the axis through the center of the interpolar space (the *quadrature axis* and the *quadrature axis*).

While two mmf's are acting upon the direct axis of the salient-pole machine, the field mmf and the armature mmf, only one mmf is acting upon the quadrature axis, namely, the armature mmf; the field mmf has no component in the quadrature axis. This indicates that, for the treatment of the salient-pole machine, the *armature mmf* must be resolved into two components, one acting upon the direct axis, the other acting upon the quadrature axis. This means that *two* armature reaction mmf's will have to be considered in the salient-pole machine (*two-reaction theory*).

It has been shown in Art. 37-1 that the field mmf  $M_f$  and the armature mmf  $M_a$  are shifted with respect to each other by an angle  $(90 - \psi)$  (see, for example, Fig. 37-1).

The same angle applies to the pole axes of field and armature. Since the direct axis coincides with the pole axis of the field,  $(90 - \psi)$  is also the angle between the direct axis and the armature mmf  $M_a$ . Fig. 38-1 shows the relative position of the direct axis, quadrature axis, and the armature

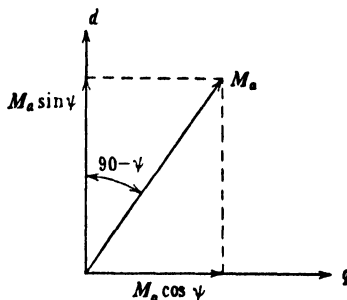


FIG. 38-1. Resolution of the armature mmf into two components, the direct-axis armature mmf and the quadrature-axis armature mmf.

mmf  $M_a$ . Resolving the armature mmf into the two components mentioned above, its component in the direct axis is  $M_a \sin \psi$  and that in the quadrature axis is  $M_a \cos \psi$ . The notations used will be

$$M_a \sin \psi = M_{ad}' \quad (38-1)$$

$$M_a \cos \psi = M_{aq}' \quad (38-2)$$

the first being the *armature mmf in the direct axis*, the second being the *armature mmf in the quadrature axis*. Thus, the mmf's  $M_f$  and  $M_{ad}'$  are acting upon the direct axis and only the mmf  $M_{aq}'$  is acting upon the quadrature axis.

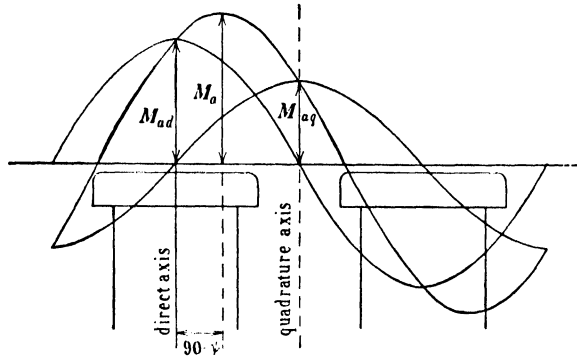


Fig. 38-2. Armature mmf wave and its two component waves in their positions relative to the direct and quadrature axes.

The armature mmf wave with the amplitude  $M_a$  and its two component waves with the amplitudes  $M_{ad}'$  and  $M_{aq}'$  in their positions relative to the direct and quadrature axes are shown in Fig. 38-2. Figs. 38-3 and 38-4 show the two component mmf waves separately.

The flux density is directly proportional to the mmf and inversely proportional to the reluctance. It is seen from Fig. 38-3 that the flux density produced by the armature mmf in the direct axis will be small in the interpolar spaces at both ends of the pole-shoe, i.e., the direct-axis armature mmf is relatively ineffective in these spaces. Introducing an effectiveness-factor  $C_d$  which takes into account the interpolar spaces, the effective armature mmf in the direct axis is (see Eq. 38-1)

$$M_{ad} = C_d M_a \sin \psi \quad (38-3)$$

The factor  $C_d$  is about 0.85.

It can be seen from Fig. 38-4 that, because of the interpolar spaces, the effectiveness of the armature mmf in the quadrature axis is much less than that of the armature mmf in the direct axis. Introducing an effective-

ness factor for the quadrature axis  $C_q$ , this factor is only about 0.45 and the effective armature mmf in the quadrature axis is (see Eq. 38-2)

$$M_{aq} = C_q M_a \cos \psi \quad (38-4)$$

The factors  $C_d$  and  $C_q$ , both smaller than 1, take into account the interpolar space. This means that calculating with the reduced mmf's in both axes,  $C_d M_a \sin \psi$  and  $C_q M_a \cos \psi$ , the gap around the stator bore is to be considered uniform, namely, of the same magnitude as that under the pole.

The phasor diagrams of the salient-pole machine can now be constructed. In the case of the unsaturated machine, three mmf's and three

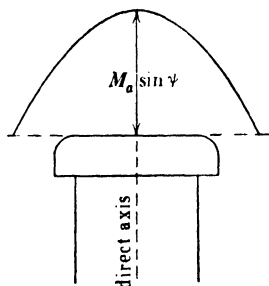


FIG. 38-3. Direct-axis armature mmf in its position relative to the direct axis.

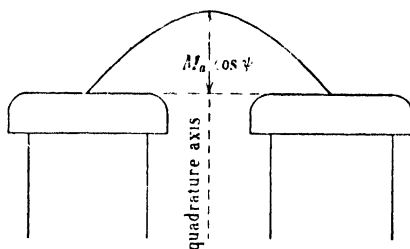


FIG. 38-4. Quadrature-axis armature mmf in its position relative to the quadrature axis.

fluxes will be considered, namely, the field flux, the armature flux in the direct axis, and the armature flux in the quadrature axis. In the case of the saturated machine three mmf's and two fluxes will be considered, namely, the flux in the direct axis produced by the resultant of the field mmf and the direct-axis armature mmf, and the armature flux in the quadrature axis.

### 38-2. Phasor diagrams of the generator and motor with salient poles. Armature reaction. First the unsaturated machine will be treated.

(a) *Machine unsaturated.* The direct-axis armature mmf  $M_{ad}$  is proportional to  $I_a \sin \psi$ ; the quadrature-axis armature mmf  $M_{aq}$  is proportional to  $I_a \cos \psi$ . The first mmf produces a flux in the direct axis; the second mmf produces a flux in the quadrature. As a consequence, the two fluxes are proportional to, and in phase with,  $I_a \sin \psi$  and  $I_a \cos \psi$  respectively. The emf's induced by the two fluxes in the armature winding are  $-jx_{ad}I_a \sin \psi$  and  $-jx_{aq}I_a \cos \psi$ . The first of these emf's is similar

to that which appears in the unsaturated machine with cylindrical rotor (see Eq. 37-1). As in the case of the latter machine,  $x_{ad}$  is the *armature reaction reactance in the direct axis*. Accordingly,  $x_{aq}$  in the second emf,  $-jx_{aq}I_a \cos \psi$ , is the *armature reaction reactance in the quadrature axis*.

Compared with the cylindrical rotor machine,  $x_{ad}$  has the same significance in both kinds of machine and  $x_{aq}$  appears only in the salient-pole machine. Furthermore, two emf's are to be considered in the arma-

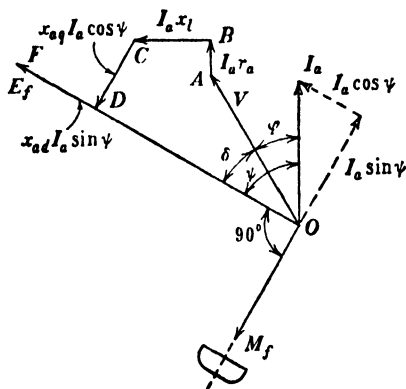


FIG. 38-5. Phasor diagram of an unsaturated, salient-pole generator with lagging current.

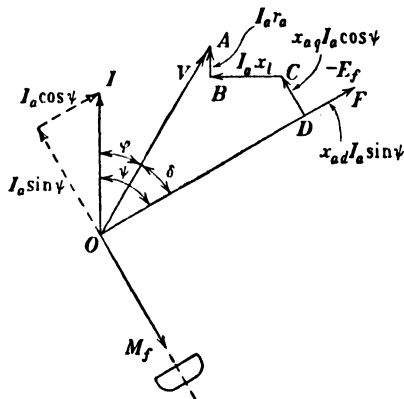


FIG. 38-6. Phasor diagram of an unsaturated, salient-pole motor with leading current.

ture winding of the salient-pole machine, one perpendicular to  $I_a \sin \psi$  and the other perpendicular to  $I_a \cos \psi$ , while only one emf, perpendicular to  $I_a$ , is to be considered in the armature winding of the cylindrical rotor machine.

Notice that  $x_{ad}$  is due to a flux the path of which is the same as that of the field winding, i.e., *along* the field poles, and  $x_{aq}$  is due to a flux which goes *across* the main poles; both of these fluxes do not take into account the leakage fluxes of the armature winding.

Kirchhoff's mesh equation for generator operation is (see Eq. 37-3)

$$V + I_a r_a + jI_a x_l + jx_{aq}I_a \cos \psi + jx_{ad}I_a \sin \psi = E_f \quad (38-5)$$

and that for motor operation (see Eq. 37-4)

$$V = -E_f + I_a r_a + jI_a x_l + jx_{aq}I_a \cos \psi + jx_{ad}I_a \sin \psi \quad (38-6)$$

Fig. 38-5 shows the phasor diagram of an unsaturated salient-pole generator for lagging current. The phasors  $V = OA$ ,  $I_a r_a = AB$  and  $BC = I_a x_l$  are drawn in the same manner as before (see, for example, Fig. 37-1). Then the phasors  $CD = x_{aq}I_a \cos \psi$  and  $DF = x_{ad}I_a \sin \psi$

are drawn. Since, according to Kirchhoff's mesh law, the phasor row  $OAB C D F$  must be balanced by the emf induced in the armature by the field flux,  $OF$  is equal to  $E_f$ .  $E_f$  lies  $90^\circ$  behind  $M_f$ . Fig. 38-6 shows the phasor diagram of an unsaturated salient-pole motor for a leading current.

It will be observed from diagrams Fig. 38-5 and 38-6 that a lagging current in a generator opposes the field mmf and also that a leading current in a motor opposes the field mmf. This is the same as in the

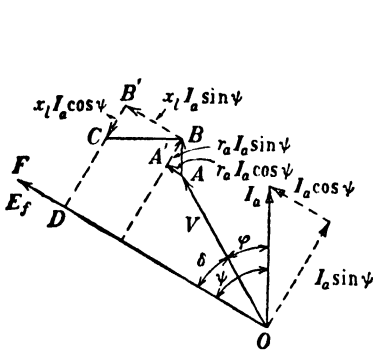


FIG. 38-7. Auxiliary diagram to Fig. 38-8.

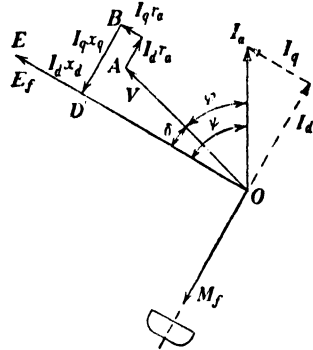


FIG. 38-8. Phasor diagram of an unsaturated, salient-pole generator with lagging current on the basis of the synchronous reactances.

machine with a cylindrical rotor. In general, the *rules of armature reaction* derived for the cylindrical rotor machine *apply also to the machine with salient poles*.

The phasor diagrams, Figs. 38-5 and 38-6, can be represented in a somewhat different form. The phasors  $AB = I_a r_a$  and  $BC = I_a x_l$  can each be resolved into two components (Fig. 38-7) so that  $AA' = I_a r_a \cos \psi$ ,  $A'B = I_a r_a \sin \psi$ ,  $BB' = I_a x_l \sin \psi$ , and  $B'C = I_a x_l \cos \psi$ . Further introducing the abbreviations  $I_a x_l \cos \psi + I_a x_{aq} \cos \psi = I_a x_q \cos \psi$ ,  $I_a x_l \sin \psi + I_a x_{ad} \sin \psi = I_a x_d \sin \psi$ ,  $I_a \cos \psi = I_q$ , and  $I_a \sin \psi = I_d$ , the phasor diagram (Fig. 38-5) for the generator with lagging current becomes as shown in Fig. 38-8.  $x_d = x_l + x_{ad}$  is the direct-axis synchronous reactance (see Eq. 37-5).

$$x_q = x_l + x_{aq} \quad (38-7)$$

is the *quadrature-axis synchronous reactance*.

Constructing the phasor diagrams (Figs. 38-5 to 38-8), it has been tacitly assumed that the angle  $\psi$  between  $I_a$  and  $E_f$  is known. Otherwise

it would not be possible to resolve  $I_a$  into the components  $I_a \sin \psi$  and  $I_a \cos \psi$ . The following artifice can be used to find the angle  $\psi$  while constructing the diagram.

In Fig. 38-9 which refers to a generator with lagging current, the phasor  $DC = I_a x_{aq} \cos \psi$  is the emf induced in the stator winding by the cross-flux of the machine, the axis of which is the quadrature axis. Since the path of the cross-flux is unsaturated, the emf  $CD = I_a x_{aq} \cos \psi$  can be found from the lower part of the no-load characteristic (air-gap

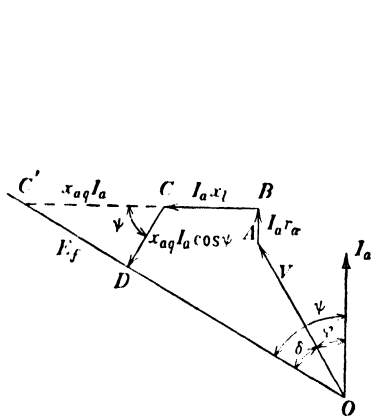


FIG. 38-9. Determination of the angle  $\psi$ .

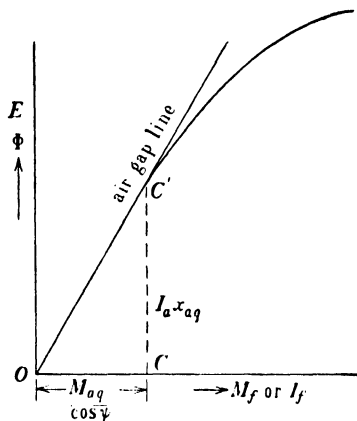


FIG. 38-10. Determination of the angle  $\psi$ .

line) as the emf corresponding to the mmf  $M_f = M_{aq} = C_q M_a \cos \psi$  (Eq. 38-4). If the line  $CB = I_a x_l$  (Fig. 38-9) is extended until it intersects the line in which  $E_f$  lies, the distance  $CC'$  is equal to  $CD/\cos \psi$ . This emf ( $= I_a x_{aq}$ ) is independent of the angle  $\psi$  and can be found just as the emf  $CD$  from the lower part of the no-load characteristic; it is the emf which corresponds to the mmf  $M_{aq}/\cos \psi = C_q M_a$  (Fig. 38-10). Hence the angle  $\psi$  can be found in the following way: Draw the phasor row  $OABC$ ; determine, from the no-load characteristic, the emf which corresponds to the mmf  $C_q M_a$ , i.e., the emf  $CC' = I_a x_{aq}$ ; extend  $BC$  by the distance  $CC' = I_a x_{aq}$ ; the line which connects the origin  $O$  with the point  $C'$  coincides with  $E_f$  and makes the angle  $\psi$  with  $I_a$ .

(b) *Machine saturated.* When the machine is saturated, only *one* flux is to be considered in the direct axis, namely, the flux produced by the resultant of the mmf's  $M_f$  and  $M_{ad}$ . Kirchhoff's mesh equation for generator operation is in this case (see Eq. 38-5)

$$\mathbf{V} + \mathbf{I}_a r_a + j \mathbf{I}_a x_l + j x_{aq} \mathbf{I}_a \cos \psi = \mathbf{E}_d \quad (38-8)$$

and for motor operation (see Eq. 38-6)

$$\mathbf{V} = -\mathbf{E}_d + \mathbf{I}_a r_a + j\mathbf{I}_a x_l + jx_{aq}\mathbf{I}_a \cos \psi \quad (38-9)$$

$E_d$  is in phase with  $E_f$  because both emf's are induced by the flux in the direct axis. However, the magnitude of  $E_d$  is different from that of  $E_f$ :  $E_d$  is due to the flux produced by the resultant mmf in the direct axis;  $E_f$  is due to the field flux alone.  $x_{ad}$  does not appear in Eqs. 38-8 and 38-9. Fig. 38-11 shows the phasor diagram of a saturated salient-pole generator

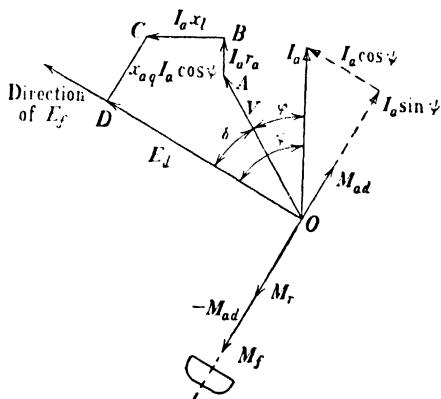


FIG. 38-11. Phasor diagram of a saturated, salient-pole generator with lagging current.

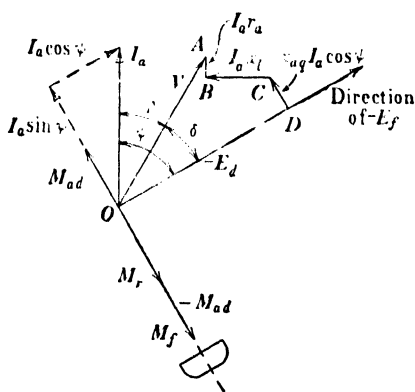


FIG. 38-12. Phasor diagram of a saturated, salient-pole motor with leading current.

with lagging current. The phasor row  $OABCD$  is the same as for the unsaturated machine (see Fig. 38-5). In the unsaturated machine, the armature mmf in the direct axis  $M_{ad}$  produces an emf  $-jx_{ad}I_a \sin \psi$  in the armature winding which is balanced by an equal component of the emf  $E_f$  produced by the field flux (Fig. 38-5). In the case of the saturated machine,  $OD$  (Fig. 38-11) is the emf induced in the armature winding by the flux due to  $\mathbf{M}_f + \mathbf{M}_{ad} = \mathbf{M}_r$ , i.e., by the flux produced by the resultant mmf  $M_r$ . This resultant mmf  $M_r$  must be determined from the no-load characteristic as the mmf which corresponds to  $E_d = OD$ , in the same way as for the saturated machine with cylindrical rotor (see Fig. 37-6). With  $M_r$  known, the field mmf is found as  $M_f = M_r + (-M_{ad})$ .

Fig. 38-12 is the phasor diagram of a saturated salient-pole motor with leading current. The construction is the same as that for the unsaturated machine (Fig. 38-6), except that here  $OD$  is the emf induced by the (single) direct-axis flux of the machine and its mmf  $M_r$  is to be determined from the no-load characteristic. Just as for the generator,  $M_f = M_r + (-M_{ad})$ .



**38-3. Generator characteristics. Voltage regulation.** Since the rules of armature reaction are the same for both cylindrical rotor and salient-pole machines and since the voltage drop  $I_a z_a = I_a(r_a + jx_l)$  also appears in both machines, the characteristics of the generator with salient-poles have the same general shape as those of the machine with a cylindrical rotor (see Art. 37-2).

The short-circuit ratio and the synchronous reactance in the direct axis,  $x_d$ , can be determined in the same way as in the case of the machine with the cylindrical rotor, namely, from the no-load and short-circuit characteristics (see Art. 37-2). Also the relation between the synchronous reactance in the direct axis,  $x_d$ , and the short-circuit ratio (SCR) is the same (see Eq. 37-10) as for the cylindrical rotor machine.

The synchronous reactance in the quadrature axis  $x_q = x_l + x_{aq}$  (Eq. 38-7) is a quantity peculiar only to the salient-pole machine. When  $x_d$  and  $x_l$  are known, then

$$x_{ad} = x_d - x_l$$

$x_{aq}$  is the armature reaction reactance in the quadrature axis;  $x_{ad}$  is that in the direct axis. The ratio of  $x_{aq}$  and  $x_{ad}$  is the same as the ratio of the armature flux in the quadrature axis and the armature flux in the direct axis, both produced by *unit current* flowing in the armature winding. The factors  $C_q$  and  $C_d$  in Eqs. 38-3 and 38-4, which take into account the interpolar space, theoretically make the air-gap uniform around the stator bore. Since the ratio of fluxes is the same as that of their mmf's, at constant air-gap, the ratio of  $x_{aq}$  and  $x_{ad}$  must be the same as that of  $M_{aq}$  and  $M_{ad}$  at unit current ( $I_a \cos \psi = 1$ ,  $I_a \sin \psi = 1$ ), i.e.,

$$\frac{x_{aq}}{x_{ad}} = \frac{C_q}{C_d} \quad (38-10)$$

from which equation  $x_{aq}$  and also  $x_q = x_l + x_{aq}$  can be determined. It can be seen that  $x_{aq}$  is much smaller than  $x_{ad}$  and therefore  $x_q$  is also much smaller than  $x_d$ .

The definition of the *voltage regulation* and the methods for determining its magnitude are the same for the salient-pole machine as for the cylindrical rotor machine. Thus the AIEE method described in Art. 37-3 can also be applied to the salient-pole machine.

**Example 38-1.** Fig. 38-13 is the no-load and gap characteristic for a 20-kva, 60-cycle, 3-phase, 440-volt, Y-connected, 6-pole, salient-pole synchronous generator. Each field pole has 400 turns. The armature is a single-circuit winding, with 72 slots and 8 series conductors per slot, coil pitch 10 slots. The armature resistance  $r_a = 0.13$  ohm, the leakage reactance  $x_l = 0.23$  ohm, and the ratio of pole arc to pole pitch  $b_p/\tau = 0.7$ .

From the armature winding data, the coil pitch is  $\frac{5}{8}$  and  $k_p = 0.966$ ,  $k_d = 0.958$ ,  $k_{dp} = 0.925$ ,  $I_a = 20,000/(440 \times 1.73) = 26.3$  rated armature current.  $C_d = 0.84$  and  $C_q = 0.46$  correspond to  $b_p/\tau = 0.7$ . From Eq. 22-20:

$$M_a = \frac{0.9mN_a I_a k_{dp}}{6} = \frac{0.9 \times 3 \times 96 \times 26.3 \times 0.925}{6} = 1050 \text{ AT per pole}$$

$M_a = 1050/400 = 2.63$  in terms of field current.  $C_q M_a = 0.46 \times 2.63 = 1.21$ . Fig. 38-9 is now constructed for  $\cos \varphi = 0.8$  lagging current.  $OA = 254$  volts,  $AB = 26.3 \times$

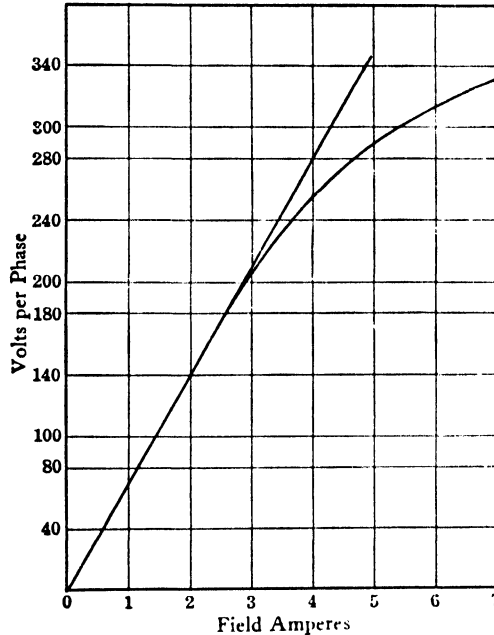


FIG. 38-13.

$0.13 = 3.42$  volts,  $BC = 26.3 \times 0.23 = 6.05$  volts. From Figs. 38-10 and 38-13 with  $OC = C_q M_a = 1.21$ ,  $CC' = x_{aq} I_a = 84$ . This is  $CC'$  in Fig. 38-9. From the latter

$$\tan \psi = \frac{V \sin \varphi + I_a x_l + I_a x_{aq}}{V \cos \varphi + I_a r_a} = \frac{254 \times 0.6 + 6.05 + 84}{254 \times 0.8 + 3.42} = 1.17, \psi = 49.6^\circ$$

$$\cos \psi = 0.648, \sin \psi = 0.761, \psi - \varphi = 12.7^\circ$$

$$\begin{aligned} E_d &= V \cos (\psi - \varphi) + I_a r_a \cos \psi + I_a x_l \sin \psi \\ &= 254 \times 0.975 + 3.42 \times 0.648 + 6.05 \times 0.761 = 254.6 \text{ volts} \end{aligned}$$

From Fig. 38-13,  $I_f$  required for  $E_d = 255$  is 4.05 amp. To this must be added  $M_{ad} = M_a C_d \sin \psi = 1050 \times 0.84 \times 0.761 = 671$  AT or  $671/400 = 1.68$  field amp to overcome  $M_{ad}$ . Hence the field current required is  $4.05 + 1.68 = 5.73$  amp. This value of  $I_f$  produces a no-load voltage of 310. The regulation is  $\epsilon = (310 - 254)/254 = 0.22$  at

0.8 power factor lagging. The characteristic reactances may be determined from the data as follows:  $M_a = 2.63$  in terms of field current for the rated current, 23.6 amp. For this same current  $I_{axl} = 26.3 \times 0.23 = 6.05$  volts. With  $I_{axl}$  and  $M_{ad} = C_d M_a$  the Potier triangle may be drawn in Fig. 38-13. The short-circuit characteristic can now be determined (see Fig. 36-2) with  $mn = M_{ad}$  and  $ml = I_{axl}$ . The no-load characteristic and short-circuit characteristic yield the unsaturated SCR = 1.593. The value for  $x_d$  is

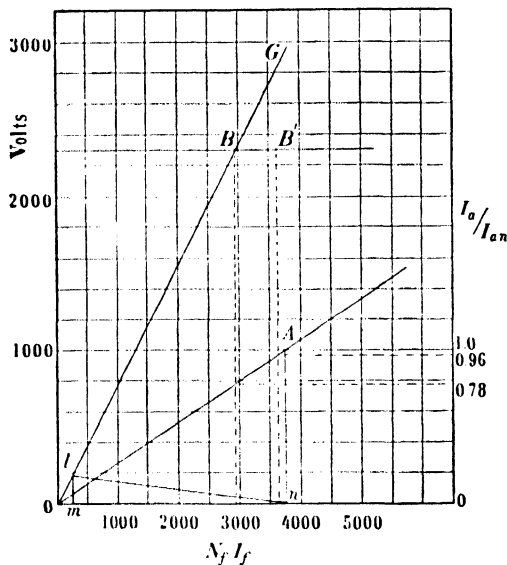


FIG. 38-14.

therefore 0.628. The unit impedance is  $254/26.3 = 9.66$  ohms and the leakage reactance in p.u.  $= 0.23/9.66 = 0.0238$ . Hence  $x_{ad} = x_d - x_l = 0.628 - 0.0238 = 0.604$ . From this  $x_{aq} = 0.604 \times 0.46/0.84 = 0.331$ . Therefore  $x_q = x_{aq} + x_l = 0.331 + 0.0238 = 0.355$  p.u.

**Example. 38-2.** The synchronous reactances in both axes will be determined for the following generator:

Output: 875 kva,  $\cos \phi = 0.80$ , 3 phases, 60 cycles, 24 poles, 2300 volts,  $I_a = 220$  amp.

Stator winding: 180 slots, 6 conductors per slot, coil pitch 6 slot pitches, pole pitch  $\tau = 9.52$  in., width of the pole arc  $b_p = 6.0$  in., no-load mmf at 2300 volts  $M_{f0} = 3610$  AT per pole and  $M_{f0g} = 2930$  AT per pole for the gap only. The leakage reactance is 0.826 ohm per phase. For the ratio  $b_p/\tau = 6.0/9.52 = 0.63$ ,  $C_d = 0.86$ ,  $C_q = 0.41$ . The number of slots per pole per phase  $q = 180/(3 \times 24) = 2.5$ ,\*  $k_d = 0.955$ ,  $k_p = \sin [(6/7.5) \times \pi/2] = 0.951$ ,  $k_{ap} = 0.908$ . The number of turns per phase

$$N_a = \frac{6 \times 180}{2 \times 3} = 180$$

\* In this example, the value of  $q$  is 2.5. Such a winding is classified as a fractional slot winding and was not considered in Chapters 21 or 22 of this text. Equation 22-6 for the distribution factor does not apply to this kind of winding.

The total armature mmf in the direct axis at  $\psi = 90^\circ$  (short circuit) is

$$M_{ad} = 0.9 \times 3 \times \frac{180}{24} \times 0.908 \times 220 \times 0.86 = 3480 \text{ AT per pole}$$

From the data given, the air-gap line  $OG$  in Fig. 38-14 may be drawn. Construct the Potier triangle with  $lm = I_a x_l = 220 \times 0.826 = 182$  volts and  $mm = 3480$  AT. To point  $n$  (3730 AT) corresponds unit armature current ( $nA$ ) on the short-circuit characteristic—draw this latter characteristic. Corresponding to  $M_{f0g} = 2930$  and  $M_{f0} = 3610$  (points  $B$  and  $B'$  respectively) the unsaturated and saturated SCR may be determined as 0.78 and 0.96 respectively. Hence:

$$\begin{aligned} x_d &= \frac{1}{0.78} = 1.28 \\ x_l &= 0.137 \\ x_{ad} &= 1.28 - 0.137 = 1.14 \\ x_{aq} &= 1.14 \times \frac{0.41}{0.86} = 0.543 \\ x_g &= x_l + x_{aq} = 0.137 + 0.543 = 0.680 \end{aligned}$$

### PROBLEMS

1. Determine the voltage regulation of the machine of Example 38-1, at unity power factor and at 0.8 power factor leading. Draw the voltage and mmf diagram to scale.

2. Determine the synchronous reactances in both axes for the following generator:  
Output: 16,500 kva,  $\cos \varphi = 0.85$ , 3 phases, 60 cycles, 52 poles, 6600 volts,  $I_a = 1442$  amp.

Stator winding: 312 slots, 2 conductors per slot, coil pitch = 5 slot pitches, pole pitch = 11.55 in., pole arc = 8.5 in., no-load mmf at 6600 volts  $M_{f0} = 6380$  AT per pole, and  $M_{f0g} = 5730$  AT per pole for the gap only. Leakage reactance of the armature winding (in p-u) = 0.187.  $C_d = 0.84$  and  $C_q = 0.48$ , corresponding to  $b_p/\tau = 0.736$ .

3. The no-load characteristic of the machine of Problem 2 is as follows, the voltage being per-phase:

AT per pole:	3020	4500	5520	6380	7080	8350
Volts:	2000	3000	3500	3810	4000	4250

Determine (a) field ampere-turns required per pole to produce rated armature current on short circuit; (b) the saturated SCR; (c) the voltage regulation at unity, 0.80 lagging, and 0.80 leading power factors. ( $r_a$  neglected.)

4. A 3-phase, 15-kva, 220-volt, Y-connected, 6-pole synchronous generator with salient poles has  $r_a = 0.10$  ohm per phase. The no-load characteristic is

$V$ (per phase):	37	70	98.4	109.3	123	142	156	166	174	181	187
$I_f$ (amp):	1.0	2.0	3.0	3.5	4.0	5.0	6	7	8	9	10

The full-load zero-power-factor characteristic is

$V$ :	0	62	88.5	109	127	132
$I_f$ :	4.05	6.35	7.43	8.5	9.7	10

The short-circuit characteristic is

$I_f$ :	2.1	4.05	6.17
$I_a$ :	20	40	60

The ratio of  $x_d$  to  $x_q$  was found to be 1.21. Construct the Potier triangle and determine  $x_l$ , and the value of  $M_a$  expressed in terms of field amperes.

5. Determine the voltage regulation of the machine of Problem 4 at unity power factor and at 0.8 power factor, leading and lagging current.

6. Determine  $x_d$  and  $x_q$  for the machine of Problem 4.

7. The following data apply to a 72-pole, 16,667-kva, 100-rpm, 13.8-kv, Y-connected, waterwheel synchronous generator:  $x_d = 0.895$ ,  $x_q = 0.62$ ,  $x_l = 0.240$  in p-u. The armature reaction  $M_a$  expressed in terms of field amperes is 135. Determine  $x_{aq}$  and  $x_{ad}$  and express all the characteristic reactances in both ohms and per-unit. Determine the value of field current required to circulate rated current in the short-circuited armature, and the SCR (unsaturated).  $I_f = 80$  amp for  $E = 3600$  v.

8. The no-load characteristic for the machine of Problem 7 is

$V$ :	2000	3600	6300	7800	8900	9550	10,000
$I_f$ :	45	80	150	200	250	300	350

The voltage is per-phase. From the data given determine the values  $BC$ ,  $CC'$  and the angles  $\psi$  and  $\delta$  of Fig. 38-9. From  $CC'$  and the no-load characteristic determine  $M_a C_q$ , and then  $C_d$  and  $C_q$ . ( $\cos \varphi = 0.8$  lagging, neglect  $r_a$ .)

9. From the data determined in Problem 8 determine the voltage regulation of the machine, at unity and at 0.8 lagging and leading power factor. Use method described in Example 38-1.

10. Repeat Problem 9, using the AIEE method, and compare results.

11. A 6000-kva, 2400-volt, 3-phase, 60-cycle, 40-pole, salient-pole generator has a resistance of 0.006 ohm per phase and is wye-connected. The characteristic curves are:

$I_f$ (amp):	25	50	75	100	125	150	175	200	255
$V$ (terminal):	690	1330	1900	2320	2600	2770	2900	3020	3160

*Full-load zero power factor*

$I_f$ (amp):	100	125	150	175	200	225	250	275	300	325
$V$ (terminal):	0	650	1170	1580	1890	2090	2240	2350	2450	2520

*Short circuit*

$I_f$ (amp):	0	50	100	150
$I_a$ (amp):	0	720	1450	2160

Construct the Potier triangle and determine  $x_l$  (in ohms and p-u) and  $M_a$  in equivalent field amperes.

12. Determine the voltage regulation for power factors of unity, 0.80 lagging, and 0.80 leading for Problem 11.

13. Determine the SCR,  $x_d$ , and  $x_q$  for the machine of Problem 11.  $C_d = 0.84$  and  $C_q = 0.50$ .

14. A 750-kva, 2400-volt, 3-phase, 60-cycle, 52-pole, salient-pole generator has an armature resistance of 0.15 ohm per phase and is wye-connected. The characteristic curves are:

*No-load*

$I_f$ (amp):	10	20	30	40	50	60	70	80	100	120	140
$V$ (terminal):	470	930	1400	1830	2150	2420	2600	2750	2960	3150	3300

*Full-load zero power factor*

$I_f$ (amp):	70	80	90	100	110	120	140	160	200
$V$ (terminal):	0	550	920	1200	1500	1740	2130	2350	2700

*Short circuit*

$I_f$ (amp):	0	31	62	93
$I_a$ (amp):	0	100	200	300

Construct the Potier triangle and determine  $x_l$  (in ohms and p-u) and  $M_a$  in equivalent field amperes.

15. Determine the voltage regulation for power factors of unity, 0.80 lagging and 0.80 leading for the machine of Problem 14.

16. Determine the SCR,  $x_d$ , and  $x_q$  for the machine of Problem 14.  $C_d = 0.85$ ,  $C_q = 0.45$ .

## Chapter 39

### TORQUE AND POWER RELATIONS. PARALLEL OPERATION OF SYNCHRONOUS GENERATORS. SYNCHRONIZING GENERATORS

**39-1. Torque and power relations.** Fig. 39-1a shows the power balance of the synchronous generator. It has been pointed out already that the iron losses ( $P_{h+c}$ ) necessary to sustain the main flux are supplied by the rotor. The total power input ( $P_{\text{inp. shaft}}$ ) is then consumed by the sum of  $P_{h+c}$ , the rotational iron losses ( $P_{\text{ir. rot}}$ ), the friction and windage losses

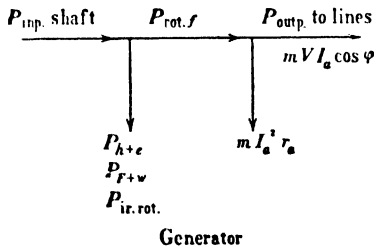


FIG. 39-1a. Power balance of a synchronous generator.

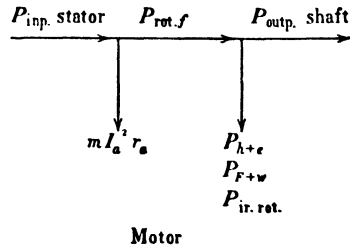


FIG. 39-1b. Power balance of a synchronous motor.

( $P_{F+w}$ ), and the electromagnetic power supplied to the stator ( $P_{\text{rot. f}}$ ). A small part of the latter power is consumed by the stator as  $I^2R$  losses, and the balance ( $m V I_a \cos \phi$ ) goes to the line. The copper losses of the field winding do not appear in the power balance of Fig. 39-1a because they are supplied by a d-c source of power. Fig. 39-1b shows the power balance of the synchronous motor.

As in all other electric machines, the electromagnetic power ( $P_{\text{rot. f}}$ ) is equal to (see Eq. 1-33 and Eq. 26-3)

$$P_{\text{rot. f}} = m E I \cos \phi \text{ watts} \quad (39-1)$$

and the electromagnetic torque

$$T = \frac{7.04}{n_s} P_{\text{rot f}} \text{ lb-ft} \quad (39-2)$$

Phasor diagram Fig. 38-8, which refers to an unsaturated salient-pole generator, will be used in order to transform Eq. 39-1 for the electromagnetic power ( $I_a r_a$  will be neglected). The result obtained also holds with satisfactory accuracy for the saturated machine. The electromagnetic power of the machine with a cylindrical rotor will appear as a special case of the machine with salient poles.

With  $I_a r_a$  neglected, the phasor diagram of Fig. 38-8 becomes as shown in Fig. 39-2. Furthermore, it follows from Figs. 39-1a and 39-1b that for  $r_a = 0$

$$P_{\text{rot f}} = m V I_a \cos \varphi \quad (39-3)$$

It can be seen from Fig. 39-2 that

$$I_a \cos \varphi = I_d \sin (\psi - \varphi) + I_q \cos (\psi - \varphi) = I_d \sin \delta + I_q \cos \delta$$

$$V \sin \delta = I_q x_q; \quad I_q = \frac{V \sin \delta}{x_q}; \quad V \cos \delta = E_f - I_d x_d$$

$$I_d = \frac{E_f - V \cos \delta}{x_d}$$

Inserting the equations for  $I_a \cos \varphi$ ,  $I_q$ , and  $I_d$  in Eq. 39-3 the equation for the electromagnetic power becomes

$$P_{\text{rot f}} = m \frac{V E_f}{x_d} \sin \delta + m V^2 \frac{x_d - x_q}{2 x_d x_q} \sin 2\delta \quad (39-4)$$

In the cylindrical rotor machine  $x_d = x_q$  since there are no interpolar spaces. Thus for the cylindrical rotor machine

$$P_{\text{rot f}} = m \frac{V E_f}{x_d} \sin \delta \quad (39-5)$$

It has been mentioned that the angle  $\delta$  between  $V$  and  $E_f$  is the basic variable of the synchronous machine. It can be seen from Eqs. 39-4 and 39-5 that for constant field current, i.e., for constant  $E_f$ , the electro-

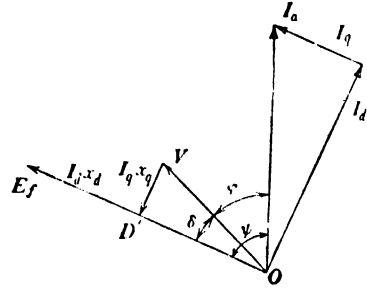


FIG. 39-2. Phasor diagram of an unsaturated, salient-pole generator — lagging current;  $-r_a$  assumed zero.



magnetic power and *torque* (Eq. 39-2) of the synchronous machine depend solely upon the angle  $\delta$ .

Fig. 39-3 is the torque-angle characteristic of the cylindrical rotor machine. The angle  $\delta$  is arbitrarily assumed positive for generator operation

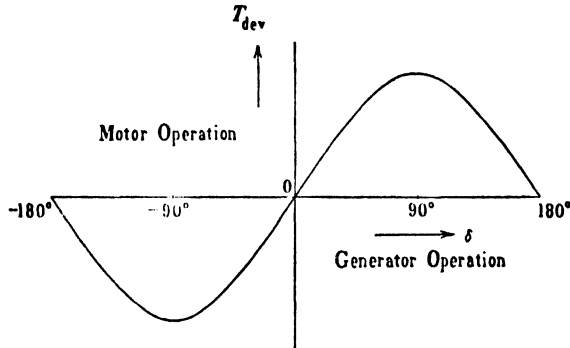


FIG. 39-3. Torque angle characteristic of a cylindrical rotor machine.

tion and negative for motor operation. The characteristic is a sinusoidal curve, and maximum torque occurs at  $\delta = \pm 90^\circ$ .

Considering Eq. 39-4 for the salient-pole machine, it is seen that the saliency ( $x_d \neq x_q$ ) appears in the second term which is a function of  $\sin 2\delta$ .

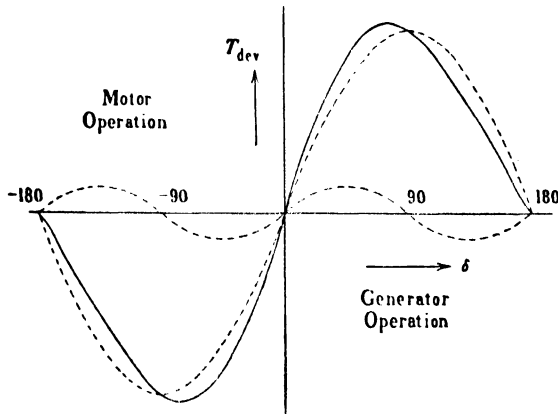


FIG. 39-4. Torque angle characteristic of a salient-pole machine.

Fig. 39-4 shows both terms of the torque of the salient-pole machine, each separately, as well as the total torque as a function of  $\delta$ . Maximum torque occurs at an angle smaller than  $90^\circ$  for both generator and motor.

An examination of Eqs. 39-4 and 39-5 shows that, when the field cur-

rent is zero ( $E_f = 0$ ), the torque of the cylindrical rotor-machine is zero while that of the salient-pole machine is not zero but has a definite value. The latter machine is able to produce a torque without field excitation and this torque depends upon the difference between the reluctances in both axes ( $x_d - x_q$ ). Synchronous motors without field windings are used for certain applications as small units; they are called *reluctance motors*.

**39-2. Parallel operation of synchronous generators.** Since qualitative rather than quantitative results are important for the consideration of machines operating in parallel, the cylindrical rotor machine, as the simpler of the two types, will be considered. Furthermore, it will be assumed that the saturation of the magnetic path is low and that the

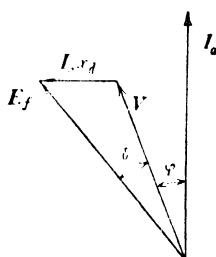


FIG. 39-5. Simplified phasor diagram of a cylindrical rotor generator—lagging current.

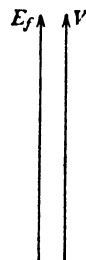


FIG. 39-6. Phasor diagram for no-load and  $E_f = V$ .

armature resistance is zero. Under these simplified conditions the phasor diagram of a generator with lagging current is shown in Fig. 39-5 (see also Fig. 37-1).

It has been shown in the foregoing article that the angle  $\delta$  between the phasors  $V$  and  $E_f$  is a measure of the power developed by the machine. Consider a synchronous generator connected to a line with a constant voltage  $V$ , at no-load. Since  $\delta = 0$  corresponds to the no-load condition, the phasors  $E_f$  and  $V$  in the phasor diagram of Fig. 39-5 must coincide. It will be assumed that the field current is adjusted in such a manner that  $E_f = V$ . The phasor diagram which corresponds to the no-load condition with  $E_f = V$  is shown in Fig. 39-6. Also according to Kirchhoff's mesh law, Eq. 37-1, the armature current  $I_a$  must be zero because  $E_f = V$ . Now let the regulator of the prime mover (for example, a turbine) be influenced in such a manner that the prime mover receives added input

(more steam) and seeks to drive the generator at an increased speed. Since the rpm of the synchronous machine is fixed by its number of poles and the line frequency (see Eq. 1-9), the increased input will result in an advance of the pole structure, i.e., considering the phasor diagram of Fig. 39-6, the phasor  $E_f$  will be moved ahead of the line voltage  $V$  to a new angle  $\delta$  (Fig. 39-7) which corresponds to the power input. Since

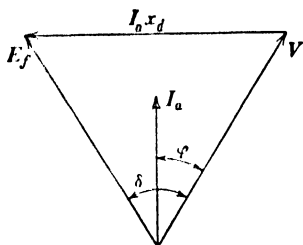


FIG. 39-7. Phasor diagram showing relative position of  $E_f$  and  $V$  of Fig. 39-6 after the input to the prime mover has been increased.

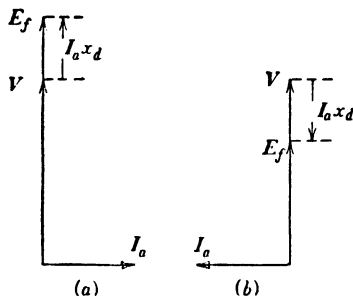


FIG. 39-8. Influence of change in field current on behavior of a synchronous generator.

$E_f \neq V$ , a current  $I_a$  will flow in the armature winding of a magnitude determined by Eq. 37-1, i.e.,  $(E_f - V) = jI_a x_d$ . It follows from Fig. 39-7 the phase displacement between the current  $I_a$  and the terminal voltage  $V$  is relatively small. This leads to the important statement that the *forward advance of the phasor  $E_f$  (of the pole structure) forces the generator to deliver a current  $I_a$  to the line which is nearly in phase with  $V$ , and which therefore yields an active power output.*

Thus, if the output of a synchronous generator which is operating in parallel with other generators is to be increased, its prime mover must be accelerated by supplying it with more power (for example, more steam) and, vice versa, if the output is to be reduced, the prime mover must be decelerated by reducing its input. This is entirely different from the operations necessary to change the load of a d-c generator or an induction generator: a change of the field current is necessary in order to change the load of a d-c generator (see Art. 6-7), and a change of the speed (of the slip) of the rotor is necessary to change the load of an induction generator (see Art. 26-4).

Consider again Fig. 39-6 which represents the phasor diagram of a generator at no-load with its field current adjusted in such a manner that  $E_f = V$ . No change will be made in the power input of the prime mover so

that the angle  $\delta$  will remain equal to zero. However, a change will be made in the field current, i.e., in  $E_f$ . First let the field current be increased so that  $E_f > V$ , as shown in Fig. 39-8a. According to Kirchhoff's mesh law, Eq. 37-1,  $jI_a x_d$  must then be in phase with  $V$ , i.e., the generator current  $I_a$  must lag  $V$  by  $90^\circ$ . Thus an increase of field current forces the generator to carry a lagging reactive current. If the field current is decreased so that  $E_f$  becomes smaller than  $V$ , as shown in Fig. 39-8b,  $jI_a x_d$  is opposite to  $V$  and the generator is forced to carry a leading reactive current.

The character of the armature current for an increase or decrease of the field current, obtained from the phasor diagrams of Figs. 39-8a and 39-8b, can also be derived from the rules of armature reaction (see Art. 37-1). If a generator or motor is connected to a line with a constant voltage  $V$ , the flux of the machine and therefore its field current are fixed by the load and the voltage  $V$ . If the field current is now increased above this fixed value, a generator will react by delivering a lagging current to the line, because in a generator a lagging current opposes the field mmf. If, on the other hand, the field current is decreased below this fixed value, a generator will react by delivering a leading current to the line, because in a generator a leading current supports the field mmf. The opposite is true of the motor.

It follows from these considerations that a *variation of the field current, at fixed load and voltage, will force the generator to deliver reactive current.*

Care must be taken that generators operating in parallel are loaded in proportion to their ratings. This applies to the active as well as to the reactive current of each generator, i.e., not only the armature current but also the field current must be properly determined and fixed. Consider, as an example, two duplicate generators operating in parallel at a fixed voltage  $V$  with an inductive load having a fixed  $\cos \phi$ . The voltage  $V$  *should* be obtained with identical field currents in both generators. However, the required voltage also can be obtained when one generator is overexcited and the other generator underexcited. In this latter case the underexcited generator, according to Eq. 37-1 and Fig. 39-8b, must carry a leading current. Since there is no place for a leading current when the load is inductive, the leading current will flow as an *internal circulating* current between the stators of the two machines, producing additional  $I^2 R$  losses and heat in the windings.

**39-3. Synchronizing of synchronous generators.** Synchronizing a synchronous generator means connecting the generator to an existing line with a terminal voltage  $V$  in such a manner that no inrush of current takes place.

As in the case of the d-c generator, several conditions must be fulfilled in order to avoid an inrush of current.

1. The terminal voltage of the incoming machine must be equal to the line voltage  $V$ .

2. Both voltages must be in phase.

3. The frequency of both voltages must be the same.

The first condition means that the voltage of the incoming machine must be exactly equal to the line voltage. If the terminal voltage of the incoming machine is greater or less than the line voltage, a current surge results upon the connection of the new machine, which subsequently causes circulating current through the armature winding of the machine, the bus-bars, and the other generators feeding the line.

The second condition, both voltages in phase, means that at the moment of connection the terminal voltage of the incoming machine and the line voltage must act in opposition to each other in the closed circuit consisting of the incoming machine, the bus-bars, and the other generators. If both voltages are not in phase at the moment of connection, the resulting voltage difference produces a surge of current which, in case of large phase displacements, can damage the machine windings.

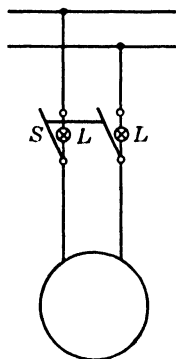


FIG. 39-9. Synchronizing a generator by means of lamps.

The in-phase condition between the line voltage and the voltage of the incoming machine and also the third condition of equal frequencies can be determined by means of lamps. Fig. 39-9 shows the arrangement of the lamps for an incoming single-phase machine. The double-pole switch  $S$  is bridged by two lamps  $L$ . If the voltages are equal and in phase, the lamps remain dark. However, if the voltages are equal but the line frequency and the frequency of the incoming machine are not the same, the lamps remain dark for only a short time, then brighten, and later become dark again. The flashing of the lamps occurs in a periodic sequence, and the frequency of fluctuation is an indication of the difference in frequency between the incoming machine and the line. The frequency of the incoming machine must

be adjusted so that the flashing of the lamps takes place very slowly, and the switch  $S$  must be closed at the moment when the lamps are dark. For a 3-phase machine, three lamps are connected to a 3-pole switch in the same manner as for the single-phase machine. Instruments called synchroscopes are also available for an accurate indication of synchronism.

## PROBLEMS

(Consider all machines unsaturated. Unit current = rated current for generators and  $= I_{HP}$  for motors.)

1. A 1500-HP, 6600-volt, 3-phase, 60-cycle, 6-pole cylindrical-rotor synchronous motor has a rated armature current of 136 amp, and an armature reactance  $x_d = 0.95$  p-u. Neglecting the resistance and assuming the input power to remain constant at 1000 kw, determine the angle  $\delta$  for values of  $E_f = 1.15, 1.20, 1.25, 1.30$  (p-u) volts respectively. Determine the power  $P_{rot.f}$  in each case.

2. For each value of  $E_f$  and the angle  $\delta$ , determined in Problem 1, calculate (a) the line current, (b) power factor of the motor. Determine the value of  $E_f$  and  $\delta$  to produce a motor power factor of unity.

3. Since  $r_a$  is neglected, the limiting value of  $\delta$  is  $90^\circ$ . For an input of 1000 kw, determine the value of  $E_f$  when  $\delta = 90^\circ$ .

4. Repeat Problem 1 for inputs of 1200 kw and for 500 kw.

5. Repeat Problem 2 for inputs of 1200 kw and for 500 kw.

6. If the motor of Problem 1 is constructed with a salient-pole rotor having an armature resistance of 0.01 p-u,  $x_d = 0.90$  p-u, and  $x_q = 0.65$  p-u, determine the power  $P_{rot.f}$  for the same  $\delta$  angles calculated using the corresponding values of  $E_f$ . Compare your results with Problem 1. Neglect resistance.

7. Two identical synchronous generators operate in parallel delivering power to a 40,000-kw load at 0.866 power factor lagging and rated terminal voltage. The machines are Y-connected and each is rated 30,000 kva, 13.2 kv and has  $x_d = 0.775$  in p-u. They are adjusted so that each is delivering its proper share of the load, and each operates at the same power factor. Determine for each machine (a) kva; (b) kw; (c) kvars; (d) the voltage  $E_f$  (per phase); (e) the angle  $\delta$ ; (f) the angle  $\psi$ , neglecting  $r_a$ . A combined graphical and analytical solution is suggested for these problems on parallel operation.

8. The excitation of one machine of Problem 7 is increased so that  $E_f = 14,000$  volts per phase, while the terminal voltage, the total load, and the power of each machine remain constant. Determine (a) the power factor of each machine; (b) the current of each machine; (c) the voltage  $E_f$  of the second machine; (d) the angle  $\delta$  for each machine; (e) the angle  $\psi$  for each machine; (f) the kva of each machine; (g) the kvars of each machine.

9. Two synchronous generators are rated as follows: machine I, 30,000 kva, 13.2 kv,  $x_d = 0.775$  per-unit; machine II, 12,250 kva, 13.2 kv,  $x_d = 1.0$  per-unit. They both are Y-connected and operate in parallel to deliver a total load of 36,000 kw at 0.866 power factor delivering current in proportion to their rating. Determine for each machine (a) the kw; (b) the kva; (c) the kvars; (d) the current; (e) the power factor; (f) the voltage  $E_f$ ; (g) the angle  $\delta$ .

## Chapter 40

### CIRCLE DIAGRAM OF THE SYNCHRONOUS MACHINE

As in the case of the induction motor the geometric locus of the stator current of the synchronous machine is a circle when the parameters ( $r_a$ ,  $x_l$ , and the main flux reactance) are constant quantities. Otherwise the geometric locus becomes a curve of higher order than the second order. Only the simplest case with constant parameters, namely, the *unsaturated* machine with constant reluctance around the stator bore, i.e., with a cylindrical rotor, will be considered.

**40-1. Circle diagrams for constant developed torque and variable field current.** Considering the synchronous motor, the power input per phase is (Fig. 39-1b)

$$P_{\text{inp.stator}} = VI_a \cos \varphi \text{ watts per phase} \quad (40-1)$$

and the electromagnetic power (the power transferred by the rotating field),  $P_{\text{rot.f}}$ , which is proportional to the developed torque of the machine,

$$P_{\text{rot.f}} = VI_a \cos \varphi - I_a^2 r_a \text{ watts per phase} \quad (40-2)$$

Consider Fig. 40-1. Let  $OL$  be the current  $I_a$  which corresponds to a fixed torque at a fixed field current. Then with a point  $M_T$  on the axis of ordinates, at first chosen arbitrarily,

$$I_a^2 \sin^2 \varphi = R_T^2 - (\overline{OM}_T - I_a \cos \varphi)^2$$

or

$$2OM_T r_a I_a \cos \varphi - I_a^2 r_a = \overline{OM}_T^2 r_a - R_T^2 r_a$$

If the point  $M_T$  is chosen in such a manner that

$$OM_T = \frac{V}{2r_a} \quad (40-3)$$

then

$$VI_a \cos \varphi - I_a^2 r_a = \frac{V^2}{4r_a} - R_T^2 r_a \quad (40-4)$$

The left side of this equation is the power transferred by the rotating field,  $P_{\text{rot.f}}$  (see Eq. 40-2). In order that this power, i.e., the torque, remain constant and independent of the value of the field current, the quantity on the right side of Eq. 40-4 must be a constant, i.e.,

$$\frac{V^2}{4r_a} - R_T^2 r_a = \text{constant} = P_{\text{rot.f}} \quad (40-5)$$

Since  $V$  and  $r_a$  are constant quantities, the quantity  $R_T$  must also be a constant, if  $P_{\text{rot.f}}$ , i.e., the torque, is to remain constant and independent

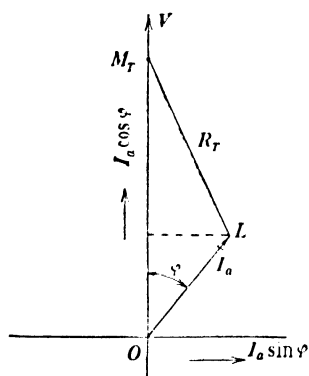


FIG. 40-1. Determination of circle diagram for constant torque and variable field current.

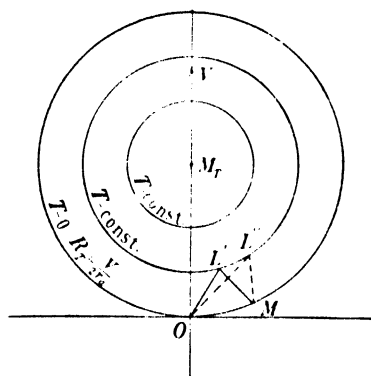


FIG. 40-2. Circle diagrams for constant torque and variable field current ( $r_a$  abnormally large).

of the magnitude of the field current. Thus, the geometric locus of the stator current for constant torque and variable field current is a *circle with  $R_T$  as the radius and  $M_T$  as the center point*, whereby  $OM_T = V/2r_a$ . To each value of the constant torque there corresponds another value of  $R_T$ , but the center point  $M_T$  is always the same for all constant-torque circles.

Solving Eq. 40-5 for the radius  $R_T$  at constant torque (constant  $P_{\text{rot.f}}$ )

$$R_T = \sqrt{\frac{V^2}{4r_a^2} - \frac{P_{\text{rot.f}} (\text{constant})}{r_a}} \quad (40-6)$$

This equation determines the radius of the circle, with  $M_T$  as a center point, which corresponds to the chosen constant value of torque ( $P_{\text{rot.f}}$ ).

The radius  $R_T$  which corresponds to zero torque is

$$R_{T0} = \frac{V}{2r_a} \quad (40-7)$$

Since  $OM_T = V/2r_a$ , the zero-torque circle goes through the origin of the coordinates  $O$ . Fig. 40-2 shows several circles for different values of



constant torque. The larger the torque, the smaller the radius (see Eq. 40-6). The influence of the variation of the field current shows up in the change of the active as well as of the reactive components of  $I_a$  at the same value of torque. The change in the active component is due to the change of the copper losses  $I_a^2 r_a$ . If these losses are assumed to be zero ( $r_a = 0$ ), then according to Eq. 40-2

$$P_{\text{rot.f}} = VI_a \cos \varphi \quad (40-8)$$

In order that the torque ( $P_{\text{rot.f}}$ ) remain constant, the power input  $VI_a \cos \varphi$  must remain constant, i.e., the geometric locus of the primary current  $I_a$  for constant torque at variable field current ( $r_a = 0$ ) becomes

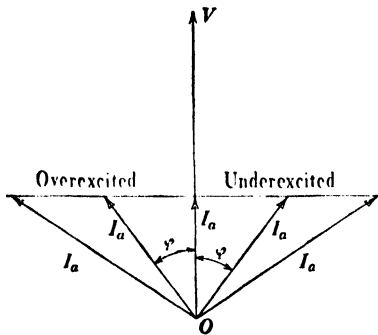


FIG. 40-3. Locus of stator current for constant torque and variable field current ( $r_a = 0$ ,  $I_a \cos \varphi = \text{constant}$ ,  $T = \text{constant}$ ).

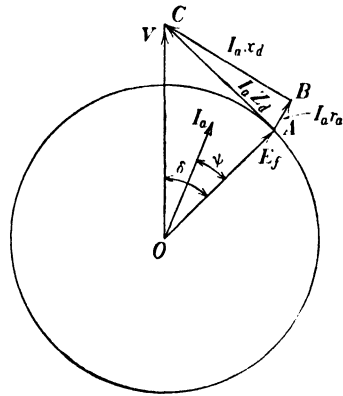


FIG. 40-4. Circle diagram of impedance drop  $I_a Z_d$  for constant field current.

a straight line as shown in Fig. 40-3. As to be expected from the rules of armature reaction (see Art. 37-1) the armature current becomes leading when the motor is overexcited, and lagging when the motor is underexcited.

**40-2. Circle diagrams of the synchronous machine for variable torque and constant field current.** The phasor diagram Fig. 40-4 refers to a motor operating with a lagging current (see Fig. 37-2); the voltage phasor  $V$  is placed in the vertical. The geometric sum of the voltage drops  $I_a r_a$  and  $jI_a x_d$  is designated as  $I_a z_d$ . This latter phasor is  $\psi_a$  degrees ahead of the current phasor  $I_a$  where

$$\tan \psi_a = \frac{x_d}{r_a} \quad (40-9)$$

If the torque is varied at constant field current, the magnitude of the phasors  $V$  and  $E_f$  will not be changed, but the torque angle  $\delta$  (see Art. 39-1) will increase with increasing torque and decrease with decreasing torque. Therefore the phasor  $I_a z_d$  changes with changing angle  $\delta$ , and with it the armature current  $I_a$  also changes.

It can be seen from Fig. 40-4 that, when  $\delta$  varies, the end-point of  $E_f$  describes a circle with the origin  $O$  as a center point. Since the end-point  $C$  of the terminal voltage phasor  $V$  is fixed, the end-point  $A$  of the phasor  $I_a z_d$  which coincides with the end-point of  $E_f$  also moves on a circle. The minimum value of  $I_a z_d$  is

$$I_a z_{d(\min)} = V - E_f \quad (40-10)$$

and the maximum value of  $I_a z_d$  is

$$I_a z_{d(\max)} = V + E_f \quad (40-11)$$

The minimum and maximum values of  $I_a z_d$  lie in the vertical, coinciding with the direction of the voltage phasor  $V$ .

If the end-point of the phasor  $I_a z_d$  moves on a circle, the same must be true of the end-point of the phasor  $I_a$  because  $z_d$  is a constant. The phasor  $I_a z_d$  is  $\psi_a$  degrees ahead of the phasor  $I_a$ . Therefore, the minimum and maximum values of  $I_a$  must lie  $\psi_a$  degrees behind the line on which the minimum and maximum values of  $I_a z_d$  lie, i.e.,  $\psi_a$  degrees behind the terminal voltage  $V$ . Thus, if a line  $OG$  is drawn which lies  $\psi_a$  degrees behind the voltage  $V$  (see Fig. 40-5),  $I_{a(\min)}$  and  $I_{a(\max)}$  lie on this line. The values of  $I_{a(\min)}$  and  $I_{a(\max)}$  are determined by Eqs. 40-10 and 40-11 as

$$I_{a(\min)} = \frac{V - E_f}{z_d}; \quad I_{a(\max)} = \frac{V + E_f}{z_d} \quad (40-12)$$

If, in Fig. 40-5,  $OP_1 = I_{a(\min)}$  and  $OP_2 = I_{a(\max)}$ , then  $P_1 P_2$  is equal to the diameter of the circle on which the end-point of  $I_a$  moves, and the center point  $M$  of the circle lies midway between the points  $P_1$  and  $P_2$ . Thus the diameter of the circle is equal to

$$D = I_{a(\max)} - I_{a(\min)} = \frac{2E_f}{z_d} \quad (40-13)$$

and the distance from center  $M$  to the origin  $O$  is

$$OM = I_{a(\max)} - \frac{D}{2} = \frac{V}{z_d} \quad (40-14)$$

i.e., the diameter of the circle depends upon the magnitude of  $E_f$  and therefore upon the field current, while the position of the center of the circle depends upon the magnitude of the terminal voltage  $V$ . The di-

ameter of the circle changes with the field current, but the center is the same for all circles. The diameter of the circle increases with increasing field current. When the field current is zero, the circle degenerates into a point, namely, the center  $M$  for which the torque is zero. Circle diagrams for variable developed torque for three different values of field current are shown in Fig. 40-7 ( $r_a = 0$ ).

In order to determine the *Torque-Line* in Fig. 40-5, two points must be found on the circle for which the torque is zero (see Art. 27-3).

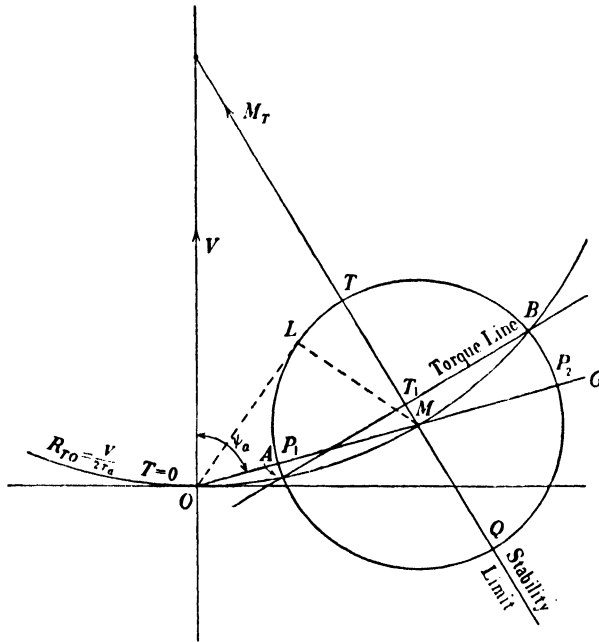


FIG. 40-5. Circle diagram for variable torque and constant field current.

In Fig. 40-2, which represents circle diagrams for constant developed torque and *variable field current*, the two zero-torque points must lie on the circle  $T = 0$ , because this circle comprises all possible values of field current and therefore includes the field current for which the circle of Fig. 40-5 is drawn. Thus, if in Fig. 40-5 a circle is drawn with the radius  $R_{T0} = V/2r_a$  (Eq. 40-7) from a center  $M_T$  on the axis of ordinates and through the origin  $O$ , this circle will intersect the circle of variable torque in two points ( $A$  and  $B$  Fig. 40-5) for which the torque is zero; the line connecting these two points is the *Torque-Line*. The machine operates as a motor on the arc  $AB$  above the *Torque-Line* and as a generator on

the arc  $AB$  below the Torque-Line. Since zero torque corresponds to the center  $M$ , this point must also lie on the  $T = 0$  circle.

The distance from a point on the circle to the axis of abscissae is proportional to the power input (see Art. 27-3), and the distance from a point on the circle to the Torque-Line is proportional to the developed torque of the machine and also to the developed mechanical power of the machine ( $P_{\text{rot.f}}$ ) which includes the windage, friction, and iron losses.

Starting with the point  $A$  (Fig. 40-5), the torque rises and reaches its maximum value (*pull-out torque*)  $TT_1$  at point  $T$ . Beyond the point  $T$  the power input and the armature current increase, but the developed

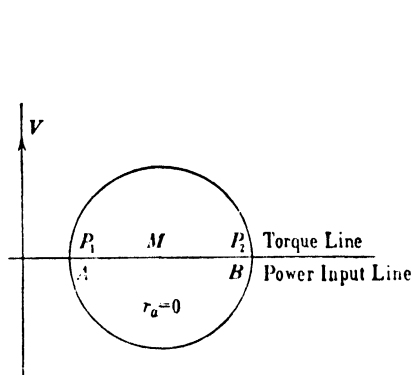


FIG. 40-6. Circle diagram for variable torque and constant field current ( $r_a = 0$ ).

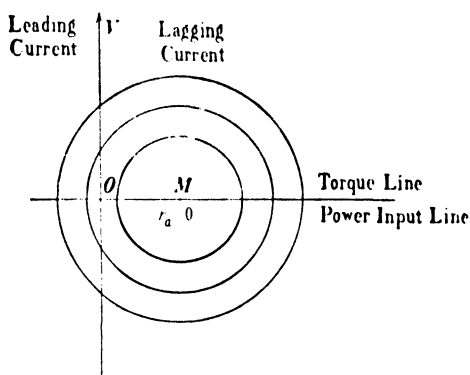


FIG. 40-7. Influence of excitation on overload capacity and power factor ( $r_a = 0$ ).

mechanical power and the torque decrease, because the copper losses increase at a greater rate than the power input. If the load torque plus the loss torque is greater than  $TT_1$ , the motor pulls out of step and comes to rest.

At point  $Q$ , which lies diametrically opposite  $T$ , the developed mechanical power of the machine as a generator reaches its maximum value  $T_1Q$ . If the power output from the prime mover is greater than  $T_1Q$  plus the losses, the prime mover runs away with the generator. The line  $TQ$  represents the *stability limits* of the machine as both a motor and a generator.

If the armature resistance  $r_a$  is neglected ( $r_a = 0$ ) in Fig. 40-5, then  $\psi_a = 90^\circ$ , and the points  $P_1$  and  $P_2$  lie on the axis of abscissae (Fig. 40-6). Therefore the center  $M$  of all circle diagrams for variable torque and constant field current lies on the axis of abscissa. Since, for  $r_a = 0$ , the radius of the  $T = 0$  circle ( $R_{T0}$ , Fig. 40-5, Eq. 40-7) becomes infinite, the geometric locus for  $T = 0$  becomes a straight line coinciding with the

axis of abscissae. Thus, for  $r_a = 0$ , the Torque-Line as well as the power input line coincide with the axis of abscissae (Fig. 40-6).

A comparison between Figs. 40-5 and 40-6, which represent the geometric locus of the stator current of the synchronous machine for variable torque, and Figs. 27-3 and 27-4, which represent the geometric locus of the primary current of the stator of the induction machine for variable torque, shows the similarity of both current diagrams. In both cases the position of the center of the circle diagram depends upon the magnitude of the resistance of the stator winding. In both cases the center of the circle lies on the axis of abscissae and the Torque-Line coincides with the axis of abscissae if the resistance of the stator winding is neglected. However, there are differences between the two types of machines. The diameter of the circle of the induction machine is determined by the parameters ( $r$  and  $x$ ) of its stator and rotor winding and by the line voltage and does not vary when the line voltage is fixed. On the other hand, the diameter of the circle of the synchronous machine depends only upon the parameters of its stator winding and not upon the parameters of its rotor windings. This is due to the fact that at synchronous speed no emf's are induced in the rotor windings. Furthermore, the diameter of the current circle of the synchronous machine can be varied, at fixed line voltage, by varying the field current, i.e.,  $E_f$ .

**40-3. Influence of field current on overload capacity and power factor. V-curves of the synchronous motor. Synchronous capacitor.** Fig. 40-7 shows several circle diagrams for variable torque and constant field current with the armature resistance neglected. The larger diameter corresponds to the larger field current. Two statements with respect to the behavior of the synchronous motor can be made on the basis of Fig. 40-7. First, an increase of the field current increases the pull-out torque, i.e., the ratio of pull-out torque to load torque (*the overload capacity*) increases with increasing field current. (Note that when the armature resistance is not neglected there is a limit to the overload capacity, which does not follow from Fig. 40-7.) Second, at a fixed load the power factor of the motor can be changed over a wide range by changing the field current. At a certain value of field current the power factor is unity; decreasing the field current below this value makes the power factor lagging, while an increase makes it leading. Since the field current influences the overload capacity, certain limits are set for the power factor. The field current of the synchronous motor is usually adjusted in such a manner that the motor operates at rated load either with  $\cos \varphi = 1$  or with a leading power factor.

Consider Fig. 40-5. For a given motor the location of the center  $M$  is fixed by the angle  $\psi_a$ , i.e., by the parameters of the armature winding and by the terminal voltage, since  $OM = V/z_d$ . The current which corresponds to an arbitrary point  $L$  on the circle is  $I_a = OL$ . Then the distance  $LM$  must be equal to  $E_f/z_d$ . This can be seen by comparing Fig. 40-5 with Fig. 40-4. In the latter figure  $OC = V$ ,  $CA = I_a z_d$ , and  $AO = E_f$ . Dividing the sides of the triangle  $OCA$  by  $z_d$  a triangle with the sides  $V/z_d$ ,  $I_a$ , and  $E_f/z_d$  results. Since, in Fig. 40-5,  $MO = V/z_d$  and  $OL = I_a$ , the third side of the triangle  $MOL$ , namely  $LM$ , must be  $E_f/z_d$ . It follows from this that when a point of the plane, for example point  $L'$  in Fig. 40-2, is connected with the origin  $O$  and the center  $M$ , which is fixed for a given motor, the distance  $OL'$  represents a current  $I_a$  and the distance  $L'M$  the quantity  $E_f/z_d$ , both for the same field current; this is true because any point of the plane can be considered as belonging

to a circle diagram for variable torque and constant field current. It should be noted (as previously stated in Art. 40-2) that the point  $M$  lies on the  $T = 0$  circle and corresponds to  $E_f = 0$ . In cylindrical rotor machines the torque developed is zero when  $E_f = 0$  (see Eqs. 39-2 and 39-5).

If the center  $M$  in Fig. 40-5 is fixed for a given motor, then the points on a constant-torque circle (Fig. 40-2) yield currents  $I_a$  ( $OL'$ ,  $OL'' \dots$ ), and the distances from the center  $M$  to these points on the circle yield the corresponding emf's ( $E_f' = L'M \times z_d$ ) ( $E_f'' = L''M \times z_d$ ) and so forth. In this way the correlation between the armature currents  $I_a$  and the emf's  $E_f$  corresponding to the currents  $I_a$  can be found for any constant-torque circle. Fig. 40-8 shows  $I_a = f(E_f)$  for three different constant values of  $T$ . These curves have the shape of a  $V$  and are called the *V-curves* of the synchronous motor.

Each constant torque circle (Fig. 40-2) has a *minimum* current at which the constant torque is produced: this is the lower intersection point of the circle with the axis of ordinates. The minimum currents for the different constant torque circles are connected in Fig. 40-8 by a dotted line: this minimum-current line is also the unity power factor line as can be seen from Fig. 40-2.

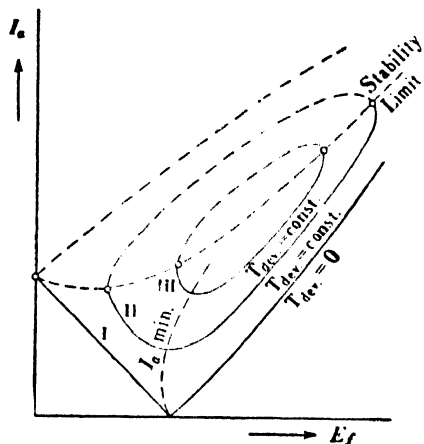


FIG. 40-8. V-curves of a synchronous motor.

It has been explained previously that the magnitude of the pull-out torque depends upon the field current. For any constant torque  $T$  (Fig. 40-8) there is a field current at which this constant torque becomes equal to the pull-out torque: at this specific field current the stability limit is reached. The field currents (emf's  $E_f$ ) which determine the stability limits are also indicated in Fig. 40-8. At large values of torque  $T$  the stability limit approaches the unity power factor field current. A relatively small underexcitation in this case may cause the motor to fall out of step. It follows that the synchronous motor must be overexcited in the region of maximum output.

If a synchronous motor is overexcited, it is forced to draw a leading current from the line (see Art. 37-1 and Fig. 40-7). The synchronous motor then performs the function of a static capacitor, i.e., it compensates for the lagging reactive currents necessary to sustain the fluxes in induction motors and transformers and thus reduces the amount of lagging current to be supplied by the generators; as a result the generators can be made smaller, since they do not have to supply the total amount of lagging current demanded by the load. Overexcited synchronous motors operating at no-load are called *synchronous capacitors* and are used to compensate for lagging reactive currents in large transmission lines. They are built only in large units.

**Example 40-1.** A plant operates with an average load of 1200 kw at 0.65 p.f. lagging. If a 500-HP 0.8-p.f. synchronous motor is added, what will be the over-all power factor when the motor operates at full-load? Assume efficiency = 94.5%; motor input =  $500 \times 0.746/0.945 = 394$  kw;  $394/0.80 = 493$  kva; kvar =  $493 \times 0.60 = 296$ ;  $1200 \times 1.17 = 1400$  kvar of original lagging load; total kw =  $1200 + 394 = 1594$ ; total kvar =  $1400 - 296 = 1104$ ;  $\tan \phi = 1104/1594 = 0.697$   $\cos \phi = 0.82$ .

**Example 40-2.** If the synchronous motor operates at  $\frac{1}{2}$  load with excitation unchanged, what will be the plant power factor? From Fig. 40-9 it is seen that the motor kva =  $493 \times 0.85 = 418$ ; kvar =  $493 \times 0.73 = 360$ ; p.f. = 0.51; kw =  $0.51 \times 418 = 214$ ; total kw =  $1200 + 214 = 1414$ ; total kvar =  $1400 - 360 = 1040$ ;  $\tan \phi = 1040/1414 = 0.734$ ;  $\cos \phi = 0.806$  or practically the same as before.

**Example 40-3.** How much additional kw should be carried by a synchronous motor added to the original plant, so as to raise the plant power factor to 0.95 but not to exceed the original kva of the feeders? What would be the power factor of the synchronous motor and about what would be its HP rating? Original load 1200 kw =  $1200/0.65 = 1845$  kva (this is the original feeder capacity),  $1200 \times 1.17 = 1400$  kvar. At 0.95 p.f.,  $1845 \times 0.95 = 1750$  kw; motor kw =  $1750 - 1200 = 550$ . Resulting kvar =  $1845 \times 0.312 = 575$ ; leading kvar =  $1400 - 575 = 825$  for motor. HP input of motor =  $550/0.746 = 736$ . Thus a synchronous motor rated 700 HP would be suitable, operating at about 0.55 p.f. at full-load.

**40-4. Starting of a synchronous motor.** It was pointed out in the treatment of the induction motor (see Art. 24-1) that a uniform torque can

be developed only when the mmf waves of both stator and rotor are stationary with respect to each other. This condition is satisfied for the synchronous motor when it runs at synchronous speed; only at this speed the stator mmf and the rotor mmf have the same speed  $n_s = 120f/p$ .

Consider the synchronous motor at standstill. If, in order to start the motor, the stator is connected to the line, the stator mmf achieves synchronous speed immediately, while the rotor mmf is still at standstill.

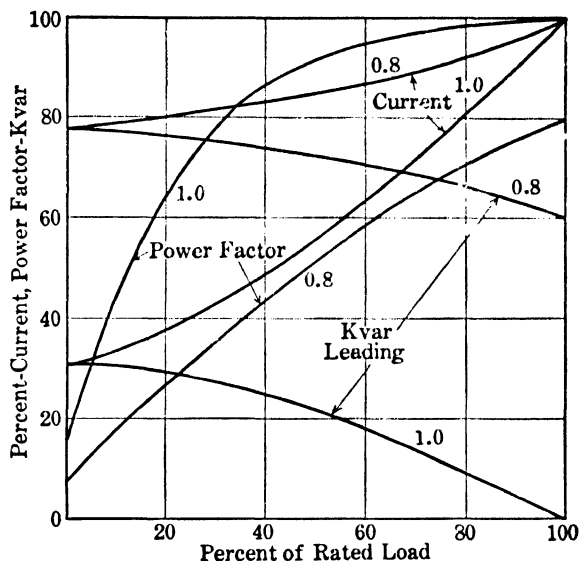


FIG. 40-9. Characteristics of unity and 0.80 power factor synchronous motors.

Therefore no starting torque is developed, and the motor will not come up to speed. The conditions are entirely different for the induction motor, because the rotor of this motor is not connected to a source of power but establishes its currents by induction from the stator. As has been explained (in Art. 24-2) the mmf waves of stator and rotor in this case are at standstill with respect to one another at *any* rotor speed, including standstill; therefore, the induction motor is capable of developing a starting torque.

In order to make it possible for a synchronous motor to start, it is supplied with a squirrel cage similar to that of the induction motor. For reasons which will become clear later (see Art. 42-4), the squirrel-cage winding is called the *damper winding*. The damper bars are placed in slots punched in the pole shoes (see Figs. 35-6 and 35-8); they are connected on both sides of the pole shoes by segments which are joined



together to make a ring connection on each side of the poles. The cage is not complete, since there are no bars in the interpolar spaces.

Just as the squirrel-cage induction motor does, the synchronous motor takes a relative large starting current from the lines. However, since the damper winding is to be used only for starting, and not for running as in the case of the induction motor, its resistance and leakage reactance can be freely adjusted to suit the required starting torque and starting current.

The rotating flux cannot induce an emf in the field winding at synchronous speed, because at this speed the flux is stationary with respect to the poles. However, it is quite different during the starting period when the speed of the field structure is less than that of the rotating flux; in this case a high emf is induced in the field winding which has a large number of turns, and this induced emf may lead to a breakdown of the insulation, if the field winding is left open during starting. In order to protect the field winding it is *closed* through a resistor during the starting period. This resistor is removed from the field circuit, and the d-c excitation is applied when the rotor reaches its maximum induction motor speed; the motor then falls into synchronism and runs as a synchronous motor. At synchronous speed the damper winding is ineffective.

The resistance inserted in the field circuit during starting is about 5 to 15 times the resistance of the field winding. Besides protecting this winding it also improves the starting performance of the motor.

When it is necessary to reduce the starting current of a synchronous motor, the same means can be employed as for the induction motor: an autotransformer, or a reactor in series with the stator winding, is quite effective. Sometimes *part-winding starting* is applied: in this case each phase of the stator winding consists of two or more parallel parts and only a part of each phase is used for starting. This increases the leakage reactance of the stator winding and thus reduces the starting current, but it also reduces the starting torque.

### PROBLEMS

(Consider all machines unsaturated. Unit current =  $I_{HP.}$ )

1. A 700-HP, 6-pole, 3-phase, 60-cycle, 4000-volt (star-connected) synchronous motor has the following data at full-load:

Efficiency	= 93%
Field current	= 25.0 amp
Total iron loss	= 5.6 kw
Friction and windage loss	= 3.2 kw
Stray load loss	= 2.0 kw

Further:

$$r_a = 0.012 \text{ p-u}$$

$$x_l = 0.10 \text{ p-u}$$

$$x_{ad} = 1.08 \text{ p-u}$$

The air-gap line is determined by:

$$I_f = 13.5 \text{ amp} \quad E = 3080 \text{ volts (line-line)}$$

It can be assumed that the rotational iron losses are equal to 2.5 kw. Construct the circle diagram for rated field current and determine the stator current, power factor, and the ratio of pull-out torque to rated torque (developed values).

2. Construct, for the motor of Problem 1, several circle diagrams for constant developed torque and draw the V-curves of the motor.

3. Repeat Problem 1 for  $r_a = 0$ .

4. Repeat Problem 2 for  $r_a = 0$ .

5. A 250-HP, 26-pole, 3-phase, 60-cycle, 2200-volt (star-connected) synchronous motor has the following data at full-load:

Efficiency	= 91%
Field current	= 36 amp
Total iron loss	= 5.0 kw
Friction and windage loss	= 0.7 kw
Stray load loss	= 0.9 kw

Further:

$$r_a = 0.014 \text{ p-u}$$

$$x_l = 0.14 \text{ p-u}$$

$$x_{ad} = 0.74 \text{ p-u}$$

The air-gap line is determined by:

$$I_f = 23.5 \text{ amp} \quad E = 2100 \text{ volts}$$

It can be assumed that the rotational iron losses are equal to 2.5 kw.

Construct the circle diagram for rated field current and determine the stator current, power factor, and ratio of pull-out to rated torque (developed values).

6. Construct, for the motor of Problem 5, several circle diagrams for constant developed torque and draw the V-curves of the motor.

7. Repeat Problem 5 for  $r_a = 0$ .

8. Repeat Problem 6 for  $r_a = 0$ .

9. Repeat Problem 1 for  $I_f = 17$  and 35 amp and draw the curve

$$\frac{T_{\text{dev. p.o.}}}{T_{\text{dev. rated}}} \text{ vs. } I_f.$$

10. Repeat Problem 5 for  $I = 25$  and 43 amp and draw the curve

$$\frac{T_{\text{dev. p.o.}}}{T_{\text{dev. rated}}} \text{ vs. } I_f.$$

## Chapter 41

### SMALL SYNCHRONOUS MOTORS

Fractional-horsepower synchronous motors are built for a wider range of output and speed than fractional-horsepower induction motors. In miniature ratings (below 0.001 HP) they are used for clocks, timing devices, control apparatus, etc.

There are two basic types of fractional-horsepower synchronous motors which do not need d-c excitation and are self-starting. These are the *reluctance* type motor and the *hysteresis* type motor.

**41-1. The reluctance motor.** The ASA defines the reluctance motor as follows: A reluctance motor is a synchronous motor similar in construction to an induction motor, in which the member carrying the secondary circuit has salient poles, without direct-current excitation. It starts as an induction motor but operates normally at synchronous speed.

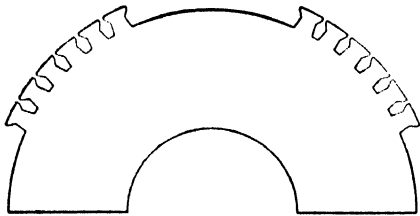


FIG. 41-1. Rotor of a reluctance motor.

Fig. 41-1 shows the rotor punching of a  $\frac{1}{2}$ -HP, 4-pole, 3-phase reluctance motor. Six teeth are removed at four places, yielding four salient poles. Since this motor starts as an in-

duction motor, the rings connecting the rotor bars must be complete, i.e., they must go around the whole rotor. The teeth can be cut out only partially, and the free spaces filled with aluminum in die-cast aluminum rotors, as shown in Fig. 41-2.

It has been shown in Art. 39-1 that a *salient-pole* machine is able to produce torque and run at synchronous speed without field excitation. Use is made of this property in the reluctance motor. Having started as an induction motor and having reached its maximum speed as an induction motor, it pulls into step and runs as a synchronous motor by virtue of its saliency.

As for the d-c excited synchronous motors, pulling-into-step is facilitated when the speed reached as an induction motor is as high as possible. This means that the rotor resistance must be made low. Furthermore, the motor pulls into step easier the lower the  $W/R^2$  of the rotating mass (rotor + load).

The stator of the reluctance motor can be polyphase or single phase. Therefore, there are:

- (a) polyphase reluctance motors,
- (b) split-phase type reluctance motors, and
- (c) capacitor-type reluctance motors.

In the case of the split-phase type, the capacitor-start, and the two-value capacitor motors the usual switch is necessary to cut out the starting winding or to change the capacitance before the motor reaches synchronous speed.

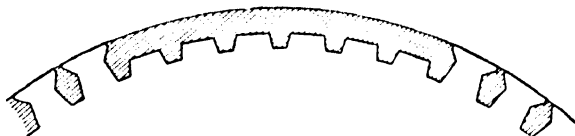


FIG. 41-2. Rotor of a reluctance motor (die-cast aluminum.)

**41-2. The hysteresis motor.** The ASA defines the hysteresis motor as follows: A hysteresis motor is a synchronous motor without salient poles and without direct-current excitation, which starts by virtue of the hysteresis losses induced in the hardened steel secondary member by the revolving field of the primary, and operates at synchronous speed *due to the retentivity of the secondary core*.

In order to explain the operation of the hysteresis motor the induction motor will be considered. During the starting of the latter motor, eddy-current and hysteresis losses appear in the rotor iron. Both kinds of losses are accompanied by torques.

It is obvious that the eddy currents in the rotor iron are able to produce a torque with the machine flux in the same way as the currents in the rotor bars do. Writing, for the eddy-current loss in the rotor (Eq. 10-4),

$$p_e = c_e f_2^2 B^2 = c_e s^2 f_1^2 B^2 \quad (41-1)$$

and applying Eq. 26-7 for the torque, the driving torque which corresponds to the eddy currents in the rotor is

$$T_e = \frac{7.04}{n_s} \frac{c_e s^2 f_1^2 B^2}{s} = \frac{7.04}{n_s} c_e s f_1^2 B^2 \quad (41-2)$$

This torque is proportional to the slip; it decreases with increasing rotor speed and becomes zero at synchronous speed.

The hysteresis losses in the rotor iron can be written (Eq. 10-3),

$$p_h = c_h f_2 B^2 = c_h s f_1 B^2 \quad (41-3)$$

Again applying Eq. 26-7 the torque which corresponds to the hysteresis losses in the rotor is

$$T_h = \frac{7.04}{n_s} c_h f_1 B^2 \quad (41-4)$$

This torque is constant and independent of the rotor speed.

In order to get a physical conception of the torque  $T_h$ , called *hysteresis torque*, consider Figs. 41-3 to 41-5. It will be assumed that the rotor of the induction motor has no secondary winding so that the driving torque is due only to the eddy-current and hysteresis losses. If there are no

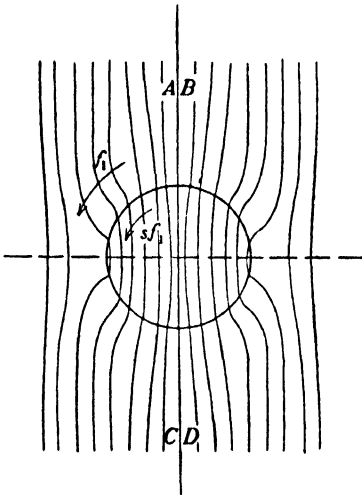


FIG. 41-3. Iron rotor without hysteresis in a magnetic field.

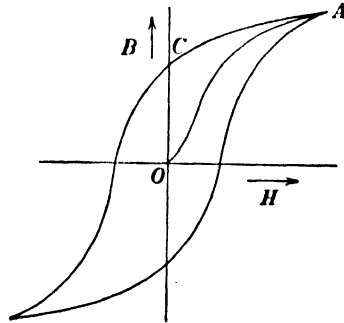


FIG. 41-4. Hysteresis loop.

hysteresis losses, the magnetization of the rotor is in phase with the stator mmf, as shown in Fig. 41-3: the magnetic axis  $AC$  of the rotor coincides with the axis  $BD$  of the stator mmf. Fig. 41-4 shows a hysteresis loop. Conforming to the meaning of the word *hysteresis*, the flux density  $B$  lags behind the magnetizing force when there are hysteresis losses. For example, starting at the point  $A$  of the loop and decreasing the magnetizing force to the value zero, the flux density will not be zero but equal to  $OC$ . If the motor considered has hysteresis losses, this lag of the magnetization behind the magnetizing force due to hysteresis results in a lag of the magnetic axis of the rotor behind the axis of the stator mmf,

as shown in Fig. 41-5. The angle of lag  $\alpha$  which causes the hysteresis torque is independent of the frequency of the magnetization of the rotor  $f_2 = sf_1$ ;

it depends only upon the hysteresis loop of the material used for the rotor and remains the same at all rotor speeds. Hence the hysteresis torque is constant and independent of the rotor speed.

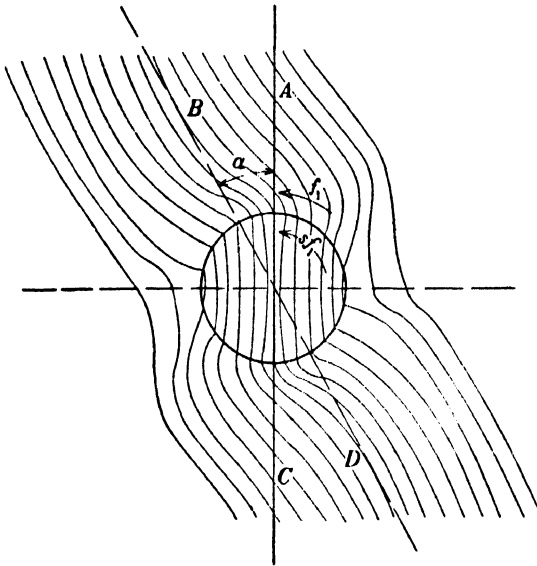


FIG. 41-5. Iron rotor with hysteresis in a magnetic field.

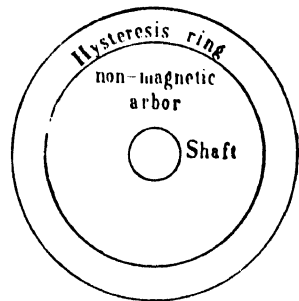


FIG. 41-6. Rotor of a hysteresis motor.

It follows from the foregoing that the rotor iron must have high hysteresis losses, i.e., a large hysteresis loop. The rotor construction of the hysteresis motor is schematically shown in Fig. 41-6. A ring of special magnetic material, such as cobalt or chrome steel, is mounted on an arbor of non-magnetic material such as aluminum. No squirrel cage is used. Starting is produced by the eddy-current *and* hysteresis torques. At synchronous speed, the eddy-current torque is zero, and the operation of the motor is accomplished exclusively by the hysteresis torque. At this speed the rotor develops magnetic poles similar to the d-c excited synchronous motor or reluctance motor. The strength of the poles is determined by the retentivity of the rotor-ring material (*OC* in Fig. 41-4).

The stator of the hysteresis motor is usually single phase. There are:

- (a) polyphase hysteresis motors
- (b) capacitor type hysteresis motors
- (c) shaded pole hysteresis motors

The hysteresis motor is the most quiet of small motors. (For other types of small synchronous motors see Ref. on A-c Machines at end of text.)

## Chapter 42

### HUNTING OF A SYNCHRONOUS MACHINE

**42-1. The synchronizing torque.** Consider a synchronous motor under load with a voltage diagram for  $r_a = 0$  as shown in Fig. 42-1. The pole structure assumes a position such that the emf phasor  $E_f$  lags the terminal

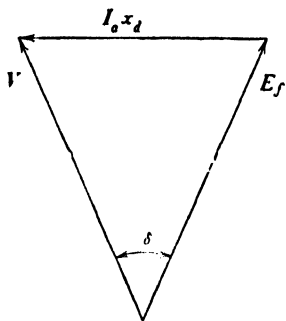


FIG. 42-1. Phasor diagram of a cylindrical rotor synchronous motor ( $r_a = 0$ ).

\*See footnote on p. 401.

voltage  $V$  by an angle  $\delta$ , the magnitude of which is fixed by the load. As is seen from Fig. 42-1, the simplest case, i.e., the unsaturated machine with cylindrical rotor, is being considered again.

Now assume that the load on the motor shaft is suddenly dropped. Then the angle  $\delta$  must become zero, i.e., the pole structure has to move forward by the angle  $\delta$ . This cannot happen suddenly because of the mass of the rotor (flywheel effect of the rotor). Consequently, in spite of the loss of the load, the armature current will not become zero at once, and the torque produced by this current, which previously served to overcome the load torque, will now accelerate the pole structure. When the pole structure reaches the zero position ( $\delta = 0$ ), its kinetic energy will cause it to swing ahead of this position. The emf  $E_f$  now leads the terminal voltage  $V$ , and the machine operates as a generator. However, since generator operation cannot continue due to the lack of a prime mover, the angle  $\delta$  must again become zero, and the action repeats itself. The entire sequence of events can be observed on the ammeters and wattmeters.

This kind of oscillation is similar to that of a flywheel (sometimes called a balance wheel) and a torsion spring. If the spring is under tension when the flywheel is at rest, and the flywheel is then released, the force of the spring seeks to bring it first to the zero position. However, since the wheel is accelerated by the force of the spring during the entire travel to

the zero position, maximum velocity occurs at  $\delta = 0$  and, therefore, the wheel swings beyond this zero position. The spring is now twisted in the opposite direction. The position of rest (end position) is again reached when the kinetic energy of the flywheel has been converted into the potential energy of the spring. The action starts again and continues until the original energy stored in the spring is absorbed by the frictional losses of the system.

The fact that the output of a synchronous machine depends upon the position of its pole structure, and that every change in the position of the poles involves a corresponding change in the output, causes the synchronous machine to act as an oscillating system. The change in output (or torque), produced by twisting the pole structure through a unit angle, may be compared to the change in the force of the spring in the mechanical system consisting of flywheel and spring, when the flywheel is twisted through a unit angle.

The *change in the torque per unit angle* is called the *synchronizing torque* of the synchronous machine. Therefore, this is the torque with which the pole structure is restored to its mid-position when it is twisted ahead of or behind this position by a unit angle.

The power transferred by the rotating flux of an  $m$ -phase synchronous machine is given by Eq. 39-5 (resistance neglected):

$$P_{\text{rot. f}} = m \frac{E_f V}{x_d} \sin \delta \quad (42-1)$$

The torque corresponding to this power is:

$$T = \frac{7.04}{n_s} m \frac{E_f V}{x_d} \sin \delta \quad (42-2)$$

and consequently the synchronizing torque is:

$$T_s = \frac{dT}{d\delta} = \frac{7.04}{n_s} m \frac{E_f V}{x_d} \cos \delta \quad (42-3)$$

In a manner similar to that of suddenly dropping the entire load on a synchronous motor, every sudden change in load of a synchronous motor or generator produces oscillations. The frequency of these oscillations depends solely upon the magnitude of the synchronizing torque and upon the magnitude of the flywheel mass to be accelerated and decelerated. Since an applied force is absent, the *system oscillates freely at its natural frequency*. These are the same oscillations which the mechanical system, consisting of flywheel and spring, executes when the flywheel is twisted and the system is then allowed to oscillate freely. The directive force



of the spring and the mass of the wheel are the factors which determine the frequency of oscillation. Here, as in the synchronous machine, damping has only a negligible influence on the frequency of oscillation.

Of greater importance than the natural oscillations are the *forced oscillations* which appear in the synchronous machine when the prime mover torque of a generator is irregular, as in a gas engine, or when the load torque of a motor is irregular, as in a compressor.

If, in the foregoing example of spring and flywheel, a force is applied which has the same period as that of flywheel and spring, then the amplitude of the oscillations becomes greater and greater; the amplitude would become infinitely great if no damping were present. The magnitude of the imparted torque is of no consequence whatever; the smallest torque suffices to produce violent oscillations. A similar condition appears, although the amplitude of the oscillations does not become as great, when the period of the applied force is not exactly the same as the natural frequency of the system but is very near to it. When an applied force is present, the frequency of oscillations is independent of the natural frequency of the system and is equal to the frequency of the applied force (*forced oscillations*). The case where the frequency of the forced oscillations is equal or close to the natural frequency of the system (resonance) is always dangerous.

It should be noted that a synchronizing torque appears only when the phasor of the terminal voltage  $V$  is fixed, as is the case of a generator operating in parallel with other generators, or of a motor (Fig. 42-1). In a singly operated synchronous generator the phasor  $V$  follows the emf phasor  $E_f$ , and there is no synchronizing torque. Again, considering the system of flywheel and spring with damping, a singly operated generator lacks the spring equivalent or, comparing the synchronous machine with a  $LCR$ -circuit, the singly operated generator behaves like a  $LR$ -circuit, whereas the generator, operated in parallel with other generators, and the synchronous motor behave as an  $LCR$ -circuit.

#### **42-2. The ratio of the amplitude of oscillation in parallel operation to the amplitude of oscillation of the single machine (the amplification factor).**

A singly operated generator follows forced oscillations just as an  $LR$ -circuit follows the magnitude and frequency of the impressed voltage. Comparing the  $LR$  and the  $LCR$ -circuits, for equal impressed terminal voltage and frequency, the frequency of the oscillations (of the current) will be the same in both circuits, but the magnitude of the oscillations (the amplitude of the current) will, in general, be different. The same applies to the singly operated generator and to the generator operated

in parallel with other generators. Considering the torque of the prime mover as consisting of a constant term, which produces the average power of the generator, and a superimposed sinusoidally varying term, which produces power oscillations, the generator operated in parallel with other generators will react differently, with respect to the oscillating torque, than the singly operated generator. The ratio of the amplitudes of oscillation for both cases will be considered in the following:

Let

$\Omega = \frac{\omega}{p/2}$  = instantaneous mechanical angular velocity of the machine;

$\Omega_m$  = mean mechanical angular velocity of the machine;

$\omega_m$  = mean electrical angular velocity of the machine;

$J$  = moment of inertia of flywheel mass;

$T_\nu$  = amplitude of the periodically varying part of the torque curve of the prime mover, having the angular velocity  $\nu\Omega_m$ .

The equation representing the motion of a *singly* operated machine is then

$$\frac{J}{p/2} \frac{d(\omega - \omega_m)}{dt} = T_\nu \sin(\nu\Omega_m t) \quad (42-4)$$

i.e., the oscillating term of the torque of the prime mover is used to accelerate the flywheel mass when it is positive, and decelerate the flywheel mass when it is negative, thus producing changes in the angular velocity of the rotating mass relative to the mean velocity.

If the machine operates in parallel with other synchronous machines, the terminal voltage produced is common for all. If the machine in consideration is subjected to forced oscillations by the prime mover, the line voltage phasor  $V$  is no longer able to take part in the oscillations as in the case of the singly operated machine, but it must retain its position. As explained in the foregoing, the hunting pole structure will then give rise to variations in the magnitude of the angle  $\delta$ , and consequently a synchronizing force appears. The *synchronizing torque*  $T_s$  is equal to the *change in the machine torque per unit angle*. For a change in the angle from  $\delta_m$  to  $\delta$ , where  $\delta_m$  corresponds to the mean position of the pole structure, the change in the machine torque is  $T_s(\delta - \delta_m)$ . The surplus (or deficiency) torque which the prime mover delivers is used now, on the one hand, for accelerating (or decelerating) the mass of the flywheel and, on the other hand, to balance the synchronizing torque.

Accordingly, the equation of motion of the synchronous machine connected to a constant voltage line is:

$$\frac{J}{p} 2 \frac{d(\omega - \omega_m)}{dt} + T_s(\delta - \delta_m) = T_v \sin (\nu \Omega_m t) \quad (42-5)$$

The solution of this latter equation is readily obtained by considering an oscillating circuit consisting of inductance and capacitance. The voltage equation of this circuit is

$$L \frac{di}{dt} + \frac{1}{C} \int i dt = E_m \sin \omega t \quad (42-6)$$

Differentiating this equation:

$$L \frac{d^2 i}{dt^2} + \frac{i}{C} = E_m \omega \cos \omega t \quad (42-7)$$

On the other hand, by differentiating Eq. 42-5,

$$\frac{J}{p} 2 \frac{d^2(\omega - \omega_m)}{dt^2} + T_s(\omega - \omega_m) = T_v \nu \Omega_m \cos (\nu \Omega_m t) \quad (42-8)$$

Equations 42-7 and 42-8 are identical in all respects. The mutually corresponding terms are

$$\begin{aligned} (\omega - \omega_m) & \dots \dots i \\ \frac{J}{p} 2 & \dots \dots L \\ T_s & \dots \dots \frac{1}{C} \end{aligned} \quad (42-9)$$

In the same manner, where the synchronizing force is zero and only mass is present, Eq. 42-4 corresponds to a circuit containing only inductance.

The similarity of the differential equations offers a means of determining the magnitude of the oscillations of the synchronous machine from the  $L$  and  $LC$  circuits. Damping has been discounted for the synchronous machine and, therefore,  $R$  must be assumed zero in the electric circuits.

The amplitude of the current in a circuit containing only inductance is given by:

$$I_{m.L} = \frac{E_m}{\omega L}$$

In a circuit containing self-inductance and capacitance the amplitude of the current is:

$$I_{m,LC} = \frac{E_m}{\omega L - \frac{1}{\omega C}}$$

The ratio of these currents is:

$$\frac{I_{m,LC}}{I_{m,L}} = \frac{\omega L}{\omega L - \frac{1}{\omega C}} = \frac{1}{1 - \frac{1}{(2\pi)^2 f^2 LC}} = \zeta \quad (42-10)$$

However,  $1/(2\pi\sqrt{LC})$  is the natural frequency ( $f_n$ ) of oscillation of an  $LC$  circuit. Consequently, the ratio of the maximum value of current in a circuit containing  $L$  and  $C$  to that in a circuit containing  $L$  alone is given by:

$$\zeta = \frac{1}{1 - \left(\frac{f_n}{f}\right)^2} \quad (42-11)$$

The same equation must apply to the hunting of a synchronous machine. The factor  $\zeta$  is called the *amplification factor* or the *modulus of resonance*. It gives the ratio of the *amplitude* of oscillation of a system containing mass and synchronizing force to that of a system in which only mass alone is present.

**42-3. The natural frequency of the synchronous machine. The danger of resonance.** The natural frequency of oscillation of a synchronous machine obtained by comparing it to a circuit consisting of inductance and capacitance is (Eq. 42-9)

$$f_n = \frac{1}{2\pi} \sqrt{\frac{(p/2)T_*}{J}} \quad (42-12)$$

The amplification factor  $\zeta$  depends on the frequency  $f$  of the forced oscillations of the prime mover, and on  $f_n$ , the natural frequency of oscillation.  $\zeta$  is the ratio of two amplitudes of oscillation, namely, that of a system with synchronizing force and mass to that of a system with mass alone. The amplitude of oscillation of the system containing mass alone has a constant finite magnitude which remains within fixed limits. *The amplification factor  $\zeta$  is, therefore, directly a measure of the magnitude of the oscillations which appear in parallel operation.*

Fig. 42-2 shows the relation between the amplification factor and the ratio ( $f_n/f$ ) in which the negative values of  $\zeta$  obtained for  $f_n > f$  are drawn upward.

Equation 42-10 and Fig. 42-2 show that the amplification factor becomes greater as the natural frequency of the machine and the frequency of the forced oscillations of the prime mover (or of the load in the

case of a motor) approach each other. If the natural frequency and the forced frequency are equal (resonance), the amplitude factor  $\zeta$  then becomes infinitely great. *In order to avoid the danger of resonance, the natural frequency of oscillation and the forced frequency of the prime mover (or load) must differ from each other.*

The values of  $\zeta$  which lie between  $\zeta = +3$  and  $\zeta = -2$  (the cross-hatched region, Fig. 42-2) are to be avoided for satisfactory parallel operation.

The adjustment of the appropriate ratio of  $f_n$  to  $f$  is essentially accomplished by a suitable selection of the moment of inertia of the rotating mass (see Eq. 42-12). The synchronizing torque  $T_s$  can be changed only within small limits.

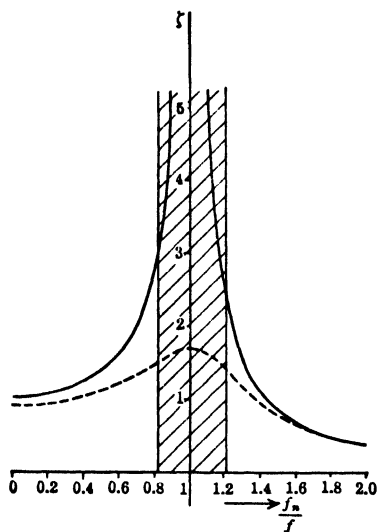


FIG. 42-2. Resonance curves.

#### 42-4. Improvement of parallel operation by means of a damper winding.

A reduction in the hunting can be achieved by a damper winding which is placed in the pole shoes in the same manner as the starting winding of the synchronous motor (see Art. 40-4), with the individual poles often not connected together. When the machine hunts, the armature flux no longer remains stationary with respect to the pole structure, but a difference in velocity between these two exists. Because of this difference, currents flow in the bars of the damper winding, which serve to reduce the oscillations.

Under some circumstances an excessively strong damping effect can be disadvantageous. If the mechanical hunting is prevented by too strong a damping effect, the flywheel mass loses its property as a reservoir of energy necessary to compensate for the torque variations of the prime mover. These torque variations are consequently transmitted to the generator so that its output and current vary in the same manner as the torque of the prime mover. This is not desirable for two reasons: first, the

other machines operating in parallel must take over the compensating effect; second, the varying current gives rise to higher copper losses.

If the pole shoes are solid, eddy currents are produced in them as a result of the relative motion between the armature field and the poles; these eddy currents act in a manner similar to a damper winding. On the other hand, in machines with laminated pole shoes the self-damping effect is slight and a damper winding has to be used. A certain amount of damping always is necessary, or otherwise the free oscillations which appear in the case of suddenly applied loads would continue undamped and thereby become of infinitely long duration.

If very strong damping is present, the resonance curve  $\zeta = f(f_n/f)$  flattens out as is indicated by the dotted curve of Fig. 42-2.

From the above it becomes clear why the squirrel cage in the pole structure of the synchronous machine is called a damper or amortisseur winding.

It should be mentioned that when an induction motor is subjected to oscillations of its speed, i.e., to hunting, it also develops a synchronizing and damping torque. (See reference on A-C Machines at end of text.)

\* Notice that in Fig. 42-1 the phasor  $E_f$  is shown without a minus sign (see Fig. 37-2). This is done in order that a single phasor diagram may be used for both generator and motor operation, in which the phasor  $V$  is *common* to both types of operation. Since  $V$  is a generated voltage in the case of a generator and an impressed voltage in the case of a motor, the phasors representing  $V$  are opposite in sign. Therefore, when  $V$  is represented by a single phasor for both motor and generator, the sign of  $-E_f$  must be reversed for motor action.

## Chapter 43

### LOSSES IN SYNCHRONOUS MACHINES HEATING AND COOLING

**43-1. The losses in the synchronous machine.** Similar to those in the d-c machine, losses in the synchronous machine are as follows:

(a) *Losses due to the main flux.* For the same reasons as given for the d-c machine (Art. 10-1) and the induction motor (Art. 34-1), the hysteresis and eddy-current losses due to the main flux are larger than those calculated from Eq. 10-5 or from iron-loss curves (given at end of text). The increase may be as high as 40 to 60% for salient-pole machines, 30 to 40% for 4-pole machines with cylindrical rotor, and 15 to 25% for 2-pole machines with cylindrical rotor.

Just as in the d-c machine, the ripple due to the slot-openings of the stator (see Fig. 10-1) causes high-frequency eddy currents in the pole surface. The losses produced by these eddy currents in per cent of the losses due to the main flux are approximately: 50 to 70% in salient-pole machines, 40 to 50% in 4-pole machines with cylindrical rotor, and 25 to 50% in 2-pole machines with cylindrical rotor.

Similar to the induction motor, the ripple produced by the slot openings causes currents not only in the iron but also in the damper winding of the salient-pole machine. The currents induced in the damper bars and their losses become considerable, if the slot pitch of the cage is much different from the stator slot pitch. A difference of up to 25% in the slot pitches keeps the losses at a low level. The losses are negligible when both slot pitches are equal to each other. Equal slot pitches can be made in salient-pole generators but not in motors, because this would produce locking torques which may prevent starting of the motor.

(b) *Losses due to the load current.* The load current produces  $I^2R$  losses in the stator winding and usually increases the  $I^2R$  losses of the field winding due to armature reaction. The additional losses due to the load current are similar to those of the induction motor.

The *cross-flux* in the slots produces skin-effect which may increase the copper loss considerably. Conductors stranded depthwise or special conductors (Roebel bars) must be used in large machines, in order to reduce the skin-effect losses. An increase of 15 to 20% in the  $I^2R$  losses due to skin-effect is reasonable.

TABLE 43-1. NO-LOAD LOSSES

Salient-pole machines.	Iron losses in the stator due to the main flux.	Pole surface losses due to slot openings.	Copper losses in the damper winding due to slot openings.	Windage and bearing friction losses.
Cylindrical rotor machines.	Iron losses in the stator due to the main flux.	Rotor surface losses due to slot openings.		Windage and bearing friction losses.

The *harmonic fluxes* produced by the stator winding produce surface losses in the rotor, in the same way as the ripple due to the slot openings. In the salient-pole machine these losses appear on the pole surfaces; in the cylindrical rotor machine, on the surface of the solid rotor. Because of the relatively large gap of the synchronous machine, these losses are usually small, about 0.05 to 0.15% of the output.

TABLE 43-2. LOAD LOSSES

Salient-pole machines.	$I^2r$ losses in stator and rotor windings.	Skin-effect losses in the stator winding.	Pole surface losses due to harmonic fluxes.	Losses in structural parts due to leakage fluxes.
Cylindrical rotor machines	$I^2r$ losses in stator and rotor windings.	Skin-effect losses in the stator winding.	Rotor surface losses due to harmonic fluxes.	Losses in structural parts due to leakage fluxes.

As in large induction motors, the *leakage fluxes of the end-windings* produce eddy-current losses in the structural parts (end plates, finger plates, bolts, etc.). The use of non-magnetic iron for the end plates and rotor retaining rings reduces these losses.

(c) *Friction and windage losses.* With respect to the friction and windage losses, the same reasoning applies as for the d-c machine and induction motor. The windage losses are quite high in 2-pole generators with cylindrical rotor. The use of hydrogen instead of air as a cooling



medium reduces the windage losses to about 10% of those which appear with air.

(d) *No-load and load losses; stray load losses.* The losses which appear at no-load and at load, respectively, are shown in Tables 43-1 and 43-2. The additional losses due to the load (items 2, 3, and 4 of Table 43-2) are called *stray load losses*.

(e) *Example of loss distribution and efficiency.* In the following tabulation is shown the loss distribution of a salient-pole generator.

875 kva, 24 poles, 60 cycles,  $\cos \phi = 0.80$

3 phase, 300 rpm, 2300 volts

Stator winding $I^2R$ . . . . .	13,500 watts
Rotor winding $I^2R$ . . . . .	9,000
Stray load loss . . . . .	4,000
Iron loss (total) . . . . .	12,000
Bearing friction and windage loss . . . . .	2,500
	<hr/> 41,000 watts

Output =  $875 \times 0.8 = 700$  kw

$$\text{Efficiency} = 100 \frac{700}{700 + 41} = 94.5\%$$

**43-2. Heating and cooling of the synchronous machine.** With respect to classes of insulation, limiting temperatures, heat conductivity, and heat transfer, the same considerations apply as in the d-c machine and induction motor. As in the d-c machine and induction motor, radial vents are used for cooling the stator of the salient-pole machine. Cylindrical rotor machines are usually long, and the problem of air flow requires very special attention.

### PROBLEMS

1. A 500-kva, 4-pole, 3-phase, 60-cycle,  $\cos \phi = 0.8$  lagging, 120/208-volt, salient-pole generator has 72 slots, 2 conductors per slot, and each conductor consisting of 16 parallel strands. The bare dimensions of the strand are 0.081 in.  $\times$  0.162 in. The mean length of a turn is 80 in. At 208 volts the winding is connected 4-parallel star. The field current at full-load is 27.2 amp, and the field resistance at 75°C is 4.55 ohms. The friction and windage loss is 4.1 kw, the total iron losses 6.2 kw and the stray load loss 1.5 kw. Determine the efficiency of this generator. Determine the current density of the stator winding.

2. An 1875-kva, 6-pole, 3-phase, 60-cycle,  $\cos \phi = 0.8$  lagging, 2400/4160-volt, salient-pole generator has 72 slots and 8 turns per coil. At 4160 volts the winding is connected 2-parallel star. The current density in the stator winding is 1835 amp per

sq in. The mean length of a turn is 90 in. and the winding is 2-layer. The leakage reactance of the stator is 0.096 (in p-u, unit current = rated current). The no-load characteristic is given by:

$$I_f \text{ (amp)} = \quad 20 \quad 30 \quad 43 \quad 51 \quad 60 \quad 66 \quad 87 \quad 100 \quad 118$$

$$E_f \text{ (volts)} = 1600 \quad 2400 \quad 3200 \quad 3600 \quad 4000 \quad 4160 \quad 4600 \quad 4800 \quad 5000$$

The field current necessary to produce rated armature current with a short-circuited armature is 74 amp. The resistance of the field winding is 0.643 ohm. The friction and windage loss is 12.5 kw. The total iron loss is 17 kw; and the stray load loss, 9.6 kw. Determine the field current at full-load and the efficiency at full-load.

3. Determine, for the generator of Problem 2, the field current and efficiency at  $\frac{3}{4}$  load,  $\cos \varphi = 0.8$  lagging, assuming that the iron loss remains the same as at full-load and that the stray load loss changes with the square of the armature current.

4. Determine, for the generator of Problem 2, the field current and efficiency at  $\frac{1}{2}$  load,  $\cos \varphi = 0.8$  lagging, assuming that the iron loss remains the same as at full-load and that the stray load loss changes with the square of the armature current.

## Chapter 44

### THE SYNCHRONOUS CONVERTER. VOLTAGE AND CURRENT RELATIONS. COPPER LOSSES COMPARED WITH THOSE OF THE D-C MACHINE

**44-1. Operation of the synchronous converter.** It has been pointed out in Art. 3-1 that the d-c machine is nothing more than an a-c machine with a special device, the commutator, which makes it possible to pick up (for generator operation) a fixed instantaneous value of voltage from the winding. It follows, therefore, that the d-c armature winding must also be able to operate as an a-c winding.

Because of the connection with the commutator, the d-c armature winding must be a closed winding (see Art. 3-1). It is represented schematically in Fig. 44-1 which shows a 2-pole machine with a closed winding wound on a ring. The end of each turn (end of each winding element) is connected to the beginning of the next following turn, and the connection point is connected to a commutator bar as in the actual d-c machine. Furthermore, three equidistant points of the winding, i.e., three points shifted 120 electrical degrees from one another, are connected to three slip rings. If such an armature is driven by a prime mover, it is able to supply d-c and a-c power simultaneously. The a-c power is 3-phase corresponding to the three slip rings. In multipole machines *each two consecutive armature paths* must be divided into three equal parts, in order to make the winding 3-phase;  $a/2$  points of the winding are then connected to each slip ring, i.e., each phase of the 3-phase winding consists of  $a/2$  parallel paths ( $a$  = number of d-c paths in the winding, see Art. 3-3).

If the winding in Fig. 44-1 is connected to two slip rings, single-phase a-c power will be obtained. The tap points must be displaced 180 electrical degrees in this case; thus in a 6-phase converter, as an example, the tap points must be displaced 60 electrical degrees, and so forth. In all cases,

each phase consists of a 2 parallel paths. A 6-pole, 3-phase rotary converter is shown in Fig. 44-2.

It has been pointed out that a machine with an armature, as shown in Fig. 44-1, is able to operate as an a-c generator-d-c generator (double-current generator). Also, it is capable of operation as an a-c motor-d-c generator or as an a-c generator-d-c motor. In the former case this machine type is called a *synchronous converter*; in the latter case it is called an *inverted converter*. The normal operation is that as a synchronous converter, i.e., the machine operates as an a-c motor-d-c generator.

Since the poles of the converter are excited with d-c, its *fundamental* character must be the same as that of a synchronous machine. For a constant frequency  $f$  the speed is constant, independent of the load, and given by the familiar equation

$$n_s = \frac{120 f}{p} \quad (44-1)$$

Apparently, the rotor must rotate against its rotating flux, in order that the latter be at stand-still with respect to the mmf of the poles. It should be remembered that this is the condition for the existence of a uniform torque (see Art. 24-1).

The synchronous converter operates as a synchronous motor on the a-c side and as a d-c generator on the d-c side. The direct current in the armature, therefore, produces a torque which opposes the motion of the rotor, i.e., the driving torque produced by the alternating current (see Fig. 7-1). Just as in the synchronous motor (see Fig. 38-6), the alternating emf phasor falls behind the phasor which represents the line voltage, and the armature takes an active current from the line of sufficient magnitude to balance the opposing torque of the direct current and the rotational loss torque. This latter torque is comparatively small. Since

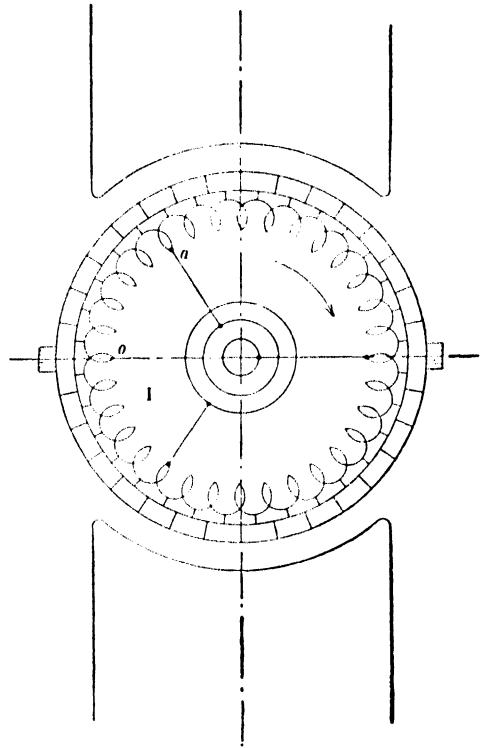


FIG. 44-1. Two-pole, 3-phase synchronous converter (schematic representation).

the mmf of the direct current and the mmf of the *active* alternating current both have their amplitudes (axes) in the interpolar space (see Figs. 4-5 and 38-4), and correspond one to generator operation, the other to motor operation, they oppose and *cancel* each other (see Figs. 7-1 and 7-2), i.e., the synchronous converter *has no cross-flux*.



Fig. 41 2 6-pole, 3-phase synchronous converter 150 kw, 275 volts, 1200 rpm.

Just as in a synchronous motor, the alternating current and voltage of a synchronous converter are in phase for some one value of excitation. If the field current is increased above this value, the machine is *overexcited* and draws a *leading current* from the line because a leading current opposes the field mmf in a synchronous motor (see Arts. 37-1). If the field current is decreased, the machine is *underexcited* and draws a *lagging current* from the line because a lagging current supports the field mmf in a synchronous motor. For reasons discussed in the following, the excitation of the synchronous converter normally is adjusted so that the voltage and current are in-phase.

Since the direct current of a synchronous converter is taken from the same winding to which the alternating current is supplied, a fixed ratio exists between the d-c and a-c voltages, as well as between the d-c and a-c currents.

**44-2. Voltage and current ratios in the synchronous converter.** In order to determine the ratio between the d-c and a-c voltages of a synchronous converter, it will first be assumed that the machine operates at no-load and is so excited that it draws no reactive current from the line. Therefore, there is no armature reaction and the main flux, produced only by the d-c field mmf, induces a fixed emf in the armature winding.

It was shown in Art. 3-4 that, when the brushes are in the neutral axis, the *amplitude* of the emf induced in the armature winding is picked up at the brushes. If a sinusoidal flux distribution is assumed, the ratio of the effective value of the emf to the maximum value is  $1/\sqrt{2}$ ; therefore, in a single-phase converter, the ratio of the alternating emf  $E_{a-c}$  (effective value) to the direct emf  $E_{d-c}$  is  $1/\sqrt{2}$ . In a multi-phase converter, with the same armature winding operating at the same speed, the value of the d-c emf does not change, but the effective value of the a-c emf per phase ( $E_{a-c}$ ) is less than  $E_{d-c}/\sqrt{2}$  and equal to the chord subtending an angle of  $2\pi/m$  radians in a circle having a diameter  $E_{d-c}/\sqrt{2}$  (Fig. 44-3);  $m$  is the number of phases. Consequently, for an  $m$ -phase converter,

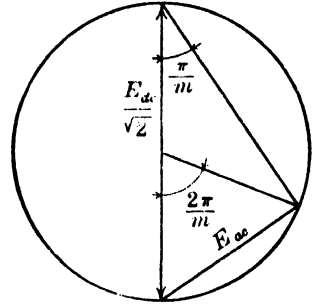


FIG. 44-3. Determination of d-c and a-c voltage ratio for the polyphase converter.

$$E_{a-c} = \frac{E_{d-c}}{\sqrt{2}} \sin \frac{\pi}{m} \quad (44-2)$$

This expression and those developed in the following also apply to the single-phase converter if  $m$  is taken as 2.

The emf transformation ratio for single-, 3-, and 6-phase converters, therefore, is

$$E_{a-c}/E_{d-c}$$

$$\text{Single-phase} = 0.707$$

$$\text{3-phase} = 0.612$$

$$\text{6-phase} = 0.354$$

At no-load the terminal voltages are practically equal to the emf's induced in the winding. Therefore, at no-load the transformation ratio of the emf's is the same as the ratio of the terminal voltages at the slip rings and at the brushes. Since the voltage drop in the armature winding

of a converter is small, the emf ratio also applies approximately to the terminal voltages under load, so that

$$\frac{V_{a-c}}{V_{d-c}} \approx \frac{1}{\sqrt{2}} \sin \frac{\pi}{m} \quad (44-3)$$

The a-c voltage available from the supply lines does not usually correspond to the d-c voltage desired at the brushes. Therefore, the synchronous converter usually requires a transformer between the line and slip rings in order to transform the line voltage to the proper value. Figs. 18-10 to 18-12 inclusive show three single-phase transformers with three different types of connections which may be used for 6-phase synchronous converters.

The tapped armature winding of a synchronous converter behaves as a closed or mesh polyphase winding. The line voltage is equal to the phase voltage, and the slip-ring current is  $2 \sin (\pi/m)$  times the phase current. If  $I_{d-c}$  is the terminal direct current,  $I_{a-c}$  the alternating current per phase, and the losses are disregarded, then the d-c power output is equal to the a-c power input:

$$V_{d-c} I_{d-c} = m V_{a-c} I_{a-c} \cos \varphi \quad (44-4)$$

From this equation and Eq. 44-3 the ratio of phase current to d-c current becomes

$$\frac{I_{a-c}}{I_{d-c}} = \frac{\sqrt{2}}{m \sin \frac{\pi}{m}} \cdot \frac{1}{\cos \varphi} \quad (44-5)$$

The ratio of slip-ring current to direct current, therefore, is:

$$\frac{I_r}{I_{d-c}} = \frac{2\sqrt{2}}{m \cos \varphi} \quad (44-6)$$

Equations 44-5 and 44-6 assume no losses whatever in the converter; they yield for a value of  $\cos \varphi = 1$  the following table of current ratios:

<i>Number of phases</i>	$I_{a-c}/I_{d-c}$	$I_r/I_{d-c}$
1	0.707	1.414
3	0.545	0.943
6	0.472	0.472

In a 3-phase converter the active component of the slip-ring current is approximately equal to the direct current, while in a 6-phase converter it is equal to about one-half the direct current.

**44-3. The copper losses in the synchronous converter.** The superposition of direct current and alternating current in the armature conductors leads to peculiar results in the copper losses.

Consider Fig. 44-1. Each phase covers 120 electrical degrees (in general  $2\pi/m$  electrical degrees). The position of phase I is assumed such that the mid-point  $O$  of the phase coincides with the mid-point of the interpolar

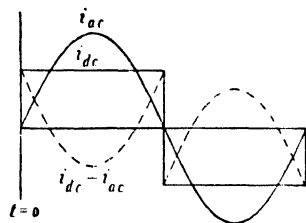


FIG. 44-4. Currents in the winding element midway between taps.

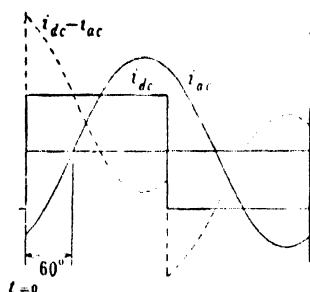


FIG. 44-5. Currents in the winding element at the tap point.

space, i.e., with the brush axis. In this position the sum of the flux lines linking phase I is maximum, and the emf induced in this phase is, therefore, zero. It will be further assumed that induced emf and current are in phase; therefore the current is also zero in phase I.

Consider the winding element  $O$ , lying midway between the taps. The alternating current in this element, as well as in the other winding elements within phase I, is zero. Since the mid-element  $O$  lies directly under the brush, the direct current is being commutated. Thus, for this element  $O$ , the direct and alternating currents go through zero at the same instant. Fig. 44-4 shows the relative positions of the d-c and a-c waves for this winding element as a function of time. The resultant current, which is the difference between the direct current and alternating current, is also shown in Fig. 44-4.

Winding element  $a$  at the tap point, which is displaced  $60^\circ$  from the mid-element in the direction of rotation, carries, at the time when commutation takes place in mid-element  $O$ , exactly the same alternating current as the mid-element but a different direct current, since commutation has taken place  $60^\circ$  earlier. The relative positions of the two current waves for the tap element  $a$  is shown in Fig. 44-5. The resultant current, which is again the difference between the direct and alternating currents, has an entirely different shape than that of the mid-element  $O$ .

The copper losses in each winding element are determined by the



resultant current in the element. Therefore, the copper losses are different in the individual coils. The losses are least in the winding element midway between tap points of a phase and greatest at the tap points.

The axis of abscissa in Fig. 44-6 represents the series order of the winding elements of one phase of a 3-phase converter between tap points, and the axis of ordinates represents the copper losses in the individual

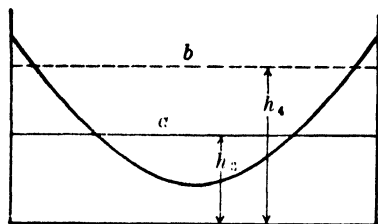


FIG. 44-6. Copper losses in the individual winding elements.

elements produced by the resultant currents. The heating effect in a winding element at the tap point is 5.4 times as great as the heating effect in the mid-element. The mean value of the losses for the entire phase, as found by planimeter measurement, is given by the distance  $h_3$  from the axis of abscissa to the straight line  $a$ . The distance  $h_4$  from the axis of abscissa to the straight line  $b$

represents the losses that would be produced by the direct current alone. Consequently  $h_3/h_4$  is the ratio of the copper losses of the machine operating as a 3-phase converter to the copper losses of the same machine operating as a d-c generator. This ratio is equal to 0.56.

**44-4. Comparison with the d-c machine.** It is seen in Fig. 44-6 that the copper losses of a 3-phase converter are much less than those of a d-c machine of the same dimensions and rating. It is shown in the following that the 6-phase and 12-phase converters are still more favorable with respect to losses than the 3-phase converter.

Fig. 44-6 refers to  $\cos \varphi = 1$  operation. When the synchronous converter is overexcited or underexcited, it carries a reactive current which increases the copper losses. The following table shows the ratio ( $r$ ) of the current losses in the synchronous converter to the corresponding losses in a d-c machine of the same dimensions and rating for various power factors on the a-c side.

No. of phases	1	3	6	12
$\cos \varphi = 1.00$	( $r$ ) = 1.38	0.56	0.27	0.21
0.90	1.85	0.84	0.48	0.40
0.80	2.51	1.23	0.77	0.67
0.70	3.46	1.80	1.19	1.06

The copper losses of a converter become less as the number of phases is increased. Furthermore, they are least when the excitation is adjusted to give unity power factor on the a-c side.

Since the current losses are proportional to the square of the current, a synchronous converter, assuming equal armature copper losses as a basis, may deliver a direct current output  $\sqrt{1/r}$  times greater than the output of a d-c machine of the same dimensions. Therefore, the magnitude  $\sqrt{1/r}$  gives the ratio of the power output of a converter to that of a d-c machine of equal dimensions. This ratio is shown in the following table:

No. of phases	1	3	6	12
$\cos \varphi = 1.00$	$\sqrt{\frac{1}{r}} = 0.85$	1.33	1.93	2.20
0.90	0.73	1.09	1.46	1.58
0.80	0.63	0.90	1.14	1.22
0.70	0.54	0.74	0.91	0.97

For any number of phases the converter output increases rapidly with an increasing value of  $\cos \varphi$ .

The 12-phase synchronous converter has little advantage over the 6-phase converter; it is quite long since it requires 12 slip rings. For this reason it is customary to design converters 6-phase. In small converters, up to 250 kw, the saving in material and the increased efficiency produced by a larger number of phases is not so important, and 3-phase design is employed.

### PROBLEMS

1. A 6-phase synchronous converter delivers 625 volts d-c to a traction system. Determine: (a) the diametrical voltage of the armature; (b) the voltage between adjacent slip rings; (c) and the voltage between alternate slip rings.

2. If a converter delivers 350 kw at 625 volts d-c determine the approximate slip-ring current, assuming the a-c supply to be: (a) single-phase; (b) 3-phase; (c) 6-phase. Assume an efficiency of 94.5% and unity power factor.

3. A 250-kw, 230-volt, 3-phase, synchronous converter receives power from a 13,200-volt, 3-phase, 60-cycle power system. The transformer bank supplying the converter is connected  $\Delta$ -Y and has an efficiency of 98%. The full load efficiency of the converter is 93%. Determine for unity power factor: (a) d-c output current of converter; (b) slip-ring current; (c) voltage, current, and kva ratings of transformer secondaries; (d) power input, current, and voltage of transformer primaries when the converter is delivering rated output. Neglect voltage drops in converter and transformers, and transformer magnetizing current.

4. Repeat Problem 3 for the same machine operated 6-phase with the transformer bank connected  $\Delta$ -diametrical.

5. Repeat Problem 3 for the same machine operated 6-phase with the transformer bank connected  $\Delta$ -double  $\Delta$ .

6. Repeat Problem 3 for a power factor of 0.90 leading. The converter efficiency is now 92% and the transformer efficiency 97.5%.

7. If the machine of Problem 3 is operated 6-phase, 0.90 power factor leading, with

a  $\Delta$ -double  $\Delta$  bank supplying the power, determine: (a) slip-ring current; (b) voltage, current, and kva ratings of transformer secondaries. Assume converter efficiency 92% and transformer efficiency 97.5%.

8. A 2500-kw, 25-cycle, 500-rpm, 230-volt, 6-phase synchronous converter supplies a 3-wire d-c system. The transformer bank supplying the converter is  $\Delta$ -double Y (neutrals connected) and receives power from a 27,000-volt, 3-phase system. The full-load converter efficiency is 95% and the full-load transformer efficiency 98.5%. For unity power factor determine: (a) d-c output current; (b) slip-ring current; (c) diametrical slip-ring voltage; (d) adjacent slip-ring voltage; (e) slip-ring to neutral voltage; (f) transformer primary current; (g) line current from 27,000-volt system.

9. Three identical single-phase transformers supply a 500-kw, 125-volt synchronous converter. The converter is 3-phase, 25-cycle, and receives power from a 27,000-volt, 3-phase distribution system, with the transformer bank connected  $\Delta$ -Y. If the converter operates at a power factor of 0.95 lagging and an efficiency of 0.94, determine the transformer voltage, current, and kva rating. If the transformer reactance drop is 5% and the converter drops are neglected, determine the d-c output voltage at full-load, unity p.f. and also 0.90 p.f. leading.

10. Three single-phase transformers connected Y-diametrical supply a 6-phase, 200-kw, 625-volt railway synchronous converter from a 13,200-volt, 3-phase line. Determine: voltage, current, and kva ratings of the transformers when the converter delivers full-load at 0.95 p.f. leading and an efficiency of 0.93. What is the ratio of transformation of the transformers?

11. A 1000-kw, 230-volt, 6-phase, 25-cycle synchronous converter supplies a 3-wire d-c system. Power is received from a 13,200-volt, 3-phase system. Write specifications for three single-phase transformers you might order, assuming primaries connected in  $\Delta$ ; (b) primaries connected in Y. Give the reasons for your selection and show connection diagram.

12. Two single-phase transformers connected in open delta supply a 250-kw, 230-volt, 3-phase synchronous converter from an 1100-volt, 3-phase line. Neglecting losses and assuming operation at unity p.f., what are the voltage, current, and kva ratings of the transformers necessary? At what p.f. do the transformers operate?

13. A 250-kw, 230-volt, 6-phase synchronous converter receives power from an 1100-volt, 3-phase line by means of two transformers connected in T-double T. Specify voltage, current, and kva ratings of the transformers necessary when operating at full-load, unity p.f. At what p.f. do the transformers operate? Neglect losses. Show diagram of connections.

14. If the converter of Problem 13 receives power from a 1100-volt, 2-phase line, specify the complete transformer ratings, neglecting losses and assuming rated output at unity p.f. Show diagram of connections.

15. Sketch the wave form of the current in a conductor located 15 electrical degrees from a tap point of a 3-phase synchronous converter for (a) unity p.f., (b) 0.90 p.f. lagging.

16. Repeat Problem 15 for a 6-phase synchronous converter.

17. If the 250-kw, 230-volt, 3-phase converter of Problem 13 receives its power from the 1100-volt, 3-phase line by means of autotransformers, specify the transformers necessary. Give voltages, tap points, and show connection diagram.

18. Specify the voltages of the autotransformers necessary to supply a 250-kw, 230-volt, 6-phase synchronous converter from an 1100-volt, 3-phase, 3-wire supply system. Show connection diagram.

## Chapter 45

### COMMUTATION OF THE SYNCHRONOUS CONVERTER. VOLTAGE REGULATION. STARTING. PARALLEL OPERATION.

**45-1. Commutation of the synchronous converter.** As in a d-c generator, the converter needs interpoles for the purpose of improving the commutation (see Art. 8-3). However, there is a difference between the d-c machine and the converter: the latter has no cross-flux (flux in the neutral axis, see Art. 44-1). As a consequence, the mmf required on the interpoles of a converter is much less than that necessary for a d-c machine of the same rating: because of the absence of a cross-flux, the interpoles must produce mainly the counter-emf equal to the emf of self- and mutual-induction in the short-circuited winding element, plus the voltage drop in the brush contact surface (see Art. 8-3). In the d-c machine the interpoles need an additional mmf to suppress the armature cross-flux, which mmf is equal to the entire armature mmf.

The absence of a cross-flux in the synchronous converter is due to the fact that the mmf of the direct current and the mmf of the active component of the alternating current cancel each other (see Art. 44-1). Since there is no mmf in the quadrature axis, a compensating winding (see Art. 4-3) is *unnecessary* in the rotary converter. This inherent cancellation of the d-c cross flux is of advantage with respect to the interpoles. However, the absence of the compensating winding is a disadvantage under transient conditions, such as change of frequency, sudden short circuit on the a-c side, or suddenly applied d-c load. In these cases the armature flux is not compensated, and high coil voltages and ring fire may appear, leading to possible damage of the commutator, brushes, and brush holders.

**45-2. Voltage regulation of the converter.** Since the ratio of direct and alternating voltages of a converter is fixed, any change in the direct

voltage requires a change in the slip-ring voltage. If the field current of a converter is changed, only the reactive component of its current is materially changed; the effect of a change in the field current on the d-c voltage is insignificant. The reactive current may change the d-c voltage slightly by changing the voltage drop in the transformer to which the converter is connected; in itself, this voltage drop is very small. Different means can be employed in order to adjust the slip-ring voltage: taps on the primary side of the transformer; a synchronous generator booster which is connected in series with the converter; an induction regulator (see Art. 30-5) the secondary winding of which is connected in series with the converter. The generator booster and the induction regulator permit a continuous regulation of the d-c voltage, which cannot be obtained with taps on the transformer. Also, a choke coil on the a-c side of the converter, in connection with variation of the field current, permits voltage regulation on the d-c side. However, in this case the converter carries reactive current which increases the copper losses.

**45-3. Starting and parallel operation of converters.** Starting of a converter can be accomplished on either the a-c or the d-c side. Since the converter behaves as a synchronous motor on the a-c side, it is not capable of starting by itself. It must be equipped, just as the synchronous motor, with a squirrel-cage winding (damper winding) to enable it to start as a squirrel-cage induction motor. In order to keep the starting current low, a reduced voltage of about  $\frac{1}{3}$  to  $\frac{1}{2}$  the rated voltage is impressed across the slip rings during the starting period. For this reason the secondary of the main transformer is suitably tapped to give this reduced voltage. When the converter is brought up to near synchronous speed as an induction motor, it will pull into step as a reluctance motor because of the salient poles (see Art. 39-1), and full voltage can be applied after it has been excited with direct current.

Just as in the conventional synchronous motor (Art. 40-4), care must be taken with the synchronous converter to see that the field winding is not punctured by high induced voltages at start. In order to avoid breakdown, the field winding is short-circuited across the armature at start or broken into several groups; in the latter case the correct connection must be made when the machine has reached synchronous speed.

If a direct-current source is available, the converter can be started from the d-c side in the same manner as a shunt motor. After reaching its rated speed, it is then synchronized with the alternating-current supply. The converter is started from the d-c side wherever this is possible. Very large converters are also started by means of special starting motors.

If several converters operate in parallel with each other, each converter normally has its own transformer. If several converters are supplied from a common transformer, then the armature windings of the machines are connected in parallel on both the a-c and the d-c sides. If, in this case, the brush-contact resistances of the machines are not equal, the direct current may enter the negative brushes of a machine and then, instead of leaving its positive brushes, follow a path through the armature, out the slip ring, over the bus-bars on the a-c side, and out the positive brushes of another machine. The brushes of this latter converter are then decidedly overloaded and sparking at the commutator results.

If a converter operates in parallel with d-c generators or with a bank of batteries, then any sudden additional load will be taken in the greater part by the converter because of its low voltage drop (in the armature winding and in the transformer). In order to obtain a uniform distribution of the load among all machines operating in parallel, and also the battery, under certain circumstances it is necessary to increase the voltage drop in the converter by using a small differentially connected series winding and a choke coil on the a-c side.

The distribution of load among rotary converters operating in parallel can be varied by changing their d-c voltages, using the means described in Art. 45-2.

As has been mentioned, a synchronous converter can also be used to transform from d-c to a-c (*inverted converter*). However, certain difficulties arise here which are not present when the synchronous converter transforms from a-c to d-c. The inverted converter operates either as a shunt or compound motor, and therefore its a-c frequency depends upon its d-c excitation. Consider the inverted converter loaded with an inductive load: an increase of the inductive current weakens the field of the converter (see Art. 37-1) and increases its speed and frequency. The increase of frequency increases the inductive reactance of the load and thus the lag angle of the current. This further reduces the field and increases the speed. The action is cumulative, and for this reason the inverted converter has to be provided with a speed-limiting device. Also, the normal rotary converter has to be provided with such a device when the possibility of inverted operation exists, as for example, in the case of a short circuit on the a-c line of a converter operating in parallel with a storage battery.

**45-4. Comparison with the motor-generator set.** A motor-generator set can be used to convert alternating current to direct current or direct current to alternating current. The motor of the a-c to d-c set can be either an

induction motor or a synchronous motor. The disadvantage of the motor-generator set in comparison with the synchronous converter is its low overall efficiency. In a motor-generator set the entire transformed energy is first transformed into mechanical energy by the motor, and then into electrical energy by the generator; in a converter the transformation is accomplished in the same armature, the winding of which carries only the difference of the two currents. The losses in the motor-generator set are, therefore, much larger than those in the synchronous converter.

The motor-generator set and the rotary converter have both been superseded by the mercury-arc rectifier and are now used only in special applications, such as speed regulating sets. An example of this application is the Ward-Leonard speed regulating system shown in Fig. 7-12.

## Chapter 46

### THE D-C ARMATURE IN AN ALTERNATING MAGNETIC FIELD

In the d-c machine and in the synchronous converter the d-c armature rotates in a magnetic field that does not vary with time and that does not move. In contrast, in a-c commutator motors a d-c armature rotates in a magnetic field that either varies with time (single-phase commutator motor), or rotates (polyphase commutator motor). A series of new phenomena, therefore, is introduced which do not appear in the case of a d-c armature rotating in a constant stationary magnetic field. The behavior of a d-c armature in an alternating field will be considered in this chapter.

**46-1. The emf of rotation and the emf of transformation in the armature winding.** It was shown in the treatment of the d-c machine that the magnetic axis of the d-c armature is determined by the position of the brushes on the commutator (see Art. 4-3). The same holds true for the d-c armature in an alternating field. However, in each armature path of the d-c machine, the magnitude and direction of the currents are constant, and the resulting armature flux, therefore, is constant; in the single-phase commutator motor, on the other hand, the current in each armature path varies with time, since the brushes carry alternating current, and as a result, the armature flux also varies with time: *the armature flux of a single-phase commutator motor is an alternating flux* the axis of which is determined by the position of the brushes on the commutator.

In the single-phase commutator motor the field (pole) winding is either a concentrated winding, similar to that in the d-c machine, or a distributed winding as in the single-phase induction machine; it produces an alternating flux. For the sake of simplicity the field winding is shown as a concentrated winding in all the figures that follow.

(a) *The emf of rotation in the armature winding.* Fig. 46-1 represents



schematically the field winding and the armature winding of a single-phase commutator motor. The brush axis is perpendicular to the axis of the pole-flux, and the armature rotates in the alternating flux produced by the field winding. The emf induced in the armature as a result of rotation and appearing at the brushes is, as in the case of the d-c machine,

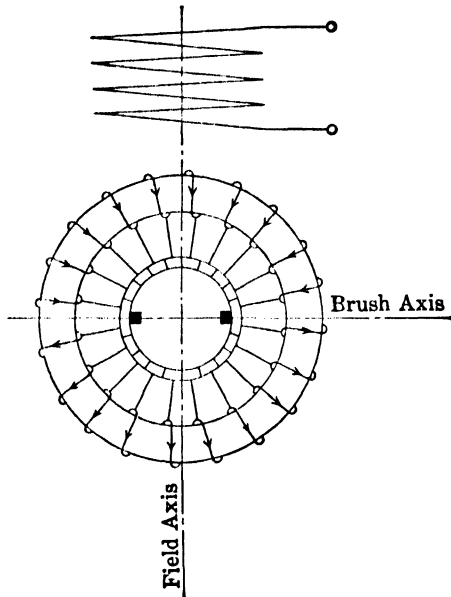


FIG. 46-1. Emf of rotation in a d-c armature winding due to an alternating flux. Brushes in the neutral.

proportional to the rpm of the armature. However, since the flux is alternating, it is not a direct emf but an alternating emf, and its *frequency is independent of the rpm of the armature and always equal to the frequency of the field current* (the frequency of the line). This is easily understood from the following consideration: The flux of a d-c machine is unvarying with time and, as a result of rotation, a direct emf is induced in the armature the magnitude of which is proportional to the rpm of the armature. If the flux of a d-c machine were to pulsate, then an alternating emf would appear between the brushes on the commutator; the frequency of this emf would correspond to the frequency of the pulsations of the flux, but its magnitude would be proportional to

the speed of the armature and independent of the frequency of the flux pulsations. From the same consideration it follows that the emf produced *by rotation in an alternating flux is in phase with the flux*: the emf is zero when the flux is zero and a maximum when the flux is a maximum.

(b) *The transformer emf in the armature winding.* In addition to the emf of rotation a second emf is induced in the armature winding *by transformer action* with the main flux. Since the pole-flux linking the individual armature winding elements is an alternating flux, it induces emf's in them just as the primary winding of a transformer induces emf's in the turns of the secondary winding; these emf's are *entirely independent of the speed*. In Fig. 46-2 the direction of the transformer emf's is shown for a certain instant of time. The emf's in the turns to the left of the axis of the field winding and the emf's in the turns to the right of the axis of the field winding have opposite directions with respect to one another, exactly the

same as do the emf's of rotation with respect to the brush axis in Fig. 46-1. These transformer emf's cannot produce *internal* (circulating) currents in the armature winding, because, with respect to the closed circuit of the armature winding, the emf's in both halves of the winding cancel one another. Furthermore the transformer emf's are ineffective with respect to the brushes lying in the axis perpendicular to the field winding (brushes *aa*, Fig. 46-2), because they cancel one another within the upper half as well as within the lower half of the armature winding; therefore the transformer emf's produce no current in the armature winding if these brushes (*aa*) are joined together. However, it is different if brushes are placed on the commutator along the field axis (brushes *ff*, Fig. 46-2). Between these brushes the transformer emf's add in both halves of the winding, and current would flow between these brushes if they were joined together.

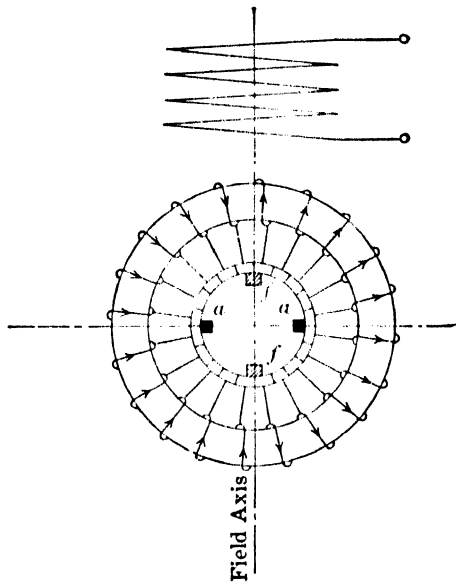


FIG. 46 2. Transformer emf in a d-c armature winding due to an alternating flux.

Thus, the emf of rotation and the transformer emf *both have the same frequency*. However, while the emf of rotation is in phase with the pole-flux producing it, and its magnitude depends upon the rpm of the armature, the transformer emf is displaced in phase  $90^\circ$  behind the flux producing it, as in every transformer, and its magnitude is independent of the rpm of the armature.

If the brushes are shifted so that the angle between the brush axis and the field axis,  $\alpha$ , is  $\geq 90^\circ$  (Fig. 46-3), then, as in the d-c machine, the emf of rotation is less than in the case when  $\alpha = 90^\circ$ ; it is proportional to  $\sin \alpha$ . Furthermore, in this case a transformer emf appears between the brushes which is proportional to  $\cos \alpha$ . This can be seen without further discussion if the flux is divided into two components, one of which,  $\Phi \sin \alpha$ , is perpendicular to the brush axis, and the other,  $\Phi \cos \alpha$ , is parallel to the brush axis (Fig. 46-3).

**46-2. The torque of the single-phase commutator motor. The compensating winding.** By means of Fig. 46-2 and the fundamental law of the force

on a conductor in a magnetic field (see Art. 1-4), it is evident that the currents produced in the armature by the transformer emf's and flowing through the brushes  $\mathcal{f}$  produce no torque in conjunction with the pole-flux: in the left half as well as in the right half of the armature the torque produced by the coils lying in the upper half of the armature oppose the

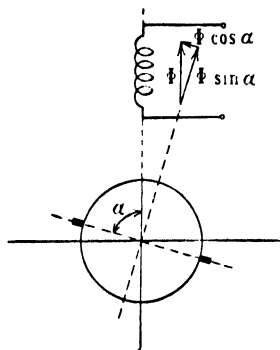


FIG. 46-3. Emf of rotation and transformer emf in a d-c armature winding due to an alternating flux. Brushes not in the neutral.

torque produced by the coils lying in the lower half of the armature. It is quite different, however, with the currents produced by the rotational emf's (Fig. 46-1): these currents and the pole-flux produce the useful torque. In the first case, where the armature currents are produced by transformer action, the axis of the armature flux coincides with the axis of the pole-flux. In the second case, where the armature currents are produced by rotation, the axis of the armature flux makes an angle of  $90^\circ$  with the axis of the pole-flux: *the greatest torque appears if the brush axis (axis of the armature flux) and the field axis make an angle of  $90^\circ$  with each other (as is usually the case in the d-c machine).*

The equation derived for the torque of a d-c machine (see Eq. 3-9) may also be employed here if the instantaneous values of brush current and flux are inserted. If the phase shift between the brush current and the flux is  $\psi$  and if the average value of the torque over a period of the current is derived, the result is

$$T = 0.1174 \frac{p}{a} \Phi_{\text{eff}} Z I \cos \psi \times 10^{-8} \text{ lb-ft} \quad (46-1)$$

where  $I$  and  $\Phi$  are effective values. If the brush axis makes an angle  $\alpha$  (Fig. 46-3) with the main field axis, then this quantity has to be multiplied by  $\sin \alpha$ , since only the component  $\Phi \sin \alpha$  of the flux is effective in producing torque. If, as usual, the maximum value of the flux  $\Phi$  is introduced, the general expression for the average value of the torque is obtained as

$$T = 0.1174 \frac{p}{a} \frac{\Phi}{\sqrt{2}} Z I \cos \psi \sin \alpha \times 10^{-8} \text{ lb-ft} \quad (46-2)$$

The torque of the single-phase commutator motor is not constant but varies between a minimum and a maximum value (see Art. 1-4). Disregarding the factors  $\cos \psi$  and  $\sin \alpha$ , the average value of the torque of

the single-phase commutator motor is less, in the ratio of  $1:\sqrt{2}$ , than the constant torque of a d-c machine with the same flux and the same armature copper losses as in the single-phase commutator motor. If the flux and current are not in phase or if the angle between the brush axis and the field (pole) axis is not equal to  $90^\circ$  ( $\psi \neq 0$ ,  $\alpha \neq 90^\circ$ ), then, in comparison with the d-c machine, the torque is still less.

*The compensating winding.* The pole-flux induces transformer emf's in the armature winding; yet, a transformer emf appears at the brushes only when the brushes are not placed on the perpendicular to the axis of the field, i.e., are not placed in the neutral axis. If the brushes are on a perpendicular to the field axis, the transformer emf between them is equal to zero, because the emf's of the individual coils in each armature path mutually cancel one another. However, the pole-flux links not only the armature winding but also the field winding; it induces a voltage of self-induction in this winding, the frequency of which is equal to the frequency of the line, and a part of the terminal voltage must be consumed in order to overcome this voltage of self-induction. This component of the terminal voltage leads the field current by  $90^\circ$ .

The armature flux has the same effect on the armature winding as the field flux has on the field winding. As described, the armature flux is an alternating flux the axis of which coincides with the brush axis. Since the armature winding behaves magnetically as a solenoid, the axis of which coincides with the brush axis (see Art. 4-3), the armature flux induces an emf of self-induction in the armature winding by transformer action, and a component of the terminal voltage again must be used to overcome this induced emf.

The emf's of self-induction in the field winding and in the armature winding introduce a phase shift between the terminal voltage and the current and would make the phase displacement of the single-phase commutator motor extraordinarily large if special means were not employed in order to avoid this effect. As in the d-c machine, the armature flux performs no part in the transfer of energy and may be nullified here just as in the d-c machine (see Art. 4-3); in consequence of this fact, *the single-phase commutator motor is, as a rule, supplied with a compensating winding* (see Art. 47-1). By means of this winding the armature flux is reduced to a small residue, the leakage fluxes, so that the emf of self-induction of the armature is small and equal to the emf induced in the armature winding by its leakage fluxes only. On the other hand, the voltage of self-induction in the field winding cannot be avoided, for this is produced by the main flux which creates the effective torque; this flux

cannot be eliminated or reduced. In order to diminish the emf of self-induction in the field winding of a single-phase series motor, the number of turns of the field winding is made as small as possible.

Similarly, as in the d-c machine, the compensating winding is made as a distributed winding and placed in slots in the stator. Its magnetic axis must coincide with the axis of the armature winding, i.e., the brush axis. Since the armature flux is alternating, it is not necessary to connect the compensating winding in series with the armature winding so that it will carry the armature current, as in the case of a d-c machine. The compensating winding will suppress the armature field if it is simply short-circuited on itself, for, with respect to the armature winding as the primary winding, it acts as the short-circuited secondary of a transformer.

**46-3. The transformer emf of a short-circuited winding element and the commutating fluxes in the single-phase commutator motor.** If commutation plays an essential role in the d-c machine and affects its performance, then this same problem enters to an even greater measure in the a-c commutator motor, because commutation takes place under much more unfavorable conditions than in the d-c machine: it is the *transformer emf in the short-circuited winding element* which makes the commutation worse in comparison to that of the d-c machine. It is evident from Fig. 46-1 that, during the time a winding element is short-circuited by the brush, the element lies in a plane that is perpendicular to the field (pole) axis, and in consequence of this it is linked by the pole-flux. Thus a transformer voltage results of the magnitude (see Eq. 12-12)

$$e_t = 4.44fN_c\phi 10^{-8} \text{ volt} \quad (46-3)$$

where  $N_c$  is the number of turns per winding element. The emf  $e_t$  induced in the short-circuited winding element thereby is independent of whether the armature rotates or is at rest and *appears at start as well as during the running of the machine*. While in the d-c machine, with the brushes located in the neutral axis, the pole-flux has no effect on the short-circuited winding element, in this case the effect of the pole-flux is present constantly in the form of a transformer emf in the short-circuited element.

The armature flux has no effect on the short-circuited winding element because it is canceled by the compensating winding. Besides the transformer emf  $e_t$ , the short-circuited element is influenced by the resistance of the short-circuit path and the *emf of self-induction*, which is the result of the change in the current during the movement of the coil from one armature path to another (see Art. 8-2). Since the armature carries an

alternating current, the reversal of current in the short-circuited element can take place at any instantaneous value of the current. The greatest emf of self-induction appears if commutation takes place at the maximum value of the current. If commutation takes place at the moment when the instantaneous value of the current is zero, then the emf of self-induction also is zero. Since maximum value of emf of self-induction occurs at the instant of maximum value of current, and zero value of emf of self-induction occurs at the instant of zero value of current, it follows that the *emf of self-induction in the short-circuited winding element is in phase with the alternating current.*

While the transformer emf in the short-circuited winding element depends upon the pole-flux and the line frequency, and lags  $90^\circ$  behind the pole-flux, the emf of self-induction in the short-circuited winding element depends upon the current and the speed of the armature and is in phase with the current. The fact that the two emf's appearing in the short-circuited element of a single-phase commutator machine have different phase angles with respect to the current, and also depend upon different quantities, makes improvement of commutation in the single-phase commutator machine rather difficult.

The cancellation of the emf of self-induction in the short-circuited winding element can be accomplished by means of interpoles in the same manner as in the d-c machine (Art. 8-3), i.e., by the *rotation* of the short-circuited element *in a commutating flux*. The strength of the commutating flux must be proportional to the current since the emf of self-induction  $e_s$  is proportional to the current. It has been found that the emf induced by *rotation* in an alternating flux is *in phase* with the alternating flux. Therefore, the phase of the commutating flux must be opposite to that of the current; then the emf induced by rotation in this flux will be exactly opposite to  $e_s$ . Fig. 46-4a shows the phasor diagram of the armature current  $I$  and the commutating flux  $\Phi_{is}$  necessary to cancel the emf of self-induction  $e_s$ . The voltage  $e_s$  is in phase with  $I$ , and the flux  $\Phi_{is}$  produces, by rotation, a voltage in the short-circuited winding element which is equal and opposite to  $e_s$ . To produce the commutating flux  $\Phi_{is}$ , the armature current has to be employed just as in the d-c machine; thus, the commutating pole winding has to carry the armature current.

It is quite different, however, with the transformer emf in the short-circuited winding element. In Fig. 46-4b  $\Phi$  is the field flux and  $e_t$  the transformer emf induced in the short-circuited element, lagging  $90^\circ$  behind the field-flux.  $e_t$  cannot be canceled by the transformer effect of a commutating flux, for this flux would have to be displaced in phase  $180^\circ$  from the field flux, and this would weaken the main flux. If  $e_t$  is to be

canceled, this must be accomplished *by rotation* in a commutating flux and this commutating flux must be  $90^\circ$  ahead of the main flux, as shown in Fig. 46-4b). For the cancellation of the transformer emf  $e_t$  in the short-circuited winding element a commutating flux  $\Phi_{it}$  of a different phase and also of a different magnitude is necessary than that required for the cancellation of the emf of self-induction  $e_s$ , because  $e_t$  is proportional to the

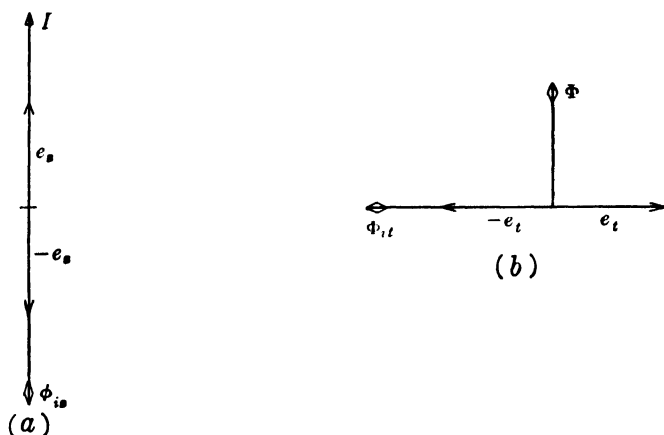


FIG. 46-4. Emfs in the short-circuited winding element and the necessary commutating fluxes.

field-flux and to the line frequency while  $e_s$  is proportional to the current and to the speed of the armature. The manner of producing both of these commutating fluxes is an important consideration in the design of single-phase commutator machines. Both emf's in the short-circuited winding element,  $e_s$  and  $e_t$ , usually are displaced nearly  $90^\circ$  from each other so that the resultant induced emf in the short-circuited path of the single-phase commutator motor is approximately equal to

$$e_r = \sqrt{e_t^2 + e_s^2} \quad (46-4)$$

As will be shown,  $e_r$  is completely canceled by the two commutating fluxes only for a fixed load. For other loads a certain residue remains. Experience shows that for good commutation, i.e., for satisfactory operation of the commutator, this remainder must not exceed 3 volts. This also sets a limit for  $e_t$ . Since the magnitude of the transformer emf  $e_t$  is independent of the armature speed and, on the other hand, since this voltage can be canceled only by *rotation* in a commutating field, it cannot be canceled at low speeds; consequently, *at standstill the transformer emf produces its full effect*. Thus, while starting, there is no means of avoiding the undesirable effect of the transformer emf in the short-circuited wind-

ing element, and it must be small (less than 3 volts), unless resistance is inserted between the winding elements and the commutator bars in order to reduce the current in the short-circuited path and the current density under the brush (see Art. 8-1).

From Eq. 46-3 it follows that  $e_r$  can be diminished if the line frequency and the field-flux are made small. This is the reason why, in the case of single-phase traction motors, a frequency of 25 cps ( $16\frac{2}{3}$  cps in Europe) is selected, and why in a-c commutator motors the pole-flux must be kept low in relation to that of other machines. The low field flux causes a low voltage per winding element. In consequence of this, the commutator of the a-c commutator machine is designed only for low voltage (about 100 volts at 50 to 60 cps, 300 volts at 25 cps, and 500 volts at  $16\frac{2}{3}$  cps). Where the line voltage is higher than these values a transformer is necessary between the line and the armature.

The limit of 3 volts for the residual voltage in the short-circuited coil is determined by the contact resistance between commutator bars and brushes. The greater this contact resistance, the smaller the current in the short-circuited path. Only hard brushes with a high contact resistance are used for a-c commutator motors; for these brushes a residual voltage of 3 volts is permissible.

### PROBLEMS

1. A 4-pole d-c armature rotates in a sinusoidally distributed alternating flux the maximum value of which is  $1.5 \times 10^6$  maxwells. The armature speed is 1200 rpm. Determine the rotational emf: (a) when the brushes are in the neutral; (b) when the brushes are in the pole axis. The number of turns per path is 80.

2. Determine, for the armature of Problem 1, the transformer emf induced between the brushes: (a) when the brushes are in the neutral; (b) when the brushes are in the pole axis. The frequency of the field current is 25 cycles.

3. Determine, for the armature of Problem 1, the average torque produced if the winding is lap wound, the brushes are in the neutral, and the armature current is 20 amp. The phase angle between armature current and flux is  $20^\circ$ .

4. Determine the ampere-conductors of the compensating winding for the armature of Problem 1 if the armature winding is lap wound and the armature current is 20 amp.



## Chapter 47

---

### THE SINGLE-PHASE SERIES COMMUTATOR MOTOR

#### 47-1. The voltage diagram of the single-phase series commutator motor.

The diagram of connections of the single-phase series motor is shown in Fig. 47-1:  $A$  is the armature,  $FW$  the field winding,  $CW$  the compensating winding, and  $IW$  the interpole winding. The brush axis is perpendicular to the field axis, and the axes of the compensating and interpole windings coincide with the brush axis. The connection of the armature, interpole, and compensating windings must be arranged in such a manner that the mmf's of the compensating and the interpole windings act in opposition to the armature mmf (see Arts. 4-3, 8-3, 46-2). Since the brush axis is perpendicular to the field (pole) axis, only an emf of rotation is induced in the armature winding by the pole-flux between the brushes, but no transformer emf whatever. The compensating winding nullifies the mmf of the armature winding. The field winding  $FW$  as well as the interpole winding  $IW$  is designed as a concentrated winding in a manner similar to the d-c machine.

Kirchhoff's mesh equation for the circuit of Fig. 47-1 is

$$V - jI\sum x = I\sum r + E_r \quad (47-1)$$

The meaning of  $\sum x$  and  $\sum r$  is explained below.  $E_r$  is in phase with  $I(\Phi)$ , as is  $I\sum r$ , and is placed together with  $I\sum r$ .

The voltage diagram corresponding to the connections of Fig. 47-1 can be established easily. All four windings carry the same current  $I$ . The pole-flux  $\Phi$  is produced by, and is in phase with, the current  $I$  (Fig. 47-2). Accordingly, the emf of rotation in the armature winding  $E_r$  is in phase with  $I$ . If  $\sum r$  represents the sum of the resistances of the four windings and  $\sum x$  the sum of the leakage reactances of armature and compensating winding plus the reactances of the field and interpole winding, then, according to Kirchhoff's mesh equation, the impressed voltage  $V$  is equal to the geometric sum of the voltage drops  $I\sum r$  and  $I\sum x$  and the emf of rotation in the armature winding  $E_r$ . The iron losses in the stator are

considered as an  $I^2R$  loss and are included in  $I\Sigma r$ . On the other hand, the iron losses of the rotor are for the greatest part of a mechanical nature similar to the windage and friction losses (see Art. 34-1) and are considered as a mechanical power loss. The reactance of the field winding constitutes the greatest part of the sum  $\Sigma x$ . In Fig. 47-2 the emf of rotation  $E_r$ , which is in phase with  $\Phi$  and  $I$ , is drawn for three different speeds. At constant current  $I$  this emf of rotation  $E_r$  is a measure of the developed

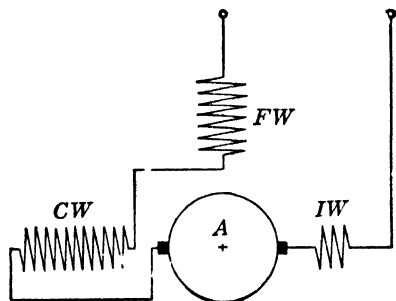


FIG. 47-1. Schematic diagram of the connections of a single-phase series commutator motor.

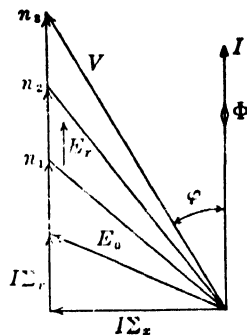


FIG. 47-2. Voltage diagram of the single-phase series commutator motor.

mechanical power of the rotor (see Art. 1-4): as such, it behaves as a dissipative resistance and is in phase with  $I\Sigma r$ . The mechanical power delivered at the shaft is less than the product  $E_r I$  by the amount of the rotational iron losses in the rotor plus the windage and friction losses.

As Fig. 47-2 shows, the phase displacement angle  $\varphi$  of the single-phase series motor decreases with decreasing  $I\Sigma x$ ; further, it decreases considerably with increasing rpm, because with increasing rpm  $E_r$  increases in comparison to  $I\Sigma x$ . For high speeds the power factor approaches a value  $\cos \varphi = 0.95$ .

Analogous to the circle diagram of the induction motor, a circle diagram for the current (at constant voltage) can also be derived for the single-phase commutator motor. However, this circle diagram is not of great value because the single-phase series motor, in contrast to the induction motor which operates over the normal working region with an almost constant flux, has a varying flux, i.e., a varying saturation of the path of the main flux and, therefore, a varying field winding reactance; this factor cannot be taken into consideration in the circle diagram.

**47-2. Commutation of the single-phase series commutator motor.** The phasor diagram of fluxes and emf's for the short-circuited winding

element is obtained by superposition of Figs. 46-4a and 46-4b where it has to be noted that  $\Phi$  is in phase with  $I$ . Fig. 47-3 shows this diagram. The resulting emf  $e_r$  in the short-circuited element lags the current by

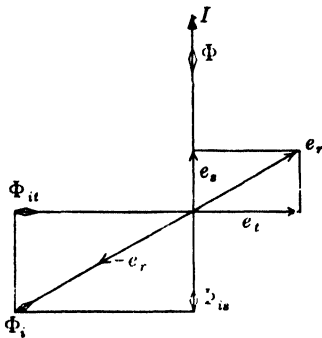


FIG. 47-3. Phasor diagram of the emf's in the short-circuited winding element and of the commutating fluxes.

a fixed angle. The generation of the oppositely directed emf  $-e_r$  is to be accomplished by means of the resulting commutating flux  $\Phi_{it}$ , and the task of the interpole winding is to furnish this flux. The interpoles cannot be excited by the armature current directly, for the resulting interpole flux  $\Phi_i$  and the armature current  $I$  are not in phase. The interpole winding must be excited by a current which lags the armature current  $I$  by the same angle by which  $e_r$  lags  $I$ . This will occur if a resistance  $R$  is connected in parallel with the interpole winding as Fig. 47-4 shows. If  $V_i$  is the voltage common to the interpole winding and the resistance  $R$  (Fig. 47-5), then

the current  $I_i$ , which flows in the interpole winding, lags behind  $V_i$  by about  $90^\circ$ , because the resistance of this winding is small in relation

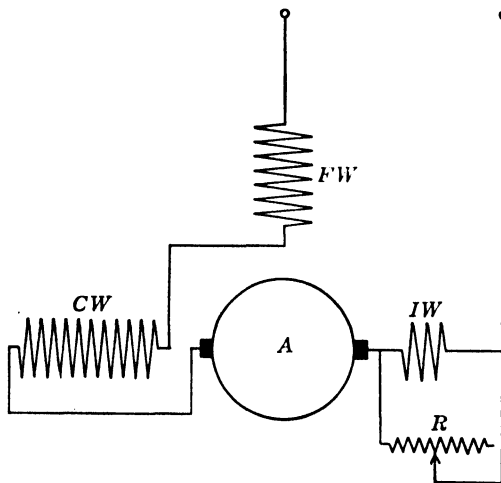


FIG. 47-4. Resistance in parallel with the interpole winding for producing the commutating fluxes according to Fig. 47-3.

to its reactance; on the other hand, the current  $I_R$ , which flows in the resistance  $R$ , is in phase with  $V_i$ . Since the geometric sum of  $I_i$  and  $I_R$  must be equal to the armature current  $I$ , the interpole current

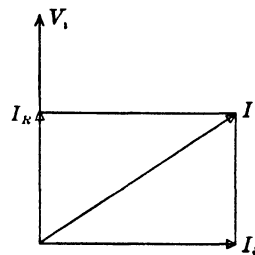


FIG. 47-5. Current diagram for interpole winding and resistance of Fig 47-4.

$I_i$  is caused, by the parallel resistance  $R$ , to lag behind the armature current, and it can therefore produce the necessary resulting commutating

flux  $\Phi_f$ . It should be remembered (see Art. 46-3) that the arrangement for improving the commutation shown in Fig. 47-4 is effective only within a certain range of motor speed; it is not effective at low speeds.

**47-3. Torque and characteristic curves of the single-phase series commutator motor.** Since the flux in the single-phase series motor is in phase with the armature current, and the brush axis makes an angle of  $90^\circ$  with the field axis, the torque, in accordance with Eq. 46-2, is

$$T = \frac{0.1174}{\sqrt{2}} \frac{p}{a} \Phi Z I \times 10^{-8} \text{ lb-ft} \quad (47-2)$$

Speed control in the single-phase series motor is accomplished by *voltage control*. For a given torque (given armature current) the counter-emf ( $E_r$  in Fig. 47-2) increases as the voltage increases and, therefore, the

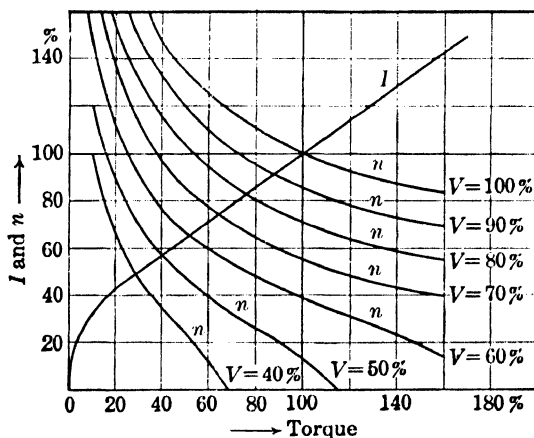


FIG. 47-6. Speed-torque characteristics and torque-current characteristic of the single-phase series motor.

speed increases with increasing voltage. For the purpose of speed control the transformer secondary is tapped, and the speed control is accomplished economically.

The relation between torque and current, as well as that between torque and speed for various voltages, is shown in Fig. 47-6. Rated values of torque, speed, etc., are taken as 100%. The general trend of the current as well as of the speed curve is the same as that in a d-c series motor. The greater the voltage, the greater will be the speed for the same torque. The line current for a given torque is independent of the magnitude of the voltage. In order to develop rated torque at start, 45 to 50% of the rated

voltage is necessary. For satisfactory commutation the speed range of the single-phase series motor is between 20 and 150% of rated speed.

**47-4. The universal motor.** The A.S.A. definition of a universal motor is as follows:

A universal motor is a series-wound or a compensated series-wound motor which may be operated either on direct current or single-phase alternating current at approximately the same speed and output. These conditions must be met when the direct-current and alternating-current voltages are approximately the same and the frequency of the alternating current is not greater than 60 cps.

As can be seen from this definition, there are two types of universal motors: the non-compensated and the compensated. The non-compensated motor has salient poles just as the d-c machine; the compensated motor has slotted stator punchings, such as the traction motor described in Art. 47-1.

The universal motor is a fractional-horsepower motor and is usually designed for speeds of 3500 rpm or less, but also up to 10,000 or 15,000 rpm. The no-load speed may be as high as 20,000 rpm. The non-compensated motor is less expensive than the compensated motor, but its operating characteristics are not as good as those of the compensated motor. For the application of universal motors see Art. 50-3.

### PROBLEMS

1. The sum of the resistances of the field winding, compensating winding, armature winding, and interpole winding of a 25-cycle, single-phase series motor is 1.5 ohms. The sum of the reactances of these windings is 4.5 ohms. At a current of 5 amp the flux per pole is  $475 \times 10^3$  maxwells. Determine the speed of the motor, if the number of poles is 4, the number of turns per path is 60, and the terminal voltage is 120 volts. Use Eq. 3-6 with  $Z = 2aN$  and remember that the brushes pick up the amplitude of the a-c voltage.

2. Determine the terminal voltage necessary to reduce the speed of the motor of Problem 1: (a) by 20%; (b) by 30%. Torque remains the same as in Problem 1.

3. Determine the terminal voltage necessary to increase the speed of the motor of Problem 1; (a) by 20%; (b) by 30%. Torque remains the same as in Problem 1.

4. Determine the torque of the motor of Problem 1 if the winding is lap wound. The brushes are in the neutral.

5. A 2-pole, 25-cycle, single-phase series motor has a total field resistance of 0.80 ohm and each pole has 150 turns. A field current of 10.0 amp produces a voltage across the field of 50 volts. Determine the reactance of the field in ohms and the pole flux. Neglect leakage.

6. The armature of the 25-cycle motor in Problem 5 is wound with winding elements having 8 turns. What is the maximum flux permitted to link a winding element if the maximum rms voltage between commutator bars is limited to 3 volts.

7. If the power input to the machine of Problem 1 is 500 watts when  $\cos \phi = 0.85$  and the terminal voltage is 71 volts, determine the emf of rotation.

## Chapter 48

### THE REPULSION MOTOR

**48-1. The voltage diagram of the repulsion motor.** The circuit of the repulsion motor is shown in Fig. 48-1. The stator winding (field winding *FW* and compensating winding *CW* in series) is connected to the line and is completely detached electrically from the armature winding; the armature is short-circuited on itself by the brushes. Since the commutator is not included in the circuit containing the stator winding, the latter may be designed for any voltage desired.

The compensating winding *CW* and the armature *constitute a transformer*; by this means the load current which is necessary to produce the torque is transferred from the lines to the armature. The compensating winding, therefore, can be designated as the *stator torque winding*. The torque is produced by the armature current and *main flux*; the brush axis is perpendicular to the field (pole) axis, exactly as in the series motor. The cross-flux in the load (horizontal) axis cannot produce torque with the armature currents, because its axis coincides with the brush axis, i.e., because with respect to this flux the current distribution in the armature is such that the torques of the individual coils mutually cancel themselves (see Art. 46-2).

*At start* the repulsion motor behaves exactly as the series motor. At start, in both motors, the voltage impressed across the terminals is consumed essentially by the field winding, because of its high reactance. At start the compensating winding and the armature winding require only a small part of the total voltage, namely, the short-circuit voltage of their leakage reactances and resistances, since the fluxes produced by

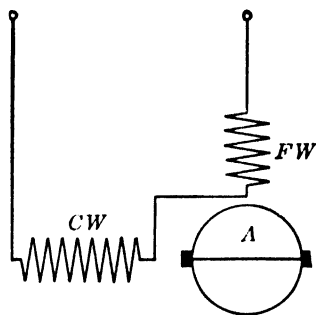


FIG. 48-1. Schematic connection diagram of the repulsion motor.

these windings cancel each other. The armature current is displaced practically  $180^\circ$  behind the pole-flux, which is produced by a current of the same phase as the current in the torque winding (winding *CW*); therefore, the conditions for developing a high starting torque are just as favorable as in the series motor.

When running, an emf is induced in the armature by the pole-flux as well as by the cross-flux. The pole-flux produces an emf of rotation  $E_r$

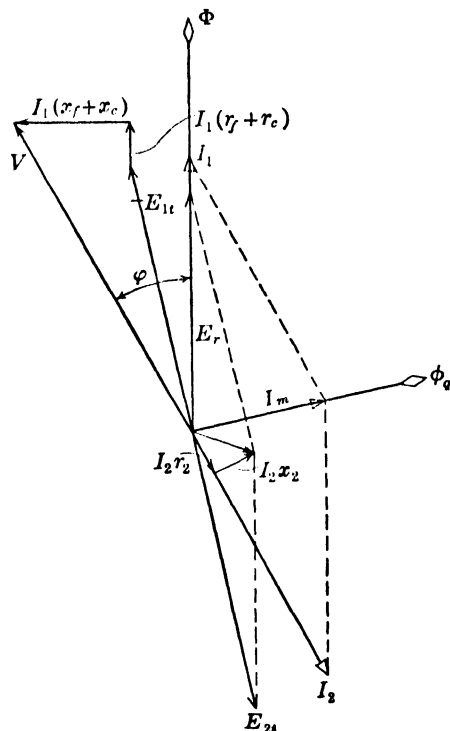


FIG. 48-2. Flux and voltage diagram of the repulsion motor.

in the armature which is in phase with this flux and the field current, and consequently with the current in the torque winding (winding *CW*), since these currents are always equal. The armature current, produced by transformer action with the torque winding, is displaced in phase nearly  $180^\circ$  from the field current, so that the emf  $E_r$  of rotation and the current transferred by transformer action are likewise displaced in phase nearly  $180^\circ$  from one another. The emf of rotation  $E_r$  consequently acts on the transformer consisting of the torque winding (winding *CW*) and the armature as the counter-voltage of an ohmic resistance; when running, the transformer appears non-inductively loaded, and the terminal voltage at the primary of the transformer, i.e., at the torque winding, must rise by an amount corresponding to the emf  $E_r$ ; therefore, when running, a voltage, in phase with the current, ap-

pears at the terminals of the torque winding *CW*, in addition to the short-circuit voltage which appears at standstill. Since this voltage at the torque winding can be produced by transformer action only, its appearance is possible if a cross-flux ( $\Phi_q$ ) is developed in the torque axis which is displaced in phase  $90^\circ$  relative to this voltage. Thus two fluxes, the pole-flux and the cross-flux, are to be considered.

Fig. 48-2 shows the voltage diagram of the repulsion motor. The stator current  $I_1$  and the pole-flux  $\Phi$  are drawn upward along the vertical.

The armature emf of rotation  $E_r$  is in phase with  $\Phi$ . The geometric sum of  $E_r$  and the emf  $E_{2t}$  induced in the armature by the transformer action of the cross-flux  $\Phi_q$  must be equal to the resistance and reactance voltage drops in the armature winding  $I_2 r_2$  and  $I_2 x_2$ . The cross-flux  $\Phi_q$  is produced in the torque winding by a magnetizing current  $I_m$ . Consequently, the stator current  $I_1$  is equal to the geometric sum of  $-I_2$  and  $I_m$ . The stator voltage  $V$  must be large enough to overcome the transformer emf of the compensating winding  $E_{1t}$  and besides provide for the resistance and reactance voltage drops of the field and compensating windings  $I_1(r_f + r_c)$  and  $I_1(x_f + x_c)$ .

The armature field is canceled in the repulsion motor in the same manner as in the series motor (Fig. 47-1). It is necessary to distinguish between the armature flux and the cross-flux  $\Phi_c$ , for the armature flux is in phase with the current  $I_2$  while the cross-flux is displaced in phase about  $90^\circ$  from the current  $I_2$ .  $x_2$  consists of only the leakage reactance of the armature winding. Correspondingly  $x_c$  consists of only the leakage reactance of the compensating winding; on the other hand,  $x_f$  includes the complete self-inductance of the field winding, as in the series motor.

As was mentioned previously, the cross-flux  $\Phi_q$ , which takes no part in the production of torque, is absolutely essential for the transfer of power from the stator to the rotor. The pole-flux  $\Phi$  and the cross-flux  $\Phi_q$  are displaced exactly  $90^\circ$  from each other in space phase and almost  $90^\circ$  in time phase. This results in a *rotating flux*. The speed of this rotating flux is

$$n_s = \frac{120f}{p}$$

if  $f$ , as in the discussions preceding, is the line frequency. Thus the repulsion motor at standstill has an alternating flux and develops a rotating flux during running.

**48-2. Commutation of the repulsion motor.** The repulsion motor has no interpoles for improvement of commutation. At standstill the transformer emf appears in the short-circuited winding element, just as in the single-phase series motor, and the current of the short-circuit path is limited by the contact resistance between brush and commutator bars. The fact that the repulsion motor develops a rotating flux while running is of importance for its commutation during running: it is evident that, when the short-circuited winding element has the same speed as the rotating flux, no voltage is induced in it by the rotating flux. Thus, at synchronous speed of the rotor, no transformer emf appears in the short-circuited winding



element. The influence of the transformer emf on commutation is largest at standstill; it decreases as the motor speed increases; it becomes zero at the synchronous speed of the motor, and increases again as the speed becomes larger than the synchronous speed. Consequently, the repulsion motor is *best operated near synchronous speed*.

**48-3. Characteristic curves of the repulsion motor.** Since the ratio of the field current to the armature current is fixed as a result of the series connection of the field and torque windings, the repulsion motor has the *characteristic of a series motor*.

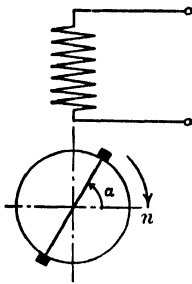


FIG. 48-3. Actual winding arrangement of the repulsion motor.

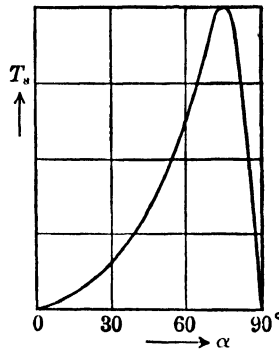


FIG. 48-4. Starting torque of the repulsion motor as a function of the brush angle.

Fig. 48-3 shows the field and compensating windings of Fig. 48-1 combined into a *single* winding. The connections of Figs. 48-1 and 48-3 are entirely equivalent to one another. This becomes evident if the stator winding of Fig. 48-3 is assumed divided into two parts, one of which has its axis in the direction of the brush axis and the other perpendicular to the brush axis. Fig. 48-3 represents the actual coil arrangement of the repulsion motor. By means of a *brush displacement* the stator winding can be distributed in any manner selected into a field and a compensating winding; in this manner the *speed and the torque of the motor can be varied*, since a variation of the number of field turns gives rise to a variation in the flux ( $\Phi$ ) which produces the torque.

The two extreme brush positions are found when the brush axis is perpendicular to the axis of the stator winding ( $\alpha = 0^\circ$ ), and when the brush axis coincides with the axis of the stator winding ( $\alpha = 90^\circ$ ). In the first case ( $\alpha = 0^\circ$ ) the armature current and torque of the motor are zero: this position is the *zero position* of the brushes. In the second case

( $\alpha = 90^\circ$ ) the motor behaves as a short-circuited transformer: this position is the *short-circuit position* of the brushes. Here, in spite of the very large current in both windings, the torque is zero because the torque-producing pole-flux is missing. Because of the large currents which can damage the windings, the motor should not be connected to the line with the brushes in this position.

At start the brushes are placed first at the zero position and then moved in one direction or the other. The *direction of rotation* of the rotor may be determined by the following considerations: if a short-circuited and movable coil is placed in the alternating field produced by a fixed

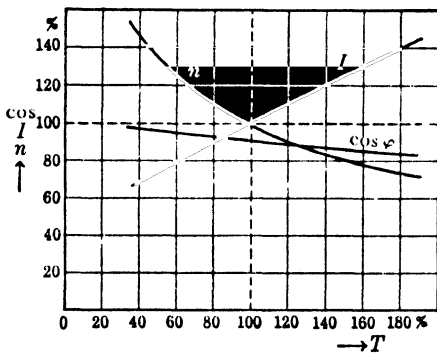


FIG. 48-5. Speed-torque characteristic and torque-current characteristic of the repulsion motor, for a fixed brush position.

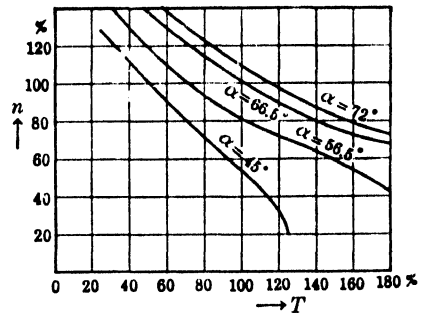


FIG. 48-6. Speed-torque characteristics of the repulsion motor for various brush positions.

coil, the movable coil seeks to adjust itself *with the shortest travel* so that the flux passing through it becomes a minimum; its axis attempts to take a position perpendicular to the axis of the field. Accordingly, the armature shown in Fig. 48-3, which may be taken as a short-circuited solenoid with the same axis as the brush axis, will try, by rotation, to bring its axis (the brush axis) to the right (clockwise) and along the horizontal. Since the brushes are immovable and the armature itself can move under the brushes, the armature itself will turn to the right (clockwise) and continue to rotate because the current distribution in the armature remains unchanged due to the fixed position of the brushes. In Fig. 48-3 the brushes are displaced by an angle  $\alpha$  from the zero position in a counterclockwise direction and the resulting rotation of the armature is clockwise. If the brushes are shifted from the zero position in a clockwise direction, the armature rotates counterclockwise; i.e., *the direction of rotation of the armature is always opposite to the displacement of the brushes from the zero position*. In order to reverse the direction of rotation of a

repulsion motor it is necessary only to place its brushes in an *opposite position* with respect to the zero position.

Fig. 48-4 shows the starting torque of the repulsion motor as a function of the brush position,  $\alpha$ . The maximum torque is obtained at a brush shift of about  $75^\circ$  to  $80^\circ$ . Starting is accomplished by shifting the brushes far enough from the zero position and against the desired direction of rotation until the magnitude of the motor torque exceeds the opposing torque of the load; the motor then runs and carries the load.

At rated load the brush shift depends upon the construction of the motor and is  $67^\circ$  to  $77^\circ$ . The relation between torque, speed, stator current, and power factor at the brush position for rated output is shown in Fig. 48-5. As in Fig. 47-6 all quantities are given as a percentage of their value at rated load. The speed torque-characteristic of the repulsion motor follows the same general trend as that of the series motor. Fig. 48-6 shows the relation between torque and speed for various brush positions,  $\alpha$ . This figure is similar to Fig. 47-6 which shows the speed of the series motor as a function of the torque for various voltages. The various voltages in Fig. 47-6 (speed control by variation of voltage) correspond to the various brush positions in Fig. 48-6 (speed control by change in the field).

## *Chapter 49*

### THE 3-PHASE SHUNT COMMUTATOR MOTOR. (THE SCHRAGE MOTOR)

Since the 3-phase shunt motor is the most widely used of the polyphase commutator motors, it will be the only one considered in this discussion.

**49-1. Connection diagram and speed control of the 3-phase shunt commutator motor.** As was explained in Art. 29-3, the speed of an induction motor can be regulated by means of a voltage impressed on its secondary winding which has the same direction and frequency as the emf induced in this winding by the rotating flux. If the voltage impressed upon the secondary winding is in phase with the induced emf, the speed of the rotor will rise, for a smaller induced emf, and consequently a smaller slip is necessary to produce the secondary current required for the opposing torque. On the other hand, if the voltage impressed on the secondary winding is displaced  $180^\circ$  in phase from the induced emf, the speed of the rotor will fall, for a greater secondary emf, and consequently a greater slip is necessary to produce the secondary current required for the opposing torque. By a suitable selection of the phase and magnitude of the impressed voltage, it is possible, therefore, to regulate the speed of an induction motor below as well as above synchronous speed.

The voltage impressed upon the secondary winding, for the purpose of regulating the speed, must have the same frequency as the emf induced in this winding by the rotating flux, i.e., the slip frequency, and it must change its frequency according to the load. In the treatment of the induction motor, it has been mentioned already that such a voltage of variable frequency can be generated by means of a polyphase commutator machine. The 3-phase shunt motor described in the following is a combination of a polyphase rotor-fed induction motor and a polyphase commutator machine in one armature and one stator.

Fig. 49-1 shows the connection diagram of the 3-phase shunt motor. Its

rotor has two windings, one of which is connected to slip rings and the other to a commutator; its stator has only one winding. The line is connected to the slip rings  $UVW$ . Neither the commutator winding of the rotor nor the stator winding is connected to the line. The three separate

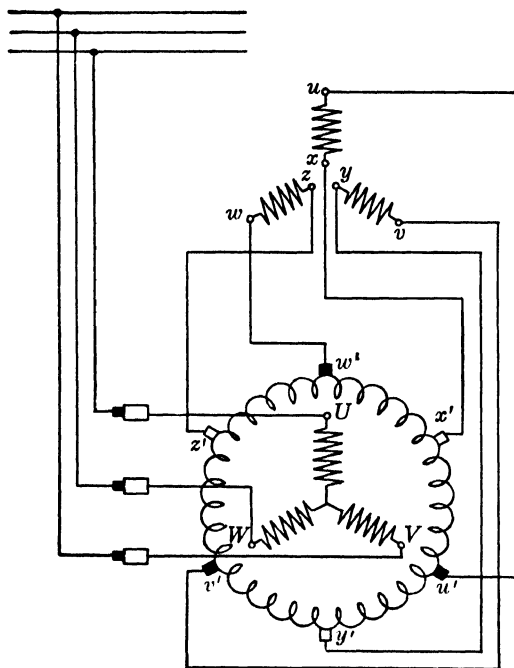


FIG. 49-1. Schematic connection diagram of the 3-phase shunt motor (Schrage motor).

phase windings of the stator are not connected to each other but are open; each of these phase windings is connected to two brushes which may be moved in *opposite* directions on the commutator. Accordingly, the 2-pole machine has 6 sets of brushes.

Relative to the *rotor* the speed of the rotating flux produced by the rotor (primary) winding is always the same,  $n_s = 120f_1/p$ . The relative velocity of the rotating flux in relation to space (stator) depends upon the speed of the rotor. As in the case of every rotor-fed induction motor, the direction of rotation of the rotor is always opposite to that of its rotating flux, for both motor and generator operation; the speed of the rotating flux relative to the *stator* is  $n_s$  at standstill and zero at synchronous speed. Consequently, the frequency of the emf's induced in the stator windings by the rotating flux is slip frequency, and rotor and stator mmf waves are at standstill with respect to one another at any rotor speed, i.e., the necessary condition for the development of a uniform torque is satisfied.

The frequency of the voltage at the commutator *brushes* can be determined from the following consideration. In a d-c machine the magnetic field is at standstill and the frequency of the current at the brushes is zero and independent of the armature speed ( $n$ ). If the brushes of a d-c machine were made to rotate with a certain speed  $n'$ , an a-c instead of a d-c voltage would be measured at the brushes and the frequency of this a-c voltage would be determined by the speed of the brushes  $n'$  but not by the armature speed  $n$ . Vice versa, if the magnetic flux (poles) of a d-c machine were made to rotate with a speed  $n'$  relative to the space, again an a-c voltage would be measured at the brushes and the frequency of this voltage would be determined solely by the speed of the magnetic flux relative to space,  $n'$ . In the 3-phase shunt motor connected according to Fig. 49-1, the magnetic flux rotates with the speed  $(n_s - n) = sn_s$  with respect to space. Therefore the frequency of the voltage at the brushes is  $sf_1$ , i.e., the same as in the stator winding, and brushes and stator winding can be connected together.

The magnitude of the voltage impressed on the stator winding (the brush voltage) is changed in the rotor-fed shunt motor by changing the spacing between the brushes of each brush pair, i.e., the distances  $u'x'$ ,  $v'y'$ , and  $w'z'$  (Fig. 49-1). The commutator voltage increases with the distance between the brushes. The greatest voltage is delivered by the commutator when the distance between the two brushes of the brush pairs is 180 electrical degrees. If both brushes of the brush pairs are on the same commutator bar, the voltage impressed on the stator winding is zero, each of the three stator windings is short-circuited, and the machine behaves as an ordinary induction motor.

The speed control is continuous, and the maximum range of control is determined by the maximum voltage available at the commutator brushes. With respect to commutation this voltage is made about one half of the voltage induced in the open stator winding at standstill: this will produce a speed range of from  $\frac{1}{2}$  to about  $1\frac{1}{2}$  times synchronous speed, i.e., a speed regulation in the ratio 1:3 is achieved.

If a *constant* brush voltage is impressed on the stator winding, the speed characteristic is displaced more or less *upward or downward* accord-

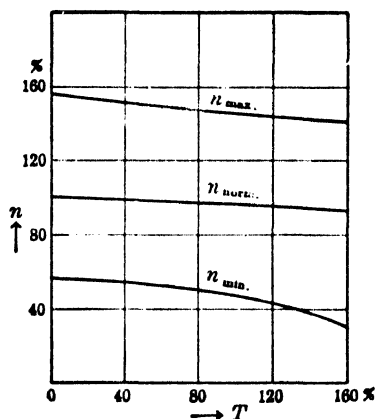


FIG. 49-2. Speed-torque characteristics for a speed ratio of 1:3 at no load.

ing to the magnitude and phase of this voltage. Fig. 49-2 shows three speed torque characteristics assuming that the regulation at no-load is in the ratio of about 1:3. The upper and lower curves show the same trend

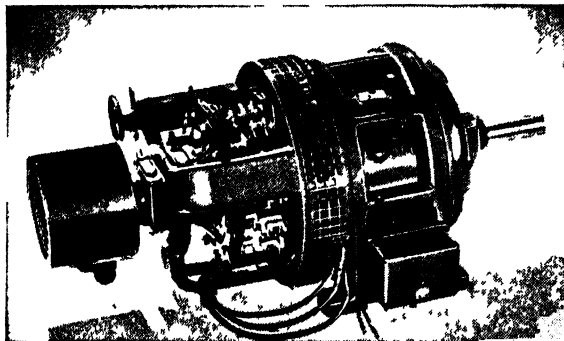


FIG. 49-3. Three-phase shunt motor (Schrage motor)

as the middle curve for which the brush voltage is equal to zero and which is, therefore, identical with the speed characteristic of the ordinary induction motor. The slip increases and therefore the speed decreases with

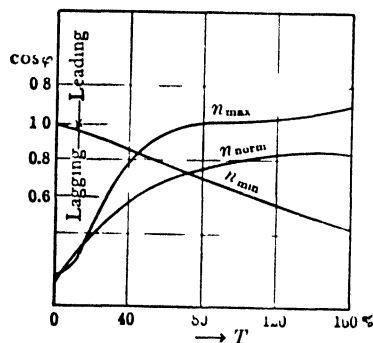


FIG. 49-4. Power factor of the 3-phase shunt motor as a function of torque

increasing torque. By inserting resistance in the stator circuit it is also possible to extend the range of regulation further downward, just as in the induction motor. The appearance of a 3-phase shunt commutator motor is shown in Fig. 49-3.

**49-2. Power-factor correction of the 3-phase shunt motor.** Power-factor correction can be attained in the induction motor by impressing a voltage on the secondary winding which leads the emf induced in it by the rotating flux by 90°. When speed regulation alone is desired, the axis of each brush pair must coincide with the axis of

the proper stator phase. The change in spacing between the brushes, in order to vary the speed, is accomplished by arranging the pairs of brushes in separate brush yokes which may be displaced from each other in opposite directions. In order to obtain power-factor correction the axis of a brush pair must be displaced from the axis of the corresponding stator phase by a fixed angle.

Assuming a regulation at no-load of about 1:3, as shown in Fig. 49-2, the relation between the power factor and the torque of the 3-phase shunt motor is given in Fig. 49-4. The power factor curve for  $n_{\text{normal}}$  is exactly the same as that of the ordinary induction motor: in this case the brush voltage is zero. The curve for the higher speed,  $n_{\text{max}}$ , produces a leading power factor at the larger values of torques in consequence of the power-factor correction. For the curve at the low speed,  $n_{\text{min}}$ , the no-load power factor must be unity or leading in order that the power factor at larger torques does not become too low.

**49-3. Commutation of the 3-phase shunt motor.** Since the rotating flux of the 3-phase shunt motor with power supply through the slip rings has a constant speed ( $n_s$ ) with respect to the armature, the emf induced by it in the short-circuited winding element is constant and independent of the speed. The emf of self-induction in the short-circuited winding element depends upon the range of speed regulation. At synchronous speed this emf is zero, for at this speed the brushes of each brush pair are placed on the same commutator bar, and commutation of current does not take place. It is low for a small range of speed variation. No special means are available to improve the commutation of a 3-phase shunt motor (such as the interpoles of a d-c motor). Therefore, the emf of the short-circuited winding must be kept small, and hard brushes with a high contact resistance must be used.

### PROBLEMS

1. The adjustable-speed, 3-phase, slip-ring fed, shunt motor (Schrage motor) is designed to increase the speed at no-load by 40% and to decrease the speed at no-load by 55%. What should be the maximum brush voltage impressed upon the stator winding in percent of the voltage of the open stator winding at standstill? Assume that the line frequency is 60 cycles. What is the frequency of the brush voltage at 140% and 45% of the no-load speed.

2. At constant torque for the motor considered in Problem 1, approximately what will be the power of the commutator winding in percent of the motor power input at 40% higher speed and at 55% lower speed.

3. The secondary frequency of the induction motor is greater than the line frequency only when its rotor runs against the rotating flux. Is it possible to produce a stator frequency in the Schrage motor larger than the line frequency, with the rotor running in the same direction as the rotating flux? If so, what should be the brush voltage, in percent of the voltage at the stator-winding terminals at standstill, in order that the secondary frequency be 130 cycles? The line frequency is 60 cycles.



## Chapter 50

### MOTOR APPLICATION

The problem of motor application consists in matching the motor to both the load and the operating conditions. To accomplish this, the motor characteristics *and* the load characteristics must be known.

Although the motor characteristics have been studied in detail in the foregoing chapters, a brief summary will be given in the discussion fol-

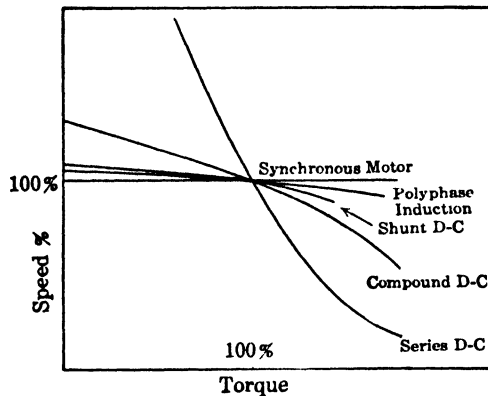


FIG. 50-1. Typical torque-speed curves of the various types of motors.

lowing. The requirements of the load vary from case to case, since the variation of torque, overload capacity, duty cycle, surrounding conditions, etc., are different for the different loads.

**50-1. Motor characteristics.** Corresponding to the variety of loads and surrounding conditions, the NEMA standards classify the motors according to:

- (a) application (general-purpose motor, special-purpose motor; etc.)
- (b) electrical type (polyphase motor, single-phase motor, d-c motor)

(c) mechanical protection and methods of cooling (open machine, drip-proof machine, splash-proof machine, semi-protected machine, totally enclosed non-ventilated machine, etc.)

(d) variability of speed (constant-speed motor, adjustable-speed motor, etc.)

(e) size (fractional-horsepower motor, integral-horsepower motor).

Considering the different electrical types and the variability of speed, an

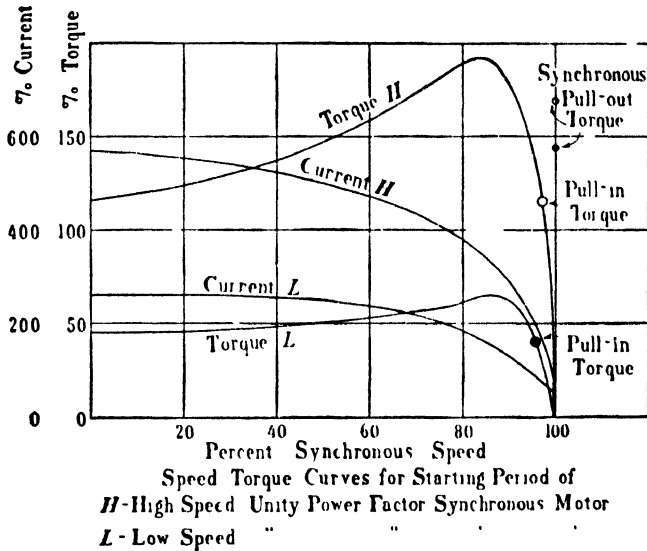


FIG. 50-2. Typical torque-speed and current-speed characteristics for synchronous motors during starting.

important motor and load characteristic is the *relation of torque to speed*. Fig. 50-1 shows typical torque-speed curves for the various industrial motors.

The *synchronous motor* is the only machine having *absolutely constant speed*. It starts, by means of the damper winding, as an induction motor (see Art. 40-4), and having reached its maximum induction motor speed, the d-c excitation is applied and the motor pulls into step. Table 1 gives the starting torques, starting currents, pull-in torques, and pull-out torques for synchronous motors on the basis of the NEMA standards. Fig. 50-2 shows the starting torque-speed curves of a high-speed and a low-speed synchronous motor, both designed for unity power factor. The *pull-in torque* given in Table 50-1 and Fig. 50-2 is the induction motor torque developed at 5% slip. The higher the speed reached while running as an induction motor and the lower the moment of inertia

TABLE 50-1. STARTING, PULL-IN, AND PULL-OUT TORQUES, AND STARTING CURRENTS OF NEMA STANDARD SYNCHRONOUS MOTORS

Type	Rpm	Starting Torque	Pull-In Torque	Pull-Out Torque	Starting Current Full-Voltage
<b>General-purpose motors</b>					
Unity pf	1800	110	110	150	550-750
(Up to 200 hp)	514-1200	110	110	175	550-750
0.8 pf	1800	125	125	200	500-700
(Up to 150 hp)	514-1200	125	125	250	500-700
<b>Large high-speed motors</b>					
Unity pf					
250 to 500 hp	514-1800	110	110	150	550-700
600 hp and above	514-1800	85	85	150	550-700
0.8 pf					
200 to 500 hp	514-1800	125	125	200	500-700
600 hp and above	514-1800	100	100	200	500-700
<b>Low-speed motors</b>					
Unity pf	less than 514	40	30	150	300-500
0.8 pf	514	40	30	200	250-400

Torques and currents are expressed in percent of rated full-load values.

Pull-in torque is based on NEMA standards for normal  $WR^2$  of the load.

of the rotating mass, the easier the motor pulls into step. The standard pull-in torques shown in Table 50-1 and Fig. 50-2 presume a normal  $WR^2$ , as specified by the NEMA standards.

It has been explained in Art. 40-3 that an overexcited synchronous motor draws leading current from the lines i.e., an overexcited syn-

TABLE 50-2. STARTING AND PULL-OUT TORQUES, STARTING CURRENT AND RATED SLIP OF A POLYPHASE 30-HP 1800-RPM INDUCTION MOTOR CORRESPONDING TO NEMA CLASSIFICATIONS A, B, C, D, AND F.

	Starting Torque	Pull-out Torque	Starting Current in Amp at 220 Volts	Rated Slip %
A	150	> 200	> 435	< 5
B	150	200	≤ 435	< 5
C	≤ 200	≤ 190	≤ 435	< 5
D	275		≤ 435	≥ 5
F	125	135	≤ 270	< 5

chronous motor behaves as a capacitance with respect to the lines. This property of the overexcited synchronous motor is used to improve the overall power factor of a plant and is the reason why synchronous

motors are rated for unity power factor *and* also for 0.8-power factor leading.

The *polyphase induction motor with squirrel-cage rotor* has nearly constant speed (Fig. 50-1), the speed variation usually being less than 10%. The NEMA standards specify five designs (A, B, C, D, and F) for polyphase squirrel-cage motors. The difference of these designs in starting torque, pull-out torque, starting current, and slip at rated load is shown for a 30-HP, 1800-rpm motor in Table 50-2 and Fig. 50-3. (For other horsepower and speeds, see NEMA standards.)

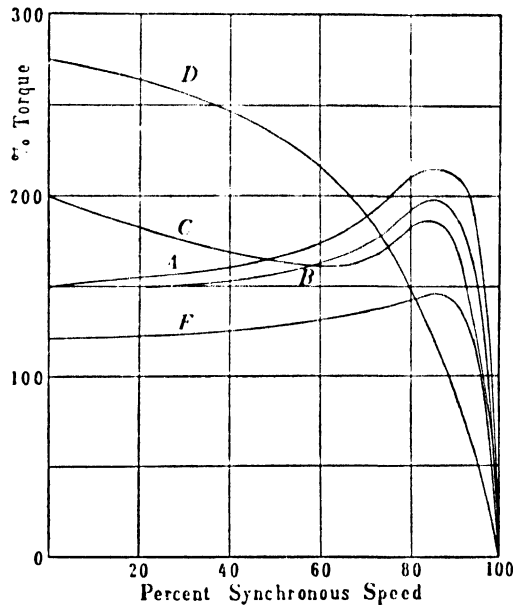


FIG. 50-3. Torque-speed curves of a 30-HP, 1800-rpm, polyphase induction motor corresponding to NEMA classifications A, B, C, D, and F.

The *polyphase induction motor with wound rotor* offers the possibility of speed control by means of a rheostat between the slip rings: the speed control is continuous but not economical (see Art. 29-3a). The starting performance of the wound-rotor motor is more efficient than that of the squirrel-cage or synchronous motor: the rheostat in the rotor circuit provides the lowest ratio of starting current to starting torque and also a high starting torque (equal to the pull-out torque, if necessary). Thus, the wound-rotor motor is used either as a varying-speed motor or as a constant-speed motor for high starting torque at low starting current. Smooth acceleration through adjustment of torque during starting is a further advantage of the wound-rotor motor.

The *d-c shunt motor*, at constant field current and constant armature voltage, operates at nearly constant speed, the speed variation usually being less than 10%. However, the speed of the d-c shunt motor can be regulated in a simple manner by field control, and also by control of its armature voltage (see Art. 7-6). The *d-c shunt motor* with field control is best suited for *wide speed ranges*.

The *d-c series motor* is a varying-speed motor able to develop a high starting torque.

The *d-c compound motor*, being a shunt and series combination, has characteristics between these two motors. Usually the shunt motor characteristic predominates.

*Single-phase induction motors* are usually fractional horsepower with a squirrel-cage rotor. The characteristic data of the various types of single-phase motors are given later in Table 50-5a and 50-5b.

**50-2. Load characteristics.** Many industrial loads operate at *constant or nearly constant speed*, the speed variation being 5 to 15%. In these cases the power output is proportional or nearly proportional to the required torque. Such loads are constant-speed blowers, compressors, crushers, fans, rubber mills, rolling mills, conveyors, pumps, grinders, concrete mixers, motor-generator sets, wood-working machines, metal-working machines, laundry machinery, looms in textile mills, saws, hammer mills, jordans, beaters, saws, etc. The synchronous motor, the induction motor, and the d-c shunt motor can be used for these loads.

Other industrial loads require that the *speed be adjustable*, i.e., that the speed be varied over a considerable range, but, when once adjusted, that it remain nearly constant. Adjustable speed loads are of three general types, namely, those in which:

- (a) the torque is essentially constant at all speeds (constant torque),
- (b) the power output is essentially constant at all speeds (constant HP),
- (c) the torque is inherently variable (variable torque).

In the first case the power output varies directly with the speed. Typical loads of this kind are certain types of conveyors and automatic machine tools. The d-c shunt motor designed for adjustable speed by field control or armature control, the wound-rotor induction motor with a resistor in the rotor circuit, and the polyphase shunt motor can be used for these loads.

In the second case, where the power output is essentially constant, the torque varies inversely with the speed. Typical loads of this kind are most machine tools. The d-c shunt motor designed for adjustable speed by field control and the wound-rotor induction motor can be used for these loads.

The third case in which the torque is inherently variable applies to fans, blowers, and centrifugal pumps. In these loads the torque increases with about the square of the speed and therefore the power output increases with about the cube of the speed. A d-c shunt motor designed for adjustable speed by field control can be used for these loads.

There are loads which require that the *speed be varying*, i.e., that the speed vary with the load, ordinarily decreasing when the load increases. Such loads are hoists, those which occur in traction, cranes, bridges, etc. The d-c series motor, the a-c single-phase commutator motor, and the repulsion motor can be used for these loads.

The *starting torque*, i.e., the torque necessary to break away from stand-still, is an important factor in determining the type of motor. Fans, blowers, centrifugal pumps, unloaded compressors, motor generator sets, etc. require a low starting torque of about 30 to 50% of rated torque. Unloaded crushers, rod mills, etc., require 100% starting torque. Other loads such as sheet mills, loaded compressors, etc., require still higher starting torques, up to 300% of normal torque. The starting torques developed by the various types of motors are given in Tables 50-1, 50-3, 50-4, and 50-5.

Another important factor is the *inertia of the mass* of the load: together with the load torque it determines the starting time and, therefore, the heat developed during starting in the rotor of a squirrel-cage motor. For loads with high inertia and high torques during starting, a squirrel-cage motor of special design or another type of motor must be used.

The *surrounding conditions* under which the motor must operate are also of importance. As has been explained in Art. 10-2 certain temperature limits are set for the insulating materials. The temperature of the winding is determined by the copper and iron losses produced in the machine and by the ambient temperature. Electric machines are usually designed for an ambient temperature of 40°C. If the ambient temperature is higher than 40°C, either an oversized machine, or high-temperature insulation (silicon), or special ventilation must be used. If the surrounding air contains dust, corrosive gases, salt air, or excessive moisture, a motor with a special enclosure to protect its windings and commutator or slip rings is required. There are splash-proof, drip-proof, dust-proof, explosion-proof, etc., enclosures available.

**50-3. Various motor types and their applications.** In the following Tables 50-3, -4, -5a and -5b the general characteristics and typical applications are given for d-c motors, polyphase induction motors, and single-phase motors.

TABLE 50-3. CHARACTERISTICS AND APPLICATIONS OF D-C MOTORS

Type	Starting Torque (%)	Max. Running Torque, Momentary (%)	Speed Regulation or Characteristic (%)	Speed Control (%)	Typical Application and General Remarks
Shunt, constant speed	Medium — usually limited to less than 250 by a starting resistor but may be increased	Usually limited to about 200 by commutation	5-10	Increase up to 200 by field control; decrease by armature voltage control	Essentially for constant-speed applications requiring medium starting torque. May be used for adjustable speed not greater than 2 to 1 range. For centrifugal pumps, fans, blowers, conveyors, woodworking machines, machine tools, printing presses.
Shunt, adjustable speed	Same as above	Same as above	10-15	6 to 1 range by field control, lowered below base speed by armature voltage control	Same as above, for applications requiring adjustable speed control, either constant torque or constant output.
Compound	High — up to 450, depending upon degree of compounding	Higher than shunt — up to 350	Varying, depending upon degree of compounding — up to 25-30	Not usually used but may be up to 125 by field control	For drives requiring high starting torque and only fairly constant speed; pulsating loads with flywheel action. For plunger pumps, shears, conveyors, crushers, bending rolls, punch presses, hoists.
Series	Very high — up to 500	Up to 400	Widely variable, high at no-load	By series rheostat	For drives requiring very high starting torque and where adjustable—varying speed is satisfactory. This motor is sometimes called the <i>traction motor</i> . Loads must be positively connected, not belted. For hoists, cranes, bridges, car dumpers. To prevent over-speed, lightest load should not be much less than 15 to 20% of full-load torque.

TABLE 50-4. CHARACTERISTICS AND APPLICATIONS OF POLYPHASE 60-CYCLE A-C MOTORS

Type Classification	Hp Range	Starting Torque (%) <sup>*</sup>	Pull-Out Torque (%) <sup>*</sup>	Starting Current (%) <sup>*</sup>	Slip (%)	Power Factor (%)	Efficiency (%)	Typical Applications
General-purpose, normal torque and starting current NEMA Class A	0.5 to 200	Poles — Torque 2 — 150 4 — 150 6 — 135 8 — 125 10 — 120 12 — 115 14 — 110 16 — 105	Up to 250 but not less than 200	500-1000	Low, 3-5	High, 87-89	High, 87-89	Constant-speed loads where excessive starting torque is not needed and where high starting current is tolerated. Fans, blowers, centrifugal pumps, most machine tools, woodworking tools, line shafting. Lowest in cost. May require reduced voltage starter. Not to be subjected to sustained overloads, because of heating. Has high pull-out torque.
General-purpose, normal torque low starting current, NEMA Class B	0.5 to 200	Same as above or larger.	About the same as Class A but may be less	About 500-550, less than average of Class A	3-5	A little lower than Class A	87-89	Same as Class A — advance over Class A is lower starting current, but power factor slightly less.
High torque, low starting current, NEMA Class C	1 to 200	200 to 250	Usually a little less than Class A but not less than 200	About same as Class B	3-7	Less than Class A	82-84	Constant-speed loads requiring fairly high starting torque and lower starting current. Conveyors, compressors, crushers, agitators, reciprocating pumps. Maximum torque at standstill.



TABLE 50-4 (Continued)

High torque, medium and high slip, NEMA Class D	0.5 to 150	Medium slip 350 high slip 250-315	Usually same as standstill torque	Medium slip 400-800, high slip 300-500	Medium 7-11, high 12-16	Low	Low	Medium slip: Highest starting torque of all squirrel-cage motors. Used for high-inertia loads such as shears, punch presses, die stamping, bulldozers, boilers. Has very high average accelerating torque. High slip used for elevators, hoists, etc., on intermittent loads.
Low starting torque, either normal starting current, NEMA Class E, or low starting current, NEMA Class F	40 to 200	Low, not less than 50	Low but not less than 135	Normal 500-1000, low 270-500	1 to 3½	About same as Class A or Class B	About same as Class A or Class B	Direct-connected loads of low inertia requiring low starting torque, such as fans and centrifugal pumps. Has high efficiency and low slip.
Wound-rotor	0.5 to 5000	Up to 300	200-250	Depends upon external rotor resistance but may be as low as 150	3-50	High, with rotor shorted same as Class A	High, with rotor shorted same as Class A, but low when used with rotor resistor for speed control	For high-starting-torque loads where very low starting current is required or where torque must be applied very gradually and where some speed control (50%) is needed. Fans, pumps, conveyors, hoists, cranes, compressors. Motor with speed control more expensive and may require more maintenance.

\* Figures are given in per cent of rated full-load values.

TABLE 50-4 (Continued)

Type Classification	Hp Range	Starting Torque (%) <sup>*</sup>	Pull-out Torque (%) <sup>*</sup>	Starting Current (%) <sup>*</sup>	Slip (%)	Power Factor (%)	Efficiency (%)	Typical Applications
Synchronous, high speed, above 500 rpm	25 to several thousand	Up to 120	Up to 200	500-700	Zero	High, but varies with load and with excitation	Highest of all motors, 92-96	Fans, blowers, d-c generators, line shafts, centrifugal pumps and compressors, reciprocating pumps and compressors. Useful for power-factor correction. Constant speed. Frequency changers.
Synchronous, low speed, below 500 rpm	Usually above 25 to several thousand	Low 40	Up to 180	200-350	Zero	High, but varies with excitation	Highest of all motors, 92-96	Lower-speed direct-connected loads such as reciprocating compressors when started unloaded, d-c generators, rolling mills, band mills, ball mills, pumps. Useful for power-factor control. Constant speed. Flywheel used for pulsating loads.

\* Figures are given in per cent of rated full-load values.

TABLE 50-5a. CHARACTERISTICS OF FRACTIONAL-HORSEPOWER MOTORS

Type Designation	Starting Torque (% of Normal)	Pull-Up Torque (% of Normal)	Pull-Out Torque (% of Normal)	Starting Current at 115 V	Power Factor	Efficiency (%)	HP Range	Application and General Remarks
General-purpose split-phase motor	90-200 Medium normal	200-250	185-250 Medium	23 amp $\frac{1}{4}$ hp	56-65	62-67	$\frac{1}{20}$ to $\frac{1}{2}$	Fans, blowers, office appliances, food-preparation machines. Low- or medium-starting-torque, low-inertia loads. Continuous operation loads. May be reversed.
High-torque split-phase motor	200-275 High	160-350 High	Up to 350	32 amp High $\frac{1}{4}$ hp	50-62	46-61	$\frac{1}{2}$ to $\frac{1}{2}$	Washing machines, sump pumps, home workshops, oil burners. Medium- to high-starting-torque loads. May be reversed.
Permanent-split-capacitor motor	60-75 Low	60-75 Low	Up to 225	Medium	80-95	55-65	$\frac{1}{20}$ to $\frac{1}{2}$	Direct-connected fans, blowers, centrifugal pumps. Low-starting-torque loads. Not for belt drives. May be reversed.
Permanent-split-capacitor motor	Up to 200 Normal	200	260		80-95	55-65	$\frac{1}{2}$ to $\frac{1}{2}$	Belt-driven or direct-drive fans, blowers, centrifugal pumps, oil burners. Moderate-starting-torque loads. May be reversed.
Capacitor-start general-purpose motor	Up to 435 Very high	265 High	Up to 400		80-95	55-65	$\frac{1}{2}$ to $\frac{1}{2}$	Dual voltage. Compressors, stokers, conveyors, pumps. Belt-driven loads with high static friction. May be reversed.


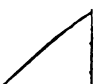








TABLE 50-5a (Continued)

Type Designation	Starting Torque (% of Normal)	Pull-Up Torque (% of Normal)	Pull-Out Torque (% of Normal)	Starting Current at 115 V	Power Factor	Efficiency (%)	HP Range	Application and General Remarks
Capacitor-start capacitor-run motor	380 High	260	Up to 260		80-95	55-65	$\frac{1}{2}$ to $\frac{3}{4}$	Compressors, stokers, conveyors, pumps. High-torque loads. High power factor. Speed may be regulated.
Repulsion-start induction-run motor	350-500 Very high	225	Up to 275	350%	70-80	55-65	Up to 10	Very-high-starting-torque loads. Pumps, compressors, conveyors, machine tools. Reversed by shifting brushes.
Shaded-pole motor	50	50	150			30-40	$\frac{1}{30}$ to $\frac{1}{15}$	Fans, toys, hair dryers, unit heaters. Low-starting-torque loads.
Series motor	400-500 Very high	High	400-500	Medium	85-95	40-60	$\frac{1}{15}$ to 1	Usually high speed, 3000 to 11,000. Hand tools, vacuum cleaners. Speed control possible with resistor or reactor. Larger sizes require compensating winding. Used on either alternating current or direct current — called "Universal" motor.
Shunt or compound d-c motor	400 Very high	400	400	Medium			$\frac{1}{20}$ to $\frac{3}{4}$	Same application as high-torque split-phase, or capacitor-start or repulsion-start motor. Speed control. May be reversed. More expensive than corresponding a-c motor.

TABLE 50-5b. CHARACTERISTICS OF FRACTIONAL-HORSEPOWER MOTORS  
(Reprinted from *Westinghouse Engineer*, March 1949, "Application of Small Motors," by T. E. M. Carville.)

Type of Motor	Wiring Diagram	Speed-Torque Characteristics	HP Range	Speed Data		Approx. Locked-Rotor Torque	Built-in Starting Mechanism	Rotor Construction	Reversibility		Radio Interference	Remarks on Applications
				Rated Speeds	Characteristics	Control			At Rest	In Motion		
Single-Phase Alternating Current	Split-Phase		$\frac{1}{8}$ to $\frac{1}{4}$	3450 1725 1140 860	Constant	None	Medium to low	Squirrel cage	Yes—change connections	No—except with special design and relay	No	For applications up to $\frac{1}{4}$ hp where low locked-rotor torque for higher ratings and medium locked-rotor torque for lower ratings is sufficient. Low locked-rotor torque minimizes light flicker making motor suitable for frequent starting, as on oil burners, office appliances, fans, and blowers.
				1725	Constant	None	Medium	Squirrel cage	Yes—change connections	No—except with special design and relay	No	For continuous and intermittent-duty applications where starting is infrequent and locked-rotor current in excess of NEMA values is not objectionable. Used for washing machines, ironers, sump pumps, and home workshop tools. Has a tendency to cause light flicker on underwired or overloaded lighting circuits.
				3450 1725 1140 860	Constant	None	High	Squirrel cage	Yes—change connections	No—except with special design and relay	No	All-purpose motor for high locked-rotor torque, low locked-rotor current, quietness, and economy. Efficiency and power factor high. Ideal for all heavy-duty drives, such as compressors, pumps, stockers, refrigerators, and air conditioners. Single voltage in lower ratings, dual voltage in higher ratings.
Single-Phase Capacitor	Permanent-Split (Single value 3-speed)		$\frac{1}{8}$ to $\frac{1}{4}$	1620 1080 820	Constant or adjustable—varying	2-speed switch or auto-transformer	Very low	Squirrel cage	Yes—change connections	No	No	For direct-connected fan drives—particularly unit heaters. Not suitable for belt drives. Same motor adaptable for 115 or 230 volts and for one-, two-, or multi-speed service by using switch or auto-transformer-type controller. Fan load must be accurately matched to motor output for proper control.
				1500 1000	Constant or adjustable—varying	Series choke or resistance	Very low	Squirrel cage	No	No	No	Constant-speed switchless motor for low-power applications. Has low locked-rotor and running torques. Used for fans, small blowers, unit heaters, hair driers, etc. With fan load accurately matched to motor output, proper speed control can be obtained by means of a series choke or resistance.
				3450 1725 1140 860	Constant	None	Medium to high	Squirrel cage	Yes—change connections	Yes—change connections	No	For all applications where polyphase circuits are available. Special designs with extra-high locked-rotor torque for such applications as hoists, motor operators, and tool traverse and clamp devices. High-frequency motors are used for high-speed applications, such as rayon spinning machines and portable tools.
Polyphase	Squirrel-cage Induction		$\frac{1}{4}$ to $\frac{1}{2}$	3450 1725 1140 860	Constant	None	Medium to high	Squirrel cage	Yes—change connections	Yes—change connections	No	

TABLE 50-5h (Continued)

Direct-Current	Shunt and Compound			$\frac{1}{16}$ to $\frac{1}{8}$ %	3450 1725 1140 860	Constant or adjustable varying	Armature resistance	Extra high	None	Drum-wound; commutator	Yes—change connections	No—except with special design	Yes	Companion d-c motor to single-phase and polyphase motors for locations where only direct current is available. Speed control of unit heaters is obtained by resistance in series with the armature. Smaller ratings are shunt wound. Starting rheostats are recommended for ratings $\frac{1}{8}$ hp and up.
	Series			$\frac{1}{16}$ to $\frac{1}{8}$ %	900 to 2000	Varying or adjustable varying	Armature resistance	Extra high	None	Drum-wound; commutator	Yes—change connections	No—except with special design	Yes	Companion d-c motor to shaded-pole motor for fan applications. Used instead of shunt motors in smaller ratings to avoid having very fine wire in the windings.
	Non-Compensated (Salient-pole winding)			$\frac{1}{16}$ to $\frac{1}{8}$ %	1500 to 15 000	Varying	Voltage control, resistance or transformer	Extra high	None	Drum-wound; commutator	No—except with special design	No—except with special design	Yes	Operates on either alternating or direct current. Inherent characteristics of the motor are high-locked-rotor torque, high speed, varying-speed regulation, and small size and light weight per horsepower, which make it particularly suitable for such applications as sewing machines, portable tools, vacuum cleaners, and motion-picture projectors. Available as parts and as complete motors. Compensated motors are recommended when higher power at lower speeds is required, as for large commercial vacuum cleaners and large portable tools.
	Compensated (Distributed winding)			$\frac{1}{16}$ to $2\frac{1}{2}$ %	2500 to 15 000	Varying	Voltage control, resistance or transformer	Extra high	None	Drum-wound; commutator	No—except with special design	No—except with special design	Yes	Governor permits utilizing the light-weight high-speed universal motor for constant-speed applications. One type of governor permits adjustment while running; it is used for typewriters, motion-picture projectors, and cameras. Another type, adjustable at standstill only, is used for constant-speed office machines.
	Governor Controlled			$\frac{1}{16}$ to $\frac{1}{8}$ %	2000 to 7500	Constant or adjustable	Adjustable governor	Extra high	None	Drum-wound; commutator	No—except with special design	No—except with special design	Yes	
A-C or D-C (Universal)														

\*Three-phase type shown; available also in two-phase type.

\*Compound winding shown.

\*Single-field type shown.

\*Each ordinate division is 100-percent of full-load torque. Each ordinate division is 20 percent of synchronous speed for a-c motors and 20 percent of full-load speed for d-c and universal motors.

# Chapter 51

## DISTRIBUTION OF POWER

Power stations usually generate power on a large scale as alternating voltage and current and also transmit this power as alternating voltage and current. The reasons for this are that a-c generators can be built for high voltages (up to 20,000 volts), that transformers are available for a further increase of the generator voltages, and that high-voltage power transmission is more economical than low-voltage power transmission. Contrary to a-c generators, large-capacity d-c generators are not practical for voltages much higher than 800 volts, and no apparatus is presently available to increase this generator-voltage considerably.

Since electric power is generated and transmitted as a-c power, it is utilized as such wherever possible. However, there are instances in which d-c power must be used and also instances in which the use of direct current offers advantages in comparison with alternating current. An example of the former instance is found in electrochemical plants; examples of the latter instance are applications in which speed control over a wide range is necessary: no motor offers better speed control than the d-c motor designed with field control. D-c also offers advantages in the congested districts of large cities, since it can be used in connection with a storage battery reserve which is an important consideration.

**51-1. Systems of d-c distribution.** D-c power is generated by d-c generators, by motor-generator sets, or by mercury-arc rectifiers. In the last two cases, a-c power is converted or rectified into d-c power.

There are two fundamental systems of distributing d-c power: the *series system* and the *multiple system*.

The series system, also called constant-current system, is used mainly for street-lighting circuits in this country. All lamps are connected in series, and a regulator is used to maintain constant current; the current required is usually less than 10 amp. The total voltage increases as the

load is increased by the addition of lamps; it lies between 2000 and 4000 volts and the line must, therefore, be carefully insulated. The advantage of the series system for street lighting is that a single wire can be run through each street (Fig. 51-1).

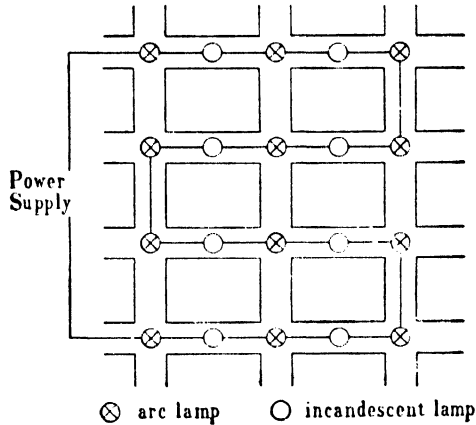


FIG. 51-1. Series system of distribution applied to street lighting.

The multiple system, also called constant voltage system, operates at approximately constant voltage while the current changes with the load demands. The various lamps and motors are all connected in parallel, and disconnecting a part of the load has no effect upon the operation of the remaining part of the load.

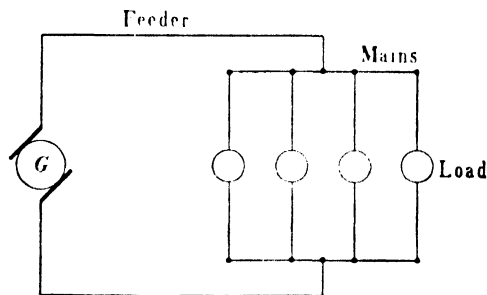


FIG. 51-2. Two-wire system of distribution. Feeders and mains.

The multiple system can be 2-wire or 3-wire. In the former case a single value of voltage is available; in the latter case two different voltages can be used.

Some arrangements of a 2-wire system are shown in Figs. 51-2, 51-3, and 51-4. Fig. 51-2 shows a common arrangement in which the voltage



is held constant at the distribution center. The voltage at the terminals of the loads changes somewhat with changing load. Fig. 51-3 shows an arrangement in which the load is sectionalized. This not only has the advantage that the voltage drop is reduced, but also an advantage in that troubles may be confined to the section in which they occur. Fig. 51-4

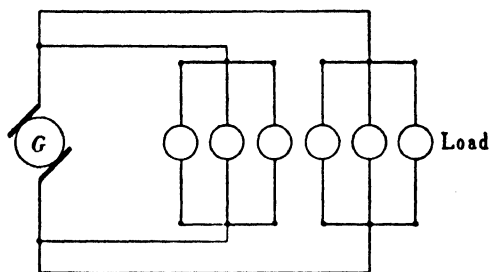


FIG. 51-3. Two-wire system of distribution with sectionalized load circuits and mains.

shows the loop connection. Here the currents flow in the same direction in the two mains, reducing the voltage drop and thus sustaining the voltage.

It follows from Figs. 51-2 and 51-3 that the voltage drop can be reduced in an overloaded system by sectionalizing the load and providing additional feeders. For the same purpose a voltage *booster* also can be used. This is a small motor-driven generator of series, shunt, or compound

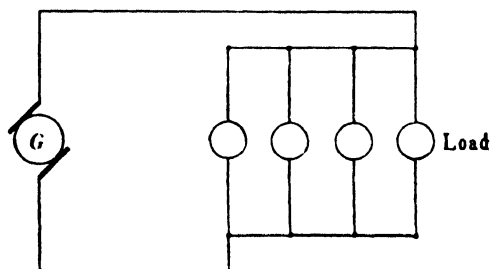


FIG. 51-4. Two-wire system of distribution with loop connection.

type, the armature of which is in series with the feeder. Such a booster is often used in connection with storage batteries for increasing the voltage during the charging period and decreasing the voltage (by reversing the polarity of the booster) during the discharge period.

The *3-wire* or *Edison system* offers the advantage of a low voltage (110 to 120 volts) for lighting, and a higher voltage (220 to 240 volts) for motor application. Fig. 51-5 shows a 3-wire system using two separate

generators which are connected in series. A middle or *neutral wire* is connected to the junction of the two generators. If the load is the same on both sides of the system, i.e., if the load is balanced, no current flows through the neutral wire. If the load is not the same on both sides, the excess current caused by the unbalance of loads flows through the neutral wire (see Fig. 51-5).

Doubling the voltage by using the 3-wire system reduces considerably the amount of copper necessary for the feeders. Assuming the same *percentage voltage drop*, for example 5% at 110 and 220 volts, the voltage drop is 5.5 volts at 110 volts and 11 volts at 220 volts. Since, for the same transmitted power, the current at 220 volts is half of that at 110 volts, the resistance of the feeders at 220 volts may be four times the resistance at 110 volts, i.e., the amount of copper necessary at 220 volts is only 25% of the amount necessary at 110 volts. This does not take into account

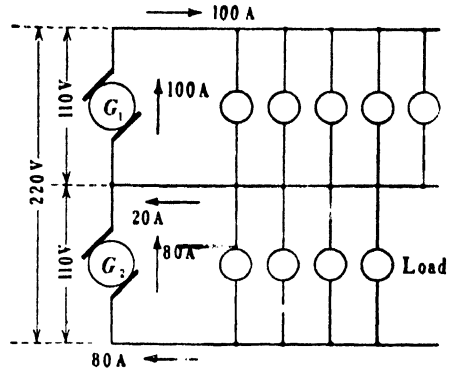


FIG. 51-5. Three-wire system of distribution with two separate generators.

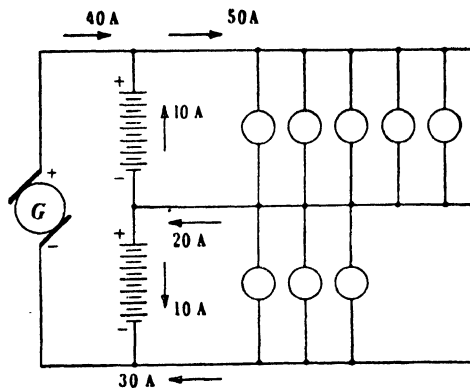


FIG. 51-6. Three-wire system of distribution with a single generator and a storage battery.

the neutral wire. If it is assumed that the neutral wire has the same cross-section as the outer wires, the 3-wire system needs  $\frac{3}{8}$  of the copper necessary for the 110-volt system for the same transmitted power.

Fig. 51-6 shows a 3-wire system consisting of a single generator and a storage battery. The neutral wire is connected to the mid-point of the battery. When the load on both sides is unbalanced, the half of the battery

on the heavier loaded side will be discharged, while the other half of the battery will be charged. The currents shown in Fig. 51-6 indicate that half of the current flowing through the neutral wire ( $= 10$  amp) returns to the positive side through the upper half of the battery discharging it to supply 10A to the load, and the other half of the current flowing through the neutral wire goes to the negative side through the lower half

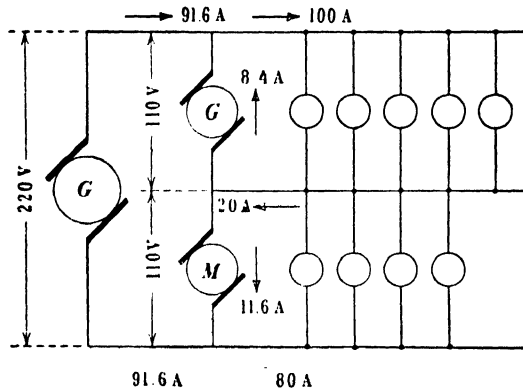


Fig. 51-7. Three-wire system of distribution with a single generator and a balancer set.

of the battery thus charging it. Since discharge is connected with a voltage drop and charge with a voltage rise, the system *voltages* must become unbalanced.

The 3-wire system, Fig. 51-5, with two separate generators is expensive; the 3-wire system, Fig. 51-6, with a single generator and a storage battery is expensive and requires a high maintenance cost for the storage battery. Furthermore, it is difficult to maintain both halves of the battery at the same condition of charge.

In Art. 9-1 a 3-wire generator (devised by Dolivo-Dobrowolsky) was described which, in connection with a coil wound on iron, yields an efficient 3-wire system (see Fig. 9-1).

Another 3-wire system employing a single generator and two small machines (a *balancer set*) is shown in Fig. 51-7. The two machines of the balancer set are mechanically coupled together and are electrically connected in series across the outer wires; the neutral wire is connected to the junction of both machines. When the load is the same on both sides, the two machines of the balancer set both operate as motors, taking enough power from the system to supply their no-load losses; the neutral wire does not carry current in this case. When the load is not the same on both sides, the unbalanced current flowing through the neutral divides between the two machines of the balancer set making one machine

operate as a motor to drive the other machine as a generator. The latter then supplies a part of the unbalanced current.

The figures shown in Fig. 51-7 are obtained under the assumption that the voltages of both sides are equal ( $= 110$  volts) and that the efficiencies of motor and generator of the balancer set are both equal to 0.85. If  $I_G$  denotes the generator current and  $I_M$  the motor current, then

$$\text{power output of the generator} = 110 \times I_G$$

$$\text{power input of the generator} = \frac{110 \times I_G}{0.85}$$

$$\text{power input of the motor} = 110 \times I_M$$

$$\text{power output of the motor} = 110 \times I_M \times 0.85$$

Since the power input of the generator equals the power output of the motor,

$$\frac{110 \times I_G}{0.85} = 110 \times I_M \times 0.85$$

Also,

$$I_G + I_M = 20$$

The two equations above yield

$$I_M = 11.6 \text{ amp} \qquad I_G = 8.4 \text{ amp}$$

The current of the main generator is

$$I = 100 - 8.4 = 80 + 11.6 = 91.6 \text{ amp}$$

**51-2. Systems of a-c distribution.** As has been mentioned, a-c power is transmitted at high voltage and mainly by the 3-phase system. The single-phase system is used to a limited extent in connection with single-phase electric railways, and the transmission of power by single-phase circuits is limited to short distances and relatively low voltage. Three-phase power transmission requires less copper than either single-phase or 2-phase power transmission.

The distribution system begins either at the substation where the power is delivered by a transmission line and stepped down by transformers or, in many cases, at the generating station. Where a large area is involved, a primary and secondary distribution system may be applied. The primary distribution system delivers power at voltages up to 15,000 to load centers where it is stepped down to 4000 or 2300 volts. Large motors are economical at 2300 to 6600 volts; small motors are designed for 440, 220, and 110 volts; incandescent lamps are most effective at

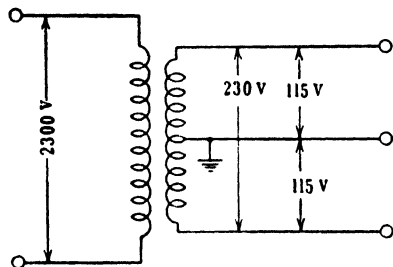


FIG. 51-8. Single-phase, 2-wire system.

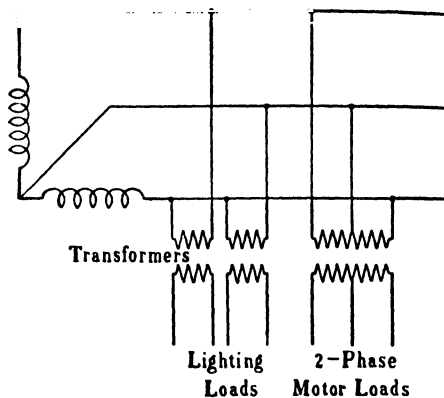


FIG. 51-9. Two-phase, 3-wire system.

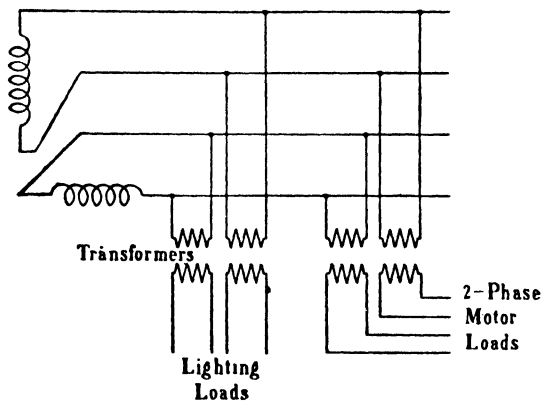


FIG. 51-10. Two-phase, 4-wire system.

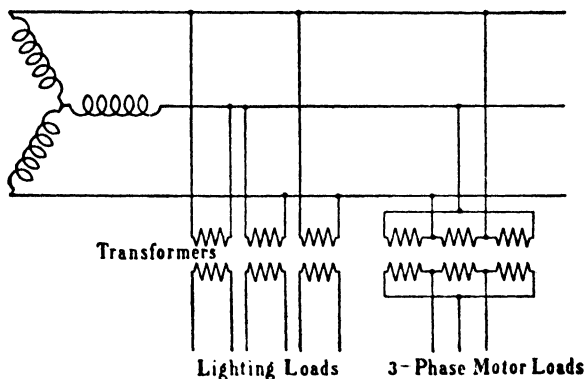


FIG. 51-11. Three-phase, 3-wire system.

110 volts. Therefore, the voltages 4000 and 2300 must be further reduced by step-down transformers for the various applications noted.

With respect to the number of phases, the following distribution systems are available for a-c power:

- (a) Single-phase, 2-wire or 3-wire (Fig. 51-8).
- (b) Two-phase, 3-wire (Fig. 51-9) or 4-wire (Fig. 51-10).
- (c) Three-phase, 3-wire (Fig. 51-11) or 4-wire (Fig. 51-12).

The single-phase 3-wire system sometimes used is identical in principle with the 3-wire d-c system. The neutral wire is connected to the center

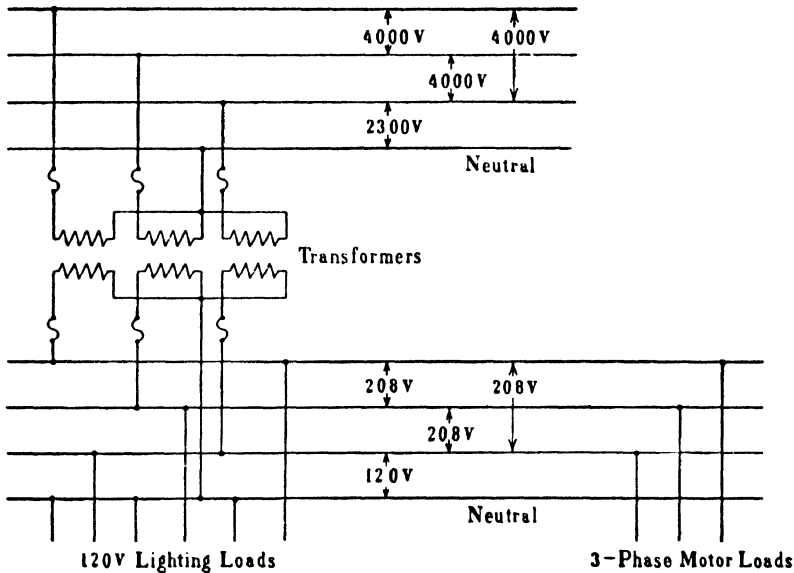


FIG. 51-12. Three-phase, 4-wire system.

of the transformer secondary. The neutral is grounded in order to protect personnel from electric shock should the transformer insulation break down, or the secondary main contact high-voltage wires.

The 2-phase system is still used in some localities. When used, the 4-wire system is preferable since the 3-wire system produces voltage unbalance because of the unsymmetrical voltage drop in the neutral wire.

The 3-phase, 3-wire and the 3-phase, 4-wire systems are both used extensively. The 3-phase, 4-wire system, Fig. 51-12, shows 4000-2300 volt distribution and 208-120 volt distribution. The higher voltage can be a primary distribution and also a secondary distribution voltage in a large area which is further stepped down to 208-120 volts.

As in the case of d-c distribution, the *series* or *multiple* method of

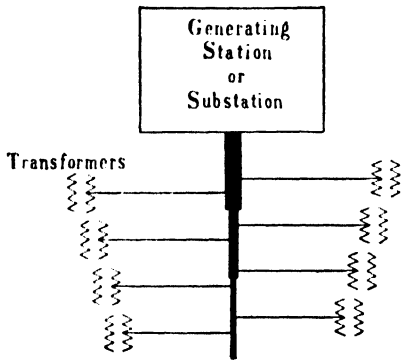


FIG. 51-13. Radial distribution. Tree system.

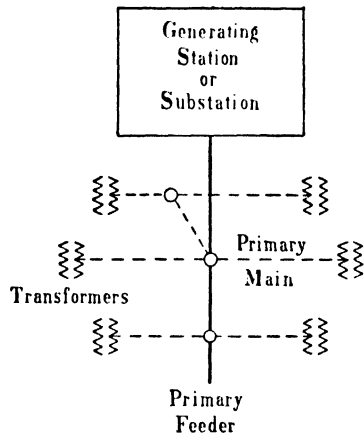


FIG. 51-14. Radial distribution with feeder and mains.

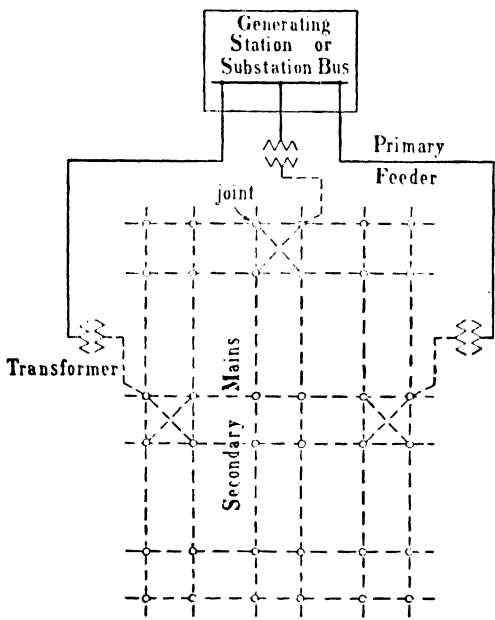


FIG. 51-15. Network distribution.

connection can be applied. In the first case special transformers for constant current are used (Fig. 20-5). The different arrangements of feeders and transformers which are used in multiple systems, in order to keep the voltage of the distribution system constant, are briefly described here. Fig. 51-13 shows a *radial distribution* of the *tree-system* type. Here a number of independent feeders branch out radially from a common

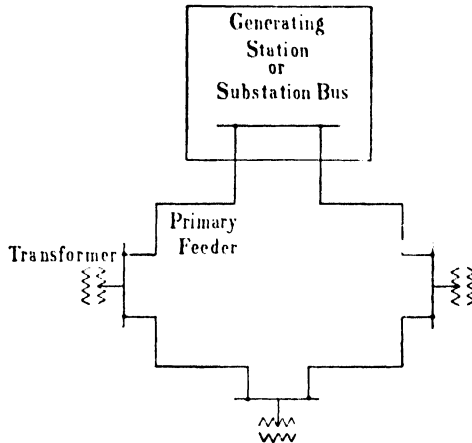


FIG. 51-16. Loop distribution.

source of supply (a substation, or a generating station), and the distribution transformers are connected to taps along the length of the feeders.

Where the tree system cannot maintain the required voltage, a *radial distribution with feeder and mains* is used (Fig. 51-14). In this case the feeder is run to a point near the load center of a district and mains connect the feeder with the transformers.

In districts with high load densities the *network distribution* system is employed (Fig. 51-15). In this case a secondary main grid is fed through distribution transformers by multiple feeders. Network distribution permits the feeding of current into a load from several directions. *Vertical* network distribution is used in tall buildings.

*Loop distribution* (Fig. 51-16) is used for supplying bulk loads. In this case the feeder normally extends from the substation or generating station to a group of customers connected in series and goes back either to the same station or to an adjacent station.

## PROBLEMS

1. A d-c load of 300 amp at 230 volts is transmitted from 250 volt bus-bars over a 500-ft copper feeder. Determine the resistance and cross-sectional area of the feeder and the feeder power loss. What is the efficiency of transmission?



2. If the load in Problem 1 was a 115-volt load, how much power could be received for the same transmission efficiency? What voltage would be necessary at the bus-bars?

3. A 75-HP d-c motor operating at an efficiency of 88% and a terminal voltage of 225 volts receives power from station bus-bars by means of two 3,000,000 circular mil feeders, each 1000 ft long. Determine the power received, bus-bar voltage, feeder power loss, transmission efficiency, and weight of the feeder.

4. A 125-volt, d-c bus-bar feeds a 20-HP motor through a switchboard with the motor 500 ft from the switchboard. If the motor terminal voltage is to be 115 volts when operating at full-load and an efficiency of 86%, determine the cross-sectional area and weight of the feeders in circular mils and pounds respectively.

5. If the motor of Problem 4 was a 230-volt, 10-HP motor of the same efficiency, and the percentage voltage drop between motor and switchboard remained unchanged, determine the cross-sectional area and weight of the feeders.

6. Determine the cross-section and weight of copper feeders necessary to transmit 100 kw of power to a 230-volt load center, if the bus-bars are 1200 ft from the load and the bus-bar voltage is 245 volts.

7. A 2400-ft street is illuminated with 16 200-watt lamps, placed 150 ft apart. The lamps are connected in multiple; assume lamp current is automatically controlled at 1.50 amp per lamp. If the line is fed from a 115-volt generator at one end, determine the voltage at each lamp. Use a No. 3 wire having a resistance of 0.196 ohm per 1000 ft for the line.

8. Repeat Problem 7 assuming the 125-volt generator to be centrally located and feeding the street lights at a junction point midway between the 8th and 9th lamps. The feeder from generator to junction is 75 ft long and consists of two No. 2 wires having a resistance of 0.156 ohm per 1000 ft.

9. A 120-240-volt, d-c, 3-wire generator supplies loads A and B over three wires each having a resistance of 0.08 ohm. Assuming the generator voltages to be 120-240 volts, determine the load voltages when load A is 25 amp and load B 25 amp.

10. Repeat Problem 9 when load A is 50 amp and load B 70 amp.

11. Repeat Problem 9 when load A is 30 amp and load B is 80 amp.

12. Determine the voltage across loads A and B in Problem 9 if the neutral wire is opened.

13. Determine the voltage across loads A and B in Problem 11 if the neutral wire is opened.

14. Load A is 1.5 kw d-c at 120 volts. Load B is 3 kw d-c at 120 volts. Load C is a 10-HP, shunt-wound d-c motor operating at full-load at 240 volts and at an efficiency of 85%. The three loads are supplied from a 3-wire system over feeders 100 ft long. The outer wires are No. 1, having an area of 83,700 circular mils, and the neutral wire No. 6, having a cross-section of 26,300 circular mils. Determine the line currents and efficiency of transmission. What are the voltages at the head end of the feeders?

15. A 115-230-volt, 3-wire a-c system supplies two loads. Load A is 115 volts, 15 kw at 0.90 p.f. lagging and load B is 115 volts, 10 kw at unity p.f. Determine the currents in the three wires.

16. Repeat Problem 15 if load A is 115 volts, 15 kw at 0.90 p.f. lagging and load B is 115 volts, 10 kw at 0.80 p.f. lagging.

17. If the loads in Problem 15 are supplied from a center-tapped transformer secondary over three wires each having a resistance of 0.08 ohm, determine the voltages at the transformer from line to ground (neutral grounded). Determine the efficiency of transmission.

18. If the loads in Problem 16 are supplied from a center-tapped transformer secondary over three wires each having a resistance of 0.08 ohm determine the voltages at the transformer from line to ground (neutral grounded). Determine the efficiency of transmission.

19. A 115-230-volt, 3-wire a-c system supplies the following: load A is 115 volts and consists of a 1.5-kw lamp load in parallel with a 3-HP single-phase motor operating at full-load, 76% efficiency and 78% power factor; load B is a 3-kw 115-volt lamp load. Determine the line currents.

20. Repeat Problem 19 if load B is a 115-volt, 2.5-kw load at 0.80 p.f. lagging.

21. A 50-HP, 440-volt, 60-cycle, 3-phase, 4-pole induction motor has a full-load efficiency of 91% and a power factor of 90%. Neglecting the reactance drops in the supply lines, determine the cross-section of the copper conductors necessary if the power bus is 100 ft from the motor and the voltage drop is not to exceed 5%. Assume 440 volts at the motor.

22. Repeat Problem 21 for a 200-HP, 440-volt, 4-pole motor having a full-load efficiency of 92% and a power factor of 89%.

23. Repeat Problem 21 for a 1000-HP, 2300-volt, 4-pole motor having a full-load efficiency of 94% and a power factor of 91%.

24. A 120/208-volt, 3-phase, 4-wire line supplies three lamp loads and a 50-HP, 3-phase, 208-volt, 60-cycle induction motor. The lamp loads are 120 volts and 10 kw, 15 kw, and 20 kw respectively. The motor is operating at full-load, 91% efficiency and 90% power factor. Determine the line currents, neutral current, and the size of feeders necessary.

25. A 3-wire, 120-volt, 2-phase system supplies two single-phase unity power factor loads. Load A is 5 kw and load B is 3.5 kw. Determine the current in the neutral (grounded) wire.

26. Repeat Problem 25 if load A is 5 kw at 0.85 p.f. lagging and load B is 3.5 kw at unity p.f.

27. Repeat Problem 25 if load A is 5 kw at 0.85 p.f. lagging and load B is 7.5 kw at 0.90 p.f. lagging.

## APPENDIX 1

(To Art. 12-2)

---

---

**Derivation of Eq. 12-6 from Ampère's Law.** The magnitude of the main flux  $\Phi$  can be determined by applying the circuital law of the magnetic field (Ampère's law) to the core structure (Fig. 12-1). Neglecting the air gap and assuming the length of the magnetic path around the center lines of the core to be  $l$ , this law yields for the amplitude of  $H$

$$Hl = N_1\sqrt{2} I_\phi \quad (\text{A1-1})$$

and, according to Eq. 1-24, for the amplitude of  $B$

$$B = \frac{0.4\pi\mu}{l} N_1\sqrt{2} I_\phi \quad (\text{A1-2})$$

Therefore (see Eqs. 1-25 to 1-27)

$$\Phi = \frac{0.4\pi}{R_m} N_1\sqrt{2} I_\phi \quad (\text{A1-3})$$

The flux interlinkage with the primary winding is

$$N_1\Phi = \frac{0.4\pi}{R_m} N_1^2\sqrt{2} I_\phi \quad (\text{A1-4})$$

On the other hand, from Eqs. 1-13 and 1-26,

$$L_m = \frac{N_1\Phi}{\sqrt{2} I_\phi} = \frac{N_1 \times 0.4\pi N_1\sqrt{2} I_\phi}{\sqrt{2} I_\phi R_m} = 0.4\pi \frac{N_1^2}{R_m} \quad (\text{A1-5})$$

Comparing Eqs. A-4 with A-5

$$N_1\Phi = L_m\sqrt{2} I_\phi \quad (\text{A1-6})$$

which is identical with Eq. 12-6.

## APPENDIX 2

(To Art. 26-2)

**Derivation of the Torque of the Polyphase Induction Motor on the Basis of Biot-Savart's Law.** Consider Fig. A2-1 which represents an elementary 2-pole machine. The flux is assumed sinusoidally distributed. Each rotor phase has a single slot per pole in which  $n_{c2}$  conductors are located, i.e., each rotor phase consists of a single coil with  $n_{c2}$  turns. The emf's induced in the coil sides are proportional to the values of  $B$  which they momentarily cut (Eq. 1-2a); hence the ordinates of the  $B$ -curve over the coil sides represent, to another scale, the emf's of the coil sides. It will be assumed that the rotor runs close to its synchronous speed, as is the case at rated load. Then the rotor current is almost in phase with the induced emf ( $r_2'/s$  large in comparison with  $x_2'$ , Eq. 25-3) and the ordinates of the  $B$ -curve over the individual coil sides also represent the currents flowing in the conductors. The currents of the three phases are shown in Fig. A2-1. For the instant chosen, the conductors of phase III lie under maximum flux density ( $B_m$ ), while for the conductors of phases I and II the flux density is half of the maximum. Therefore the current in phase III will be a maximum and the currents in phases I and II half of the maximum value. Corresponding to Biot-Savart's law (Eq. 1-28b), the tangential force per pole is

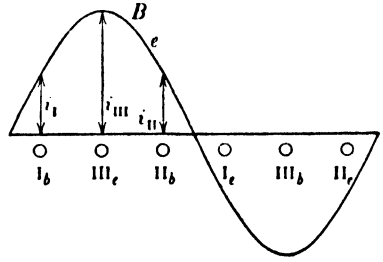


FIG. A2-1.

$$F = 8.85 \times 10^{-8} n_{c2} l_e \left[ \frac{B_m}{2} \frac{I_{2m}}{2} + B_m I_{2m} + \frac{B_m}{2} \frac{I_{2m}}{2} \right]$$

$$F = 18.75 \times 10^{-8} n_{c2} l_e B_m I_2 \text{ lb} \quad (\text{A2-1})$$

$l_e$  is the effective core length (see Art. 3-7).

If each phase of the rotor has  $q_2$  slots per pole and the coils are chorded (fractional-pitch winding), the value of  $F$  must be multiplied by  $q_2$  and by the winding factor  $k_{a2} \times k_{p2}$  of the rotor (see Eq. 22-8). Further,  $F$  must be multiplied by the number of poles  $p$ . This yields for the total tangential force around the armature

$$F = 6.25 \times 10^{-8} \times l_e Z_2 k_{a2} k_{p2} B_m I_2 \text{ lb} \quad (\text{A2-2})$$

where  $Z_2 = 3n_{c2}q_2p$  is the total number of conductors of the rotor.

The developed torque (in lb-ft) is obtained by multiplying  $F$  by the radius  $R = \frac{D}{2} \times \frac{1}{12} = \frac{p\tau}{\pi \times 2} \times \frac{1}{12}$  ft. Introducing

$$Z_2 = N_2 \times 2m_2$$

where  $N_2$  is the number of turns per rotor phase and  $m_2$  the number of rotor phases, and also Eqs. 24-5, 24-4, and 1-32

$$E_2 = 4.44f_1N_2k_{d2}k_{p2}\Phi 10^{-8}$$

$$f_1 = \frac{pn_s}{120} \quad \Phi = \frac{2}{\pi} \tau l_s B_m$$

the torque becomes

$$T = \frac{7.04}{n_s} m_2 E_2 I_2 \text{ lb-ft} \quad (\text{A2-3})$$

This equation has been derived under the assumption that the rotor current is in phase with its emf. If this is not the case, as for example at starting, the cosine of the angle between  $E_2$  and  $I_2$  ( $\cos \psi_{2s}$ , Eq. 25-1) has to be introduced into Eq. A2-3. The considerations are the same as for the determination of the power of a circuit with voltage and current in phase or out of phase. Thus, in general,

$$T = \frac{7.04}{n_s} m_2 E_2 I_2 \cos \psi_{2s} = \frac{7.04}{n_s} m_1 E_2' I_2' \cos \psi_{2s} \quad (\text{A2-4})$$

Observing that  $E_2' \cos \psi_{2s} = I_2' \times \frac{r_2'}{s}$  (see Fig. 25-1 or Eq. 25-3),

$$T = \frac{7.04}{n_s} m_1 I_2'^2 \frac{r_2'}{s} \quad (\text{A2-5})$$

## APPENDIX 3

(To Art. 26-3)

**Derivation of the Currents of the Polyphase Induction Motor from the Equations for the Electric Circuits and Magnetic Circuit.** Eqs. 25-2 to 25-5 with the abbreviations

$$\mathbf{Z}_1 = r_1 + jx_1 \quad \mathbf{Z}_2' = \frac{r_2'}{s} + jx_2' \quad (\text{A3-1})$$

yield the following equations for the primary and secondary currents

$$\mathbf{I}_1 = \mathbf{V}_1 \frac{1 + \mathbf{Y}_m \mathbf{Z}_2'}{\mathbf{Z}_1 + \mathbf{Z}_2' + \mathbf{Z}_1 \mathbf{Z}_2' \mathbf{Y}_m} \quad (\text{A3-2})$$

$$\mathbf{I}_2' = -\mathbf{V}_1 \frac{1}{\mathbf{Z}_1 + \mathbf{Z}_2' + \mathbf{Z}_1 \mathbf{Z}_2' \mathbf{Y}_m} \quad (\text{A3-3})$$

where

$$\mathbf{Z}_1 \mathbf{Y}_m = (r_1 g_m + x_1 b_m) + j(x_1 g_m - r_1 b_m)$$

There will be no noticeable error if the assumption is made that

$$\mathbf{Z}_1 \mathbf{Y}_m \approx x_1 b_m \left( 1 - j \frac{r_1}{x_1} \right) \quad (\text{A3-4})$$

Introducing the primary and secondary leakage coefficients

$$\tau_1 = \frac{x_1}{x_m} \quad \tau_2 = \frac{x_2'}{x_m} \quad (\text{A3-5})$$

and the abbreviations

$$\begin{aligned} r_t &= r_1 + (1 + \tau_1)r_2' & x_t &= x_1 + (1 + \tau_1)x_2' \\ f &= g_m \frac{r_2'}{s} + (1 + \tau_2) & h &= g_m x_2' - b_m \frac{r_2'}{s} \\ l &= (1 + \tau_2)r_1 + (1 + \tau_1) \frac{r_2'}{s} & m &= x_t - b_m r_1 \frac{r_2'}{s} \end{aligned} \quad (\text{A3-6})$$

the primary and secondary currents become

$$\mathbf{I}_1 = \mathbf{V}_1 \frac{\sqrt{f^2 + h^2}}{\sqrt{l^2 + m^2}} \quad (\text{A3-7})$$

$$\mathbf{I}_2' = \mathbf{V}_1 \frac{1}{\sqrt{l^2 + m^2}} \quad (\text{A3-8})$$

and the phase angle between the primary current and primary voltage is

$$\varphi_1 = \tan^{-1} \frac{h}{f} - \tan^{-1} \frac{m}{l} \quad (\text{A3-9})$$

For medium-sized and larger machines the term  $-j(r_1/x_1)$  can be neglected in Eq. (A3-4). Then

$$l = r_1 + (1 + \tau_1) \frac{\tau_2'}{s}, \quad m = x_t \quad (\text{A3-10})$$

For larger values of  $s$  the main flux is small and  $g_m \approx 0$ . Thus the inrush (starting current) of the induction motor

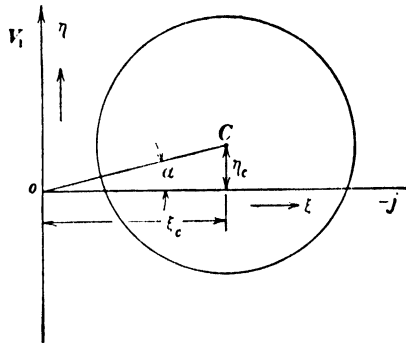
$$I_{1(s=1)} \approx V_1 \frac{1 + \tau_2}{\sqrt{r_t^2 + x_t^2}} \quad (\text{A3-11})$$

$$\tan \varphi_{1(s=1)} = \frac{x_t}{r_t} \quad (\text{A3-12})$$

(To Art. 27-1)

**Derivation of the Circle Diagram of the Polyphase Induction Motor.** With the aid of Eqs. A3-4, A3-5, and A3-6, Eq. A3-2 for the primary current of the polyphase induction motor can be written as

$$\frac{\mathbf{I}_1}{\mathbf{V}_1} = \frac{r_2' (a_m - j b_m) + [(1 + \tau_2) + j j_m x_2'] s}{r_2' [(1 + \tau_1) - j r_1 b_m] + [r_1 (1 + \tau_2) + j x_1] s} \quad (\text{A4-1})$$



**FIG. A4-1.**

$\mathbf{V}_1$  will be assumed in the real axis (axis of ordinates). Then  $\mathbf{V}_1 = V_1$ . With the abbreviations

$$\begin{aligned} r_2' (g_m - j b_m) &= \mathbf{A} & (1 + \tau_2) + j g_m x_2' &= \mathbf{B} \\ r_2' [(1 + \tau_1) - j r_1 b_m] &= \mathbf{C} & \tau_1 (1 + \tau_2) + j x_t &= \mathbf{D} \end{aligned} \quad (\text{A4-2})$$

Eq. (A4-1) becomes

$$\frac{I_1}{V_1} = \frac{A + B_s}{C + D_s} \quad (A4-3)$$

In order to determine the radius and the coordinates of the center of the circle, Cartesian coordinates  $\xi$  and  $\eta$  (Fig. A4-1) will be introduced in such a manner that  $\xi$  coincides with the imaginary axis and  $\eta$  with the real axis. (Contrary to the text, Art. 27-1, where the symbols  $x'$  and  $y'$  are used for the Cartesian coordinates, here the symbols  $\xi$  and  $\eta$  are used in order to avoid confusion with the reactances  $x_1$  and  $x_2'$ .)



With these coordinates

$$\mathbf{I}_1 = \eta - j\xi \quad (\text{A4-4})$$

$$\mathbf{V}_1 = \mathbf{V}_\eta = \mathbf{V}_1$$

Rewriting Eq. A4-3

$$(\mathbf{I}_1 \mathbf{C} - \mathbf{V}_1 \mathbf{A}) = (\mathbf{V}_1 \mathbf{B} - \mathbf{I}_1 \mathbf{D})s \quad (\text{A4-5})$$

From Eq. A4-2

$$\begin{aligned} \mathbf{A} &= \mathbf{A}_\eta + j\mathbf{A}_\xi & \mathbf{B} &= \mathbf{B}_\eta + j\mathbf{B}_\xi \\ \mathbf{C} &= \mathbf{C}_\eta + j\mathbf{C}_\xi & \mathbf{D} &= \mathbf{D}_\eta + j\mathbf{D}_\xi \end{aligned} \quad (\text{A4-6})$$

where

$$\begin{aligned} r_2' g_m &= A_\eta, \quad (1 + \tau_2) = B_\eta, \quad r_2'(1 + \tau_1) = C_\eta, \quad r_1(1 + \tau_2) = D_\eta \\ -r_2' b_m &= A_\xi, \quad g_m x_2' = B_\xi, \quad -r_2' r_1 b_m = C_\xi, \quad x_t = D_\xi \end{aligned} \quad (\text{A4-7})$$

Inserting Eqs. A4-4 and A4-6 in Eq. A4-5 and separating the real terms from the imaginary, two equations are obtained:

$$\begin{aligned} \eta C_\eta + \xi C_\xi - V_1 A_\eta &= (V_1 B_\eta - \eta D_\eta - \xi D_\xi)s \\ \eta C_\xi - \xi C_\eta - V_1 A_\xi &= (V_1 B_\xi - \eta D_\xi + \xi D_\eta)s \end{aligned} \quad (\text{A4-8})$$

Elimination of the slip  $s$  from these equations yields the equation of a circle in Cartesian coordinates with the coordinates of the center  $(\xi_c, \eta_c)$  and the radius  $R_c$ :

$$\xi_c = \frac{V_1}{2} \frac{\alpha_3}{\alpha_2}, \quad \eta_c = \frac{V_1}{2} \frac{\alpha_4}{\alpha_2} \quad (\text{A4-9})$$

$$R_c = \sqrt{\xi_c^2 + \eta_c^2 + V_1^2 \frac{\alpha_1}{\alpha_2}} \quad (\text{A4-10})$$

where

$$\begin{aligned} \alpha_1 &= A_\xi B_\eta - A_\eta B_\xi, & \alpha_3 &= (B_\eta C_\eta + B_\xi C_\xi) - (A_\eta D_\eta + A_\xi D_\xi) \\ \alpha_2 &= C_\eta D_\xi - C_\xi D_\eta, & \alpha_4 &= (A_\eta D_\xi - A_\xi D_\eta) - (B_\eta C_\xi - B_\xi C_\eta) \end{aligned} \quad (\text{A4-11})$$

The angle  $\alpha$  (Fig. A4-1), between the axis of abscissae and the line  $OC$  which connects the origin with the center, is according to Eqs. A4-7, A4-9, and A4-11

$$\tan \alpha = \frac{\eta_c}{\xi_c} \approx \frac{2r_1(1 + \tau_2)}{x_m + 2x_t} \approx \frac{2r_1}{x_m[1 + 2\tau_1 + \tau_2]} \quad (\text{A4-12})$$

wherein  $x_m$  is substituted for  $1/b_m$  (see Eq. 25-7).

In the problems encountered in practice, the no-load point and the locked rotor point ( $s = 1$ ) of the circle as well as the motor parameters are given, either by test or by computation. From these points and the angle  $\alpha$  the circle can be drawn.

## APPENDIX 5

---

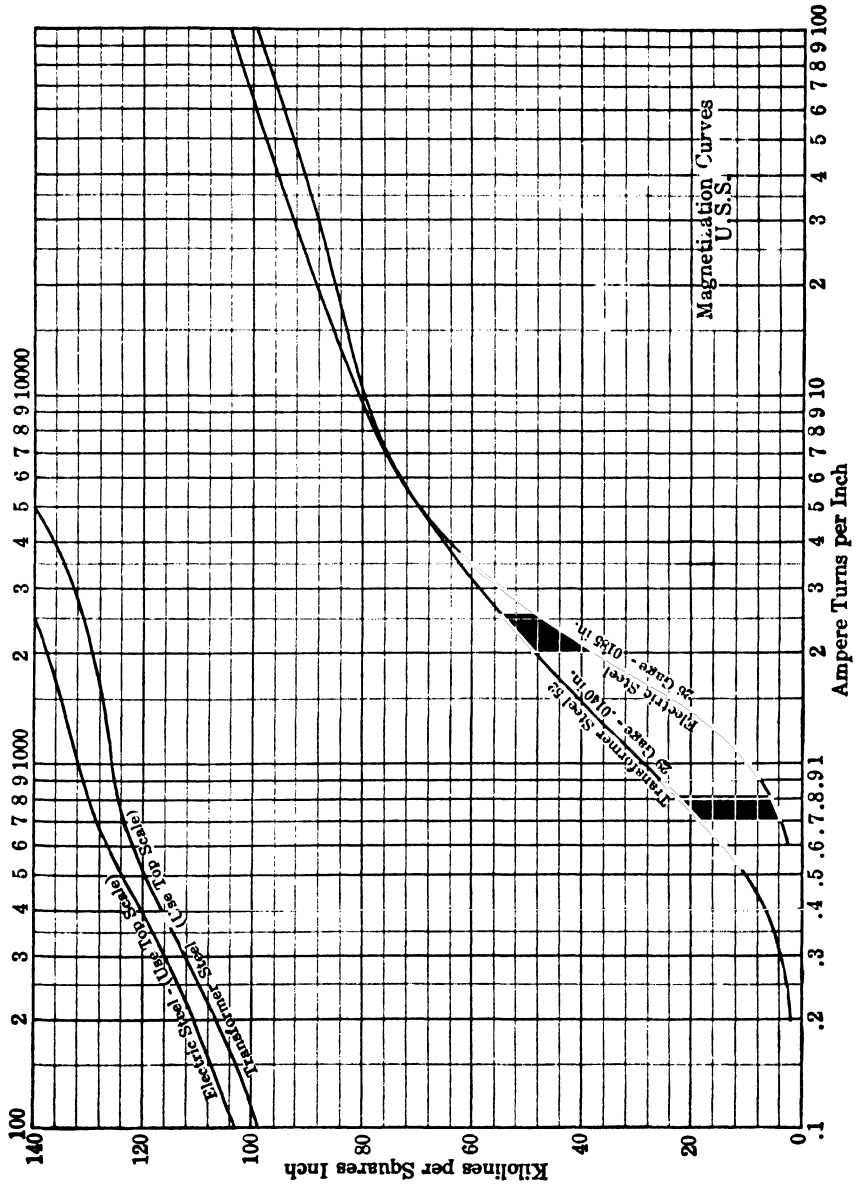


Fig. A5-1. Magnetization curves for transformer steel and dynamo steel.

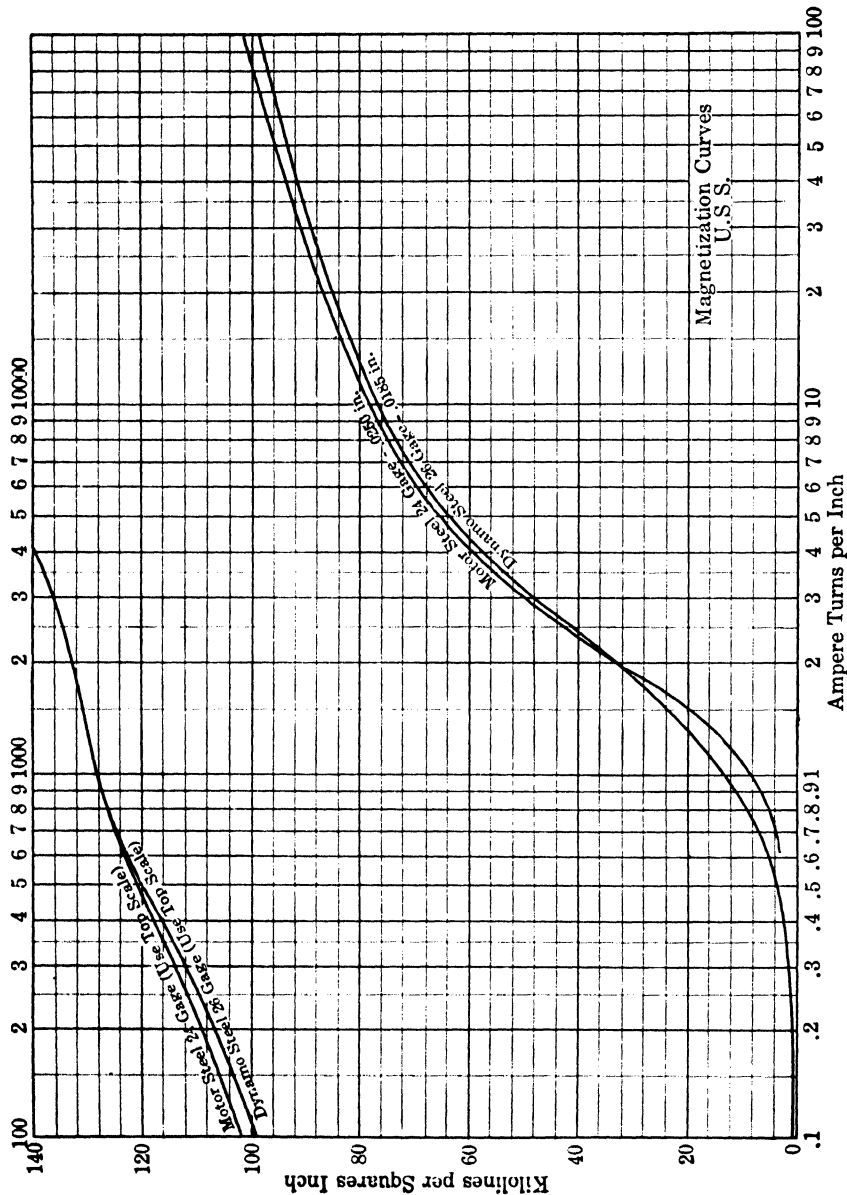


FIG. A5-2. Magnetization curves for dynamo steel.

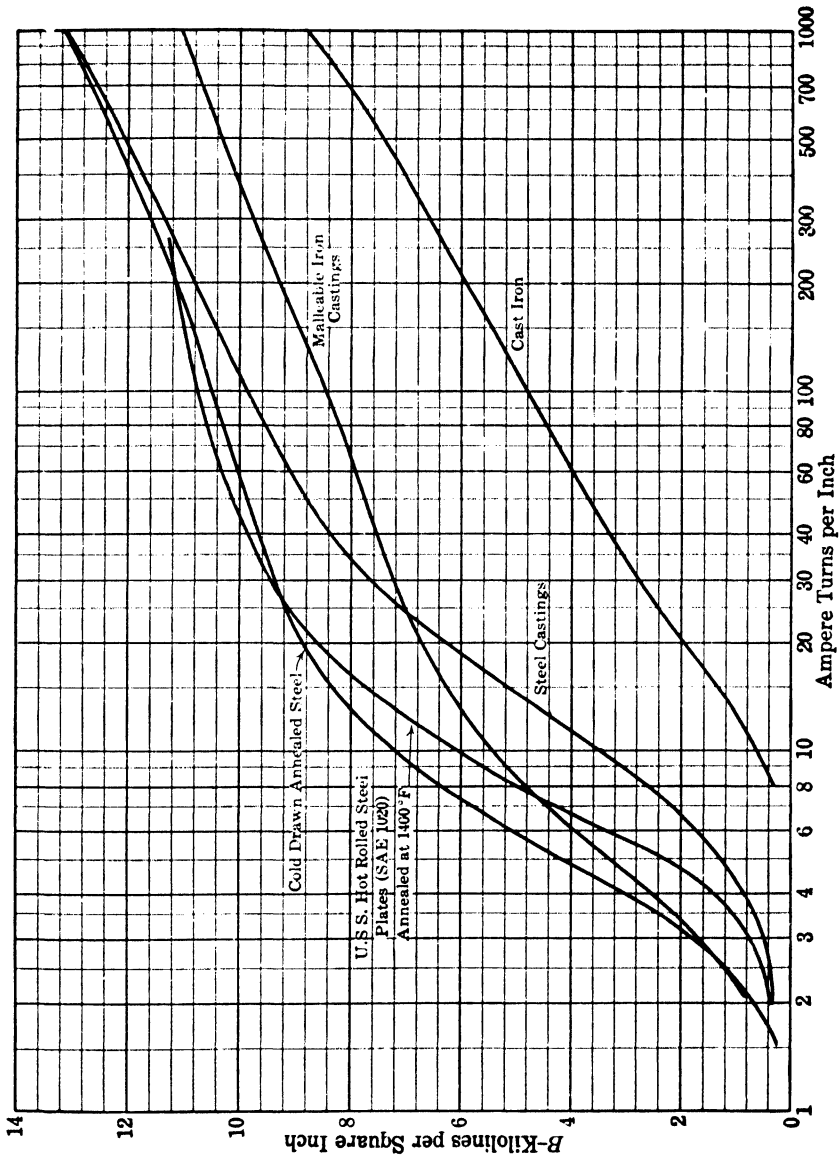


FIG. A5-3. Magnetization curves for cast iron, steel castings, cold-drawn annealed steel, and hot-rolled steel.

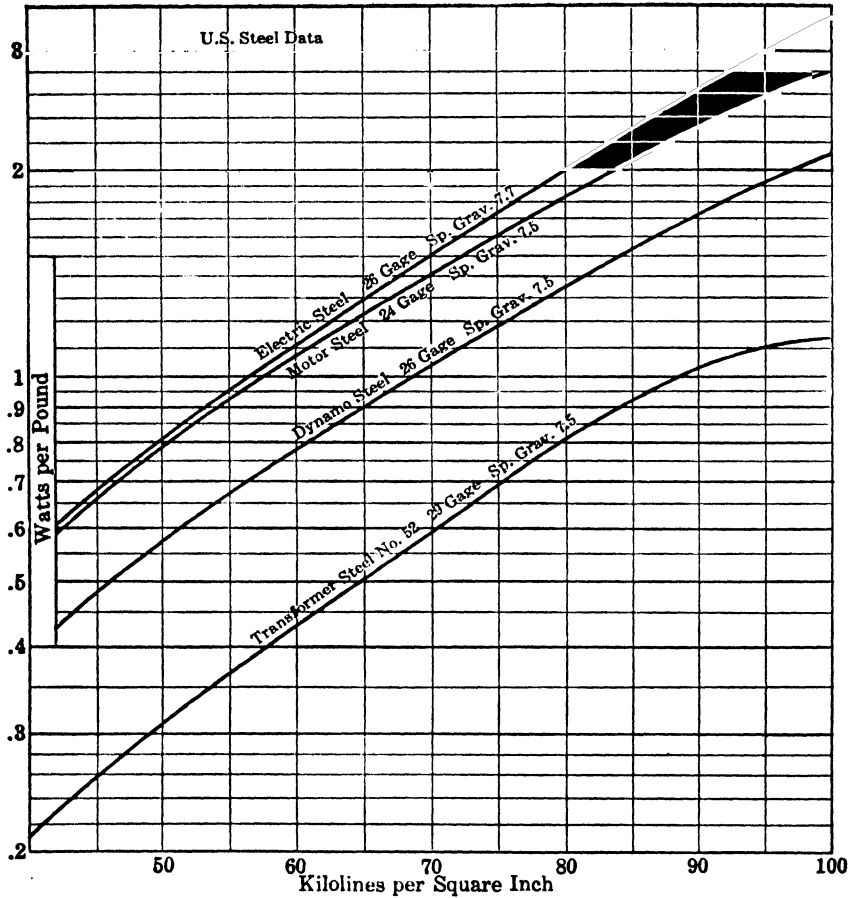


FIG. A5-4. 60-cycle loss curves for transformer steel and dynamo steel.

## LIST OF SYMBOLS

---

### *A, a*

<i>A</i>	area
AT	ampere turns
<i>a</i>	number of paths in d-c armature
<i>a</i>	transformation ratio of transformer

### *B, b*

<i>B</i>	flux density
<i>B<sub>g</sub></i>	flux density in air gap
<i>B<sub>t</sub></i>	flux density in teeth
<i>B<sub>y</sub></i>	flux density in yoke
<i>B<sub>p</sub></i>	flux density in pole
<i>b</i>	width
<i>b<sub>e</sub></i>	effective width
<i>b<sub>v</sub></i>	width of ventilating duct
<i>b<sub>p</sub></i>	pole face width
<i>b<sub>m</sub></i>	main flux susceptance

### *C, c*

<i>C</i>	constant
<i>C<sub>d</sub></i>	effectiveness factor in direct axis of salient pole synchronous machine.
<i>C<sub>q</sub></i>	effectiveness factor in quadrature axis of salient pole synchronous machine.

### *D, d*

<i>D</i>	diameter
<i>d<sub>i</sub></i>	inside diameter

### *E, e*

<i>E</i>	effective value of induced emf (a-c)
<i>E</i>	induced emf (d-c)
<i>E<sub>1</sub></i>	primary induced emf (transformer)

$E_1$	stator induced emf per phase (induction motor)
$E_2$	secondary induced emf (transformer)
	rotor induced emf per phase (induction motor)
$E_2'$	$E_2$ referred to primary winding (transformer)
	$E_2$ referred to stator (induction motor)
$E_c$	emf induced in coil
$E_f$	emf induced in armature of synchronous machine by field flux
$E_r$	emf due to rotation
$E_t$	emf due to transformer action
$E_{d-c}$	d-c emf of synchronous converter
$E_{a-c}$	a-c emf of synchronous converter
$E_0$	emf at no-load, d-c machine
$E_{2s}$	emf induced in rotor by rotating flux (induction motor)
$E_{2s}'$	$E_{2s}$ referred to stator
$E_{avg}$	average value of emf
$E_m$	maximum value of emf
$E_{s1}$	stator induced emf (resolver)
$E_{s2}$	stator induced emf (resolver)
$E_{r1}$	rotor induced emf (resolver)
$E_{r2}$	rotor induced emf (resolver)
$e$	instantaneous induced emf
$e_s$	emf of self induction (instantaneous value)
$e_t$	transformer emf (instantaneous value)
$e_r$	resultant of $e_s$ and $e_t$ (commutator machine)

 $F, f$ 

$F$	force
$F$	amplitude of mmf
$f$	mmf
$f$	force on a conductor
$f$	frequency in cycles per second
$f_n$	frequency of $n$ -th harmonic
$f_n$	natural frequency of oscillation
$f_1$	line frequency
$f_2$	rotor frequency in induction motor

 $G, g$ 

$g$	air gap length
$g_m$	main flux conductance

 $H, h$ 

$H$	magnetizing force
HP	horsepower
$h$	height

$I, i$ 

$I$	effective value of current (a-c)
$I_a$	armature current (d-c machine)
$I_a$	armature current (synchronous machine)
$I_f$	field current
$I_m$	maximum value of current (a-c)
$I_m$	magnetizing current
$I_n$	normal or rated current
$I_0$	no-load current
$I_\Phi$	reactive component of magnetizing current
$I_{h+c}$	hysteresis and eddy current component
$I_1$	primary current (transformer)
	stator phase current (induction motor)
$I_2$	secondary current (transformer)
	rotor phase current (induction motor)
$I_2'$	$I_2$ referred to primary (transformer)
	$I_2$ referred to stator (induction motor)
$I_{sc}$	short circuit current
$I_L$	locked-rotor current
$I_L$	line current
$I_{HP}$	output component of current (induction motor)
$I_{2f}$	forward rotor current (single phase motor)
$I_{2b}$	backward rotor current (single phase motor)
$I_{2f}'$	$I_{2f}$ referred to stator (single phase motor)
$I_{2b}'$	$I_{2b}$ referred to stator (single phase motor)
$I_M$	main winding current (single phase motor)
$I_S$	starting winding current (single phase motor)
$I_d$	component of armature current in phase with $E_f$ (salient pole synchronous machine)
$I_q$	component of armature current in quadrature with $E_f$ (salient pole synchronous machine)
$I_{d-c}$	direct current of synchronous converter
$I_{a-c}$	alternating current of synchronous converter
$I_r$	slip ring current of synchronous converter
$I_i$	interpole current
$I_{\min}$	minimum current
$I_{\max}$	maximum current
$i$	instantaneous current
$i_a$	current per path in d-c armature

 $J$ 

$J$	polar moment of inertia
-----	-------------------------

 $K, k$ 

$k$	number of commutator bars
-----	---------------------------



$k_i$	stacking factor
$k_p$	pitch factor
$k_{p1}$	pitch factor for fundamental
$k_{p1}$	stator pitch factor (induction motor)
$k_{pn}$	pitch factor for $n$ -th harmonic
$k_d$	distribution factor
$k_{d1}$	distribution factor for fundamental
$k_{d1}$	stator distribution factor (induction motor)
$k_{dn}$	distribution factor for $n$ -th harmonic
$k_{p2}$	rotor pitch factor (induction motor)
$k_{d2}$	rotor distribution factor (induction motor)
$k_{dp}$	winding factor
$k_{dpn}$	winding factor for $n$ -th harmonic
$k_s$	saturation factor
$k_{WM}$	winding factor (main winding, single phase motor)
$k_{WS}$	winding factor (starting winding, single phase motor)

 $L, l$ 

$L$	length
$L$	coefficient of self-inductance
$L_{11}$	coefficient of self-inductance due to primary or stator leakage flux
$L_{21}$	coefficient of self-inductance due to secondary or rotor leakage flux
$L_{21}'$	$L_{21}$ referred to primary or stator
$L_m$	coefficient of self-inductance due to main flux
$l$	length
$l_c$	length of core
$l_e$	effective or equivalent length
$l_y$	length of yoke
$l_p$	length of pole
$l_t$	length of teeth

 $M, m$ 

$M$	coefficient of mutual inductance
$M_a$	armature mmf
$M_f$	field mmf
$M_r$	resultant mmf
$M_{ad}$	armature mmf in direct axis
$M_{aq}$	armature mmf in quadrature axis
$M_d$	resultant mmf in direct axis
$m$	number of phases
$m_1$	number of primary or stator phases
$m_2$	number of secondary or rotor phases

 $N, n$ 

$N$	turns
$N_a$	number of armature turns (d-c machines)

$N_a$	turns per phase (polyphase machines)
$N_c$	turns per coil
$N_e$	turns per winding element
$N_e$	effective number of turns
$N_1$	number of primary turns (transformer)
	number of stator turns per phase (induction motor)
$N_2$	number of secondary turns (transformer)
	number of rotor turns per phase (induction motor)
$N_f$	shunt field turns per pole
$N_S$	number of turns on starting winding
$N_M$	number of turns on main winding
$n_c$	turns per coil
$n_s$	conductors per slot
$n$	rpm
$n_n$	normal or rated speed
$n_0$	no-load speed
$n_s$	synchronous speed
$n_r$	rotor speed

 $P, p$ 

$P$	power
$P_{co}$	copper loss
$P_e$	eddy current loss
$P_h$	hysteresis loss
$P_{h+e}$	hysteresis plus eddy current loss
$P_{ir.rot}$	iron loss due to rotation
$P_{rot.f}$	power of rotating field
$P_{F+W}$	friction and windage loss
$P_{m.dev}$	mechanical power developed
$P_{m.del}$	mechanical power delivered
$P_{sc}$	short circuit power input
$P_L$	locked rotor power input
$P_0$	no-load power input
$P_{inp}$	power input
$P_{outp}$	power output
$p$	instantaneous power
$p$	number of poles

 $Q, q$ 

$Q$	number of slots
$Q_1$	number of stator slots
$Q_2$	number of rotor slots
$q_1$	slots per pole per phase (stator)

$q_2$  slots per pole per phase (rotor)

$R, r$

$R$  resistance  
 $R$  radius  
 $R_e$  effective resistance  
 $R_{sc}$  short-circuit resistance  
 $R_L$  locked-rotor resistance  
 $R_s$  starting resistance  
 $R_2$  load resistance (transformer)  
 $R_2'$   $R_2$  in terms of primary  
 $r$  resistance  
 $r_a$  armature resistance  
 $r_c$  compensating winding resistance  
 $r_i$  interpole winding resistance  
 $r_f$  field winding resistance  
 $r_1$  primary resistance (transformer)  
 stator resistance per phase (induction motor)  
 $r_2$  secondary resistance (transformer)  
 rotor resistance per phase (induction motor)  
 $r_2'$   $r_2$  referred to primary (transformer)  
 $r_2$  referred to stator (induction motor)  
 $r_m$  main flux resistance

$S, s$

SCR short circuit ratio  
 $s$  slip  
 $s_n$  normal slip  
 $s_{po}$  pull-out slip  
 $s_b$  slip with respect to backward rotating flux

$T, t$

$T$  period in seconds  
 $T$  torque  
 $T_c$  period of commutation in seconds  
 $T_f$  forward torque  
 $T_b$  backward torque  
 $T_s$  synchronizing torque  
 $T_v$  periodic torque variation  
 $t$  time in seconds

$V, v$

$V$  effective terminal voltage (a-c)  
 $V_L$  line terminal voltage

$V_L$	locked-rotor terminal voltage (induction motor)
$V_{sc}$	short-circuit terminal voltage (transformer)
$V_1$	primary terminal voltage
	stator terminal voltage per phase
$V_2$	secondary terminal voltage
	rotor terminal voltage per phase
$V_2'$	$V_2$ referred to primary
	$V_2$ referred to stator
$V_s$	secondary terminal voltage of induction voltage regulator
$V_n$	normal or rated terminal voltage
$V_{d-c}$	d-c terminal voltage of synchronous converter
$V_{a-c}$	a-c terminal voltage of synchronous converter
$V_r$	slip ring terminal voltage of synchronous converter
$v$	velocity
$v$	instantaneous terminal voltage

$W, w$

$W$	coil width
-----	------------

$X, x$

$X$	reactance
$X_e$	equivalent reactance
$X_2'$	load reactance in primary terms (transformer)
$X_{sc}$	short-circuit reactance
$X_L$	locked-rotor reactance
$x$	distance
$x$	reactance
$x_1$	primary leakage reactance (transformer)
	stator leakage reactance per phase (induction motor)
$x_2$	secondary leakage reactance (transformer)
	rotor leakage reactance per phase (induction motor)
$x_2'$	$x_2$ in primary terms (transformer)
	$x_2$ in stator terms (induction motor)
$x_m$	main flux reactance
$x_l$	leakage reactance (synchronous machine)
$x_d$	direct axis synchronous reactance
$x_q$	quadrature axis synchronous reactance
$x_{ad}$	armature reaction reactance in direct axis
$x_{aq}$	armature reaction reactance in quadrature axis
$x_f$	field winding reactance
$x_c$	compensating winding reactance

$Y, y$

$Y$	admittance
$Y_m$	main flux admittance

$y$	distance
$y$	winding pitch
$y_b$	back pitch
$y_f$	front pitch

*Z, z*

$Z$	impedance
$Z$	number of conductors
$Z_m$	main flux impedance
$Z_1$	primary winding impedance (transformer) stator impedance per phase (induction motor)
$Z_2$	secondary winding impedance (transformer) rotor impedance per phase (induction motor)
$Z_2'$	$Z_2$ referred to primary (transformer) $Z_2$ referred to stator (induction motor)
$Z_e$	equivalent impedance
$Z_{sc}$	short-circuit impedance
$Z_L$	locked-rotor impedance
$Z_f$	impedance (forward, single phase motor)
$Z_b$	impedance (backward, single phase motor)
$Z_d$	direct axis synchronous impedance

*Alpha*

$\alpha$	ratio of pole arc to pole pitch
$\alpha$	angle
$\alpha_s$	angle between slots

*Beta*

$\beta$	angle
---------	-------

*Delta*

$\Delta$	lamination thickness
$\Delta$	increment
$\Delta$	delta connection
$\delta$	torque angle (synchronous machine)

*Epsilon*

$\epsilon$	voltage regulation
$\epsilon$	voltage drop

*Zeta*

$\zeta$	amplification factor (hunting, synchronous machine)
---------	---

*Eta*

$\eta$	efficiency
--------	------------

*Mu* $\mu$  permeability*Rho* $\rho$  resistivity*Sigma* $\sigma_h$  hysteresis loss constant $\sigma_e$  eddy current loss constant*Tau* $\tau$  pitch $\tau_p$  pole pitch $\tau_s$  slot pitch $\tau_c$  commutator pitch $\tau_1$  primary leakage coefficient $\tau_2$  secondary leakage coefficient*Phi* $\Phi$  flux per pole $\Phi_1$  total primary flux $\Phi_2$  total secondary flux $\Phi_{l1}$  primary leakage flux $\Phi_{l2}$  secondary leakage flux $\Phi_f$  field flux $\Phi_d$  direct axis flux $\Phi_q$  quadrature axis flux $\Phi_i$  interpole flux $\varphi$  power factor angle $\varphi_0$  no-load power factor angle $\varphi_1$  primary power factor angle (transformer) $\varphi_2$  secondary power factor angle (transformer) $\varphi_L$  locked rotor power factor angle*Psi* $\psi$  angle between  $I_a$  and  $E_f$  (synchronous machine) $\psi_{2s}$  angle between  $sE_2$  and  $I_2$  in rotor of induction motor*Omega* $\Omega$  mechanical angular velocity $\omega$  electrical angular velocity

## CONVERSION TABLE

<i>Multiply</i>	<i>by</i>	<i>to obtain</i>
Centimeters	0.3937	Inches
Centimeters	0.01	Meters
Circular mils	$0.7854 \times 10^{-6}$	Square inches
Square centimeters	0.1550	Square inches
Square centimeters	$10^{-4}$	Square meters
Square inches	6.45	Square centimeters
Dynes	$10^{-5}$	Newtons
Dynes	$2.25 \times 10^{-6}$	Pounds
Dyne-centimeters	$10^{-7}$	Newton-meters
Dyne-centimeters	$7.38 \times 10^{-8}$	Pound-feet
Ergs	$10^{-7}$	Joules or watt-seconds
Joules	0.738	Foot-pounds
Foot-pounds	$3.77 \times 10^{-7}$	Kilowatt hours
Kilowatt-hours	3413	B.T.U.
Kilowatt-hours	1.34	Horsepower-hours
Kilowatt-hours	$3.6 \times 10^6$	Joules
Kilowatt-hours	860	Kilogram-calories
Foot-pounds per second	$1.356 \times 10^{-3}$	Kilowatts
Horsepower	746	Watts
Abamperes	10	Amperes
Abvolts	$10^{-8}$	Volts
Abohms	$10^{-9}$	Ohms
Ohm-centimeters	0.01	Ohm-meters
Ohm-centimeters	$6.02 \times 10^6$	Ohms "per mil foot"
Kilolines	1000	Maxwells (lines)
Maxwells (lines)	$10^{-8}$	Webers
Gausses	6.45	Lines per square-inch
Gausses	$10^{-4}$	Webers per square-centimeter
Ampere-turns	1.257	Gilberts
Ampere-turns per inch	39.37	Ampere-turns per meter
Ampere-turns per inch	0.495	Oersteds
Abhenries	$10^{-9}$	Henries
Abfarads	$10^9$	Farads

## REFERENCES

---

It is to be observed that the following list of references is by no means complete. It contains only a few of the books and papers which may be useful to the reader. For a more complete list see *Electric Machinery*, Vol. I and II, by M. Liwshitz-Garik assisted by C. C. Whipple, D. Van Nostrand Co., 1946.

### *Electromagnetic Field Theory*

1. *Electric and Magnetic Fields*, S. S. Attwood, Wiley, 1941.
2. *Electromagnetic Fields*, Vol. I, E. Weber, Wiley, 1951.
3. *Electromagnetic Theory*, G. A. Stratton, McGraw-Hill, 1941.
4. *Two Dimensional Fields in Electrical Engineering*, I. Bewley, Macmillan, 1948.
5. *Classic Theory of Electricity and Magnetism*, M. Abraham and R. Becker, Blackie and Sons, 1932.
6. "Graphical Flux Mapping," J. F. Calvert and A. M. Harrison, *Electric Journal*, Vol. 25, 1928.

### *Circuits*

1. *Principles of Electrical Engineering*, W. H. Timbie, V. Bush, assisted by G. B. Hoadley, Wiley, 1951.
2. *Principles of Electric and Magnetic Fields*, W. B. Boast, Harper Brothers, 1948.
3. *Electrical Engineering — Basic Analysis*, E. M. Strong, Wiley, 1943.
4. *Basic Electrical Engineering*, G. F. Corcoran, Wiley, 1949.
5. *Electrical Engineering Fundamentals*, G. F. Corcoran and E. B. Kurtz, Wiley, 1941.
6. *Alternating-Current Circuits*, R. M. Kerchner and G. F. Corcoran, Wiley, 1951.
7. *Alternating-Current Circuits*, K. Y. Tang, International Textbook Co., 1951.
8. *Circuits in Electrical Engineering*, C. R. Vail, Prentice-Hall, 1950.
9. *Alternating-Current Circuit Theory*, M. B. Reed, Harper Brothers, 1948.
10. *Introduction to Circuit Analysis*, A. R. Knight and G. H. Fett, Harper Brothers, 1943.
11. *Electric Circuits*, E. E. Staff M.I.T. Wiley, 1940.
12. *Magnetic Circuits and Transformers*, E. E. Staff M.I.T. Wiley, 1943.

### *Direct-Current Machines*

1. *D. C. Machines*, E. Arnold and J. L. LaCour: Vol. I and II, Springer, Germany, 1927.
2. *Electric Machinery*, R. Richter: Vol. I, Birkhauser, Basel, Switzerland, 1951.
3. *Electric Machinery*: Vol. I, II, III, M. Liwshitz-Garik, Teubner, Germany, 1934.
4. *Principles of D-C Machines*, A. S. Langsdorf, McGraw-Hill, 1940.
5. *Direct-Current Machinery*, R. G. Kloeffler, R. M. Brenneman and J. L. Kerchner, Macmillan, 1948.
6. *Electric Machinery*: Vol. I, M. Liwshitz-Garik assisted by C. C. Whipple, Van Nostrand, 1946.

### *Alternating-Current Machines*

1. *A. C. Machines*, E. Arnold and J. L. LaCour: Vol. IV, V-1, V-2, Springer, Germany, 1913.



2. *A. C. Machines*, R. Richter: Vol. III, IV, and V. Springer, Germany, 1934, 1947.
3. *Principles of Alternating-Current Machinery*, R. R. Lawrence. McGraw-Hill, 1940.
4. *Theory of Alternating-Current Machinery*, A. S. Langsdorf. McGraw-Hill, 1937.
5. *Alternating-Current Machines*, A. F. Puchstein and T. C. Lloyd. Wiley, 1942.
6. *Alternating-Current Machinery*, L. V. Bewley. Macmillan, 1949.
7. *Electric Machinery*: Vol. I, II and III, M. Liwschitz-Garik. Teubner, Germany, 1934.
8. *Electric Machinery*, Vol. II, M. Liwschitz-Garik assisted by C. C. Whipple. Van Nostrand, 1946.
9. *Synchronous Machines*, C. Concordia. Wiley, 1952.
10. *The Nature of Polyphase Induction Machines*, P. L. Alger. Wiley, 1951.
11. *Winding Alternating-Current Machines*, M. Liwschitz-Garik assisted by C. Gentilini. Van Nostrand, 1950.
12. *Fractional Horsepower Electric Motors*, C. G. Veinott. McGraw-Hill, 1948.
13. *Alternating-Current Machinery*, J. Tarboux. International Textbook Co., 1947.
14. *Fundamentals of Alternating-Current Machines*, A. Pen-Tung Sah. McGraw-Hill, 1946.
15. *Alternating-Current Machinery*, T. C. MacFarland. Van Nostrand, 1948.
16. *Alternating-Current Machines*, G. V. Mueller. McGraw-Hill, 1951.
17. *Design of Electrical Apparatus*, J. H. Kuhlmann. Wiley, 1950.
18. *Transformer Engineering*, L. F. Blume. Wiley, 1938.
19. "Induction Motor Damping and Synchronizing Torques," C. Concordia. *AIEE Transactions*, 1952.

## ANSWERS TO PROBLEMS

---

The answers given below are, in many cases, determined on the basis of information obtained from plotted curves, sometimes requiring interpolation or extrapolation. The student should not expect to arrive at exactly the same result in all cases.

### CHAPTER 1

1. 0.096
2. 41.67 fpm
3. 225 rpm
4. 0.0015 v
5. 292 turns
6. 22.6 v, 14.4 v
7. 200,000 maxwells, 3.33 v, 7.5 v
8. 2.8 v, 1.4 v
9. 7.07 v
10. 2040 rpm
11. 320,000, 2 v, 1.6 v, 0 v, 2.52 v
12.  $3.2 \times 10^8$ , 3.2 mh
13.  $12.8 \times 10^8$ , 12.8 mh
14. 0.283 h, 0.488 h
15. 2450 v
16. 5250 v
17. 5 h, 40 joules, 80 v
18. 30 h
19.  $60 \times 10^8$ ,  $240 \times 10^8$ , 85.7 h
20. 362 v
21. 1280
22. 2260
23. 680, -300
24. 4.0, 7.2, 12.3, 20, 24 amp
25. 135 lines/sq in., 85,000 lines/sq. in.
26. 100 kilolines per sq in., 315,000 maxwells
27. 46,000 maxwells, 13,100 lines/sq in.
28. 9350 gaussess, 60,300 lines/sq in.
29. 0.213 amp
30. 0.685 lb, 0.441 lb ft
31. 2.98 lb ft
32. 2.11 lb ft
33. 1.49 lb ft
34. 9420 lines/sq in.

### CHAPTER 3

1. 216 bars, 216 bars, both symmetrical
2. 240 v, 480 v
3. 720 v, 3:1
6. 4, 180 bars
7. 860 rpm
8. simplex lap,  $y_b = 48$  bars,  $y_f = 47$  bars
9. 0.0469
10. yes
11. simplex lap,  $y_b = 25$  slots,  $y_f = 24$  slots
12. 400 amp, 85.3 kw
13.  $0.897 \times 10^6$  maxwells
14. 68.2 lb ft
15. 1970 lb ft
16. 3990 lb ft
17. 571 lb ft

### CHAPTER 4

1. 100% voltage, AT/pole = 3160
2. 100% voltage, AT/pole = 4250
3. 100% voltage, AT/pole = 3850
4. 100% voltage, AT/pole = 1430

### CHAPTER 6

1. 249.8 v
2. 260 kw
3. 1530 lb ft
4. 0.957
5. 93.7 lb (for 90% efficiency)
6. 1530 lb ft
7. 17.6% reduction
8. 385 v
9. 180 v (external resistance zero)
10. 231 v
11. 350 v

12. 3.85 amp; 5.55 amp
13. 50.8 ohms, 630 v, 0.05
14. 12.3 ohms, 626 v, 0.043; 89 ohms, 640 v, 0.067
15. 597 v
16. 595 v
17. 67,000 lines/sq in.
18. lap winding,  $7.5 \times 10^6$  maxwells, 281.6 lb ft
19. 146 ohms, 1845 AT, 1080 AT, 337 v, 2.31 amp, 3160 AT
20. 76 ohms, 303 v
21. 280 v
22. 3
23. (a) 339, 1161; (b) 555 v
24. 230.4 v, 480 kw, 120 kw, 2080 amp, 520 amp

## CHAPTER 7

1. (a) 1885 rpm, (b) 1925 rpm, (c) 67.4 lb ft
2. (a) 1710 rpm, (b) 1755 rpm, (c) 61.5 lb ft
3. 69.8 amp, 0.922 amp
4. 71.6 amp, 14 turns
5. (a) 1920 rpm, (b) 73.2 amp, (c) 0.965 amp
6. (a) 1752 rpm, (b) 80.1 amp, (c) 0.812 amp
7. (a) 1896 rpm, (b) 1840 rpm, (c) 70.2 lb ft
8. (a) 1715 rpm, (b) 1655 rpm, (c) 65.2 lb ft
9. 0.248 ohm
10. 1590 rpm, 68 lb ft
11. 1747 rpm, 68 lb ft
12. 17.9, 35.8, 53.7, 71.6, 89.7 lb ft, 1778, 1769, 1750, 1739, 1720 rpm
13. 0.878
14. 1885 rpm, 246 volt
15. 1510 rpm, 71.3 lb ft
16. 18.2, 36.7, 55.7, 75.0, 94.6 lb ft; 1752, 1717, 1684, 1660, 1620 rpm
17. 39.3 amp
18. 37.7%
19. 4.27 ohms
20. 17.35 lb ft, 0.792
21. 7.16 amp, 12.1 ohm
22. 153 lb ft, 0.745 ohm
23. 2.84 amp, 4.96 lb ft
24. 1272 rpm, 1030 rpm
25. 49.0 lb ft, 1550 rpm
26. (a) 1925 rpm, (b) 1650 rpm
28. 14.3% increase
29. 16 amp, 1000 rpm, 766 lb ft
30. 862 rpm, 868 lb ft
31. 0, 365, 662, 908, 1112, 1290, 1530
32. 850 rpm
33. 1235 rpm
34. 94.2 amp, 232 lb ft
35. 232 lb ft, 942 rpm
36. 49.9 amp, 53.1 lb ft
37. use 50 HP motor; 168 amp
38. (a) 33.8 HP, (b) 51 amp, (c) 98  $\epsilon$

## CHAPTER 8

1.  $11.86 \times 10^{-6}$  sec,  $5.05 \times 10^6$  amp/sec
2.  $18.1 \times 10^{-6}$  sec,  $2.76 \times 10^6$  amp/sec
3.  $20.2 \times 10^{-6}$  sec,  $0.624 \times 10^6$  amp/sec
4.  $10.8 \times 10^{-6}$  sec,  $96.5 \times 10^6$  amp/sec

## CHAPTER 10

1. 5400 lb ft, 0.912
2. 0.921
3. 0.945, 0.911, 0.920, 0.916, 0.912
4. 553 HP, 0.86
5. (a) 0.788, (b) 9790 w, (c) 9.72 amp

## CHAPTER 12

1. 79.5 w, pf = 0.476, 94,000 lines
2. 73,200 lines/sq in., 1.30 amp (assuming 0.0015" air gaps)
3. 544 turns
4. 1098.5 v, 109.85 v,  $5.15 \times 10^6$  maxwells
5. 1098 v, 1098 v
6. pf = 0.290, 2299 v, 0.0870 amp, 0.287 amp
7. 1350 turns, 110 turns, 240 sq in.
9. 0.214 amp, 1.22 amp, 1.24 amp, pf = 0.172
10. 0.418 amp, 2.44 amp, 2.48 amp, pf = 0.172
11. 0.836 amp, 4.88 amp, 4.96 amp, pf = 0.172

## CHAPTER 14

1. 41.4 amp, 0.996, 0.895 amp, 0.950
2. 6.48 amp, 0.995, 0.255 amp, 0.982
3. 44.5 amp, 0.866, 0.92 amp, 0.984
4. 14.85 amp, 0.77, 0.389 amp, 0.989

## CHAPTER 17

1.  $r_1 = 6.80$ ,  $r_2' = 3.73$ ,  $x_1 = x_2' = 11.15$ ,  $r_m = 77.6$ ,  $x_m = 2440$  ohms
2.  $r_1 = 9.55$ ,  $r_2' = 5.35$ ,  $x_1 = x_2' = 32.8$ ,  $r_m = 8600$ ,  $x_m = 32,400$  ohms

3.  $r_1 = 0.191$ ,  $r_2' = 0.105$ ,  $x_1 = x_2' = 1.24$ ,  $r_m = 112.4$ ,  $x_m = 885$  ohms
4. 0.0227, 0.972; 0.0454, 0.965; 0.968, 0.975, 0.975; 0.960, 0.970, 0.970
5. 0.0123, 0.978; 0.0387, 0.973; 0.955, 0.973, 0.978; 0.944, 0.966, 0.971
6. 0.00955, 0.987; 0.0451, 0.983; 0.976, 0.985, 0.988; 0.970, 0.981, 0.983
7. 0.0745, 0.0775, -0.00142
8. 0.0148, 0.0444, -0.0211
9. 0.00722, 0.0241, -0.0127
10. 0.0109, 0.0382, -0.0212
11. 0.0105, 0.0212, -0.00444; 0.980, 0.975, 0.975
12. 0.971
13. 0.986
14. 0.167, 0.0359, -0.00940; 0.975, 0.968, 0.968; 0.947, 0.965, 0.970, 0.966
16. 235.3 v
15. (A) 100 kw, 1.0 pf, (B) 50 kw, 0.50 pf
16. Main:  $a = 5$ , 1100/220 v, 524/2620 amp  
Teaser:  $a = 5$ , 952/191 v, 524/2620 amp
17. 115 v,  $120^\circ$
18. Main: Pri. 26.9 kva, Sec. 23.3 kva  
Teaser: Pri. 23.3 kva, Sec. 23.3 kva
19. 79.6 kw
20. 58.4 kw
21. For 625-v converter:  
Pri. 11,500 v, 25.1 amp, 166.7 kva,  $a = 26$   
Sec. 442 v, 377 amp, 166.7 kva
22. Pri. 11,500 v, 25.1 amp, 166.7 kva,  $a = 30.1$   
Sec. 382 v, 218 amp, 166.7 kva
23. Pri. 11,500 v, 25.1 amp, 166.7 kva,  $a = 52$   
Sec. 221 v, 377 amp, 166.7 kva

## CHAPTER 18

1. (a) 7620/220 v, 437/15,100 amp, 3333 kva,  $a = 34.6$   
(b) 7620/127 v, 437/26,200 amp, 3333 kva,  $a = 60$   
(c) 13200/127 v, 252/26,200 amp, 3333 kva,  $a = 104$   
(d) 13200/220 v, 252/15100 amp, 3333 kva,  $a = 60$
2.  $N_1 = 34.1$ ,  $N_2 = 29.6$
3. (a) 6600 v, 15.1 amp  
(b) 120 v, 832 amp  
(c) 55
4. Primary 6350 v, 30.8 amp  
Secondary 1100 v, 179 amp
5. Primary 11,000 v, 17.8 amp  
Secondary 635 v, 309 amp
6. Primary 11,000 v, 17.8 amp  
Secondary 1100 v, 179 amp
8. (a) 947 amp, (b) 17.2 amp,  $I_{\text{line}} = 29.8$  amp, (c) 0.998 lagging
9. 2660/440 v, 2.62/158 amp, 69 kva,  $a = 60.5$
10. (a) 33.3 kva, 28.8 kw, (b) 33.3 kva, 28.8 kw, (c) 71 kva, 68.8 kw
11. Main:  $a = 10.46$ , Pri. 176 kva, Sec. 204 kva  
Teaser:  $a = 12.1$ , Pri. 176 kva, Sec. 204 kva
12. Main: 150 kw, Teaser 150 kw
13. Main: 1100/220 v, 29.2/126 amp  
Teaser: 952/220 v, 29.2/126 amp
14. (A) 75 kw, 0.866 pf, (B) 75 kw, 0.866 pf

## CHAPTER 19

1. (a) I: 0.025, 0.01, 0.0229; 121, 48.4, 111 ohms  
II: 0.035, 0.008, 0.0341; 33.9, 7.74, 33.0 ohms  
(b) I: 0.980, 0.976, 0.976  
II: 0.985, 0.980, 0.980  
(c) I: 0.0103, 0.0218, -0.00545  
II: 0.00858, 0.0271, -0.0136
2. I: 250 amp, 109 kw, 0.989, 0  
II: 890 amp, 391 kw, 0.999, 0
3. I: 250 amp, 96.2 kw, 0.876, 0  
II: 890 amp, 303.8 kw, 0.775, 0
4. I: 290 amp, 1646 kw, 0.860, 0  
II: 241 amp, 1330 kw, 0.837, 0
5. I: 54.5 amp, 121 kw, 0.964, 1.32 amp  
II: 221.5 amp, 448 kw, 0.878, 1.32 amp
6. I: 56.4 amp, 124.5 kw, 0.958, 0  
II: 219.5 amp, 444.5 kw, 0.880, 0
7. Losses (Problem 5) = 1.02 Losses (Problem 6)

## CHAPTER 20

1. (a) 12/11, 11; (b) 183.3, 200, 16.7 amp; (c) 40.3 kva; (d) 3.67 kva
2. 60 kva, 36.4, 45.5, 9.1 amp, 50 kva, 10 kva
7. 2 autotransformers; (a) 208/230 center-tapped; (b) 180/230 v.
8. 3 autotransformers; Pri. 133 v; Sec. taps + 150 v, -150 v

## CHAPTER 22

- $2.56 \times 10^6$  maxwells, 1995 v
- $k_{p7} = 0.259$   $k_{p11} = 0.966$   $k_{p13} = -0.966$   $k_{d7} = 0.259$   $k_{d11} = 0.966$   $k_{d13} = -0.966$
- $k_{p6} = 0.174$   $k_{p7} = 0.766$   $k_{p11} = 0.766$   $k_{p13} = -0.174$   $k_{d5} = 0.217$   $k_{d7} = -0.177$   $k_{d11} = -0.177$   $k_{d13} = 0.217$
- $k_{p11} = 0.766$   $k_{p13} = -0.174$   $k_{d11} = -0.177$   $k_{p13} = 0.217$
- (a) 33.2 rms v, (b) 35.8 rms v
- 16 v, FF = 1.11, 15.4 v
- (a) 306 v, (b) 296 v, (c) 283 v
- 10,860 v

## CHAPTER 24

- 0.667, 1.0, 2.0, 3.33 cps
- (a)  $s = 0.022$ , (b)  $72^\circ$
- (a) 720 rpm, (b) 16 rpm, (c) 720 rpm, (d) 0
- (a)  $k_p = 0.966$ ,  $k_d = 0.958$   
(b) 673,000 maxwells
- 2.14
- 0.865 v
- (a)  $k_p = 0.940$ ,  $k_d = 0.960$ ,  
(b) 512,000 maxwells
- 2.22
- 0.624 v

## CHAPTER 26

- $I_{st} = 166$  amp;  $T_{st} = 28.8$  lb ft  
 $I_1 = 21.2$  amp, pf = 0.81,  $\eta = 0.88$ ,  
 $T_{dev} = 12.5$  lb ft,  $T_{del} = 11.7$  lb ft
- $I_{st} = 241$  amp,  $T_{st} = 78.2$  lb ft  
 $I_1 = 32.7$  amp, pf = 0.85,  $\eta = 0.87$ ,  
 $T_{dev} = 39.7$  lb ft,  $T_{del} = 37.5$  lb ft
- $I_{st} = 144$  amp,  $T_{st} = 120$  lb ft  
 $I_1 = 22.4$ , pf = 0.77,  $\eta = 0.90$ ,  
 $T_{dev} = 74.5$  lb ft,  $T_{del} = 71.5$  lb ft

## CHAPTER 28

- 10.1, 9.40, 8.85, 7.52, 5.53, 3.50,  
1.40 (p-u) amp  
0.616, 0.632, 0.668, 0.707, 0.791,  
0.867, 0.785
- 26.7, 28.2, 30.5, 31.2, 29.9, 23.1, 8.95  
lb ft
- 11.5, 10.8, 9.80, 8.55, 6.35, 4.05,  
1.65 (p-u) amp  
0.534, 0.633, 0.666, 0.538, 0.839, 0.867,  
0.784
- 8.58, 8.00, 7.53, 6.40, 4.67, 2.96, 1.21  
(p-u) amp

- 0.618, 0.634, 0.670, 0.707, 0.790, 0.869,  
0.786
- 35.6, 37.5, 37.3, 40.7, 41.3, 31.6, 12.0  
lb ft
- 19.5, 20.3, 22.1, 22.7, 21.6, 16.6, 6.5 lb  
ft
- $I_1$  (inrush) = 28.1 amp,  $T_{dev} = 30.4$   
lb ft
- $I_1 = 4.15$  amp, pf = 0.797,  $T_{dev} =$   
8.66 lb ft,  $P_{out} = 279$  HP, eff =  
0.828
- saturation factor 1.04,  $s_{po} = 0.324$ ,  
 $T_{po} = 31$  lb ft
- (a) 1.25, (b) 2.42 ohms, (c) 0.64
- $r_1 = 0.103$ ,  $r_2' = 0.143$ ,  $x_1 = 0.710$ ,  
 $x_2' = 0.710$ ,  $r_m = 0.547$ ,  $x_m = 30.2$   
(unsat)  
 $r_1 = 0.103$ ,  $r_2' = 0.143$ ,  $x_1 = 0.54$ ,  
 $x_2' = 0.54$ ,  $r_m = 0.547$ ,  $x_m =$   
30.2
- 567 HP output, eff 0.937, 127 amp,  
 $T_{dev} = 0.747$  (p-u)
- 1195 amp,  $T_{dev} = 0.985$  (p-u)
- 7.96, 7.78, 7.57, 6.65, 5.46, 4.27, 0.847  
(p-u) amp  
0.212, 0.243, 0.284, 0.334, 0.485, 0.707,  
0.895
- 0.985, 1.18, 1.49, 1.71, 2.29, 2.81, 0.747  
(p-u) lb ft
- 9.16, 8.95, 8.62, 7.56, 6.25, 4.92, 0.97  
(p-u) amp  
0.218, 0.242, 0.282, 0.333, 0.483, 0.722,  
0.893
- 6.77, 6.65, 6.40, 5.65, 4.68, 3.96, 0.806  
(p-u) amp  
0.221, 0.243, 0.284, 0.333, 0.502, 0.691,  
0.924
- 1.32, 1.56, 1.93, 2.23, 3.01, 3.73, 0.970  
(p-u) lb ft
- 0.712, 0.855, 1.05, 1.22, 1.67, 2.39,  
0.687 (p-u) lb ft
- 0.102, 2.81 (p-u) lb ft
- (a) 0.90 ohm per phase; (b) 0.46  
ohm per phase
- $r_1 = 1.20$ ,  $r_2' = 0.72$ ,  $x_1 = 2.31$ ,  $x_2' =$   
2.40,  $r_m = 2.04$ ,  $x_m = 41.2$  ohms  
(unsat)  
 $r_1 = 1.20$ ,  $r_2' = 1.01$ ,  $x_1 = 1.80$ ,  $x_2' =$   
1.80,  $r_m = 2.04$ ,  $x_m = 41.2$
- 4.87 HP output, eff. 0.836, 1.36 (p-u)  
amp, 30.6 lb ft
- 8.33 (p-u) amp; 63.0 lb ft
- 8.33, 8.10, 7.74, 6.75, 5.29, 3.72, 1.36  
(p-u) amp

- 0.515, 0.533, 0.564, 0.582, 0.674, 0.800, 0.762
27. 63.0 66.0, 74.0, 76.5, 83.8, 80.7, 30.6 lb ft
28. 0.157, 84.0 lb ft
29. 9.63, 9.34, 8.90, 7.75, 6.08, 4.28, 1.575 (p-u) amp  
0.516, 0.533, 0.563, 0.584, 0.672, 0.800, 0.758
30. 7.06, 6.88, 6.56, 5.72, 4.50, 3.16, 1.16 (p-u) amp  
0.521, 0.535, 0.559, 0.585, 0.675, 0.800, 0.759
31. 81.9, 88.4, 89.6, 102, 112, 106, 41.1 lb ft
32. 43.9, 48.2, 53.8, 55.7, 56.5, 58.4, 22.1 lb ft

## CHAPTER 29

1. 12.1 ohms per phase
2. 3.12 ohms per phase
3. 63.9 lb ft (1.46 p-u)
4.  $I_1 = 5.63$  (p-u),  $T_{dev} = 0.695$  p-u = 30.4 lb ft, no
5. 15.9 ohms per phase, 1.073 (p-u) = 15.8 amp, squirrel-cage motor,  $I = 5.00 - 10.00$  (p-u)
6. Voltage ratio 3:2;  $T_{st} = 0.238$  (p-u) 130 lb ft
7. 9.66 ohms per phase; 72 kw
8.  $T_{st} = 0.238$  (p-u)
9. 5.22 ohms per phase
10.  $T_{st} = 0.238$  (p-u)
11. (a) 0.314; (b) 0.94 ohm per phase
12.  $T_{st}$  (auto) =  $16 \times T_{st}$  (resistor)
13.  $I_2' = 66.6$  amp; 0.956; 750 lb ft (2.5% rotational losses)
14. 795 v ( $\cos \phi = 0.90$ )
15. approximately 246 v, 450 kva

## CHAPTER 30

3.  $87.25^\circ$
4.  $99.4^\circ$ ,  $93.4^\circ$
5.  $110.8^\circ$ ,  $116.3^\circ$ ,  $121.8^\circ$
6. 350, 110 v

## CHAPTER 32

1.  $I_1 = 3.1$  amp, pf = 0.574,  $T_{dev} = 13.6$  oz ft,  $T_L = 12.2$  oz ft,  $\eta = 0.577$
2. 8.12, 7.45, 6.63, 4.47, 3.85, 3.20 amp  
0.795, 0.805, 0.810, 0.768, 0.716, 0.595
3. 32.9, 34.2, 33.5, 25.7, 20.5, 13.8 oz ft  
0.165 HP, eff = 0.59 at  $s = 0.046$

5.  $r_1 = 1.71$ ,  $r_m = 1.61$ ,  $r_2' = 1.22$  ohms  
 $x_1 = 1.90$ ,  $x_m = 28.0$ ,  $x_2' = 0.95$
6.  $I_1 = 4.86$  amp, pf = 0.70,  $T_{dev} = 18.0$  oz ft,  $T_{del} = 16.02$  oz ft,  $\eta = 0.642$
7. 14.8, 13.6, 12.1, 7.84, 6.50, 4.85 amp  
0.820, 0.835, 0.849, 0.840, 0.812, 0.700
8. 41.1, 42.6, 43.0, 33.4, 28.0, 18.0 oz ft
9.  $r_m = 2.77$  ohms
10.  $I_1 = 2.54$  amp, pf = 0.70,  $T_{dev} = 9.32$  oz ft,  $T_{del} = 8.1$  oz ft,  $\eta = 0.62$
11. 7.25, 6.67, 5.97, 3.96, 3.32, 2.54 amp  
0.795, 0.811, 0.827, 0.826, 0.798, 0.70
12. 18.6, 19.4, 19.9, 16.3, 13.6, 9.32 oz ft
13.  $r_1 = 2.44$ ,  $r_m = 1.505$ ,  $r_2' = 1.796$  ohms  
 $x_1 = 2.57$ ,  $x_m = 36.2$ ,  $x_2' = 1.285$
14.  $I_1 = 3.55$  amp, pf = 0.675,  $T_{dev} = 12.7$  oz ft,  $T_{del} = 11.62$  oz ft,  $\eta = 0.661$
15. 10.35, 9.40, 8.34, 5.43, 4.56, 3.55 amp  
0.830, 0.844, 0.855, 0.827, 0.786, 0.675
16. 29.4, 29.8, 29.9, 22.7, 19.0, 12.7 oz ft

## CHAPTER 34

1. 8.90, 0.0906, 68.4 lb ft, 0.882, 0.790  
4.25, 0.0533, 31.4 lb ft, 0.788, 0.779  
0.667, 0.0227, 4.78 lb ft, 0.287, 0.470
2. (a) 4130; (b) 4000; (c) 4320;  
(d) 0.864; (e) 0.0315 (f) 16.15 lb ft
3. (a) 4975; (b) 4788; (c) 5220;  
(d) 0.857; (e) 0.0376; (f) 19.5 lb ft
4. 0.895, 0.843
5. 0.892, 0.895; 0.898, 0.910
6. 449 HP, 0.928, 0.880
7. 343 HP, 0.930, 0.864; 555 HP, 0.921, 0.872

## CHAPTER 37

2. (a) 5.50 ohms, 0.191 p-u; (b) 35 amp;  
(c) 31.3 ohms, 1.08 p-u
3. 0.163, 0.263, -0.084
4. 1.06, 0.92
5. (a) 1.21 ohms, 0.15 p-u; (b) 194 amp; (c) 11.1 ohms, 1.37 p-u
6. 0.31, 0.02
7. 0.73, 0.83
8. (a) 0.404 ohms, 0.15 p-u; (b) 371 amp; (c) 3.68 ohms, 1.37 p-u
9. 0.22, 0.31, 0.02

## CHAPTER 38

1. 0.083, -0.181

2.  $x_d = 1.25$ ,  $x_{ad} = 1.06$ ,  $x_{aq} = 0.61$ ,  $x_q = 0.79$
3. (a) 7175; (b) sat. SCR = 0.89; unsat. SCR = 0.80; (c) 0.122 at unity pf
4.  $x_l = 0.861$  ohm, 0.235 p-u,  $M_a = 3.2$  amp
5. 0.252, 0.0236, 0.410
6.  $x_d = 1.14$ ,  $x_q = 0.944$  p-u values
7.  $x_{ad} = 0.655$  p-u = 7.48 ohms,  $x_{aq} = 0.380$  p-u = 4.35 ohms, SCR = 1.12, 178 amp
8.  $BC = 1910$  v,  $CC' = 3030$  v,  $\psi = 56.7^\circ$ ,  $\delta = 19.8^\circ$ ,  $M_a C_q = 68$  amp,  $C_q = 0.504$ ,  $C_d = 0.869$
9. 0.142, 0.261, -0.178
10. 0.153, 0.272, -0.160
11. 0.259 ohm, 0.271 p-u, 77 amp
12. 0.125, 0.312, -0.0334
13. SCR = 0.89,  $x_d = 1.12$  (p-u),  $x_q = 0.78$  (p-u)
14. 2.02 ohms, 0.262 p-u, 57 amp
15. 0.175, 0.317, 0.0625
16. SCR = 0.90,  $x_d = 1.11$  p-u,  $x_q = 0.71$  p-u

## CHAPTER 39

1.  $47.6^\circ$ ,  $45.0^\circ$ ,  $42.7^\circ$ ,  $40.8^\circ$ ; 1000 kw
2. (a) 90.6, 88.9, 87.9, 87.5 amp  
(b) 0.965, 0.984, 0.995, 0.999 lag  
40.4, 8630 v
3. 3320 v
4.  $62.2^\circ$ ,  $58.1^\circ$ ,  $54.5^\circ$ ,  $51.6^\circ$ ; 1200 kw  
 $21.7^\circ$ ,  $20.8^\circ$ ,  $19.8^\circ$ ,  $19^\circ$ ; 500 kw
5. (a) 115.3, 111.6, 108.8, 107 amp  
(b) 0.910, 0.940, 0.965, 0.981 lag  
(a) 44.4, 45.5, 47.4, 49.7 amp  
(b) 0.985, 0.961, 0.923, 0.880 lead
6. 1168 kw
7. (a) 23,100 kva, (b) 20,000 kw,  
(c) 11,550 kvar, (d) 10,650 v,  
(e)  $21.8^\circ$ , (f)  $51.8^\circ$   
(a) 23,100 kva, (b) 20,000 kw,  
(c) 11,550 kvar, (d) 10,650 v,  
(e)  $21.8^\circ$ , (f)  $51.8^\circ$
8. (a) 0.561 lag, (b) 1564, (c) 7460,  
(d)  $16.3^\circ$ , (e)  $72.2^\circ$ , (f) 35,600,  
(g) 29,400 lag  
(a) 0.952 lead, (b) 921, (d)  $31.8^\circ$ ,  
(e)  $14^\circ$ , (f) 20,950, (g) 6,400 lead
9. (a) 25,550 kw, (b) 29,550 kva,  
(c) 14,800 kvar, (d) 1292 amp,  
(e) 0.866, (f) 11,660 v, (g)  $25.5^\circ$
- (a) 10,450 kw, (b) 12,050 kva,  
(c) 6,000 kvar, (d) 528 amp,  
(e) 0.866, (f) 13,170 v, (g)  $30.1^\circ$

## CHAPTER 43

1. 0.955, 1650 amp/sq in.
2. 133.6 amp, 0.964
3. 113.7 amp, 0.960
4. 96.4 amp, 0.950

## CHAPTER 44

1. (a) 442, (b) 221, (c) 383 v
2. (a) 837 amp, (b) 559 amp, (c) 280 amp
3. (a) 1086 amp, (b) 1100 amp, (c) 81.4 v, 1100 amp, 89.5 kva, (d) 91.4 kw, 6.92 amp, 13,200 v
4. (a) 1086 amp, (b) 552 amp, (c) 162.8 v, 552 amp, 89.5 kva, (d) 91.4 kw, 6.92 amp, 13,200 amp
5. (a) 1086 amp, (b) 552 amp, (c) 141 v, 319 amp, 89.5 kva, (d) 91.4 kw, 6.92 amp, 13,200 v
6. (a) 1086 amp, (b) 1238 amp, (c) 81.4 v, 1238 amp, 101 kva, (d) 93 kw, 7.83 amp, 13,200 v
7. (a) 1086 amp, (b) 619 amp, (c) 141 v, 357 amp, 101 kva, (d) 93 kw, 7.83 amp, 13,200 v
8. (a) 10,860 amp, (b) 5400 amp, (c) 162.8 v, (d) 81.4, v (e) 81.4 v, (f) 33 amp, (g) 57.1 amp
9. Pri: 27,000 v, 6.93 amp, 186.5 kva  
Sec: 44.2 v, 4220 amp, 186.5 kva  
125 v, 122 v, 128 v
10. Pri: 7620 v, 9.90 amp, 75.5 kva  
Sec: 442 v, 171 amp, 75.5 kva
12. Pri: 1100 v, 131 amp, 144.5 kva, pf = 0.866  
Sec: 141 v, 1023 amp, 144.5 kva
13. Main: Pri: 1100 v, 131 amp, 144.5 kva,  
a = 7.8, pf = 0.866  
Sec: 141 v, 512 amp, 144.5 kva  
Teaser: Pri: 951 v, 131 amp, 125 kva,  
a = 7.8, pf = unity  
Sec: 122 v, 512 amp, 125 kva
14. Main: Pri: 1100 v, 114 amp, 125 kva  
Sec: 141 v, 512 amp, 144 kva  
Teaser: Pri: 1100 v, 114 amp, 125 kva  
Sec: 122 v, 512 amp, 125 kva
17. 3 autotransformers Pri: 635 v, Sec. tap 81.4 v
18. 3 autotransformers Pri: 635 v, Sec. taps +81.4 v, -81.4 v

## CHAPTER 46

1. 136, 0
2. 0, 84.8
3. 14.95 lb ft
4. 3200 total

## CHAPTER 47

1. 4110
2. (a) 88.3, (b) 77.4
3. (a) 132.7, (b) 144
4. 0.95 lb ft
5. 4.93, 150,000
6. 338,000 maxwells
7. 48 v

## CHAPTER 49

1. 55%, 24 and 33 cps
2. Approximately 55%
3. Yes. Approximately 217%

## CHAPTER 51

1. 0.0667 ohm per 1,000 ft, 156,000 cm, 6 kw, 0.92
2. 17.4 kw, 125 v
3. 63.6 kw, 227 v, 552 w, 0.991, 19,040 lb
4. 157,000 cm, 475 lb
5. 19,580 cm, 59 lb
6. 723,000 cm, 5220 lb

7.  $V_1 = 113.6$  v,  $V_5 = 108.8$ ,  $V_{10} = 104.97$ ,  $V_{16} = 103.1$  v
8.  $V_1 = V_{16} = 122.25$  v,  $V_5 = V_{12} = 123.13$ ,  $V_7 = V_{10} = 124.1$  v
9. 118 v
10. 119.6 v, 112.8 v
11. 121.6 v, 109.6 v
12. 118 v
13. 174.3 v, 58.8 v
14. 120.1 v, 121.3 v, 241.4 v  
49.0 amp, 12.5 amp, 61.5 amp, 0.993
15. 144.9  $\angle -25.9^\circ$  amp, 87.0  $\angle 0^\circ$ , 76.6  $\angle -55.8^\circ$
16. 144.9  $\angle -25.9^\circ$  amp, 108.6  $\angle -36.8^\circ$ , 43.0  $\angle 2.53^\circ$
17. 129.3  $\angle -4.59^\circ$  v, 117.5  $\angle 2.47^\circ$ , 0.989
18. 129.5  $\angle -1.5^\circ$  v, 125.4  $\angle -1.5^\circ$
19. 43.7  $\angle -28^\circ$  amp, 23.9  $\angle -58.4^\circ$ , 26.1  $\angle 0^\circ$
20. 43.7  $\angle -28^\circ$  amp, 8.67  $\angle -29^\circ$ , 27.2  $\angle -36.9^\circ$
21. 9300 cir. mils
22. 37,300 cir. mils
23. 6500 cir. mils
24. 205, 245, 288 amp; 72 amp
25. 50.9 amp
26. 68.9 amp
27. 89.0 amp





## INDEX

---

- AIEE** regulation, synchronous machine, 353
- Air gap**, 223, 227
- Air gap line**, 73, 339, 346
- Air flow in d-c machine**, 120
- Ampère's law**, 1, 130, 133, 470
- Amplidyne**, 108, 109
- Angular velocity**, 5
- Amplifiers, rotating**, 107-112
- Armature reaction**
- d-c machines, 55-59, 67
    - brush shift, 58
    - cross flux, 56
    - distortion, 57
    - demagnetizing flux, 56
    - reduction in flux, 56-59
  - single-phase commutator motor, 423
  - synchronous machines, 343-353
    - cylindrical rotor, saturated, 346
    - cylindrical rotor, unsaturated, 343
    - salient-pole, saturated, 362
    - salient-pole, unsaturated, 359
- Armature windings**, 30-48, 189-198
- d-c machines, 30-48
    - lap, 30, 31, 34, 35, 36
    - wave, 30, 31, 36, 37, 38
  - a-c machines
    - polyphase lap, 189-193
    - polyphase wave, 193
    - single phase, 193
    - squirrel cage, 217, 220, 268
- Application of motors**, 444-456
- Autosyn**, 291
- Autotransformer**, 181 (*see* Transformers)
- Balancer set**
- Back pitch, 31
  - Backward rotating flux, 301
  - Biot-Savart law, 1, 471
  - Brush rigging, 26
  - Brush shift motor, 436, 439
- Capacitor motor**, 319
- Capacitor-start motor**, 318
- Chorded windings**, 192, 211
- Circuit law**, 1, 12, 50, 204
- Coefficient of self-inductance**, 8, 133
- Coefficient of mutual-inductance**, 9
- Commutation**
- d-c machine, 98-104
    - accelerated, 100
    - accelerated by interpoles or main flux, 102-104
    - delayed, 101
    - emf of self-induction, 101, 102
    - emf due to armature flux, 101
    - linear, 98, 99
    - period, 98
  - repulsion motor, 435,
  - Schrage motor, 443
  - series a-c motor, 429
  - synchronous converter, 415
- Commutating flux**, 102
- Commutator operation**, 40
- Compensating windings**
- d-c machines, 57
  - a-c machines, 423, 433
- Constant current transformer**, 186, 467
- Converters, *see* Synchronous Converter**
- Cooling**
- d-c machines, 118
  - induction motors, 326
  - synchronous machines, 404
  - transformers, 127
- Cores, transformer**, 122-125
- Core loss curve**, 480
- Counter-emf**, 83
- Current transformer**, 182
- Damping torques**
- induction motors, 401
  - synchronous machines, 400
- Damping winding**, 331, 382, 385, 399
- Deep bar rotor**, 268
- Differential compound generator**, 79
- Differential compound motor**, 88

- Differential leakage, 225
- Direct axis, 341
- Direct axis reactance, 343, 351
- Distributed windings, 30-40, 189-198
- Distribution factor, 200
- Distribution of power, 458-467
  - d-c, 458
  - single-phase, 464
  - three-phase, 464-465
  - two-phase, 464
- Double squirrel-cage rotor, 218, 268
- Doubly fed motor, 287
- Dynamic braking, 88
- Dynamotor, 107
- Eddy-current losses**, 114, 301
- Efficiency
  - all-day, 160
  - d-c machine, 86
  - polyphase induction motors, 250, 266
  - single-phase motors, 315
  - synchronous machines, 404, 453
  - transformers, 145, 156, 159
- Electrical neutral, 58
- Electromagnetic power, 84, 242, 370
- Emf, average value, 4
- Emf, effective value, 6, 7, 200
- Emf of mutual induction, 8, 11
- Emf of rotation, 45, 83, 200, 419
- Emf of self-induction, 1, 8, 11, 101, 131, 423
- Emf, sinusoidal, 5
- Emf, transformer, 227, 419, 420
- Emf maximum, 6, 7
- End winding leakage, 101
- Equalizer connections, 42
- Equivalent circuits
  - polyphase induction motor, 238, 263, 473
  - single phase induction motor, 304
  - synchronous machine, 340
  - transformer, 142, 154, 155, 156, 175
- Excitation methods, 61-65
  - compound, 63
  - separate, 61
  - series, 61
  - shunt, 62
- Exciters, synchronous machines, 33, 337
- External characteristics
  - compound generator, 74
  - series generator, 71
  - shunt generator, 69, 72
  - synchronous generator, 360
- Faraday's law**, 1, 7, 58, 82
- Fibreglas, 119
- Field construction, 25, 26
- Field excitation, 61-65
- Field winding, 25, 85
- Flash-over, 415
- Flux
  - alternating, 204, 419
  - backward, 301
  - commutating, 424
  - distribution, 4, 5, 47
  - end winding, 101
  - forward, 301
  - interlinkage, 8
  - rotating, 204
  - transformer, 130, 148
- Force on conductor, 14, 471
- Forward pitch, 31
- Fractional HP motors, 27, 300, 432, 448, 454-457
- Fractional pitch coils, 192
- Frequency, 6, 227, 232, 284
- Fundamental laws, 1, 18
- Generators, d-c**, 66-79
  - applications, 79
  - compound cumulative, 74
  - compound differential, 79
  - distribution factor, 204
  - external characteristics, 67, 71, 72, 74
  - flux distribution, 47
  - no-load characteristics, 67, 70, 71, 74
  - regulation, 70, 73
  - series, 70
  - shunt, 71
- Generators, a-c, *see* Synchronous generator
- Harmonics**, influence of
  - induction motor, 220, 270
  - transformers, 205
  - transformer connections, 161
- Harmonic leakage, 225
- Heating
  - d-c machines, 118
  - induction motors, 327
  - synchronous machines, 404
- Hunting
  - generators, 394-401
  - synchronous motors, 394
- Hysteresis losses, 114
- Hysteresis motor, 391
- Induction motor, polyphase**, 214-289

- Induction motor, air gap, 223, 227
  - brake operation, 246
  - circle diagram, 253-260, 475-476
  - construction, 254, 260, 475
  - delivered mechanical power, 255
  - developed mechanical power, 255
  - maximum output, 256
  - pull-out torque, 257
  - torque line, 256
  - slip line, 259
  - cooling, 327
  - double-cage rotor, 218, 268
  - efficiency, 250, 266, 451
  - electromagnetic coupling, 291
  - end winding leakage, 225
  - equivalent circuit, 238
    - no-load, 263
  - load, 238-241
  - locked rotor, 264
    - generator operation, 246
  - harmonics, influence of, 270
  - heating, 266, 327
  - leakage fluxes, 225
    - end winding, 225
    - harmonic or differential, 225
    - slot, 225
    - tooth-top, 225
  - locked rotor test, 264
  - losses
    - friction and windage, 242, 325
    - harmonics, 243, 324
    - load, 260, 324
    - main flux, 243, 323
    - rotation, 243
  - magnetizing current, 226, 238
  - main flux, 223
    - admittance, 233, 238
    - conductance, 238, 263
    - susceptance, 238
    - resistance, 238, 263
    - reactance, 238, 263
    - impedance, 233, 238
  - main wave, 225
  - mechanical elements, 214-223
  - no-load current, 236, 262
  - no-load test, 262
  - parameters of equivalent circuit, 262, 265
  - performance, equivalent circuit, 249-251, 270
  - per-unit values, 265
  - phasor diagram, 237
  - power balance, 242
- Induction motor, power developed, 242, 255
  - power delivered, 244, 255
  - power of rotating field, 242, 260
  - pull-out torque, 246
  - ratio of transformation, 227
  - reduction factors, 230
  - rotating flux, 204
  - rotor
    - construction, 214
    - die cast, 217, 220
    - deep bar, 268
    - double cage, 218, 238
    - polyphase winding, 234
    - skin-effect, 268
    - squirrel cage, 217
    - wound, 216, 219, 225
  - saturation, influence of, 269
  - saturation factors, 275
  - skin effect factors, 275
  - slip, 231, 246, 440, 451
  - special motors, 290-297
  - speed control, 282-288
    - by changing number of poles, 283
    - double-feeding, 287
    - Kramer cascade, 285
    - rotor emf, 284
    - Schrage, 439
    - speed regulating set, 284, 287
    - wound rotor, 283, 447
  - speed-torque characteristics, 245, 270, 282
  - starting, 278-282
    - autotransformer, 279
    - reactor, 278
    - resistor, 278
    - wound rotor, 280
  - stator, 214
    - leakage reactance, 226, 230
    - mmf distribution, 212
    - windings, 189
  - synchronous speed, 227
  - torque
    - delivered, 244
    - developed, 228, 244, 260
    - pull-out, 246, 266, 446, 451
    - starting, 249, 266, 446, 451
- Induction motor, single phase, 300-322
  - circle diagram, 305
  - cooling, 327
  - efficiency, 315
  - equivalent circuit, 304-309
    - no-load, 307
    - load, 304

- Induction motor, single phase, locked-**
  - rotor, 309
  - heating, 327
  - locked rotor test, 309
  - losses
    - friction and windage, 308, 325
    - load, 308, 312, 324
    - main flux, 308, 323
    - no-load, 311, 325
    - rotor, 312
    - stray load, 315
  - magnetizing current, 307
  - main winding, 193, 317
  - main flux reactance, 308, 311
    - resistance, 309, 312
  - mechanical elements, 300, 322
  - no-load current, 307
  - no-load test, 307
  - performance, 310-315
  - repulsion induction, 321
  - repulsion start, 321
  - rotating flux, 209, 300
  - rotor, 300
  - split phase, 317
  - starting, 317, 321
  - starting winding, 317
  - torque, 301
  - torque. pull-out, 454
  - torque, starting, 302, 318, 454
- Induction voltage regulator, 295-297**
  - polyphase, 296
  - single phase, 295
- Inertol, 129**
- Instrument transformers**
  - current, 182
  - potential, 182
- Interpoles, 26, 104, 415, 430**
- Insulating materials, 119**
- Inverted converter, 407, 417**
- Iron loss curves, 480**
- Kramer cascade control, 285**
- Kirchhoff's laws, 1, 9, 11**
  - d-c generator, 66
  - d-c motor, 83
  - polyphase induction motor, 226, 238, 473
  - single-phase induction motor, 303
  - single-phase series motor, 428
  - synchronous machines, 343, 346, 359, 361
  - transformers, 131, 139, 143
- Leakage flux**
  - d-c machine, 51, 101
  - induction motor, 225
  - transformer, 131
- Leakage reactance**
  - polyphase induction motor, 230, 269
  - single-phase induction motor, 309
  - synchronous machine, 349
  - transformer, 131, 138
- Lenz's law, 1**
- Load characteristics, 69-74**
  - compound generator, 74
  - series generator, 70
  - shunt generator, 69, 71
  - synchronous machine, 348
- Load division**
  - d-c generators, 77
  - synchronous generators, 375
  - transformers, 177
- Locked-rotor test, 264, 309**
- Loop distribution, 467**
- Losses, d-c and a-c machines, 113-118, 323-327, 402-404**
  - armature copper, 115, 260, 324, 402
  - eddy current, 114
  - field, 117
  - friction, 116, 242, 325, 403
  - hysteresis, 114
  - main flux, 113, 243, 308, 323, 342, 402
  - stray load, 117, 315, 404
  - windage, 116, 242, 325, 403
- Magnetic circuit, 50-60**
  - d-c machine, 50-60
  - induction motor, 222
  - synchronous motor, 331
  - transformer, 130, 148
- Magnetization curves, 447-449**
- Magnetizing current**
  - polyphase induction motor, 226, 238
  - repulsion motor, 434
  - single-phase induction motor, 307
  - transformer, 132, 139
- Magnetomotive force, 14, 205, 212, 228**
- Main flux**
  - d-c machine, 21, 51
  - polyphase induction motor, 225
  - transformer, 131
- Main flux losses, 145, 243, 323**
- Modulus of resonance, 399**
- Moment of inertia, 397**
- Motor application, 444-457**
  - characteristics, 444

**Motor application, load characteristics, 448**  
 types, 448  
**Motors, d-c, 84-94**  
 compound, 88, 444  
 series, 87, 444  
 shunt, 84, 444  
 speed control, 89, 90, 445, 447, 450  
 types, comparison, 88, 444  
 voltage variation, effect of, 89  
**Mutual reactance, 12**  
  
**Neutral axis, 58**  
**Noise, 218**  
**No-load characteristics**  
 d-c machine, 55, 67, 70, 72  
 synchronous machine, 339, 346  
**No-load test**  
 polyphase induction motor, 262  
 single-phase induction motor, 307  
 transformer, 154  
  
**Oil, insulating, 129**  
**Oil-cooled transformer, 129**  
**Oscillations of synchronous machine, 395**  
  
**Parallel operation**  
 d-c generators, 77-79  
 synchronous generators, 373-376  
 transformers, 174  
**Permeability, 13**  
**Per-unit parameters**  
 polyphase induction motor, 265  
 synchronous machine, 377  
 transformer, 156  
**Phasor, definition, 6**  
**Pitch factor, 200**  
**Plugging, 248**  
**Polarity of transformers, 161-163**  
 lead designation, 161  
 tests, 162  
**Pole leakage, 52**  
**Pole pitch, 4, 30**  
**Position indicators, 294**  
**Potential transformer, 182**  
**Potier triangle, 347**  
**Power developed**  
 induction motor, 242  
 synchronous motor, 371  
**Power factor correction, 386, 442**  
**Primary distribution, 463**  
**Pull-in torque, 416, 445, 446**  
**Pull-out torque, 246, 266, 446, 451, 453**  
**Pyranol, 129**

**Quadrature axis, 358, 359**  
**Quadrature axis reactance, 361**  
  
**Ratio of transformation, 134, 137, 227**  
**Reactance, leakage**  
 polyphase induction motor, 230, 269  
 single-phase induction motor, 309  
 synchronous machine  
 direct axis, 343, 351  
 quadrature axis, 361  
 transformers, 138  
**Regulation, speed, 87, 450**  
**Regulation, voltage**  
 d-c generator, 67, 70, 73  
 synchronous generator, 350-355, 364  
 transformer, 146, 150, 159  
**Regulators, induction, 295-299**  
**Reluctance, 14**  
**Reluctance motor, 390**  
**Reluctance torque, 371, 390**  
**Repulsion motor, 321, 433**  
**Repulsion-start motor, 321**  
**Rotating amplifier, 107**  
**Rheostatic speed control, 91**  
**Rotating flux**  
 polyphase winding, 204  
 single-phase winding, 209, 301  
**Rotors**  
 cylindrical, 330  
 salient pole, 329, 331, 332  
 squirrel cage, 217, 220  
 wound, 216, 219, 225  
**Rototrol, 109-112**  
**Resolvers, 297**  
  
**Saturation curve, 477, 478, 479**  
**Saturation factors, 275**  
**Schrage motor (BTA), 439**  
**Scott connection, 168**  
**Secondary network, 466**  
**Self-synchronizers, 291**  
**Selsyns, 291**  
**Series distribution, 458**  
**Series generator, 70**  
**Series motor, a-c, 428**  
**Series motor, d-c, 87**  
**Shaded pole motor, 322**  
**Short-circuit characteristic, 347**  
**Short-circuit ratio, 351**  
**Short-circuit tests, 155**  
**Shunt generator, 71**  
**Shunt motor, 84**  
**Silicones, 119**

- Skewing, 211
- Skin effect factor, 275
- Skin effect losses, 117
- Skin effect rotor, 268
- Slot ripple, 115, 323
- Split phase motor, 318
  - capacitor, 319
  - capacitor start, 318
  - resistor start, 318
  - reactor start, 318
- Starting
  - d-c motor, 85
  - polyphase induction motor, 278-288
  - single-phase motor, 317, 321
  - synchronous motor, 386
- Surface losses, 115, 324
- Synchronizing generators, 375
- Synchroscope, 376
- Synchronous converter, 406-418
  - armature winding, 406
  - armature paths, 406
  - armature reaction, 415
  - commutation, 415
  - comparison with d-c generator, 412
  - comparison with m-g set, 417
  - cross flux, 408
  - current ratios, 410
  - efficiency, 413
  - field current, 408
  - hunting, *see* Synchronous motor
  - interpoles, 415
  - inverted operation, 407, 417
  - losses, 411
  - operation, 416
  - parallel operation, 416
  - power factor, 408
  - starting, 416
  - taps on winding, 410-412
  - transformers, 164-171
  - voltage regulation, 415
  - voltage ratios, 409
  - wave shapes, 411
- Synchronous generator
  - AIEE regulation, 353
  - air gap line, 339, 347
  - armature reaction, 344, 360
  - armature winding, 189-193
  - construction, 329-337
  - cooling, 404
  - cylindrical rotor machine, 333
  - damping, 331, 332, 399
  - direct axis mmf, 341, 358
  - Synchronous generator direct axis synchronous reactance, 343, 351
  - effectiveness factors, 358, 359
  - efficiency, 404
  - equivalent circuit, 340
  - external characteristic, 360
  - excitation, 333, 337
  - heating, 404
  - hunting, 394-401
  - leakage reactance, 349
  - losses, *see* Synchronous motor
  - main flux reactance, 340, 341, 360
  - main flux path, 331
  - mmf, resultant, 345
  - mmf, armature reaction, 344, 360
  - no-load characteristic, 339, 346, 347
  - oscillations, 395
  - parallel operation, 373-376
    - circulating current, 375
    - synchronizing, 375
  - per-unit quantities, 377
  - phasor diagrams, 345-347, 359-363
  - Potier triangle, 347
  - power balance, 370
  - power of rotating field, 370, 371
  - quadrature axis mmf, 341, 358
  - quadrature axis synchronous reactance, 361
  - regulation, voltage
    - cylindrical rotor, 350-355
    - salient pole rotor, 364
  - salient pole machine, 330
  - saturated machine
    - cylindrical rotor, 345
    - salient pole rotor, 362
  - short-circuit characteristic, 347
  - short-circuit ratio, 351
  - synchronous reactance, 343, 351, 361
  - torque, 371
  - torque angle, 372
  - two reaction theory, 357
  - unsaturated machine
    - cylindrical rotor, 343
    - salient pole rotor, 359
  - windings
    - stator, 189-193
    - rotor, 333, 334
  - zero power factor characteristic, 348
- Synchronous induction motor, 290
- Synchronous motor
  - circle diagram, 378-384
  - capacitor operation, 384, 386
  - construction, 329-337

**Synchronous motor, damping winding,**  
     331, 332, 385  
 efficiency, 453 (*see* Losses)  
 excitation, 333  
 hunting, 394  
 losses  
     friction and windage, 403  
 load current, 402  
     main flux, 342, 402  
     stray load, 404  
 moment of inertia, 397  
 phasor diagrams, 345-347, 359-363  
 Potier triangle, 347  
 power balance, 370  
 power factor correction, 386  
 reluctance torque, 371, 390, 416  
 rotors  
     cylindrical, 330  
     salient pole, 329, 331, 332  
 stability, 383  
 starting, 386  
 synchronizing power, 395  
 torque  
     developed, 338, 382  
     pull-in, 416, 445, 446  
     pull-out, 445, 446, 453  
     starting, 387, 446, 453  
     synchronizing, 394  
     torque angle, 371, 372  
     two-reaction theory, 357  
 V curves, 384  
**Synchrotie apparatus, 291**  
**Teaser transformer, 167**  
**Three-phase commutator motor, 439**  
**Three-phase power distribution, 464**  
**Three-wire generator, 106, 462**  
**Two-phase distribution, 464**  
**Torque, on conductor, 16**  
**Torque developed**  
     a-c commutator motors, 422, 431  
     d-c machine, 46, 48, 83-86  
     hysteresis torque, 392  
     induction motor, 244, 471  
     repulsion motor, 436  
     single-phase induction motor, 301, 454  
     synchronous motor, 338, 382  
**Torque, starting, 387**  
     d-c machine, 450  
     induction motor, 228, 249, 266, 446  
     single-phase motor, 302, 317  
     synchronous motor, 371, 378, 446, 453  
**Two-reaction theory, 357**

**Transformers**  
 all-day efficiency, 160  
 autotransformer, 181  
 connections, polyphase  
      $\Delta$ - $\Delta$ , 164  
     Y-Y, 165  
      $\Delta$ -Y, 166  
     Y- $\Delta$ , 166  
     diametrical, 169  
     double delta, 171  
     double wye, 170  
     open delta, 167  
     Scott, 168  
     T, 167, 171  
 constant current, 186  
 construction, 122, 147  
 cooling, 127  
 copper loss, 156  
 cores, 122-125  
 current ratio, 136, 138  
 efficiency, 145, 156, 159  
 equivalent circuit, 142, 144  
     load, 142  
     no-load, 154  
     short circuit, 156  
 equivalent values of parameters, 143,  
     151, 156  
 harmonics, 165  
 induced emf, 133, 136  
 instrument  
     current, 182  
     potential, 182  
 insulation, 126  
 Kapp diagram, 150  
 leakage flux, 131  
 leakage reactance, 131, 138  
 losses, 145  
 main flux, 131, 136  
     admittance, 133  
     impedance, 134, 154  
 magnetization curves, 477  
 magnetizing current, 132, 137, 139  
 no-load current, 130, 139  
 no-load test, 154  
 oil, 129  
 parallel operation, 174  
 per-unit values, 156  
 phasor diagrams, 132, 137, 141  
 polarity, 161, 162, 163  
     leads, 161  
     tests, 162  
 ratio of transformation, 134  
 reduction factors, 137



**Transformers**, regulation, 146, 150, 159

short-circuit test, 155

teaser, 167

temperature, 156

three-phase, 147

types, 121

voltage ratio, 136, 138

windings, 125

**Universal motor**, 432

**V curves**, 384

**Ventilation**, 120, 326, 334

**Voltage equations**

d-c generator, 66

d-c motor, 82

polyphase induction motor, 226, 233, 238

single-phase induction motor, 303

**Voltage equations**, synchronous generator, 343, 346, 359, 361

synchronous motor, 343, 346, 359, 361

transformer, 131, 139, 143

**Voltage regulation**

d-c generator, 70, 73

synchronous generator, 350-355, 364-367

transformer, 150-153

**Ward Leonard system**, 91

**Windings**,

d-c, 30-48

a-c polyphase, 189-195

a-c single phase, 193-198

**Winding element**, 31

**Winding factor**, 203, 318

**Winding pitch**, 31, 32

**Zero power factor characteristic**, 348





